frontiers | Research Topics

Exploring the intersection of cancer metabolism, metastasis and immunotherapy

Edited by
Lei Huang and Pengpeng Liu

Published in
Frontiers in Immunology
Frontiers in Oncology

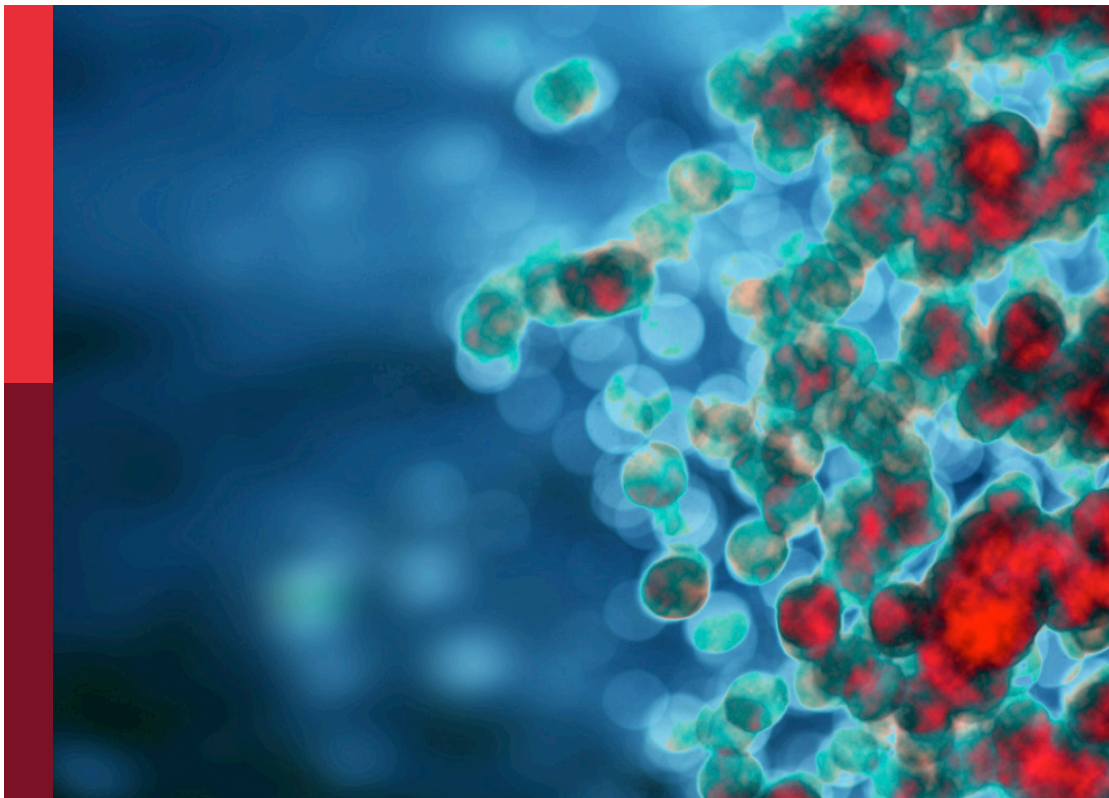

ISSN 1664-8714
ISBN 978-2-8325-7036-4
DOI 10.3389/978-2-8325-7036-4

Generative AI statement
Any alternative text (Alt text) provided alongside figures in the articles in this ebook has been generated by Frontiers with the support of artificial intelligence and reasonable efforts have been made to ensure accuracy, including review by the authors wherever possible. If you identify any issues, please contact us.

About Frontiers

Frontiers is more than just an open access publisher of scholarly articles: it is a pioneering approach to the world of academia, radically improving the way scholarly research is managed. The grand vision of Frontiers is a world where all people have an equal opportunity to seek, share and generate knowledge. Frontiers provides immediate and permanent online open access to all its publications, but this alone is not enough to realize our grand goals.

Frontiers journal series

The Frontiers journal series is a multi-tier and interdisciplinary set of open-access, online journals, promising a paradigm shift from the current review, selection and dissemination processes in academic publishing. All Frontiers journals are driven by researchers for researchers; therefore, they constitute a service to the scholarly community. At the same time, the *Frontiers journal series* operates on a revolutionary invention, the tiered publishing system, initially addressing specific communities of scholars, and gradually climbing up to broader public understanding, thus serving the interests of the lay society, too.

Dedication to quality

Each Frontiers article is a landmark of the highest quality, thanks to genuinely collaborative interactions between authors and review editors, who include some of the world's best academicians. Research must be certified by peers before entering a stream of knowledge that may eventually reach the public - and shape society; therefore, Frontiers only applies the most rigorous and unbiased reviews. Frontiers revolutionizes research publishing by freely delivering the most outstanding research, evaluated with no bias from both the academic and social point of view. By applying the most advanced information technologies, Frontiers is catapulting scholarly publishing into a new generation.

What are Frontiers Research Topics?

Frontiers Research Topics are very popular trademarks of the *Frontiers journals series*: they are collections of at least ten articles, all centered on a particular subject. With their unique mix of varied contributions from Original Research to Review Articles, Frontiers Research Topics unify the most influential researchers, the latest key findings and historical advances in a hot research area.

Find out more on how to host your own Frontiers Research Topic or contribute to one as an author by contacting the Frontiers editorial office: frontiersin.org/about/contact

Exploring the intersection of cancer metabolism, metastasis and immunotherapy

Topic editors

Lei Huang — University of Massachusetts Medical School, United States

Pengpeng Liu — University of Massachusetts Medical School, United States

Citation

Huang, L., Liu, P., eds. (2025). *Exploring the intersection of cancer metabolism, metastasis and immunotherapy*. Lausanne: Frontiers Media SA.

doi: 10.3389/978-2-8325-7036-4

Table of contents

frontiers | Frontiers in Immunology

TYPE Review
PUBLISHED 07 February 2025
DOI 10.3389/fimmu.2025.1539396

OPEN ACCESS

EDITED BY
Renjun Gu,
Nanjing University of Chinese Medicine, China

REVIEWED BY
Wenqing Liang,
Zhoushan Hospital of Traditional Chinese Medicine Affiliated to Zhejiang Chinese Medical University, China
Weihu Ma,
Ningbo No.6 Hospital, China
Yizheng Wu,
Zhejiang University, China

*CORRESPONDENCE
JunFeng Hu
hujunfengsx2024@163.com

RECEIVED 04 December 2024
ACCEPTED 15 January 2025
PUBLISHED 07 February 2025

CITATION
Li B, Zhang C, Xu X, Shen Q, Luo S and Hu J (2025) Manipulating the cGAS-STING Axis: advancing innovative strategies for osteosarcoma therapeutics.
Front. Immunol. 16:1539396.
doi: 10.3389/fimmu.2025.1539396

Manipulating the cGAS-STING Axis: advancing innovative strategies for osteosarcoma therapeutics

BingBing Li[1], Cheng Zhang[1], XiaoJuan Xu[1], QiQin Shen[2], ShuNan Luo[3] and JunFeng Hu[4*]

[1]Department of Pediatrics, Shaoxing Central Hospital, The Central Affiliated Hospital of Shaoxing University, Shaoxing, Zhejiang, China, [2]Department of Orthopedics, Shaoxing Central Hospital, The Central Affiliated Hospital of Shaoxing University, Shaoxing, Zhejiang, China, [3]Department of Surgery, Shaoxing People's Hospital, Shaoxing, Zhejiang, China, [4]Department of Pain, Shaoxing People's Hospital, Shaoxing, Zhejiang, China

This paper explored the novel approach of targeting the cyclic guanosine monophosphate (GMP)-adenosine monophosphate (AMP) synthase-stimulator of interferon genes (cGAS-STING) pathway for the treatment of osteosarcoma (OS). Osteosarcoma is a common malignancy in adolescents. Most patients die from lung metastasis. It reviewed the epidemiology and pathological characteristics of OS, highlighting its highly malignant nature and tendency for pulmonary metastasis, underscoring the importance of identifying new therapeutic targets. The cGAS-STING pathway was closely associated with the malignant biological behaviors of OS cells, suggesting that targeting this pathway could be a promising therapeutic strategy. Currently, research on the role of the cGAS-STING pathway in OS treatment has been limited, and the underlying mechanisms remain unclear. Therefore, further investigation into the mechanisms of the cGAS-STING pathway in OS and the exploration of therapeutic strategies based on this pathway are of great significance for developing more effective treatments for OS. This paper offered a fresh perspective on the treatment of OS, providing hope for new therapeutic options for OS patients by targeting the cGAS-STING pathway.

KEYWORDS

osteosarcoma, cGAS-STING, treatment target, drug, tumor immunity

1 Introduction

OS is a malignant bone tumor that primarily affects children and adolescents, particularly those in a rapid growth phase. According to literature reports, the incidence of OS has tripled since 2000, with the highest incidence observed in individuals aged 10 to 24 years, reaching 7.2 cases per million (95% CI: 6.9-7.5) (1). Although the overall incidence is relatively low, its highly malignant nature and tendency for pulmonary metastasis contribute to a high mortality rate, posing a significant threat to the health of adolescents.

Current treatment primarily has involved a combination of surgery, chemotherapy, and radiotherapy. Traditional treatments for osteosarcoma include surgical resection and systemic chemotherapy. Surgery is mainly divided into amputation and limb-salvage surgery. Surgery means complete removal of the tumor. Amputation requires that the osteotomy plane is at least 5 cm away from the tumor-free boundary. If the lesion cannot be completely removed during limb-salvage surgery, the local recurrence rate can be as high as 25% (2). At best, only 10% of all patients with osteosarcoma can be cured by tumor resection alone, and most develop local recurrence and/or lung metastases months later. Adjuvant systemic chemotherapy can significantly improve a patient's chance of cure (3–5). Adjuvant systemic chemotherapy includes postoperative chemotherapy used to remove lesions that cannot be completely removed by surgery and preoperative chemotherapy to improve the success rate of limb-sparing surgery and reduce the risk of recurrence, which have significantly improved the 5-year survival rate of patients with osteosarcoma. However, it is impossible to avoid the systemic side effects caused by chemotherapy, including liver and kidney damage, bone marrow suppression, neurotoxicity, gastrointestinal reactions, etc. For example, doxorubicin can cause permanent myocardial damage, and cisplatin can cause high-frequency hearing loss. wait (6–8). Although radiotherapy can be used for patients whose tumors cannot be surgically removed or remain at the resection margin, and for OS patients whose tumors do not respond well to chemotherapy, the actual sensitivity of OS to radiotherapy is not high (9). While these treatments improve survival rates, they also present challenges such as chemotherapy resistance and high recurrence rates, indicating the need for better treatment options and improved patient quality of life (4, 10). Immunotherapy is a hot research direction at present and is considered to be one of the breakthroughs in the treatment of osteosarcoma (11–15). The tumor microenvironment exists as an immune cell network with complex functions that can promote OS growth. Tumor-derived exosomes can drive bone cell behavior and create conditions for tumor cell homing (16). On the other hand, exosomes also widely promote immunosuppression, such as inhibiting the activity of T cells and NK cells, inducing T cell apoptosis, etc., to help osteosarcoma cells escape immune system (17–19). In addition, many factors such as specific proteins in OS-derived exosomes, cancer-associated fibroblasts, TGF-β, VEGF, tumor-associated macrophages, etc. have their own roles in the osteosarcoma microenvironment, some of which mediate the downregulation of immune cells, some of which provide support for tumor growth, regulate tumor progression, or affect the immune response (20, 21). A strongly suppressive immune microenvironment is associated with overactivation of multiple immunosuppressive pathways, so there is an urgent need to gain a deeper understanding of the osteosarcoma immune system and use its immune markers to develop targeted immunotherapy (22). The abnormal regulation of the immune system is crucial for the occurrence of OS. During interactions between the bone microenvironment and OS cells, the loss or dysfunction of the fatty acid synthase protein within OS cells allows them to evade immune surveillance, particularly in metastatic environments such as the lungs, which constitutively express fatty acid synthase ligands. It allows tumor cells to bypass the host's defense mechanisms, significantly reducing the efficacy of immune monitoring and clearance. Additionally, the macrophage migration inhibitory factor in OS activates the RAS/MAPK pathway, further promoting tumor cell escape and invasion (23). The formation of an immunosuppressive microenvironment and chronic inflammation provides a conducive environment for tumor growth. Metastatic cells with osteolytic potential in bone metastases can induce OS cells to produce factors such as parathyroid hormone-related protein, transforming growth factor-beta, or interleukin 11, which interact with the RANKL-RANK pathway between osteoblasts and osteoclasts, stimulating osteoclast activation. Simultaneously, the expression of RANK enhances the invasive ability of tumor cells. In environments with impaired immune function, this increases the risk of pulmonary metastasis, contributing to bone tumor progression. These abnormal immune responses not only exacerbate OS progression but also complicate immunotherapy, highlighting the immune system as a potential target for treatment. Therefore, understanding these abnormal regulatory mechanisms is crucial for developing more effective OS treatment strategies (24). (Figure 1) The cGAS-STING pathway is closely related to the regulation of the tumor's immune microenvironment. In recent years, the cGAS-STING pathway has received increasing attention in the immunotherapy research of osteosarcoma (25, 26). Therefore, we chose cGAS-STING pathway for discussion in this review, although Jordan et al. recently published a review with a similar theme (27). The main focus of these two reviews is different. Our main focus is on the cGAS-STING pathway and its upstream and downstream molecular mechanisms. The paper published by Jordan et al. mainly focuses on the application of nanotechnology in targeting the cGAS-STING pathway.

Traditional treatment methods for osteosarcoma include surgical resection, chemotherapy, and radiotherapy as adjuvant therapies. However, due to limitations such as restricted surgical anatomical locations, high tumor recurrence rates, poor aesthetic outcomes, significant systemic side effects of chemotherapy, and low sensitivity to radiotherapy, the advantages of immunotherapy have come to the fore. Studies indicate that immunological agents such as human interferon α, interferon α-2b and liposomal muramyl tripeptide phosphatidylethanolamine can effectively inhibit or reduce osteosarcoma cells.

The cGAS-STING pathway is a well-studied immune pathway. It activates innate immunological responders(IRs), forming a broadly applicable surveillance mechanism to defend against tissue damage and pathogen invasion (28). The pathway recognizes cytoplasmic double-stranded DNA (dsDNA) and promotes type I interferon (IFN) inflammatory signaling responses, while also influencing processes such as autophagy, cell survival, and senescence. It interacts with other innate immune pathways, regulating responses to infections, inflammatory diseases, and cancer, contributing to the impacts of immunotherapy (29). The cGAS-STING pathway is abnormally activated in various tumors, including hepatocellular carcinoma, acute myeloid leukemia, and OS, and plays a role in their occurrence and development (30–32). In OS, the abnormal activation of this

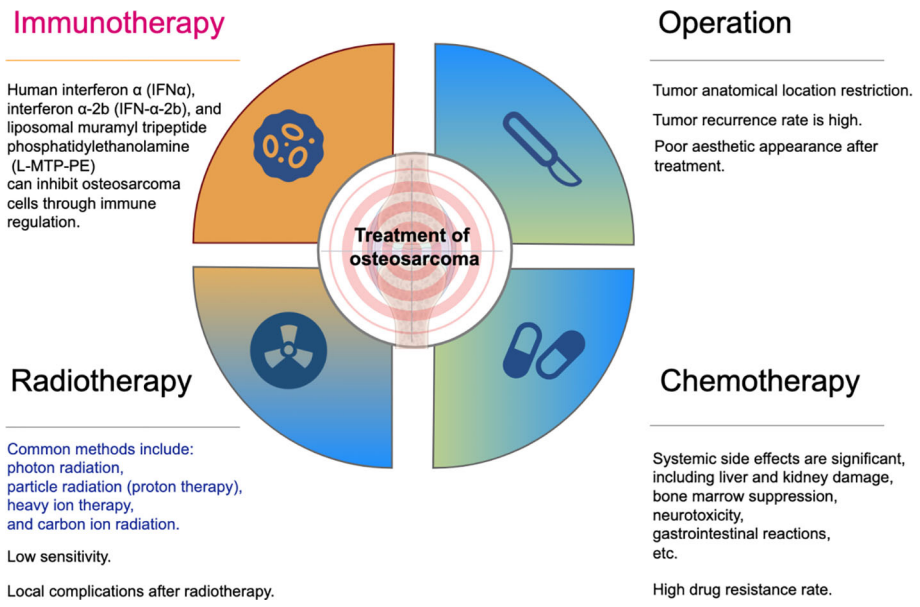

FIGURE 1
Current treatment of OS.

pathway is closely associated with the malignant biological behaviors of tumor cells (25). This paper aimed to explore the mechanisms of the cGAS-STING pathway in OS and identify therapeutic strategies based on this pathway. We outlined the structure and function of the cGAS-STING pathway and its role in innate IRs, and analyzed the abnormal activation of this pathway in OS and its relationship with tumor cell proliferation, invasion, and metastasis. We also discussed therapeutic strategies (including small molecule inhibitors alongside immunotherapy), and the challenges and prospects of targeting this pathway for OS treatment, providing a new perspective on OS treatment.

2 Structure and function of cGAS and STING proteins

cGAS is composed of a double-globular domain with two spherical structures connected by a groove. Its C-terminal portion contains a nucleotide transferase domain, which includes a catalytic domain and two DNA binding sites (A and B). DNA binding site A induces conformational changes in the protein, repositioning the catalytic pocket to allow catalysis with ATP and GTP substrates. The unique structure of cGAS enables it to effectively recognize and bind to DNA, cGAMP synthesis, and activate the IRs. STING (stimulator of interferon genes) is a protein composed of four transmembrane helices, a cytoplasmic ligand-binding domain (LBD), and a C-terminal tail. The LBD undergoes conformational changes upon binding to cGAMP, promoting STING oligomerization. cGAS and STING are key proteins in the cGAS-STING pathway, playing important roles in DNA recognition and activation of downstream signaling. cGAS catalyzes cGAMP synthesis, which acts as a second messenger to activate STING. STING then recruits and activates TBK1, initiating downstream signaling that leads to an IR. When dsDNA, whether exogenous or endogenous, is detected in the cytoplasm due to DNA damage or pathogen infection, cGAS catalyzes the synthesis of cGAMP. STING, located on the endoplasmic reticulum, recognizes and binds cGAMP, triggering conformational changes, including a 180° rotation and inward folding of the LBD, promoting STING oligomerization. Activated STING is transported from the endoplasmic reticulum to the Golgi apparatus via specific signaling pathways, where it recruits and activates numerous TBK1 molecules. Upon activation, TBK1 phosphorylates interferon regulatory factor 3 (IRF3) and nuclear factor kappa B transcription factors, promoting their translocation into the nucleus and the expression of IFN-α/β and tumor necrosis factor-alpha genes. These genes enhance innate IRs and initiate adaptive IRs (33–35). In addition to this classical pathway, STING can also mediate autonomous defense functions through gene transcription, with autophagy playing a key role. The activation of STING not only triggers antiviral IRs but also induces cellular "senescence" and eventually leads to cell death. Autophagy, senescence, and apoptosis are crucial mechanisms by which the cGAS-STING pathway combats pathological changes and maintains cellular homeostasis (33, 35, 36).

3 Relationship of cGAS-STING pathway with different diseases

The cGAS-STING pathway plays a crucial role in tumor immunology. For example, tumor cells can produce DNA damage, activate the cGAS-STING pathway, and trigger inflammatory responses and cell senescence, thereby inhibiting tumor growth. Additionally, tumor cells can evade immune destruction by degrading cGAS, STING, or TBK1 proteins.

Radiation therapy, a traditional cancer treatment, plays an important role in clinical applications. It directly kills tumor cells and also activates the cGAS-STING pathway, regulating downstream signals to improve the effectiveness of cancer treatment. Studies have found that expression levels of genes related to the cGAS-STING pathway are low in non-small cell lung cancer cells. Researchers used the cGAS-STING pathway activator diABZI and the small molecule human polynucleotide kinase/phosphatase inhibitor A12B4C3 (which promotes DNA damage) to enhance the activation of this pathway. The results showed that both diABZI and DNA damage increased the sensitivity of NSCLC cells to radiotherapy by promoting apoptosis, offering a new direction for combining radiotherapy with immunotherapy (37). In liver cancer research, a nanoplatform was used to activate the cGAS-STING pathway and enhance the effectiveness of immunotherapy. This platform uses manganese ions (Mn^{2+}) and β-paclitaxel to activate the cGAS-STING pathway, upregulate programmed death-ligand 1 (PD-L1), enhance T cell responses, and inhibit tumor growth and metastasis (38). Another study has demonstrated the potential of the cGAS-STING pathway in treating gastric cancer, where metformin can promote the release of downstream inflammatory factors by activating this pathway, enhancing antitumor IRs. The mechanism lies in the fact that metformin inhibits protein kinase B (AKT) phosphorylation, downregulating the expression of the transcription factor sex-determining region Y-box 2 (SOX2). SOX2 downregulation inhibits the AKT signaling pathway, thereby activating the cGAS-STING pathway (39). While cell senescence has a double-edged role in cancer, it can inhibit tumor progression by halting the cell cycle and enhancing immune surveillance (40). In breast cancer treatment, nanomaterials have been used to activate the cGAS-STING pathway, producing hydrogen sulfide and carbon monoxide gases. These gases induce mitochondrial dysfunction and tumor cell apoptosis while stimulating inflammation and dendritic cell maturation, ultimately promoting antitumor IRs and inhibiting the growth and metastasis of breast cancer (41). Many studies also suggest that various factors in multiple cancers activate the cGAS-STING pathway to enhance antitumor IRs (42).

Immune checkpoints are molecules that interact between immune cells, and under normal conditions, they regulate IRs and prevent excessive damage to the body's own tissues (43). However, in the tumor microenvironment (TME), tumor cells exploit immune checkpoints to suppress immune cell activity, evading immune surveillance and promoting tumor growth and metastasis. Immune checkpoint blockade (ICB) therapy targets these immune checkpoints, relieving their inhibitory effects, reactivating immune cells, and enhancing antitumor IRs (44–46). The cGAS-STING pathway, a cytoplasmic DNA sensor, can recognize dsDNA in the cytoplasm and activate innate IRs. Studies have found that the cGAS-STING pathway works synergistically with ICB therapy to enhance antitumor IRs. This is because the ataxia telangiectasia mutated protein, a key factor in DNA damage repair, is absent, leading to increased cytoplasmic DNA levels, which activate the cGAS-STING pathway, enhancing the efficacy of ICB therapy (47).

The cGAS-STING pathway plays a key role in infectious diseases. During infection, pathogen DNA is released into the cytoplasm, where cGAS recognizes and binds to this DNA, catalyzing the synthesis of cGAMP and activating STING protein. STING then initiates downstream signaling, activating TBK1 and IRF3, which induce the production of type I IFNs and inflammatory factors. These factors activate immune cells and trigger inflammatory and adaptive IRs to eliminate pathogens. The cGAS-STING pathway plays an important role in various infectious diseases. For example, during Kaposi's sarcoma-associated herpesvirus infection, the pathway is activated, inhibiting viral replication and enhancing IRs. The viral IFN regulatory factor 1 protein encoded by KSHV can inhibit STING-mediated DNA sensing, affecting viral replication and host IRs (48). Another study found that human glial cells express high levels of cGAS and downstream STING proteins in both resting and activated states, improving their ability to recognize viral DNA, activate IRF3, and express IFN-β mRNA, enhancing antiviral capacity (49). In dengue virus infections, which involve an RNA virus, the cGAS-STING pathway is activated, triggering antiviral IRs. Dengue virus can activate this pathway through mechanisms such as IL-1β-induced mitochondrial DNA (mtDNA) release and direct activation of cGAS. However, dengue virus infection can also inhibit the cGAS-STING pathway, such as through the degradation of cGAS or inhibition of STING signal transduction, demonstrating the dual nature of the pathway in viral infections (50–52). In bacterial infections, the cGAS-STING pathway plays an important role in host defense. It recognizes bacterial DNA and regulates innate IRs through a cascade of reactions. In a respiratory tract infection model, STING knockout mice exhibited higher bacterial loads, indicating the cGAS-STING pathway's importance in controlling Brucella infection (53). Similarly, following Mycobacterium bovis infection, the cGAS-STING pathway promotes the maturation and activation of DCs and enhances CD4+ T cell proliferation, bolstering adaptive IRs to clear the infection (54). In fungal infections, the cGAS-STING pathway is a key pattern recognition receptor in host defense, particularly in corneal epithelial cells. Fungal DNA or RNA hybrids are recognized by cGAS in the cytoplasm, triggering the pathway, promoting IFNs and inflammatory cytokines, and initiating IRs to clear fungal pathogens. Additionally, the pathway induces autophagic flux by enhancing the formation of microtubule-associated protein 1 light chain 3-, participating in clearing intracellular DNA and viruses, which helps the host fight fungal infections (55). Therefore, the cGAS-STING pathway plays an essential role in various infectious diseases, acting as the body's first line of defense against pathogen invasion. By activating this pathway, the body effectively responds to diverse infectious challenges and achieves self-protection (36, 56–58) (Table 1).

TABLE 1 The role of cGAS-STING signaling pathway in different types of diseases.

Disease Type	Disease	Effects of cGAS-STING signaling pathway	Reference
Cance	Lung cancer	diABZI and promotion of DNA damage activate the cGAS-STING pathway and increase the sensitivity of NSCLC cells to radiotherapy.	(37)
	Liver cancer	It enhances T cell responses and inhibits tumor growth and metastasis by upregulating programmed death-ligand 1.	(38)
	Gastric cancer	It promotes the release of downstream inflammatory factors and enhance anti-tumor immune response	(39)
	Breast cancer	It promotes anti-tumor immune response and inhibit the growth and metastasis of breast cancer.	(41)
infection	Kaposi sarcoma-associated herpes virus	It inhibits viral replication and enhance immune response	(48)
	Dengue virus	Activation of the cGAS-STING pathway can induce cell damage and apoptosis	(50)
	Brucella	STING knockout mouse model of respiratory infection exhibits higher bacterial load	(53)
	Mycobacterium bovis	It enhances adaptive immune responses to clear and fight infection	(54)
	Aspergillus fumigatus	It promotes the expression of IFNs and other inflammatory cytokines, triggering host immune responses and clearing fungal pathogens.	(55)

4 Role of cGAS-STING pathway in OS

The TME is a highly dynamic and evolving system, making accurate prediction challenging. The TME functions like nutrient-rich soil, providing nourishment for tumor cell proliferation while restricting anti-tumor immunity (59). The cGAS-STING pathway supports tumor survival and proliferation by promoting the formation of an immunosuppressive TME (60). Zhang et al. (61) constructed a Cox proportional hazards regression model and found that high expression of C–C motif chemokine ligand 5 was associated with a favorable prognosis in children with OS. The mechanism involves high expression of C–C motif chemokine ligand 5 significantly increasing the infiltration levels of macrophages (M0, M1), CD8+ T cells, and regulatory T cells in tumor tissues. Henrich et al. (62) developed a model for Ewing's sarcoma and discovered that ubiquitin-specific protease 6 significantly enhanced the infiltration of macrophages (F4/80+), DCs (CD11c+), and myeloid cells (CD11b+) in primary Ewing's sarcoma tumors through the synergistic effect of inducing chemokines such as C–X–C motif chemokine ligand 10, resulting in a significant improvement in overall survival rates. C–C motif chemokine ligand 5 and 10 can promote the infiltration of DCs and immune effector cells in OS. Radiotherapy can elevate the expression levels of C–C motif chemokine ligand 5 and 10 (63); however, this effect is not universally present in all cells. In U2OS OS cells with low STING expression, this effect is not observed. The use of STING agonists can alter this phenomenon (63). STING signaling is essential for radiation-induced expression of C–C motif chemokine ligand 5 and 10 in OS cells. Therefore, enhancing STING signaling may be beneficial for OS treatment. Sodium-glucose cotransporter 2 is a mediator of epithelial glucose transport and is highly expressed in many tumor types. Inhibition of Sodium-glucose cotransporter 2 can exert anticancer effects in various tumors, including HCC, pancreatic cancer, prostate cancer, colorectal cancer, lung cancer, and breast cancer (64–67). Wei et al. found that Sodium-glucose cotransporter 2 inhibitors can upregulate the cGAS-STING pathway and induce immune cell infiltration. Furthermore, the combination of Sodium-glucose cotransporter 2 inhibitors and the STING agonist 2'3'-cGAMP exhibited synergistic antitumor effects in OS (32). However, whether STING has an antitumor effect in tumor treatment remains controversial (68). Inducing apoptosis is a commonly employed antitumor strategy. The IFN gamma inducible protein 16/p53 pathway is a mechanism of cell apoptosis. Studies have shown that STING can promote the degradation of IFN gamma inducible protein 16. Additionally, overexpression of STING inhibits p53 serine 392 phosphorylation, p53 transcriptional activity, p53 target gene expression, and p53-dependent mitochondrial depolarization and apoptosis (69). Therefore, further research is needed to identify the therapeutic targets of the cGAS-STING pathway in OS.

The biological characteristics of OS have driven a surge of interest in developing new antitumor drugs based on tissue engineering. One promising approach involves targeting reactive oxygen species (ROS), which are by-products of cellular oxygen metabolism, such as superoxide anion, hydrogen peroxide, hydroxyl radical, and nitric oxide. These ROS are mainly generated by complexes I and III of the mitochondrial inner membrane respiratory chain and by nicotinamide adenine dinucleotide phosphate oxidase on the cell membrane. While

ROS play a crucial role in cellular signaling and homeostasis, they are also associated with the occurrence and progression of cancer. Under normal conditions, cells maintain a balance in ROS levels via the antioxidant defense system. However, when this balance is disrupted, excessive ROS can lead to DNA damage, genomic instability, and carcinogenic mutations, thus promoting cancer progression (70, 71). In tumor cells, this imbalance is often caused by mitochondrial dysfunction, which leads to an impaired electron transport chain, reduced mitochondrial membrane potential, increased nicotinamide adenine dinucleotide phosphate oxidase expression, and iron metabolism disorders. These factors, coupled with the excessive proliferation of tumor cells and reduced antioxidant enzyme activity, contribute to elevated intracellular ROS levels (72). Based on this mechanism, Xiang et al. developed composite nanoparticles composed of ROS-sensitive amphiphilic polymers designed to activate the cGAS-STING pathway. These nanoparticles dissociate within the cell in response to ROS, releasing Pt(IV)-C12 and NLG919. The former induces DNA damage, which activates the cGAS-STING pathway and promotes the infiltration of CD8+ T cells into the TME, while the latter enhances the activity of these CD8+ T cells, boosting the IR against cancer cells. For patients with inoperable or metastatic OS, radiotherapy is a critical treatment method. However, in some TMEs with strong immunosuppression, low-dose radiotherapy can lead to radio resistance in tumor cells (73, 74), whereas high-dose radiotherapy may cause damage to immune cells and healthy tissues. Experimental studies have shown that a Ta-Zr co-doped metal-organic framework has significant synergistic effects in enhancing radiotherapy sensitization, photodynamic therapy, and immunotherapy in OS cells. The radiotherapy-radiotherapy dynamic therapy effect mediated by Ta-Zr co-doped metal-organic framework induces DNA damage, which activates the cGAS-STING pathway, stimulating antitumor IRs. Notably, PD-L1 expression stimulated by the cGAS-STING pathway in the Ta-Zr co-doped metal-organic framework+X-ray group was twice that of the control and unirradiated Ta-Zr co-doped metal-organic framework groups, promoting a stronger antitumor IR in radiotherapy.

5 Therapeutic strategies targeting the cGAS-STING pathway

Given the significant potential of cGAS-STING pathway in tumor treatment, many researchers are actively investigating therapies that target this pathway. Here, we summarized recent findings related to drug treatments aimed at modulating cGAS-STING activity across various cancers.

Several commonly used chemotherapeutic drugs have been shown to activate the cGAS-STING pathway, contributing to their antitumor effects. For instance, Hu et al. (75) demonstrated *in vitro* that paclitaxel could activate cGAS signaling in certain triple-negative breast cancer cell lines, inducing the polarization of macrophages toward the M1 phenotype and recruiting lymphocytes to the TME, and improving patient survival when combined with other treatments. However, this lymphocyte infiltration does not occur in all triple-negative breast cancer cases, and corresponding *in vivo* studies are lacking. Future research could address this gap and explore the variability in response to paclitaxel. In another study, Li et al. (76) found that arsenic trioxide-induced mitochondrial damage could activate the cGAS-STING pathway in hepatocellular carcinoma cells, enhancing the expression of IFNs. At the same time, STING activation was also associated with increased expression of the immune checkpoint protein PD-L1 in tumor cells. arsenic trioxide treatment improved antitumor immunity and immunogenicity in arsenic trioxide-sensitive hepatocellular carcinoma cells, although arsenic trioxide-insensitive hepatocellular carcinoma cells showed limited response. Future research could focus on improving arsenic trioxide sensitivity in these resistant cells. Notably, when arsenic trioxide-pretreated tumor cells were injected into mice, the treatment also showed both preventive and therapeutic effects, significantly reducing tumor growth, providing a new avenue for the development of hepatocellular carcinoma vaccines. In addition to chemotherapeutic agents, some drugs traditionally used for non-cancer treatments have also been found to activate the cGAS-STING pathway in tumors. Metformin, a classic drug for type 2 diabetes, has been found in recent years to have antitumor effects in several cancers, including lung, pancreatic, breast, prostate, and colon cancer (77–79). Most of these antitumor mechanisms were found to be independent of cGAS-STING pathway. However, Shen et al. (39) found that metformin could activate the cGAS-STING pathway via the SOX2/AKT axis in gastric cancer cells, promoting the release of inflammatory factors and enhancing the effectiveness of immunotherapy. This raises the question of whether metformin may exert similar cGAS-STING-mediated effects in the treatment of other tumors, warranting further investigation.

Lovastatin, an inhibitor of 3-hydroxy-3-methylglutaryl coenzyme A reductase, is widely used to treat hyperlipidemia but also shows promise in cancer treatment. Huang et al. (80) demonstrated that lovastatin activated the cGAS-STING pathway by increasing the abundance of mtDNA in the cytoplasm through mitochondrial damage. This activation resulted in growth inhibition and apoptosis across various cancer cell types. In HCT116 xenograft tumor models, lovastatin effectively inhibited tumor growth via the cGAS-STING pathway. Knocking out cGAS or STING diminished its antitumor effects. Nonsteroidal anti-inflammatory drugs also play a role in tumor treatment. Kosaka et al. (81) found that celecoxib, a selective cyclooxygenase-2 inhibitor, enhanced the antitumor effect of the STING agonist cGAMP in a T cell-dependent manner, inducing systemic tumor-specific IRs in mouse models. Additionally, Zhu et al. (82) showed that aspirin, a targeted drug for inhibiting cGAS-STING signaling, significantly improved asymptomatic orchitis induced by airborne particulate matter. Tumor immunomodulators have been integrated into cGAS-STING targeted therapy. Anlotinib, effective against various tumors such as hepatocellular carcinoma, renal cell carcinoma, and non-small cell lung cancers, glioblastoma, refractory metastatic cervical cancer, and refractory epithelial ovarian cancer, has been shown to enhance tumor control and improve long-term survival (83–88). Yuan et al. (89) established a gastric cancer mouse model and found that anlotinib treatment reduced cell proliferation and invasion by activating the cGAS-STING/IFN-β

pathway. Nanotechnology-based targeted therapies focusing on cGAS-STING are gaining attention. Mn^{2+} can enhance antitumor IRs by activating the cGAS-STING pathway (90, 91). Excessive zinc ions (Zn^{2+}), which can induce mutant p53 prevalent in many cancers, may relieve inhibition of the cGAS-STING pathway and lead to tumor immunosuppression (92, 93). To harness the synergistic effects of Mn^{2+} and Zn^{2+}, Sun et al. (94) constructed MnO_2-modified zeolitic imidazolate framework 8 nanoparticles, which not only deliver individual ions but also provide dsDNA for the activation of cGAS-STING pathway, enhancing cGAS-STING-mediated antitumor immunotherapy. Fang et al. (95) constructed a manganese-based nanosystem that activates the cGAS-STING pathway to promote the maturation of DCs and enhance the infiltration of cytotoxic T lymphocytes, thereby increasing the sensitivity to ICB immunotherapy. Additionally, Li et al. (96) created an iron-based metal-organic framework nanoparticle reactor loaded with dihydroartemisinin that induces DNA damage to activate the cGAS-STING pathway, facilitating the binding of STING and IRF3 and promoting anticancer immunotherapy. Scutellarein, a natural compound isolated from schisandra lignans, has also been shown to activate the cGAS-STING pathway, inhibiting hepatitis B virus replication and chronic hepatitis B (97). Yang et al. (98) further found that SC reduced tumor growth by enhancing type I IFN responses in a cGAS-STING pathway-dependent manner. Moreover, when combined with platinum chemotherapy, Scutellarein enhanced the antitumor effects of cisplatin while mitigating side effects. These findings highlight the potential of cGAS-STING-targeted therapies and nanotechnology in cancer treatment Figure 2, Table 2.

The DNA binding site of cGAS A induces conformational changes in the protein, repositioning the catalytic pocket to allow catalysis with ATP and GTP substrates. The LBD undergoes conformational changes upon binding to cGAMP, promoting STING oligomerization. cGAS catalyzes cGAMP synthesis, which acts as a second messenger to activate STING. STING then recruits and activates TBK1, initiating downstream signaling that leads to an IR. Then TBK1 phosphorylates IRF3 and nuclear factor kappa B transcription factors, promoting their translocation into the nucleus and the expression of IFN-α/β and tumor necrosis factor-alpha

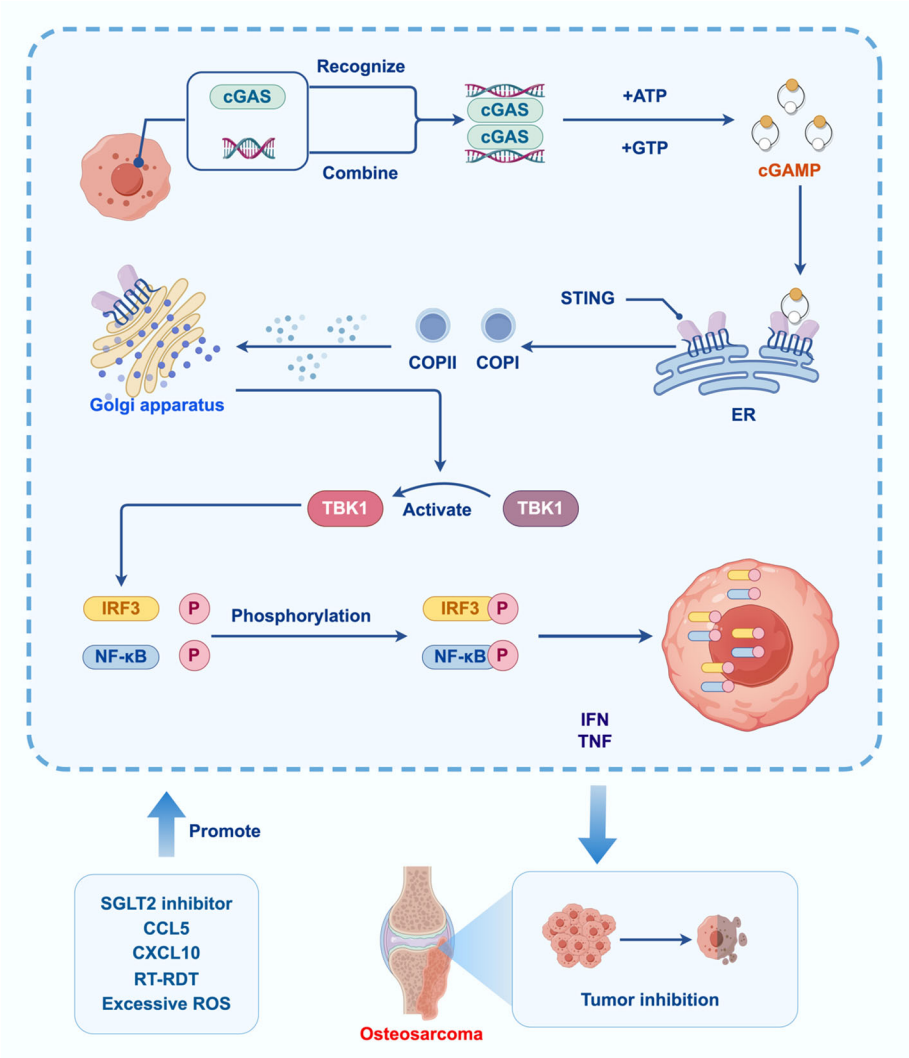

FIGURE 2
Effect of cGAS-STING signaling pathway in OS.

TABLE 2 Tumor treatment of drugs targeting the cGAS-STING pathway.

Drug name	dose	cell lines	*In Vivo* Studies	Effects	References
Metformin	5 mmol/L	BGC823, AGS, SGC7901	none	Metformin exerts an anti-tumor effect in gastric cancer immunotherapy by inhibiting SOX2/AKT activation of the cGAS/STING signaling pathway.	(39)
Anlotinib	8μM	AGS,HS746T	Subcutaneous tumor model	Anlotinib may inhibit the proliferation, migration, and immune evasion of gastric cancer cells by activating the cGAS-STING/IFN-β pathway.	(89)
Schisandrin C	30 mg/kg	MC38,4T1	Subcutaneous tumor model	Schisandrin C reduces tumor growth by enhancing type I IFN response in a cGAS-STING-dependent manner.	(98)
Lovastatin	10 μM	HCT116,HEK293T	Subcutaneous tumor model	Lovastatin triggers accumulation of mitochondrial DNA in the cytoplasm through oxidative mitochondrial DNA damage, thus activating the cGAS-STING pathway in CRC.	(80)
Arsenic trioxide	3 mg/kg	Hepa1-6,Huh7,MHCC97H, Hep G2, Hep 3B,H22	Subcutaneous tumor model	Arsenic trioxide activates the cGAS/STING/IFN cascade through induction of mitochondrial damage and mtDNA release, exerting an immunostimulatory effect.	(76)
Paclitaxel	10nM	MDA-MB-231,BT-549, MDA-MB-468,MDA-MB-436,MDA-MB-453, Hs578T, HCC1806	none	Paclitaxel induces macrophage polarization to M1 phenotype in a cGAS-dependent manner, and may help with lymphocyte recruitment in some TNBC samples and better survival in patients receiving combination therapy.	(75)
Celecoxib	200 ppm	4T1-Luc RRID, CVCL_J239, E0771 RRID: CVCL_GR23,CT26	Orthotopic tumor model	Combination treatment with cGAMP and celecoxib significantly inhibits tumor growth through T cell-mediated and STING signaling responses.	(81)

genes. Activation of the cGAS-STING signaling pathway leads to osteosarcoma. inhibitory effect. SGLT2 inhibitors, CCL5, CXCL10, RT-RDT, ROS and other factors affect the activation of the cGAS-STING signaling pathway.

6 Clinical research

The cGAS-STING signaling pathway is a popular molecular mechanism in recent years. There are few clinical studies related to the cGAS-STING signaling pathway. The cGAS-STING signaling pathway is of great significance in the treatment of tumors. Eribulin is a regulator of the cGAS-STING signaling pathway that can improve the tumor microenvironment. Candace et al. found that the combination of Eribulin and pembrolizumab in metastatic soft tissue sarcoma can achieve better therapeutic effects in liposarcomas and angiosarcomas, and serum IFNα and IL4 levels are associated with clinical benefits (99). Manganese is necessary for cGAS-STING to defend against cytoplasmic dsDNA (100). Lv et al. found in a phase I clinical trial that manganese and anti-PD-1 antibodies were used in combination in patients with a variety of metastatic solid tumors. The results showed that the combined application showed promising efficacy, exhibiting type I IFN induction, manageable safety and revived responses to immunotherapy (90). Combining activators of the cGAS-STING signaling pathway has advantages for tumor treatment. In addition to research on tumors, the cGAS-STING signaling pathway has also been clinically studied in diseases such as anemia and infection (101, 102). There are no reports on clinical studies of the cGAS-STING signaling pathway in osteosarcoma.

7 Summary and outlook

The cGAS-STING pathway is emerging as a crucial component in tumor immunology, particularly in OS. Research has shown that this pathway is abnormally activated in OS, correlating with the malignant biological behaviors of tumor cells. Targeting the cGAS-STING pathway presents a promising new approach for the treatment of OS. Recent studies indicate that various small molecule drugs and nanomaterials aimed at the cGAS-STING pathway may serve as potential therapies for OS. For example, SGLT2 inhibitors can upregulate the cGAS-STING pathway and induce immune cell infiltration, while Mn^{2+} can activate the cGAS-STING pathway *in vivo*, promoting antitumor IRs. These findings suggest new ideas for developing OS treatment based on the cGAS-STING pathway. However, research on the role of the cGAS-STING pathway in OS treatment remains limited, and the underlying mechanisms are not fully understood. Therefore, further investigation into the mechanisms of cGAS-STING in OS and the exploration of targeted treatment strategies are of great significance for the development of more effective treatment options for OS. While effective therapies for OS are still lacking, the significance of the cGAS-STING pathway in tumor diseases might provide a new perspective for its treatment. In future, targeted therapies based on the cGAS-STING pathway may offer new hope for OS patients.

Author contributions

BL: Conceptualization, Data curation, Formal analysis, Funding acquisition, Investigation, Methodology, Project administration,

Resources, Software, Supervision, Validation, Visualization, Writing – original draft, Writing – review & editing. CZ: Conceptualization, Data curation, Formal analysis, Funding acquisition, Writing – review & editing. XX: Conceptualization, Investigation, Methodology, Project administration, Writing – review & editing. QS: Supervision, Validation, Visualization, Writing – review & editing. SL: Software, Supervision, Validation, Visualization, Writing – review & editing. JH: Conceptualization, Data curation, Formal analysis, Funding acquisition, Investigation, Methodology, Project administration, Resources, Software, Supervision, Validation, Visualization, Writing – original draft, Writing – review & editing.

Funding

The author(s) declare that no financial support was received for the research, authorship, and/or publication of this article.

Conflict of interest

The authors declare that the research was conducted in the absence of any commercial or financial relationships that could be construed as a potential conflict of interest.

Generative AI statement

The author(s) declare that no Generative AI was used in the creation of this manuscript.

Publisher's note

References

1. Cole S, Gianferante DM, Zhu B, Mirabello L. Osteosarcoma: A Surveillance, Epidemiology, and End Results program-based analysis from 1975 to 2017. *Cancer*. (2022) 128:2107–18. doi: 10.1002/cncr.v128.11

2. Kha ST, Sharma J, Kenney D, Daldrup-Link H, Steffner R. Assessment of the interval to diagnosis in pediatric bone sarcoma. *Pediatr Emerg Care*. (2023) 39:963–7. doi: 10.1097/PEC.0000000000003031

3. Zarghooni K, Bratke G, Landgraf P, Simon T, Maintz D, Eysel P. The diagnosis and treatment of osteosarcoma and ewing's sarcoma in children and adolescents. *Dtsch Arztebl Int*. (2023) 120:405–12. doi: 10.3238/arztebl.m2023.0079

4. Jafari F, Javdansirat S, Sanaie S, Naseri A, Shamekh A, Rostamzadeh D, et al. Osteosarcoma: A comprehensive review of management and treatment strategies. *Ann Diagn Pathol*. (2020) 49:151654. doi: 10.1016/j.anndiagpath.2020.151654

5. Tsuda Y, Tsoi K, Parry MC, Stevenson JD, Fujiwara T, Sumathi V, et al. Impact of chemotherapy-induced necrosis on event-free and overall survival after preoperative MAP chemotherapy in patients with primary high-grade localized osteosarcoma. *Bone Joint J*. (2020) 102-b:795–803. doi: 10.1302/0301-620X.102B6.BJJ-2019-1307.R1

6. Fontes GS, Bourne KL, Bracha S, Curran KM, Cook M, Lapsley JM, et al. Development of non-pulmonary soft-tissue metastasis is not a poor prognostic indicator in dogs with metastatic appendicular osteosarcoma. *Can Vet J*. (2024) 65:1061–70.

7. Shkalim-Zemer V, Ash S, Toledano H, Kollender Y, Issakov J, Yaniv I, et al. Highly effective reduced toxicity dose-intensive pilot protocol for non-metastatic limb osteogenic sarcoma (SCOS 89). *Cancer Chemother Pharmacol*. (2015) 76:909–16. doi: 10.1007/s00280-015-2865-x

8. Basit Q, Qazi HS, Tanveer S. Osteosarcoma and its advancement. *Cancer Treat Res*. (2023) 185:127–39. doi: 10.1007/978-3-031-27156-4_8

9. Sun C, Li S, Ding J. Biomaterials-boosted immunotherapy for osteosarcoma. *Adv Healthc Mater*. (2024) 13:e2400864. doi: 10.1002/adhm.202400864

10. Meltzer PS, Helman LJ. New horizons in the treatment of osteosarcoma. *N Engl J Med*. (2021) 385:2066–76. doi: 10.1056/NEJMra2103423

11. Wu C, Tan J, Shen H, Deng C, Kleber C, Osterhoff G, et al. Exploring the relationship between metabolism and immune microenvironment in osteosarcoma based on metabolic pathways. *J BioMed Sci*. (2024) 31:4. doi: 10.1186/s12929-024-00999-7

12. Zhu T, Han J, Yang L, Cai Z, Sun W, Hua Y, et al. Immune microenvironment in osteosarcoma: components, therapeutic strategies and clinical applications. *Front Immunol*. (2022) 13:907550. doi: 10.3389/fimmu.2022.907550

13. Orrapin S, Moonmuang S, Udomruk S, Yongpitakwattana P, Pruksakorn D, Chaiyawat P. Unlocking the tumor-immune microenvironment in osteosarcoma: insights into the immune landscape and mechanisms. *Front Immunol*. (2024) 15:1394284. doi: 10.3389/fimmu.2024.1394284

14. Wen Y, Tang F, Tu C, Hornicek F, Duan Z, Min L. Immune checkpoints in osteosarcoma: Recent advances and therapeutic potential. *Cancer Lett*. (2022) 547:215887. doi: 10.1016/j.canlet.2022.215887

15. Ying H, Li ZQ, Li MP, Liu WC. Metabolism and senescence in the immune microenvironment of osteosarcoma: focus on new therapeutic strategies. *Front Endocrinol (Lausanne)*. (2023) 14:1217669. doi: 10.3389/fendo.2023.1217669

16. Ong JLK, Jalaludin NFF, Wong MK, Tan SH, Angelina C, Sukhatme SA, et al. Exosomal mRNA Cargo are biomarkers of tumor and immune cell populations in pediatric osteosarcoma. *Transl Oncol*. (2024) 46:102008. doi: 10.1016/j.tranon.2024.102008

17. Fan Q, Wang Y, Cheng J, Pan B, Zang X, Liu R, et al. Single-cell RNA-seq reveals T cell exhaustion and immune response landscape in osteosarcoma. *Front Immunol*. (2024) 15:1362970. doi: 10.3389/fimmu.2024.1362970

18. Wang S, Ma F, Feng Y, Liu T, He S. Role of exosomal miR–21 in the tumor microenvironment and osteosarcoma tumorigenesis and progression (Review). *Int J Oncol*. (2020) 56:1055–63. doi: 10.3892/ijo.2020.4992

19. Yang X, Zhang W, Xu P. NK cell and macrophages confer prognosis and reflect immune status in osteosarcoma. *J Cell Biochem*. (2019) 120:8792–7. doi: 10.1002/jcb.v120.5

20. Yang L, Long Y, Xiao S. Osteosarcoma-associated immune genes as potential immunotherapy and prognosis biomarkers. *Biochem Genet*. (2024) 62:798–813. doi: 10.1007/s10528-023-10444-3

21. Tuohy JL, Somarelli JA, Borst LB, Eward WC, Lascelles BDX, Fogle JE. Immune dysregulation and osteosarcoma: Staphylococcus aureus downregulates TGF-β and heightens the inflammatory signature in human and canine macrophages suppressed by osteosarcoma. *Vet Comp Oncol*. (2020) 18:64–75. doi: 10.1111/vco.12529

22. Yu S, Yao X. Advances on immunotherapy for osteosarcoma. *Mol Cancer*. (2024) 23:192. doi: 10.1186/s12943-024-02105-9

23. Wang C, Zhou X, Li W, Li M, Tu T, Ba X, et al. Macrophage migration inhibitory factor promotes osteosarcoma growth and lung metastasis through activating the RAS/MAPK pathway. *Cancer Lett*. (2017) 403:271–9. doi: 10.1016/j.canlet.2017.06.011

24. Alfranca A, Martinez-Cruzado L, Tornin J, Abarrategi A, Amaral T, de Alava E, et al. Bone microenvironment signals in osteosarcoma development. *Cell Mol Life Sci*. (2015) 72:3097–113. doi: 10.1007/s00018-015-1918-y

25. Liu K, Zan P, Li Z, Lu H, Liu P, Zhang L, et al. Engineering bimetallic polyphenol for mild photothermal osteosarcoma therapy and immune microenvironment remodeling by activating pyroptosis and cGAS-STING pathway. *Adv Healthc Mater*. (2024) 13:e2400623. doi: 10.1002/adhm.202400623

26. Li T, Gao M, Wu Z, Yang J, Mo B, Yu S, et al. Tantalum-zirconium co-doped metal-organic frameworks sequentially sensitize radio-radiodynamic-immunotherapy for metastatic osteosarcoma. *Adv Sci (Weinh)*. (2023) 10:e2206779. doi: 10.1002/advs.202206779

27. O'Donoghue JC, Freeman FE, Make it STING. nanotechnological approaches for activating cGAS/STING as an immunomodulatory node in osteosarcoma. *Front Immunol*. (2024) 15:1403538. doi: 10.3389/fimmu.2024.1403538

28. Chen C, Xu P. Cellular functions of cGAS-STING signaling. *Trends Cell Biol*. (2023) 33:630–48. doi: 10.1016/j.tcb.2022.11.001

29. Wan D, Jiang W, Hao J. Research advances in how the cGAS-STING pathway controls the cellular inflammatory response. *Front Immunol*. (2020) 11:615. doi: 10.3389/fimmu.2020.00615

30. Curran E, Chen X, Corrales L, Kline DE, Dubensky TW Jr., Duttagupta P, et al. STING pathway activation stimulates potent immunity against acute myeloid leukemia. *Cell Rep*. (2016) 15:2357–66. doi: 10.1016/j.celrep.2016.05.023

31. Lv H, Zong Q, Chen C, Lv G, Xiang W, Xing F, et al. TET2-mediated tumor cGAS triggers endothelial STING activation to regulate vasculature remodeling and anti-tumor immunity in liver cancer. *Nat Commun*. (2024) 15:6. doi: 10.1038/s41467-023-43743-9

32. Wu W, Zhang Z, Jing D, Huang X, Ren D, Shao Z, et al. SGLT2 inhibitor activates the STING/IRF3/IFN-β pathway and induces immune infiltration in osteosarcoma. *Cell Death Dis*. (2022) 13:523. doi: 10.1038/s41419-022-04980-w

33. Decout A, Katz JD, Venkatraman S, Ablasser A. The cGAS-STING pathway as a therapeutic target in inflammatory diseases. *Nat Rev Immunol*. (2021) 21:548–69. doi: 10.1038/s41577-021-00524-z

34. Wang Y, Luo J, Alu A, Han X, Wei Y, Wei X. cGAS-STING pathway in cancer biotherapy. *Mol Cancer*. (2020) 19:136. doi: 10.1186/s12943-020-01247-w

35. Samson N, Ablasser A. The cGAS-STING pathway and cancer. *Nat Cancer*. (2022) 3:1452–63. doi: 10.1038/s43018-022-00468-w

36. Zhang X, Bai XC, Chen ZJ. Structures and mechanisms in the cGAS-STING innate immunity pathway. *Immunity*. (2020) 53:43–53. doi: 10.1016/j.immuni.2020.05.013

37. Xue A, Shang Y, Jiao P, Zhang S, Zhu C, He X, et al. Increased activation of cGAS-STING pathway enhances radiosensitivity of non-small cell lung cancer cells. *Thorac Cancer*. (2022) 13:1361–8. doi: 10.1111/1759-7714.14400

38. Wang X, Liu Y, Xue C, Hu Y, Zhao Y, Cai K, et al. A protein-based cGAS-STING nanoagonist enhances T cell-mediated anti-tumor immune responses. *Nat Commun*. (2022) 13:5685. doi: 10.1038/s41467-022-33301-0

39. Shen Q, Yang L, Li C, Wang T, Lv J, Liu W, et al. Metformin promotes cGAS/STING signaling pathway activation by blocking AKT phosphorylation in gastric cancer. *Heliyon*. (2023) 9:e18954. doi: 10.1016/j.heliyon.2023.e18954

40. Schmitt CA, Wang B, Demaria M. Senescence and cancer - role and therapeutic opportunities. *Nat Rev Clin Oncol*. (2022) 19:619–36. doi: 10.1038/s41571-022-00668-4

41. Wang K, Li Y, Wang X, Zhang Z, Cao L, Fan X, et al. Gas therapy potentiates aggregation-induced emission luminogen-based photoimmunotherapy of poorly immunogenic tumors through cGAS-STING pathway activation. *Nat Commun*. (2023) 14:2950. doi: 10.1038/s41467-023-38601-7

42. Si W, Liang H, Bugno J, Xu Q, Ding X, Yang K, et al. Lactobacillus rhamnosus GG induces cGAS/STING- dependent type I interferon and improves response to immune checkpoint blockade. *Gut*. (2022) 71:521–33. doi: 10.1136/gutjnl-2020-323426

43. Johnson DB, Nebhan CA, Moslehi JJ, Balko JM. Immune-checkpoint inhibitors: long-term implications of toxicity. *Nat Rev Clin Oncol*. (2022) 19:254–67. doi: 10.1038/s41571-022-00600-w

44. Topalian SL, Forde PM, Emens LA, Yarchoan M, Smith KN, Pardoll DM. Neoadjuvant immune checkpoint blockade: A window of opportunity to advance cancer immunotherapy. *Cancer Cell*. (2023) 41:1551–66. doi: 10.1016/j.ccell.2023.07.011

45. Yadav D, Kwak M, Chauhan PS, Puranik N, Lee PCW, Jin JO. Cancer immunotherapy by immune checkpoint blockade and its advanced application using bio-nanomaterials. *Semin Cancer Biol*. (2022) 86:909–22. doi: 10.1016/j.semcancer.2022.02.016

46. Liu H, Zhao Q, Tan L, Wu X, Huang R, Zuo Y, et al. Neutralizing IL-8 potentiates immune checkpoint blockade efficacy for glioma. *Cancer Cell*. (2023) 41:693–710.e8. doi: 10.1016/j.ccell.2023.03.004

47. Hu M, Zhou M, Bao X, Pan D, Jiao M, Liu X, et al. ATM inhibition enhances cancer immunotherapy by promoting mtDNA leakage and cGAS/STING activation. *J Clin Invest*. (2021) 131:e139333. doi: 10.1172/JCI139333

48. Ma Z, Jacobs SR, West JA, Stopford C, Zhang Z, Davis Z, et al. Modulation of the cGAS-STING DNA sensing pathway by gammaherpesviruses. *Proc Natl Acad Sci U.S.A*. (2015) 112:E4306–15. doi: 10.1073/pnas.1503831112

49. Jeffries AM, Marriott I. Human microglia and astrocytes express cGAS-STING viral sensing components. *Neurosci Lett*. (2017) 658:53–6. doi: 10.1016/j.neulet.2017.08.039

50. Aarreberg LD, Esser-Nobis K, Driscoll C, Shuvarikov A, Roby JA, Gale M Jr. Interleukin-1β Induces mtDNA Release to Activate Innate Immune Signaling via cGAS-STING. *Mol Cell*. (2019) 74:801–815.e6. doi: 10.1016/j.molcel.2019.02.038

51. Bhattacharya M, Bhowmik D, Tian Y, He H, Zhu F, Yin Q. The Dengue virus protease NS2B3 cleaves cyclic GMP-AMP synthase to suppress cGAS activation. *J Biol Chem*. (2023) 299:102986. doi: 10.1016/j.jbc.2023.102986

52. Ng WC, Kwek SS, Sun B, Yousefi M, Ong EZ, Tan HC, et al. A fast-growing dengue virus mutant reveals a dual role of STING in response to infection. *Open Biol*. (2022) 12:220227. doi: 10.1098/rsob.220227

53. Alonso Paiva IM, A Santos R, Brito CB, Ferrero MC, Ortiz Wilczyński JM, Carrera Silva EA, et al. Role of the cGAS/STING pathway in the control of Brucella abortus infection acquired through the respiratory route. *Front Immunol*. (2023) 14:1116811. doi: 10.3389/fimmu.2023.1116811

54. Li Q, Liu C, Yue R, El-Ashram S, Wang J, He X, et al. cGAS/STING/TBK1/IRF3 signaling pathway activates BMDCs maturation following mycobacterium bovis infection. *Int J Mol Sci*. (2019) 20(4):895. doi: 10.3390/ijms20040895

55. Han F, Guo H, Wang L, Zhang Y, Sun L, Dai C, et al. The cGAS-STING signaling pathway contributes to the inflammatory response and autophagy in Aspergillus fumigatus keratitis. *Exp Eye Res*. (2021) 202:108366. doi: 10.1016/j.exer.2020.108366

56. Wu Y, Zhang M, Yuan C, Ma Z, Li W, Zhang Y, et al. Progress of cGAS-STING signaling in response to SARS-CoV-2 infection. *Front Immunol*. (2022) 13:1010911. doi: 10.3389/fimmu.2022.1010911

57. Erttmann SF, Swacha P, Aung KM, Brindefalk B, Jiang H, Härtlova A, et al. The gut microbiota prime systemic antiviral immunity via the cGAS-STING-IFN-I axis. *Immunity*. (2022) 55:847–861.e10. doi: 10.1016/j.immuni.2022.04.006

58. Liu N, Pang X, Zhang H, Ji P. The cGAS-STING pathway in bacterial infection and bacterial immunity. *Front Immunol*. (2021) 12:814709. doi: 10.3389/fimmu.2021.814709

59. Dong W, Chen M, Chang C, Jiang T, Su L, Chen C, et al. Remodeling of tumor microenvironment by nanozyme combined cGAS-STING signaling pathway agonist for enhancing cancer immunotherapy. *Int J Mol Sci*. (2023) 24(18):13935. doi: 10.3390/ijms241813935

60. Liu Z, Wang D, Zhang J, Xiang P, Zeng Z, Xiong W, et al. cGAS-STING signaling in the tumor microenvironment. *Cancer Lett*. (2023) 577:216409. doi: 10.1016/j.canlet.2023.216409

61. Zhang Z, Liu C, Liang T, Yu C, Qin Z, Zhou X, et al. Establishment of immune prognostic signature and analysis of prospective molecular mechanisms in childhood osteosarcoma patients. *Med (Baltimore)*. (2020) 99:e23251. doi: 10.1097/MD.0000000000023251

62. Henrich IC, Jain K, Young R, Quick L, Lindsay JM, Park DH, et al. Ubiquitin-specific protease 6 functions as a tumor suppressor in ewing sarcoma through immune activation. *Cancer Res*. (2021) 81:2171–83. doi: 10.1158/0008-5472.CAN-20-1458

63. Withers SS, Moeller CE, Quick CN, Liu CC, Baham SM, Looper JS, et al. Effect of stimulator of interferon genes (STING) signaling on radiation-induced chemokine expression in human osteosarcoma cells. *PloS One*. (2023) 18:e0284645. doi: 10.1371/journal.pone.0284645

64. Laeeq T, Ahmed M, Sattar H, Zeeshan MH, Ali MB. Role of SGLT2 inhibitors, DPP-4 inhibitors, and metformin in pancreatic cancer prevention. *Cancers (Basel)*. (2024) 16(7):1325 doi: 10.3390/cancers16071325

65. Ali A, Mekhaeil B, Biziotis OD, Tsakiridis EE, Ahmadi E, Wu J, et al. The SGLT2 inhibitor canagliflozin suppresses growth and enhances prostate cancer response to radiotherapy. *Commun Biol*. (2023) 6:919. doi: 10.1038/s42003-023-05289-w

66. Luo J, Hendryx M, Dong Y. Sodium-glucose cotransporter 2 (SGLT2) inhibitors and non-small cell lung cancer survival. *Br J Cancer*. (2023) 128:1541–7. doi: 10.1038/s41416-023-02177-2

67. Dutka M, Bobiński R, Francuz T, Garczorz W, Zimmer K, Ilczak T, et al. SGLT-2 inhibitors in cancer treatment-mechanisms of action and emerging new perspectives. *Cancers (Basel)*. (2022) 14(23):5811. doi: 10.3390/cancers14235811

68. Xu Y, Chen C, Liao Z, Xu P. cGAS-STING signaling in cell death: Mechanisms of action and implications in pathologies. *Eur J Immunol*. (2023) 53:e2350386. doi: 10.1002/eji.202350386

69. Li D, Xie L, Qiao Z, Mai S, Zhu J, Zhang F, et al. STING-mediated degradation of IFI16 negatively regulates apoptosis by inhibiting p53 phosphorylation at serine 392. *J Biol Chem*. (2021) 297:100930. doi: 10.1016/j.jbc.2021.100930

70. Cheung EC, Vousden KH. The role of ROS in tumor development and progression. *Nat Rev Cancer*. (2022) 22:280–97. doi: 10.1038/s41568-021-00435-0

71. Chen Z, Wu FF, Li J, Dong JB, He HY, Li XF, et al. Investigating the synergy of Shikonin and Valproic acid in inducing apoptosis of osteosarcoma cells via ROS-mediated EGR1 expression. *Phytomedicine*. (2024) 126:155459. doi: 10.1016/j.phymed.2024.155459

72. Jelic MD, Mandic AD, Maricic SM, Srdjenovic BU. Oxidative stress and its role in cancer. *J Cancer Res Ther*. (2021) 17:22–8. doi: 10.4103/jcrt.JCRT_862_16

73. Dahl O, Dale JE, Brydøy M. Rationale for combination of radiation therapy and immune checkpoint blockers to improve cancer treatment. *Acta Oncol*. (2019) 58:9–20. doi: 10.1080/0284186X.2018.1554259

74. Gómez V, Mustapha R, Ng K, Ng T. Radiation therapy and the innate immune response: Clinical implications for immunotherapy approaches. *Br J Clin Pharmacol*. (2020) 86:1726–35. doi: 10.1111/bcp.14351

75. Hu Y, Manasrah BK, McGregor SM, Lera RF, Norman RX, Tucker JB, et al. Paclitaxel induces micronucleation and activates pro-inflammatory cGAS-STING signaling in triple-negative breast cancer. *Mol Cancer Ther*. (2021) 20:2553–67. doi: 10.1158/1535-7163.MCT-21-0195

76. Li X, Pan YF, Chen YB, Wan QQ, Lin YK, Shang TY, et al. Arsenic trioxide augments immunogenic cell death and induces cGAS-STING-IFN pathway activation in hepatocellular carcinoma. *Cell Death Dis*. (2024) 15:300. doi: 10.1038/s41419-024-06685-8

77. Vallianou NG, Evangelopoulos A, Kazazis C. Metformin and cancer. *Rev Diabetes Stud*. (2013) 10:228–35. doi: 10.1900/RDS.2013.10.228

78. Ye J, Cai S, Feng Y, Li J, Cai Z, Deng Y, et al. Metformin escape in prostate cancer by activating the PTGR1 transcriptional program through a novel super-enhancer. *Signal Transduct Target Ther*. (2023) 8:303. doi: 10.1038/s41392-023-01516-2

79. Yang J, Zhou Y, Xie S, Wang J, Li Z, Chen L, et al. Metformin induces Ferroptosis by inhibiting UFMylation of SLC7A11 in breast cancer. *J Exp Clin Cancer Res*. (2021) 40:206. doi: 10.1186/s13046-021-02012-7

80. Huang X, Liang N, Zhang F, Lin W, Ma W. Lovastatin-Induced Mitochondrial Oxidative Stress Leads to the Release of mtDNA to Promote Apoptosis by Activating cGAS-STING Pathway in Human Colorectal Cancer Cells. *Antioxidants (Basel)*. (2024) 13(6):679. doi: 10.3390/antiox13060679

81. Kosaka A, Yajima Y, Yasuda S, Komatsuda H, Nagato T, Oikawa K, et al. Celecoxib promotes the efficacy of STING-targeted therapy by increasing antitumor CD8(+) T-cell functions via modulating glucose metabolism of CD11b(+) Ly6G(+) cells. *Int J Cancer*. (2023) 152:1685–97. doi: 10.1002/ijc.v152.8

82. Zhu T, Chen X, Qiu H, Liu Y, Mwangi J, Zhao L, et al. Aspirin Alleviates Particulate Matter Induced Asymptomatic Orchitis of Mice via Suppression of cGAS-STING Signaling. *Front Immunol*. (2021) 12:734546. doi: 10.3389/fimmu.2021.734546

83. Shen G, Zheng F, Ren D, Du F, Dong Q, Wang Z, et al. Anlotinib: a novel multi-targeting tyrosine kinase inhibitor in clinical development. *J Hematol Oncol*. (2018) 11:120. doi: 10.1186/s13045-018-0664-7

84. Xu Q, Wang J, Sun Y, Lin Y, Liu J, Zhuo Y, et al. Efficacy and safety of sintilimab plus anlotinib for PD-L1-positive recurrent or metastatic cervical cancer: A multicenter, single-arm, prospective phase II trial. *J Clin Oncol*. (2022) 40:1795–805. doi: 10.1200/JCO.21.02091

85. Liang L, Hui K, Hu C, Wen Y, Yang S, Zhu P, et al. Autophagy inhibition potentiates the anti-angiogenic property of multikinase inhibitor anlotinib through JAK2/STAT3/VEGFA signaling in non-small cell lung cancer cells. *J Exp Clin Cancer Res*. (2019) 38:71. doi: 10.1186/s13046-019-1093-3

86. Song Y, Yihebali C, Yang L, Cui CX, Zhang W, Sun YK, et al. Long term follow-up results of anlotinib in the treatment of advanced renal cell carcinoma. *Zhonghua Zhong Liu Za Zhi*. (2020) 42:765–70. doi: 10.3760/cma.j.cn112152-20200214-00089

87. Cheng Y, Wang Q, Li K, Shi J, Wu L, Han B, et al. Anlotinib for patients with small cell lung cancer and baseline liver metastases: A *post hoc* analysis of the ALTER 1202 trial. *Cancer Med*. (2022) 11:1081–7. doi: 10.1002/cam4.v11.4

88. Ji Y, Li X, Qi Y, Zhao J, Zhang W, Qu P. Anlotinib exerts inhibitory effects against cisplatin-resistant ovarian cancer *in vitro* and *in vivo*. *Molecules*. (2022) 27 (24):8873. doi: 10.3390/molecules27248873

89. Yuan M, Guo XL, Chen JH, He Y, Liu ZQ, Zhang HP, et al. Anlotinib suppresses proliferation, migration, and immune escape of gastric cancer cells by activating the cGAS-STING/IFN-β pathway. *Neoplasma*. (2022) 69:807–19. doi: 10.4149/neo_2022_211012N1441

90. Lv M, Chen M, Zhang R, Zhang W, Wang C, Zhang Y, et al. Manganese is critical for antitumor immune responses via cGAS-STING and improves the efficacy of clinical immunotherapy. *Cell Res*. (2020) 30:966–79. doi: 10.1038/s41422-020-00395-4

91. Zhang K, Qi C, Cai K. Manganese-based tumor immunotherapy. *Adv Mater*. (2023) 35:e2205409. doi: 10.1002/adma.202205409

92. Labuschagne CF, Zani F, Vousden KH. Control of metabolism by p53 - Cancer and beyond. *Biochim Biophys Acta Rev Cancer*. (2018) 1870:32–42. doi: 10.1016/j.bbcan.2018.06.001

93. Garufi A, Trisciuoglio D, Porru M, Leonetti C, Stoppacciaro A, D'Orazi V, et al. A fluorescent curcumin-based Zn(II)-complex reactivates mutant (R175H and R273H) p53 in cancer cells. *J Exp Clin Cancer Res*. (2013) 32:72. doi: 10.1186/1756-9966-32-72

94. Sun L, Gao H, Wang H, Zhou J, Ji X, Jiao Y, et al. Nanoscale Metal-Organic Frameworks-Mediated Degradation of Mutant p53 Proteins and Activation of cGAS-STING Pathway for Enhanced Cancer Immunotherapy. *Adv Sci (Weinh)*. (2024) 11: e2307278. doi: 10.1002/advs.202307278

95. Fang M, Zheng J, Wang J, Zheng C, Leng X, Wen E, et al. Amplifying STING activation and alleviating immunosuppression through a mn(2+)-based metal-organic framework nanosystem for synergistic cancer therapy. *Biomater Res*. (2024) 28:0028. doi: 10.34133/bmr.0028

96. Li LG, Yang XX, Xu HZ, Yu TT, Li QR, Hu J, et al. A dihydroartemisinin-loaded nanoreactor motivates anti-cancer immunotherapy by synergy-induced ferroptosis to activate cgas/STING for reprogramming of macrophage. *Adv Healthc Mater*. (2023) 12: e2301561. doi: 10.1002/adhm.202301561

97. Zhao J, Xu G, Hou X, Mu W, Yang H, Shi W, et al. Schisandrin C enhances cGAS-STING pathway activation and inhibits HBV replication. *J Ethnopharmacol*. (2023) 311:116427. doi: 10.1016/j.jep.2023.116427

98. Yang H, Zhan X, Zhao J, Shi W, Liu T, Wei Z, et al. Schisandrin C enhances type I IFN response activation to reduce tumor growth and sensitize chemotherapy through antitumor immunity. *Front Pharmacol*. (2024) 15:1369563. doi: 10.3389/fphar.2024.1369563

99. Haddox CL, Nathenson MJ, Mazzola E, Lin JR, Baginska J, Nau A, et al. Phase II study of eribulin plus pembrolizumab in metastatic soft-tissue sarcomas: clinical outcomes and biological correlates. *Clin Cancer Res*. (2024) 30:1281–92. doi: 10.1158/1078-0432.CCR-23-2250

100. Wang C, Guan Y, Lv M, Zhang R, Guo Z, Wei X, et al. Manganese Increases the Sensitivity of the cGAS-STING Pathway for Double-Stranded DNA and Is Required for the Host Defense against DNA Viruses. *Immunity*. (2018) 48:675–687.e7. doi: 10.1016/j.immuni.2018.03.017

101. Tumburu L, Ghosh-Choudhary S, Seifuddin FT, Barbu EA, Yang S, Ahmad MM, et al. Circulating mitochondrial DNA is a proinflammatory DAMP in sickle cell disease. *Blood*. (2021) 137:3116–26. doi: 10.1182/blood.2020009063

102. Ruiz-Moreno JS, Hamann L, Shah JA, Verbon A, Mockenhaupt FP, Puzianowska-Kuznicka M, et al. The common HAQ STING variant impairs cGAS-dependent antibacterial responses and is associated with susceptibility to Legionnaires' disease in humans. *PloS Pathog*. (2018) 14:e1006829. doi: 10.1371/journal.ppat.1006829

frontiers | Frontiers in Immunology

TYPE Original Research
PUBLISHED 14 February 2025
DOI 10.3389/fimmu.2025.1540998

OPEN ACCESS

EDITED BY
Renjun Gu,
Nanjing University of Chinese Medicine, China

REVIEWED BY
Chen Li,
Free University of Berlin, Germany
Yue Liu,
The University of Texas at Austin,
United States

*CORRESPONDENCE
Changmin Wang
vcin68130840628@163.com
Zhiwei Li
zhiyuan83644@163.com

RECEIVED 06 December 2024
ACCEPTED 27 January 2025
PUBLISHED 14 February 2025

CITATION
Li Z, Wang Q, Liu Y, Yang S, Zhao J, Wu C and Wang C (2025) Role of MLIP in burn-induced sepsis and insights into sepsis-associated cancer progression.
Front. Immunol. 16:1540998.
doi: 10.3389/fimmu.2025.1540998

Role of MLIP in burn-induced sepsis and insights into sepsis-associated cancer progression

Zhiwei Li[1]*, Qian Wang[1], Yezi Liu[1], Shuting Yang[1], Jin Zhao[1], Changdong Wu[2] and Changmin Wang[1]*

[1]Clinical Laboratory Center, People's Hospital of Xinjiang Uygur Autonomous Region, Urumqi, Xinjiang, China, [2]Xinjiang Emergency Center, People's Hospital of Xinjiang Uygur Autonomous Region, Urumqi, Xinjiang, China

Introduction: Burn-induced sepsis is a critical clinical challenge marked by systemic inflammation, immune dysregulation, and high mortality. Macrophage-driven inflammatory pathways are central to sepsis pathogenesis, while immune cell metabolic reprogramming plays a key role in both sepsis and cancer progression.

Methods: Bioinformatics analyses using GEO, TCGA, and GTEx datasets identified MLIP-modulated genes linked to immune responses and prognosis. *In vitro*, LPS-stimulated HUVEC cells were used to study MLIP's effects on inflammation and macrophage function through cell viability, ROS levels, cytokine expression, qRT-PCR, and immunofluorescence assays.

Results: MLIP-modulated genes were associated with immune-related metabolic pathways in both sepsis and cancer. Epigenetic analysis showed MLIP expression is regulated by promoter methylation and chromatin accessibility. Prognostic analyses revealed MLIP's impact on survival outcomes across cancer types. *In vitro*, MLIP reduced inflammation, oxidative stress, and macrophage hyperactivation.

Conclusions: MLIP regulates immune-metabolic dynamics in burn-induced sepsis, influencing macrophage activity and oxidative stress. Its role in metabolic reprogramming suggests MLIP as a potential therapeutic target linking immune modulation and cancer progression. Further research on MLIP's role in immune evasion and tumor metabolism may inform novel therapeutic strategies.

KEYWORDS

burns, sepsis, MLIP, macrophage activation, bioinformatics, inflammation, gene expression, prognosis

Introduction

Currently, burns, sepsis, and cancer represent significant global public health challenges, all of which involve complex immune responses characterized by inflammation, cellular injury, and subsequent repair mechanisms. A comprehensive understanding of the unique pathophysiological processes underlying these conditions is crucial for advancing therapeutic strategies. Furthermore, identifying pathways that can alleviate disease progression, rather than allowing it to worsen, holds substantial therapeutic value. Elucidating the mechanisms behind these interconnected yet distinct health issues, by synthesizing global and regional data, enables a systematic analysis of key aspects such as disease epidemiology, risk factors, and disease burden. This knowledge provides critical evidence for the development of effective control strategies and facilitates the formulation of targeted and impactful interventions (1–3).

Sepsis is notably characterized by its rapid onset and high mortality rate, primarily attributed to the excessive release of cytokine that initiates a cascade of immune imbalances leading to immunosuppression and, ultimately, multiorgan failure (4, 5). A considerable body of research has focused on the pathophysiological mechanisms through which sepsis induces organ dysfunction. With the support of immunological approaches, basic research has increasingly concentrated on the role of macrophages in various organs during this process, while also showing significant interest in the regulatory mechanisms of macrophages in the context of infection. Although macrophages play a central role, other immune cells, such as neutrophils and T cells, are equally critical in the progression of both sepsis and cancer. A thorough understanding of the immune responses of various immune cell types is vital for developing comprehensive therapeutic strategies. Understanding the role of cytokines in immune responses provides valuable insights for the development of effective treatment strategies for a range of diseases. Through research into cytokine signaling and immune regulation mechanisms, scientists have identified numerous potential therapeutic targets (6). Burn injuries induce widespread inflammatory responses and immune dysregulation, often resulting in immunosuppression and increased susceptibility to sepsis. Severe burns can lead to systemic inflammatory response syndrome (SIRS), a pathway similar to sepsis, frequently culminating in organ failure and high mortality rates (7). Investigating the immune and inflammatory alterations triggered by burns is critical for devising preventive strategies against burn-induced sepsis (8, 9).In this context, a significant number of macrophages may become hyperactivated, releasing immune mediators in a rapid, burst-like manner. This amplified immune response can shift the individual's focus from managing the initial inflammatory phase to addressing secondary infections, which are frequently observed following severe burns and critically influence the prognosis of burn-induced sepsis. When designing therapeutic interventions, it is essential to consider the dynamic temporal patterns of macrophage activation, particularly during the acute and chronic phases of sepsis and burns, as well as their interplay with metabolic shifts. These metabolic changes can further exacerbate immune dysfunction, influencing the effectiveness of immune responses and the overall recovery process.

Additionally, the immunosuppressive state induced by burn injuries can impair the body's capacity to detect and combat emerging cancers, potentially heightening the risk for certain malignancies (10, 11). Cellular regeneration following burn injuries may foster conditions conducive to abnormal cell growth and cancerous lesions. Such an environment could contribute to carcinogenesis (12, 13). In the pursuit of understanding the underlying mechanisms, recent research advancements in the field of molecular biology have provided valuable insights. Transcriptomics has emerged as a crucial tool, as it plays a significant role in revealing the immune microenvironment and holds great importance for the diagnosis and prognosis of various diseases (14, 15). Through transcriptome analysis and single - cell techniques, researchers are now able to identify the functional characteristics and molecular markers of different cancer - associated fibroblast (CAF) sub - populations, thereby providing a solid theoretical foundation for the development of precise treatment strategies (16). Moreover, the immune escape mechanisms prevalent in the tumor microenvironment and their subsequent promotion of tumor progression have been identified as potential therapeutic targets for novel targeted treatment approaches (17). Single - cell transcriptomics analysis has demonstrated that diverse signaling pathways and immune regulatory factors play critical roles in antigen - specific cell functional exhaustion and immune escape, offering essential guidance for optimizing treatment regimens (18, 19). By leveraging single - cell RNA sequencing and bioinformatics analysis, researchers have been successful in identifying important molecules and pathways associated with the tumor microenvironment, thus charting new directions for precision medicine (20). Additionally, single - cell transcriptomics has been applied to analyze the repair process, shedding light on the underlying mechanisms (21). Concurrently, bioinformatics analysis and experimental validation of potential biomarkers have furnished crucial indicators for disease diagnosis and prognosis assessment (22–24). The advent of novel technologies and advanced molecular research methods has had a profound impact on disease research and treatment (25). In the realm of cancer treatment, for instance, antibody - drug conjugates and photodynamic therapy have witnessed continuous development. Through meticulous mechanism research, rigorous clinical validation, and the integration of bioinformatics analysis of clinical data, these advancements have propelled cancer treatment to new heights (26). Modern bioinformatics and big data technologies are increasingly indispensable in disease diagnosis, prognosis evaluation, and treatment. The application of these cutting - edge technologies and methodologies has not only spurred the growth of biomedical research but has also laid a robust foundation for the realization of precision medicine (27, 28). Gaining insight into how burns may facilitate cancer formation could inform the development of strategies to mitigate the risk of advanced-stage cancer (13, 29). However, the specific mechanisms by which burn-induced immune-metabolic changes impact cancer development across different cancer types should be further elucidated, as this connection is not yet fully understood.

Sepsis, with its extensive infectious inflammation, similarly poses a potential pathway for cancer development (30, 31). The prolonged inflammatory state associated with sepsis may lead to genomic instability and the accumulation of mutations, creating conditions that disrupt local cellular environments and potentially transform cells into malignant tumors (32, 33). Addressing chronic sepsis-related inflammation and bolstering immune function could play a pivotal role in modulating cancer risk and progression (31, 34). Furthermore, various macrophage cell death pathways, such as pyroptosis, autophagy, and ferroptosis, play a significant role in organ damage during sepsis. These mechanisms add complexity to the immune response in sepsis and may serve as potential therapeutic targets for modulating immune responses and preventing multiorgan failure. The heterogeneity of tumor microenvironments across different cancer types may limit the generalizability of findings related to the impact of sepsis-induced immune alterations on cancer development. Moderate exercise has long been recognized for its positive effects on immune function, strengthening the body's defense mechanisms. Such exercise may enhance management strategies for conditions like burns, sepsis, and cancer (35, 36). Exercise supports recovery from burn injuries, reduces the risk of sepsis, and mitigates some irreversible side effects of cancer therapies, while also boosting the efficacy of treatments (37, 38). Thus, this emerging perspective could foster a more integrated approach to patient care, treating these conditions in concert rather than in isolation (39, 40). Research has found that nicorandil can relieve joint contracture and fibrosis by inhibiting the RhoA/ROCK and TGF - β1/Smad signaling pathways, providing potential drug targets for joint diseases (41).

The fields of cell therapy and biologic agent therapy are developing rapidly. Studies on engineered extracellular vesicles and exosomes derived from stem cells have delved deep into their mechanisms of action and actual treatment effects in tissue repair and regeneration (42). Moreover, exploring the relationship between exercise-induced metabolites and macrophage activity offers a promising area for research. Insights from this field could reveal novel methods for immune regulation and open pathways for resolving sepsis-associated inflammation. In summary, the combined effects of conditions such as burns and sepsis may increase the risk of cancer, a factor that warrants attention both medically and socially (31, 43). Moreover, by investigating the role of macrophages and their immune functions in sepsis, we aim to identify novel therapeutic targets to reduce multiorgan dysfunction and improve patient survival rates. Moving forward, it is essential to further explore the complex interconnections between burns, sepsis, and cancer, with the goal of optimizing treatment strategies based on these findings, ultimately offering better therapeutic prospects for patients.

Materials and methods

Exercise-induced modulation of pan-cancer gene expression in the context of burns and sepsis

We applied the Wilcoxon rank sum test (also known as the Mann-Whitney U test), a nonparametric method, to assess gene expression differences between cancerous and normal tissue across multiple cancer types (44, 45). This test was chosen for its suitability with non-normally distributed data, unlike parametric alternatives that require normal distribution assumptions. Statistical significance was established at $\alpha = 0.05$, indicating meaningful divergence between the median values of two independent sample groups. We analyzed de-identified gene expression data, represented as transcripts per million (TPM), from The Cancer Genome Atlas (TCGA) for tumor samples and late-stage normal tissue samples from the Genotype-Tissue Expression (GTEx) project. These datasets were accessed via the UCSC Xena database. To mitigate inter-dataset variability, the gene expression values were normalized using Z-scores, allowing for consistent dimensional comparisons. Our primary analysis centered on the glioblastoma multiforme (GBM) dataset, through which we investigated gene expression disparities between cancerous and non-cancerous tissues. This detailed comparison allowed us to observe exercise-induced changes in gene expression, providing insights into potential therapeutic implications for managing burns and sepsis within the cancer context.

Promoter methylation analysis of genes linked to exercise impacts on burns and sepsis

This study provides an overview of methylation levels across diverse genomic regions, including the TSS1500 region (200–1500 bp upstream of the transcription start site), the proximal promoter region (the first 200 bp upstream from the TSS), the first exon, and the 5' untranslated region (UTR) (46, 47). For each sample, median methylation values within these regions were determined to represent the sample's overall methylation status. To investigate the correlation between methylation levels and gene expression, we applied Spearman's rank correlation, a non-parametric test ideal for assessing relationships between variables that may not exhibit linear patterns. In this analysis, methylation levels served as the independent variables, while gene expression levels were treated as dependent variables. The strength of these associations was quantified using the Spearman rank correlation coefficient. Additionally, we employed the Wilcoxon rank sum test to compare methylation levels between tumor and normal tissue samples. This non-parametric test is appropriate for comparing two independent sample groups without assuming a specific data distribution, thereby enabling a reliable distinction between tumor and normal tissue methylation patterns across different sample sources. Through this approach, we identified significant methylation differences, enhancing our understanding of tumor biology and the potential role of exercise in modulating responses to burns and sepsis.

ATAC-seq analysis of exercise-related gene modulation in burns and sepsis

In this study, we employed ChIPseeker, an R package tailored for analyzing and visualizing both ChIP-seq and ATAC-seq data (48, 49).

Utilizing ChIPseeker's annotatePeak function, we conducted an in-depth analysis of transcription start sites (TSS) within promoter regions of genes. We set the parameter tssRegion = c (-3000, 3000) to cover the 3000 base pairs upstream and downstream of the TSS, enabling a comprehensive examination of genomic elements, including transcription factor binding sites and histone modifications. To visualize coverage, we utilized ChIPseeker's covplot function, generating plots that illustrate the distribution of peaks across the genome in human ATAC-seq data. These coverage plots reveal not only the spatial distribution of peaks along chromosomes but also offer detailed insights, including gene names, tumor types, chromosomal positions, and genetic distances, conveniently displayed on the left side of the graph. This visual approach provides researchers with a holistic and precise representation of the ATAC-seq data, enhancing our understanding of exercise-induced gene regulation in the context of burns and sepsis.

Prognostic assessment of exercise-related genes in burns and sepsis across pan-cancer

To evaluate the prognostic significance of various genes, we applied a univariate Cox regression model using the survival package in R (50, 51). For each gene, we derived hazard ratios along with their 95% confidence intervals by fitting the data into a Cox proportional hazards model through the coxph() function. The results were visualized in a heatmap to facilitate comparative analysis and enhance interpretability.

Genomic profiling of exercise-related genes in burns, sepsis, and pan-cancer contexts

To investigate the impact of exercise on genes associated with burns and sepsis across various cancer types, we analyzed copy number alterations and DNA methylation data from The Cancer Genome Atlas (TCGA) (52, 53). Patient samples were organized in a structured matrix format, with rows representing samples and columns representing genes or genomic regions. After quality control steps to exclude low-quality samples and probes, data were standardized to minimize technical variation. Using tools like GISTIC and CNAnorm, we identified and categorized genomic amplification and deletion events, quantifying their frequencies across the genome. DNA methylation levels at gene promoter regions were assessed on the UALCAN platform, comparing differences between normal and cancerous tissues to elucidate the influence of exercise on wound healing and infection responses. For methylation pattern analysis in specific cancer-associated genes, we utilized the 'gene visualization' module available in MethSurv. To further understand genomic impacts, Mutation Annotation Files (MAF) from TCGAbiolinks and tumor mutation burden (TMB) calculations via maftools allowed us to explore links between these genomic features and immunotherapy responsiveness. Statistical analyses, including correlation and survival analyses, were conducted on copy number alteration, DNA methylation, and TMB data to assess their associations with exercise-modulated gene expression in wound healing and infection. These analyses aimed to evaluate the potential impact of these genomic variations on tumor progression and patient outcomes.

Gene set enrichment analysis across pan-cancer types

This study utilized data from The Cancer Genome Atlas (TCGA) repository, incorporating tumor and normal tissue samples from a specific cancer type (54, 55). The data underwent stringent quality control processes, during which invalid samples and probes were excluded to ensure robustness. Following quality filtering, normalization was applied to mitigate technical variability inherent in the dataset, including adjustments for background noise, often present in raw files. We employed the "limma" package within the R environment, which facilitates background correction, normalization, and statistical analyses for identifying genes with significant differential expression. The criteria for selection involved both log2 fold change (log_2FC) and p-values. Log_2FC quantified the relative changes in gene expression, while the p-value assessed statistical significance. For gene set enrichment analysis (GSEA), we used the "clusterProfiler" package in R to annotate and visualize enriched pathways associated with differentially expressed genes in public databases such as KEGG, GO, and Reactome. We relied on the Enrichment Score (ES), which ranges from 0 to 1, as a metric to determine the relevance of pathway alterations in relation to gene expression changes. Finally, to visualize the findings, we utilized R packages, including "ggplot2," to create various graphical representations. This included simple bar charts, scatter plots, and heatmaps, allowing a clear interpretation of the results. This methodological framework provides a structured approach to interpreting the molecular implications of gene expression variations in cancer.

Cell culture

Human umbilical vein endothelial cells (HUVECs) were seeded in culture flasks and maintained in Dulbecco's modified Eagle medium (DMEM, low glucose), supplemented with 10% fetal bovine serum (FBS), 1% endothelial cell growth supplement, and 1% penicillin-streptomycin solution. The cells were incubated at 37°C in a humidified chamber with 5% CO_2 under normoxic conditions. To establish an *in vitro* model, HUVECs were subsequently exposed to 1 μg/mL of lipopolysaccharide (LPS). Eight hours before the experiments, cells were cultured in serum-free DMEM. For differentiation, THP-1 cells were treated with 100 ng/mL phorbol 12-myristate 13-acetate (PMA) for five days to induce macrophage-like characteristics. RAW 264.7 mouse macrophages (ATCC, Rockville, MD, USA) were cultured in DMEM containing 10% heat-inactivated FBS, 100 U/mL penicillin, and 100 μg/mL streptomycin, and incubated at 37°C in a 5% CO_2 atmosphere.

Cell viability assay

HUVECs, seeded at a density of 5×10^3 cells per well, were transfected with MLIP knockdown, overexpression, or control plasmids and plated in 96-well plates to assess proliferation. After an initial 16-hour incubation, the cells were either stimulated with LPS or left untreated for 0, 6, and 24-hour intervals. Cell proliferation was measured using the Cell Counting Kit-8 (CCK-8; Beyotime, Beijing, China, Cat#C0038), in accordance with the manufacturer's protocol. Absorbance was recorded at 450 nm using a BioTek microplate reader (BioTek, U.S.A.).

Real-time reverse transcription polymerase chain reaction

Total RNA was isolated from the three experimental groups using Trizol reagent (Invitrogen, USA). The isolated RNA was reverse-transcribed into complementary DNA (cDNA) using the PrimeScript II 1st Strand cDNA Synthesis Kit (Takara, Shiga, Japan). Real-time RT-PCR was performed with the SYBR Premix Ex Taq II (Takara, Shiga, Japan) on a StepOnePlus Real-Time PCR system (Applied Biosystems, CA, USA). The relative mRNA expression levels were quantified using the 2^−ΔΔCt method, with GAPDH as the internal control.

Measurement of oxidative stress and LDH release assay

Cytotoxicity was assessed by quantifying lactate dehydrogenase (LDH) release using a commercial assay kit, following the manufacturer's instructions. Briefly, 50 µL of supernatant from each well was collected and incubated with reduced nicotinamide adenine dinucleotide (NADH) and pyruvate for 15 minutes at 37°C. The reaction was terminated with the addition of 0.4 mol/L NaOH. LDH activity was measured by recording the absorbance at 440 nm on a SpectraMax M2 spectrophotometer (Molecular Devices, Sunnyvale, CA, USA) and expressed as U/g protein. Additionally, oxidative stress markers, including superoxide dismutase (SOD) and glutathione peroxidase (GSH-Px) activities, along with reactive oxygen species (ROS) and malondialdehyde (MDA) levels, were measured using commercially available kits, following the manufacturer's protocols.

Flow cytometry analysis

Apoptosis and cell polarization were evaluated in both treated and untreated cells using flow cytometry. Following treatment, cells were harvested and stained with FITC-Annexin V and propidium iodide (PI) for 10 minutes at room temperature, following the protocol provided by the Annexin V-EGFP Apoptosis Detection Kit (KeyGEN BioTECH). For polarization assessment, cells were additionally stained with antibodies targeting M1 polarization markers when required. Data acquisition and analysis were conducted on a Fluorescence-Activated Cell Sorting (FACS) Calibur flow cytometer (Becton-Dickinson, Sparks, MD, USA) with associated software. For the colony formation assay, cells were plated in 6-well plates and treated with designated drugs for 6 hours according to the experimental groups for reactive oxygen species (ROS) detection. A fluorescent probe, DCFH-DA (10 µM; Solarbio, China), was diluted in a serum-free medium, and cells were incubated with it for 30 minutes at 37°C. FITC signals were subsequently detected via flow cytometry.

Immunofluorescence analysis

Cells were plated in 6-well culture plates and incubated overnight to ensure adherence. The cells were then fixed with 3.7% paraformaldehyde at room temperature for 15 minutes and subsequently permeabilized in cold methanol at -20°C for 15 minutes. Blocking was performed using a buffer containing 5% normal goat serum and 0.5% Triton X-100 in PBS for 1 hour at room temperature. Primary antibodies were added, and cells were incubated overnight at 4°C. After washing three times with PBS for 10 minutes each, cells were incubated at room temperature with Alexa Fluor 488-conjugated goat anti-rabbit secondary antibody (Cat# A-11034) and Alexa Fluor 594-conjugated goat anti-mouse secondary antibody (Cat# A-11004; Thermo Fisher), both diluted 1:500 in blocking buffer. Prior to imaging, nuclei were stained with DAPI (Cat# D9542; Sigma) for 30 minutes at room temperature. Images were obtained using a Nikon Eclipse E800 fluorescence microscope.

Statistical analysis

Data are presented as mean ± standard deviation (SD). Statistical analyses were conducted using GraphPad Prism 8 software. Group differences were assessed using either Student's t-test or analysis of variance (ANOVA), depending on the experimental design. A p-value of less than 0.05 ($P < 0.05$) was considered statistically significant.

Results

Gene expression and pathway enrichment analysis

In our study, we investigated gene expression differences and pathway enrichment between two sample groups using a variety of analytical approaches. The UMAP plot (Figure 1A) revealed distinct clustering between the groups, indicating significant differences in gene expression profiles. This clustering suggests that the gene expression profiles of the groups are sufficiently divergent to merit further investigation into the underlying molecular mechanisms. The volcano plot (Figure 1B) highlighted differentially expressed genes. This visualization not only underscores the extent of differential expression but also aids in the identification of key genes that may be crucial in the context of burn-induced sepsis and its potential association with cancer. GSEA identified significantly enriched pathways (Figure 1C), including those related to immune response activation, metabolic pathways, and

10.3389/fimmu.2025.1540998

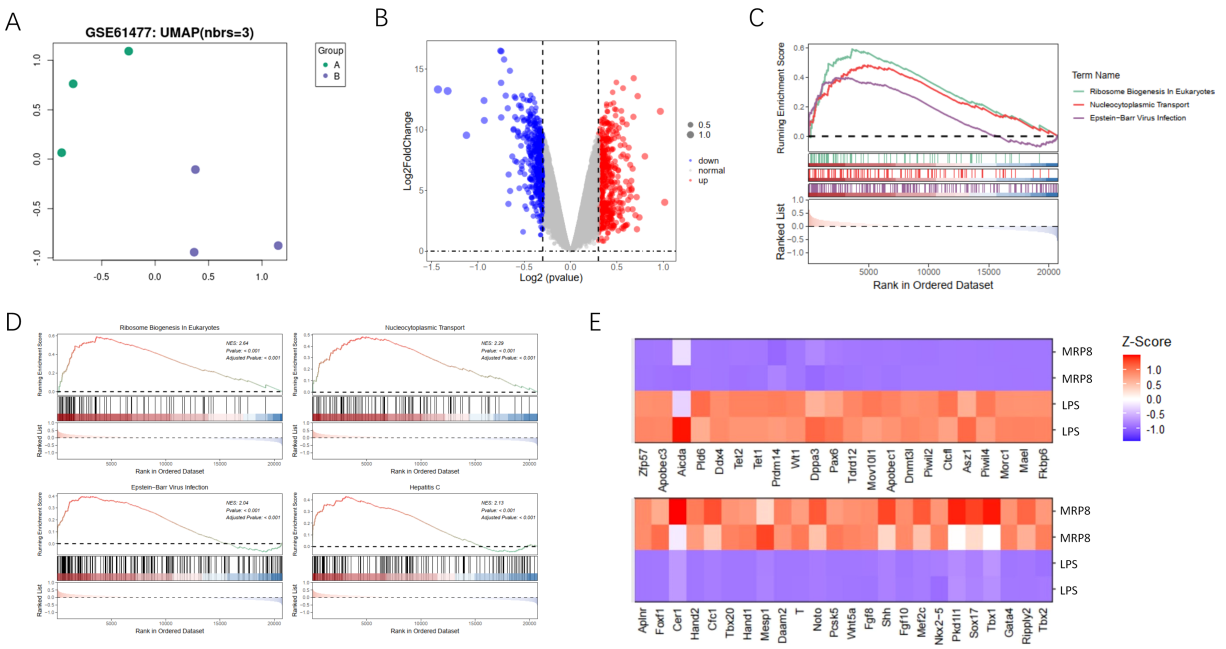

FIGURE 1
Analysis of gene expression and pathway enrichment between two sample groups. **(A)** The UMAP plot shows the two-dimensional distribution of the two sample groups visualized using Uniform Manifold Approximation and Projection (UMAP). Each point represents an individual sample, color-coded by group, and illustrates clustering patterns based on gene expression profiles. **(B)** The volcano plot presents differential gene expression analysis between the two groups. The x-axis displays the log2 fold change in gene expression between groups, and the y-axis shows the -log10 adjusted p-value to indicate statistical significance. Red points highlight significantly upregulated genes, blue points represent significantly downregulated genes, and grey points indicate genes without significant changes. **(C)** The GSEA plot illustrates gene set enrichment analysis, highlighting pathways with significant enrichment. The enrichment score is plotted across the rank-ordered gene list for three specific pathways: Immune Response in Activation, Metabolic Pathways, and Tumor Suppressor Inhibition, each represented by different colors and line types. **(D)** The GSEA top pathways display the four most significantly enriched pathways individually through GSEA. Each panel includes an enrichment score curve, indicating the positions of genes within the pathway on the ranked gene list, revealing the distribution and relevance of genes contributing to pathway enrichment. **(E)** The heatmap visualizes the expression levels of genes identified in the enriched pathways. Each row represents a specific gene, and each column corresponds to a sample. Gene expression levels are normalized to z-scores, with red indicating high expression and blue indicating low expression, allowing a visual comparison of expression patterns across samples in each group.

tumor suppressor inhibition. The top four enriched pathways (Figure 1D) were further explored, with the enrichment scores and the specific positions of genes within these pathways clearly displayed. A heatmap (Figure 1E) illustrates the Z-scores of gene expression for genes within these pathways, providing a clear visualization of expression patterns across all samples. This comprehensive analysis highlights significant differences in gene expression and pathway enrichment between the two groups, emphasizing key pathways involved in disease mechanisms and pinpointing potential therapeutic targets. These findings lay the groundwork for identifying therapeutic targets and biomarker candidates, which could play a crucial role in the development of more effective treatment strategies for burn-induced sepsis and its potential link to cancer.

Differential gene expression and pathway enrichment analysis

Our study aimed to identify differentially expressed genes (DEGs) and significantly enriched pathways between tumor and normal tissue samples. To achieve this, we utilized a combination of statistical and computational tools, with the results presented in various figures to provide clarity and a comprehensive understanding of the findings. Figure 2A presents a volcano plot that illustrates the distribution of DEGs between tumor and normal groups. The dashed lines represent thresholds for statistical significance, enabling the clear identification of the most relevant genes affected by the conditions under investigation. GSEA was conducted to identify significantly enriched pathways, with Figure 2B depicting the statistical significance of these pathways. This figure reveals the biological processes most influenced by the differential gene expression patterns observed between tumor and normal tissues. The pathways selected based on their statistical significance offer valuable insights into the biological processes that are most affected by the differentially expressed genes. Further GSEA results highlighted the top four enriched pathways, as shown in Figure 2C. Additionally, the gene distribution within these pathways is shown, offering a clearer understanding of how specific genes contribute to pathway enrichment and their potential role in tumor development. Figure 2D displays a heatmap that visualizes gene expression levels across all samples, specifically focusing on genes related to the identified pathways. Each row in the heatmap corresponds to a unique gene, while each column represents an individual sample. Collectively, these analyses provide a detailed view of the molecular alterations occurring in tumor and normal tissues. The identification of significantly enriched pathways and

10.3389/fimmu.2025.1540998

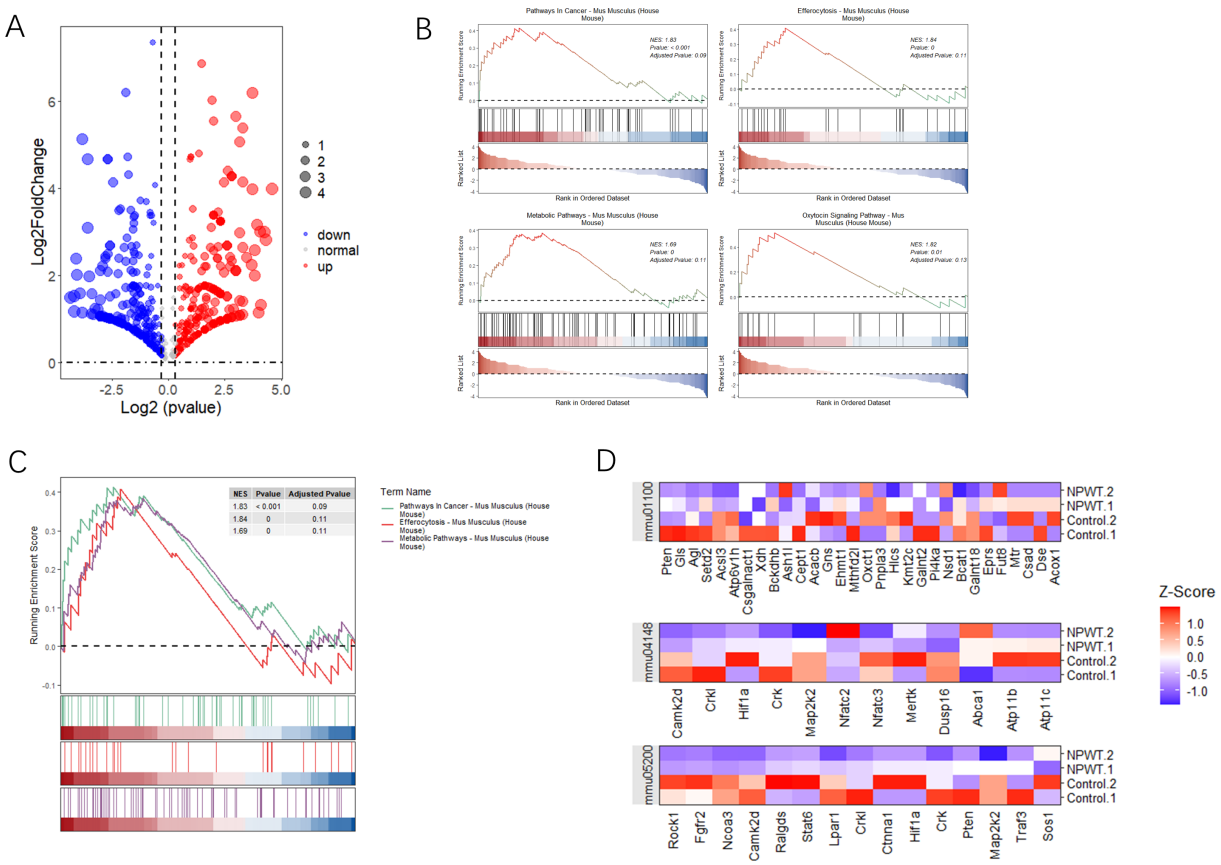

FIGURE 2
Analysis of differential gene expression and pathway enrichment. **(A)** The volcano plot illustrates the differential expression of genes between two groups. The x-axis represents log2 fold change, while the y-axis shows -log10(p-value). Red highlights genes with significant upregulation, blue indicates downregulated genes, and dashed lines mark the thresholds for statistical significance. **(B)** Gene Set Enrichment Analysis (GSEA) plots illustrate the enrichment of three pathways with significant results. The y-axis displays the enrichment score (ES), and the x-axis shows the rank of genes within the ordered dataset. Key pathways enriched in this analysis are emphasized based on their statistical significance. **(C)** Additional GSEA plots present the top four pathways with notable enrichment scores, further emphasizing the relevance of pathways that show substantial statistical enrichment. **(D)** A heatmap shows the expression levels of genes across significant pathways, normalized by Z-score across all samples. Each row represents a gene, and each column represents a sample, with color gradation indicating expression levels—red for high expression and blue for low. This comparison includes gene expression data from both tumor and normal tissue samples, allowing a comparative analysis of gene expression under different conditions.

differentially expressed genes contributes to a deeper understanding of the biological functions and pathways involved in tumorigenesis.

Expression landscape of exercise-influenced genes in pan-cancer analysis

In this study, we analyzed the expression landscape of exercise-influenced genes associated with burns and sepsis. The datasets used included GSE193428, GSE61477, and a dataset of exercise-related genes, collectively providing a comprehensive profile of gene expression. By integrating data from these diverse sources, we aimed to investigate the shared and unique gene expression patterns influenced by exercise in the context of burns, sepsis, and cancer. As shown in Figure 3A, a Venn diagram illustrates the overlap and unique characteristics of DEGs across the datasets. Specifically, 626 genes were unique to GSE193428, 911 were specific to GSE61477, and 194 were exclusive to the exercise-related genes. Additionally, 53 genes overlapped between GSE193428 and GSE61477, while 10 genes were common between GSE61477 and the exercise-related gene dataset. Key genes identified among these, such as FARSA, SVIL, LAMP2, and COL12A1, were found to be influenced by exercise in both burns and sepsis, suggesting their potential roles in exercise-mediated recovery processes. These genes are involved in critical biological functions such as protein synthesis, cell signaling, and tissue repair, all of which are vital for enhancing the body's response to burns, sepsis, and potentially cancer development. Figures 3B, C present the differential expression analysis of these genes across various cancer types. Figure 3B illustrates the expression levels using non-paired samples, capturing the variability in gene expression due to exercise, burns, and sepsis. In contrast, Figure 3C employs paired samples to compare tumor and adjacent normal tissues, providing a more refined analysis that controls for individual variability and highlights consistent exercise-influenced expression patterns. Expanding on these analyses, Figure 3D integrates data from both

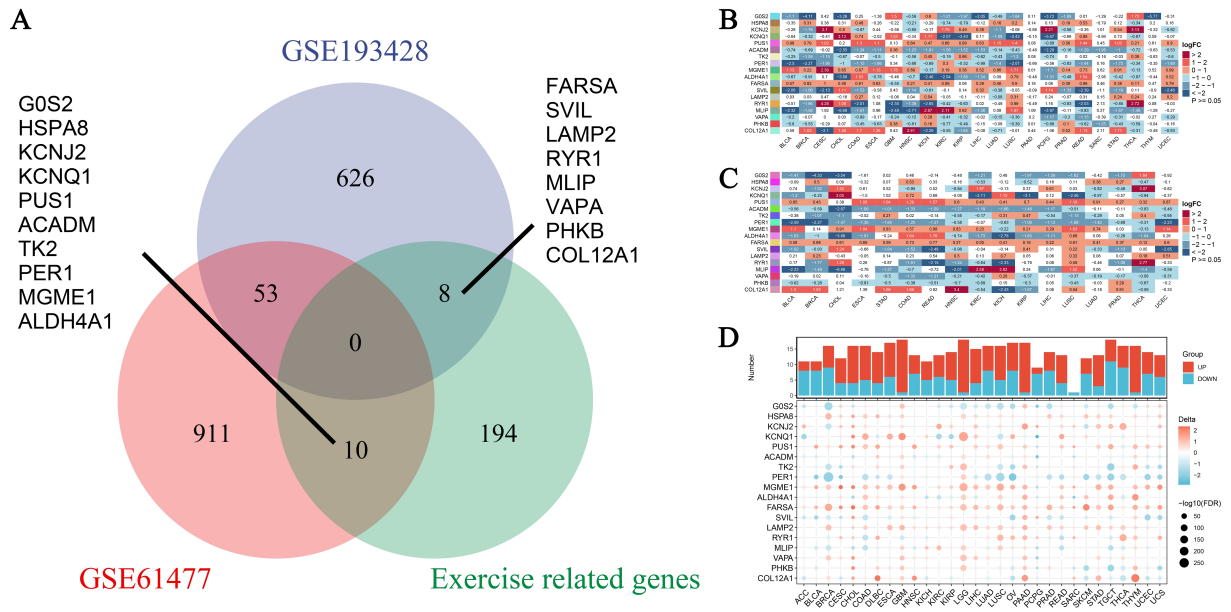

FIGURE 3
Expression profiles of exercise-modulated genes related to burns and sepsis in pan-cancer analysis. **(A)** The Venn diagram illustrates the overlap of differentially expressed genes (DEGs) identified from two datasets, GSE193428 and GSE61477, including a subset of genes associated with exercise. This visualization distinguishes DEGs unique to each dataset from those shared between them, underscoring genes commonly modulated by exercise, burns, and sepsis. Specific genes unique to each condition are labeled outside the Venn circles. **(B)** Differential expression analysis was conducted on exercise-modulated genes linked to burns and sepsis using non-paired samples across multiple cancer types. The resulting heatmap depicts the expression levels of these genes, with color intensity reflecting the extent of expression change. The data, drawn from various cancer types, showcases gene expression variations influenced by exercise, burns, and sepsis. **(C)** A subsequent differential expression analysis was performed on the same gene set, using paired samples from individual patients. This heatmap presents refined insights into gene expression changes by comparing tumor tissue directly with adjacent normal tissue from the same patient. Analyzing paired samples helps control for individual variability, revealing more consistent gene expression patterns related to exercise influences. **(D)** Additional differential expression analysis incorporates data from the TCGA-GTEx projects, providing a comprehensive comparison of gene expression across cancerous and normal tissues. This analysis examines exercise's influence on genes associated with burns and sepsis. At the top, a bar chart details the number of samples analyzed, while the heatmap below indicates shifts in gene expression, with color coding denoting increased or decreased levels.

the TCGA and GTEx projects, enabling a comprehensive comparison of gene expression profiles in malignant and healthy tissues. This figure offers further insights into how physical activity may modulate expression changes associated with burns and sepsis. At the top of Figure 3D, the sample sizes for each cancer type are displayed. Below, a heatmap uses color coding to represent upregulated and downregulated genes, highlighting the expression patterns across cancer types. These findings underscore the significant influence of exercise on transcriptional patterns associated with burns and sepsis in the context of cancer. The consistent expression changes observed in exercise-influenced genes across various datasets suggest that exercise may be a critical modulator of recovery from both sepsis and burns, with potential implications for cancer prevention and survival.

Analysis of promoter methylation of burn and sepsis-related genes influenced by exercise

Figure 4 provides an in-depth analysis of promoter methylation levels and their impact on mRNA expression in burn- and sepsis-related genes affected by physical activity. Figure 4A presents a heatmap that displays variations in promoter methylation levels for genes such as ACADM, ALDH4A1, COL12A1, FARS2, G6PC, HSP90A, KCNJ2, KCNQ1, PER1, PHKB, PUS1, RYR1, SVIL, TK2, and VAPA. In this heatmap, red represents hypermethylation, blue indicates hypomethylation, and white denotes no significant change. The analysis compares methylation patterns across patient samples, distinguishing those who underwent exercise intervention from those who did not, revealing notable differences that suggest the influence of exercise on the epigenetic regulation of these genes. Figure 4B illustrates the relationship between promoter methylation levels and corresponding mRNA expression levels, employing the same color scheme: red for a negative correlation, blue for a positive correlation, and white for no significant correlation. This heatmap demonstrates how changes in promoter methylation can impact gene expression, with hypermethylation generally associated with reduced mRNA expression and hypomethylation linked to increased expression levels. The analysis was conducted with rigorous statistical evaluations, examining parameters such as distribution, mean, median, standard deviation, and variance to ensure objectivity and precision in data interpretation. These findings highlight the potential regulatory role of exercise in gene expression related to burn and sepsis recovery, emphasizing the significance of considering epigenetic modifications in therapeutic strategies and suggesting the potential benefits of exercise

10.3389/fimmu.2025.1540998

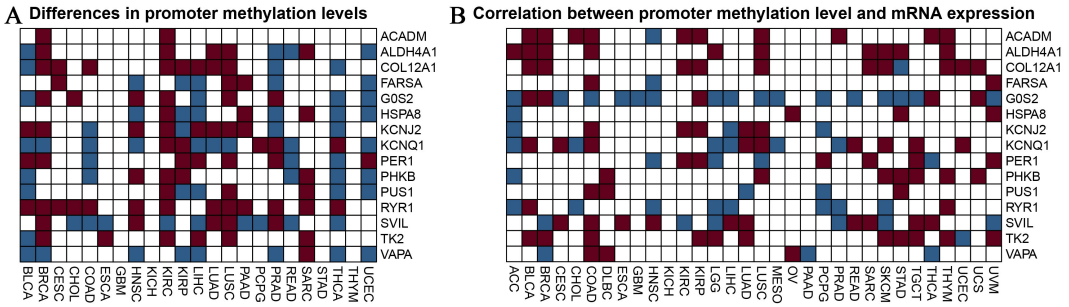

FIGURE 4
Analysis of promoter methylation in exercise-modulated genes related to nurns and sepsis. **(A)** The heatmap visualizes differences in promoter methylation for specific genes associated with burns and sepsis, including ACADM, ALDH4A1, COL12A1, FARS2, G6PC, HSP90A, KCNJ2, KCNQ1, PER1, PHKB, PUS1, RYR1, SVIL, TK2, and VAPA. The colors in the heatmap represent methylation levels, with red indicating hypermethylation, blue indicating hypomethylation, and white showing no significant change. This analysis compares samples from patients receiving exercise treatment with those who did not. **(B)** The heatmap examines the correlation between promoter methylation and mRNA expression levels for the same set of genes. It visually represents the relationship between changes in methylation and mRNA expression, using the same color scheme as in panel **(A)**. Red indicates a negative correlation, blue indicates a positive correlation, and white shows no significant correlation. This analysis seeks to understand how variations in promoter methylation impact gene expression.

interventions in clinical settings. Future research should aim to further elucidate the mechanisms behind these epigenetic modifications and their implications for recovery in burn and sepsis. Investigating how specific exercise interventions might influence gene methylation pathways and understanding their functional consequences on gene expression will provide deeper insights into the potential therapeutic benefits of exercise. This analysis provides valuable insights into the influence of exercise on promoter methylation and gene expression, making a substantial contribution to the growing field of exercise genomics and its role in medical treatments.

Promoter methylation analysis of burn and sepsis-related genes affected by exercise

Promoter methylation analysis revealed varying methylation patterns across burn and sepsis-related genes influenced by exercise. ACADM showed mainly unmethylated or low methylation, with variable CpG site methylation (Supplementary Figure 1A). ALDH4A1 had predominantly unmethylated sites (Supplementary Figure 1B), while COL12A1 exhibited low to medium methylation hotspots (Supplementary Figure 1C). FARSA had a balanced methylation pattern with some sites highly methylated (Supplementary Figure 1D). G0S2 showed low methylation levels with specific CpG site variation (Supplementary Figure 1E). HSPA8 and LAMP2 were primarily lowly methylated (Supplementary Figures 1F, I). KCNJ2 and KCNQ1 exhibited medium to high methylation (Supplementary Figures 1G, H). MGME1 and SVIL had balanced methylation with significant site-specific methylation (Supplementary Figures 1J, P). MLIP showed varied methylation, notably high levels (Supplementary Figure 1K), while PER1 and PHKB had low to medium methylation (Supplementary Figures 1L, M). PUS1 had medium to high methylation (Supplementary Figure 1N), and RYR1 was largely unmethylated (Supplementary Figure 1O). TK2 mainly exhibited low methylation (Supplementary Figure 1Q), and VAPA was mostly unmethylated or lowly methylated (Supplementary Figure 1R). These results highlight exercise's potential role in regulating the epigenetic modification of these genes, providing insight into the underlying molecular mechanisms and potential therapeutic applications.

Correlation of burn and sepsis-related gene expression with tumor prognosis

Our study examined the correlation between the expression of burn- and sepsis-related genes and tumor prognosis, specifically focusing on Disease-Free Interval (DFI), Disease-Specific Survival (DSS), Overall Survival (OS), and Progression-Free Interval (PFI) (Figure 5). In the Disease-Free Interval (DFI) panel (Figure 5A), a heatmap displays the relationship between gene expression and DFI in tumor patients. Here, red squares denote genes associated with increased risk, while blue squares indicate protective genes, with significant correlations marked ($p < 0.05$). Similarly, the Disease-Specific Survival (DSS) panel (Figure 5B) presents a heatmap that illustrates the correlation between gene expression and DSS, maintaining the same color scheme and significance threshold. The Overall Survival (OS) panel (Figure 5C) shows correlations between gene expression and OS, with red indicating risky genes and blue representing protective genes. Only statistically significant correlations ($p < 0.05$) are displayed to emphasize meaningful relationships. Lastly, the Progression-Free Interval (PFI) panel (Figure 5D) provides a heatmap showing the correlation between gene expression and PFI, using consistent color coding and significance criteria. These findings highlight the significant influence of specific gene expressions on various tumor prognosis metrics, offering valuable insights that could guide the development of potential therapeutic targets. The study emphasizes the importance of considering the molecular landscape shaped by burn and sepsis-related genes, which may provide novel opportunities for personalized treatments in cancer patients, particularly those recovering from burns or sepsis.

10.3389/fimmu.2025.1540998

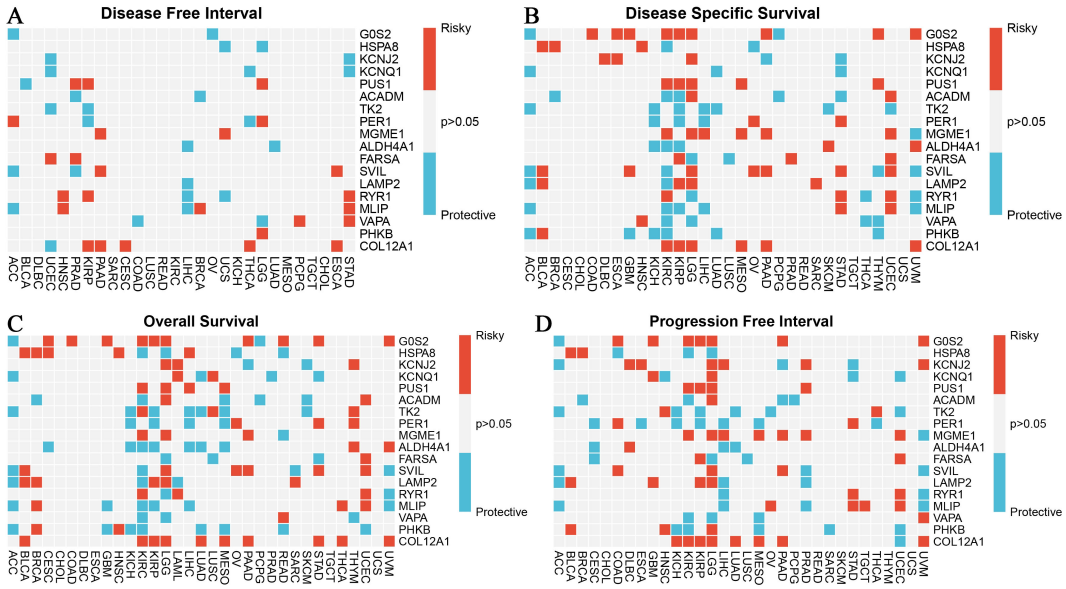

FIGURE 5
Association of burn and sepsis-related gene expression with tumor prognosis indicators (DFI, DSS, OS, PFI). **(A)** The heatmap shows the correlation between the expression of burn and sepsis-associated genes and the disease-free interval in cancer patients. Red squares represent genes correlated with an increased risk (risky), while blue squares indicate genes with a protective effect. Only significant correlations ($p<0.05$) are shown. **(B)** The heatmap illustrates the relationship between gene expression and disease-specific survival in cancer patients, following the same color coding as in panel **(A)**. Red squares denote risky genes, and blue squares indicate protective genes, with only significant associations ($p<0.05$) included. **(C)** This panel provides a heatmap that demonstrates the correlation between gene expression and overall survival in cancer patients. Genes associated with a higher risk are shown in red, while those with protective associations are in blue. Only significant correlations ($p<0.05$) are highlighted. **(D)** The heatmap examines the correlation between gene expression and progression-free interval in cancer patients. As in the previous panels, red indicates risky genes, and blue represents protective genes. Only statistically significant correlations ($p<0.05$) are displayed.

Comprehensive analysis of exercise-influenced burn and sepsis-related genes across pan-cancer

This study explores the impact of exercise on genes associated with burns and sepsis across various cancer types, revealing several key findings. Supplementary Figure 2A shows mutation frequencies of these genes in 20 cancer types, with color intensity representing mutation rates. A waterfall plot (Supplementary Figure 2B) highlights mutation variability across categories. Figures 2C, D illustrate the correlation between gene expression and Tumor Mutation Burden (TMB), with bubble sizes indicating correlation significance and colors reflecting the strength and direction. Figures 2E, F categorize samples by copy number amplifications, identifying the most common cancer types. Figure 2G presents cumulative copy number alterations, while Figure 2H compares amplifications and deletions across cancer types. Finally, Figure 2I displays a correlation matrix of gene expression in different cancers, with bubble sizes representing p-values. These findings highlight the heterogeneous genomic effects of exercise on burn- and sepsis-related genes in cancers, offering insights into potential therapeutic targets and informing personalized cancer treatment strategies.

Exercise-influenced gene expression in cancer and microbiomes

Our analysis of gene expression following exercise across multiple cancer types revealed notable enrichments in genomic features and microbiome signatures. In Figure 6A, we observed distinctive gene expression patterns associated with burns and sepsis that correlate with CNVs. In this figure, circle sizes denote significance levels, while color gradients indicate delta values, highlighting differential expression. Similarly, Figure 6B shows the relationship between gene expression and promoter methylation, with blue representing negative correlations and red indicating positive correlations. Figures 6C, D explore the expression of these genes within different microbiomes. A heatmap in Figure 6C presents normalized expression levels, while hierarchical clustering in Figure 6D reveals co-regulated gene clusters influenced by microbial presence. Figure 6E provides a GSEA across various cancers, identifying enriched pathways. Bubble sizes correspond to the number of genes involved, and colors reflect enrichment scores, with red indicating higher scores. These findings suggest that exercise modulates gene expression in ways that affect cancer biology and microbial interactions, offering potential insights for therapeutic development. The interaction between exercise, gene expression, and microbiome modulation highlights new avenues for improving cancer treatment strategies through holistic approaches that consider genetic, epigenetic, and microbial factors.

Pan-cancer GSVA enrichment analysis

This study performed an extensive pan-cancer analysis of burn- and sepsis-related gene sets influenced by exercise across various

10.3389/fimmu.2025.1540998

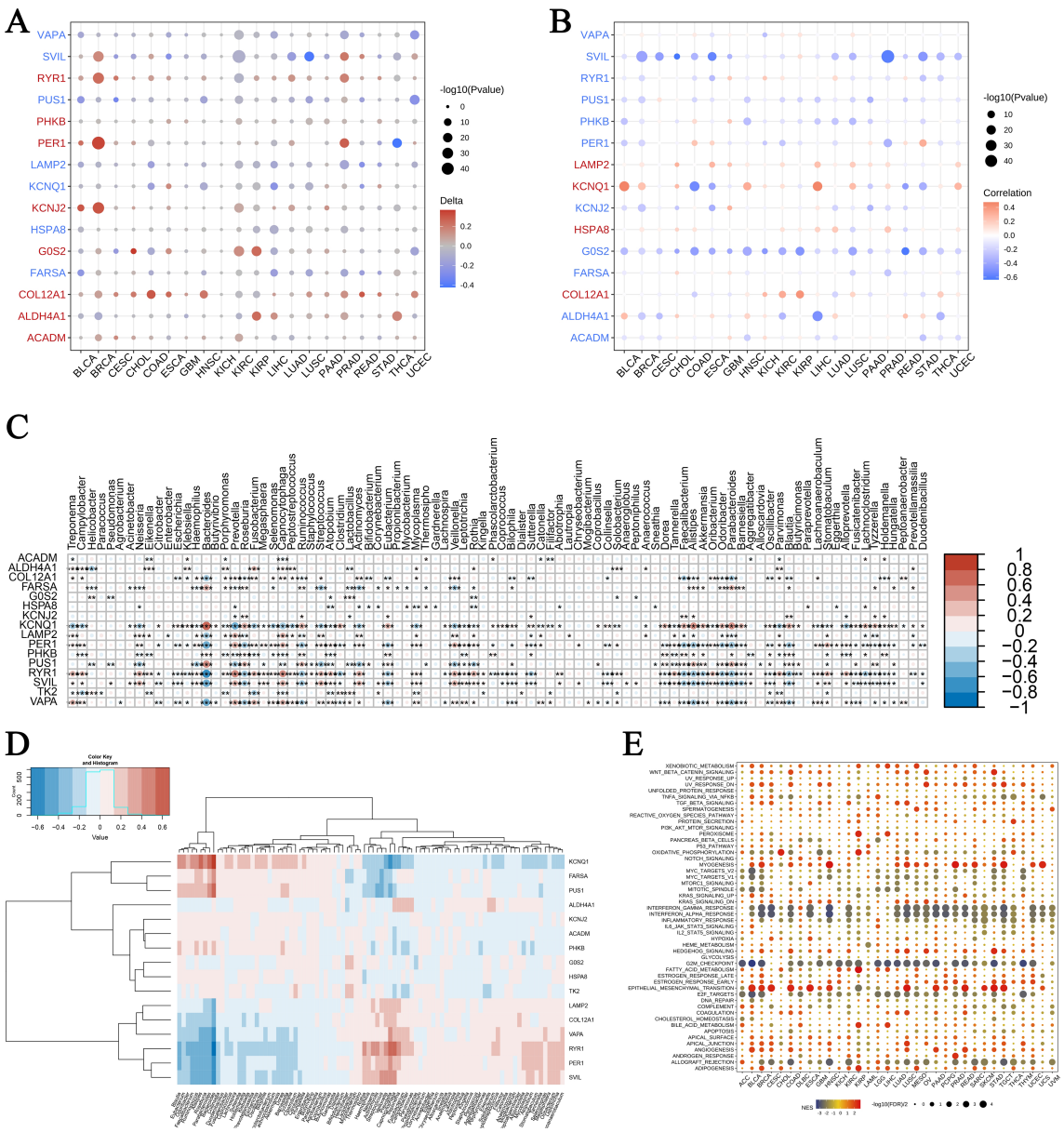

FIGURE 6
Pan-cancer enrichment analysis and gene expression in microbiomes. **(A)** Association of exercise-influenced burn and sepsis gene expression with CNV in multiple cancer types: This panel presents the correlation between the expression of exercise-modulated genes associated with burns and sepsis and copy number variations (CNV) across various cancer types. Circle size corresponds to the significance level (-log10 p-value), while the color gradient indicates delta values, with red representing upregulation and blue indicating downregulation. **(B)** Association of gene expression with promoter methylation across cancer types: This panel displays the correlation between gene expression and promoter methylation levels for exercise-influenced genes related to burns and sepsis across multiple cancers. Circle size reflects the significance level (-log10 p-value), while the color gradient denotes correlation values, with blue indicating negative correlation and red showing positive correlation. **(C, D)** Expression of exercise-influenced genes in microbiomes: The heatmap in panel **(C)** illustrates expression levels of these genes across various microbiomes, with color intensity representing normalized expression levels. Panel **(D)** depicts hierarchical clustering of gene expression data, with a color scale from blue (low expression) to red (high expression), showing distinct clustering patterns. **(E)** GSEA pathway enrichment analysis in different cancers: This bubble plot illustrates the pathways enriched in different cancers, with bubble size representing the number of genes involved and color indicating the enrichment score—red for a higher enrichment score and blue for a lower score. The symbols *, **, and *** represent statistical significance levels corresponding to p<0.05, p<0.01, and p<0.001, respectively.

cancer types using four scoring methods: combined z-scores, GSVA z-scores, PLAGE z-scores, and ssGSEA z-scores. Results in Supplementary Figure 3 reveal significant differences in gene set enrichment between normal and tumor tissues. Supplementary Figure 3A presents the combined z-scores, showing notable statistical significance in cancers such as KIRC and BLCA, which suggests differential gene expression. Supplementary Figure 3B displays the GSVA z-scores, with marked variations in THCA and KICH, pointing to potential implications for tumor biology. In Supplementary Figure 3C, the PLAGE z-scores highlight

significant differences in KIRP and BLCA, underscoring the influence of exercise on gene set activity. Finally, Supplementary Figure 3D shows the ssGSEA z-scores, revealing substantial changes across multiple cancers, suggesting therapeutic potential for exercise-modulated genes in cancer treatment. This analysis provides key insights into the role of exercise-related genes in cancer biology, emphasizing their potential therapeutic applications. It opens avenues for future research, particularly in identifying cancer types that could benefit from exercise-based interventions and exploring the molecular mechanisms underlying exercise-induced gene expression changes in cancer.

MLIP modulates inflammation, oxidative stress, and macrophage polarization in LPS-induced RAW264.7 cells

This study investigated the role of MLIP in regulating inflammation, oxidative stress, and macrophage polarization in LPS-induced RAW264.7 cells. Figure 7A shows that MLIP overexpression (MLIP-OE) significantly enhanced the expression of target genes, while MLIP knockdown (sh-MLIP) notably reduced expression, highlighting MLIP's regulatory function. Figure 7B reveals that LPS treatment upregulated TNF-α, IL-6, and IL-1β mRNA levels, indicating an intensified inflammatory response. MLIP-OE attenuated these cytokine levels, suggesting its potential to suppress inflammation, while LPS + sh-MLIP further elevated inflammatory markers, indicating that MLIP inhibition exacerbates inflammation. Figure 7C demonstrates increased ROS production in the LPS group, reflecting heightened oxidative stress. MLIP-OE reduced ROS levels compared to LPS treatment alone, indicating that MLIP mitigates oxidative stress, while sh-MLIP further increased ROS levels. Figure 7D illustrates that superoxide dismutase (SOD) activity, a key antioxidant enzyme, was reduced by LPS but partially restored with MLIP-OE, underscoring the antioxidative role of MLIP. Figures 7E, F explore MLIP's effects on macrophage polarization. MLIP-OE reduced the expression of the M1 marker CD86 and IL-1β, while increasing the expression of the M2 marker CD206, suggesting MLIP's role in promoting a balanced macrophage polarization. IL-10 levels remained highest in the LPS group, reflecting the influence of LPS on anti-inflammatory responses. Figure 7G, through immunofluorescence staining, shows reduced IL-6 and IL-1β expression in the MLIP-OE group compared to the LPS and sh-MLIP groups, further supporting MLIP's anti-inflammatory effects. Finally, Figure 7H presents flow cytometry data showing shifts in macrophage polarization profiles: MLIP-OE promoted a less inflammatory state, while sh-MLIP favored pro-inflammatory polarization. Overall, these results highlight the significant role of MLIP in modulating inflammation, oxidative stress, and macrophage polarization in LPS-induced RAW264.7 cells. These findings suggest that MLIP could serve as a potential therapeutic target for inflammatory diseases, particularly those involving macrophage polarization, such as autoimmune disorders, infections, and chronic inflammatory conditions.

The role of MLIP in regulating inflammation, oxidative stress, and cell proliferation in HUVECs, with implications for burn-induced sepsis and cancer progression

This study explores MLIP's role in modulating gene expression, inflammation, oxidative stress, and cell proliferation in human umbilical vein endothelial cells (HUVECs). Additionally, it investigates MLIP's potential involvement in burn-induced sepsis and subsequent cancer progression. As illustrated in Figure 8A, MLIP overexpression markedly increased the relative mRNA levels of target genes, whereas MLIP knockdown reduced these levels, underscoring its significant function in gene regulation. Figure 8B demonstrates that MLIP overexpression enhances cell viability, as indicated by the CCK-8 assay, while knockdown decreases proliferation, suggesting MLIP's supportive role in cell growth. Further, Figure 8C compares the expression levels of pro-inflammatory cytokines TNFα, IL-6, and IL-1β across different treatments. The LPS + MLIP-OE group displayed lower cytokine levels than the LPS-only group, underscoring MLIP's potential anti-inflammatory effect. Conversely, increased cytokine levels in the LPS + sh-MLIP group suggest that MLIP inhibition may amplify inflammatory responses. Immunofluorescence analysis of IL-6 and IL-1β (Figures 8D, E) corroborates these findings, showing reduced inflammatory marker expression with MLIP overexpression and elevated levels with knockdown. Moreover, flow cytometry analysis of ROS production (Figure 8F) reveals that MLIP overexpression alleviates LPS-induced oxidative stress, while knockdown elevates ROS levels, highlighting MLIP's regulatory influence on oxidative stress. Apoptosis analysis (Figure 8G) indicates that MLIP overexpression mitigates LPS-induced apoptosis, whereas its inhibition increases apoptosis rates, suggesting a protective role against cell death. Figure 9 provides a comprehensive view of MLIP's involvement in burn-induced sepsis and its implications for cancer progression related to sepsis. The left panel traces the progression from burns to systemic inflammation and sepsis, showing MLIP's role in immune modulation. Central bioinformatics analysis demonstrates differential gene expression, pathway enrichment, and pan-cancer analysis, elucidating MLIP's influence on specific pathways and epigenetic regulation during sepsis. Prognostic analysis suggests MLIP's potential relevance across various cancer types, while microbiome interactions hint at its immunomodulatory properties. The right panel integrates findings from *in vitro* studies on an LPS-induced endothelial model of sepsis, linking MLIP's effects on cell proliferation, ROS levels, and inflammatory cytokine expression. Collectively, these findings highlight MLIP as a pivotal modulator of cellular responses under inflammatory conditions, offering a foundation for its therapeutic potential in managing sepsis and reducing cancer risk associated with inflammation. These results support the notion that MLIP may act as a central mediator of cellular responses in inflammation, oxidative stress, and immune modulation, with important implications for inflammatory diseases and cancer treatment.

10.3389/fimmu.2025.1540998

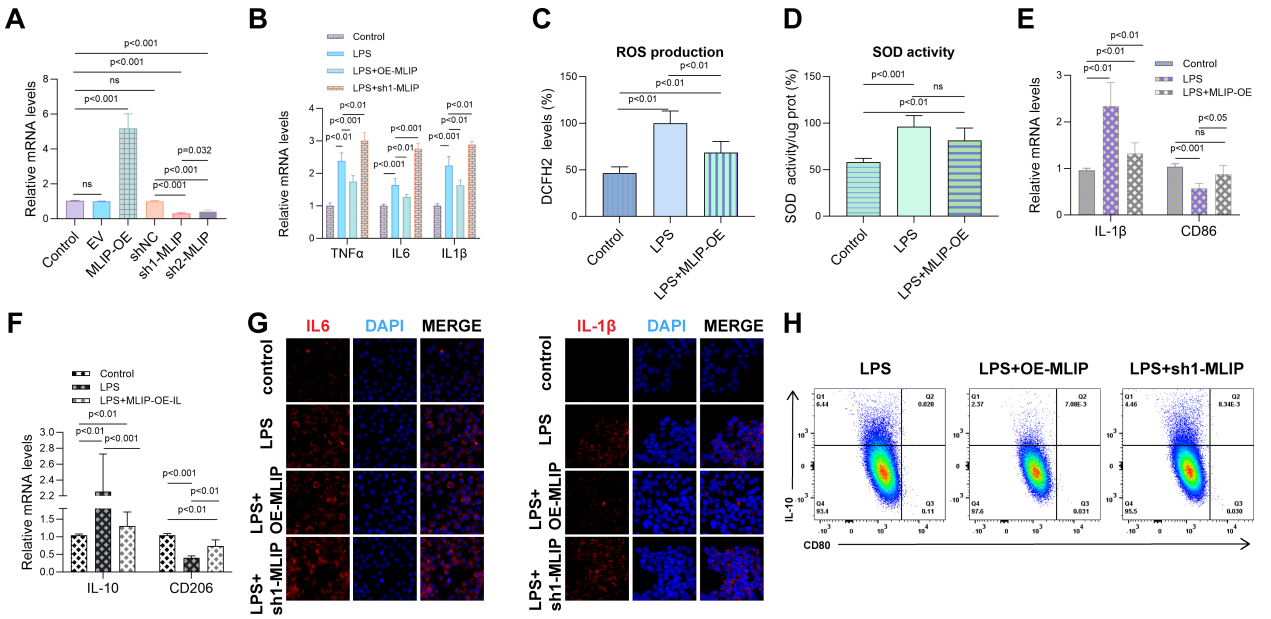

FIGURE 7
MLIP's role in modulating inflammation, oxidative stress, and polarization in LPS-induced RAW264.7 cells. **(A)** Quantitative RT-PCR analysis of target gene expression in RAW264.7 cells across various treatment groups, including Control, MLIP overexpression (MLIP-OE), MLIP knockdown (sh-MLIP), and LPS-stimulated cells. Expression levels are normalized to the Control group and reported as mean ± SD, with $p < 0.05$ indicating statistical significance. **(B)** Quantitative RT-PCR analysis showing relative mRNA levels of TNF-α, IL-6, and IL-1β in Control, LPS, LPS + MLIP-OE, and LPS + sh-MLIP groups, demonstrating MLIP's role in modulating inflammation in the context of LPS treatment. **(C)** DCFH-DA assay results illustrate the effects of different treatments on intracellular reactive oxygen species (ROS) levels. The Control group serves as the baseline, while LPS treatment induces ROS production, and LPS + MLIP-OE treatment reduces ROS, suggesting an antioxidative role for MLIP. **(D)** Measurement of SOD activity across Control, LPS, and LPS + MLIP-OE groups. LPS significantly reduces SOD activity, while MLIP overexpression restores SOD function in treated cells. Data are expressed as mean ± SD, with $p < 0.05$ indicating statistical significance. **(E)** qRT-PCR analysis of M1 macrophage markers IL-1β and CD86 in Control, LPS, and LPS + MLIP-OE groups, highlighting MLIP's influence on macrophage polarization. **(F)** Comparison of IL-10 and CD206 expression levels in Control, LPS, and LPS + MLIP-OE groups using qRT-PCR. Data are shown as mean ± SD, with $p < 0.05$ denoting statistical significance. **(G)** Immunofluorescence staining of inflammatory cytokines: Representative immunofluorescence images illustrating IL-6 and IL-1β expression in RAW264.7 cells across Control, LPS, LPS + MLIP-OE, and LPS + sh-MLIP groups. Cells are stained with DAPI (blue) to label nuclei, with IL-6 or IL-1β (red) indicating cytokine localization and expression. **(H)** Flow cytometry analysis of macrophage polarization: Flow cytometric plots showing the impact of LPS, LPS + MLIP-OE, and LPS + sh-MLIP treatments on macrophage polarization, measured by surface marker expression. Data illustrate shifts in polarization states influenced by MLIP modulation. The results represent three independent experiments. ns, not significant.

Discussion

Burn-induced sepsis presents not only a clinical emergency but also a significant public health concern, as supported by epidemiological data. This alarming statistic highlights the critical nature of burn-induced sepsis and underscores the urgent need for enhanced preventive strategies, diagnostic methods, and therapeutic interventions (56, 57). Given macrophages' pivotal role in immune response, their involvement is central to sepsis pathology. Understanding macrophage-mediated inflammatory responses offers a promising avenue for identifying potential therapeutic targets in treating burn-induced sepsis.

Recent advancements in the medical research field have provided great hope in addressing the complexities of burn-induced sepsis. This study establishes a solid theoretical foundation for improving intervention strategies and discovering new therapeutic targets (58). Given these findings, an appropriate exercise regimen for burn patients could potentially enhance immune function and recovery, thereby reducing susceptibility to sepsis. Significant progress has also been made in nanotechnology. Through bioinformatics, scientists have gained a deeper understanding of the relationship between the microstructure and properties of nanomaterials. This has enabled precise control over pore size, porosity, and composition, leading to broad applications in catalysis, adsorption, and biomedicine (59, 60). For instance, the development of near-infrared light-activated upconversion nanoparticles/curcumin mixed nanomedicines has shown promising potential in inducing glioma stem cell differentiation and effective eradication (61). While this research primarily focuses on gliomas, the concept of using nanomaterials for targeted therapy can be applied to burn-induced sepsis. Researchers have successfully identified potential biomarkers and developed risk prediction models, offering new perspectives for personalized treatment strategies (62–64). Large datasets have also been utilized for bioinformatics analysis, facilitating the precise identification of biomarkers, the exploration of signaling pathways, and the systematic study of immune characteristics (65–67). In the context of burn-induced sepsis, this could lead to early detection through the identification of sepsis-specific biomarkers. Moreover, assessing patients' immune profiles allows for more accurate prognosis, enabling timely adjustments to treatment strategies.

10.3389/fimmu.2025.1540998

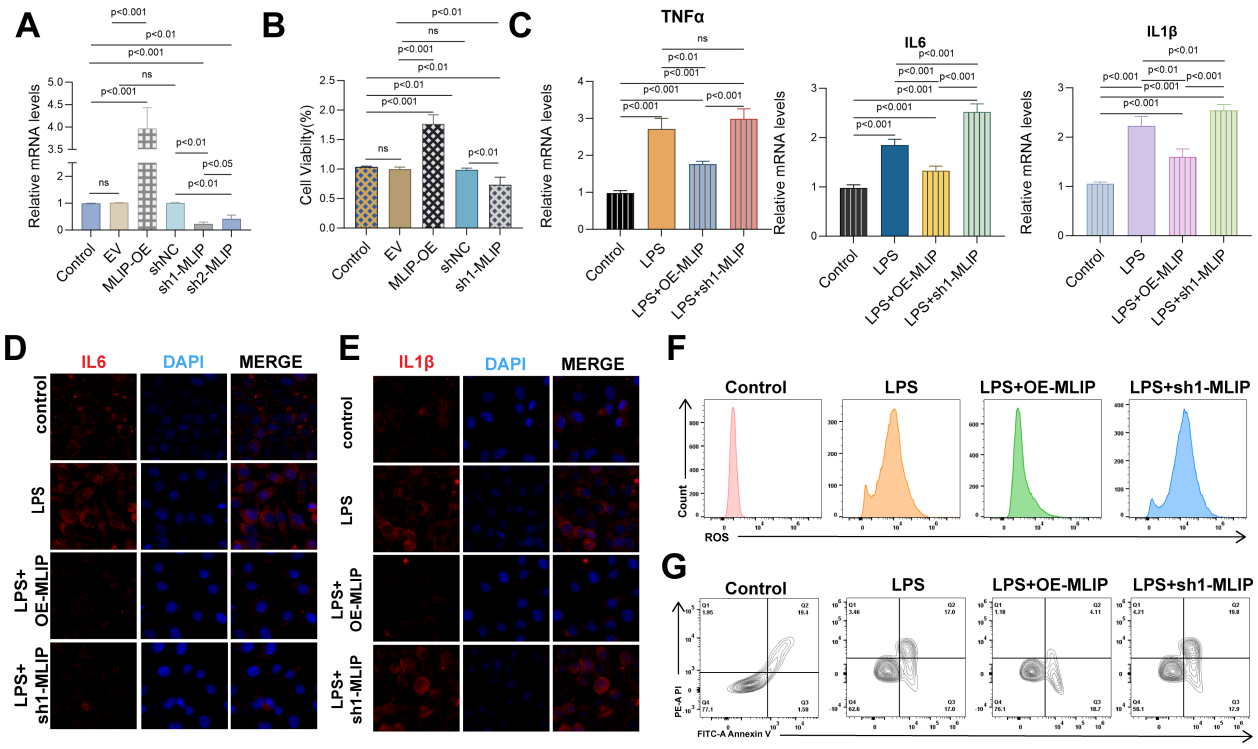

FIGURE 8
Effects of MLIP on gene expression, cell viability, inflammation, ROS levels, and apoptosis in HUVECs across treatment conditions. **(A)** The relative mRNA expression levels of target genes were analyzed via qRT-PCR across treatment groups, with the Control group as a baseline. The EV (empty vector) group serves as a negative control, MLIP-OE represents MLIP overexpression, and sh-MLIP indicates MLIP knockdown. Data represent mean ± SD from three independent experiments, with *p < 0.05 denoting statistical significance. **(B)** HUVEC proliferation was measured under various conditions. Control represents untreated cells, EV serves as the empty vector control, MLIP-OE represents MLIP overexpression, and sh-MLIP indicates MLIP silencing. Results are expressed as mean ± SD, with *p < 0.05 indicating significant differences. **(C)** mRNA levels of inflammatory cytokines were measured by qRT-PCR in Control, LPS-stimulated, LPS + MLIP-OE, and LPS + sh-MLIP groups. LPS stimulation models inflammation, and subsequent treatments assess MLIP's role in modulating cytokine expression. Data are presented as mean ± SD, with *p < 0.05 indicating significance. **(D)** Immunofluorescence staining of IL-6 (red) with DAPI (blue) was performed on HUVECs to assess IL-6 expression under different treatment conditions, including LPS stimulation and MLIP modulation. **(E)** Cells were stained for IL-1β (red) and DAPI (blue), revealing IL-1β expression changes due to LPS treatment, MLIP overexpression, and MLIP knockdown. **(F)** Flow cytometry quantified ROS levels in HUVECs under Control, LPS, LPS + MLIP-OE, and LPS + sh-MLIP conditions, highlighting MLIP's role in regulating oxidative stress during inflammation. **(G)** The percentage of apoptotic cells was measured across treatment groups: Control, LPS-stimulated, LPS + MLIP-OE, and LPS + sh-MLIP. Data underscore MLIP's influence on LPS-induced apoptosis, illustrating differences in apoptosis rates between groups. ns, not significant.

Our research focuses on gene expression profiles and epigenetic modifications in the context of burn - induced sepsis and cancer. These processes are essential for understanding how sepsis and tumorigenesis are interlinked, as they may facilitate tumor cell proliferation and survival while also potentially enhancing immune evasion (31, 68). For instance, cytokines such as TNF-α and IL-6, produced during sepsis, play a key role in organizing inflammatory responses and may indirectly support tumor formation (31, 69). Additionally, oxidative stress associated with sepsis can result in DNA double-strand breaks and genomic instability, creating a genetic foundation conducive to tumor initiation and progression (70). These findings highlight the need for further exploration into the impact of sepsis on tumor microenvironments, particularly in terms of immune suppression and the initiation of genomic instability, both of which could present novel therapeutic opportunities. Examining how macrophage dysfunction during sepsis contributes to site-specific organ damage may provide novel insights into controlling inflammation and preventing cancer progression, depending on the affected sites. We are investigating how exercise influences gene expression profiles and epigenetic modifications across medical conditions such as burns, sepsis, and cancer (71, 72). The Wilcoxon rank - sum test was applied to analyze gene expression differences between tumor and normal tissues. Sourcing data from relevant databases and performing necessary normalizations, we also analyzed methylation levels in specific genomic regions.

These findings underscore the particular significance and timeliness of our study. By investigating the mechanisms of burn-induced sepsis, we aim to provide deeper insights into this clinical issue from both molecular and biological perspectives (73). Our research contributes not only to the development of new preventative and therapeutic strategies to reduce sepsis risk and improve outcomes for burn patients but also to the understanding of the intricate link between inflammation and tumor development. By expanding scientific knowledge on the connections between burn-induced sepsis and tumorigenesis, we can provide valuable data to support informed policy development, potentially leading to

10.3389/fimmu.2025.1540998

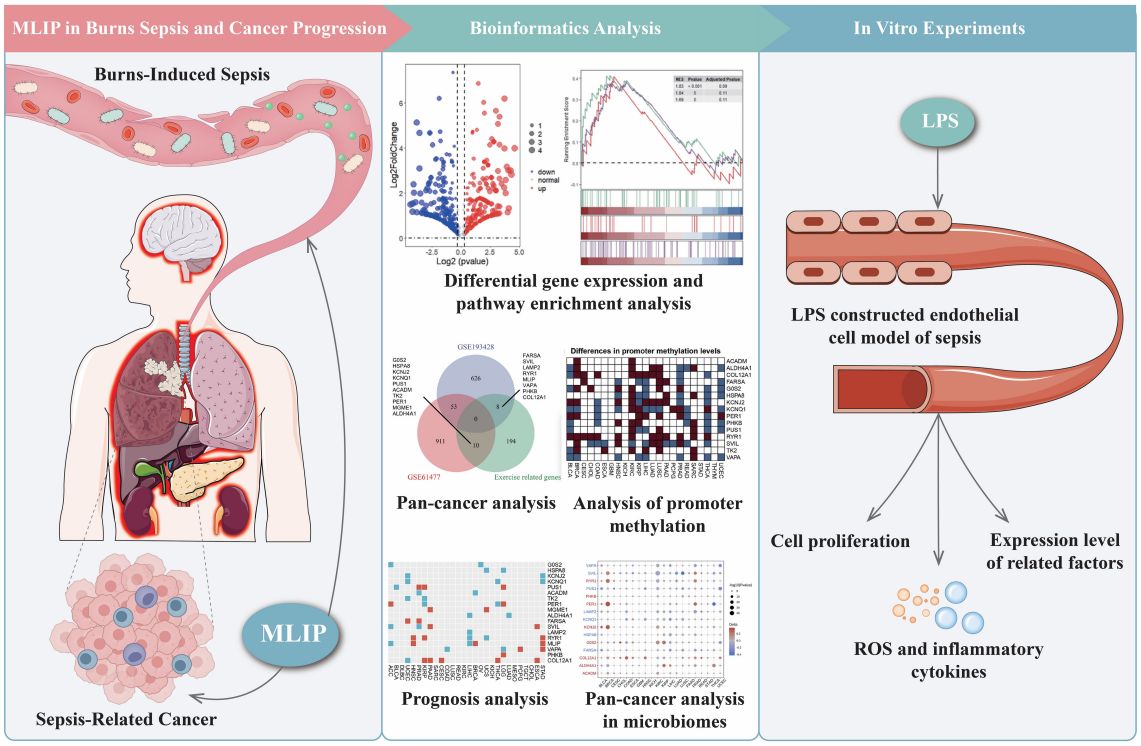

FIGURE 9
Comprehensive analysis of MLIP's role in burns-induced sepsis and cancer progression through bioinformatics and *in vitro* studies. *In vivo* findings highlight MLIP's role in modulating immune responses, suggesting its potential in preventing the transition from sepsis to cancer. The middle section focuses on bioinformatics, analyzing differential gene expression, pathway enrichment, and Gene Set Enrichment Analysis (GSEA) using RNA-seq data. The right section describes *in vitro* experiments using an endothelial cell model of sepsis, where cells are treated with lipopolysaccharide (LPS). These experiments assess cell proliferation, inflammatory markers, ROS, and cytokine levels, shedding light on immune responses during septic conditions. This comprehensive figure explores MLIP's involvement in burns-induced sepsis and cancer progression, presenting potential therapeutic targets.

measurable reductions in the incidence and healthcare costs of these diseases on a broader scale (13, 31).

This study employed a multitude of approaches to explore the therapeutic potential of molecular targets, with bioinformatics playing a pivotal role in data interpretation. From a microscopic perspective of molecules and cells, the combination of transcriptomics and proteomics has delved deep into disease mechanisms, revealing the crucial regulatory mechanisms of transcription factor networks and protein modifications in diseases. This has laid a theoretical foundation for developing novel treatment strategies (74). Through the combined analysis of metabolomics and proteomics, the metabolic pathways and their significant roles in cell functions have been explored multiple times (75). In cell - level research, an in - depth exploration of cell polarization and its role in immune regulation and treatment strategies has provided important evidence for understanding cell functions and immune regulation mechanisms (76). The advancements in proteomics technology have enabled a more thorough study of protein - protein interaction networks, their modifications, and regulatory mechanisms. This helps uncover the complex signal transduction processes within cells, laying the groundwork for understanding the essence of life activities and developing new targeted treatment strategies (77, 78). Through bioinformatics analysis, key genes associated with specific diseases were identified, and their roles in immune infiltration were explored, indicating the direction for disease diagnosis and the search for treatment targets (79, 80). Notably, the inclusion of bioinformatics tools in the analysis has provided insights into the molecular underpinnings of burn-induced sepsis and their connections to cancer-related pathways. Bioinformatics tools were applied to annotate gene functions and conduct pathway enrichment analyses, revealing potential signaling pathways and regulatory networks involved in burn - induced sepsis and its connection to cancer - related pathways. *In vivo* studies using animal models further substantiated these findings. For instance, RNA-seq allows researchers to quantify gene expression across various tumor types in comparison to normal tissues, identifying gene expression profiles associated with cancer development (81, 82). High - throughput sequencing technologies, like RNA - seq, combined with bioinformatics analysis, were used to investigate gene expression profiles in tumor and normal tissues, identifying profiles associated with cancer development.

Bisulfite sequencing (BS-seq) and chromatin accessibility assays offer insights into epigenetic regulatory mechanisms by inferring the DNA methylation status of gene promoters. This is crucial for understanding epigenetic modifications that lead to the activation or silencing of transcription start sites (TSS) (83, 84). Additionally, ATAC-seq technology identifies open chromatin regions that may interact with transcription factors and other regulatory proteins,

playing a vital role in controlling gene expression (85, 86). We anticipate that future work will further explore how these epigenetic modifications could potentially serve as therapeutic targets in burn-induced sepsis and cancer. This approach may ultimately assist in identifying novel biomarkers for early cancer detection, particularly in individuals who have experienced burn-induced sepsis. GSEA can be applied to immune-related gene sets, providing an integrated perspective on immune regulatory mechanisms within the tumor microenvironment (87). Additionally, microbial differential expression studies enable the examination of gene expression profiles within microbial communities in tumor contexts, shedding light on the relationships between microbes, tumor development, and treatment responses (88).

This study systematically investigated the role of MLIP in RAW264.7 cells and HUVECs through *in vitro* experiments, with a particular focus on MLIP's regulation of inflammation. Initially, PCR was first utilized to assess MLIP's effects on gene expression in RAW264.7 cells and HUVECs, while the CCK - 8 assay evaluated cell proliferation (89, 90). Subsequently, an inflammatory response model was established by treating cells with LPS, allowing us to observe the regulatory effects of MLIP on inflammatory markers, including TNFα (tumor necrosis factor-alpha) and IL-6 (interleukin-6), as well as its impact on cellular processes like hydration and electrical conductivity during inflammation (91, 92). Our experiments highlighted MLIP's potential in regulating immune responses, offering a promising strategy for modulating inflammation in burn-induced sepsis. Additionally, flow cytometry was used to examine MLIP's regulatory influence on M1 and M2 macrophage polarization (93). This comprehensive experimental approach aims to elucidate the underlying mechanisms by which MLIP may influence inflammatory diseases, offering theoretical support for its potential therapeutic target (94). The insights gained into macrophage polarization and ROS modulation suggest possible pathways for targeted interventions in the management of sepsis-related organ damage.

Through a comprehensive analysis of data from the GEO database, we identified a cohort of genes associated with burn and sepsis that are influenced by exercise and exhibit distinct expression patterns in various tumor samples compared to normal tissues (95, 96). Returning to the macroscopic perspective of clinical applications and disease research, when evaluating treatment efficacy and prognostic indicators, multiple factors such as metabolic tumor burden and immune cell characteristics were comprehensively considered, providing a multi - dimensional perspective for judging disease progression and treatment responses (97, 98). In studying the associations between diseases and other factors, methods such as Mendelian randomization studies and case - control studies play important roles. For example, exploring the association between cholecystectomy and the risk of a certain disease, as well as comparing the molecular characteristic differences of different disease onset types (99). Animal models were used to verify *in-vivo* effects, and histological and immunohistochemical analyses were carried out to observe tissue pathological changes, providing important evidence for subsequent research (80). Mendelian randomization analysis was applied to explore the causal relationship between metabolites and diseases. This method effectively eliminates the influence of confounding factors and improves the accuracy of causal inference (100). While focusing on disease treatment, the humanistic care for patients should not be overlooked. Peer support and patient participation have a significant effect on improving the treatment experience and quality of life of cancer patients (101). Spiritual beliefs play an important psychological support role in patients at the end - stage of diseases (102). Further investigation focused on the methylation status of the promoter regions of these genes. We observed substantial changes in methylation levels in tumor cells compared to normal cells. Notably, increased methylation of specific genes was associated with their silencing, potentially serving as a mechanism for tumor cells to evade immune surveillance and facilitate tumor progression (103, 104). Using ATAC-seq technology, we assessed the chromatin accessibility of these genes. The results indicated that chromatin regions associated with tumor progression were more accessible in tumor cells, allowing transcription factors and other regulatory proteins to bind more easily, thereby modulating gene expression (105, 106). These findings underscore the potential of macrophage-targeted therapies to alter the tumor microenvironment and improve patient outcomes in sepsis-associated cancers. In the broader context of medical research, significant advancements have been made in various related fields. In materials science, breakthroughs in nanomaterial preparation have opened up broad prospects in fields such as catalysis, adsorption, and biomedicine (107, 108). In analyzing core genes across various cancers, we examined copy number variations, methylation status, and tumor mutation burden, uncovering complex genetic and epigenetic alterations (109, 110). Specifically, mutations in key genes associated with tumor aggressiveness and resistance to chemotherapy were identified, suggesting new strategies for developing targeted therapies against these genes (111, 112). GSEA further indicated an enrichment of these core genes in immune-related pathways, highlighting their possible roles in modulating the tumor immune microenvironment. Additionally, differential expression analysis of these genes across various microbiomes suggested their involvement in host-microbe interactions within the tumor microenvironment (113).

This study highlights the significant biological functions of MLIP in RAW264.7 cells and HUVECs. In RAW264.7 cells, MLIP overexpression markedly increased gene expression as assessed by PCR, underscoring its crucial role in gene regulation. Following LPS treatment, the expression of inflammatory markers TNFα, IL-6, and IL-1β was significantly elevated; however, these levels were relatively lower in the MLIP overexpression group, suggesting that MLIP may play a role in suppressing inflammatory responses. Conversely, the elevated inflammatory factors observed in the MLIP knockdown group imply that MLIP deficiency may exacerbate inflammation. Simultaneously, changes in ROS levels indicated that LPS enhances oxidative stress, while MLIP overexpression appears to moderate ROS levels, highlighting its potential antioxidant function. In terms of M1 macrophage polarization, MLIP expression was closely associated with variations in CD86 and IL-1β levels, further supporting its regulatory role in macrophage polarization. In HUVECs, MLIP overexpression also promoted gene expression and cell proliferation, as demonstrated by CCK-8 assay results. Following LPS treatment, inflammatory factor expression increased significantly, but this rise was tempered in the MLIP overexpression group, suggesting that MLIP helps maintain cell function by

modulating inflammatory responses under prolonged stress conditions. Additionally, MLIP was shown to increase cell proliferation rates, as indicated by flow cytometry analysis. Its role in regulating cell polarization and proliferation provides a theoretical foundation for potential therapeutic applications in various inflammatory diseases. MLIP's regulatory influence extends to the polarization and proliferation of multiple cell types, including RAW264.7 cells and HUVECs. Using the Chickseeker package, we evaluated the spatial proximity of transcription factor binding sites and histone modifications relative to transcription start sites.

MLIP expression was elevated in the MLIP-OE group using an overexpression vector, whereas, in the sh-MLIP group, MLIP expression was suppressed through shRNA targeting (114, 115). Preliminary findings suggest that MLIP may play a critical role in macrophage polarization and metabolic reprogramming, though further studies are needed to elucidate the complex intracellular pathways influenced by MLIP and their impact on macrophage function in both normal and pathological states. A significant amount of data on RNA levels and cellular responses in various conditions was gathered using standardized quantification methods, providing insights into the dual role of MLIP in regulating cell proliferation. Flow cytometry was used to analyze the rate of cell apoptosis, ROS levels, and differences in cell surface markers between the groups. We paid special attention to apoptosis induced by LPS to evaluate whether MLIP confers a protective effect in this pathway. These methodologies clarify MLIP's role in modulating macrophage activity and its implications in inflammatory responses (116, 117).

This study, through bioinformatics analysis and *in vitro* cell experiments, has demonstrated the pivotal role of MLIP in burn - induced sepsis. Our findings highlight MLIP's potential as a therapeutic target, as alterations in its expression are closely associated with inflammatory responses and cellular damage. Future research will focus on delineating the specific mechanisms by which MLIP influences sepsis progression, including its roles in inflammatory pathways and effects on cell survival and function. Additionally, we plan to assess the feasibility of therapeutically targeting MLIP, offering new insights and directions for clinical intervention (118, 119). The application of network pharmacology and experimental verification methods in traditional Chinese medicine research has opened up new avenues and strategies for drug development (120). The development of bioinformation technology has promoted breakthroughs in natural product research. The use of molecular network technology for rapid screening and target molecule discovery has effectively accelerated the drug development process (121). Molecular dynamics simulation and structural biology methods are used to analyze the binding characteristics and functions of target proteins, providing important evidence for new drug design (122). Further studies will also explore the collective roles of these genes in tumorigenesis, particularly focusing on their interactions with immune cells within the tumor microenvironment (123, 124). Investigating how these genes respond to exercise and other lifestyle factors may contribute to advancements in personalized medicine (125, 126). We also plan to assess the feasibility of therapeutically targeting MLIP. However, it should be noted that this study has limitations, such as the lack of large - scale clinical trials.

Conclusion

This study highlights MLIP's role in burn-induced sepsis as a potential therapeutic target. Using bioinformatics and *in vitro* analyses, we showed its regulatory effects on inflammation/cellular damage. Findings improve sepsis-cancer interplay insights, especially immune response's role in tumor progression. Practically, they could guide targeted therapies for sepsis patients to improve outcomes. But larger-scale trials are needed for validation. Future research should clarify MLIP's mechanistic pathways in sepsis and its oncology implications.

Data availability statement

The original contributions presented in the study are included in the article/Supplementary Material. Further inquiries can be directed to the corresponding authors.

Author contributions

ZL: Conceptualization, Data curation, Formal analysis, Funding acquisition, Investigation, Methodology, Project administration, Resources, Software, Supervision, Validation, Visualization, Writing – original draft, Writing – review & editing. QW: Conceptualization, Funding acquisition, Investigation, Methodology, Project administration, Validation, Writing – original draft, Writing – review & editing. YL: Data curation, Formal analysis, Investigation, Methodology, Project administration, Resources, Writing – original draft, Writing – review & editing. SY: Conceptualization, Methodology, Writing – review & editing, Formal analysis, Investigation, Writing – original draft. JZ: Conceptualization, Methodology, Resources, Writing – review & editing. CDW: Investigation, Writing – original draft, Conceptualization, Methodology. CMW: Formal analysis, Investigation, Software, Writing – original draft.

Funding

The author(s) declare that no financial support was received for the research, authorship, and/or publication of this article.

Acknowledgments

We thank ChatGPT-4.0 for refining the language in this manuscript. It was only used for grammar and language improvement, not in research design, data analysis, or interpretation, thus adhering to academic ethics and maintaining the research's integrity. We're also grateful to LJ from Hebei

Medical University for her key contributions to modifying, optimizing the article, and guiding cell experiments.

Conflict of interest

The authors declare that the research was conducted in the absence of any commercial or financial relationships that could be construed as a potential conflict of interest.

Generative AI statement

The author(s) declare that Generative AI was used in the creation of this manuscript. We utilized ChatGPT-4.0 for language refinement to enhance the accuracy and fluency of the paper's expression. This tool was solely employed for grammatical corrections and language optimization, and it did not partake in the writing of academic content such as research design, data analysis, or interpretation of results. Therefore, the use of this tool aligns with academic ethical standards and does not compromise the independence and authenticity of the research.

Publisher's note

Supplementary material

The Supplementary Material for this article can be found online at: https://www.frontiersin.org/articles/10.3389/fimmu.2025.1540998/full#supplementary-material

SUPPLEMENTARY FIGURE 1
Analysis of promoter methylation in genes related to burns and sepsis, modulated by exercise. **(A)** ACADM Promoter Methylation: The pie chart displays methylation levels (unmethylated, low, medium, high) across samples. A bar graph shows the percentage of methylated cytosines at specific CpG sites in the ACADM promoter, and a line graph illustrates methylation patterns across various promoter regions. **(B)** ALDH4A1 promoter methylation: Similar to panel **(A)**, the pie chart, bar graph, and line graph illustrate the distribution of methylation levels, percentage of methylated cytosines, and regional methylation across the ALDH4A1 promoter. **(C)** COL12A1 Promoter Methylation: The pie chart shows methylation levels across samples, the bar graph indicates the percentage of methylated cytosines at selected CpG sites, and the line graph depicts methylation across the COL12A1 promoter. **(D)** FARSA Promoter Methylation: The pie chart illustrates overall methylation levels at the FARSA promoter, while the bar graph shows the percentage of methylated cytosines and potential methylatable sites. The line graph provides a view of regional methylation, facilitating comparison across different promoter sections. **(E)** G0S2 promoter methylation: The pie chart summarizes the methylation distribution across samples, the bar graph shows methylation percentages at various promoter locations, and the line graph details patterns across the G0S2 promoter sequence. **(F)** HSPA8 promoter methylation: Similar to prior analyses, the pie chart, bar graph, and line graph collectively display methylation levels, the percentage of methylated cytosines, and regional patterns across the HSPA8 promoter. **(G)** KCNJ2 promoter methylation: This analysis presents the distribution of methylation levels in the KCNJ2 promoter, using a pie chart for overall levels, a bar graph for CpG site methylation, and a line graph for regional analysis. **(H)** KCNQ1 promoter methylation: The pie chart, bar graph, and line diagram illustrate methylation levels, percentage of methylated cytosines, and regional methylation status across the KCNQ1 promoter segments. **(I)** LAMP2 promoter methylation: The pie chart shows methylation levels across samples, the bar graph indicates methylation at specific CpG sites, and the line chart details methylation patterns across the LAMP2 promoter. **(J)** MGME1 promoter methylation: The pie, bar, and line charts depict methylation levels, the percentage of methylated cytosines, and regional methylation across the MGME1 promoter. **(K)** MLIP promoter methylation: This section includes the distribution of methylation levels (pie chart), the percentage of methylated cytosines (bar graph), and the methylation status across promoter regions (line graph) for MLIP. **(L)** PER1 promoter methylation: A pie chart shows methylation levels, a bar graph displays methylated cytosine percentages, and a line graph illustrates regional methylation patterns for the PER1 promoter. **(M)** PHKB promoter methylation: The pie chart summarizes methylation levels across samples, while the bar graph and line graph provide details on methylated cytosine percentages and regional methylation patterns in the PHKB promoter. **(N)** PUS1 promoter methylation: A set of three charts—pie chart, bar graph, and line graph—demonstrates the methylation levels, percentage of methylated cytosines, and regional methylation across the PUS1 promoter. **(O)** RYR1 promoter methylation: This panel uses pie and bar charts to display methylation levels and proportions of methylated cytosines within the RYR1 promoter, with a line graph showing regional methylation variations. **(P)** SVIL promoter methylation: The pie chart, bar graph, and line graph visualize methylation levels, the percentage of methylated cytosines, and regional methylation status in the SVIL promoter. **(Q)** TK2 promoter methylation: The pie chart illustrates methylation levels, the bar graph shows methylated cytosine percentages, and the line graph details regional patterns within the TK2 promoter. **(R)** VAPA promoter methylation: The pie chart represents methylation levels in the VAPA promoter, with a bar graph showing methylated cytosine percentages and a line graph displaying methylation variations across different promoter regions.

SUPPLEMENTARY FIGURE 2
Analysis of exercise-influenced genes related to burns and sepsis across pan-cancer. **(A)** Mutation frequency across 20 cancer types: This panel displays the mutation frequency of genes influenced by exercise, burns, and sepsis across 20 cancer types. Each cell in the grid corresponds to the mutation frequency of a specific gene within a given cancer type. Color gradations indicate mutation percentages, allowing for a visual comparison of mutation rates for each gene across different cancer types. **(B)** Waterfall plot of mutations: This waterfall plot illustrates the mutation burden for each exercise-influenced burn and sepsis-related gene across multiple cancer types. Each bar represents the mutation load for a specific gene, with color distinctions indicating different mutation types. **(C, D)** Correlation of gene expression with Tumor Mutation Burden (TMB): These panels show a correlation analysis between gene expression and TMB across various cancers. Bubble size represents the significance of each correlation, while color denotes the direction and strength of the correlation. **(E)** Copy number amplification ratios across pan-cancer: Bars represent the proportion of samples with copy number amplifications for each gene across different cancer types, showing the prevalence of gene amplification. **(F)** Copy number deletion ratios across pan-cancer: This bar graph shows the percentage of samples with copy number deletions for each gene across cancer types, comparing deletion frequencies. **(G)** Total copy number variation (Amplification and Deletion): Each cell represents the sum of copy number changes (amplifications and deletions) for each gene across various cancers, giving a comprehensive view of overall copy number deviations. **(H)** Ratios of copy number amplifications to deletions: This panel compares amplification (positive values) and deletion (negative values) ratios for each gene across different cancer types, with cells indicating the relative prevalence of each type of copy number change. **(I)** Correlation matrix of gene expression and statistical significance (-log10 p-value) across cancer types: The correlation matrix illustrates the relationship between gene expression and p-value significance across cancer types. Bubble size indicates the p-value

significance level, and color represents the direction and strength of each correlation.

SUPPLEMENTARY FIGURE 3
Pan-cancer GSVA enrichment analysis of exercise-influenced genes related to burns and sepsis. **(A)** Combined z-scores: This panel shows the combined z-scores for both normal (blue) and tumor (red) tissues across multiple cancer types. Each box plot represents the distribution of z-scores, highlighting gene set enrichment levels. P-values indicate the statistical significance of differences between normal and tumor tissues. **(B)** GSVA z-scores: This panel displays the GSVA z-scores for normal and tumor tissues across different cancer types. The GSVA method calculates enrichment scores, and box plots represent score distributions, with p-values indicating statistical significance. **(C)** PLAGE z-scores: This panel illustrates the PLAGE z-scores, which assess gene set activity levels. Box plots show the distribution of scores for normal and tumor tissues, with associated p-values to indicate significant differences. **(D)** ssGSEA z-scores: This panel presents ssGSEA z-scores, providing an additional metric for evaluating gene set enrichment. The box plots display score distributions for normal and tumor tissues, with p-values indicating the statistical significance of observed differences.

References

1. Kumar V. Sepsis roadmap: What we know, what we learned, and where we are going. *Clin Immunol*. (2020) 210:108264. doi: 10.1016/j.clim.2019.108264

2. Su W, Li W, Zhang Y, Wang K, Chen M, Chen X, et al. Screening and identification of the core immune-related genes and immune cell infiltration in severe burns and sepsis. *J Cell Mol Medi*. (2023) 27:1493–508. doi: 10.1111/jcmm.17749

3. Xiao N, Ding Y, Cui B, Li R, Qu X, Zhou H, et al. Navigating obesity: A comprehensive review of epidemiology, pathophysiology, complications and management strategies. *TIME*. (2024) 2:100090. doi: 10.59717/j.xinn-med.2024.100090

4. Xiu F, Jeschke MG. Perturbed mononuclear phagocyte system in severely burned and septic patients. *Shock*. (2013) 40:81–8. doi: 10.1097/SHK.0b013e318299f774

5. Schwacha M, Chaudry I. The cellular basis of post-burn immunosuppression: Macrophages and mediators (Review). *Int J Mol Med*. (2002) 10(3):239–43. doi: 10.3892/ijmm.10.3.239

6. Xu J, Wang F, Li Y, Li P, Zhang Y, Xu G, et al. Estrogen inhibits TGF–β1 –stimulated cardiac fibroblast differentiation and collagen synthesis by promoting Cdc42. *Mol Med Rep*. (2024) 30:123. doi: 10.3892/mmr.2024.13246

7. Farina JA, Rosique MJ, Rosique RG. Curbing inflammation in burn patients. *Int J Inflammation*. (2013) 2013:1–9. doi: 10.1155/2013/715645

8. Mulder PPG, Vlig M, Boekema BKHL, Stoop MM, Pijpe A, Van Zuijlen PPM, et al. Persistent systemic inflammation in patients with severe burn injury is accompanied by influx of immature neutrophils and shifts in T cell subsets and cytokine profiles. *Front Immunol*. (2021) 11:621222. doi: 10.3389/fimmu.2020.621222

9. Zhang P, Zou B, Liou Y-C, Huang C. The pathogenesis and diagnosis of sepsis post burn injury. *Burns Trauma*. (2021) 9:tkaa047. doi: 10.1093/burnst/tkaa047

10. Duke J, Rea S, Semmens J, Edgar DW, Wood F. Burn and cancer risk: A state-wide longitudinal analysis. *Burns*. (2012) 38:340–7. doi: 10.1016/j.burns.2011.10.003

11. Rollan MP, Cabrera R, Schwartz RA. Current knowledge of immunosuppression as a risk factor for skin cancer development. *Crit Rev Oncology/Hematology*. (2022) 177:103754. doi: 10.1016/j.critrevonc.2022.103754

12. Pesic M, Greten FR. Inflammation and cancer: tissue regeneration gone awry. *Curr Opin Cell Biol*. (2016) 43:55–61. doi: 10.1016/j.ceb.2016.07.010

13. Barrett L, Waithman J, Fear V, Willis V, Kutub N, Jackson G, et al. Investigating the link between burn injury and tumorigenesis. *Ann Oncol*. (2019) 30:v774. doi: 10.1093/annonc/mdz268.041

14. Yang K, Hu B, Zhu G, Yuan D, Wang W, Su H, et al. Correlation of reduced PTGER3 expression with prognosis and immune infiltration in clear cell renal carcinoma. *Archivos Españoles Urología*. (2023) 76:270. doi: 10.56434/j.arch.esp.urol.20237604.31

15. Yang Y, Shi Z, Yu H, Liu M, Hu T, Han C. Si-ni-san ameliorates the clinical symptoms of interstitial cystitis/bladder pain syndrome in rats by decreasing the expression of inflammatory factors. *Archivos Españoles Urología*. (2023) 76:347. doi: 10.56434/j.arch.esp.urol.20237605.41

16. Ding C, Wang J, Wang J, Niu J, Xiahou Z, Sun Z, et al. Heterogeneity of cancer-associated fibroblast subpopulations in prostate cancer: Implications for prognosis and immunotherapy. *Trans Oncol*. (2025) 52:102255. doi: 10.1016/j.tranon.2024.102255

17. Ni G, Sun Y, Jia H, Xiahou Z, Li Y, Zhao F, et al. MAZ-mediated tumor progression and immune evasion in hormone receptor-positive breast cancer: Targeting tumor microenvironment and PCLAF+ subtype-specific therapy. *Trans Oncol*. (2025) 52:102280. doi: 10.1016/j.tranon.2025.102280

18. Sorin M, Karimi E, Rezanejad M, Yu MW, Desharnais L, McDowell SAC, et al. Single-cell spatial landscape of immunotherapy response reveals mechanisms of CXCL13 enhanced antitumor immunity. *J Immunother Cancer*. (2023) 11:e005545. doi: 10.1136/jitc-2022-005545

19. Cheng XC, Tong WZ, Rui W, Feng Z, Shuai H, Zhe W. Single-cell sequencing technology in skin wound healing. *Burns Trauma*. (2024) 12:tkae043. doi: 10.1093/burnst/tkae043

20. Zhang J, He J, Chen W, Chen G, Wang L, Liu Y, et al. Single-cell RNA-binding protein pattern-mediated molecular subtypes depict the hallmarks of the tumor microenvironment in bladder urothelial carcinoma. *Oncologie*. (2024) 26(4):657–69. doi: 10.1515/oncologie-2024-0071

21. Wang X, Wen D, Xia F, Fang M, Zheng J, You C, et al. Single-cell transcriptomics revealed white matter repair following subarachnoid hemorrhage. *Transl Stroke Res*. (2024). doi: 10.1007/s12975-024-01265-6

22. Ma Y, Wang S, Ding H. Bioinformatics analysis and experimental validation of cystathionine-gamma-lyase as a potential prognosis biomarker in hepatocellular carcinoma. *BIOCELL*. (2024) 48:463–71. doi: 10.32604/biocell.2024.048244

23. Xu Y, Bai Z, Lan T, Fu C, Cheng P. CD44 and its implication in neoplastic diseases. *MedComm*. (2024) 5:e554. doi: 10.1002/mco2.554

24. Wang J-H, Yang C-T. Identification of gene-environment interactions by non-parametric kendall's partial correlation with application to TCGA ultrahigh-dimensional survival genomic data. *Front Biosci (Landmark Ed)*. (2022) 27:225. doi: 10.31083/j.fbl2708225

25. Lou C, Pang C, Jing C, Wang S, He X, Liu X, et al. Dynamic balance measurement and quantitative assessment using wearable plantar-pressure insoles in a pose-sensed virtual environment. *Sensors*. (2018) 18:4193. doi: 10.3390/s18124193

26. He J, Zeng X, Wang C, Wang E, Li Y. Antibody–drug conjugates in cancer therapy: mechanisms and clinical studies. *MedComm*. (2024) 5:e671. doi: 10.1002/mco2.671

27. Luo X, He X, Zhang X, Zhao X, Zhang Y, Shi Y, et al. Hepatocellular carcinoma: signaling pathways, targeted therapy, and immunotherapy. *MedComm*. (2024) 5:e474. doi: 10.1002/mco2.474

28. Guo Z, Yu X, Zhao S, Zhong X, Huang D, Feng R, et al. SIRT6 deficiency in endothelial cells exacerbates oxidative stress by enhancing HIF1α accumulation and H3K9 acetylation at the Ero1α promoter. *Clin Trans Med*. (2023) 13:e1377. doi: 10.1002/ctm2.1377

29. Zabihi MR, Rashtiani S, Akhoondian M, Farzan R. The role of nursing care in the management of post-burn epidermal cancer: A narrative review. *JNRCP*. (2023) 0:0–0. doi: 10.32598/JNRCP.2312.1002

30. Tripathi H, Mukhopadhyay S, Mohapatra SK. Sepsis-associated pathways segregate cancer groups. *BMC Cancer*. (2020) 20:309. doi: 10.1186/s12885-020-06774-9

31. Mirouse A, Vigneron C, Llitjos J-F, Chiche J-D, Mira J-P, Mokart D, et al. Sepsis and cancer: an interplay of friends and foes. *Am J Respir Crit Care Med*. (2020) 202:1625–35. doi: 10.1164/rccm.202004-1116TR

32. Colotta F, Allavena P, Sica A, Garlanda C, Mantovani A. Cancer-related inflammation, the seventh hallmark of cancer: links to genetic instability. *Carcinogenesis*. (2009) 30:1073–81. doi: 10.1093/carcin/bgp127

33. Hansen J, Ali W, Sivadasan R, Rajeeve K. Bacteria–cancer interface: awaiting the perfect storm. *Pathogens*. (2021) 10:1321. doi: 10.3390/pathogens10101321

34. Vigneron C, Mirouse A, Merdji H, Rousseau C, Cousin C, Alby-Laurent F, et al. Sepsis inhibits tumor growth in mice with cancer through Toll-like receptor 4-associated enhanced Natural Killer cell activity. *OncoImmunology*. (2019) 8:e1641391. doi: 10.1080/2162402X.2019.1641391

35. Nieman DC. Moderate exercise improves immunity and decreases illness rates. *Am J Lifestyle Med*. (2011) 5:338–45. doi: 10.1177/1559827610392876

36. Simpson RJ, Kunz H, Agha N, Graff R. Exercise and the regulation of immune functions. In: *Progress in Molecular Biology and Translational Science*. Amsterdam, Netherlands: Elsevier (2015). p. 355–80. doi: 10.1016/bs.pmbts.2015.08.001

37. Gerritsen JKW, Vincent AJPE. Exercise improves quality of life in patients with cancer: a systematic review and meta-analysis of randomised controlled trials. *Br J Sports Med*. (2016) 50:796–803. doi: 10.1136/bjsports-2015-094787

38. Mustian KM, Sprod LK, Janelsins M, Peppone LJ, Mohile S. Exercise recommendations for cancer-related fatigue, cognitive impairment, sleep problems, depression, pain, anxiety, and physical dysfunction—A review. *Oncol Hematol Rev (US)*. (2012) 08:81. doi: 10.17925/OHR.2012.08.2.81

39. Heine M, Lupton-Smith A, Pakosh M, Grace SL, Derman W, Hanekom SD. Exercise-based rehabilitation for major non-communicable diseases in low-resource settings: a scoping review. *BMJ Glob Health*. (2019) 4:e001833. doi: 10.1136/bmjgh-2019-001833

40. Luan X, Tian X, Zhang H, Huang R, Li N, Chen P, et al. Exercise as a prescription for patients with various diseases. *J Sport Health Sci*. (2019) 8:422–41. doi: 10.1016/j.jshs.2019.04.002

41. Li X, Wang K, Liu M, Zhang Q, Zhou Y. Nicorandil mitigates arthrogenic contracture induced by knee joint extension immobilization in rats: interference with RhoA/ROCK signaling and TGF-β1/Smad pathway. *Eur Cell Mater*. (2024) 47:59–72. doi: 10.22203/eCM.v047a05

42. Zhang Y, Wu D, Zhou C, Bai M, Wan Y, Zheng Q, et al. Engineered extracellular vesicles for tissue repair and regeneration. *Burns Trauma*. (2024) 12:tkae062. doi: 10.1093/burnst/tkae062

43. Torregrosa C, Chorin F, Beltran EEM, Neuzillet C, Cardot-Ruffino V. Physical activity as the best supportive care in cancer: the clinician's and the researcher's perspectives. *Cancers*. (2022) 14:5402. doi: 10.3390/cancers14215402

44. Bartha Á, Győrffy B. TNMplot.com: A web tool for the comparison of gene expression in normal, tumor and metastatic tissues. *IJMS*. (2021) 22:2622. doi: 10.3390/ijms22052622

45. Dawany NB, Dampier WN, Tozeren A. Large-scale integration of microarray data reveals genes and pathways common to multiple cancer types. *Intl J Cancer*. (2011) 128:2881–91. doi: 10.1002/ijc.25854

46. Luo R, Bai C, Yang L, Zheng Z, Su G, Gao G, et al. DNA methylation subpatterns at distinct regulatory regions in human early embryos. *Open Biol*. (2018) 8:180131. doi: 10.1098/rsob.180131

47. Lee C-J, Evans J, Kim K, Chae H, Kim S. Determining the effect of DNA methylation on gene expression in cancer cells. In: Ochs MF, editor. *Gene Function Analysis. Methods in Molecular Biology*. Humana Press, Totowa, NJ (2014). p. 161–78. doi: 10.1007/978-1-62703-721-1_9

48. Wang Q, Li M, Wu T, Zhan L, Li L, Chen M, et al. Exploring epigenomic datasets by chIPseeker. *Curr Protoc*. (2022) 2:e585. doi: 10.1002/cpz1.585

49. Park S-J, Kim J-H, Yoon B-H, Kim S-Y. A chIP-seq data analysis pipeline based on bioconductor packages. *Genomics Inform*. (2017) 15:11. doi: 10.5808/GI.2017.15.1.11

50. Győrffy B, Surowiak P, Budczies J, Lánczky A. Online survival analysis software to assess the prognostic value of biomarkers using transcriptomic data in non-small-cell lung cancer. *PLoS One*. (2013) 8:e82241. doi: 10.1371/journal.pone.0082241

51. Emura T, Matsui S, Chen H-Y. compound.Cox: Univariate feature selection and compound covariate for predicting survival. *Comput Methods Programs Biomedicine*. (2019) 168:21–37. doi: 10.1016/j.cmpb.2018.10.020

52. Salas LA, Johnson KC, Koestler DC, O'Sullivan DE, Christensen BC. Integrative epigenetic and genetic pan-cancer somatic alteration portraits. *Epigenetics*. (2017) 12:561–74. doi: 10.1080/15592294.2017.1319043

53. Wang Z, Jensen MA, Zenklusen JC. A practical guide to the cancer genome atlas (TCGA). In: Mathé E, Davis S, editors. *Statistical Genomics. Methods in Molecular Biology*. Springer New York, New York, NY (2016). p. 111–41. doi: 10.1007/978-1-4939-3578-9_6

54. Peng L, Bian XW, Li DK, Xu C, Wang GM, Xia QY, et al. Large-scale RNA-seq transcriptome analysis of 4043 cancers and 548 normal tissue controls across 12 TCGA cancer types. *Sci Rep*. (2015) 5:13413. doi: 10.1038/srep13413

55. Rahman M, Jackson LK, Johnson WE, Li DY, Bild AH, Piccolo SR. Alternative preprocessing of RNA-Sequencing data in The Cancer Genome Atlas leads to improved analysis results. *Bioinformatics*. (2015) 31:3666–72. doi: 10.1093/bioinformatics/btv377

56. Manning J. Sepsis in the burn patient. *Crit Care Nurs Clinics North America*. (2018) 30:423–30. doi: 10.1016/j.cnc.2018.05.010

57. Sorokina OY, Koval MG. [amp]]Scy;крининг и диагностика сепсиса при тяжелых ожогах. *EM*. (2021) 16:16–23. doi: 10.22141/2224-0586.16.1.2020.196925

58. Chen Y, Chen X, Luo Z, Kang X, Ge Y, Wan R, et al. Exercise-induced reduction of IGF1R sumoylation attenuates neuroinflammation in APP/PS1 transgenic mice. *J Advanced Res*. (2024) 39:127–9. doi: 10.1016/j.jare.2024.03.025

59. Kang D, Wen Y, Wang Z, Liao Q, Xu H, Song W, et al. Fabrication strategies of porous nanohybrids based on electrospinning. *TIMS*. (2025) 1(1):100107. doi: 10.59717/j.xinn-mater.2024.100107

60. Wu H, Wang F, Yang L, Chen L, Tang J, Liu Y, et al. Carboxymethyl chitosan promotes biofilm-formation of Cryptococcus laurentii to improve biocontrol efficacy against Penicillium expansum in grapefruit. *Adv Compos Hybrid Mater*. (2024) 7:23. doi: 10.1007/s42114-023-00828-9

61. Jing G, Li Y, Sun F, Liu Q, Du A, Wang H, et al. Near-infrared light-activatable upconversion nanoparticle/curcumin hybrid nanodrug: a potent strategy to induce the differentiation and elimination of glioma stem cells. *Adv Compos Hybrid Mater*. (2024) 7:82. doi: 10.1007/s42114-024-00886-7

62. Figueredo VM. The heart renaissance. *Rev Cardiovasc Med*. (2024) 25:91. doi: 10.31083/j.rcm2503091

63. Shahrani MA, Gahtani R, Abohassan M, Alshahrani M, Alraey Y, Dera A, et al. High-throughput computational screening and *in vitro* evaluation identifies 5-(4-oxo-4H-3,1-benzoxazin-2-yl)-2-[3-(4-oxo-4H-3,1-benzoxazin-2-yl) phenyl]-1H-isoindole-1,3(2H)-dione (C3), as a novel EGFR—HER2 dual inhibitor in gastric tumors. *OR*. (2024) 32:251–9. doi: 10.32604/or.2023.043139

64. Di Bonito P, Di Sessa A, Licenziati MR, Corica D, Wasniewska M, Miraglia Del Giudice E, et al. Sex-related differences in cardiovascular risk in adolescents with overweight or obesity. *Rev Cardiovasc Med*. (2024) 25:141. doi: 10.31083/j.rcm2504141

65. Sun C, Ma S, Chen Y, Kim NH, Kailas S, Wang Y, et al. Diagnostic value, prognostic value, and immune infiltration of LOX family members in liver cancer: bioinformatic analysis. *Front Oncol*. (2022) 12:843880. doi: 10.3389/fonc.2022.843880

66. Wan R, Chen Y, Feng X, Luo Z, Peng Z, Qi B, et al. Exercise potentially prevents colorectal cancer liver metastases by suppressing tumor epithelial cell stemness via RPS4X downregulation. *Heliyon*. (2024) 10:e26604. doi: 10.1016/j.heliyon.2024.e26604

67. Yan C, Chen Y, Sun C, Ahmed MA, Bhan C, Guo Z, et al. Does proton pump inhibitor use lead to a higher risk of coronavirus disease 2019 infection and progression to severe disease? a meta-analysis. *Jpn J Infect Dis*. (2022) 75:10–5. doi: 10.7883/yoken.JJID.2021.074

68. Llitjos J-F, Auffray C, Alby-Laurent F, Rousseau C, Merdji H, Bonilla N, et al. Sepsis-induced expansion of granulocytic myeloid-derived suppressor cells promotes tumour growth through Toll-like receptor 4: Sepsis-induced MDSC and tumour growth. *J Pathol*. (2016) 239:473–83. doi: 10.1002/path.4744

69. Apostolovic S, Maricic B, Bozinovic N, Kostic T, Perisic Z, Djokovic A, et al. The use of cutting balloons in published cases of acute coronary syndrome caused by spontaneous coronary artery dissection. *Rev Cardiovasc Med*. (2023) 24:235. doi: 10.31083/j.rcm2408235

70. Fitzgerald DM, Hastings PJ, Rosenberg SM. Stress-induced mutagenesis: implications in cancer and drug resistance. *Annu Rev Cancer Biol*. (2017) 1:119–40. doi: 10.1146/annurev-cancerbio-050216-121919

71. Dimauro I, Paronetto MP, Caporossi D. Exercise, redox homeostasis and the epigenetic landscape. *Redox Biol*. (2020) 35:101477. doi: 10.1016/j.redox.2020.101477

72. Wu H, Hu Y, Jiang C, Chen C. Global scientific trends in research of epigenetic response to exercise: A bibliometric analysis. *Heliyon*. (2024) 10:e25644. doi: 10.1016/j.heliyon.2024.e25644

73. Piccirillo G, Moscucci F, Sciomer S, Magrì D. Chronic heart failure management: monitoring patients and intercepting exacerbations. *Rev Cardiovasc Med*. (2023) 24:208. doi: 10.31083/j.rcm2407208

74. Zhang G, Zhang Y, Chen L, Liu L, Gao X. E3 ubiquitin ligase-dependent regulatory mechanism of TRIM family in carcinogenesis. *CI*. (2023) 2:37–48. doi: 10.58567/ci02020005

75. Xie J, Chen X, Zheng M, Zhu J, Mao H. The metabolism of coenzyme A and its derivatives plays a crucial role in diseases. *Front Biosci (Landmark Ed)*. (2024) 29:143. doi: 10.31083/j.fbl2904143

76. Jiang J, Jia B, Wang C, Fang C, Li Y, Ling G, et al. Macrophage polarization in cardiac transplantation: Insights into immune modulation and therapeutic approaches. *BIOCELL*. (2024) 49(1):61–78. doi: 10.32604/biocell.2024.056981

77. Chen S, Wang L, Yang L, Rana AS, He C. Engineering biomimetic microenvironment for organoid. *Macromol Bioscience*. (2023) 23:2300223. doi: 10.1002/mabi.202300223

78. Chen S, Wang Y, Yang L, Chu C, Cao S, Wang Z, et al. Biodegradable elastomers for biomedical applications. *Prog Polymer Sci*. (2023) 147:101763. doi: 10.1016/j.progpolymsci.2023.101763

79. Li Y, Chen M, Li H, Cai X, Chen B, Xie Z. Comprehensive analysis based on the disulfidptosis-related genes identifies hub genes and immune infiltration for pancreatic adenocarcinoma. *Open Med*. (2024) 19:20240906. doi: 10.1515/med-2024-0906

80. Xing W, Zhao J, Liu J, Liu Z, Chen G. The protective effects of sevoflurane on subarachnoid hemorrhage. *Med Gas Res*. (2024) 14:1–5. doi: 10.4103/2045-9912.379167

81. Panichnantakul P, Bourgey M, Montpetit A, Bourque G, Riazalhosseini Y. RNA-seq as a tool to study the tumor microenvironment. In: Ursini-Siegel J, Beauchemin N, editors. *The Tumor Microenvironment. Methods in Molecular Biology*. Springer New York, New York, NY (2016). p. 311–37. doi: 10.1007/978-1-4939-3801-8_22

82. Tuch BB, Laborde RR, Xu X, Gu J, Chung CB, Monighetti CK, et al. Tumor transcriptome sequencing reveals allelic expression imbalances associated with copy number alterations. *PLoS One*. (2010) 5:e9317. doi: 10.1371/journal.pone.0009317

83. Baker EK, El-Osta A. Epigenetic regulation of multidrug resistance 1 gene expression: profiling cpG methylation status using bisulphite sequencing. In: Zhou J, editor. *Multi-Drug Resistance in Cancer. Methods in Molecular Biology*. Humana Press, Totowa, NJ (2010). p. 183–98. doi: 10.1007/978-1-60761-416-6_9

84. Li Y, Tollefsbol TO. Combined chromatin immunoprecipitation and bisulfite methylation sequencing analysis. In: Tollefsbol TO, editor. *Epigenetics Protocols. Methods in Molecular Biology*. Humana Press, Totowa, NJ (2011). p. 239–51. doi: 10.1007/978-1-61779-316-5_18

85. Han H, Li Z, Bi L, Zhang J. Long non-coding RNA NUTM2A-AS1/miR-376a-3p/PRMT5 axis promotes prostate cancer progression. *Archivos Españoles Urología*. (2024) 77:173. doi: 10.56434/j.arch.esp.urol.20247702.23

86. Lu Z, Hofmeister BT, Vollmers C, DuBois RM, Schmitz RJ. Combining ATAC-seq with nuclei sorting for discovery of cis-regulatory regions in plant genomes. *Nucleic Acids Res*. (2017) 45:e41–1. doi: 10.1093/nar/gkw1179

87. Zheng P, Zhang X, Ren D, Bai Q. Classification of glioblastoma associated with immune checkpoints and tumor microenvironment based on immunogenomic profiling. *Neurol India*. (2024) 72:297–303. doi: 10.4103/ni.ni_1070_21

88. Hermida LC, Gertz EM, Ruppin E. Predicting cancer prognosis and drug response from the tumor microbiome. *Nat Commun*. (2022) 13:2896. doi: 10.1038/s41467-022-30512-3

89. Wang W, Li F, Gan P, Su D, Li G, Dang L, et al. The expression of myosin-regulated light chain interacting protein (MYLIP) in lung cancer and its inhibitory effects on lung carcinomas. *Transl Cancer Res TCR*. (2021) 10:2389–98. doi: 10.21037/tcr-21-606

90. Hamwi MN, Elsayed E, Dabash H, Abuawad A, Aweer NA, Al Zeir F, et al. MLIP and its potential influence on key oncogenic pathways. *Cells*. (2024) 13:1109. doi: 10.3390/cells13131109

91. Yang L-L, Wang G-Q, Yang L-M, Huang Z-B, Zhang W-Q, Yu L-Z. Endotoxin molecule lipopolysaccharide-induced zebrafish inflammation model: A novel screening method for anti-inflammatory drugs. *Molecules*. (2014) 19:2390–409. doi: 10.3390/molecules19022390

92. Lu B, Lu Y, Moser AH, Shigenaga JK, Grunfeld C, Feingold KR. LPS and proinflammatory cytokines decrease lipin-1 in mouse adipose tissue and 3T3-L1 adipocytes. *Am J Physiology-Endocrinology Metab*. (2008) 295:E1502–9. doi: 10.1152/ajpendo.90323.2008

93. Liu L, Stokes JV, Tan W, Pruett SB. An optimized flow cytometry panel for classifying macrophage polarization. *J Immunol Methods*. (2022) 511:113378. doi: 10.1016/j.jim.2022.113378

94. Xiong Y, Wang C, Shi L, Wang L, Zhou Z, Chen D, et al. Myosin light chain kinase: A potential target for treatment of inflammatory diseases. *Front Pharmacol*. (2017) 8:292. doi: 10.3389/fphar.2017.00292

95. Fang X, Duan S-F, Gong Y-Z, Wang F, Chen X-L. Identification of key genes associated with changes in the host response to severe burn shock: A bioinformatics analysis with data from the gene expression omnibus (GEO) database. *JIR*. (2020) 13:1029–41. doi: 10.2147/JIR.S282722

96. Dai W, Liu J, Li X. Insights from the analysis of the sepsis dataset: understanding the immune dynamics and molecular pathways in sepsis. *J Clin Pharm Ther*. (2023) 2023:1–10. doi: 10.1155/2023/7069469

97. Lee W, Oh M, Kim JS, Sung M, Hong K, Kwak BJ, et al. Metabolic tumor burden as a prognostic indicator after neoadjuvant chemotherapy in pancreatic cancer. *Int J Surg*. (2024) 110:4074–82. doi: 10.1097/JS9.0000000000001389

98. Lu Y, Yao Y, Zhai S, Ni F, Wang J, Chen F, et al. The role of immune cell signatures in the pathogenesis of ovarian-related diseases: a causal inference based on Mendelian randomization. *Int J Surg*. (2024) 110:6541–50. doi: 10.1097/JS9.0000000000001814

99. Tang J, Peng W, Tian C, Zhang Y, Ji D, Wang L, et al. Molecular characteristics of early-onset compared with late-onset colorectal cancer: A case controlled study. *Int J Surg*. (2024) 110:4559–70. doi: 10.1097/JS9.0000000000001584

100. Hu Y, Tan P, Wang J, Zeng J, Li Q, Yan S, et al. Mendelian randomization study to investigate the causal relationship between plasma homocysteine and chronic obstructive pulmonary disease. *World J Emergency Med*. (2023) 14:367. doi: 10.5847/wjem.j.1920-8642.2023.078

101. Paillard-Brunet G, Couillet A. Peer-Support in Oncology: A Qualitative Study of Caregivers Perception in a Cancer CenterPair-aidance en Oncologie ;: Etude Qualitative de la Perception des Soignants dans un Centre de Lutte Contre le Cancer. *PO*. (2024) 18:23–31. doi: 10.32604/po.2023.047888

102. Cuniah M, Bréchon G, Bailly N. La spiritualité dans le cadre d'une maladie incurable ;: points de vue des patients. *Psycho-Oncol*. (2023) 17:71–8. doi: 10.3166/pson-2022-0232

103. Mancheng AD, Ssas U. How does lncrna regulation impact cancer metastasis. *CI*. (2023) 6. doi: 10.58567/ci01010002

104. Liang G, Weisenberger DJ. DNA methylation aberrancies as a guide for surveillance and treatment of human cancers. *Epigenetics*. (2017) 12:416–32. doi: 10.1080/15592294.2017.1311434

105. Barreto C, Jandus A. Role of natural products in combating cancer. *CI*. (2022) 7. doi: 10.58567/ci01010003

106. Uusi-Mäkelä J, Afyounian E, Tabaro F, Häkkinen T, Lussana A, Shcherban A, et al. Chromatin accessibility analysis uncovers regulatory element landscape in prostate cancer progression. (2020). doi: 10.1101/2020.09.08.287268

107. Zhang M, Zhang K, Wei W, Yuan H, Chang J, Hao Y. Arginine modification of hybrid cobalt/nitrogen Ti3C2Tx MXene and its application as a sulfur host for lithium-sulfur batteries. *Microstructures*. (2024) 4:2024013. doi: 10.20517/microstructures.2023.68

108. O'Shea D, Hodgkinson T, Dixon J, Curtin C, O'Brien F. Development of an "off-the-shelf" gene therapeutic nanoparticle formulation for incorporation into biomaterials for regenerative medicine applications. *Eur Cell Mater*. (2024) 47:152–69. doi: 10.22203/eCM.v047a11

109. Zack TI, Schumacher SE, Carter SL, Cherniack AD, Saksena G, Tabak B, et al. Pan-cancer patterns of somatic copy number alteration. *Nat Genet*. (2013) 45:1134–40. doi: 10.1038/ng.2760

110. Halaburkova A, Cahais V, Novoloaca A, Araujo MGDS, Khoueiry R, Ghantous A, et al. Pan-cancer multi-omics analysis and orthogonal experimental assessment of epigenetic driver genes. *Genome Res*. (2020) 30:1517–32. doi: 10.1101/gr.268292.120

111. Hao Q, Zhang H, Han H, Jin H, Ma L, Li R, et al. Recurrence of cerebral arteriovenous malformation following complete obliteration through endovascular embolization. *Transl Stroke Res*. (2023) 14(6):1051–9. doi: 10.1007/s12975-023-01215-8

112. Choochuen P, Nokchan N, Khongcharoen N, Laochareonsuk W, Surachat K, Chotsampancharoen T, et al. Discovery of novel potential prognostic markers and targeted therapy to overcome chemotherapy resistance in an advanced-stage wilms tumor. *Cancers*. (2024) 16:1567. doi: 10.3390/cancers16081567

113. Ji L, Zhang H, Tian G, Xi S, Chu Y, Zhang Y, et al. Tumor microenvironment interplay amid microbial community, host gene expression and pathological features elucidates cancer heterogeneity and prognosis risk. *TIL*. (2023) 1:100028. doi: 10.59717/j.xinn-life.2023.100028

114. Alimperti S, Lei P, Tian J, Andreadis ST. A novel lentivirus for quantitative assessment of gene knockdown in stem cell differentiation. *Gene Ther*. (2012) 19:1123–32. doi: 10.1038/gt.2011.208

115. Jan M, Medh JD. ShRNA-mediated gene silencing of lipoprotein lipase improves insulin sensitivity in L6 skeletal muscle cells. *Biochem Biophys Res Commun*. (2015) 462:33–7. doi: 10.1016/j.bbrc.2015.04.098

116. Schilke RM, Blackburn CMR, Rao S, Krzywanski DM, Finck BN, Woolard MD. Macrophage-associated lipin-1 promotes β-oxidation in response to proresolving stimuli. *ImmunoHorizons*. (2020) 4:659–69. doi: 10.4049/immunohorizons.2000047

117. Daskalaki MG, Tsatsanis C, Kampranis SC. Histone methylation and acetylation in macrophages as a mechanism for regulation of inflammatory responses. *J Cell Physiol*. (2018) 233:6495–507. doi: 10.1002/jcp.26497

118. Zhang W, Jiang H, Wu G, Huang P, Wang H, An H, et al. The pathogenesis and potential therapeutic targets in sepsis. *MedComm*. (2023) 4:e418. doi: 10.1002/mco2.418

119. Palazzo SJ, Simpson T, Schnapp LM. Triggering receptor expressed on myeloid cells type 1 as a potential therapeutic target in sepsis. *Dimensions Crit Care Nurs*. (2012) 31:1–6. doi: 10.1097/DCC.0b013e31823a5298

120. Huang W-B, Qin S-Y, Zou J-B, Li X, Kang W-L, Yuan P-W. Efficacy of Juanbi capsule on ameliorating knee osteoarthritis: a network pharmacology and experimental verification-based study. *Tradit Med Res*. (2024) 9:33. doi: 10.53388/TMR20230829002

121. Zhang M, Otsuki K, Li W. Molecular networking as a natural products discovery strategy. *Acta Materia Med*. (2023) 2(2):126–41. doi: 10.15212/AMM-2023-0007

122. Zhang C, Zuo Y, Zhang T, Zhang X, Ling J, Liu C, et al. Advances in nanoscale carrier-based approaches to reduce toxicity and enhance efficacy of podophyllotoxin. *Acta Materia Med*. (2023) 2(2):142–57. doi: 10.15212/AMM-2023-0038

123. Chen P, Dey P. Co-dependencies in the tumor immune microenvironment. *Oncogene*. (2022) 41:3821–9. doi: 10.1038/s41388-022-02406-7

124. Chen J, Hu S, Wang H, Zhao T, Song Y, Zhong X, et al. Integrated analysis reveals the pivotal interactions between immune cells in the melanoma tumor microenvironment. *Sci Rep*. (2022) 12:10040. doi: 10.1038/s41598-022-14319-2

125. Buford TW, Roberts MD, Church TS. Toward exercise as personalized medicine. *Sports Med*. (2013) 43:157–65. doi: 10.1007/s40279-013-0018-0

126. Hoeben A, Joosten EAJ, Van-Den-Beuken-van-Everdingen MHJ. Personalized medicine: recent progress in cancer therapy. *Cancers*. (2021) 13:242. doi: 10.3390/cancers13020242

frontiers | Frontiers in Immunology

TYPE Original Research
PUBLISHED 03 March 2025
DOI 10.3389/fimmu.2025.1559396

OPEN ACCESS

EDITED BY
Lei Huang,
University of Massachusetts Medical School, United States

REVIEWED BY
Yuejia Deng,
Texas A and M University, United States
Yue Liu,
The University of Texas at Austin, United States

*CORRESPONDENCE
Dejun Cui
cuidejun@gz5055.com
Chen Li
chen.li.scholar@outlook.com

†These authors have contributed equally to this work and share first authorship

RECEIVED 12 January 2025
ACCEPTED 17 February 2025
PUBLISHED 03 March 2025

CITATION
Chen L, He Y, Duan M, Yang T, Chen Y, Wang B, Cui D and Li C (2025) Exploring NUP62's role in cancer progression, tumor immunity, and treatment response: insights from multi-omics analysis. *Front. Immunol.* 16:1559396. doi: 10.3389/fimmu.2025.1559396

Exploring NUP62's role in cancer progression, tumor immunity, and treatment response: insights from multi-omics analysis

Lihong Chen[1†], Youfu He[2†], Menghui Duan[3], Tianwen Yang[4], Yin Chen[1], Bo Wang[5], Dejun Cui[1*] and Chen Li[6*]

[1]Department of Gastroenterology, Guizhou Provincial People's Hospital, Guiyang, Guizhou, China, [2]Department of Cardiology, Guizhou Provincial People's Hospital, Guiyang, Guizhou, China, [3]Department of Critical Care Medicine, The First Hospital of China Medical University, Shenyang, Liaoning, China, [4]Department of Orthopaedics, Guizhou Second People's Hospital, Guiyang, Guizhou, China, [5]Department of General Surgery, Guizhou Provincial People's Hospital, Guiyang, Guizhou, China, [6]Department of Pharmacy, the First Affiliated Hospital of Guangxi Medical University, Nanning, Guangxi, China

Background: NUP62, a key component of the nuclear pore complex, is closely associated with cellular functions and cancer progression. However, its expression patterns, prognostic value, and relationship with tumour immunity and drug sensitivity across multiple cancers have not been systematically studied. This study used multi-omics analyses combined with experimental validation in gastric cancer to investigate the expression, functional characteristics, and clinical relevance of NUP62 in cancer.

Methods: Data from TCGA, GTEx, and CPTAC databases were used to analyse the expression, mutation characteristics, and clinical associations of NUP62. Tools such as SangerBox, TIMER 2.0, and GSEA were employed to evaluate the relationship between NUP62 and the tumour immune microenvironment, as well as its involvement in signalling pathways. Immunohistochemistry and RT-PCR were used to validate the expression of NUP62 in gastric cancer tissues. PRISM and CTRP databases were utilised to assess the correlation between NUP62 expression and drug sensitivity.

Results: NUP62 was significantly upregulated in multiple cancers and was associated with poor prognosis in cancers such as clear cell renal carcinoma (KIRC), lower-grade glioma (LGG), and adrenocortical carcinoma (ACC), while playing a protective role in others, such as bladder cancer (BLCA) and stomach cancer (STAD). Functional analyses showed that NUP62 is involved in cell cycle regulation, DNA damage repair, and tumour immunity. High NUP62 expression was significantly correlated with increased infiltration of immune cells, such as macrophages and T cells, and a higher response rate to immunotherapy. Drug sensitivity analysis identified NUP62 as a marker of sensitivity to various chemotherapeutic agents. Validation experiments demonstrated that NUP62 mRNA and protein levels were significantly higher in gastric cancer tissues than in adjacent normal tissues.

Conclusions: NUP62 plays a critical role in multiple cancers and shows potential as a biomarker for cancer diagnosis, prognosis, and therapeutic response prediction. Its role in tumour immunity and signalling pathways highlights its potential as a target for immunotherapy and precision medicine.

KEYWORDS

Nup62, immune, pan cancer, gastric cancer, immune cell infiltration

1 Background

Cancer represents a major public health issue worldwide and is the second leading cause of death in the United States. In 2022, there will be nearly 20 million new cases of cancer, while 9.7 million people will die of cancer. About one in five men or women will develop cancer in their lifetime, while about one in nine men and one in 12 women will die of cancer (1). The rate of decline in cancer mortality has risen from about 1 percent per year in the 1990s, to 1.5 percent per year in the 2000s, to 2 percent per year between 2015 and 2020 (2).This trend reflects the increasing depth of human research into cancer, which is closely related to advancements in early cancer diagnosis and targeted therapy (3–5). Pan-cancer analysis, which integrates multiple databases, can aid in the identification of cancer biomarkers and therapeutic targets (6, 7).

Metabolic reprogramming is a hallmark of tumors, whereby tumors undergo reprogramming of nutrient acquisition and metabolic pathways to meet the bioenergetic, biosynthetic, and redox demands of malignant cells (8, 9). There exists a close interaction between metabolism and signaling pathways in cancer cells, and several signaling pathways associated with cell proliferation also regulate metabolic pathways that integrate nutrients into biomacromolecules (10). Consequently, certain cancer-related mutations enable cancer cells to acquire and metabolize nutrients in a manner conducive to proliferation, rather than efficiently producing ATP (11, 12). To fulfill the demands of proliferation, cancer cells utilize processes such as glycolysis, glutaminolysis, and fatty acid oxidation to meet their energy requirements and metabolic synthesis processes (13, 14). Studies have indicated that oxidative phosphorylation represents an emerging target in cancer therapy (15). Furthermore, immune cells within the tumor microenvironment (TME) exhibit metabolic shifts similar to the glycolytic metabolic profile, leading to competition for nutrients between cancer cells and tumor-infiltrating cells (16). On the other hand, metabolic disturbances characterized by hypoxia and elevated metabolite levels (especially lactate) in the TME can result in immunosuppression (17, 18). Simultaneously, metabolic dysregulation and imbalances in immune cells within the TME can drive immune evasion and compromise treatment outcomes (19).

The primary function of the nuclear pore complex (NPC) is to mediate transport between the nucleus and cytoplasm. Studies have shown that nucleoporins exert effects independently of the NPC in both nuclear and cytoplasmic compartments, directly regulating gene expression and participating in the regulation of development and the cell cycle (20). Nucleoporin 62 (NUP62), a structural component of the NPC, may mediate the localization of glucocorticoid receptors to the nucleus after binding to steroids (21). Additionally, NUP62 can interact with OSBP-related protein 8 (ORP8), which has the ability to regulate hepatic lipogenesis and plasma lipid levels (22). Furthermore, numerous studies have demonstrated that NUP62 mediates selective nucleocytoplasmic transport and is associated with various cancers through chromosomal translocations that generate fusion proteins, alterations in protein expression levels, and single-point mutations (23–27). Specifically, high expression of NUP62 contributes to preventing epidermal differentiation in squamous cell carcinomas originating from stratified epithelia (27, 28).

2 Materials and methods

2.1 Data collection and processing

We obtained expression levels and related clinical characteristics of NUP62 from the Cancer Genome Atlas (TCGA, http://cancergenome.nih.gov/) and the Genotype-Tissue Expression (GTEx, https://gtexportal.org/) databases through the Xena platform at the University of California, San Diego. The mutation frequency of NUP62 in the TCGA cohort was calculated using the cBioPortal database (https://www.cbioportal.org/). Pan-cancer analysis of TCGA samples was conducted using the online bioinformatics tool SangerBox 3.0 (http://sangerbox.com/) (29). Various immune infiltration algorithms in the TIMER 2.0 database (http://timer.cistrome.org) were utilized to characterize the correlation between NUP62 expression and the tumor immune microenvironment.

Expression profiles of human normal tissues and cancer cell lines were obtained from the Human Protein Atlas (HPA, https://www.proteinatlas.org/). Relevant chemotherapy data were retrieved from the Genomics of Drug Sensitivity in Cancer (GDSC, https://www.cancerrxgene.org/), Cancer Therapeutics Response Portal (CTRP, http://portals.broadinstitute.org/ctrp/), and PRISM databases to illustrate the relationship between NUP62 expression and drug sensitivity. Cancer immune cycle data originated from the

Tracking Immune Phenotypes in Cancer (TIP, https://biocc.hrbmu.edu.cn/TIP/), while Immune Phenotype Scores (IPS) data were obtained from the TCIA website (https://tcia.at/home).

2.2 Expression and variation analysis

To investigate whether there were differences in NUP62 expression between tumor and normal tissues, we first compared the expression of NUP62 mRNA between tumor and normal tissues using the "wilcox" test. Subsequently, a paired "wilcox" test was conducted on matched samples to validate protein expression at the external gene transcriptome level in the GEO and CPTAC databases. Additionally, we used the "gganatogram" R package to visualize the expression of NUP62 in different human organs. The cBioPortal website (http://www.cbioportal.org) served as a powerful tool to search for NUP62 mutation frequency, types, copy number alteration (CNA) data, and gene alteration traits. Furthermore, we employed the "pROC" R package to calculate the Area Under the Curve (AUC) value, illustrating the importance of NUP62 in pan-cancer diagnosis.

2.3 Survival and clinical outcome analysis

Survival data were sourced from the TCGA database. We analyzed the relationship between NUP62 expression and these prognostic indicators, including Overall Survival (OS), Disease-Specific Survival (DSS), Progression-Free Interval (PFI), and Disease-Free Interval (DFI), using the "survival" and "survminer" R packages. Kaplan-Meier (KM) analysis and univariate COX analysis were combined to assess whether NUP62 was a protective or risk factor, resulting in the creation of high-confidence survival landscapes for NUP62. Additionally, the "forestplot" R package was utilized for visual analysis of COX survival data.

2.4 Subtyping of NUP62 and immunotherapy analysis

Researchers conducted extensive immunogenomic analysis on over 10,000 tumor samples encompassing 33 different cancer types from the TCGA database. Across tumor types, they successfully identified six immune subtypes by evaluating macrophage or lymphocyte markers, Th1 to Th2 cell ratios, the range of genetic heterogeneity among tumors, aneuploidy, neoantigen burden range, total cell landscape, immune-regulatory gene expression, and prognosis. The six subtypes are introduced as follows:

C1 (Tissue Healing) subtype exhibits elevated angiogenic gene expression, a high proliferation rate, and significant acquired immune infiltration with a Th2 bias. Primary associated cancers include colorectal adenocarcinoma (COAD), rectal adenocarcinoma (READ), lung squamous cell carcinoma (LUSC), luminal A subtype of breast invasive ductal carcinoma (BRCA), classical subtype of head and neck squamous cell carcinoma (HNSC), and chromosomally unstable gastrointestinal subtype.

C2 (IFN-γ Dominant) subtype demonstrates the highest M1/M2 macrophage polarization, strong CD8 signaling, and, like the C6 subtype, the highest TCR diversity. Additionally, the C2 subtype has a high proliferation rate, with primary associated cancers including hypermutated BRCA, gastric cancer, ovarian cancer, HNSC, and cervical squamous cell carcinoma and endocervical adenocarcinoma (CESC).

C3 (Inflammatory) subtype shows elevated Th17 and Th1 gene expression but fails to effectively inhibit tumor cell proliferation. Like the C5 subtype, C3 has fewer aneuploidies and overall cellular copy number alterations compared to other subtypes. Primary associated cancers include most kidney cancers, prostate adenocarcinoma (PRAD), pancreatic adenocarcinoma (PAAD), and thyroid papillary carcinoma (THCA).

C4 (Lymphocyte-Depleted) subtype is characterized by prominent macrophage features, Th1 suppression, and high M2 responsiveness. Primary associated cancers include specific subtypes of adrenocortical carcinoma (ACC), pheochromocytoma and paraganglioma (PCPG), hepatocellular carcinoma (LIHC), and gliomas.

C5 (Immunologically Silent) subtype has the lowest lymphocyte count, the highest macrophage response, and is dominated by M2 macrophages. This subtype is primarily a subtype of low-grade gliomas (LGG) of the brain, including glioma CpG island methylator phenotype-high (CIMP-H), 1p/19q codeleted subtype, and fibrillary astrocytoma-like (PA-like) type. Additionally, the remaining types are mainly within the C4 subtype, while isocitrate dehydrogenase mutant types are more prevalent in the C5 subtype than in the C4 subtype.

C6 (TGF-β Dominant) subtype is a smaller group composed of a mix of cancers and does not dominate any TCGA subtype. This subtype has the highest TGF-β signature and high lymphatic infiltration, with equal distribution of Type I and Type II T cells.

This study further explored the relationship between NUP62 and patient prognosis in external datasets using the BEST database and investigated the correlation between NUP62 expression and the immunotherapy response in cancer patients (30).

2.5 Pathway and mechanism of action analysis

To delve into the mechanism of action of NUP62-related pathways, we classified various tumor samples based on NUP62 expression levels (the top 30% as the high-expression group and the bottom 30% as the low-expression group). Subsequently, we employed Gene Set Enrichment Analysis (GSEA) to investigate the differential activation or inhibition states of 50 characteristic genomic signatures and 83 metabolic genomic signatures between the high and low NUP62 expression groups across different malignancies. Utilizing the "GSVA" R package, we quantitatively analyzed 14 functional status genomic signatures using the "z-score" algorithm. Based on the z-score values of each genomic

signature, we conducted subsequent data processing and analysis. Furthermore, we applied "Pearson" correlation analysis to assess the statistical correlation between the z-score of each genomic signature and NUP62 expression levels. Additionally, we identified genes that underwent significant changes in both high and low NUP62 expression groups.

2.6 Identification of chemicals interacting with NUP62

To explore the potential association between NUP62 expression and drug sensitivity, we leveraged the GSCA database (http://bioinfo.life.edu.cn/web/GSCALite/). Through the GSCA platform, we obtained information on small molecule drugs from the GDSC and CTRP databases. Furthermore, we identified genes differentially expressed between the high and low NUP62 expression groups across various malignancies. To screen for biomarkers closely related to NUP62, we selected the top 150 significantly upregulated and downregulated genes. Simultaneously, we downloaded the CMAP_gene_signatures RData file, which contains 1,288 attributes associated with compound functional characteristics.

3 Results

3.1 Expression and mutation of NUP62 in humans

Using unpaired and paired sample data from the TCGA database, we conducted an in-depth analysis at the mRNA level and observed an upward trend in NUP62 expression across multiple cancer types, including Bladder Urothelial Carcinoma (BLCA), Breast Invasive Carcinoma (BRCA), COAD, Esophageal Carcinoma (ESCA), HNSC, Kidney Renal Clear Cell Carcinoma (KIRC), Kidney Renal Papillary Cell Carcinoma (KIRP), LIHC, Lung Adenocarcinoma (LUAD), LUSC, and Stomach Adenocarcinoma (STAD) (Figures 1A, C). Additionally, we further validated these findings in the CPTAC database (Figure 1B). Figure 1D depicts the expression profile of NUP62 in different human organs. Notably, NUP62 expression levels were significantly upregulated in most cancer types, while they exhibited a downward trend in testicular tissue. NUP62 displayed variable expression patterns in most cancers, with mutation sites distributed as shown in Figure 1E. Leveraging the cBioPortal (TCGA, Pan-cancer Atlas) database, we comprehensively assessed the pan-cancer mutational characteristics of the NUP62 gene. The results indicated that the most common types of variations in NUP62 included mutations, amplifications, and deep deletions, with Endometrial Cancer, Cervical Cancer, and Bladder Cancer having the highest mutation rates (Figure 1F). Subsequently, we conducted an in-depth analysis of the distribution characteristics of NUP62 mutations across different cancers and explored the types of single nucleotide variants (SNVs). The results showed that missense mutations dominated among various types of variations (Figure 1G). Finally, we conducted a comprehensive analysis of the distribution of NUP62 and other genes in cancer samples. The results revealed that among all cancer types, NUP62 was most widely distributed in UCEC, while the TP53 signal was significantly distributed in most cancers (Figure 1H).

3.2 Expression of NUP62 in cells

Based on fluorescence images provided by the Human Protein Atlas (HPA), we observed that NUP62 is primarily localized within the cell nucleus (Supplementary Figure 1A). Researchers systematically analyzed normal tissues such as the cerebral cortex, liver, colon, kidney, and pancreas, as well as tumor tissues such as lung cancer, liver cancer, colorectal cancer, pancreatic cancer, and breast cancer, using immunohistochemical techniques. The results indicated that compared to normal tissues, the expression level of NUP62 in tumor tissues exhibited a significant upward trend (Supplementary Figure 1B).

3.3 Correlation between NUP62 and clinical characteristics across various cancer types

As shown in Figure 2A, gender differences in NUP62 expression levels are observed in sarcoma (SARC), KIRP, and the Pan-kidney cohort (KIPAN), with significantly higher expression in female patients compared to male patients. Additionally, the expression level of NUP62 is closely related to age. In KIRP, PCPG, and ESCA, there is a negative correlation between age and NUP62 expression (Figure 2G). Furthermore, the expression of NUP62 is associated with various cancer stages. In KIPAN and LIHC, differences in NUP62 expression are observed among tumor patients with different T stages (Figure 2B). In KIRP and ACC, NUP62 expression exhibits certain differences across different N stages (Figure 2C). Only in ACC is there an association between NUP62 expression and its M stage (Figure 2D). In glioma (GBMLGG), LGG, HNSC, and LIHC, significant differences in NUP62 expression are found among tumor patients with different G stages (Figure 2E). In LIHC, NUP62 expression is correlated with its stage classification (Figure 2F).

3.4 Diagnostic value of NUP62 in pan-cancer

We evaluated the diagnostic capacity of NUP62 for various cancers in both the TCGA dataset and the combined TCGA-GTEx dataset (Figure 3A). The results indicated that the AUC value of NUP62 in ESCA was >0.9, suggesting a high diagnostic value for ESCA. Additionally, the AUC values in BRCA, LUSC, COAD, STAD, READ, KIRC, and HNSC were all between 0.8 and 0.9, indicating that NUP62 also has diagnostic value for these tumors. Figures 3B, C depict the ROC curves of NUP62 in ESCA and BRCA, respectively. Therefore, NUP62 is an effective diagnostic biomarker across various cancer types.

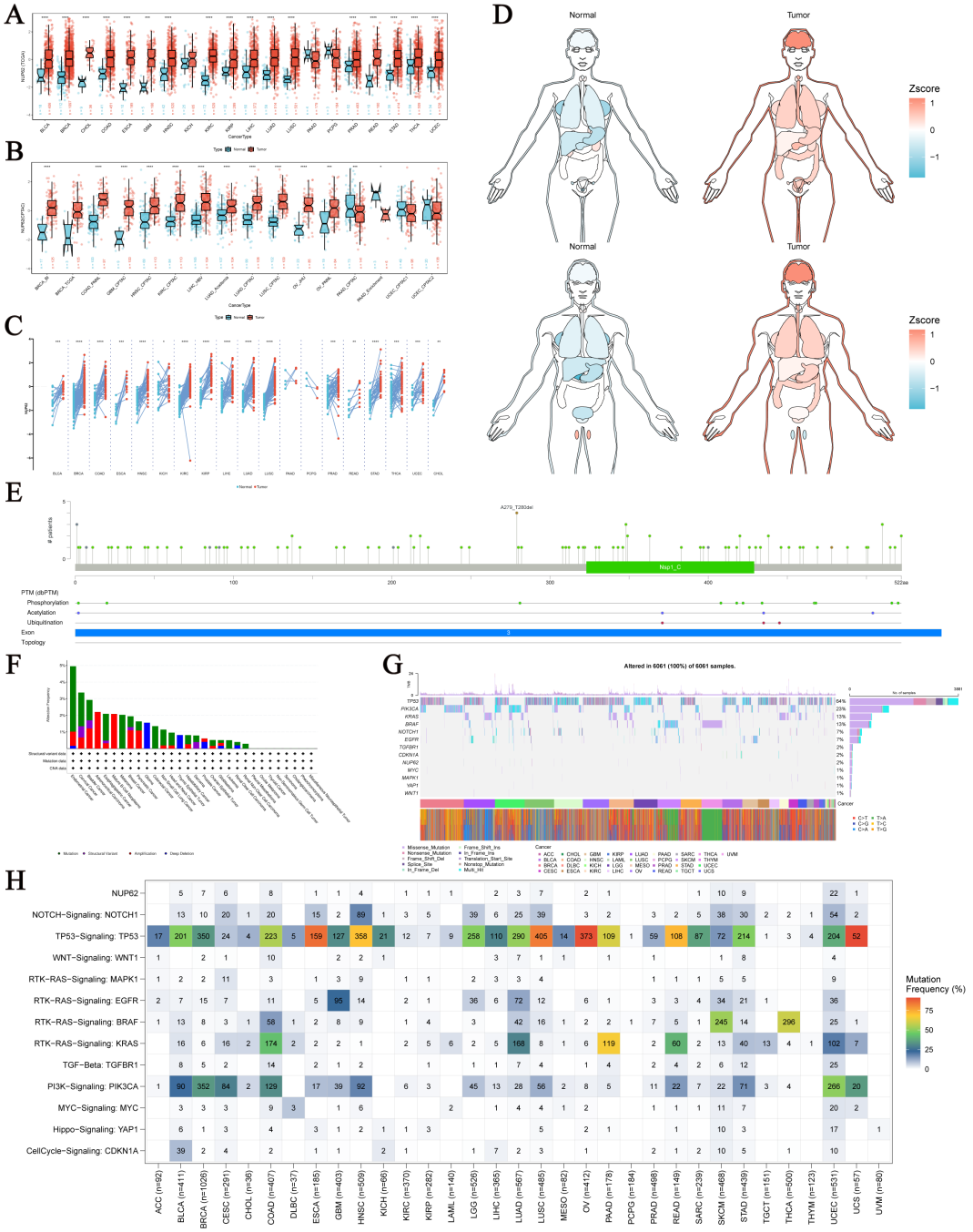

FIGURE 1
Expression and Mutation of NUP62. **(A)** Expression of NUP62 mRNA in tumor and normal tissues. **(B)** Expression of NUP62 in tumor and normal tissues from the CPTAC database. **(C)** Expression of NUP62 in tumor and paired adjacent normal tissues. **(D)** Expression and distribution of NUP62 in organs of tumor and normal tissues. **(E)** Mutation sites of NUP62. **(F)** Mutation frequencies and corresponding mutations of NUP62 in different cancers. **(G)** Gene alteration sites and numbers of NUP62 in different cancers. **(H)** Distribution of NUP62 and other signals in cancers. *P<0.05. **P<0.01. ***P<0.001. ****P<0.0001.

3.5 Correlation between NUP62 expression and pan-cancer prognosis

To gain deeper insights into the clinical significance of NUP62 in the field of cancer, we analyzed its prognostic value in multiple malignant tumors. The results in Figure 4A clearly show that NUP62 expression levels are significantly associated with poor prognosis in various cancers, serving as a risk factor for their prognosis. Figures 4B–M present the KM survival curves for overall survival (OS) based on NUP62 expression levels in some cancers. The results indicate that high expression of NUP62 is significantly associated with shorter OS in KIRP, KIRC, ACC, LGG, LIHC, mesothelioma (MESO), skin cutaneous melanoma (SKCM), and SARC ($p < 0.05$). However, in uveal melanoma (UVM), BLCA, STAD, and CESC, high expression of NUP62 is associated with longer survival, potentially playing a protective role.

10.3389/fimmu.2025.1559396

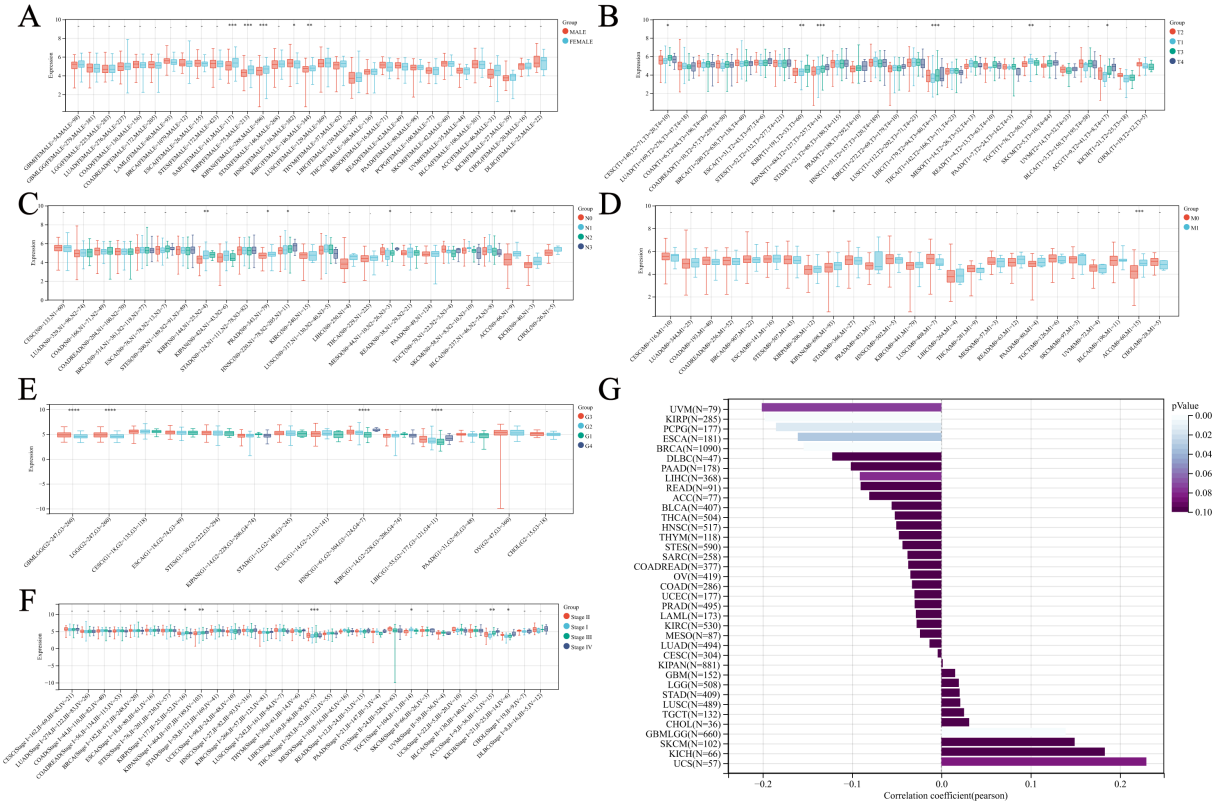

FIGURE 2
Relationship between NUP62 Expression and Clinical Characteristics Across Various Cancer Types. **(A)** Correlation between gender and NUP62 expression in pan-cancer. **(B)** Correlation between NUP62 expression and T stage in pan-cancer. **(C)** Correlation between NUP62 expression and N stage in pan-cancer. **(D)** Correlation between NUP62 expression and M stage in pan-cancer. **(E)** Correlation between NUP62 expression and G stage in pan-cancer. **(F)** Correlation between NUP62 expression and tumor stage in pan-cancer. **(G)** Correlation between age and NUP62 expression. *P<0.05. **P<0.01. ***P<0.001. ****P<0.0001.

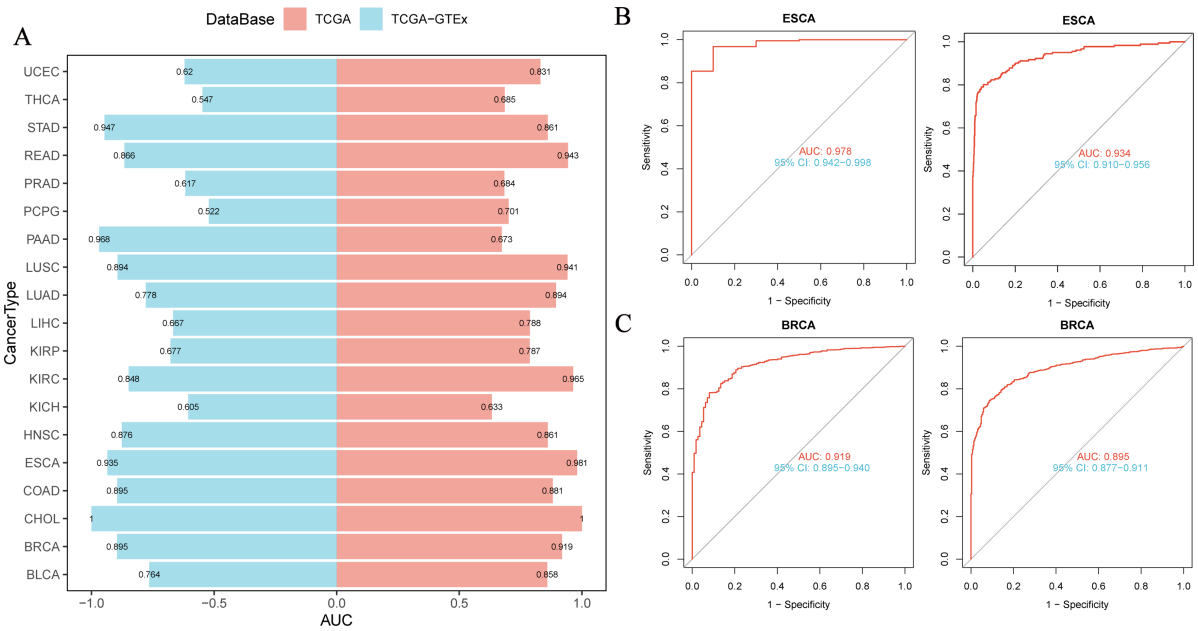

FIGURE 3
Correlation between NUP62 Expression and Diagnosis of Various Cancer Types. **(A)** Diagnostic value of NUP62 across various cancer types; **(B, C)** ROC curves of NUP62 in ESCA and BRCA.

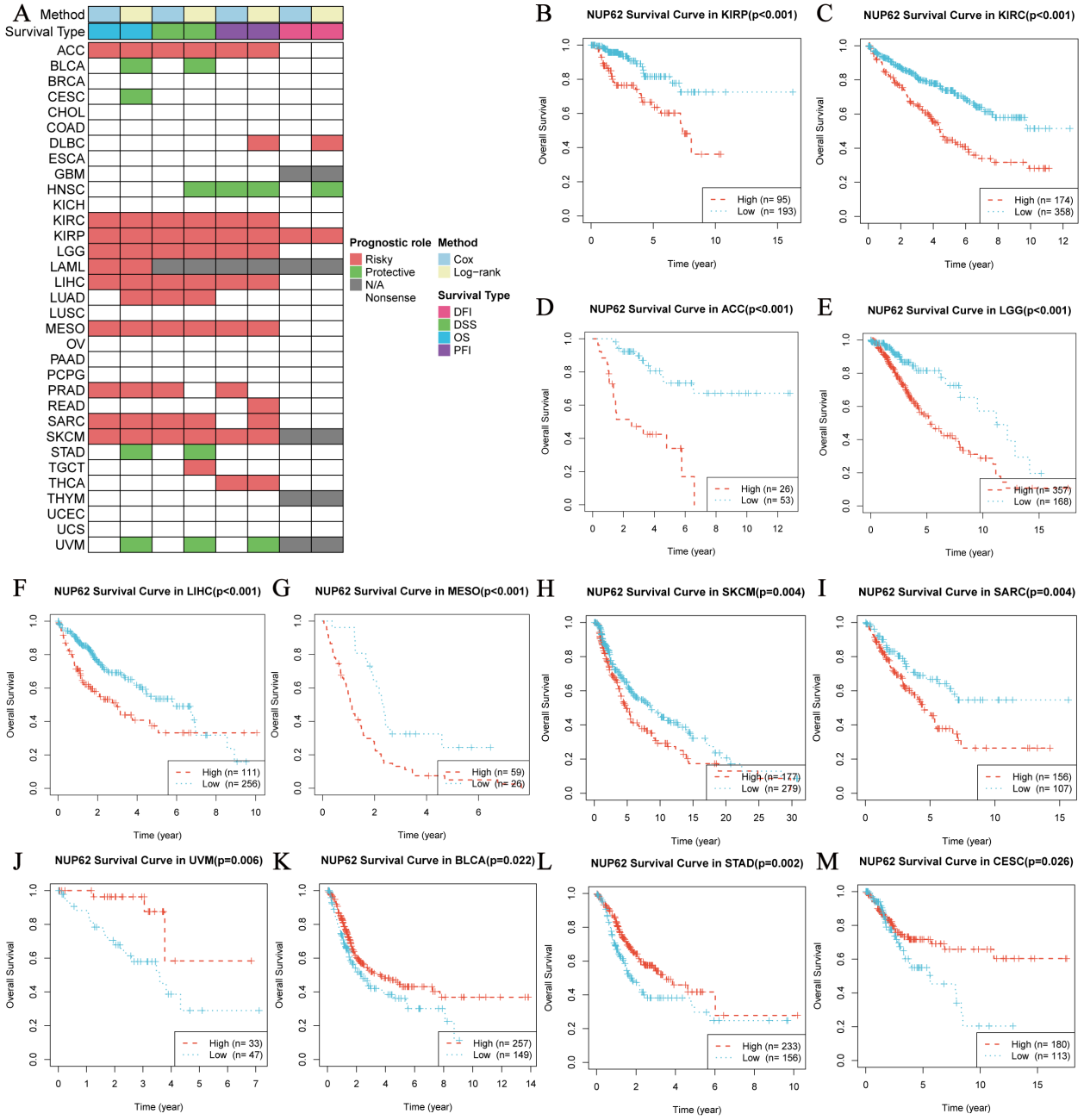

FIGURE 4
Survival Analysis Spectrum of NUP62 Across Multiple Cancer Types. **(A)** Correlation between NUP62 expression levels and OS, disease-specific survival (DSS), disease-free interval (DFI), and progression-free interval (PFI). **(B-M)** Relationship between NUP62 expression levels and OS in patients with different cancer types.

3.6 The role of NUP62 in cancer pathways

To delve deeper into the potential roles and specific functions of NUP62 in cancer, we employed an integrated analysis of signature gene expression to assess the activity status of NUP62 pathways. We utilized the z-score parameter from Gene Set Variation Analysis (GSVA) to quantify and evaluate 14 functional status gene sets, covering angiogenesis, apoptosis, cell cycle regulation, cell differentiation, DNA damage response, DNA repair mechanisms, epithelial-mesenchymal transition (EMT), hypoxic adaptation, inflammatory response, invasive behavior, metastatic potential, cell proliferation, cellular quiescence, and cellular stemness features. From this, composite z-scores were obtained. Subsequently, we calculated the Pearson correlation coefficients between NUP62 and each functional status gene set score (Figure 5A). The results revealed significant positive correlations between NUP62 expression levels and cell cycle regulation, DNA damage response, and DNA repair mechanisms. Additionally, we

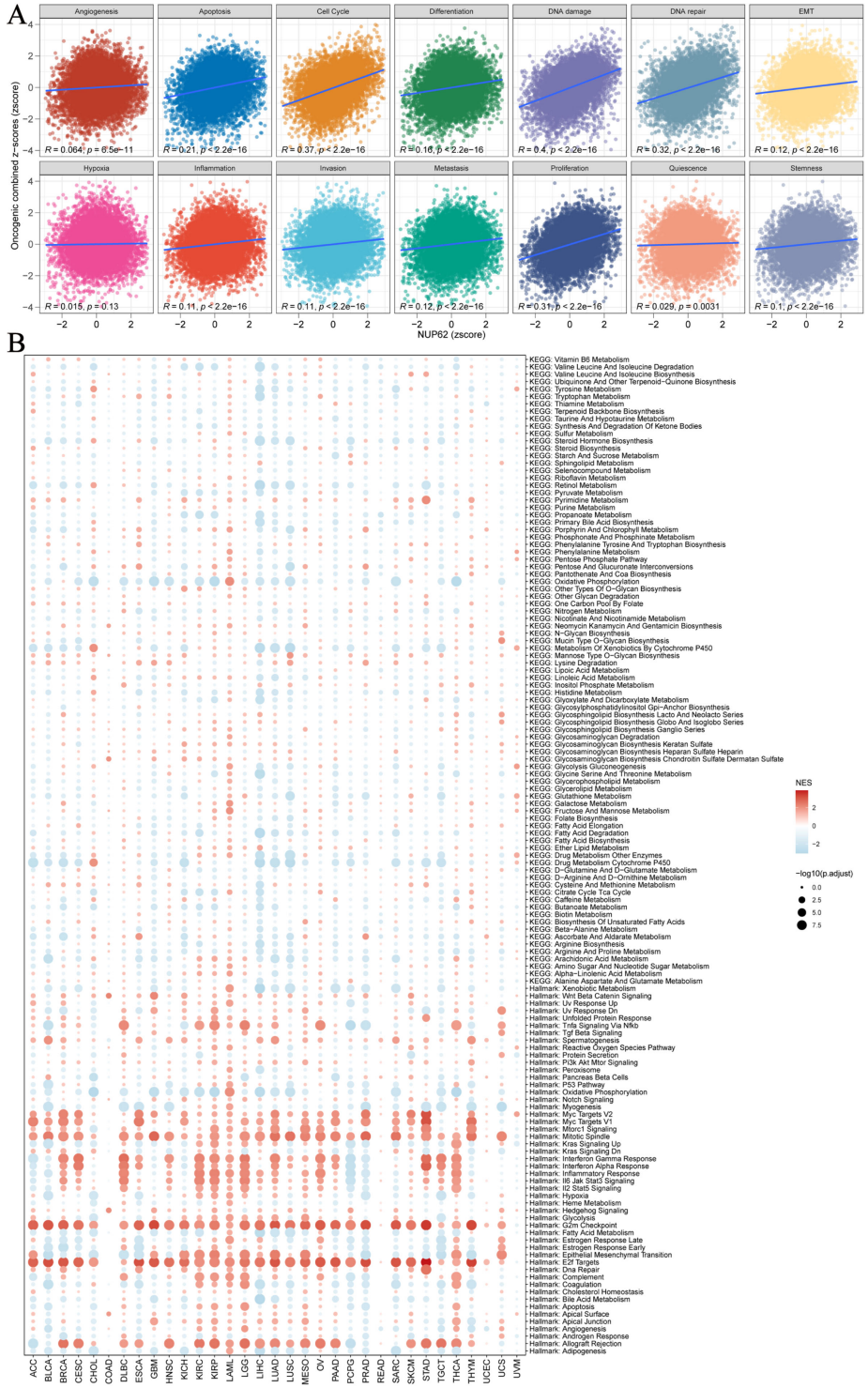

FIGURE 5
(A) Relationships between NUP62 and 14 malignant features of cancer; **(B)** Enrichment differences of NUP62 in 50 HALLMARK and 83 metabolic gene sets.

collected datasets from cancer patients and conducted Gene Set Enrichment Analysis (GSEA). The analysis results indicated that NUP62 may be involved in various tumor-related pathways and metabolic regulatory processes, such as the G2/M checkpoint, E2F transcription factor target genes, allograft rejection, and mitotic spindle formation (Figure 5B).

3.7 The relationship between NUP62 and cellular pathways

Utilizing the TCGA database, we conducted an in-depth exploration of the interaction between NUP62 and functional proteins within the TCGA database, and found that NUP62

exhibits significant correlations with multiple key functional proteins across various cancer types. Specifically, in UVM, the expression level of NUP62 is significantly positively correlated with CASPASE8, CYCLIN D1, CRAF (pS338), AKT, and RB proteins, while it is significantly negatively correlated with the expression levels of ACC-pS79, ACC1, CKIT, ATM, and PKCα. In ACC, the expression of NUP62 is positively correlated with the expression of CABL protein and negatively correlated with the expression of FOXO3A protein (Figure 6A). Figure 6B illustrates the relationships between cancer and 10 cancer-related pathways, where the activation of apoptosis, activation, cell cycle, and DNA damage promotes the occurrence of cancer. Subsequently, we detailed the most significantly correlated functional proteins of NUP62 in ACC and UVM from the TCPA database (Figures 6C, D).

3.8 The relationship between NUP62 and immune subtypes and immunotherapy

Based on nearly 10,000 cancer samples from the TCGA database, we subclassified them into six distinct immune subtypes. The analysis revealed that C1, C2, C3, and C4 subtypes dominate among all immune subtypes. Additionally, in cancer samples with high NUP62 expression, the proportion of the C2 subtype was significantly higher than that in samples with low NUP62 expression; conversely, in patients with low NUP62 expression, the proportions of C3 and C5 subtypes were significantly higher than those in patients with high NUP62 expression (Figure 7A). Subsequently, we delved into the correlation between NUP62 expression levels and immunotherapy response in clinical trials. Among the two immunotherapy cohorts included in the study, patients with high NUP62 expression had a significantly higher response rate to immunotherapy than those with low expression (Figure 7B). Notably, we evaluated the potential efficacy of NUP62 as a predictor of immunotherapy response using ROC curve analysis (Figure 7C). By comparing the impact of two different immunotherapy regimens on patients' overall survival, we found that patients with elevated NUP62 expression had a significantly longer overall survival compared to those with decreased NUP62 expression (Figure 7D).

3.9 The relationship between NUP62 and immunity

Immunotherapy has emerged as a primary modality in cancer treatment, prompting our investigation into the potential association

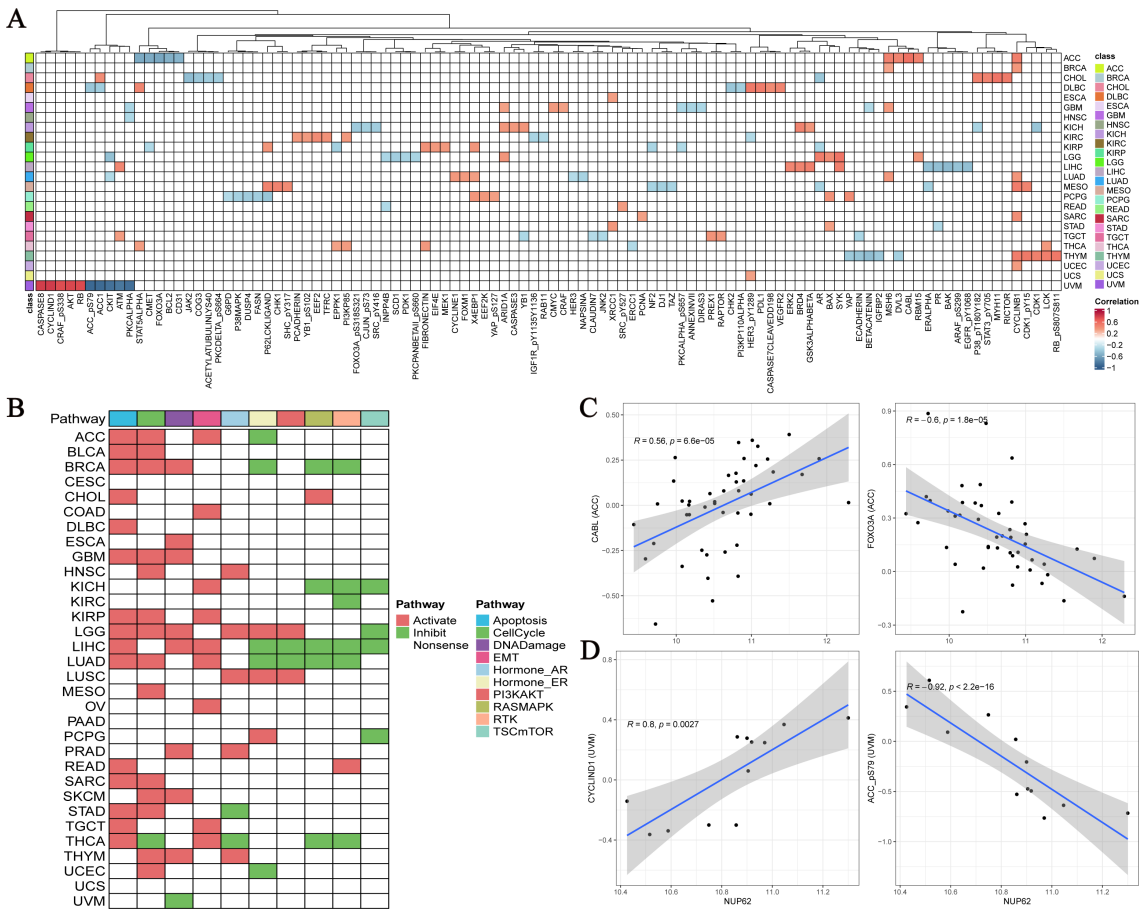

FIGURE 6
(A) Top five functionally related proteins of NUP62 across various cancers in the TCGA database; **(B)** Relationships between cancer and 10 cancer-related pathways; **(C, D)** NUP62-related functional proteins in ACC and UVM from the TCPA database.

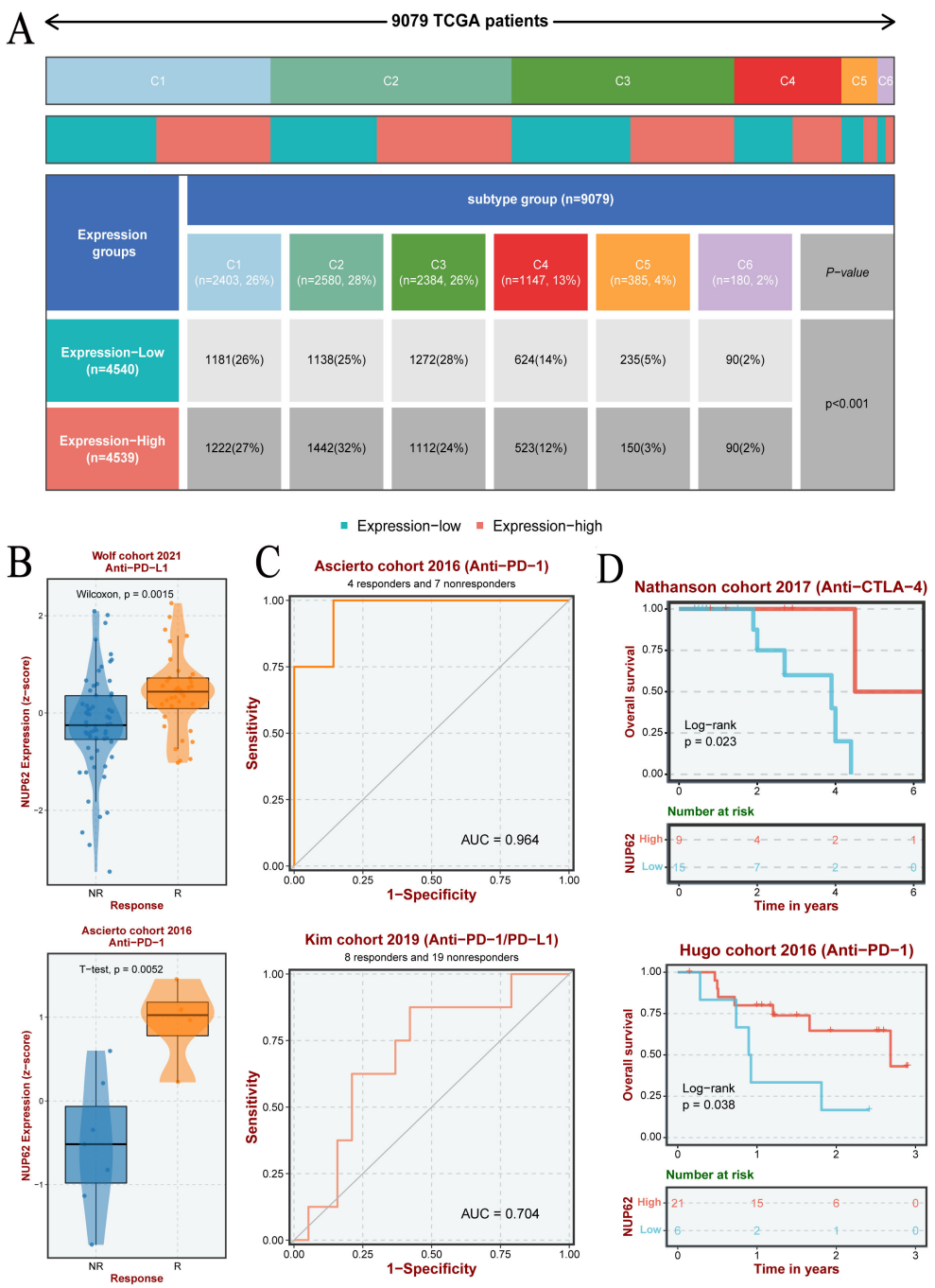

FIGURE 7
(A) Differences in the number of pan-cancer immune subtypes between the high and low NUP62 expression groups. **(B)** Expression of NUP62 in responders and non-responders within different immunotherapy cohorts. **(C)** Diagnostic value of NUP62 in different immunotherapy settings. **(D)** Correlation between NUP62 expression and survival rates in different immunotherapy cohorts.

between NUP62 and cancer immunity. Our results indicate that across various cancer types, the expression level of NUP62 significantly correlates with the expression of immune-related genes, such as those in THCA, KIRC, KIRP, and PCPG (Figure 8A). Furthermore, by examining the levels of immune cell infiltration in the TME, we found that the expression of NUP62 is significantly correlated with the infiltration levels of multiple immune cell types, including Th1 cells, Th2 cells, dendritic cells (DC-TIMER), M0 and M1 macrophages (Macrophages-M0-CIBERSORT), neutrophils (neutrophil-TIMER), T cells (T-cells-MCPcounter), and regulatory T cells (T-cells-regulatory-CIBERSORT), among others, across several cancer types (Figure 8B). These findings suggest that NUP62 may play a crucial role in the tumor immune microenvironment, potentially affecting tumor growth and the efficacy of immunotherapy by regulating the expression of immune cells or immune-modulating genes.

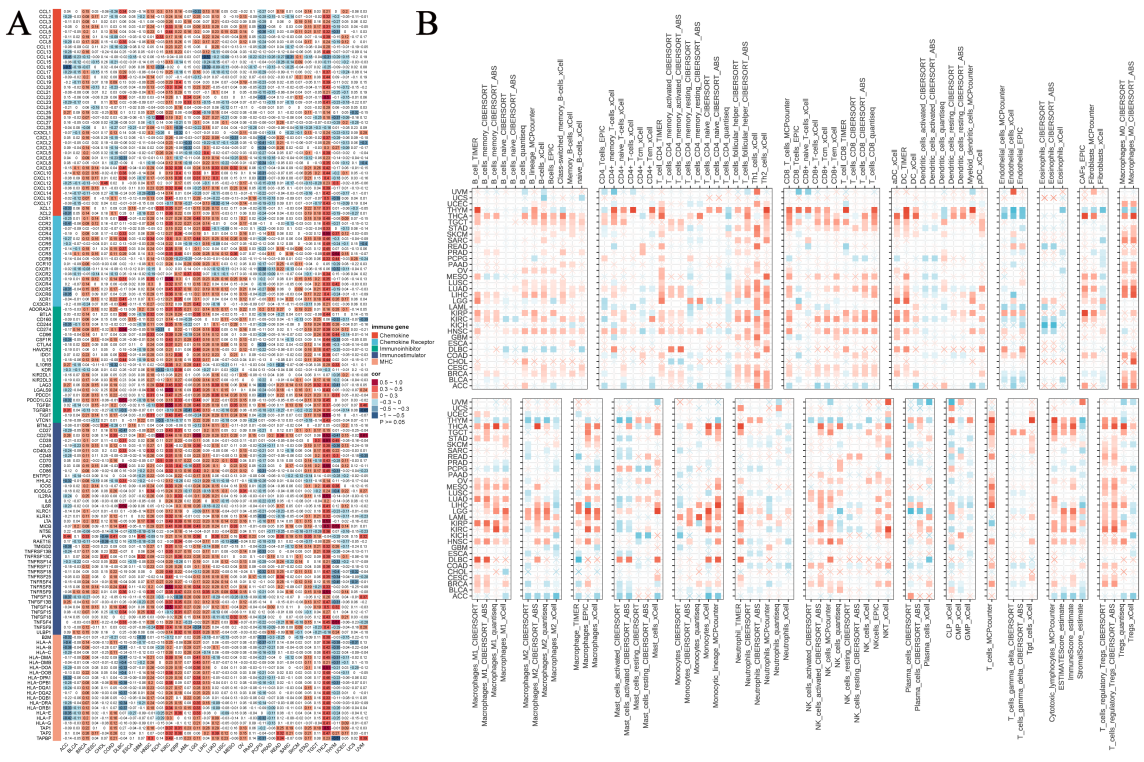

FIGURE 8
The relationship between NUP62 expression and immune infiltration. **(A)** Heatmap showing the correlation between NUP62 mRNA expression and the expression of chemokines, chemokine receptors, immune inhibitors, immune stimulators, and MHC genes. **(B)** Correlation between NUP62 expression and tumor immune infiltration.

3.10 NUP62 may influence chemotherapy response

We further delved into the potential association between NUP62 expression levels and drug sensitivity. Results from both PRISM and CTRP drug sensitivity experiments revealed a significant correlation between NUP62 mRNA expression levels and drug sensitivity. The PRISM drug sensitivity experiment showed that the top three drugs positively correlated with NUP62 expression levels were trametinib, Ro-4987655, and AS-703026, while the top three negatively correlated drugs were idronoxil, sirolimus, and LY3023414 (Figure 9A). Similarly, the CTRP drug sensitivity experiment also demonstrated that the top three drugs positively correlated with NUP62 expression levels were selumetinib, saracatinib, and PD318088, while the top three negatively correlated drugs were axitinib, indisulam, and PRIMA-1 (Figure 9B). The discovery of compounds that can significantly modulate NUP62 activity holds important potential value for developing novel and effective tumor treatment regimens. We found that arachidonyltrifluoromethane significantly impacts NUP62 expression across multiple tumor types (Figure 9C). Subsequently, we detailed the specific effects of various compounds on NUP62 in different tumor types and highlighted the significant diagnostic and prognostic predictive value of NUP62 in these tumor types (Figures 9D–F).

3.11 Validation of NUP62 expression levels in gastric cancer

To validate our initial hypothesis, we employed immunohistochemical techniques to conduct an in-depth analysis of NUP62 protein expression levels in gastric cancer tissues and their adjacent non-cancerous tissues. Figure 10A visually demonstrates the distribution and intensity of NUP62 expression in both non-cancerous and gastric cancer tissues. The research findings indicate that the expression level of NUP62 in gastric cancer tissues is significantly higher than that in their adjacent non-cancerous tissues (see Figure 10B). Furthermore, through quantitative PCR analysis, we found that the mRNA expression level of NUP62 in gastric cancer tissues is also significantly elevated compared to their adjacent non-cancerous tissues.

4 Discussion

Firstly, our study determined the expression and mutation status of NUP62 in humans. The results indicated that NUP62 expression is generally higher in cancer cells compared to normal cells. Mutations in NUP62 within tumors may lead to functional abnormalities of NUP62, affecting normal cellular functions and playing a role in tumorigenesis and progression. HPA fluorescence

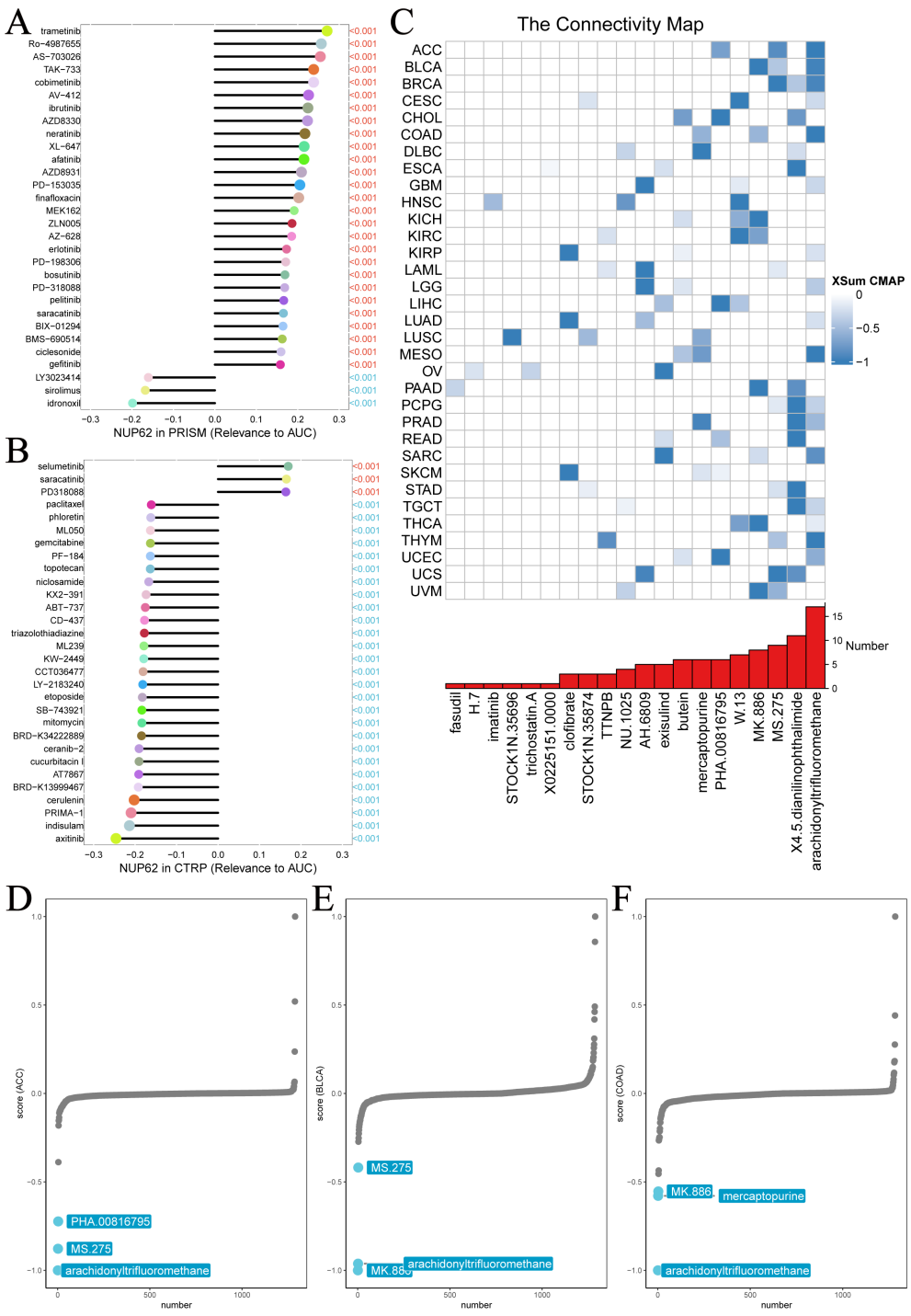

FIGURE 9
Chemotherapy resistance analysis. Two different databases were utilized to investigate the association between NUP62 expression and drug sensitivity. **(A)** PRISM. **(B)** CTRP. **(C)** Identification of NUP62-targeting compounds through cMap analysis. **(D-F)** NUP62-targeting compounds with clinical significance.

images and staining data demonstrated that NUP62 is primarily localized in the nucleus, consistent with its role as a component of the NPC (20, 31). Further stratification according to patients' clinical characteristics revealed that NUP62 is associated with the stages of multiple cancers, suggesting its role in tumor progression, invasion, and metastasis (32–34). The expression of NUP62 is also closely related to gender and age, which may be associated with hormones, cellular aging, decreased DNA damage repair capacity, and increased cancer risk (35–37). In the TCGA dataset and the combined TCGA-GTEx dataset, NUP62 exhibited high AUC values across various cancers. Notably, in ESCA, the AUC value was >0.9, indicating that NUP62 has significant value for the screening and diagnosis of multiple cancers, particularly ESCA (38–40). Next, our research found that NUP62 expression is associated with the

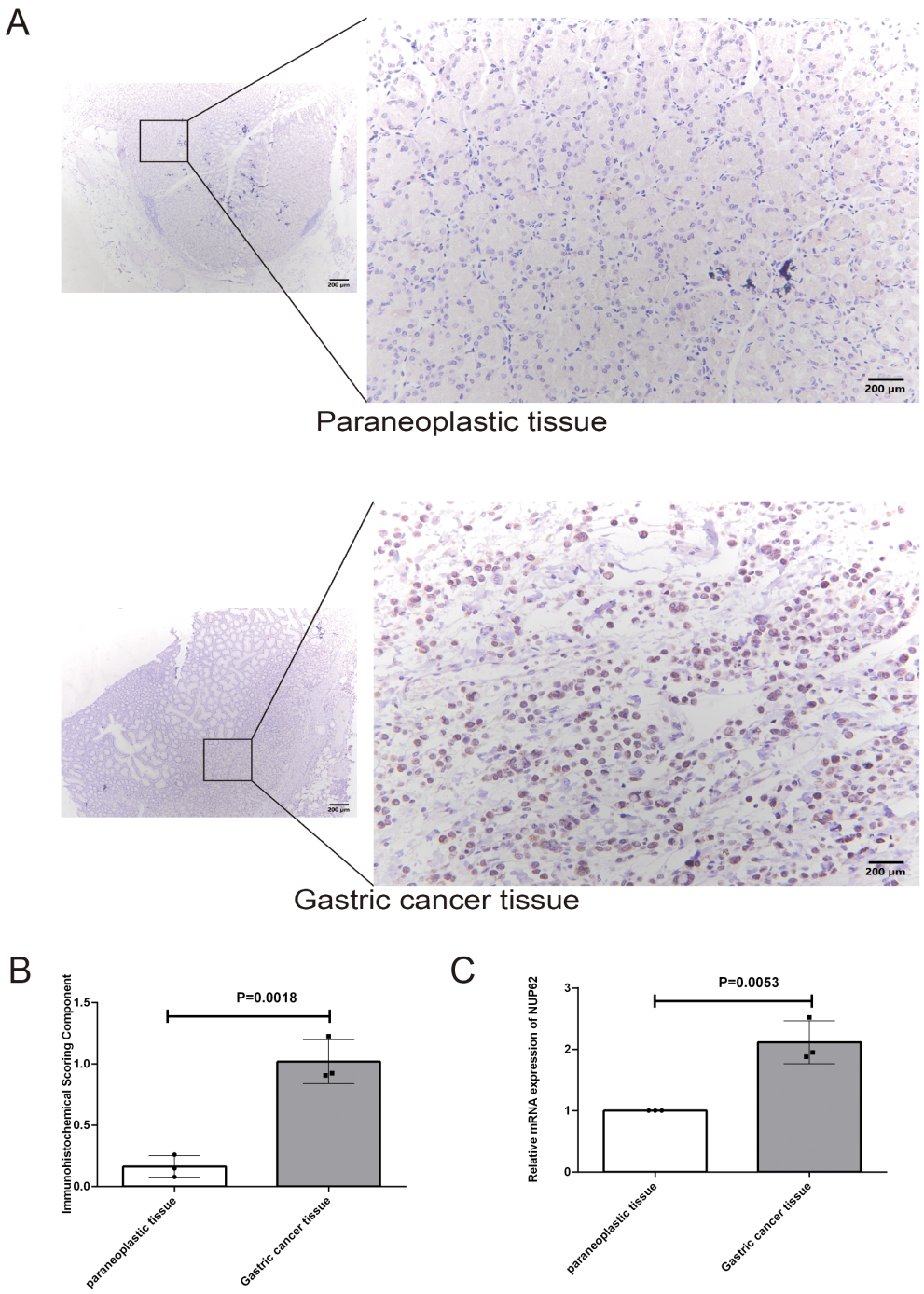

FIGURE 10
(A, B) Represent the protein expression levels of NUP62 in gastric cancer tissues and their adjacent non-cancerous tissues. **(C)** Illustrates the mRNA expression levels of NUP62 in gastric cancer tissues versus their adjacent non-cancerous tissues.

prognosis of cancer patients, with differential expression observed in different types of cancer patients, as confirmed by KM curves. This suggests that NUP62 can serve as a prognostic marker for some cancers to guide the selection of treatment regimens for cancer patients, taking into account individual differences and formulating personalized treatment plans (41–43). Further GSEA analysis revealed that NUP62 is significantly associated with the cell cycle, DNA damage, and DNA repair, which may be related to NUP62's involvement in numerous tumor-related pathways and metabolic processes, including the G2/M checkpoint, E2F target genes, allograft rejection, and mitotic spindle. These pathways and processes play crucial roles in cancer cell proliferation, invasion, metastasis, and drug resistance, emphasizing the complexity and diversity of NUP62 in tumors (44–48). Subsequently, we

investigated the relationship between NUP62 and TCPA functional proteins, further demonstrating the important role of NUP62 in regulating the cell cycle of cancer patients.

We noted a decreasing trend in the expression level of NUP62 in testicular cancer tissues, which contrasts with the upregulation of NUP62 expression in most cancers. This difference in expression patterns may reflect the unique biology of testicular cancer. Therefore, we believe that testicular cancer is a validated experimental subject worthy of further study. By deeply exploring the expression regulation mechanism of NUP62 in testicular cancer, it is expected to provide new ideas and methods for the diagnosis and treatment of testicular cancer. We have not validated this for the time being, but it will be an important direction for future research.

Although our study found that high expression of NUP62 was associated with longer survival in these tumors, this does not mean that NUP62 is necessarily protective in these tumors. It is possible that the expression level of NUP62 is affected by a variety of factors, which may have different roles in different types of tumors. Therefore, the specific mechanism of action of NUP62 in these tumors and its interrelationship with other biomarkers can be further explored in subsequent studies, with the aim of providing more accurate targets for the treatment of these tumors.

Nuclear pore complex core proteins were shown to be extensively involved in metabolic reprogramming, such as NUP37, Nup210 (49–51). Therefore we speculated that NUP62 might be involved in metabolic pathways in tumors. In the subsequent analysis, we comprehensively analyzed the metabolic pathways in which NUP62 might be involved in pan-cancer by performing GSEA analysis on the KEGG metabolic gene set. The results indicated that NUP62 may inhibit multiple metabolic pathways in most tumors, such as steroid hormone synthesis, fatty acid synthesis, and glucose metabolism. This finding reveals a novel function of NUP62 as a nuclear pore complex core protein in tumor metabolism. Traditionally, NUP62 is mainly thought to be involved in the regulation of nuclear-plasmic transport and cellular signaling, whereas this study links it to metabolic pathways in tumors, providing a new perspective for understanding the role of NUP62 in tumorigenesis and progression.

Simultaneously, our research also revealed that the expression of NUP62 is significantly correlated with the infiltration levels of various immune cells, indicating that NUP62 can regulate the tumor immune microenvironment by influencing immune cells (52–55).

We delved into the correlation between NUP62 expression levels and immunotherapy response. The results showed that in clinical trials of immunotherapy, the response rate to immunotherapy was significantly higher in patients with high NUP62 expression than in patients with low expression. This suggests that NUP62 may be an important biomarker for predicting response to immunotherapy (56). By detecting patients' NUP62 expression levels, physicians may be able to more accurately predict which patients are more likely to benefit from immunotherapy, thereby optimizing the treatment regimen and improving the therapeutic efficacy. The results of the ROC curve analysis showed the potential efficacy of NUP62 in predicting immunotherapy response, which provides a new way of thinking for the development of immunotherapy evaluation methods (57). Traditional immunotherapy assessment methods mainly rely on indicators such as changes in tumor size, but these indicators often suffer from lag and inaccuracy. In contrast, biomarker-based prediction methods may be able to assess immunotherapy effects earlier and more accurately, thus guiding the adjustment and optimization of treatment regimens (58, 59). The study also found that the overall survival of patients with high NUP62 expression in immunotherapy was significantly longer than that of patients with low expression. This suggests that NUP62 may be associated with immunotherapy resistance (60). Through in-depth study of the mechanism of NUP62's role in immunotherapy resistance, it may provide new strategies and methods for overcoming immunotherapy resistance, thereby improving the effectiveness of immunotherapy and patient survival (61, 62).

The significant negative correlation of NUP62 with CTLA-4 may imply that the low expression of NUP62 in these two cancers is associated with an attenuated immunosuppressive state (63). This suggests that NUP62 expression in these cancers may not be the primary factor promoting immune evasion or that it interacts in a complex manner with other immune regulatory mechanisms. The significant correlation of NUP62 with the expression of immune-related genes (e.g., THCA, KIRC, KIRP, and PCPG) in multiple cancer types suggests that it may play a role in a wide range of immune regulatory processes (64). This further supports the idea that NUP62 serves as an important node in the cancer immunoregulatory network. Given the significant correlation of NUP62 with immune-related genes, it could be a potential target for immunotherapy (65). By regulating the expression or function of NUP62, it may be able to influence the activity of immune cells and the immune status in the tumor microenvironment, thus providing new strategies for immunotherapy. In the future, further in-depth studies can be conducted to investigate how NUP62 interacts with immune-related genes and how these interactions affect the tumor immune microenvironment and immunotherapeutic effects (66).

The findings suggest that NUP62 expression level may become a marker for predicting the efficacy of specific drugs (67). This means that in future clinical practice, physicians can select the most likely effective drugs based on a patient's NUP62 expression level, enabling more precise and personalized treatment (68). By understanding the relationship between NUP62 and drug sensitivity, drug developers can design new drugs in a more targeted manner, especially for those drugs that are positively or negatively correlated with NUP62 expression levels (69). This biomarker-based drug development strategy is expected to improve the success rate and clinical application of new drugs. In addition, by monitoring changes in NUP62 expression levels, physicians can make timely adjustments to treatment regimens to avoid or delay the onset of drug resistance. In addition, the efficacy of certain drugs, such as those negatively correlated with NUP62 expression levels, may be affected by NUP62 expression levels, and therefore, other alternative drugs or combination strategies may need to be explored in specific patient populations (70, 71). The present study reveals a novel role of NUP62 in drug sensitivity, which provides important clues for an in-depth understanding of its biological functions and regulatory mechanisms. This can help to further expand the application areas of biomarker research and improve the diagnosis and treatment of diseases such as cancer (72–74).

Additionally, we validated the differential expression of NUP62 between gastric cancer tissues and their adjacent non-cancerous tissues.

In summary, this study revealed the expression characteristics of NUP62 in multiple malignancies and its associations with tumor-related pathways, clinical features, prognosis, and tumor immunity. These findings provide crucial insights into our understanding of the role of NUP62 in tumors and offer new targets for future tumor diagnosis and immunotherapy. However, to fully uncover the mechanisms of NUP62 in tumors, further in-depth research and exploration are required.

Data availability statement

The original contributions presented in the study are included in the article/Supplementary Files, further inquiries can be directed to the corresponding authors.

Ethics statement

The studies involving humans were approved by the Ethics Committee of the Guizhou Provincial People's Hospital. The studies were conducted in accordance with the local legislation and institutional requirements. The participants provided their written informed consent to participate in this study.

Author contributions

LC: Conceptualization, Data curation, Formal analysis, Investigation, Methodology, Project administration, Resources, Software, Supervision, Validation, Visualization, Writing – original draft. YH: Conceptualization, Data curation, Formal analysis, Funding acquisition, Investigation, Methodology, Project administration, Resources, Software, Supervision, Validation, Visualization, Writing – original draft. MD: Conceptualization, Data curation, Formal analysis, Investigation, Methodology, Resources, Software, Supervision, Validation, Visualization, Writing – original draft. TY: Data curation, Investigation, Methodology, Software, Writing – original draft. YC: Data curation, Investigation, Methodology, Writing – original draft. BW: Data curation, Investigation, Methodology, Software, Writing – original draft. DC: Investigation, Software, Writing – review & editing. CL: Investigation, Methodology, Software, Supervision, Writing – review & editing.

Funding

The author(s) declare that financial support was received for the research, authorship, and/or publication of this article. This work was supported by the [Guizhou Provincial Health and Wellness Commission] under Grant [gzwkj 2021-102]; The National Natural Science Foundation of China (No. 82260084); Guizhou Provincial Science and Technology Agency Project (Qian Ke He Foundation ZK [2023] General 217); and Support by Key Advantageous Discipline Construction Project of Guizhou Provincial Health Commission in 2023.

Conflict of interest

The authors declare that the research was conducted in the absence of any commercial or financial relationships that could be construed as a potential conflict of interest.

Generative AI statement

The author(s) declare that no Generative AI was used in the creation of this manuscript.

Publisher's note

Supplementary material

The Supplementary Material for this article can be found online at: https://www.frontiersin.org/articles/10.3389/fimmu.2025.1559396/full#supplementary-material

SUPPLEMENTARY FIGURE 1
Expression Levels of NUP62 in Cell Line Models, Cancerous, and Normal Tissues. **(A)** Immunofluorescence images and merged images of the nuclei, NUP62 protein, microtubules, and endoplasmic reticulum (ER) in A-431, U2OS, and U-251MG cell lines obtained from the HPA database. **(B)** IHC images of NUP62 protein expression in normal and tumor tissues obtained from the HPA database.

References

1. Sun S, Wang YH, Gao X, Wang HY, Zhang L, Wang N, et al. Global cancer statistics 2022: GLOBOCAN estimates of incidence and mortality worldwide for 36 cancers in 185 countries. *CA. Cancer J Clin*. (2024) 74:229–63. doi: 10.3322/caac.21834

2. Siegel RL, Miller KD, Wagle NS, Jemal A. Cancer statistics, 2023. *CA. Cancer J Clin*. (2023) 73:17–48. doi: 10.3322/caac.21763

3. Wu F, Yang J, Liu J, Wang Y, Mu J, Zeng Q, et al. Signaling pathways in cancer-associated fibroblasts and targeted therapy for cancer. *Signal Transduction Targeting Ther*. (2021) 6:1–35. doi: 10.1038/s41392-021-00641-0

4. Punekar SR, Velcheti V, Neel BG, Wong K-K. The current state of the art and future trends in RAS-targeted cancer therapies. *Nat Rev Clin Oncol*. (2022) 19:637–55. doi: 10.1038/s41571-022-00671-9

5. Pérez-Herrero E, Fernández-Medarde A. Advanced targeted therapies in cancer: Drug nanocarriers, the future of chemotherapy. *Eur J Pharm Biopharm*. (2015) 93:52–79. doi: 10.1016/j.ejpb.2015.03.018

6. Zhang Y, Yan L, Liu A, Li F, Li Y, Zhang Y. Cell polarity-related gene PTK7, a potential diagnostic biomarker in pan-cancer. *Curr Med Chem*. (2024) 31:1–18. doi: 10.2174/0109298673313999240816103054

7. Zhang Y, Xue Y, Gao Y, Zhang Y. Prognostic and predictive value of pathohistological features in gastric cancer and identification of SLITRK4 as a potential biomarker for gastric cancer. *Sci Rep*. (2024) 14:29241. doi: 10.1038/s41598-024-80292-7

8. Cordani M, Dando I, Ambrosini G, González-Menéndez P. Signaling, cancer cell plasticity, and intratumor heterogeneity. *Cell Commun Signal*. (2024) 22:255. doi: 10.1186/s12964-024-01643-5

9. DeBerardinis RJ, Chandel NS. Fundamentals of cancer metabolism. *Sci Advances*. 2(5):e1600200. doi: 10.1126/sciadv.1600200

10. Vaghari-Tabari M, Ferns GA, Qujeq D, Andevari AN, Sabahi Z, Moein S. Signaling, metabolism, and cancer: An important relationship for therapeutic intervention. *J Cell Physiol*. (2021) 236:5512–32. doi: 10.1002/jcp.v236.8

11. Vander Heiden MG, Cantley LC, Thompson CB. Understanding the warburg effect: the metabolic requirements of cell proliferation. *Science*. (2009) 324:1029–33. doi: 10.1126/science.1160809

12. Gyamfi J, Kim J, Choi J. Cancer as a metabolic disorder. *Int J Mol Sci*. (2022) 23:1155. doi: 10.3390/ijms23031155

13. Dey P, Kimmelman AC, DePinho RA. Metabolic codependencies in the tumor microenvironment. *Cancer Discovery*. (2021) 11:1067–81. doi: 10.1158/2159-8290.CD-20-1211

14. Koppenol WH, Bounds PL, Dang CV. Otto Warburg's contributions to current concepts of cancer metabolism. *Nat Rev Cancer*. (2011) 11:325–37. doi: 10.1038/nrc3038

15. Ashton TM, McKenna WG, Kunz-Schughart LA, Higgins GS. Oxidative phosphorylation as an emerging target in cancer therapy. *Clin Cancer Res*. (2018) 24:2482–90. doi: 10.1158/1078-0432.CCR-17-3070

16. Chelakkot C, Chelakkot VS, Shin Y, Song K. Modulating glycolysis to improve cancer therapy. *Int J Mol Sci*. (2023) 24:2606. doi: 10.3390/ijms24032606

17. Wang Z-H, Peng W-B, Zhang P, Yang X-P, Zhou Q. Lactate in the tumour microenvironment: From immune modulation to therapy. *eBioMedicine*. (2021) 73. doi: 10.1016/j.ebiom.2021.103627

18. Ngwa VM, Edwards DN, Philip M, Chen J. Microenvironmental metabolism regulates antitumor immunity. *Cancer Res*. (2019) 79:4003–8. doi: 10.1158/0008-5472.CAN-19-0617

19. Chuang Y-M, Tzeng S-F, Ho P-C, Tsai C-H. Immunosurveillance encounters cancer metabolism. *EMBO Rep*. (2024) 25:471–88. doi: 10.1038/s44319-023-00038-w

20. Kalverda B, Pickersgill H, Shloma VV, Fornerod M. Nucleoporins directly stimulate expression of developmental and cell-cycle genes inside the nucleoplasm. *Cell*. (2010) 140:360–71. doi: 10.1016/j.cell.2010.01.011

21. Echeverría PC, Mazaira G, Erlejman A, Gomez-Sanchez C, Piwien Pilipuk G, Galigniana MD. Nuclear import of the glucocorticoid receptor-hsp90 complex through the nuclear pore complex is mediated by its interaction with nup62 and importin β. *Mol Cell Biol*. (2009) 29:4788–97. doi: 10.1128/MCB.00649-09

22. Zhou T, Li S, Zhong W, Vihervaara T, Beaslas O, Perttila J, et al. OSBP-related protein 8 (ORP8) regulates plasma and liver tissue lipid levels and interacts with the nucleoporin nup62. *PloS One*. (2011) 6:e21078. doi: 10.1371/journal.pone.0021078

23. Simon DN, Rout MP. Cancer and the nuclear pore complex. In: Schirmer EC, de las Heras JI, editors. *Cancer biology and the nuclear envelope: recent advances may elucidate past paradoxes*. Springer, New York, NY (2014). p. 285–307. doi: 10.1007/978-1-4899-8032-8_13

24. Singh U, Bindra D, Samaiya A, Mishra RK. Overexpressed Nup88 stabilized through interaction with Nup62 promotes NF-κB dependent pathways in cancer. *Front Oncol*. (2023) 13. doi: 10.3389/fonc.2023.1095046

25. Betancor YZ, Ferreiro-Pantin M, Anido-Herranz U, Fuentes-Losada M, Leon-Mateos L, Garcia-Acuna SM, et al. A three-gene expression score for predicting clinical benefit to anti-PD-1 blockade in advanced renal cell carcinoma. *Front Immunol*. (2024) 15. doi: 10.3389/fimmu.2024.1374728

26. Liu H, Yan Y, Chen R, Zhu M, Lin J, He C, et al. Integrated nomogram based on five stage-related genes and TNM stage to predict 1-year recurrence in hepatocellular carcinoma. *Cancer Cell Int*. (2020) 20:140. doi: 10.1186/s12935-020-01216-9

27. Borlido J, D'Angelo MA. Nup62-mediated nuclear import of p63 in squamous cell carcinoma. *EMBO Rep*. (2018) 19:3–4. doi: 10.15252/embr.201745497

28. Hazawa M, Lin DC, Kobayashi A, Jiang YY, Xu L, Dewi FRP, et al. ROCK-dependent phosphorylation of NUP62 regulates p63 nuclear transport and squamous cell carcinoma proliferation. *EMBO Rep*. (2018) 19:73–88. doi: 10.15252/embr.201744523

29. Shen W, Song Z, Zhong X, Huang M, Shen D, Gao P, et al. Sangerbox: A comprehensive, interaction-friendly clinical bioinformatics analysis platform. *Imeta* (2022) 1(3):e36. doi: 10.1002/imt2.36

30. Liu Z, Liu L, Weng S, Xu H, Xing Z, Ren Y, et al. BEST: a web application for comprehensive biomarker exploration on large-scale data in solid tumors. *J Big Data*. (2023) 10:165. doi: 10.1186/s40537-023-00844-y

31. Madheshiya PK, Shukla E, Singh J, Bawaria S, Ansari MY, Chauhan RJMBotC. Insights into the role of Nup62 and Nup93 in assembling cytoplasmic ring and central transport channel of the nuclear pore complex. *Mol Biol Cell*. (2022) 33(14):ar139. doi: 10.1091/mbc.E22-01-0027

32. Klein CA. Cancer progression and the invisible phase of metastatic colonization. *Nat Rev Cancer*. (2020) 20:681–94. doi: 10.1038/s41568-020-00300-6

33. Kumar R, Paul AM, Amjesh R, George B, Pillai MR. Coordinated dysregulation of cancer progression by the HER family and p21-activated kinases. *Cancer Metastasis Rev*. (2020) 39:583–601. doi: 10.1007/s10555-020-09922-6

34. Wang L, Guo X-L. Molecular regulation of galectin-3 expression and therapeutic implication in cancer progression. *Biomed Pharmacother*. (2016) 78:165–71. doi: 10.1016/j.biopha.2016.01.014

35. Iwatsubo T, Ishihara R, Morishima T, Maekawa A, Nakagawa K, Arao M, et al. Impact of age at diagnosis of head and neck cancer on incidence of metachronous cancer. *BMC Cancer*. (2019) 19:3. doi: 10.1186/s12885-018-5231-7

36. Pawelec G, Derhovanessian E, Larbi A. Immunosenescence and cancer. *Crit Rev Oncol Hematol*. (2010) 75:165–72. doi: 10.1016/j.critrevonc.2010.06.012

37. Muermann MM, Wassersug RJ. Prostate cancer from a sex and gender perspective: A review. *Sex Med Rev*. (2022) 10:142–54. doi: 10.1016/j.sxmr.2021.03.001

38. Menz A, Weitbrecht T, Gorbokon N, Buscheck F, Luebke AM, Kluth M, et al. Diagnostic and prognostic impact of cytokeratin 18 expression in human tumors: a tissue microarray study on 11,952 tumors. *Mol Med*. (2021) 27:16. doi: 10.1186/s10020-021-00274-7

39. Krings G, Nystrom M, Mehdi I, Vohra P, Chen Y-Y. Diagnostic utility and sensitivities of GATA3 antibodies in triple-negative breast cancer. *Hum Pathol*. (2014) 45:2225–32. doi: 10.1016/j.humpath.2014.06.022

40. Ding N, Li M, Zhao X. PHF5A is a potential diagnostic, prognostic, and immunological biomarker in pan-cancer. *Sci Rep*. (2023) 13:17521. doi: 10.1038/s41598-023-44899-6

41. Zhang L, Barritt GJ. TRPM8 in prostate cancer cells: a potential diagnostic and prognostic marker with a secretory function? *Endocr. Relat Cancer*. (2006) 13:27–38. doi: 10.1677/erc.1.01093

42. Mesci A, Lucien F, Huang X, Wang EH, Shin D, Meringer M, et al. RSPO3 is a prognostic biomarker and mediator of invasiveness in prostate cancer. *J Transl Med*. (2019) 17:125. doi: 10.1186/s12967-019-1878-3

43. Schinke H, Shi E, Lin Z, Quadt T, Kranz G, Zhou J, et al. A transcriptomic map of EGFR-induced epithelial-to-mesenchymal transition identifies prognostic and therapeutic targets for head and neck cancer. *Mol Cancer*. (2022) 21:178. doi: 10.1186/s12943-022-01646-1

44. Icard P, Fournel L, Wu Z, Alifano M, Lincet H. Interconnection between metabolism and cell cycle in cancer. *Trends Biochem Sci*. (2019) 44:490–501. doi: 10.1016/j.tibs.2018.12.007

45. Evan GI, Vousden KH. Proliferation, cell cycle and apoptosis in cancer. *Nature*. (2001) 411:342–8. doi: 10.1038/35077213

46. Lord CJ, Ashworth A. The DNA damage response and cancer therapy. *Nature*. (2012) 481:287–94. doi: 10.1038/nature10760

47. Basu AK. DNA damage, mutagenesis and cancer. *Int J Mol Sci*. (2018) 19:970. doi: 10.3390/ijms19040970

48. Kang T-H. DNA damage, repair, and cancer metabolism. *Int J Mol Sci*. (2023) 24:16430. doi: 10.3390/ijms242216430

49. Liu Z, Hu Q, Luo Q, Zhang G, Yang W, Cao K, et al. NUP37 accumulation mediated by TRIM28 enhances lipid synthesis to accelerate HCC progression. *Oncogene*. (2024) 43:3255–67. doi: 10.1038/s41388-024-03167-1

50. Zaitsava H, Gachowska M, Bartoszewska E, Kmiecik A, Kulbacka J. The potential of nuclear pore complexes in cancer therapy. *Molecules*. (2024) 29:4832. doi: 10.3390/molecules29204832

51. Han F, Fan X, Hu M, Wen J, Wang J, Zhang D, et al. Nup210 promotes colorectal cancer progression by regulating nuclear plasma transport. *Lab Invest*. (2024) 104. doi: 10.1016/j.labinv.2024.102149

52. Gajewski TF, Schreiber H, Fu Y-X. Innate and adaptive immune cells in the tumor microenvironment. *Nat Immunol*. (2013) 14:1014–22. doi: 10.1038/ni.2703

53. Fu T, Dai L-J, Wu S-Y, Xiao Y, Ma D, Jiang Y-Z, et al. Spatial architecture of the immune microenvironment orchestrates tumor immunity and therapeutic response. *J Hematol Oncol.J Hematol Oncol*. (2021) 14:98. doi: 10.1186/s13045-021-01103-4

54. Lv B, Wang Y, Ma D, Cheng W, Liu J, Yong T, et al. Immunotherapy: reshape the tumor immune microenvironment. *Front Immunol*. (2022) 13. doi: 10.3389/fimmu.2022.844142

55. Mei K, Chen Z, Huang L, Wang J, Wei Y. Correlation between the immune microenvironment and bladder cancer based on a prognostic miRNA risk model. *Cancer Insight*. (2024) 3:14–25. doi: 10.58567/ci03020002

56. Liu Y, Zhang B, Wu X, Wang F, Yang Z, Li M, et al. A facile liquid biopsy assay for highly efficient CTCs capture and reagent-less monitoring of immune checkpoint PD-L1 expression on CTCs with non-small cell lung cancer patients. *Biosens. Bioelectron*. (2025) 275:117236. doi: 10.1016/j.bios.2025.117236

57. Zhang N, Li C, Zhao Z, Jiang B, Wang W, Sun F, et al. Immune microenvironment features underlying the superior efficacy of neoadjuvant

immunochemotherapy over chemotherapy in local advanced gastric cancer. *Front Immunol*. (2025) 16. doi: 10.3389/fimmu.2025.1497004

58. Wang X, Li J, Zhu Y, Shen H, Ding J, Zeng T, et al. Targeting ADAR1 with a small molecule for the treatment of prostate cancer. *Nat Cancer*. (2025) 1–19. doi: 10.1038/s43018-025-00907-4

59. Naing A, McKean M, Tolcher A, Victor A, Hu P, Gao W, et al. TIGIT inhibitor M6223 as monotherapy or in combination with bintrafusp alfa in patients with advanced solid tumors: a first-in-human, phase 1, dose-escalation trial. *J Immunother. Cancer*. (2025) 13:e010584. doi: 10.1136/jitc-2024-010584

60. Ghorbaninezhad F, Nour MA, Farzam OR, Saeedi H, Vanan AG, Bakhshivand M, et al. The tumor microenvironment and dendritic cells: Developers of pioneering strategies in colorectal cancer immunotherapy? *Biochim Biophys Acta BBA - Rev Cancer*. (2025) 1880:189281. doi: 10.1016/j.bbcan.2025.189281

61. Sardar P, Beresford-Jones BS, Xia W, Shabana O, Suyama S, Ramos RJF, et al. Gut microbiota-derived hexa-acylated lipopolysaccharides enhance cancer immunotherapy responses. *Nat Microbiol 1–13*. (2025). doi: 10.1038/s41564-025-01930-y

62. Pan S, Wang Z. Antiviral therapy can effectively suppress irAEs in HBV positive hepatocellular carcinoma treated with ICIs: validation based on multi machine learning. *Front Immunol*. (2025) 15. doi: 10.3389/fimmu.2024.1516524

63. Wu Y, Yin M, Xia W, Dou B, Liu X, Sun R. Enhancing NK cell antitumor activity with natural compounds: research advances and molecular mechanisms. *Phytother. Res*. (2025). doi: 10.1002/ptr.8456

64. Yang J, Tang S, Saba NF, Shay C, Teng Y. Tumor secretome shapes the immune landscape during cancer progression. *J Exp Clin Cancer Res*. (2025) 44:47. doi: 10.1186/s13046-025-03302-0

65. Huang M, Huang Z, Miao S, Chen X, Tan Y, Zhou Y, et al. Bioinformatics Analysis of coagulation-related genes in lung adenocarcinoma: unveiling prognostic indicators and treatment pathways. *Sci Rep*. (2025) 15:4972. doi: 10.1038/s41598-025-87669-2

66. Liu R, Ji Z, Wang X, Zhu L, Xin J, Ma L, et al. Regorafenib plus sintilimab as a salvage treatment for microsatellite stable metastatic colorectal cancer: a single-arm, open-label, phase II clinical trial. *Nat Commun*. (2025) 16:1481. doi: 10.1038/s41467-025-56748-3

67. Sharma D, Arumugam S. Pharmacophore-based identification and in Silico characterization of microbial metabolites as potential modulators of Wnt signaling pathway in colorectal cancer therapy. *Mol Divers*. (2025). doi: 10.1007/s11030-024-11103-4

68. Wan X, Jiang M, Madan S. Research progress of nanomedicine for tumor immunotherapy. *Cancer Insight*. (2023) 3:83–98. doi: 10.2174/0109298673313999240816103054

69. Zhang C, Chen YY, Chen S, Wang Y, Yuan Y, Yang X, et al. Characterization of an enhancer RNA signature reveals treatment strategies for improving immunotherapy efficacy in cancer. *Cancer Res*. (2025). doi: 10.1158/0008-5472.CAN-24-2289

70. Long H, Zhou J, Zhou C, Xie S, Wang J, Tan M, et al. Proteomic characterization of liver cancer cells treated with clinical targeted drugs for hepatocellular carcinoma. *Biomedicines*. (2025) 13:152. doi: 10.3390/biomedicines13010152

71. Zhao L, Shang J, Meng X, He X, Zhang Y, Liu JX. Adaptive multi-kernel graph neural network for drug-drug interaction prediction. *Interdiscip. Sci Comput Life Sci*. (2025). doi: 10.1007/s12539-024-00684-1

72. Kuai X, Wei C, He X, Wang F, Wang C, Ji J. The potential value of RPS27A in prognosis and immunotherapy: from pan-cancer analysis to hepatocellular carcinoma validation. *ImmunoTargets Ther*. (2024) 13:673–90. doi: 10.2147/ITT.S493217

73. Liu S, He M, Sun H, Wu Y, Jin W. 5-hydroxytryptamine G-protein-coupled receptor family genes: key players in cancer prognosis, immune regulation, and therapeutic response. *Genes*. (2024) 15:1541. doi: 10.3390/genes15121541

74. Zhou T, Zhang DD, Jin J, Xie J, Yu J, Zhu C, et al. Multiomic characterization, immunological and prognostic potential of SMAD3 in pan-cancer and validation in LIHC. *Sci Rep*. (2025) 15:657. doi: 10.1038/s41598-024-84553-3

frontiers | Frontiers in Immunology

TYPE Original Research
PUBLISHED 10 April 2025
DOI 10.3389/fimmu.2025.1560717

OPEN ACCESS

EDITED BY
Lei Huang,
University of Massachusetts Medical School, United States

REVIEWED BY
Haocai Chang,
South China Normal University, China
Hong Kwan Kim,
Sungkyunkwan University, Republic of Korea

*CORRESPONDENCE
Qiancheng Luo
luoqiancheng14@163.com;
qufrrzwqryrd@hotmail.com
Kailiang Xu
xkl01934@glhospital.com;
kamkwhfedomxw@hotmail.com

†These authors have contributed equally to this work

RECEIVED 14 January 2025
ACCEPTED 28 February 2025
PUBLISHED 10 April 2025

CITATION
Liu R, Jia L, Yu L, Lai D, Li Q, Zhang B, Guo E, Xu K and Luo Q (2025) Interaction between post-tumor inflammation and vascular smooth muscle cell dysfunction in sepsis-induced cardiomyopathy.
Front. Immunol. 16:1560717.
doi: 10.3389/fimmu.2025.1560717

Interaction between post-tumor inflammation and vascular smooth muscle cell dysfunction in sepsis-induced cardiomyopathy

Rui Liu[1†], Lina Jia[2†], Lin Yu[1], Detian Lai[1], Qingzhu Li[1], Bingyu Zhang[1], Enwei Guo[1], Kailiang Xu[1*] and Qiancheng Luo[1*]

[1]Department of Critical Care Medicine, Shanghai Pudong New Area Gongli Hospital, Shanghai, China, [2]Hebei Medical University, Shijiazhuang, China

Background: Sepsis-induced cardiomyopathy (SIC) presents a critical complication in cancer patients, contributing notably to heart failure and elevated mortality rates. While its clinical relevance is well-documented, the intricate molecular mechanisms that link sepsis, tumor-driven inflammation, and cardiac dysfunction remain inadequately explored. This study aims to elucidate the interaction between post-tumor inflammation, intratumor heterogeneity, and the dysfunction of VSMC in SIC, as well as to evaluate the therapeutic potential of exercise training and specific pharmacological interventions.

Methods: Transcriptomic data from NCBI and GEO databases were analyzed to identify differentially expressed genes (DEGs) associated with SIC. Weighted gene co-expression network analysis (WGCNA), gene ontology (GO), and KEGG pathway enrichment analyses were utilized to elucidate the biological significance of these genes. Molecular docking and dynamics simulations were used to investigate drug-target interactions, and immune infiltration and gene mutation analyses were carried out by means of platforms like TIMER 2.0 and DepMap to comprehend the influence of DVL1 on immune responsiveness.

Results: Through the utilization of the datasets, we discovered the core gene DVL1 that exhibited remarkable up-regulated expression both in SIC and in diverse kinds of cancers, which were associated with poor prognosis and inflammatory responses. Molecular docking revealed that Digoxin could bind to DVL1 and reduce oxidative stress in SIC. The DVL1 gene module related to SIC was identified by means of WGCNA, and the immune infiltration analysis demonstrated the distinctive immune cell patterns associated with DVL1 expression and the impact of DVL1 on immunotherapeutic resistance.

Conclusions: DVL1 is a core regulator of SIC and other cancers and, therefore, can serve as a therapeutic target. The present study suggests that targeted pharmacological therapies to enhance response to exercise regimens may be a

novel therapeutic tool to reduce the inflammatory response during sepsis, particularly in cancer patients. The identified drugs, Digoxin, require further *in vivo* and clinical studies to confirm their effects on SIC and their potential efforts to improve outcomes in immunotherapy-resistant cancer patients.

KEYWORDS

sepsis induced cardiomyopathy, DVL1, intratumor heterogeneity, oxidative stress, drug therapy, immunotherapy resistance, molecular docking, exercise training

1 Background

Sepsis-induced cardiomyopathy (SIC) is a common serious complication in critically ill cancer patients (1, 2). This condition leads to cardiac dysfunction, which is strongly associated with multiple organ failure, thereby increasing the risk of death (1, 2). Epidemiological studies have shown that SIC has a high incidence in critically ill patients, especially in cancer patients with accompanying sepsis, where its mortal (3, 4). This may be closely related to factors such as cancer-related chronic inflammation and immune dysfunction (5, 6). In recent years, an increasing number of studies have focused on the mechanisms of SIC in cancer patients, finding that the tumor microenvironment (TME) may interact with the immune imbalance related to sepsis, thus aggravating the development of SIC (7, 8). In addition, immunotherapy, chemotherapy, and targeted therapy may have an impact on the cardiovascular system and further increase the susceptibility to SIC in cancer patients (9, 10). In recent years, with technological advances, through RNA sequencing and spatial transcriptomics, scientists have revealed the functions and interactions of immune cells in the tumor microenvironment (11–13). Therefore, the systematic investigation of the molecular mechanisms of SIC and the exploration of potential therapeutic strategies may have important clinical implications for improving the prognosis of cancer patients (14). The pathomechanisms of SIC involve systemic inflammation, oxidative stress, mitochondrial dysfunction, as well as immune dysregulation (15, 16). In sepsis, a large number of proinflammatory cytokines (TNF- α, IL-6, IL-1 β) are released, triggering a cascade of inflammatory responses, leading to cardiomyocyte damage, mitochondrial collapse, deregulation of calcium homeostasis and, ultimately,myocardial contractile dysfunction (4, 17). In addition, oxidative stress and overproduction of ROS not only exacerbate cellular damage but may also further worsen the progression of SIC by inducing the loss of mitochondrial membrane potential and abnormal energy metabolism (18, 19). Increasing awareness of the role of cell death and metabolic regulation in disease progression is providing new targets and strategies for developing drugs (20–22). In cancer patients, the occurrence of SIC is also significantly affected by the tumor microenvironment. Macrophage polarization is closely related to changes in the immune microenvironment and crosstalk between immune cells (23, 24). Immunosuppressive cytokines secreted by tumors, such as TGF-β and IL-10, weaken the body's ability to resist infection and inhibit the normal regulation of inflammatory response, leading to more severe sepsis-related myocardial injury (25, 26). At the same time, patients resistant to immunotherapy may exhibit more severe sepsis-associated cardiac damage, as TME-driven immune escape mechanisms may further contribute to inflammatory imbalance and immune hyperactivation in a septic setting (27, 28). Although the molecular mechanisms of SIC have been well studied in typical sepsis patients, the specific characteristics of SIC, immune-metabolic interactions, and their responses to existing treatment options in cancer patients are still underexplored (29, 30). Cancer-induced chronic inflammation and immunosuppression may exacerbate the development and progression of SIC, highlighting the importance of studying the role of tumor-associated immune regulation in the progression of sepsis-associated cardiomyopathy (31). In particular, considering the complexity of the cancer microenvironment, which includes different genetic, cellular, and tissue characteristics, leading to different therapeutic responses (32, 33).

The pathogenesis of SIC is closely related to the systemic inflammatory response, excessive cytokine release, and oxidative stress (34, 35). Hyperactivation of the immune system during sepsis leads to the massive release of pro-inflammatory cytokines such as tumor necrosis factor- α (TNF- α), interleukin-6 (IL-6), and interleukin-1 β (IL-1 β) (36, 37). These inflammatory mediators disrupt cardiac function, induce mitochondrial damage, dysregulation of calcium homeostasis, and promote cardiomyocyte apoptosis (38, 39). This inflammatory cascade is more complex in cancer patients, further exacerbated by tumor-induced immunosuppression. Tumor cells can secrete immunosuppressive cytokines such as transforming growth factor- β (TGF- β) and interleukin-10 (IL-10), which can inhibit the activation of cytotoxic immune cells and promote the formation of an immunotolerant tumor microenvironment (40, 41). Moreover, oxidative stress is also a key factor in the development of SIC. Reactive oxygen species (ROS) accumulation causes cell damage and apoptosis, which further deteriorates cardiac function and intensifies cardiac dysfunction (42, 43). Bioinformatics technologies have played a key role in the study of gene expression and regulatory mechanisms, providing an essential basis for understanding biological processes (44, 45).

The high incidence rate and the high intratumoral heterogeneity of tumors show the high pathological characteristics of SIC in cancer patients, as well as the high variability of treatment (46, 47). This heterogeneity is implicated by genetic variation and phenotypic heterogeneity, directly modulating the effectiveness of various treatment modalities, including immunotherapy. This variation presents a barrier to consistent clinical results (2, 48). Hence, it is crucial to understand the interaction between systemic inflammation, genetic variation, and the tumor microenvironment for the development of personalized treatment strategies for SIC in cancer patients (49, 50). While SIC is commonly associated with acute cardiac insufficiency and with symptoms such as hypotension and arrhythmia, clinically, it is associated with a decreased survival rate (1, 2). Continuous deterioration in cardiac function is associated with a marked reduction in quality of life. Still, it may also enhance the onset of complications, including chronic heart failure (CHF) and systemic multiorgan dysfunction (SOD) (51, 52). Thus, an in-depth understanding of the underlying pathogenic mechanisms of SIC will contribute to the exploration of therapeutic strategies with higher targeting and clinical applicability (53, 54). Individualized precision medicine intervention strategy combining several factors could be more beneficial to improve the therapeutic outcome of SIC (55). Despite extensive research on the inflammatory response and cellular damage mechanisms of SIC, there remain significant gaps in understanding the role of specific cell types, such as VSMCs, in sepsis-associated cardiac dysfunction (56). Most of the existing studies have focused on the effects of cytokine release on cardiomyocytes and ignored the role of VSMCs as an essential component of the cardiovascular system in the development of SIC (57, 58). VSMCs are mainly responsible for maintaining vascular stability and regulating vascular tone, enabling blood vessels to adapt to dynamic changes in blood pressure and blood flow (59, 60).VSMCs can transition from a contractile to a synthetic form in a sepsis-induced inflammatory setting, displaying both pro-inflammatory and pro-oxidative traits (61, 62). This pathological remodeling not only exacerbates the vascular dysfunction but also may further drive the progression of SIC by worsening the myocardial microcirculation and exacerbating cardiac inflammation (48, 63). Single-cell multi-omics analysis can analyze the complex physiological processes at the single-cell level, facilitate a deep understanding of the transplant immune mechanism, and provide support for the optimization of treatment options (64, 65). Therefore, studying the mechanism of VSMCs in sepsis-related cardiac dysfunction will not only contribute to a deep understanding of the pathogenesis of SIC but may also provide new potential therapeutic targets to lay the foundation for precise intervention of SIC.

In this study, the DVL1 protein has become a key point. DVL1 is a core regulator of the Wnt/β -catenin signaling pathway and is capable of regulating cell proliferation, differentiation, and apoptosis (48, 63). In various cancers, abnormal DVL1 expression is associated with poor prognosis, indicating its relevance in tumor biology (66). Advances in big data technologies and bioinformatics tools have driven the identification and validation of disease markers, especially in the areas of immune microenvironment, cellular signaling, and metabolic regulation (67, 68). In a septic setting, abnormal activation of DVL1 may affect macrophage polarization and disrupt the balance between proinflammatory M1 and immunosuppressive M2 macrophages, thereby exacerbating the systemic inflammatory response and inhibiting immune recovery, accelerating SIC progression (58). In cancer metabolism, DVL1 may regulate glycolysis and mitochondrial bioenergetic metabolism through the Wnt signaling pathway (58, 69). It is shown that DVL1 overexpression may enhance the metabolic plasticity of tumor-associated immune cells and cardiomyocytes, leading to abnormal glucose utilization and impaired oxidative phosphorylation, thus aggravating the myocardial energy crisis in SIC (31, 70). Moreover, DVL1 may affect cardiac dysfunction through oxidative stress associated with mitochondrial signaling (71, 72). Studies have shown that overexpression of DVL1 can increase reactive oxygen species (ROS) generation, directly disrupt cardiomyocytes, and perturb the mitochondrial membrane potential (73, 74). Wnt signaling can also affect mitochondrial biosynthesis by interacting with PGC-1 α, exacerbating metabolic and function decline in SIC (75, 76). Although DVL1 is recognized as a key factor in gastrointestinal cancer and SIC, its specific molecular roles and pathways in sepsis, cancer metabolism,and cardiac dysfunction have not been fully explored (70, 77). Further exploration of the mechanism by which DVL1 regulates SIC could provide new ideas for the treatment of SIC (69, 78).

This research seeks to examine how post-tumor inflammation interacts with VSMC dysfunction, aiming to bridge a significant gap in the understanding of SIC mechanisms. Subsequently, determine potential therapeutic targets to alleviate the treatment burden of SIC in individuals with cancer (56, 79). Paying particular attention to the DVL1 expression pattern in gastrointestinal cancers and evaluating the potential utility of FDA approved drugs in the treatment of SIC(37,38). This study also combines bibliometric analysis to judge the application trend of computer-assisted drug design in SIC-targeted therapy, and to provide a theoretical basis for the development of new therapeutic strategies in the future (80, 81). The application of network pharmacology and experimental validation methods in drug research provides new approaches and strategies for drug research and development, such as studying the mechanism of action and efficacy of a drug in the treatment of new diseases (82, 83).

New technologies and molecular research methods have played an essential role in disease research and treatment (84, 85). This study adopted a multi-level integration strategy to integrate transcriptomic data analysis (86). Through the deep mining of a large number of transcriptomic data, key genes and signaling pathways closely related to various physiological and pathological processes can be screened out, and potential targets for drug development can be identified (87, 88). Meanwhile, the key genes and signaling pathways associated with SIC were systematically analyzed (89, 90). The study of the regulatory mechanisms of multiple biological processes provides a basis for the optimization of intervention strategies (91–93). In recent years, precision-targeted intervention strategies targeting specific proteins or gene pathways have made breakthroughs in improving treatment specificity or clinical efficacy. The combination of transcriptomics

with proteomics reveals key regulatory mechanisms of transcription factor networks and protein modification in disease (94, 95). This experimental study provides a successful experience for the individualized treatment of SIC (96, 97). This study further revealed the regulatory mechanism of VSMC dysfunction in SIC by post-tumor inflammation, focusing on immune cell infiltration, genetic heterogeneity, and its association with cardiovascular injury and assessing the potential of pharmacological intervention to alleviate pathological effects (98, 99). These findings enhance the comprehension of SIC's pathogenic mechanisms and support the creation of personalized treatment approaches (43, 48). By integrating bioinformatics, transcriptomics, and pharmacological techniques, we will study the specific role of A fresh perspective on precision treatment for SIC patients provided by DVL1 in SIC (100, 101).

2 Materials and methods

2.1 Analysis of differential gene expression in sepsis-related cardiomyopathy

Transcriptomic datasets concerning sepsis-related cardiomyopathy were sourced from the NCBI and GEO databases (http://www.ncbi.nlm.nih.gov/geo/) (102, 103). For this study, two specific datasets were chosen: GSE172270, containing 20 peripheral blood samples from healthy individuals and 47 from patients with acute myocardial infarction (AMI), and GSE57065, which includes 25 samples from healthy controls alongside 28 from individuals diagnosed with sepsis (103, 104). Differential gene expression analysis was conducted using the limma package, applying a threshold of an adjusted P-value < 0.05 and |log2 fold change (log_2FC)| > 1.00 to identify differentially expressed genes (DEGs). Volcano plots were employed to visualize the DEGs. To pinpoint common genes linked to sepsis-induced cardiomyopathy, Venn diagrams were used for comparative analysis. Subsequently, Gene Set Enrichment Analysis (GSEA) was performed to elucidate the functional roles of gene sets implicated in sepsis-related cardiomyopathy.

2.2 Development of a weighted gene co-expression network

To investigate gene expression patterns associated with sepsis-induced cardiomyopathy, genes exhibiting variance levels above the upper quartile were initially selected (90, 105). These selected genes were subsequently analyzed using the "WGCNA" package within R software to establish a weighted gene co-expression network (WGCNA) specific to sepsis-induced cardiomyopathy (55). The optimal soft-thresholding power (β) was determined by clustering the samples and using a scale-free network model to establish the association network by calculating the gene connection adjacency matrix. The topological overlap matrix (TOM) was used to measure gene similarity and create a hierarchical clustering tree. Dynamic tree-cutting methods were then employed to identify and refine gene modules from a constructed gene dendrogram. After the modules were established, the module eigengenes (MEs) for each cluster were calculated, followed by correlation with clinical characteristics of the AMI patients. To calculate the correlation between MEs and clinical traits, Pearson correlation was computed to find a module associated most closely with AMI, which was termed the key hub module. Further analyses were performed on this module, including validation of differentially expressed genes and functional enrichment. WGCNA was performed to screen hub genes, which were then overlapped with differentially expressed genes in sepsis-induced cardiomyopathy. This resulted in the identification of core genes closely associated with sepsis-induced cardiomyopathy. Using the clusterProfiler gene ontology (GO), common target genes for sepsis-induced cardiomyopathy were examined. R package in R and Perl. To elucidate the biological functions of these targets, this analysis involved the main GO categories, namely Cellular Component (CC), Molecular Function (MF), and Biological Process (BP). KEGG pathway enrichment analysis was also conducted using the clusterProfilerKEGG. R package, and pathway visualization performed using the path view package. The enrichment factor was used to assess the relevance of core pathway enrichments, revealing biological functions and signaling pathways that are involved in the pathophysiology of sepsis-induced cardiomyopathy.

2.3 Screening of FDA-approved drug library and molecular docking analysis

A library of 2,568 small molecules, all approved by the FDA (Food and Drug Administration), was selected for screening (106, 107). The molecular structures of these compounds were retrieved in SDF format from the DrugBank database (https://go.drugbank.com/) (108, 109). These molecules were imported into Chem3D software, where the structural optimization and energy minimization were performed using the MMFF94 force field (Halgren, 1999) within the Calculation module, and the optimized structures were saved in mol2 format. Core protein domains in pdb format were obtained from the PDB database (http://www.rcsb.org/), and preliminary processing, including solvent removal, was performed using PyMol software. Further preparations, including the addition of hydrogen atoms and assignment of charges, were executed using AutoDockTools, with both the protein targets and small molecules saved in pdbqt format. Grid parameters, including positions and dimensions, were defined, and the molecular docking between the ligands and target proteins was performed using Autodock-Vina. The results were analyzed using clustering heatmaps generated in R software, and PyMol was used for visualizing the docking interactions, yielding detailed molecular docking model diagrams.

2.4 Molecular dynamics simulation

Molecular dynamics (MD) simulations were performed using Gromacs version 2019.6 (110, 111). The optimal protein-ligand

docking model, as determined from docking outcomes, was selected as the starting conformation for the simulation, with GAPDH used as a positive control (112, 113). The protein was modeled using the amber14sb force field, whereas the small molecule was represented with the Gaff2 force field. Using the TIP3P water model, the complex system was solvated, and a water box was formed with sodium ions to neutralize its charge. The Verlet and cg algorithms were used for elastic simulations, with Particle-Mesh Ewald (PME) handling electrostatic interactions. The system was subjected to energy minimization through the steepest descent method with a set step limit. The cutoff distances for Coulomb and van der Waals forces were set at 1.4 nm. Equilibration was achieved through both the constant volume (NVT) and constant pressure (NPT) ensembles, followed by a 100 ns MD simulation under standard temperature and pressure conditions. During the MD run, the LINCS algorithm was used to constrain hydrogen bonds with a two fs integration time step. PME calculations utilized a cutoff distance of 1.2 nm, while a 10 Å cutoff was set for non-bonded interactions. Temperature was kept at 300 K using the V-rescale thermostat, and pressure was stabilized at 1 bar with the Berendsen barostat. A 30 ps equilibration period was conducted under both NVT and NPT conditions at 300 K, preceding the 100 ns MD simulation of the protein-ligand complex. Local conformational shifts during the simulation were assessed using the root mean square fluctuation (RMSF) with a threshold of 0.2. The radius of gyration (Rg) was used to evaluate the structural compactness of the system, while RMSF offered insights into specific site fluctuations throughout the simulation.

2.5 Expression landscape analysis of DVL1 in gastrointestinal tumors

Recognizing the close association between gastrointestinal tumors and sepsis, this study performed a comprehensive analysis of DVL1 expression in various gastrointestinal cancers (COAD, ESCA, READ, and STAD) by comparing its expression in tumor and adjacent normal tissues to elucidate its role in tumor development (114, 115). Data from the TCGA and GTEx databases were integrated to investigate disparities in DVL1 expression between healthy individuals and cancer patients. The ability of DVL1 levels to distinguish between cancerous and healthy tissues was assessed using the pROC package, which included calculating the 95% confidence interval, the area under the curve (AUC), and creating ROC curves. Additionally, expression patterns of DVL1 in various cell subpopulations were analyzed using single-cell datasets associated with gastrointestinal tumors.

For methylation analysis, emphasis was placed on the TSS1500, TSS200, 1st Exon, and 5' UTR regions, using Spearman correlation analysis to examine the relationship between methylation status and gene expression—particularly appropriate for analyzing correlations in non-normally distributed data. Copy number variation (CNV) analysis was carried out on 451 samples using the GISTIC scoring method, and the results were presented through bar charts. Chromosomal alterations were quantified, with indicators defined from C1 to C5. To explore expression differences among gene subgroups, ANOVA and TukeyHSD were employed for multiple comparisons.

Pathway activity was evaluated using the GSVA package with four parameters—z-score, GSVA, ssGSEA, and PLAGE—standardizing the results to Z-Score values. Differences in expression between tumor and normal tissues were tested using the Wilcoxon Rank Sum Test and visualized through boxplots using the ggplot2 package. The pan-cancer mutation landscape of the DVL1 gene was illustrated using the plotmafSummary function from the maftools package. Additionally, immune infiltration data from TCGA samples were retrieved from the TIMER 2.0 database to evaluate the presence of different immune cell types in the tumor microenvironment and their correlation with DVL1 expression. Correlations between immune cell abundance and gene expression were clearly illustrated using bar-scatter plots, showing correlation coefficients.

2.6 Spatial transcriptomic analysis of core genes at the single-cell level

In this paper, gene expression data obtained from the TISCH database for rectal cancer at the single-cell level up to October 2023 were analysed (116, 117). Heatmap of Gene Expression Patterns at the Single Cell Level in Different Cancer Types In order to detect and preserve gene expression patterns in different types of cancers, hierarchical clustering was performed using Euclidean distance and Ward's minimum variance method. Due to the use of UMAP (Uniform Mobility Approximation and Projection) for high-dimensional data exploration, the original data structure was preserved as part of an algorithm designed specifically for non-linear data. Using UMAP to elucidate biological differences in gene expression in our cohort. The Kruskal-Wallis rank sum test was used to determine differences in gene expression between cell types. The Wilcoxon rank sum test is a non-parametric test used to determine if there is a significant difference between two independent groups. It does not assume that the data follow a normal distribution. The AUCell score, which quantifies the variability of pathway activity in single cells, was also used, as well as UMAP for visualisation. This approach provides a comprehensive view of the distribution of pathway activity and helps to identify potential biological differences.

2.7 Cell culture

RAW 264.7 Mouse macrophages (ATCC, Rockville, USA) were cultured in DMEM medium containing 10% heat-inactivated foetal bovine serum (FBS), 100 U/mL penicillin, and 100 µg/mL streptomycin at 37°C under 5% CO_2. Digoxin and general HPLC reagents were purchased from Sigma (St. Louis, MO, USA). Cell culture media and supplements were provided by Invitrogen (Carlsbad, USA). THP-1 human monocytes (ATCC, Rockville, USA) were cultured in RPMI 1640 medium, which also contained 10% FBS, 100 U/mL penicillin, and 100 µg/mL streptomycin, and

incubated under the same conditions at 37°C and 5% CO_2 conditions. To induce differentiation into macrophages, THP-1 monocytes were exposed to PMA (100 ng/mL) for 5 days. To investigate the effect of Digoxin on P-glycoprotein (P-gp) activity in macrophages, RAW 264.7 cells were treated with 0.2 μM Digoxin for 4 hours (118, 119). Digoxin concentrations used in the treatments included 0, 0.025 mM (low), 0.05 mM (medium), and 0.1 mM (high).

Human colorectal cancer cell lines, including HCT116, SW480, CX-1, SW620, LoVo, COLO 205, LS-174T, and the normal colonic mucosa cell line FHC, were purchased from the American Typical Culture Collection (ATCC, Manassas, VA, USA). HCT116 cells were cultured in DMEM/F12 medium supplemented with 10% fetal bovine serum (FBS). SW480, SW620, and LoVo cells were maintained in DMEM containing 10% FBS. CX-1 and COLO 205 cells were grown in RPMI-1640 medium containing 10% FBS. In contrast, LS-174T cells were grown in Eagle Minimum Essential Medium (MEM) supplemented with 1% non-essential amino acids, 1 mM sodium pyruvate, and 10% FBS. Eagle Minimum Essential Medium (MEM) supplemented with 1% non-essential amino acids and 10% FBS. All cells were incubated at 37°C in a humidified environment with 5% CO_2.

2.8 Statistical analysis

All statistical analyses were carried out with the help of GraphPad Prism 8.0 software. Descriptive statistics were used to summarise general data (120). For quantitative data, a t-test was used to compare means between two groups using an independent samples t-test. One-way analysis of variance (ANOVA) was used to assess differences in means between groups. P-values less than 0.05 were considered to indicate statistical significance.

3 Result

3.1 Core genes and pathways in sepsis-induced myocardial dysfunction: the role of DVL1

The transcriptome analysis of Sepsis-Induced Myocardial Dysfunction (SIMD) across datasets, including GSE122720 for Acute Myocardial Infarction (AMI) and GSE57065 for sepsis, revealed significant differential expression patterns, with five core genes (KIF11, TOP2A, DVL1, RRM2, SERPINB2) being consistently differentially expressed across both conditions (Figures 1A–E). The hierarchical clustering of these genes highlighted distinct expression profiles, emphasizing their potential role in SIMD (Figure 1C). Subsequent Gene Ontology (GO) and KEGG pathway enrichment analyses identified key biological processes and pathways, such as the Wnt signaling pathway and complement cascades, which are implicated in the disease's pathophysiology (Figures 1D–E). Further exploration using Weighted Gene Co-expression Network Analysis (WGCNA) pinpointed the MEturquoise module as significantly correlated with SIMD, containing numerous hub genes, including the core gene DVL1, which was consistently upregulated in SIMD (Figures 1F–I). The relative expression analysis of DVL1 across different patient groups further supported its potential as a biomarker, with significant upregulation observed in SIMD cases (Figure 1I). Supplementary analyses extended these findings to gastrointestinal tumors, where DVL1 was linked to poor prognosis and altered immune landscapes, reinforcing its role as a critical gene across multiple conditions (Supplementary Figure 1). Together, these results highlight the central role of DVL1 in SIMD and its broader implications in disease, positioning it as a promising target for future therapeutic strategies.

3.2 Molecular docking and dynamics simulation of DVL1 as a drug target

The identification of DVL1 as a drug target was conducted through a combination of molecular docking and molecular dynamics (MD) simulations, revealing significant insights into its interactions with FDA-approved drugs. Table 1 presents the binding affinity and docking scores of various compounds interacting with the DVL1 protein, as determined by molecular docking simulations using Autodock-Vina and Discovery Studio 2019 (Table 1). As shown in Figure 2, virtual screening highlighted small molecules with high binding affinity for DVL1, with docking scores visualized through a heat map (Figure 2A), where red represents strong binding affinity and blue represents weaker interactions. Among the top candidates, Digoxin was selected for further analysis due to its balanced docking score. Detailed molecular docking models (Supplementary Figures 2B–G) demonstrated the interaction of DVL1 with selected ligands, showcasing various conformations and key molecular interactions such as hydrogen bonds and hydrophobic contacts. MD simulations provided additional insights, with RMSD analysis (Figure 2H) showing fluctuations in the DVL1-Digoxin complex around 5 ns, stabilizing after 10 ns, indicating initial instability followed by equilibrium. The Radius of Gyration (RG) analysis (Figure 2I) revealed significant fluctuations in DVL1-Digoxin, suggesting transitions between unstable states, contrasting with the more stable GAPDH-Digoxin complex. RMSF analysis (Figure 2J) highlighted the flexibility of specific residues, with DVL1 showing considerable conformational changes. The Solvent Accessible Surface Area (SASA) analysis (Figure 2K) indicated a stable decrease in SASA for the DVL1-Digoxin complex, reflecting favorable binding and structural compactness. Finally, the Hydrogen Bond Number (HBNUM) analysis (Figure 2L) showed consistent hydrogen bond formation in both complexes, correlating with their stability. Overall, these findings underscore DVL1's potential as a drug target, with Digoxin emerging as a promising ligand due to its strong binding and stability, as revealed through the comprehensive simulations.

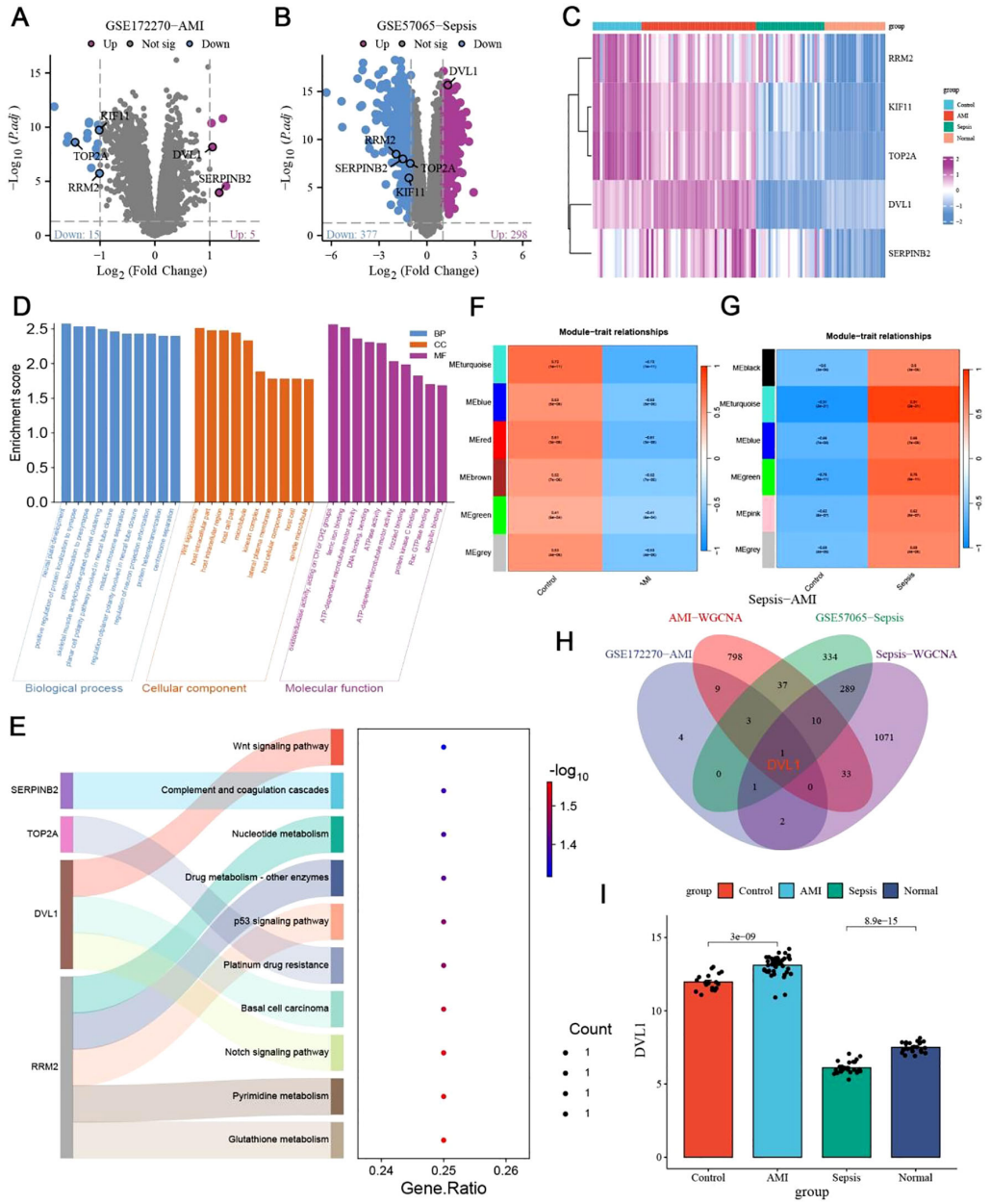

FIGURE 1
Identification of core genes in sepsis-induced myocardial dysfunction. **(A, B)** Volcano plots depicting differentially expressed genes (DEGs) in sepsis-Induced myocardial dysfunction. **(A)** DEGs from the GSE122720 dataset related to Acute Myocardial Infarction (AMI). Genes with significant upregulation (Log2 FC > 1, p < 0.05) are highlighted in red, while those significantly downregulated (Log2 FC < -1, p < 0.05) are shown in blue. Notable genes such as SERPINH1 and RRAD are labeled. **(B)** DEGs from the GSE57065 dataset related to sepsis. Significant upregulated and downregulated genes are indicated similarly, with DVL1 and SERPINH1 highlighted. **(C)** Heatmap of differentially expressed genes associated with Sepsis-Induced Myocardial Dysfunction. Hierarchical clustering of DEGs shows distinct expression patterns across different patient groups, with clustering performed on both gene expression profiles and patient samples. Key genes such as SERPINH1, TOP2A, and DVL1 are labeled, with expression levels indicated by the color gradient (from blue to pink representing low to high expression). **(D, E)** GO and KEGG pathway enrichment analysis of differentially expressed genes in Sepsis-Induced Myocardial Dysfunction. **(D)** GO enrichment analysis indicates significant biological processes, cellular components, and molecular functions associated with DEGs. **(E)** KEGG pathway enrichment analysis showing pathways such as Wnt signaling, complement and coagulation cascades, and nucleotide metabolism. The gene ratio indicates the proportion of DEGs involved in each pathway, with the color gradient representing the significance level [-log10(p-value)]. **(F, G)** Weighted Gene Co-expression Network Analysis (WGCNA) of Sepsis-Induced Myocardial Dysfunction. **(F)** Module-trait relationships identified in the AMI dataset, highlighting correlations between gene modules and clinical traits. **(G)** Module-trait relationships in the sepsis dataset, identifying key gene modules associated with disease severity. Color scale indicates the strength and direction of correlations. **(H)** Venn diagram illustrating the intersection of key genes identified across the datasets (GSE122720-AMI, GSE57065-Sepsis, AMI-WGCNA, Sepsis-WGCNA). This diagram highlights the core genes common to both conditions, emphasizing genes like DVL1 and SERPINH1 that are central to the disease process. **(I)** Relative expression analysis of the DVL1 gene across different patient groups (Control, AMI, Sepsis, Normal). The bar graph shows the mean ± standard deviation of DVL1 expression, with statistical significance denoted by p-values (e.g., p < 0.05). This analysis underscores the differential expression of DVL1 in Sepsis-Induced Myocardial Dysfunction, suggesting its potential role as a biomarker or therapeutic target.

TABLE 1 Molecular docking results of selected compounds with DVL1 protein (PDB ID: 6TTK) using autodock-vina and discovery studio 2019.

Protein (Binding Site)	Compound	Vina (kcal·mol^{-1})	RMSD	DS (LibDockScore)
DVL1 (6TTK)	**Digoxin**	-4.5	1.619	165.304
DVL1 (6TTK)	**Paromomycin**	-3.7	2.095	158.73
DVL1 (6TTK)	**Cabazitaxel**	-4.5	1.829	152.19
DVL1 (6TTK)	**Paclitaxel**	-4.6	1.516	151.868
DVL1 (6TTK)	**Streptomycin**	-4.6	2.614	148.925
DVL1 (6TTK)	**Toposar**	-5.2	0.452	147.71

This table presents the binding affinity and docking scores of various compounds interacting with the DVL1 protein, as determined by molecular docking simulations using Autodock-Vina and Discovery Studio 2019. The Vina score (expressed in kcal·mol^{-1}) reflects the binding affinity, where more negative values indicate stronger interactions between the compound and the protein. The RMSD (Root Mean Square Deviation) values provide insight into the stability and accuracy of the binding pose, with lower values indicating a more stable interaction. The DS (LibDockScore) from Discovery Studio 2019 represents the strength of interaction, with higher scores suggesting better binding affinity. The bold values in the table are the binding energies calculated by autodock - vina (Vina values, in kcal·mol- ^{1}), the root - mean - square deviations (RMSD), and the LibDockScore values calculated in Discovery Studio, which are used to measure the binding characteristics of compounds to the DVL1 protein.

3.3 Comprehensive analysis of DVL1 expression and mutation in gastrointestinal cancers

In this study, we investigated the role of DVL1 in gastrointestinal cancers, focusing on its expression pattern, diagnostic potential and prognostic significance. Analysis of DVL1 expression in four gastrointestinal tumors - COAD, STAD, ESCA and READ - showed significant overexpression in tumor tissues compared to normal tissues (Figure 3A, C). DVL1 gene expression levels varied in different organs of cancer patients, and the expression levels varied with the anatomical location of the tumor (Figure 3B). The ROC analysis demonstrated that DVL1 has strong diagnostic potential, with high AUC values in COAD, ESCA, and READ (Supplementary Figures 3D–F). Kaplan-Meier survival curves indicated that elevated DVL1 expression correlates with poorer survival outcomes in these cancers, suggesting its value as a prognostic marker (Supplementary Figures 3G–I). Figures 3D–I display the related analyses of DVL1 in gastrointestinal tumors, including ROC curves and survival curves for different tumor types. These figures intuitively demonstrate the important roles of DVL1 in diagnosis and prognosis. Further investigation revealed heterogeneity in DVL1 expression across different cellular populations within tumors (Figure 3J) and significant differences in expression across various immune subtypes (Figure 3K). Correlation analyses between DVL1 expression and oncogenic pathways highlighted its involvement in tumor biology (Figure 3L). A summary of clinical data from 1181 TCGA patients indicated that higher DVL1 expression is associated with advanced tumor stages and poorer outcomes (Figure 3M). In colorectal cancer, DVL1 showed a somatic mutation rate of 1.61%, with several mutation hotspots identified (Supplementary Figure 2A). Pan-cancer analysis confirmed DVL1 as one of the most mutated genes, emphasizing its potential role in carcinogenesis (Supplementary Figure 2B). Additionally, DVL1 expression varied significantly across different MSI subtypes, implicating it in MSI-driven tumorigenesis (Supplementary Figure 2C). Protein expression analysis using HPA data showed differential DVL1 expression in colorectal and stomach cancer tissues, supporting its involvement in cancer pathophysiology (Supplementary Figure 2D). These findings collectively suggest that DVL1 is a critical biomarker in gastrointestinal cancers, with significant implications for its use in diagnosis and prognosis.

3.4 Expression and prognostic significance of DVL1 in colorectal cancer

Our study reveals that DVL1 is significantly overexpressed in colorectal cancer (COAD) tissues compared to adjacent normal tissues, as demonstrated by both immunohistochemical staining and RNA-seq analysis (Figures 4A–C). The ROC curves further confirm the diagnostic and prognostic value of DVL1, with AUC values indicating its potential to distinguish between tumor and normal tissues, and to predict patient outcomes (Figures 4D, E). High DVL1 expression correlates with poorer overall survival, as shown by Kaplan-Meier survival curves and a comparative analysis of clinical characteristics (Figures 4F–H). The observed changes in DVL1 phosphorylation sites between normal and tumor tissues suggest possible post-translational modifications contributing to its oncogenic role (Figure 4I). Thermal profiling data delineate significant covariations between DVL1 transcriptional activity and immunological biomarkers within COAD, establishing mechanistic insights into its regulatory potential within tumor-associated immune landscapes (Figure 4J). Additionally, the analysis of DVL1 expression across different tumor stages and its correlation with various COAD-related genes indicates a strong association with disease progression, although survival analysis did not show a significant difference between high and low-expression groups (Supplementary Figures 3A–G). Functional analyses, covering CRISPR-Cas9 screening as well as pathway enrichment studies, further highlighted the critical role of DVL1 in cancer biology, with significant enrichment in pathways associated with tumor progression (Supplementary Figures 4A–I). These findings suggest that DVL1 plays a crucial role in the development of COAD and could serve as a potential therapeutic target.

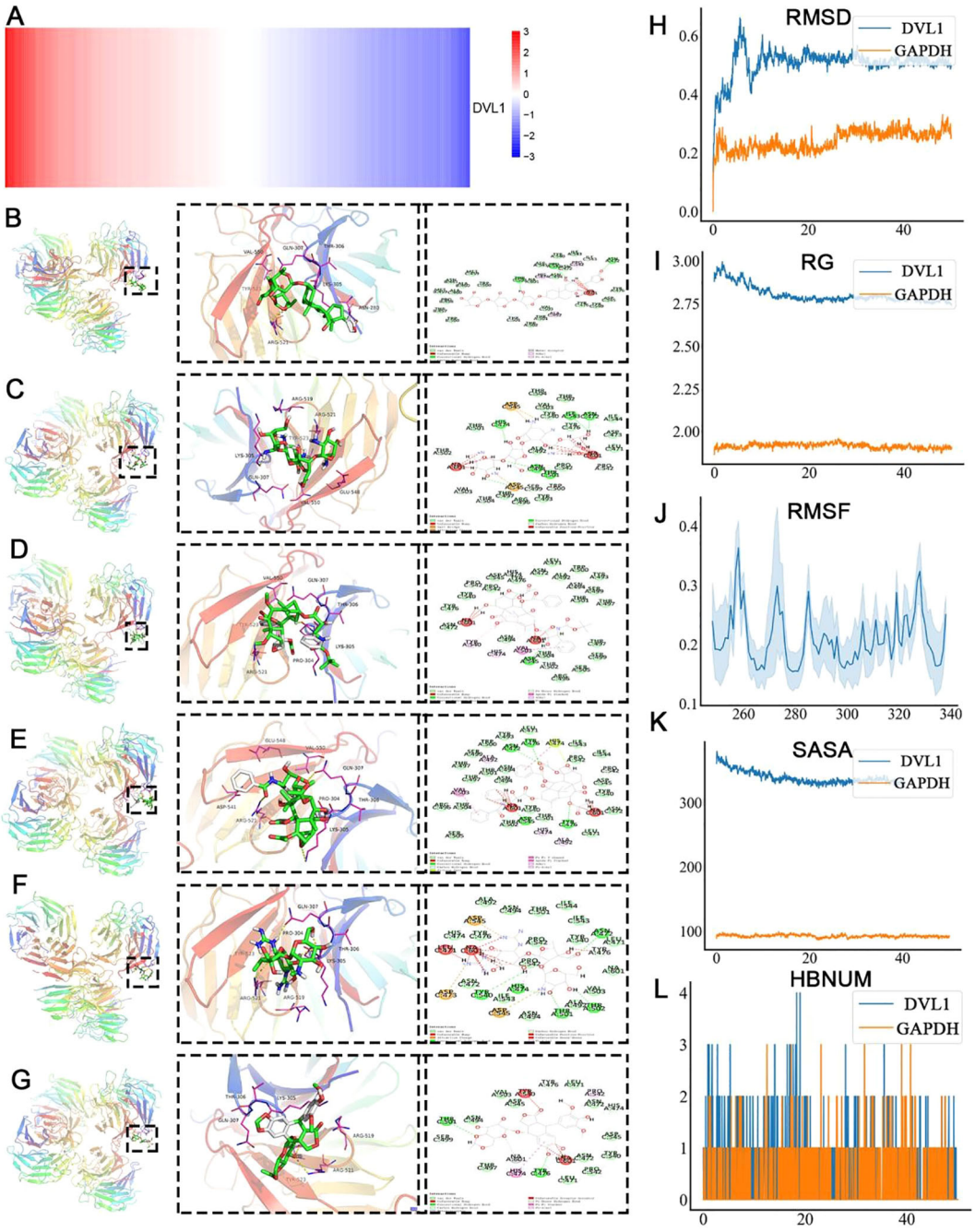

FIGURE 2
Molecular dynamics simulation and virtual screening of core protein DVL1. **(A)** Heat map representation of the virtual screening of core protein DVL1 against the FDA-approved drug library. The color gradient from red to blue represents the binding affinity, with red indicating high binding affinity and blue indicating low binding affinity. **(B-G)** Molecular docking models of the core protein DVL1 with selected ligands. Each panel shows the overall structure of DVL1 in a ribbon diagram (left), a zoomed-in view of the ligand-binding site with interacting residues highlighted (middle), and a 2D interaction diagram depicting the molecular interactions between DVL1 and the ligand (right). The models illustrate the different conformations of DVL1 when bound to various ligands, highlighting key interactions such as hydrogen bonds, hydrophobic contacts, and electrostatic interactions. **(H-L)** Molecular dynamics (MD) simulation analysis comparing DVL1 (blue) with the positive control protein GAPDH (orange). The analysis includes: **(H)** Root Mean Square Deviation (RMSD) analysis over the simulation time, showing the structural stability of DVL1 and GAPDH. **(I)** Radius of Gyration (RG) indicating the compactness of the protein structures. **(J)** Root Mean Square Fluctuation (RMSF) analysis, providing insight into the flexibility of specific residues within the protein structures. **(K)** Solvent Accessible Surface Area (SASA) analysis, representing the extent of exposure of the protein surface to the solvent. **(L)** Hydrogen Bond Number (HBNUM) analysis, illustrating the number of hydrogen bonds formed during the simulation, which correlates with protein stability.

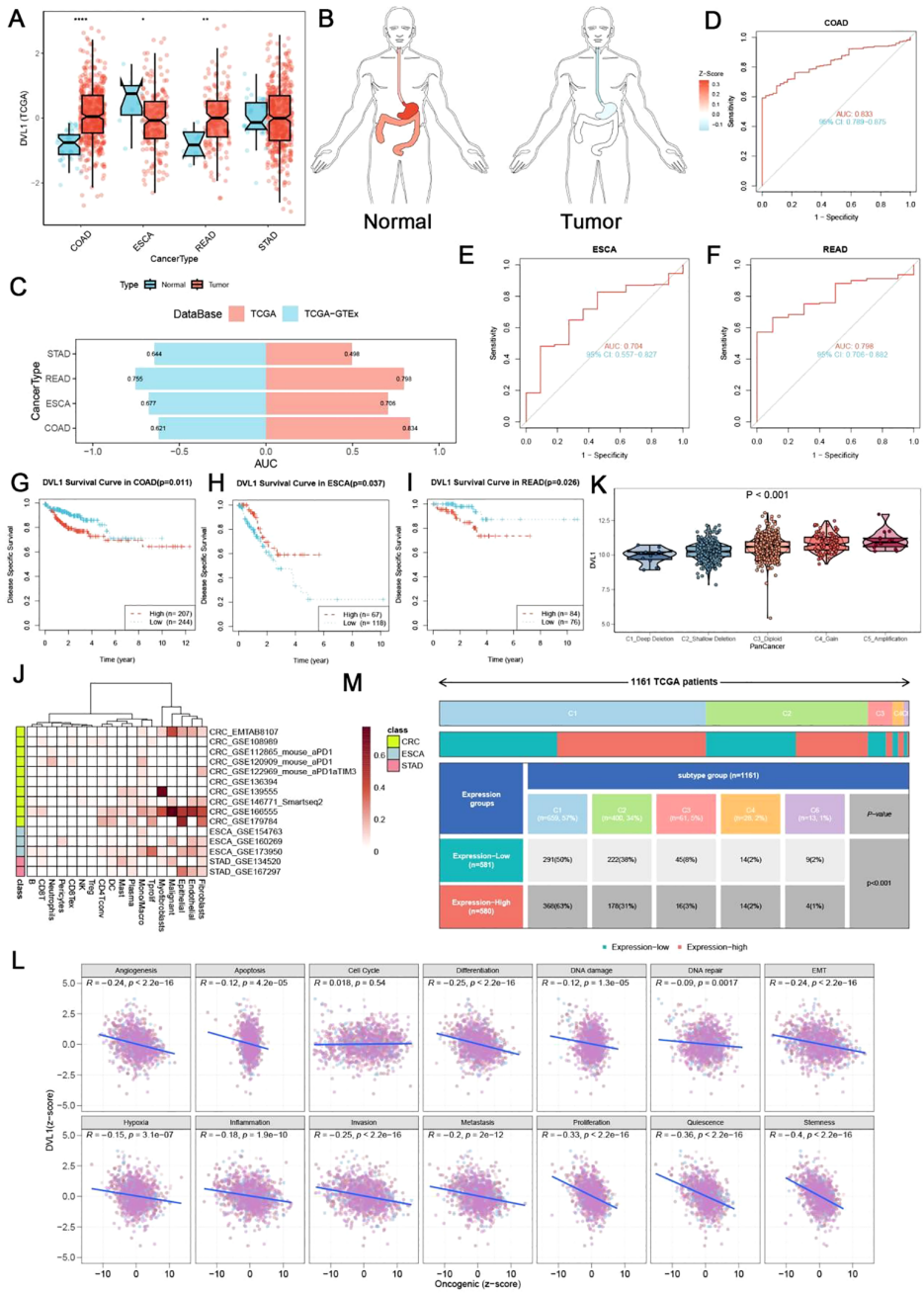

FIGURE 3
Landscape of DVL1 expression in gastrointestinal tumors. **(A, C)** DVL1 gene expression levels across four types of gastrointestinal tumors (COAD, STAD, ESCA, and READ) are depicted. Panel **(A)** shows a comparison between normal and tumor tissues based on data from the TCGA and GTEx databases, demonstrating differential expression patterns with statistical significance (indicated by p-values). Panel **(C)** provides a summary of the area under the curve (AUC) values for the receiver operating characteristic (ROC) analysis, reflecting the diagnostic potential of DVL1 in these cancers. **(B)** Illustration of DVL1 gene expression distribution across different organs in cancer patients, highlighting the variation in expression levels depending on the anatomical location of the tumor. **(D-F)** Receiver operating characteristic (ROC) curves for DVL1 gene in three types of gastrointestinal tumors (COAD, ESCA, and READ) are presented. The curves show the diagnostic accuracy of DVL1 expression, with each panel detailing the AUC values, sensitivity, and specificity metrics for each cancer type. **(G-I)** Kaplan-Meier survival curves analyzing the prognostic significance of DVL1 expression in three types of gastrointestinal tumors (COAD, ESCA, and READ). The survival analysis indicates the correlation between DVL1 expression levels and patient survival outcomes, with log-rank test p-values provided to denote statistical significance. **(J)** Heatmap showing DVL1 gene expression across different cell subgroups in four gastrointestinal tumors. This panel illustrates the heterogeneity in DVL1 expression among various cellular populations within the tumors. **(K)** Violin plot depicting the expression of DVL1 across different immune subtypes within gastrointestinal tumors. The plot demonstrates significant differences in DVL1 expression depending on the immune landscape of the tumor ($p < 0.001$). **(L)** Scatter plots examining the relationship between DVL1 expression and 14 different tumor phenotypes. Each plot includes regression lines and correlation coefficients, providing insight into the association between DVL1 expression and oncogenic pathways. **(M)** Summary of clinical data for 1181 TCGA patients with four types of gastrointestinal tumors, classified based on DVL1 expression levels. The panel provides an overview of clinical characteristics such as tumor stage, survival status, and molecular subtypes, highlighting the relevance of DVL1 expression in the clinical context. The symbols *, **, and **** represent statistical significance levels corresponding to p<0.05, p<0.01, and p<0.0001.

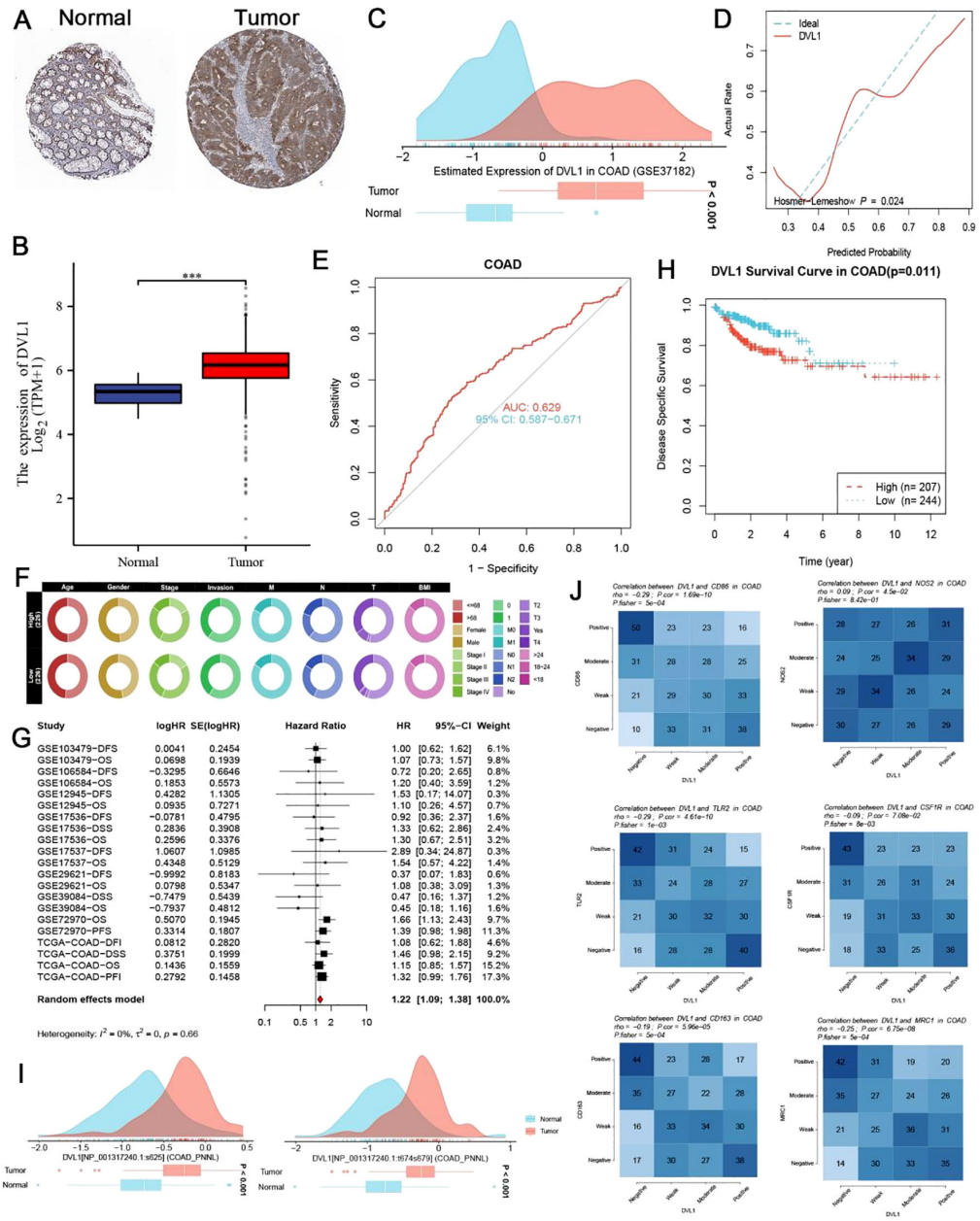

FIGURE 4
Expression and prognostic significance of DVL1 in colorectal cancer (COAD). **(A, B)** Immunohistochemical (IHC) staining for DVL1 in colorectal cancer tissues and adjacent normal tissues demonstrats increased expression of DVL1 in tumor tissues compared to normal tissues. Representative images from the study cohort are shown, with higher DVL1 expression observed in the tumor samples. Data were obtained using the Human Protein Atlas (HPA) database. **(C)** Distribution of DVL1 gene expression in colorectal cancer versus normal tissues, analyzed using the GSE37182 dataset. The data is presented as density plots, showing a significant upregulation of DVL1 in tumor tissues compared to normal tissues. **(D)** Receiver Operating Characteristic (ROC) curve assessing the diagnostic performance of DVL1 expression in distinguishing tumor tissues from normal tissues. The area under the curve (AUC) and the model's discriminatory ability are shown, indicating a good diagnostic value for DVL1 expression in COAD. **(E)** ROC curve evaluating the prognostic performance of DVL1 expression in predicting outcomes in colorectal cancer patients. The AUC value and the 95% confidence interval (CI) are provided, highlighting the prognostic relevance of DVL1 expression in COAD. **(F)** Comparative analysis of clinical characteristics between high and low DVL1 expression groups in COAD patients. The circular heatmap visualizes the distribution of various clinical traits (e.g., age, gender, BMI, stage) between the two groups, illustrating significant associations with DVL1 expression. **(G)** Forest plot summarizing the univariate analysis of DVL1 expression across multiple datasets for COAD patients. Hazard ratios (HR) and 95% confidence intervals (CI) are depicted for each study, with a pooled HR calculated from the meta-analysis, indicating the overall prognostic impact of DVL1. The analysis shows a significant association between high DVL1 expression and poor prognosis. **(H)** Kaplan-Meier survival curve comparing overall survival between high and low DVL1 expression groups in COAD patients. The survival analysis shows a statistically significant difference (p = 0.011), with high DVL1 expression associated with worse survival outcomes. **(I)** Analysis of phosphorylation site changes in the DVL1 protein between normal and tumor tissues, indicating potential post-translational modifications that may contribute to altered function in colorectal cancer. The density plots depict the distribution of phosphorylation levels at specific sites, showing significant differences between normal and tumor groups. **(J)** Correlation heatmaps show the association between DVL1 expression and various immune markers in COAD, highlighting the positive and negative correlations with immune-related genes. The analysis provides insights into the potential role of DVL1 in modulating the immune microenvironment in COAD. The symbols *** represent statistical significance levels corresponding to p<0. 001.

3.5 Analysis of DVL1 in colorectal cancer

In this research, we probed into the function of the DVL1 in COAD, concentrating on its expression patterns among tumor stages and its connection with key cancer-related pathways. Supplementary Figure 4A presents the distribution of DVL1 expression across four clinical stages of COAD (Stage I to IV). Statistical analysis shows that there are no remarkable differences in DVL1 expression levels among stages ($P = 0.87$). Likewise, a comparison between the early-stage (Stage I to II) and the late-stage (Stage III to IV) of COAD in Supplementary Figure 4B also reveals no significant difference ($P = 0.995$).To further explore the functional role of DVL1, we analyzed its dependency across various cancer types using CRISPR-Cas9 screening data from the DepMap database, as illustrated in Figure 4C. This analysis highlights variable DVL1 dependency across cancer cell lines, indicating its essential role in certain types of cancers. Next, we performed KEGG pathway enrichment analysis (Supplementary Figure 4D), which identified several cancer-related pathways associated with DVL1 expression, including the Wnt signaling pathway and pathways involved in cell cycle regulation. GSEA was conducted to assess hallmark gene sets, revealing significant enrichment in cellular processes related to proliferation, DNA repair, and apoptosis, particularly in the high DVL1 expression group, as shown in Supplementary Figure 4E. Additionally, Supplementary Figure 4F presents a LocusCompare analysis, which demonstrates specific genetic loci correlated with DVL1 expression. Finally, functional enrichment analysis for transcription factors associated with DVL1 expression was performed. The GO term analysis (Supplementary Figure 4G) highlights biological processes related to transcriptional regulation, while KEGG pathway analysis (Supplementary Figure 4H) indicates significant involvement in pathways such as p53 signaling and RNA polymerase activity. The Friends analysis in Figure 4I identifies key transcription factors, such as FOXM1 and NFKB2, which are strongly correlated with DVL1 expression and may contribute to its regulatory network in cancer. Collectively, these findings suggest that while DVL1 expression remains consistent across COAD stages, its dependency and functional interactions highlight its critical role in cancer biology, particularly in cell survival and proliferation pathways.

3.6 Comprehensive analysis of DVL1 in colorectal adenocarcinoma: gene interaction, immune landscape, and therapeutic implications

The DVL1 gene plays a critical role in COAD, as demonstrated by a series of comprehensive analyses involving gene set enrichment, immune landscape evaluation, and upstream transcription factor studies. As illustrated in Figure 5A, a gene interaction network centered on DVL1 reveals significant associations with various genes, underscoring its involvement in essential cellular processes. Differential expression analysis (Figure 5B) further highlights the extensive alteration in gene expression associated with DVL1, implicating its pivotal role in tumor development. Gene set enrichment analysis (GSEA) and gene set variation analysis (GSVA) results (Supplementary Figures 5C, E, F) show significant pathway alterations between high and low DVL1 expression groups, particularly in hallmark gene sets, reinforcing DVL1's influence on tumorigenesis. The immune response correlation (Figure 5H) and its association with immunostimulatory genes (Figure 5I) reveal a complex relationship between DVL1 expression and immune system activity, further supported by the immunomodulatory landscape in COAD (Figure 5J). Upstream transcription factors were analyzed to uncover potential regulatory mechanisms affecting DVL1 expression, with significant correlations observed between ATAC-Peak signals and specific transcription factors (Figure 6A). Figure 6C presents transcription factors associated with DVL1 identified via Friends analysis, offering critical insights for exploring the regulatory mechanisms of this signaling molecule. These transcription factors, highlighted in the differential expression analysis (Figure 6B) and prognostic forest plots (Supplementary Figures 6D–G), suggest potential targets for therapeutic intervention. The correlation of DVL1 with SMAD2 and XBP1 (Figure 6H) further suggests a collaborative role in COAD progression. In terms of therapeutic implications, DVL1's role in predicting drug sensitivity and immunotherapy response is evidenced by the ROC-AUC analysis (Supplementary Figure 5A) and its significant correlation with drug sensitivity metrics (Supplementary Figures 5B–D). Notably, DVL1 expression correlated with increased sensitivity to the drug BI.2536 (Supplementary Figures 5E, F), suggesting that DVL1 could serve as a potential biomarker of drug response. Mutation analysis (Supplementary Figures 6K–M) provided insights into the mutational status of DVL1 and its impact on components of the tumor microenvironment (Supplementary Figures 6N–P), further cementing its relevance in colorectal cancer pathogenesis and treatment. Together, these findings highlight the importance of DVL1 as a key player in colorectal cancer, providing valuable insights for targeted therapy and prognostic assessment.

3.7 Comprehensive analysis of DVL1 expression in colorectal cancer using single-cell and spatial transcriptomics

The comprehensive analysis of DVL1 expression in colorectal cancer, combining single-cell sequencing and spatial transcriptomics, reveals critical insights into the gene's role within the tumor microenvironment. Through UMAP visualization of major cell lineages (Figure 7A), distinct clusters such as T cells, B cells, epithelial cells, and fibroblasts were identified, with Figure 7B highlighting varying levels of DVL1 expression across these populations. The comparison of cell type proportions between

10.3389/fimmu.2025.1560717

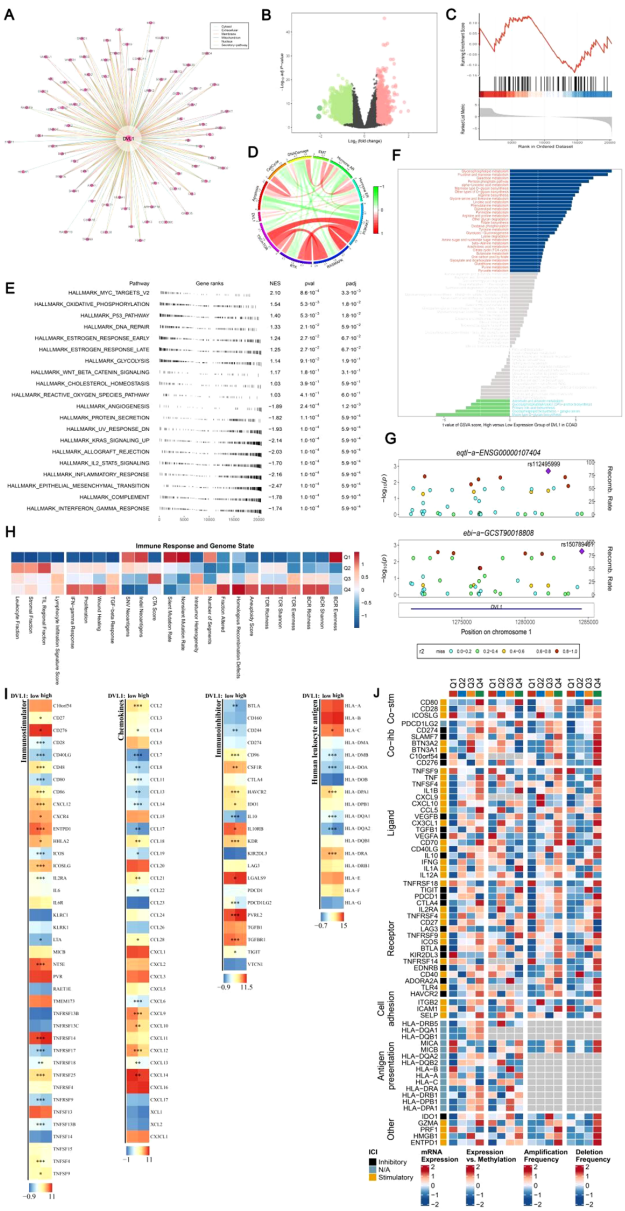

FIGURE 5
DVL1 gene enrichment analysis and associated immune landscape in COAD. **(A, D)** DVL1 gene interaction network: A network analysis illustrating the interactions of genes closely related to DVL1. Panel **(A)** shows a comprehensive gene-gene interaction network with DVL1 at the center, highlighting both direct and indirect interactions with associated genes. Panel **(D)** further details the connections and functional relationships among these genes using a circular plot. **(B)** Differential expression analysis of DVL1-associated genes: A volcano plot showing the differentially expressed genes associated with DVL1. Genes are categorized into upregulated (green), downregulated (red), and non-significant (black) groups based on log2 fold changes and statistical significance (p-value). **(C)** GSEA enrichment analysis of differentially expressed genes associated with DVL1: A line graph representing the Gene Set Enrichment Analysis (GSEA) results for DVL1-related differentially expressed genes, focusing on key gene sets that show significant enrichment or depletion. **(E)** Hallmark gene set enrichment analysis (GSEA): A dot plot visualizing the enrichment scores and significance levels of various hallmark gene sets associated with DVL1 expression. The pathways are ranked based on normalized enrichment score (NES) and statistical significance. **(F)** GSVA pathway enrichment scores comparing DVL1 high-expression versus low-expression groups: A bar chart depicting the difference in pathway activity scores between high and low DVL1 expression groups, identified using Gene Set Variation Analysis (GSVA). Pathways with significantly altered activity are color-coded based on their upregulation (blue) or downregulation (red) in high DVL1 expression groups. **(G)** Visualization analysis using gassocplot package: Scatter plots displaying the association between specific genetic variants and phenotypic traits related to DVL1, across various chromosomal locations. Points are color-coded according to their significance and categorized by variant type, with annotation of significant SNPs and genomic regions. **(H)** Immune response and genome state: A heatmap representing the correlation between DVL1 expression and various immune-related genes or pathways. Data points are color-coded to indicate the strength and direction of correlation, providing insights into the relationship between DVL1 and immune system activity. **(I)** Landscape of DVL1 in immunostimulator analysis: Heatmaps illustrating the association of DVL1 expression levels with various immunostimulatory genes across different sample sets. The analysis highlights significant correlations, with color intensities representing the degree of association. **(J)** Complex heatmap of immunomodulators in COAD: A detailed heatmap depicting the expression patterns, copy number variations, and mutation frequencies of key immunomodulatory genes in colorectal adenocarcinoma (COAD). The rows represent individual genes, and the columns represent different patient samples or conditions. The heatmap is annotated to show expression levels, amplification, deletion frequencies, and the presence of mutations, providing a comprehensive overview of the immunomodulatory landscape in relation to DVL1 expression in COAD. The symbols *, **, and *** represent statistical significance levels corresponding to p<0.05, p<0.01, and p<0. 001, respectively.

10.3389/fimmu.2025.1560717

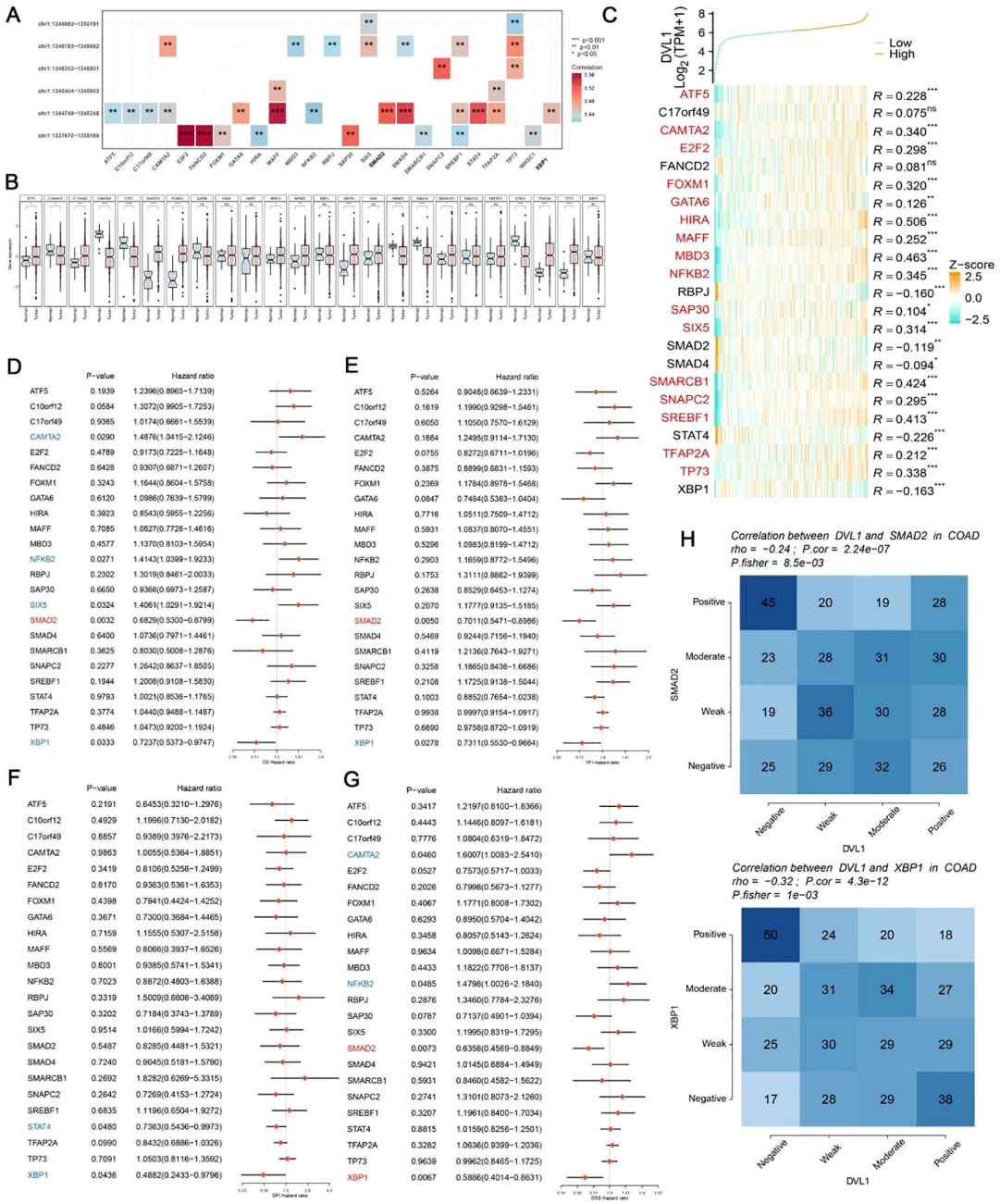

FIGURE 6
Analysis of upstream transcription factors of DVL1 gene. **(A)** Spearman correlation analysis between ATAC-Peak and transcription factors. This panel illustrates the Spearman correlation coefficients between ATAC-Peak signals and various transcription factors, providing insight into the potential regulatory relationships affecting DVL1 expression. The analysis highlights transcription factors with significant correlations, denoted by color-coded squares representing the strength and direction of correlation (positive in red, negative in blue). **(B)** Differential expression analysis of transcription factors associated with the DVL1 gene. Box plots display the expression levels of transcription factors across different sample groups, with statistical significance indicated for factors showing a differential expression. This analysis identifies transcription factors that are differentially regulated in association with DVL1, highlighting potential key regulators. **(C)** Friends analysis of the DVL1 gene to identify correlated transcription factors. A heatmap shows the correlation between DVL1 and selected transcription factors, identified through Friends analysis. Transcription factors with positive and negative correlations are listed alongside their correlation coefficients (R-values). The analysis helps to pinpoint transcription factors that may co-regulate with DVL1 or are part of the same regulatory network. **(D-G)** Forest plots screening prognostically relevant transcription factors through multi-gene analysis. These panels show hazard ratios and confidence intervals for multiple transcription factors in relation to overall survival in a cohort of cancer patients. The forest plots identify transcription factors significantly associated with prognosis, highlighting those with potential as biomarkers or therapeutic targets in conjunction with DVL1. **(H)** Correlation analysis between the DVL1 gene and transcription factors SMAD2 and XBP1. Heatmaps present the correlation strength between DVL1 and SMAD2/XBP1 across various samples, categorized into positive, moderate, weak, and negative correlations. The analysis provides a detailed view of the interaction between DVL1 and these specific transcription factors, offering insights into their potential collaborative roles in the biological processes studied. The symbols *, **, ***and ****represent statistical significance levels corresponding to p<0.05, p<0.01,p<0. 001 and p<0. 0001, respectively. ns, not significant.

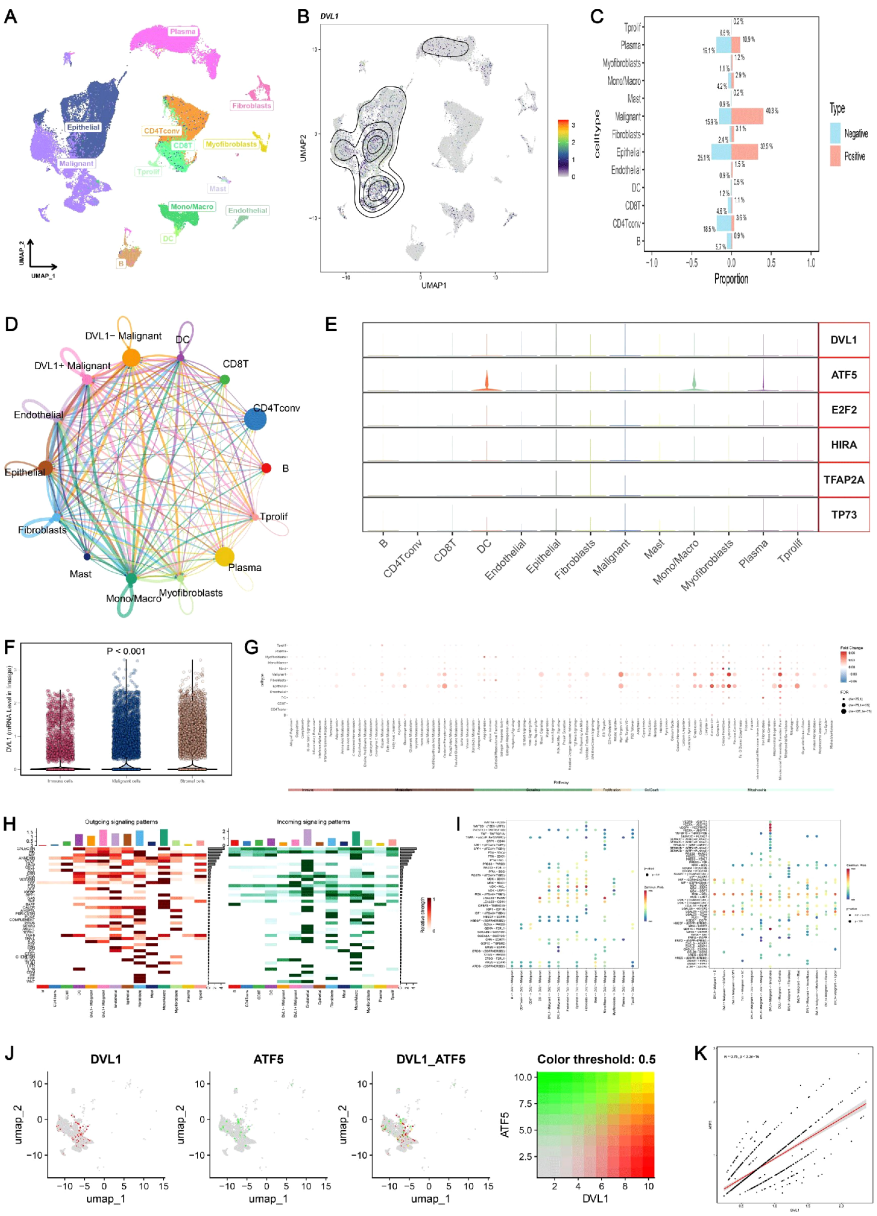

FIGURE 7
Single-cell sequencing analysis of DVL1 in colorectal cancer. **(A, B)** UMAP visualization of major cell lineages and DVL1 single-gene expression in single cells from colorectal cancer samples. **(A)** displays the distribution of the main cell lineages identified in the dataset, including T cells, B cells, epithelial cells, fibroblasts, myofibroblasts, mast cells, and others, with distinct clusters representing each lineage. **(B)** shows the UMAP plot highlighting the expression levels of the DVL1 gene across individual cells, with a gradient indicating varying expression levels. **(C)** Comparison of the proportions of different cell types between DVL1-positive and DVL1-negative groups. The bar graph presents the proportion of each cell type (e.g., T cells, B cells, fibroblasts) stratified by DVL1 expression status. The data suggest differential representation of cell types depending on DVL1 gene expression, with statistically significant differences noted. **(D)** Interaction network of different cell subsets in colorectal cancer. This network diagram illustrates the inferred interactions between various cell subsets within the tumor microenvironment, highlighting connections involving DVL1+ malignant cells and their interactions with other cell types such as CD8+ T cells, fibroblasts, and endothelial cells. The thickness of the lines corresponds to the strength or frequency of interactions. **(E)** Differential expression of DVL1 and upstream transcription factors across different cell types. The expression patterns of DVL1 and associated transcription factors such as ATF5, E2F2, HIRA, TFAP2A, and TP73 are shown across various cell types, including malignant cells, fibroblasts, and T cells. Each panel represents the distribution of expression levels across the cell types. **(F)** Variability in DVL1 expression across different tumor cell states. Box plots illustrate the differential expression of DVL1 among various tumor cell states, indicating statistically significant differences ($P < 0.001$). This comparison underscores the heterogeneity of DVL1 expression in distinct tumor microenvironments. **(G)** Pathway differences between DVL1-positive and DVL1-negative groups across different cell types. A dot plot shows the differential pathway activity scores between cells grouped by DVL1 expression status, across various cell types. Each dot represents a pathway, with size and color intensity reflecting the significance and magnitude of pathway activation differences. **(H, I)** Pathway enrichment differences between cell types. Heatmaps depict the enrichment of signaling pathways across different cell types in the tumor microenvironment. **(H)** displays outgoing signaling pathways, while **(I)** focuses on incoming signaling pathways. The data show distinct enrichment patterns, highlighting the unique roles of different cell types in signal transduction within the tumor context. **(J, K)** Correlation analysis of gene expression levels. **(J)** presents UMAP visualizations of the co-expression patterns of two specific genes, including DVL1 and ATF5, both individually and in combination. **(K)** shows a scatter plot demonstrating the correlation between the average expression levels of these two genes, with a color-coded threshold (0.5) indicating the strength of the correlation. This analysis reveals a significant positive correlation, suggesting potential regulatory interactions between DVL1 and ATF5.

DVL1-positive and DVL1-negative groups (Figure 7C) underscores the differential representation of cell types, notably a higher presence of fibroblasts and T cells in DVL1-positive samples. Furthermore, the interaction network in Figure 7D demonstrates the significant role of DVL1+ malignant cells in coordinating cellular interactions, particularly with CD8+ T cells and fibroblasts. Differential expression analysis in Figure 7E highlights the association between DVL1 and transcription factors like ATF5 and E2F2 across various cell types. The variability in DVL1 expression across tumor cell states (Figure 7F) and pathway activity differences between DVL1-positive and DVL1-negative cells (Figure 7G) emphasize the gene's influence on tumor heterogeneity and pathway activation. The pathway enrichment of different cell types in the tumor microenvironment (TME) revealed the differential activity of pro-inflammatory and immune regulation-related signaling pathways (e. g. Wnt/β -catenin, NF- κ B, TGF- β) in immune cells, fibroblasts and tumor cells (Figures 7H, I) Tumor-associated fibroblasts (CAF) showed high activity in TGF- β and ECM-related pathways, while Treg cells were enriched in IL-10-mediated anti-inflammatory pathways, suggesting unique roles for different cell types in TME regulation. Correlation analysis between DVL1 and ATF5 (Figures 7J, K) suggests a regulatory interaction, potentially impacting tumor progression. Spatial transcriptomics provides a refined visualization of DVL1 expression within tumor tissue, revealing its heterogeneous spatial distribution (Figure 8A). A robust correlation is noticed between the expression of DVL1 and key microenvironmental constituents (Supplementary Figures 7A–D). Spatial mapping further accentuates the enhanced expression of DVL1 in malignant areas, indicating its potential engagement in tumor progression and aggression (Figures 8B–D). Altogether, these discoveries emphasize the crucial role of DVL1 in coordinating the cellular and spatial dynamics of colorectal cancer, molding microenvironmental interactions and influencing tumor behavior.

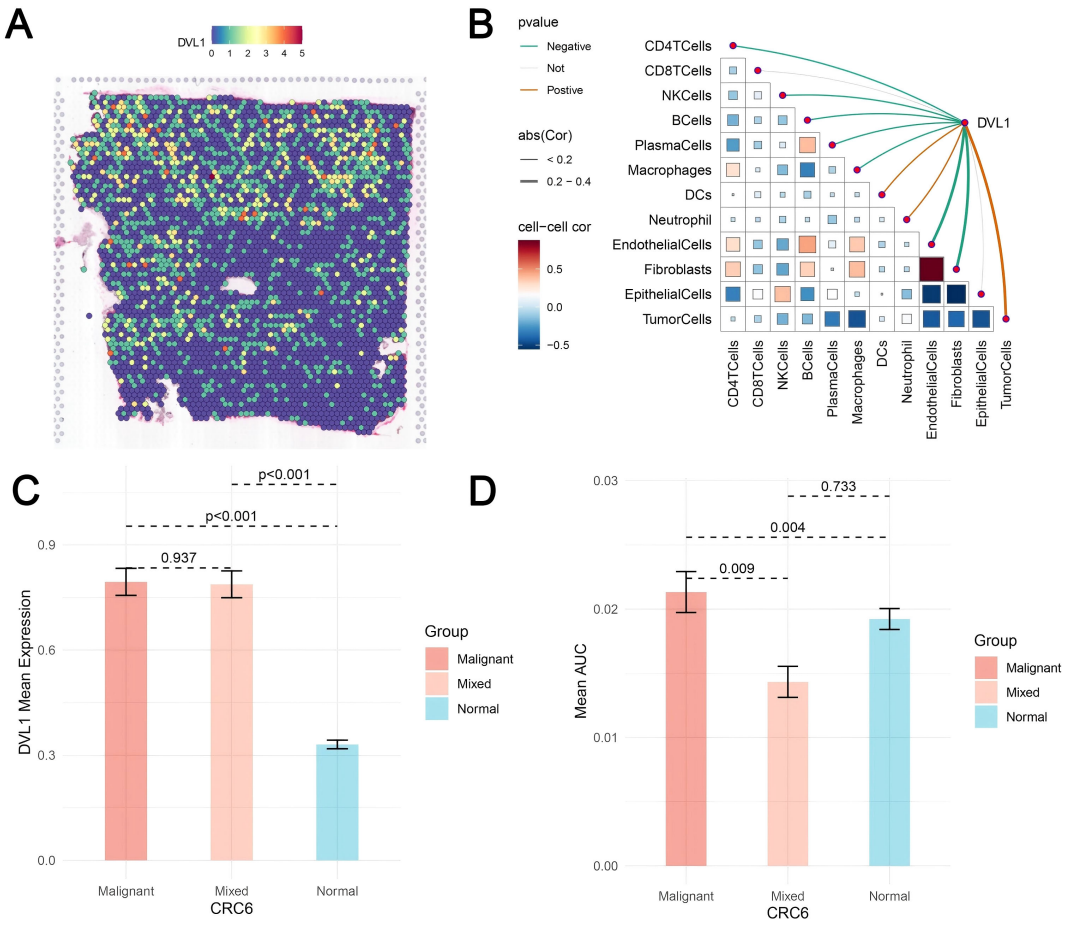

FIGURE 8
Spatial transcriptomics analysis of DVL1 in colorectal cancer. **(A)** Spatial distribution of DVL1 expression across the tissue sample. The heatmap illustrates expression levels, with higher intensities indicating elevated DVL1 expression. **(B)** Spearman correlation analysis between DVL1 expression and tumor microenvironment components. The correlation matrix represents the relationships between DVL1 and various cell types, with color gradients reflecting positive and negative correlations. Statistically significant correlations are highlighted. **(C)** Comparison of DVL1 mean expression levels among malignant, mixed, and normal tissue regions. Statistical significance is indicated by p-values. **(D)** Mean AUC values of a specific gene set across different tissue compositions, highlighting significant differences in tumor microenvironment interactions.

3.8 DVL1 expression and its role in modulating cell proliferation and tumor progression

The study investigated the expression of DVL1 and its impact on cell proliferation and tumor progression across various cell lines, including SW620, HCT116, and RAW264.7. Quantitative PCR analysis, as shown in Figure 9A, revealed that DVL1 mRNA levels were significantly downregulated in response to different concentrations of Digoxin, particularly at high concentrations ($p < 0.001$). Among the tested cell lines, HCT116 and SW620 exhibited the most substantial reductions in DVL1 expression, suggesting that Digoxin effectively suppresses DVL1 expression. Additionally, Figure 9D highlights a significant upregulation of DVL1 in RAW264.7 cells compared to THP-1 cells ($p < 0.001$). To assess the functional role of DVL1, a CCK-8 assay was performed, revealing a dose-dependent decrease in cell viability in HCT116 and SW620 cells treated with Digoxin, with the greatest inhibition observed at high concentrations, as illustrated in Figure 9B ($p < 0.05$). This suggests that Digoxin-mediated DVL1 downregulation contributes to reduced tumor cell proliferation. Moreover, the expression of inflammatory cytokines was measured using qPCR across different treatments, showing significant changes in SW620, HCT116, and RAW264.7 cells (Figure 9C, $p < 0.001$), indicating a role of DVL1 in modulating inflammatory responses. Further analysis involved DVL1 overexpression and knockdown models, where Figure 9E demonstrated that overexpression significantly promoted cell proliferation, whereas knockdown markedly inhibited growth ($p < 0.001$). The plate colony formation assay results, depicted in Figure 9H, supported these findings, showing enhanced colony formation with DVL1 overexpression and a reduction with knockdown. CCK-8 proliferation assays demonstrated that DVL1 overexpression enhances cellular growth kinetics in both HCT116 and SW620 colorectal cancer models, whereas genetic silencing of DVL1 exerted potent growth-suppressive effects (Figure 9F). Finally, Figure 9G showed a substantial decrease in DVL1 mRNA levels in SW620, HCT116, and RAW264.7 cells following DVL1 knockdown ($p < 0.001$). Collectively, these results suggest that DVL1 plays a critical role in promoting cell proliferation and tumor progression, and that down-regulation of its expression by pharmacological agents or gene knockdown significantly inhibits these processes.

3.9 The effects of digoxin and DVL1 overexpression on inflammatory responses, cell viability, migration, and protein expression in cancer cells

This study investigated the impact of Digoxin and OE-DVL1 on various cellular processes in SW620 and HCT116 cell lines, focusing on inflammatory cytokine expression, EMT markers, cell viability, migration, proliferation, apoptosis, and protein expression. qRT-PCR analysis showed that Digoxin and OE-DVL1 significantly reduced the expression of pro-inflammatory cytokines TNFα, IL6, and IL1β compared to the LPS-treated group, suggesting an anti-inflammatory effect (Figure 10A). The expression of key EMT markers such as CDH1, VIM, and MMP9 was modulated by the combination of Digoxin and OE-DVL1, suggesting its role in inhibiting EMT-related changes (Figure 10A). CCK-8 demonstrated that Digoxin, particularly at high doses, significantly reduced the viability of SW620 and HCT116 cells, with further decreases when combined with OE-DVL1, highlighting their combined inhibitory effect on cell proliferation (Figure 10B). Transwell migration assays confirmed that both Digoxin and OE-DVL1 significantly reduced cell migration, further supporting their role in inhibiting metastatic potential (Figure 10C). Colony formation assays showed a marked decrease in the number of colonies formed in cells treated with Digoxin, with an additional reduction observed when combined with OE-DVL1, suggesting enhanced anti-proliferative effects (Figure 10D). Flow cytometry analysis indicated increased apoptosis levels in cells treated with Digoxin, particularly when combined with OE-DVL1, highlighting the pro-apoptotic effects of these treatments (Figure 10E). Immunofluorescence staining revealed decreased expression of EMT markers ZEB2 and MMP9, as well as cell cycle regulators CDC6 and PCNA, indicating alterations in EMT status and cell cycle progression following treatment (Figures 10F, G). Furthermore, Figure 11 illustrates the broader role of DVL1 in SICand multiple cancers, with oxidative stress identified as a critical mediator linking DVL1 to these conditions. Digoxin emerges as a potential therapeutic agent targeting DVL1, modulating its activity and downstream signaling pathways. The combined results from transcriptomic analyses, drug susceptibility screening, and spatial transcriptomics provide a comprehensive view of DVL1's involvement in both SIC and cancer, positioning Digoxin as a promising therapeutic strategy for regulating these pathways.

4 Discussion

SIC is a serious complication in critically ill cancer patients and is closely associated with heart failure and high mortality (2, 121). TME-driven immune imbalance may exacerbate the development and progression of SIC (122, 123). The interaction mechanisms between tumor-associated inflammation, dysfunction of VSMC, and myocardial injury are still poorly elucidated (56, 124). Therefore, it is crucial to investigate the pathogenesis. In this study, the role of DVL1 in SIC was investigated by integrating transcriptome analysis, WGCNA, molecular docking and drug screening, and explored the possibility of DVL1 as a potential therapeutic target for SIC.

This study revealed the critical role of DVL1 gene in SIC in cancer patients (2). Multiomic analysis indicates that DVL1 is significantly upregulated in SIC and various gastrointestinal cancers, and is closely associated with the occurrence of poor prognosis and enhanced inflammatory response (115, 125). These findings not only highlight the role of DVL1 in the progression of SIC, but also elucidate its underlying mechanism in immune regulation within the tumor microenvironment. Furthermore, these insights have important

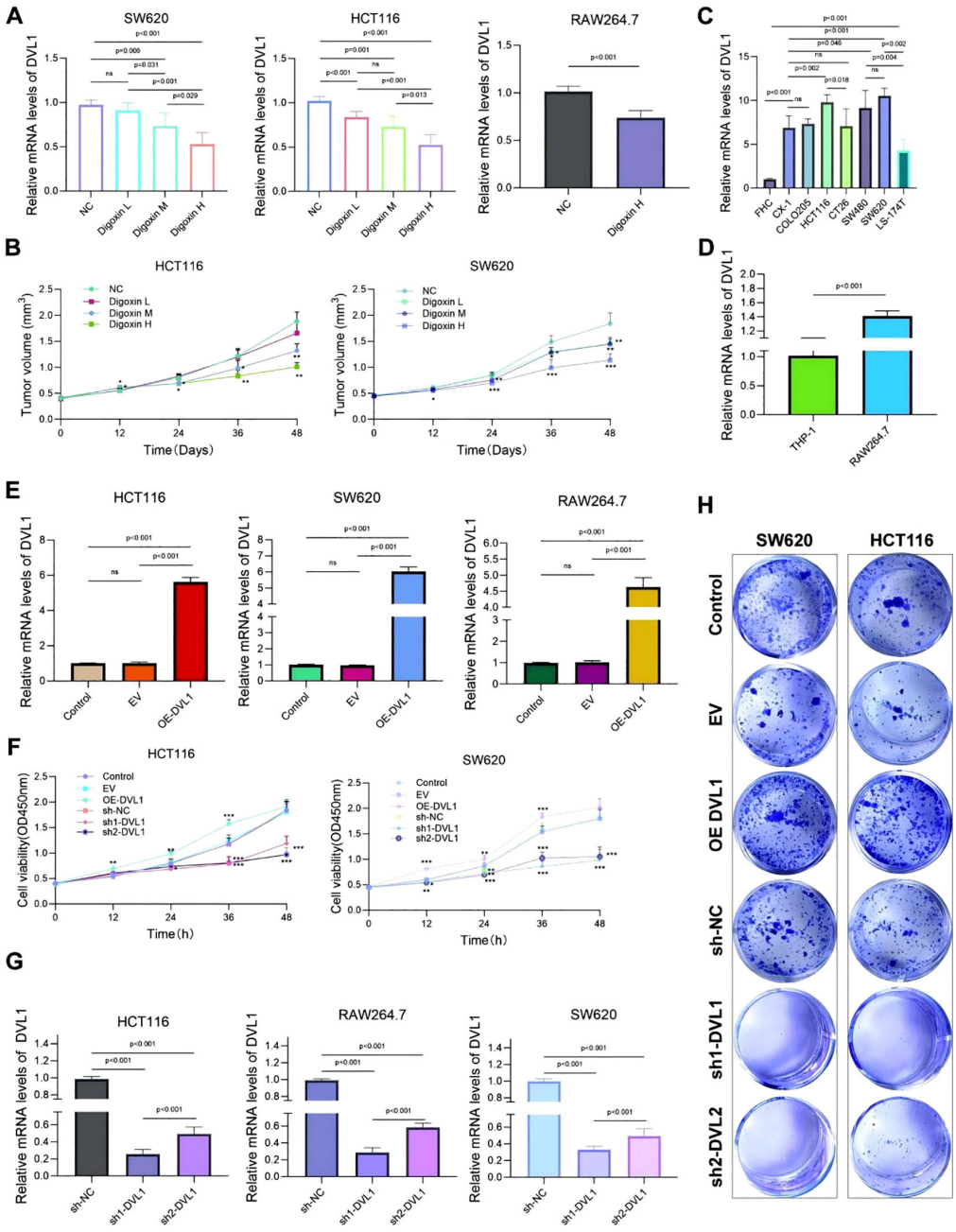

FIGURE 9
Analysis of DVL1 expression and its effects on cell proliferation and tumor progression across various cell lines. **(A)** Quantitative PCR Analysis: Relative mRNA levels of DVL1 in SW620, HCT116, and RAW264.7 cell lines following treatment with different concentrations of Digoxin (H, High; M, Medium; L, Low) were assessed using qPCR. The expression of DVL1 is significantly downregulated in cells treated with Digoxin, especially at high concentrations ($p < 0.001$). **(B)** CCK-8 Assay: Cell viability analysis of HCT116 and SW620 cells treated with different concentrations of Digoxin (H, M, L) over 48 hours using the CCK-8 assay. The results indicate a dose-dependent reduction in tumor volume in both cell lines, with Digoxin H showing the greatest inhibitory effect on proliferation ($p < 0.05$). **(C)** Inflammatory Cytokine Expression: Quantitative PCR was used to detect the mRNA expression levels of key inflammatory cytokines in multiple cell lines, including SW620, HCT116, and RAW264.7, treated with various conditions. Notable changes in cytokine expression are evident across different treatments ($p < 0.001$). **(D)** DVL1 Expression in THP-1 and RAW264.7 Cells: qPCR analysis of DVL1 mRNA levels in THP-1 and RAW264.7 cell lines, highlighting significant upregulation in RAW264.7 cells compared to THP-1 ($p < 0.001$). **(E)** DVL1 Expression in Various Cell Lines: qPCR results show the expression of DVL1 in SW620, HCT116, and RAW264.7 cells. The data indicate distinct differences in DVL1 expression levels among cell lines, with overexpression observed in specific groups ($p < 0.001$). **(F)** Impact of DVL1 on Cell Proliferation: The effect of DVL1 on cell proliferation in HCT116 and SW620 cells was evaluated using a CCK-8 assay. Results indicate that overexpression of DVL1 promotes cell proliferation, whereas knockdown significantly inhibits growth in both cell lines ($p < 0.001$). **(G)** DVL1 Expression Post-Knockdown: Quantitative PCR analysis of DVL1 expression in SW620, HCT116, and RAW264.7 cells following DVL1 knockdown. Results demonstrate a significant decrease in DVL1 mRNA levels across all tested cell lines after knockdown treatment ($p < 0.001$). **(H)** Plate Colony Formation Assay: Assessment of DVL1's impact on colony-forming ability in SW620 and HCT116 cells through plate cloning experiments. Images depict colonies from control, EV (empty vector), DVL1 overexpression (OE-DVL1), and DVL1 knockdown groups (sh-DVL1). The data suggest that DVL1 overexpression enhances colony formation, while knockdown reduces it. The symbols *, **, and *** represent statistical significance levels corresponding to $p<0.05$, $p<0.01$, and $p<0.\ 001$, respectively. ns, not significant.

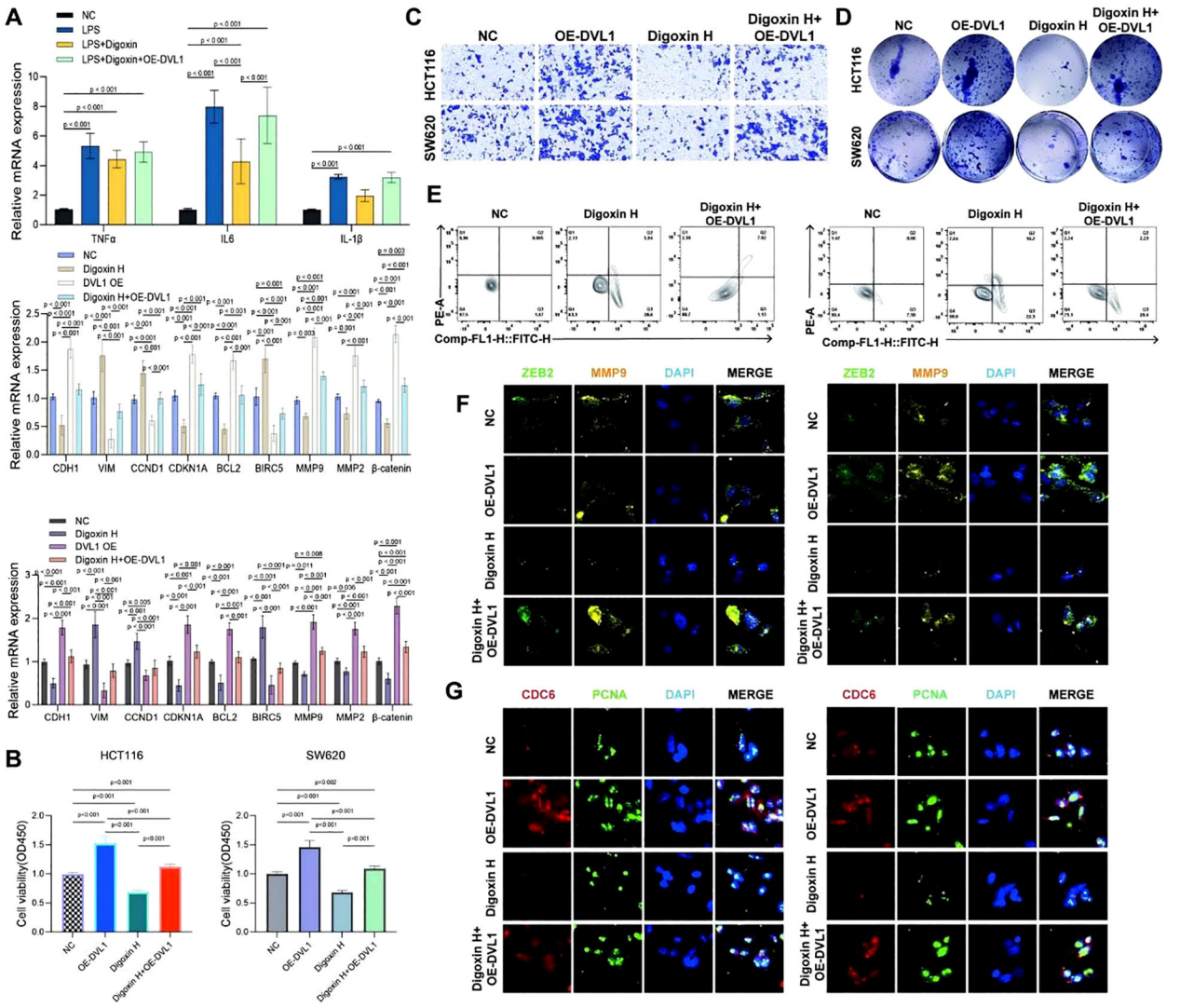

FIGURE 10
The effects of digoxin and DVL1 overexpression on inflammatory cytokine expression, cell viability, migration, proliferation, apoptosis, and key protein expression in SW620 and HCT116 cell lines. **(A)** Relative mRNA expression levels of inflammatory cytokines (TNFα, IL6, IL1β) and key EMT markers (CDH1, VIM, CDK1A, CDKN1, BCL2, BIRC5, MMP9, MMP2, β-catenin) were assessed in SW620 and HCT116 cell lines under different treatment conditions: Control group (NC), LPS, Digoxin, OE-DVL1, and the combination of LPS and Digoxin with OE-DVL1 overexpression. Data are presented as mean ± SD, with statistical significance indicated by p-values. **(B)** The effects of varying concentrations of Digoxin (High, Medium, Low) and OE-DVL1 on the viability of SW620 and HCT116 cells were measured using the CCK-8 assay. Significant decreases in viability were observed in cells treated with Digoxin H compared to controls, with further reductions upon OE-DVL1 overexpression. **(C)** The migratory capacity of SW620 and HCT116 cells was assessed using Transwell chambers. Cells treated with Digoxin H and those overexpressing DVL1 showed reduced migration compared to the control group, highlighting the role of Digoxin and DVL1 in inhibiting cell migration. **(D)** Proliferative ability was evaluated by plating SW620 and HCT116 cells. Colony formation was significantly reduced in the Digoxin H treatment group, with a further decrease in the combination of Digoxin H and OE-DVL1, indicating the suppressive effect of these treatments on cell proliferation. **(E)** Apoptosis was measured using flow cytometry in SW620 and HCT116 cells under various treatments. Increased levels of apoptosis were observed in cells treated with Digoxin H, especially when combined with OE-DVL1, compared to untreated controls. **(F, G)** Immunofluorescence staining of ZEB2, MMP9, CDC6, and PCNA: The expression of EMT marker ZEB2 and matrix metalloproteinase MMP9, as well as the cell cycle regulators CDC6 and PCNA, were visualized by immunofluorescence in SW620 and HCT116 cells. Cells treated with Digoxin H and those overexpressing OE-DVL1 displayed significant changes in these protein expressions, indicating alterations in EMT and cell cycle progression.

implications for understanding the differentiated response patterns during patient immunotherapy (63, 126). We used a variety of experimental methods to study the function of DVL1 in SIC and selected FDA-approved drugs such as Digoxin and paromomycin as potential inhibitors of DVL1. Among them, Digoxin reduces the level of sepsis-induced oxidative stress by targeting DVL1, thereby improving the survival rate of cardiomyocytes. The results of this study provide a new direction for pharmacological intervention in SIC. Approved drugs (repurposed drugs) may be used to improve clinical outcomes in patients with SIC. Especially in cancer patients, the impact of SIC on cardiac function may be more severe, and thus DVL1-targeted therapies may be an important complement to personalised immunotherapy. WGCNA further identified a turquoise module that is closely associated with SIC. This module

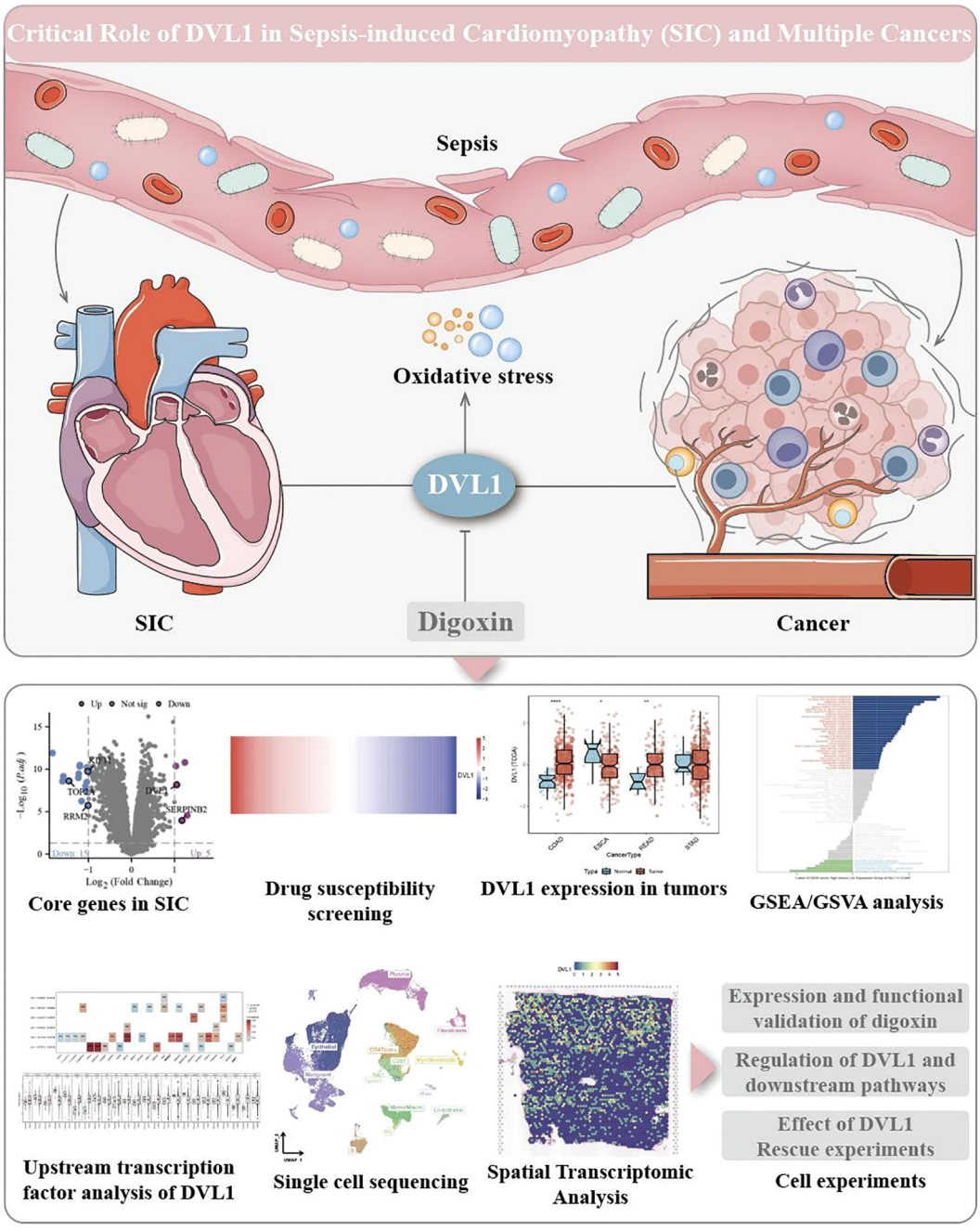

FIGURE 11
Critical role of DVL1 in sepsis-induced cardiomyopathy (SIC) and multiple cancers. This figure illustrates the central role of DVL1 in the progression of sepsis-induced cardiomyopathy and its association with various cancers, emphasizing the role of oxidative stress as a key mediator. The upper part of the image depicts sepsis-induced systemic inflammation leading to increased oxidative stress, which impacts the cardiovascular system, resulting in SIC. The illustration also highlights DVL1's involvement in cancer development and progression through its effects on tumor microenvironments. Positioned centrally, DVL1 acts as a crucial node that links oxidative stress responses to both cardiac dysfunction and oncogenic processes. Digoxin is indicated as a potential therapeutic agent that targets DVL1, offering a promising approach for modulating DVL1 activity and its downstream pathways. The lower section of the figure provides an overview of various experimental analyses related to DVL1's function. It includes differential expression analysis of core genes in SIC, highlighting significant alterations in gene expression (e.g., DVL1) through a volcano plot. Drug susceptibility screening results are presented in a heatmap, identifying the responsiveness of SIC-associated cells to potential therapeutic agents. Additionally, the figure shows DVL1 expression across different tumor types through box plots, revealing its dysregulation in multiple cancers. Gene set enrichment analysis (GSEA) and gene set variation analysis (GSVA) further demonstrate DVL1's involvement in critical signaling pathways. Transcription factor analysis and single-cell sequencing provide insights into the regulatory mechanisms and cellular heterogeneity associated with DVL1 expression. Spatial transcriptomic analysis maps the spatial distribution of DVL1 in tissue samples, while cell-based experiments validate the functional impact of DVL1, including the effects of Digoxin treatment and DVL1 knockdown on downstream signaling and cell viability.

contains a set of key genes that may synergistically contribute to the ground inflammatory response during sepsis. Immune infiltration analyses showed that increased DVL1 expression levels were closely associated with increased infiltration of pro-inflammatory immune cells (e.g., macrophages and T-cells), suggesting that DVL1 may influence the susceptibility of SIC patients by modulating the behavior of immune cells in the sepsis microenvironment. These results suggest that SIC is, at least in part, an immune-mediated disease and further reveal a central role for 138DVL1 in the regulation of inflammation.

In a broader biological context, this study revealed DVL1 as a key molecular link between sepsis, cancer, and cardiac dysfunction (31, 127).DVL1 is a core regulator of the Wnt signaling pathway and plays important roles in biological processes such as cell proliferation, differentiation, and migration (128, 129). Through bioinformatics analysis and experimental verification, studying the association of signaling pathways and diseases has become an important direction of current medical research, among which the research on the Wnt signaling pathway has yielded fruitful results (130).These studies provide new targets and ideas of disease treatment, further highlighting the significance for SIC therapy in the research focusing on DVL1 and the Wnt signaling pathway.DVL1, as a central mediator of the Wnt signaling pathway, modulates downstream signaling upon Wnt signaling activation by interacting with the frizzled receptor as well as Lrp5/6. It promotes the accumulation of β-cyclins by inhibiting GSK-3β and bringing it into the nucleus, which ultimately affects the expression of downstream genes (131, 132). Aberrant activation of the Wnt signaling pathway may promote pathological remodeling of cardiac tissue associated with SIC, especially in cancer patients in a hyperinflammatory state (133, 134). Because to the central role of Wnt signaling in immune regulation, this mechanism can help to understand the emergence of immunotherapy resistance in certain cancer subtypes.

This study also explored the epigenetic mechanisms of DVL1 transcriptional regulation, combined with ATAC-seq data. The methods of this study borrowed and combineed advanced technology and experimental procedures of several documents (135–137). In this process, big data and bioinformatics technologies play a key role. Their use in biomarker identification is increasingly important to aid in the diagnosis and prognostic assessment of the disease (138). We found that the open chromatin state of the DVL1 promoter and enhancer regions is closely associated with the binding of multiple transcription factors, including key transcriptional regulators such as MYC, NF- κ B and STAT 3. These transcription factors all play important roles in the inflammatory response, tumor progression, and immune regulation. The abnormal activation of MYC may aggravate the inflammatory response in the tumor microenvironment by enhancing DVL1 expression, and the synergistic action of NF- κ B and STAT 3 may further drive the pathological progression of SIC. It has been shown that the open state of chromatin not only determines gene accessibility, but also affects the extent to which tumor cells respond to immunotherapy. In the study of cancer immunotherapy, new mechanisms of immune cells have been explored from the aspects of epigenetic modification, metabolic regulation and intercellular communication to provide a theoretical basis for the optimization of cancer immunotherapy strategies (139). These studies highlight the important role of bioinformatics and transcriptomic approaches in resolving the tumor immune microenvironment and provide new perspectives for the development of future targeted therapeutic protocols (140, 141). This has similarities with our study on the role of DVL1 in SIC and the therapeutic strategy. Therefore, we hypothesized that targeted regulation of DVL1-associated epigenetic regulatory networks may help to optimize therapeutic strategies for SIC and related tumors. The study of biomarkers is a key link in early disease diagnosis and precision treatment (142). Using multi-omics analysis technology and combined with bioinformatics means it can reveal the potential markers of diseases from the molecular level, such as the identification of disease-related MicroRNAs, metabolic fingerprint maps and extracellular vesicle surface proteins from biological samples such as bile and serum, opening up a new way for the early detection of diseases and disease monitoring (143). The open chromatin regions revealed by ATAC-seq data can be used to screen patients who respond to DVL1 targeted therapy to enable precision treatment. Moreover, combined with single-cell sequencing technology, it is expected to further investigate the role of DVL1 in different immune cell subsets and reveal its dynamic changes in the remodeling of the immune microenvironment. These findings provide new perspectives for future research on targeted intervention strategies for DVL1. Despite the importance of this study, some limitations remain. First, we focused on the direct effect of DVL1 on cardiomyocytes, and did not deeply investigate its specific role in VSMCs in SIC (48, 56). VSMCs play a key role in maintaining vascular homeostasis and vascular remodeling processes, and their response during sepsis may influence the pathological progression of SIC (60, 144). Future studies investigating DVL1 function in VSMCs and analyzing its effects on vascular dysfunction should be performed to refine the mechanism of DVL1 action in the pathogenesis of SIC. Second, although this study explored the pharmacological intervention strategies for DVL1, its synergy with non-pharmacological interventions (e.g., exercise) has not been fully evaluated (145, 146). Exercise has been shown to improve the course of SIC by modulating the Wnt signaling pathway and reducing oxidative stress and inflammation.

In the future, further research can be made to investigate whether exercise improves SIC by affecting the DVL1 signaling pathway and evaluate the effect of combined exercise and drug intervention to optimize the comprehensive treatment regimen of SIC. Moreover, this study has some limitations in terms of sample size and dataset. The sample size may not be sufficiently representative of all potential patient population characteristics.The data in the database used may also have geographical, ethnic and other bias, thus affecting the generalizability of the study results. Future studies should also cover a wider range of cell types and explore in-depth the function of DVL1 in different microenvironments (e.g., tumor microenvironment and immune system).At the same time, the development of “off-the-shelf” gene therapy nanoparticles based on existing drugs or the use of CRISPR technology also provides new possibilities for clinical applications in medicine (147, 148). Furthermore, through in-depth analysis of patient engagement and social support systems, the investigators revealed the important

impact of these factors on disease management and patient mental health (149, 150). Future studies on SIC can consider including these psychosocial factors in the research category, comprehensively evaluate their interaction with biological factors, develop more comprehensive and effective treatment and management programs, and promote the overall recovery of patients.DVL1 expression is upregulated in a variety of cancers (such as colorectal and gastric cancers) and is closely associated with the abnormal activation of the Wnt signaling pathway. Understanding these interactions could provide new insights into how DVL1 mediates immune responses in the SIC. Finally, the main conclusions of this study are based on *in vitro* experiments and bioinformatics analysis, and lack support from *in vivo* experimental and clinical data. In the future, mouse SIC models should be constructed to verify the efficacy of DVL1 inhibitors (such as Digoxin) in SIC treatment and evaluate the correlation of DVL1 expression level and the prognosis of SIC patients combined with clinical data. The further development of animal experiments and clinical research will provide stronger evidence for the wide application of DVL1-targeted drugs in SIC treatment. Although this study focuses on the interaction of post-tumor inflammation with the dysfunction of VSMC and the mechanism of DVL1 in sepsis-induced cardiomyopathy (SIC), the field of medical research is broad and interconnected (43, 151). The coding research of the biological meta-universe explores the progress and challenges in the neural field from the macro level to the micro level, combined with the simulation of the nervous system information transmission, and lays the foundation for the future development of human-computer interaction and neuroregulation technology (152). In terms of microbial research, the study of the gut microbiome has always been a hot topic (153, 154). Using metagenomic sequencing technology combined with bioinformatics data analysis to deeply explore the interactions between microorganisms in the gut,is important for understanding the relationship between human health and disease. Microorganisms are also emerging in drug delivery. bacteria-based drug delivery systems have opened up new ways for the treatment of non-neoplastic diseases, showing unique therapeutic advantages (155). In this study, although the microbiome-related content was not directly involved, the microbiome combined with bioinformatics analysis can also open up new ways for the diagnosis and treatment of diseases (156, 157). In the future, in the study of SIC and related diseases, we may learn from the ideas and methods of microbial research, use bioinformatics to analyze the pathogen genome and host immune response data, deeply explore the relationship between microorganisms and diseases in SIC patients, and provide multi-dimensional support for the development of more effective treatment strategies (158, 159). This also suggests that in future studies, we should focus on the integration of research results in different fields and explore the pathogenesis and treatment strategies of SIC from a broader perspective (8, 121). In conclusion, this study reveals the critical role of DVL1 in the pathogenesis of SIC and provides strong evidence as a novel therapeutic target, providing important clues for precision medicine of SIC. Moreover, the synergistic effects of pharmacological and non-pharmacological interventions still deserve intensive investigation in the hope of providing more effective personalized treatment options for patients with SIC (160).In this process, big data and bioinformatics technologies play a pivotal role, particularly in biomarker identification, which is increasingly important for aiding the diagnosis and prognostic assessment of diseases (138). In the future, combining big data analysis, bioinformatics means, and multi-level experimental validation, it is expected to further elucidate the regulatory network of DVL1 and optimize its targeted intervention strategies (161, 162). The findings of this study not only deepen the understanding of the molecular mechanisms of DVL1, but also establish the theoretical basis for future personalized treatment strategies for patients with SIC (163, 164). Research of biomarkers is crucial for the early diagnosis and precise treatment of diseases (142, 165). In this study, multi-omics analysis techniques and bioinformatics means were used to study the DVL1 gene as a potential biomarker (125, 166). In the future, further research is expected to identify potential markers such as MicroRNAs, metabolic fingerprints, and extracellular vesicle surface proteins from more biological samples so as to provide more ways for early disease detection and disease monitoring and promote the development of personalized treatment for SIC and related diseases (143). With the continuous advancement of research, DVL1 will become a new breakthrough in the treatment of SIC and even cancer-related cardiovascular diseases, contributing to the development of new treatment methods (167–169).

5 Conclusion

This study highlights DVL1 as a key gene in SIC and its association with poor outcomes in cancer, particularly in the context of immunotherapy resistance. DVL1's upregulation is linked to increased inflammation and unfavorable prognosis, suggesting its role in the complex landscape of intratumor heterogeneity. Molecular docking identified Digoxin as a promising candidate for targeting DVL1, with the potential to reduce oxidative stress and modulate immune responses in SIC. WGCNA further confirmed the central role of DVL1 in the gene network driving disease progression. These findings underscore the potential of targeting DVL1 to improve therapeutic outcomes in SIC and cancer, particularly when integrated with pharmacotherapy and exercise regimens. By addressing the challenges posed by intratumor heterogeneity, this study offers new insights into the molecular mechanisms underlying SIC and its overlap with cancer progression. Further clinical research is needed to validate the therapeutic potential of targeting DVL1, aiming to enhance immunotherapy effectiveness and provide more personalized treatment strategies for patients facing both SIC and cancer.

Data availability statement

The original contributions presented in the study are included in the article/Supplementary Material. Further inquiries can be directed to the corresponding authors.

Ethics statement

As this study solely involves cell-based experiments, no ethical approval or informed consent was required.

Author contributions

RL: Conceptualization, Data curation, Formal Analysis, Investigation, Methodology, Resources, Software, Supervision, Writing – original draft, Writing – review & editing. LJ: Conceptualization, Formal Analysis, Investigation, Methodology, Writing – original draft, Writing – review & editing, Project administration, Resources, Supervision, Validation, Visualization. LY: Conceptualization, Data curation, Investigation, Methodology, Writing – original draft, Writing – review & editing, Formal Analysis, Software. DL: Data curation, Investigation, Methodology, Writing – original draft, Writing – review & editing, Conceptualization. QZL: Data curation, Formal Analysis, Investigation, Writing – original draft, Writing – review & editing, Methodology. BZ: Writing – original draft, Writing – review & editing, Data curation, Formal Analysis, Investigation. EG: Writing – original draft, Writing – review & editing, Project administration, Supervision. KX: Conceptualization, Writing – original draft, Writing – review & editing, Methodology, Visualization. QCL: Conceptualization, Formal Analysis, Writing – original draft, Writing – review & editing, Data curation.

Funding

The author(s) declare that financial support was received for the research and/or publication of this article. This work was supported by the The Academic Leaders Training Program of Shanghai Pudong New Area Health Commission (Grant Number: PWRd2022-14), The Medical Discipline Construction Program of Shanghai Pudong New Area Health Commission (the Specialty Program) (Grant Number: PWZzb2022-21), and The Scientific Research Program of Shanghai Pudong New Area Health Commission (Grant Number: PW2023A-51). Shanghai Pudong New Area Science and Technology Development Foundation Public Welfare Research Project (Grant Number: PKJ2022-Y14) and Shanghai Pudong New Area Health System Discipline Training Project (Grant Number: PWRd2024-21).

Acknowledgments

We want to thank the language editing team for their assistance in polishing the manuscript. We also express our gratitude to the Shanghai Pudong New Area Health Commission for their financial and resource support.

Conflict of interest

The authors declare that the research was conducted in the absence of any commercial or financial relationships that could be construed as a potential conflict of interest.

Generative AI statement

The author(s) declare that Generative AI was used in the creation of this manuscript. We also acknowledge the use of ChatGPT-4.0 for language optimization, limited to grammatical adjustments, ensuring no influence on the research content or academic integrity.

Publisher's note

All claims expressed in this article are solely those of the authors and do not necessarily represent those of their affiliated organizations, or those of the publisher, the editors and the reviewers. Any product that may be evaluated in this article, or claim that may be made by its manufacturer, is not guaranteed or endorsed by the publisher.

Supplementary material

The Supplementary Material for this article can be found online at: https://www.frontiersin.org/articles/10.3389/fimmu.2025.1560717/full#supplementary-material

References

1. Lin Y-M, Lee M-C, Toh HS, Chang W-T, Chen S-Y, Kuo F-H, et al. Association of sepsis-induced cardiomyopathy and mortality: a systematic review and meta-analysis. *Ann Intensive Care*. (2022) 12:112. doi: 10.1186/s13613-022-01089-3

2. Hanumanthu BKJ, Nair AS, Katamreddy A, Gilbert JS, You JY, Offor OL, et al. Sepsis-induced cardiomyopathy is associated with higher mortality rates in patients with sepsis. *Acute Crit Care*. (2021) 36:215–22. doi: 10.4266/acc.2021.00234

3. Wang Y, Zhou J, Wu K. High 28-day mortality in critically ill patients with sepsis and concomitant active cancer. *J Int Med Res*. (2018) 46:5030–9. doi: 10.1177/0300060518789040

4. Nazer L, Lopez-Olivo MA, Cuenca JA, Awad W, Brown AR, Abusara A, et al. All-cause mortality in cancer patients treated for sepsis in intensive care units: a systematic review and meta-analysis. *Support Care Cancer*. (2022) 30:10099–109. doi: 10.1007/s00520-022-07392-w

5. Kanterman J, Sade-Feldman M, Baniyash M. New insights into chronic inflammation-induced immunosuppression. *Semin Cancer Biol*. (2012) 22:307–18. doi: 10.1016/j.semcancer.2012.02.008

6. Shalapour S, Karin M. Immunity, inflammation, and cancer: an eternal fight between good and evil. *J Clin Invest*. (2015) 125:3347–55. doi: 10.1172/JCI80007

7. Mirouse A, Vigneron C, Llitjos J-F, Chiche J-D, Mira J-P, Mokart D, et al. Sepsis and cancer: an interplay of friends and foes. *Am J Respir Crit Care Med*. (2020) 202:1625–35. doi: 10.1164/rccm.202004-1116TR

8. Williams B, Zou L, Pittet J-F, Chao W. Sepsis-induced coagulopathy: A comprehensive narrative review of pathophysiology, clinical presentation, diagnosis, and management strategies. *Anesth Analg*. (2024) 23. doi: 10.1213/ANE.0000000000006888

9. Palaskas NL, Ali H-J, Koutroumpakis E, Ganatra S, Deswal A. Cardiovascular toxicity of immune therapies for cancer. *BMJ*. (2024) 385:e075859. doi: 10.1136/bmj-2023-075859

10. Totzeck M, Schuler M, Stuschke M, Heusch G, Rassaf T. Cardio-oncology - strategies for management of cancer-therapy related cardiovascular disease. *Int J Cardiol*. (2019) 280:163–75. doi: 10.1016/j.ijcard.2019.01.038

11. Heller G, Fuereder T, Grandits AM, Wieser R. New perspectives on biology, disease progression, and therapy response of head and neck cancer gained from single cell RNA sequencing and spatial transcriptomics. *Oncol Res*. (2024) 32:1–17. doi: 10.32604/or.2023.044774

12. Guo J, Tong C, Shi J, Li X, Chen X. A prognosis model for predicting immunotherapy response of esophageal cancer based on oxidative stress-related signatures. *Oncol Res*. (2024) 32:199–212. doi: 10.32604/or.2023.030969

13. Xu J, Wang F, Li Y, Li P, Zhang Y, Xu G, et al. Estrogen inhibits TGF–β1 –stimulated cardiac fibroblast differentiation and collagen synthesis by promoting Cdc42. *Mol Med Rep*. (2024) 30:123. doi: 10.3892/mmr.2024.13246

14. Gao D, Ge G. Exploring the underlying biology of cancer and potential therapeutic strategies: a special issue focused on mechanism-based studies. *Acta Biochim Biophys Sin*. (2023) 55:891–2. doi: 10.3724/abbs.2023114

15. Hu D, Sheeja Prabhakaran H, Zhang Y-Y, Luo G, He W, Liou Y-C. Mitochondrial dysfunction in sepsis: mechanisms and therapeutic perspectives. *Crit Care*. (2024) 28:292. doi: 10.1186/s13054-024-05069-w

16. Galley HF. Oxidative stress and mitochondrial dysfunction in sepsis. *Br J Anaesth*. (2011) 107:57–64. doi: 10.1093/bja/aer093

17. Mourad M, Chow-Chine L, Faucher M, Sannini A, Brun JP, De Guibert JM, et al. Early diastolic dysfunction is associated with intensive care unit mortality in cancer patients presenting with septic shock. *Br J Anaesth*. (2014) 112:102–9. doi: 10.1093/bja/aet296

18. Tirichen H, Yaigoub H, Xu W, Wu C, Li R, Li Y. Mitochondrial reactive oxygen species and their contribution in chronic kidney disease progression through oxidative stress. *Front Physiol*. (2021) 12:627837. doi: 10.3389/fphys.2021.627837

19. Sanderson TH, Reynolds CA, Kumar R, Przyklenk K, Hüttemann M. Molecular mechanisms of ischemia–reperfusion injury in brain: pivotal role of the mitochondrial membrane potential in reactive oxygen species generation. *Mol Neurobiol*. (2013) 47:9–23. doi: 10.1007/s12035-012-8344-z

20. Arba F, Ferretti S, Leigh R, Fara A, Warach SJ, Luby M, et al. Cerebral small vessel disease and infarct growth in acute ischemic stroke treated with intravenous thrombolysis. *Transl Stroke Res*. (2024) 24. doi: 10.1007/s12975-024-01277-2

21. Zhang W, Liu Y, Zhou J, Qiu T, Xie H, Pu Z. Chicoric acid advanced PAQR3 ubiquitination to ameliorate ferroptosis in diabetes nephropathy through the relieving of the interaction between PAQR3 and P110α pathway. *Clin Exp Hypertens*. (2024) 46:2326021. doi: 10.1080/10641963.2024.2326021

22. Xu W, Gao X, Luo H, Chen Y. FGF21 attenuates salt-sensitive hypertension via regulating HNF4α/ACE2 axis in the hypothalamic paraventricular nucleus of mice. *Clin Exp Hypertens*. (2024) 46:2361671. doi: 10.1080/10641963.2024.2361671

23. Chen D, Zhang X, Li Z, Zhu B. Metabolic regulatory crosstalk between tumor microenvironment and tumor-associated macrophages. *Theranostics*. (2021) 11:1016–30. doi: 10.7150/thno.51777

24. Wang N, Liang H, Zen K. Molecular mechanisms that influence the macrophage M1â€"M2 polarization balance. *Front Immunol*. (2014) 5:614. doi: 10.3389/fimmu.2014.00614

25. Thakur A, Banerjee R, Thakur S, Kumar G, Thakur SS. Role of macrophage polarization in cancer progression and their association with COVID-19 severity. *Cancer Insight*. (2023) 24. doi: 10.58567/ci02010005

26. Wang Y, Liu W, Zhang J, Geng P, Jin X. The role of crosstalk between cerebral immune cells and peripheral immune cells in the damage and protection of blood–brain barrier after intracerebral hemorrhage. *Brain Hemorrhages*. (2024) 5:117–30. doi: 10.1016/j.hest.2024.02.002

27. Peters Van Ton AM, Kox M, Abdo WF, Pickkers P. Precision immunotherapy for sepsis. *Front Immunol*. (2018) 9:1926. doi: 10.3389/fimmu.2018.01926

28. Patil NK, Bohannon JK, Sherwood ER. Immunotherapy: A promising approach to reverse sepsis-induced immunosuppression. *Pharmacol Res*. (2016) 111:688–702. doi: 10.1016/j.phrs.2016.07.019

29. Rudiger A, Singer M. Mechanisms of sepsis-induced cardiac dysfunction. *Crit Care Med*. (2007) 35:1599–608. doi: 10.1097/01.CCM.0000266683.64081.02

30. Potz B A, Sellke FW, Abid MR. Endothelial ROS and impaired myocardial oxygen consumption in sepsis-induced cardiac dysfunction. *J Intensive Crit Care*. (2016) 02:24. doi: 10.21767/2471-8505.100020

31. Huang H, Wang Q, Ma L, Wu Y. ITGAM: A pivotal regulator in macrophage dynamics and cardiac function during sepsis-induced cardiomyopathy. *Cureus*. (2024) 24. doi: 10.7759/cureus.59342

32. Del Bufalo D, Bagnato A, Fusco A, Milella M. Lost in translation: bridging the gap between cancer research and effective therapies. *Cell Death Differ*. (2011) 18:1082–4. doi: 10.1038/cdd.2010.186

33. Stanczak MA, Läubli H. Siglec receptors as new immune checkpoints in cancer. *Mol Aspects Med*. (2023) 90:101112. doi: 10.1016/j.mam.2022.101112

34. Clària J, Arroyo V, Moreau R. The acute-on-chronic liver failure syndrome, or when the innate immune system goes astray. *J Immunol*. (2016) 197:3755–61. doi: 10.4049/jimmunol.1600818

35. Alonso De Vega JM, Díaz J, Serrano E, Carbonell LF. Oxidative stress in critically ill patients with systemic inflammatory response syndrome. *Crit Care Med*. (2002) 30:1782–6. doi: 10.1097/00003246-200208000-00018

36. Zanotti S, Kumar A, Kumar A. Cytokine modulation in sepsis and septic shock. *Expert Opin Investig Drugs*. (2002) 11:1061–75. doi: 10.1517/13543784.11.8.1061

37. Houschyar KS, Pyles MN, Rein S, Nietzschmann I, Duscher D, Maan ZN, et al. Continuous hemoadsorption with a cytokine adsorber during sepsis – a review of the literature. *Int J Artif Organs*. (2017) 40:205–11. doi: 10.5301/ijao.5000591

38. Mann DL. Stress-activated cytokines and the heart: from adaptation to maladaptation. *Annu Rev Physiol*. (2003) 65:81–101. doi: 10.1146/annurev.physiol.65.092101.142249

39. Mehra VC, Ramgolam VS, Bender JR. Cytokines and cardiovascular disease. *J Leukoc Biol*. (2005) 78:805–18. doi: 10.1189/jlb.0405182

40. Williams JC, Ford ML, Coopersmith CM. Cancer and sepsis. *Clin Sci*. (2023) 137:881–93. doi: 10.1042/CS20220713

41. Drosatos K, Lymperopoulos A, Kennel PJ, Pollak N, Schulze PC, Goldberg IJ. Pathophysiology of sepsis-related cardiac dysfunction: driven by inflammation, energy mismanagement, or both? *Curr Heart Fail Rep*. (2015) 12:130–40. doi: 10.1007/s11897-014-0247-z

42. D'Oria R, Schipani R, Leonardini A, Natalicchio A, Perrini S, Cignarelli A, et al. The role of oxidative stress in cardiac disease: from physiological response to injury factor. *Oxid Med Cell Longev*. (2020) 2020:1–29. doi: 10.1155/2020/5732956

43. Liu Y-C, Yu M-M, Shou S-T, Chai Y-F. Sepsis-induced cardiomyopathy: mechanisms and treatments. *Front Immunol*. (2017) 8:1021. doi: 10.3389/fimmu.2017.01021

44. Yao J-Y, Yang Y-L, Chen W-J, Fan H-Y. Exploring the therapeutic potential of Qi Teng Mai Ning recipe in ischemic stroke and vascular cognitive impairment. *Tradit Med Res*. (2024) 9:57. doi: 10.53388/TMR20240214001

45. Pourbagheri-Sigaroodi A, Fallah F, Momeny M, Rezaei N, Bashash D. Unveiling the predictive power of bacterial response-related genes signature in hepatocellular carcinoma: with bioinformatics analyses and experimental approaches. *BIOCELL*. (2024) 48:1781–804. doi: 10.32604/biocell.2024.055848

46. Lv X, Mao Z, Sun X, Liu B. Intratumoral heterogeneity in lung cancer. *Cancers*. (2023) 15:2709. doi: 10.3390/cancers15102709

47. Janiszewska M. The microcosmos of intratumor heterogeneity: the space-time of cancer evolution. *Oncogene*. (2020) 39:2031–9. doi: 10.1038/s41388-019-1127-5

48. Zaky A, Deem S, Bendjelid K, Treggiari MM. Characterization of cardiac dysfunction in sepsis: an ongoing challenge. *Shock*. (2014) 41:12–24. doi: 10.1097/SHK.0000000000000065

49. Comen EA, Bowman RL, Kleppe M. Underlying causes and therapeutic targeting of the inflammatory tumor microenvironment. *Front Cell Dev Biol*. (2018) 6:56. doi: 10.3389/fcell.2018.00056

50. McAllister SS, Weinberg RA. The tumour-induced systemic environment as a critical regulator of cancer progression and metastasis. *Nat Cell Biol*. (2014) 16:717–27. doi: 10.1038/ncb3015

51. Nieminen MS, Dickstein K, Fonseca C, Serrano JM, Parissis J, Fedele F, et al. The patient perspective: Quality of life in advanced heart failure with frequent hospitalisations. *Int J Cardiol*. (2015) 191:256–64. doi: 10.1016/j.ijcard.2015.04.235

52. Sila CA. Cognitive impairment in chronic heart failure. *Cleve Clin J Med*. (2007) 74:S132–2. doi: 10.3949/ccjm.74.Suppl_1.S132

53. Omerovic E. Did Jesus die of a 'broken heart'? *Eur J Heart Fail*. (2009) 11:729–31. doi: 10.1093/eurjhf/hfp095

54. Oyinbo C. Secondary injury mechanisms in traumatic spinal cord injury: a nugget of this multiply cascade. *Acta Neurobiol Exp (Warsz)*. (2011) 71:281–99. doi: 10.55782/ane-2011-1848

55. Song J, Ren K, Zhang D, Lv X, Sun L, Deng Y, et al. A novel signature combing cuproptosis- and ferroptosis-related genes in sepsis-induced cardiomyopathy. *Front Genet*. (2023) 14:1170737. doi: 10.3389/fgene.2023.1170737

56. Sorokin V, Vickneson K, Kofidis T, Woo CC, Lin XY, Foo R, et al. Role of vascular smooth muscle cell plasticity and interactions in vessel wall inflammation. *Front Immunol*. (2020) 11:599415. doi: 10.3389/fimmu.2020.599415

57. Orr AW, Hastings NE, Blackman BR, Wamhoff BR. Complex regulation and function of the inflammatory smooth muscle cell phenotype in atherosclerosis. *J Vasc Res*. (2010) 47:168–80. doi: 10.1159/000250095

58. Sergi C, Shen F, Lim DW, Liu W, Zhang M, Chiu B, et al. Cardiovascular dysfunction in sepsis at the dawn of emerging mediators. *BioMed Pharmacother*. (2017) 95:153–60. doi: 10.1016/j.biopha.2017.08.066

59. Zanotti-Cavazzoni SL, Hollenberg SM. Cardiac dysfunction in severe sepsis and septic shock. *Curr Opin Crit Care*. (2009) 15:392–7. doi: 10.1097/MCC.0b013e3283307a4e

60. Strela FB, Brun BF, Berger RCM, Melo S, De Oliveira EM, Barauna VG, et al. Lipopolysaccharide exposure modulates the contractile and migratory phenotypes of vascular smooth muscle cells. *Life Sci*. (2020) 241:117098. doi: 10.1016/j.lfs.2019.117098

61. Tang H-Y, Chen A-Q, Zhang H, Gao X-F, Kong X-Q, Zhang J-J. Vascular smooth muscle cells phenotypic switching in cardiovascular diseases. *Cells*. (2022) 11:4060. doi: 10.3390/cells11244060

62. Ashraf JV, Al Haj Zen A. Role of vascular smooth muscle cell phenotype switching in arteriogenesis. *Int J Mol Sci*. (2021) 22:10585. doi: 10.3390/ijms221910585

63. Nie Q, Zhang J, He B, Wang F, Sun M, Wang C, et al. A novel mechanism of protection against isoproterenol-induced cardiac inflammation via regulation of the SIRT1/NRF2 signaling pathway with a natural SIRT1 agonist. *Eur J Pharmacol*. (2020) 886:173398. doi: 10.1016/j.ejphar.2020.173398

64. Wang R, Peng X, Yuan Y, Shi B, Liu Y, Ni H, et al. Dynamic immune recovery process after liver transplantation revealed by single-cell multi-omics analysis. *Innovation*. (2024) 5:100599. doi: 10.1016/j.xinn.2024.100599

65. Zhang J, He J, Chen W, Chen G, Wang L, Liu Y, et al. Single-cell RNA-binding protein pattern-mediated molecular subtypes depict the hallmarks of the tumor microenvironment in bladder urothelial carcinoma. *Oncologie*. (2024) 26:657–69. doi: 10.1515/oncologie-2024-0071

66. Raines EW, Ferri N. Thematic Review Series: The Immune System and Atherogenesis. Cytokines affecting endothelial and smooth muscle cells in vascular disease. *J Lipid Res*. (2005) 46:1081–92. doi: 10.1194/jlr.R500004-JLR200

67. Feng D, Li D, Wang J, Wu R, Zhang C. Senescence-associated lncRNAs indicate distinct molecular subtypes associated with prognosis and androgen response in patients with prostate cancer. *Acta Mater Med*. (2023) 2:24. doi: 10.15212/AMM-2023-0025

68. Zhang M, Otsuki K, Li W. Molecular networking as a natural products discovery strategy. *Acta Mater Med*. (2023) 2:24. doi: 10.15212/AMM-2023-0007

69. Vanhoutte D, Schellings MWM, Götte M, Swinnen M, Herias V, Wild MK, et al. Increased expression of syndecan-1 protects against cardiac dilatation and dysfunction after myocardial infarction. *Circulation*. (2007) 115:475–82. doi: 10.1161/CIRCULATIONAHA.106.644609

70. Shimada BK, Boyman L, Huang W, Zhu J, Yang Y, Chen F, et al. Pyruvate-driven oxidative phosphorylation is downregulated in sepsis-induced cardiomyopathy: A study of mitochondrial proteome. *Shock*. (2022) 57:553–64. doi: 10.1097/SHK.0000000000001858

71. Verma SK, Garikipati VNS, Kishore R. Mitochondrial dysfunction and its impact on diabetic heart. *Biochim Biophys Acta BBA - Mol Basis Dis*. (2017) 1863:1098–105. doi: 10.1016/j.bbadis.2016.08.021

72. Lin J, Kirshenbaum LA. Wnt-1 dishevelled signaling functionally links calcium-calmodulin–dependent protein kinase II and cardiac dysfunction. *Hypertension*. (2015) 65:287–8. doi: 10.1161/HYPERTENSIONAHA.114.04616

73. Chen Y-R, Zweier JL. Cardiac mitochondria and reactive oxygen species generation. *Circ Res*. (2014) 114:524–37. doi: 10.1161/CIRCRESAHA.114.300559

74. Gao D, Yang J, Wu Y, Wang Q, Wang Q, Lai EY, et al. Targeting dynamin 2 as a novel pathway to inhibit cardiomyocyte apoptosis following oxidative stress. *Cell Physiol Biochem*. (2016) 39:2121–34. doi: 10.1159/000447908

75. Costa R, Peruzzo R, Bachmann M, Montà GD, Vicario M, Santinon G, et al. Impaired mitochondrial ATP production downregulates wnt signaling via ER stress induction. *Cell Rep*. (2019) 28:1949–1960.e6. doi: 10.1016/j.celrep.2019.07.050

76. Arrázola MS, Silva-Alvarez C, Inestrosa NC. How the Wnt signaling pathway protects from neurodegeneration: the mitochondrial scenario. *Front Cell Neurosci*. (2015) 9:166. doi: 10.3389/fncel.2015.00166

77. Kuroshima T, Kawaguchi S, Okada M. Current perspectives of mitochondria in sepsis-induced cardiomyopathy. *Int J Mol Sci*. (2024) 25:4710. doi: 10.3390/ijms25094710

78. Haybar H, Shahrouzian M, Gatavizadeh Z, Saki N, Maniati M, Deris Zayeri Z. Cyclin D1: A golden gene in cancer, cardiotoxicity, and cardioprotection. *Jundishapur J Chronic Dis Care*. (2021) 10. doi: 10.5812/jjcdc.112413

79. Ramel D, Gayral S, Sarthou M-K, Augé N, Nègre-Salvayre A, Laffargue M. Immune and smooth muscle cells interactions in atherosclerosis: how to target a breaking bad dialogue? *Front Pharmacol*. (2019) 10:1276. doi: 10.3389/fphar.2019.01276

80. Sabe VT, Ntombela T, Jhamba LA, Maguire GEM, Govender T, Naicker T, et al. Current trends in computer aided drug design and a highlight of drugs discovered via computational techniques: A review. *Eur J Med Chem*. (2021) 224:113705. doi: 10.1016/j.ejmech.2021.113705

81. Wu Z, Chen S, Wang Y, Li F, Xu H, Li M, et al. Current perspectives and trend of computer-aided drug design: a review and bibliometric analysis. *Int J Surg*. (2024) 24. doi: 10.1097/JS9.0000000000001289

82. Huang W-B, Qin S-Y, Zou J-B, Li X, Kang W-L, Yuan P-W. Efficacy of Juanbi capsule on ameliorating knee osteoarthritis: a network pharmacology and experimental verification-based study. *Tradit Med Res*. (2024) 9:33. doi: 10.53388/TMR20230829002

83. Zhang J, Zhao F, Ma B, Shen X, Geng Y. Fluoxetine inhibited RANKL-induced osteoclastic differentiation *in vitro*. *Open Med*. (2024) 19:20241094. doi: 10.1515/med-2024-1094

84. Lou C, Pang C, Jing C, Wang S, He X, Liu X, et al. Dynamic balance measurement and quantitative assessment using wearable plantar-pressure insoles in a pose-sensed virtual environment. *Sensors*. (2018) 18:4193. doi: 10.3390/s18124193

85. Hussen BM, Taheri M, RKh Y, Gh A, Sr A, Rk K, et al. Revolutionizing medicine: recent developments and future prospects in stem-cell therapy. *Int J Surg*. (2024) 110:8002–24. doi: 10.1097/JS9.0000000000002109

86. Zhou W, Wu J, Zhang J, Liu X, Guo S, Jia S, et al. Integrated bioinformatics analysis to decipher molecular mechanism of compound Kushen injection for esophageal cancer by combining WGCNA with network pharmacology. *Sci Rep*. (2020) 10:12745. doi: 10.1038/s41598-020-69708-2

87. Chu C, Sun W, Chen S, Jia Y, Ni Y, Wang S, et al. Squid-inspired anti-salt skin-like elastomers with superhigh damage resistance for aquatic soft robots. *Adv Mater*. (2024) 36:2406480. doi: 10.1002/adma.202406480

88. Ni Y, Li B, Chu C, Wang S, Jia Y, Cao S, et al. One-step fabrication of ultrathin porous Janus membrane within seconds for waterproof and breathable electronic skin. *Sci Bull*. (2024) S2095927324009502. doi: 10.1016/j.scib.2024.12.040

89. Liu D, Wang T, Wang Q, Dong P, Liu X, Li Q, et al. Identification of key genes in sepsis-induced cardiomyopathy based on integrated bioinformatical analysis and experiments *in vitro* and *in vivo*. *PeerJ*. (2023) 11:e16222. doi: 10.7717/peerj.16222

90. Li J, Zhou L, Li Z, Yang S, Tang L, Gong H. Identification of crucial genes and infiltrating immune cells underlying sepsis-induced cardiomyopathy via weighted gene co-expression network analysis. *Front Genet*. (2021) 12:812509. doi: 10.3389/fgene.2021.812509

91. Chen Y, Chen X, Luo Z, Kang X, Ge Y, Wan R, et al. Exercise-induced reduction of IGF1R sumoylation attenuates neuroinflammation in APP/PS1 transgenic mice. *J Adv Res*. (2024) S2090123224001279. doi: 10.1016/j.jare.2024.03.025

92. Chen Y, Huang L, Luo Z, Han D, Luo W, Wan R, et al. Pantothenate-encapsulated liposomes combined with exercise for effective inhibition of CRM1-mediated PKM2 translocation in Alzheimer's therapy. *J Controlled Release*. (2024) 373:336–57. doi: 10.1016/j.jconrel.2024.07.010

93. Chen Y, Luo Z, Sun Y, Li F, Han Z, Qi B, et al. Exercise improves choroid plexus epithelial cells metabolism to prevent glial cell-associated neurodegeneration. *Front Pharmacol*. (2022) 13:1010785. doi: 10.3389/fphar.2022.1010785

94. Wu Y, Li Y, Wu T, Yang H. The dual roles of S-nitrosylation of proteins in cancer: molecular mechanisms and recent advancements. *Cancer Insight*. (2024) 3:37–48. doi: 10.58567/ci03020005

95. Yuan L, Liu Y, Sun Y, Ren L, Gu X, Chen L, et al. Puerarin attenuates remifentanil–induced postoperative hyperalgesia via targeting PAX6 to regulate the transcription of TRPV1. *Mol Med Rep*. (2024) 29:81. doi: 10.3892/mmr.2024.13204

96. Yauch RL, Settleman J. Recent advances in pathway-targeted cancer drug therapies emerging from cancer genome analysis. *Curr Opin Genet Dev*. (2012) 22:45–9. doi: 10.1016/j.gde.2012.01.003

97. Nicolaides NC, Sass PM, Grasso L. Advances in targeted therapeutic agents. *Expert Opin Drug Discovery*. (2010) 5:1123–40. doi: 10.1517/17460441.2010.521496

98. Chistiakov DA, Orekhov AN, Bobryshev YV. Vascular smooth muscle cell in atherosclerosis. *Acta Physiol*. (2015) 214:33–50. doi: 10.1111/apha.12466

99. Clarke MCH, Figg NL, Bennett MR. Vascular smooth muscle cell apoptosis induces interleukin-1–directed inflammation: effects of hyperlipidemia-mediated inhibition of phagocytosis. *Circ Res*. (2010) 106:363–72. doi: 10.1161/CIRCRESAHA.109.208389

100. Marques L, Costa B, Pereira M, Silva A, Santos J, Saldanha L, et al. Advancing precision medicine: A review of innovative in silico approaches for drug development, clinical pharmacology and personalized healthcare. *Pharmaceutics*. (2024) 16:332. doi: 10.3390/pharmaceutics16030332

101. Maggi E, Patterson NE, Montagna C. Technological advances in precision medicine and drug development. *Expert Rev Precis Med Drug Dev*. (2016) 1:331–43. doi: 10.1080/23808993.2016.1176527

102. Chen M, Kong C, Zheng Z, Li Y. Identification of biomarkers associated with septic cardiomyopathy based on bioinformatics analyses. *J Comput Biol*. (2020) 27:69–80. doi: 10.1089/cmb.2019.0181

103. Long Q, Li G, Dong Q, Wang M, Li J, Wang L. Exploration of the shared gene signatures between myocardium and blood in sepsis: evidence from bioinformatics analysis. *BioMed Res Int*. (2022) 2022:1–16. doi: 10.1155/2022/3690893

104. Huang D, Zheng S, Liu Z, Zhu K, Zhi H, Ma G. Machine learning revealed ferroptosis features and a novel ferroptosis-based classification for diagnosis in acute myocardial infarction. *Front Genet*. (2022) 13:813438. doi: 10.3389/fgene.2022.813438

105. Cirulis MM, Beesley SJ, Wilson EL, Stubben C, Olsen TD, Hirshberg EL, et al. The peripheral blood transcriptome in septic cardiomyopathy: an observational, pilot study. *Intensive Care Med Exp*. (2019) 7:57. doi: 10.1186/s40635-019-0271-0

106. Wu P, Nielsen TE, Clausen MH. Small-molecule kinase inhibitors: an analysis of FDA-approved drugs. *Drug Discovery Today*. (2016) 21:5–10. doi: 10.1016/j.drudis.2015.07.008

107. Lin H-H, Zhang L-L, Yan R, Lu J-J, Hu Y. Network analysis of drug–target interactions: A study on FDA-approved new molecular entities between 2000 to 2015. *Sci Rep*. (2017) 7:12230. doi: 10.1038/s41598-017-12061-8

108. Wishart DS, Feunang YD, Guo AC, Lo EJ, Marcu A, Grant JR, et al. DrugBank 5.0: a major update to the DrugBank database for 2018. *Nucleic Acids Res*. (2018) 46: D1074–82. doi: 10.1093/nar/gkx1037

109. Vilar S, Harpaz R, Uriarte E, Santana L, Rabadan R, Friedman C. Drug—drug interaction through molecular structure similarity analysis. *J Am Med Inform Assoc*. (2012) 19:1066–74. doi: 10.1136/amiajnl-2012-000935

110. Khatami MH, Bromberek M, Saika-Voivod I, Booth V. Molecular dynamics simulations of histidine-containing cod antimicrobial peptide paralogs in self-assembled bilayers. *Biochim Biophys Acta BBA - Biomembr*. (2014) 1838:2778–87. doi: 10.1016/j.bbamem.2014.07.013

111. Vo ATN, Murphy MA, Stone TW, Phan PK, Baskes MI, Prabhu RK. Molecular dynamics simulations of phospholipid bilayer mechanoporation under different strain states—a comparison between GROMACS and LAMMPS. *Model Simul Mater Sci Eng*. (2021) 29:055015. doi: 10.1088/1361-651X/abfeaf

112. Alves KMA, Cardoso FJB, Honorio KM, De Molfetta FA. Design of inhibitors for glyceraldehyde-3-phosphate dehydrogenase (GAPDH) enzyme of leishmania mexicana. *Med Chem*. (2020) 16:784–95. doi: 10.2174/1573406415666190712111139

113. Guterres H, Im W. Improving protein-ligand docking results with high-throughput molecular dynamics simulations. *J Chem Inf Model*. (2020) 60:2189–98. doi: 10.1021/acs.jcim.0c00057

114. Zhao W. Cyclin D1 in various cancers: Mechanisms and clinical implications. *Theor Nat Sci*. (2024) 29:87–91. doi: 10.54254/2753-8818/29/20240752

115. He R, Chen Y, Qian C, Hu Y, Huang X, Tao R. Dishevelled segment polarity protein 2 promotes gastric cancer progression through Wnt/β-catenin pathway. *Tissue Cell*. (2023) 82:102119. doi: 10.1016/j.tice.2023.102119

116. Yang X, Qi Q, Pan Y, Zhou Q, Wu Y, Zhuang J, et al. Single-cell analysis reveals characterization of infiltrating T cells in moderately differentiated colorectal cancer. *Front Immunol*. (2021) 11:620196. doi: 10.3389/fimmu.2020.620196

117. Sun D, Wang J, Han Y, Dong X, Ge J, Zheng R, et al. TISCH: a comprehensive web resource enabling interactive single-cell transcriptome visualization of tumor microenvironment. *Nucleic Acids Res*. (2021) 49:D1420–30. doi: 10.1093/nar/gkaa1020

118. Wang Y, Ma Q, Zhang S, Liu H, Zhao B, Du B, et al. Digoxin enhances the anticancer effect on non-small cell lung cancer while reducing the cardiotoxicity of adriamycin. *Front Pharmacol*. (2020) 11:186. doi: 10.3389/fphar.2020.00186

119. Zha W, Wang G, Xu W, Liu X, Wang Y, Zha BS, et al. Inhibition of P-glycoprotein by HIV protease inhibitors increases intracellular accumulation of berberine in murine and human macrophages. *PloS One*. (2013) 8:e54349. doi: 10.1371/journal.pone.0054349

120. Hardin J, Kloke J. Statistical analyses. *Curr Protoc Essent Lab Tech*. (2017) 14:24. doi: 10.1002/cpet.10

121. Han Z, Quan Z, Zeng S, Wen L, Wang H. Utilizing omics technologies in the investigation of sepsis-induced cardiomyopathy. *IJC Heart Vasc*. (2024) 54:101477. doi: 10.1016/j.ijcha.2024.101477

122. Chen C, Wang Z, Ding Y, Qin Y. Tumor microenvironment-mediated immune evasion in hepatocellular carcinoma. *Front Immunol*. (2023) 14:1133308. doi: 10.3389/fimmu.2023.1133308

123. De Visser KE, Joyce JA. The evolving tumor microenvironment: From cancer initiation to metastatic outgrowth. *Cancer Cell*. (2023) 41:374–403. doi: 10.1016/j.ccell.2023.02.016

124. Wiejak J, Murphy FA, Maffia P, Yarwood SJ. Vascular smooth muscle cells enhance immune/vascular interplay in a 3-cell model of vascular inflammation. *Sci Rep*. (2023) 13:15889. doi: 10.1038/s41598-023-43221-8

125. Sharma M, Castro-Piedras I, Rodgers AD, Pruitt K. Genomic profiling of DVL-1 and its nuclear role as a transcriptional regulator in triple negative breast cancer. *Genes Cancer*. (2021) 12:77–95. doi: 10.18632/genesandcancer.217

126. Iba T, Nisio MD, Levy JH, Kitamura N, Thachil J. New criteria for sepsis-induced coagulopathy (SIC) following the revised sepsis definition: a retrospective analysis of a nationwide survey. *BMJ Open*. (2017) 7:e017046. doi: 10.1136/bmjopen-2017-017046

127. Li J, Zhang Y, Zhang D, Li Y. The role of long non-coding RNAs in sepsis-induced cardiac dysfunction. *Front Cardiovasc Med*. (2021) 8:684348. doi: 10.3389/fcvm.2021.684348

128. Gentzel M, Schambony A. Dishevelled paralogs in vertebrate development: redundant or distinct? *Front Cell Dev Biol*. (2017) 5:59. doi: 10.3389/fcell.2017.00059

129. Alshahrani SH, Rakhimov N, Rana A, Alsaab HO, Hjazi A, Adile M, et al. Dishevelled: An emerging therapeutic oncogene in human cancers. *Pathol - Res Pract*. (2023) 250:154793. doi: 10.1016/j.prp.2023.154793

130. Ding C, Wang J, Wang J, Niu J, Xiahou Z, Sun Z, et al. Heterogeneity of cancer-associated fibroblast subpopulations in prostate cancer: Implications for prognosis and immunotherapy. *Transl Oncol*. (2025) 52:102255. doi: 10.1016/j.tranon.2024.102255

131. National Cancer Institute. DVL1 gene.," Definitions. *Qeios*. (2020). doi: 10.32388/7Z8HQ4

132. Gan X, Wang J, Xi Y, Wu Z, Li Y, Li L. Nuclear Dvl, c-Jun, β-catenin, and TCF form a complex leading to stabiLization of β-catenin–TCF interaction. *J Cell Biol*. (2008) 180:1087–100. doi: 10.1083/jcb.200710050

133. Wang W, Xu H, Lin H, Molnar M, Ren H. The role of the cholinergic anti-inflammatory pathway in septic cardiomyopathy. *Int Immunopharmacol*. (2021) 90:107160. doi: 10.1016/j.intimp.2020.107160

134. Zhang W, Xu X, Kao R, Mele T, Kvietys P, Martin CM, et al. Cardiac fibroblasts contribute to myocardial dysfunction in mice with sepsis: the role of NLRP3 inflammasome activation. *PloS One*. (2014) 9:e107639. doi: 10.1371/journal.pone.0107639

135. Liang Y, Zhang R, Biswas S, Bu Q, Xu Z, Qiao L, et al. Integrated single-cell transcriptomics reveals the hypoxia-induced inflammation-cancer transformation in NASH-derived hepatocellular carcinoma. *Cell Prolif*. (2024) 57:e13576. doi: 10.1111/cpr.13576

136. Sui S, Tian Y, Wang X, Zeng C, Luo OJ, Li Y. Single-cell RNA sequencing gene signatures for classifying and scoring exhausted CD8+ T cells in B-cell acute lymphoblastic leukaemia. *Cell Prolif*. (2024) 57:e13583. doi: 10.1111/cpr.13583

137. Sui S, Wei X, Zhu Y, Feng Q, Zha X, Mao L, et al. Single-cell multiomics reveals TCR clonotype-specific phenotype and stemness heterogeneity of T- ALL cells. *Cell Prolif*. (2024) e13786. doi: 10.1111/cpr.13786

138. Yuan J, Liao Y, Zhang T, Tang Y, Yu P, Liu Y, et al. Integrating bulk RNA and single-cell sequencing data unveils efferocytosis patterns and ceRNA network in ischemic stroke. *Transl Stroke Res*. (2024). doi: 10.1007/s12975-024-01255-8

139. Qin S, Xie B, Wang Q, Yang R, Sun J, Hu C, et al. New insights into immune cells in cancer immunotherapy: from epigenetic modification, metabolic modulation to cell communication. *MedComm*. (2024) 5:e551. doi: 10.1002/mco2.551

140. Ni G, Sun Y, Jia H, Xiahou Z, Li Y, Zhao F, et al. MAZ-mediated tumor progression and immune evasion in hormone receptor-positive breast cancer: Targeting tumor microenvironment and PCLAF+ subtype-specific therapy. *Transl Oncol*. (2025) 52:102280. doi: 10.1016/j.tranon.2025.102280

141. Ma Y, Wang S, Ding H. Bioinformatics analysis and experimental validation of cystathionine-gamma-lyase as a potential prognosis biomarker in hepatocellular carcinoma. *BIOCELL*. (2024) 48:463–71. doi: 10.32604/biocell.2024.048244

142. Al Ghamdi ASM, Alalawi RO, Almalki ASA, Alzahrani AM, Nezamuldeen A, Alshikhey MA, et al. Critical analysis of laboratory biomarker discovery: bridging biomedical research with clinical diagnostics for early disease detection. *J Ecohumanism*. (2024) 3:24. doi: 10.62754/joe.v3i8.5314

143. Liu DSK, Puik JR, Venø MT, Mato Prado M, Rees E, Patel BY, et al. MicroRNAs as Bile-based biomarkers in pancreaticobiliary cancers (MIRABILE): a cohort study. *Int J Surg*. (2024) 110:6518–27. doi: 10.1097/JS9.0000000000001888

144. Zhuge Y, Zhang J, Qian F, Wen Z, Niu C, Xu K, et al. Role of smooth muscle cells in Cardiovascular Disease. *Int J Biol Sci*. (2020) 16:2741–51. doi: 10.7150/ijbs.49871

145. Yang F, Zhao LN, Sun Y, Chen Z. Levosimendan as a new force in the treatment of sepsis-induced cardiomyopathy: mechanism and clinical application. *J Int Med Res*. (2019) 47:1817–28. doi: 10.1177/0300060519837103

146. Tan Y, Chen S, Zhong J, Ren J, Dong M. Mitochondrial injury and targeted intervention in septic cardiomyopathy. *Curr Pharm Des*. (2019) 25:2060–70. doi: 10.2174/1381612825666190708155400

147. O'Shea D, Hodgkinson T, Dixon J, Curtin C, O'Brien F. Development of an "off-the-shelf" gene therapeutic nanoparticle formulation for incorporation into biomaterials for regenerative medicine applications. *Eur Cell Mater*. (2024) 47:152–69. doi: 10.22203/eCM.v047a11

148. Graham J, Werba L, Federico I, Gonzalez-Fernandez T. Crispr strategies for stem cell engineering: a new frontier in musculoskeletal regeneration. *Eur Cell Mater*. (2023) 46:91–118. doi: 10.22203/eCM.v046a05

149. Lamore KA. Constantly Evolving Journal: Reflecting on 2023Une revue en constante évolution : retour sur l'année 2023. *Psycho-Oncol*. (2024) 18:1–3. doi: 10.32604/po.2024.050518

150. Dutheil S, Bacqué M-F, Lamore K. Promoting Health DemocracyFavoriser la démocratie en santé. *Psycho-Oncol*. (2024) 18:5–7. doi: 10.32604/po.2024.050924

151. Nong Y, Wei X, Yu D. Inflammatory mechanisms and intervention strategies for sepsis-induced myocardial dysfunction. *Immun Inflammation Dis*. (2023) 11:e860. doi: 10.1002/iid3.860

152. Cai Y, Hu W, Pei Y, Zhao H, Yu G. Encoding biological metaverse: Advancements and challenges in neural fields from macroscopic to microscopic. *Innovation*. (2024) 5:100627. doi: 10.1016/j.xinn.2024.100627

153. Chen S. The impact of the human microbiome on gut health: recent research. *Int J Clin Case Rep*. (2024). doi: 10.5376/ijccr.2024.14.0004

154. Kwa WT, Sundarajoo S, Toh KY, Lee J. Application of emerging technologies for gut microbiome research. *Singapore Med J*. (2023) 64:45–52. doi: 10.4103/Singaporemedj.SMJ-2021-432

155. Cao Z, Pang Y, Pu J, Liu J. Bacteria-based drug delivery for treating non-oncological diseases. *J Controlled Release*. (2024) 366:668–83. doi: 10.1016/j.jconrel.2024.01.020

156. Wang Z. Research on microbial data modeling and disease prediction by fusion and integration of deep learning. *Appl Math Nonlinear Sci*. (2024) 9:20240884. doi: 10.2478/amns-2024-0884

157. Vo D, Singh SC, Safa S, Sahoo D. Boolean implication analysis unveils candidate universal relationships in microbiome data. *BMC Bioinf*. (2021) 22:49. doi: 10.1186/s12859-020-03941-4

158. Kumar AR, Nair B, Kamath AJ, Nath LR, Calina D, Sharifi-Rad J. Impact of gut microbiota on metabolic dysfunction-associated steatohepatitis and hepatocellular carcinoma: pathways, diagnostic opportunities and therapeutic advances. *Eur J Med Res*. (2024) 29:485. doi: 10.1186/s40001-024-02072-3

159. Duan J, Li Q, Cheng Y, Zhu W, Liu H, Li F. Therapeutic potential of Parabacteroides distasonis in gastrointestinal and hepatic disease. *MedComm*. (2024) 5:e70017. doi: 10.1002/mco2.70017

160. Rasha F, Boligala GP, Yang MV, Martinez-Marin D, Castro-Piedras I, Furr K, et al. Dishevelled 2 regulates cancer cell proliferation and T cell mediated immunity in HER2-positive breast cancer. *BMC Cancer*. (2023) 23:172. doi: 10.1186/s12885-023-10647-2

161. Benstead-Hume G, Wooller SK, Pearl FMG. [amp]]lsquo;Big data' approaches for novel anti-cancer drug discovery. *Expert Opin Drug Discovery*. (2017) 12:599–609. doi: 10.1080/17460441.2017.1319356

162. Chen B, Butte A. Leveraging big data to transform target selection and drug discovery. *Clin Pharmacol Ther*. (2016) 99:285–97. doi: 10.1002/cpt.318

163. Christaki E, Giamarellos-Bourboulis EJ. The beginning of personalized medicine in sepsis: small steps to a bright future. *Clin Genet*. (2014) 86:56–61. doi: 10.1111/cge.12368

164. Itenov TS, Murray DD, Jensen JUS. Sepsis: personalized medicine utilizing 'Omic' Technologies—A paradigm shift? *Healthcare*. (2018) 6:111. doi: 10.3390/healthcare6030111

165. Sireesha V, Fatima F, Sultana S, Kumar MSS, Pravarsha Y, Tatikonda RR. A comprehensive review on biomarker and its role in diseases. *Cardiol Angiol Int J*. (2024) 13:75–81. doi: 10.9734/ca/2024/v13i1395

166. Rosati D, Palmieri M, Brunelli G, Morrione A, Iannelli F, Frullanti E, et al. Differential gene expression analysis pipelines and bioinformatic tools for the identification of specific biomarkers: A review. *Comput Struct Biotechnol J*. (2024) 23:1154–68. doi: 10.1016/j.csbj.2024.02.018

167. Petersen BK, Yang J, Grathwohl WS, Cockrell C, Santiago C, An G, et al. Deep reinforcement learning and simulation as a path toward precision medicine. *J Comput Biol*. (2019) 26:597–604. doi: 10.1089/cmb.2018.0168

168. Palma P, Rello J. Precision medicine for the treatment of sepsis: recent advances and future prospects. *Expert Rev Precis Med Drug Dev*. (2019) 4:205–13. doi: 10.1080/23808993.2019.1626714

169. Sharma M, Castro-Piedras I, Simmons GE, Pruitt K. Dishevelled: A masterful conductor of complex Wnt signals. *Cell Signal*. (2018) 47:52–64. doi: 10.1016/j.cellsig.2018.03.004

frontiers | Frontiers in Immunology

TYPE Review
PUBLISHED 15 April 2025
DOI 10.3389/fimmu.2025.1561560

OPEN ACCESS

EDITED BY
Renjun Gu,
Nanjing University of Chinese Medicine, China

REVIEWED BY
Xuxu Liu,
Harbin Medical University, China
Qi Wang,
Jiangsu University, China

*CORRESPONDENCE
Dong Yang
yangdongyi2010@126.com

†These authors have contributed equally to this work

RECEIVED 16 January 2025
ACCEPTED 28 March 2025
PUBLISHED 15 April 2025
CORRECTED 09 July 2025

CITATION
Huang B, Yuan Q, Sun J, Wang C and Yang D (2025) Thymidine phosphorylase in nucleotide metabolism: physiological functions and its implications in tumorigenesis and anti-cancer therapy. *Front. Immunol.* 16:1561560. doi: 10.3389/fimmu.2025.1561560

Thymidine phosphorylase in nucleotide metabolism: physiological functions and its implications in tumorigenesis and anti-cancer therapy

Bo Huang[1,2†], Qihang Yuan[2†], Jiaao Sun[2†], Chao Wang[1] and Dong Yang[1*]

[1]Liaoning Cancer Hospital & Institute, Shenyang, China, [2]First Affiliated Hospital of Dalian Medical University, Dalian, China

Thymidine phosphorylase (TYMP), a protein found in both prokaryotic and eukaryotic cells, is encoded by a gene located in the q13 region of chromosome 22. With a relative molecular mass of 55,000, TYMP exists as a homodimer. Recent research has increasingly illuminated the diverse functions of TYMP. It is known to facilitate platelet activation, osteoclast differentiation, and angiogenesis. Mutations in the TYMP gene are linked to mitochondrial neurogastrointestinal encephalomyopathy. Beyond its physiological roles, TYMP contributes significantly to tumor growth and cancer progression, where it promotes angiogenesis, modulates epigenetic genes, inhibits apoptosis, and acts as a critical enzyme in the nucleoside metabolic rescue pathway. Moreover, TYMP holds substantial implications in cancer treatment and prognosis. Given its involvement in cancer progression, TYMP inhibitors may prove valuable in inhibiting tumor growth and metastasis. Interestingly, while TYMP can drive tumor growth, certain concentrations of TYMP also enhance the cytotoxic effects of chemotherapy drugs such as 5-fluorouracil (5-FU). Although challenges exist—such as the potential disruption of normal physiological functions when inhibiting TYMP—the protein remains a promising target for cancer treatment. Ongoing research on TYMP could deepen our understanding of human physiology and the pathogenesis of cancer and open new avenues for therapeutic interventions. This article provides a comprehensive review of TYMP's structure, physiological functions, and its role in tumorigenesis and anti-tumor therapy.

KEYWORDS

nucleotide metabolism, thymidine phosphorylase, physiological functions, tumorigenesis, anticancer therapy

1 Introduction

Thymidine phosphorylase (TYMP) was first isolated and purified from animal tissues by Friedkin and Roberts in 1954, with the enzyme subsequently named thymidine phosphorylase, now commonly referred to as TYMP (1). Due to the technological limitations of the time, research on TYMP was limited following its discovery. It wasn't until 1978 that Kubilus and Baden isolated and purified human TYMP from human amniotic membrane, confirming its existence in humans (2). This marked the beginning of a deeper exploration into the presence and functions of TYMP within the human body. Over time, TYMP's essential biological roles, including promoting platelet activation, osteoclast differentiation, angiogenesis, and its involvement in tumor angiogenesis, epigenetic gene modification, apoptosis resistance, and nucleoside metabolic salvage, have been gradually unveiled. As such, TYMP has become a critical target in cancer research. Despite significant advancements, ongoing studies continue to deepen our understanding of TYMP's full potential, yet much remains to be uncovered.

Cancer remains the leading cause of death worldwide (3–5). Its insidious nature means that by the time clinical symptoms become apparent, the disease is often in its advanced stages (6). While outcomes vary among patients, many advanced cancer cases can benefit from careful preoperative assessment and postoperative neoadjuvant chemotherapy, leading to improved prognoses (7, 8). However, these approaches do not diminish the significance of targeted cancer therapies in the treatment landscape. In recent years, the development of targeted cancer therapies, coupled with clinical trials, has provided promising alternative treatment options, offering patients greater choices. Therefore, understanding the underlying mechanisms of cancer and identifying viable therapeutic targets, such as TYMP, has become an essential focus in cancer research.

2 Structure of TYMP

2.1 Gene and molecular structure of TYMP

The TYMP gene is located on chromosome 22q13.32-qter (9). Whether in mammals or bacteria, TYMP exhibits structural conservation, existing as an anionic protein composed of two homodimers with a relative molecular mass of 55,000. Notably, when investigating the three-dimensional structure of *Escherichia coli* thymidine phosphorylase, researchers determined its active site by differentiating thymine and thymidine binding. This marked the first reported identification of a possible molecular structure of TYMP with thymine in the active site (10). Furthermore, human TYMP shares 39% sequence homology with *Escherichia coli* TYMP (11). Human TYMP possesses a proline-rich N-terminus (12), a feature absent in bacterial TYMP, potentially explaining the functional differences between the two. For instance, human TYMP plays a role in promoting platelet activation and hemostasis, functions that bacteria do not require.

2.2 TYMP enzyme activity and TYMP inhibitors

TYMP serves as a rate-limiting enzyme (13), exhibiting the common characteristic where enzyme structure influences its activity (14–16). Tipiracil hydrochloride (TPI) has been identified as a potent TYMP inhibitor, demonstrating high binding affinity to the enzyme. Moreover, TPI can function as an imaging agent for assessing TYMP expression *in vivo*, owing to its stability post-18 F labeling (17). Another notable TYMP inhibitor is the tritylated inosine derivative 5'-O-triynyl sugar (formerly KIN59), which is a non-competitive inhibitor (16). KIN59 binds to TYMP, inducing a conformational change that inhibits enzymatic activity without affecting substrate binding, underscoring the impact of TYMP conformational alterations on its enzymatic function. Additionally, Karen et al. identified polycyclic nitrogen heterocycles as potential TYMP inhibitors (18). Utilizing molecular docking techniques, their research demonstrated the interaction between polycyclic nitrogen heterocycles and TYMP's active binding site. These findings highlight TYMP inhibitors as a promising class of drugs with significant research potential. For the development of TYMP-targeted therapies in the medical field, understanding the binding site and conformational changes of TYMP will be crucial for optimizing drug efficacy.

3 Physiological functions of TYMP

3.1 Downstream activation pathways of TYMP

TYMP performs a variety of functions, with its activities often relying on multiple signal transduction pathways. In recent years, research into TYMP has advanced significantly, leading to a deeper understanding of its mechanisms. Among the key mechanisms of TYMP are the following:

Platelets, which play a pivotal role in thrombosis, rely on platelet activation as a critical factor in the thrombotic process. Collagen-induced platelet activation is primarily mediated through glycoprotein VI (GPVI). GPVI exists in both monomeric and dimeric forms on the cell surface and is associated with various effectors, including the Fc receptor γ chain (FcRγ), spleen tyrosine kinase, phospholipase Cγ, protein kinase Cδ, and bisphosphoinositide polyphosphate phosphodiesterase 1 (19). During platelet activation, LYN and FYN kinases bind to the cytoplasmic domain of one GPVI molecule, while the other GPVI molecule associates with the FcRγ chain dimer, thereby activating the GPVI signaling pathway that mediates platelet activation (20). Src family kinases (SFKs) play a pivotal role in this activation cascade (21), with FYN acting as the primary stimulator of SFKs, which in turn influence platelet activation. LYN can suppress collagen-induced platelet activation by promoting phosphorylation of the immunoreceptor tyrosine inhibitory motif (ITIM) domain of platelet endothelial cell adhesion molecule 1 (PECAM1) (22, 23). TYMP interacts with the phosphate group on p-LYN, removing it and impairing LYN's ability

to mediate PECAM-1/ITIM phosphorylation. This action reduces LYN's inhibitory function on collagen-induced platelet activation, thereby indirectly promoting platelet activation and thrombosis (12). This mechanism of TYMP's role in platelet activation is summarized in Figure 1. Consequently, targeting TYMP with specific drugs may offer a promising approach for developing new anti-platelet and anti-thrombotic treatments.

The receptor activator of nuclear factor-κB ligand (RANKL)-associated signaling pathway plays a critical role in osteoclastogenesis and is potentially linked to inflammation (24). Osteoclasts (OCs) are multinucleated hematopoietic cells capable of bone resorption. Their formation is supported by macrophage colony-stimulating factor (M-CSF) and RANKL, which binds to the RANK receptor on OC precursors (25). The RANK-RANKL interaction recruits tumor necrosis factor receptor-associated factor 6 (TRAF6), which activates the NF-κB and AP-1 transcription factors (26, 27), initiating the signaling cascade. This activation promotes the expression of key molecules such as c-Fos, Cathepsin K, and T cell nuclear factor cytoplasmic 1 (NFATc1), thereby facilitating OC differentiation (28, 29) (Figure 1). Once differentiated, OC cells are rapidly driven toward apoptosis. FYN plays a key role in stimulating osteoclastogenesis by enhancing the proliferation and differentiation of OC precursors (30). This effect is primarily mediated through phosphorylation. A Japanese research team identified TYMP as a factor that induces osteoclast differentiation by activating FYN signaling. After TYMP stimulation, they observed a marked increase in phosphorylated FYN levels and enhanced FYN gene expression in macrophages. Additionally, sedimentation experiments revealed that TYMP binds to a complex containing integrin β1 (ITGβ1) and FYN. Furthermore, in TYMP-stimulated cells, there was a significant upregulation of phosphorylated protein kinase 1/2 (MEK1/2) and phosphorylated extracellular signal-regulated kinase 1/2 (ERK1/2). These findings suggest that TYMP activates FYN signaling, leading to the activation of MAPK and NF-κB pathways, thereby promoting osteoclast differentiation (31). The detailed mechanism by which TYMP promotes osteoclast differentiation is summarized in Figure 1.

3.2 Pro-angiogenic function of TYMP

Angiogenesis, the process of forming new blood vessels from existing ones, is promoted by TYMP. TYMP is highly expressed not only in tumor cells but also in normal cells, including macrophages, stromal cells, glial cells, and certain epithelial cells (32). Notably, the elevated expression of TYMP in macrophages and skin plays a critical role in maintaining systemic thymidine homeostasis.

TYMP catalyzes the conversion of thymidine (TdR) into deoxyribose-1-phosphate (dR-1-P) and thymine, producing a molecular structure that contains deoxyribose (dR) (33). This dR component can further participate in angiogenesis (34). Since TYMP catalyzes this reaction and indirectly influences angiogenesis, its pro-angiogenic effect is closely tied to its enzymatic activity. Consequently, inhibiting TYMP's enzymatic activity with TYMP inhibitors to block its pro-angiogenic effects presents a potential therapeutic strategy. Furthermore, TYMP can directly induce angiogenic factors such as interleukin-8, basic fibroblast growth factor, and tumor necrosis factor α, which promote angiogenesis and stimulate endothelial cell migration and invasion (33). However, research into TYMP's role in

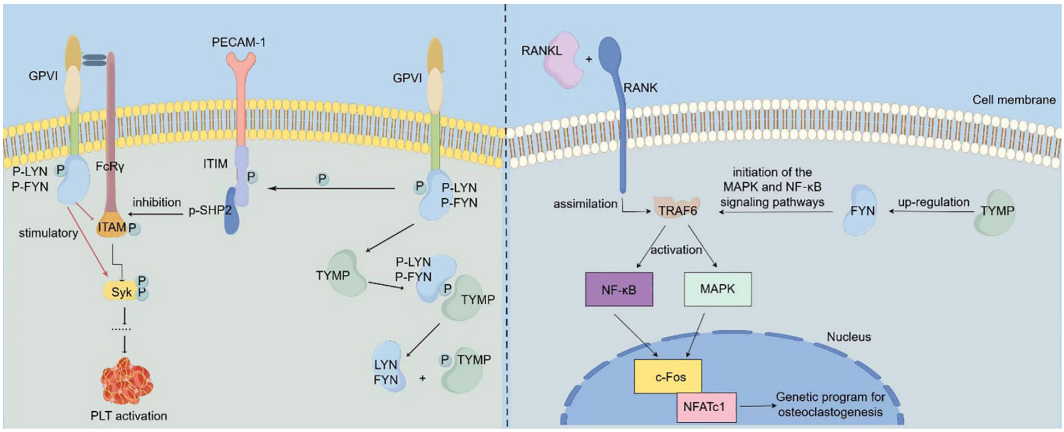

FIGURE 1
Mechanisms via which TYMP promotes platelet activation and osteoclast differentiation [The left-hand panel was adapted from Li et al. (2014) (12)]. LYN and FYN bind to the cytoplasmic domain of one GPVI molecule, while the other GPVI molecule interacts with the FcRγ chain dimer, thereby initiating the GPVI signaling pathway. Activation of this pathway results in LYN and FYN stimulating the phosphorylation of ITAM and Syk, which in turn activates platelet activation. Concurrently, LYN inhibits collagen-induced platelet activation by promoting the phosphorylation of the immunoreceptor tyrosine inhibitory motif (ITIM) domain of platelet endothelial cell adhesion molecule 1 (PECAM1). TYMP binds to the phosphate group of p-LYN, dephosphorylating it and causing the loss of its ability to mediate PECAM-1/ITIM phosphorylation. This action attenuates LYN's inhibitory function on collagen-induced platelet activation, thereby indirectly promoting platelet activation and contributing to thrombosis. In OC precursor cells, RANKL binds to the RANK receptor on OC precursors, leading to the recruitment of TRAF6, which activates NF-kB and AP-1 transcription factors, triggering downstream signaling pathways. This activation promotes the expression of c-Fos and NFATc1, key drivers of osteoclast differentiation. In TYMP-stimulated cells, the expression of FYN is significantly increased. TYMP activates FYN signaling, which subsequently promotes the activation of MAPK and NF-kB signaling pathways, thereby facilitating osteoclast differentiation.

angiogenesis remains limited, and it is unclear whether additional pro-angiogenic mechanisms exist. Therefore, the full extent of TYMP's involvement in angiogenesis is not yet fully understood, and further investigation is necessary.

3.3 Genetic disorders caused by TYMP deficiency

Mitochondrial neurogastrointestinal encephalomyopathy (MNGIE) is a rare autosomal recessive disorder caused by mutations in the TYMP gene, resulting in the loss of TYMP function (35). This disease leads to dysfunction in the digestive and nervous systems, presenting with clinical symptoms such as cachexia, ptosis, external ophthalmoplegia, peripheral neuropathy, and leukoencephalopathy (36–38). While no significant side effects have been reported for TYMP inhibitors as emerging drugs, the existence of MNGIE serves as a reminder that TYMP inhibitors could have previously unrecognized side effects. Therefore, extensive research is still needed before TYMP inhibitors can be applied clinically.

4 Role of TYMP in the occurrence and progression of cancer

TYMP is overexpressed in various cancers, including breast cancer (38), gastric cancer (39), esophageal cancer (40), oral squamous cell carcinoma (41), lung cancer (42), colorectal cancer (43), cervical cancer (44), and bladder cancer (45). Furthermore, plasma levels of TYMP in individuals with certain cancers are significantly higher than in healthy individuals (46) (Figure 2).

4.1 TYMP-driven tumorigenesis through angiogenesis

The most well-established function of TYMP is its role in promoting angiogenesis. For tumors to proliferate extensively, they require a constant supply of oxygen and nutrients, which depend on blood circulation. Thus, a fully developed vascular system is essential for tumor growth and progression. TYMP's angiogenesis-promoting effect addresses this need. As previously

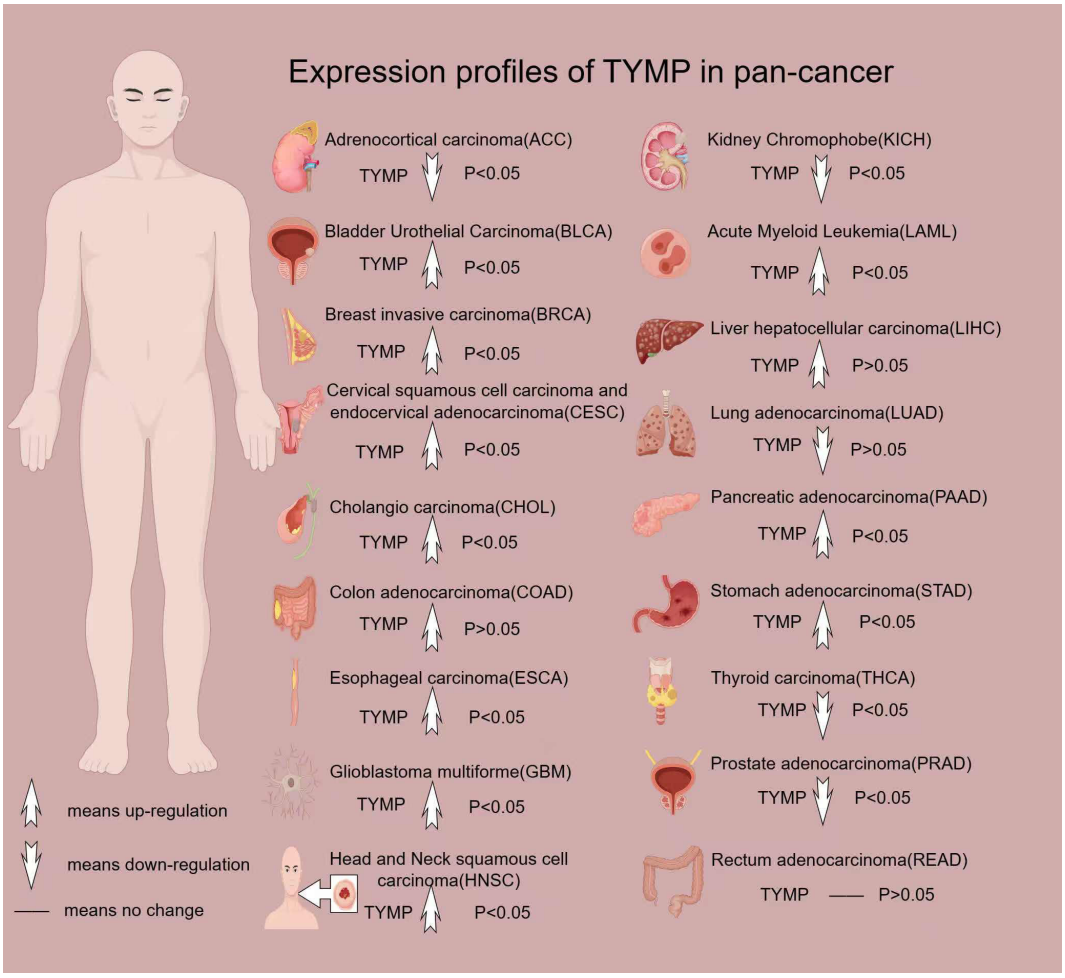

FIGURE 2
Expression profile of TYMP in pan-cancer. All data in this image are sourced from the GEPIA2 platform.

mentioned, TYMP facilitates angiogenesis through the dR component in its metabolites and by directly stimulating angiogenic factors, which in turn influence tumor growth and development. Consequently, inhibiting TYMP enzymatic activity using TYMP inhibitors has emerged as a viable therapeutic approach for slowing cancer progression. However, not all tumors depend on TYMP for angiogenesis. Some tumors, despite having dense microvascular networks, show no significant increase in TYMP levels (47). This suggests that additional, yet unexplored, mechanisms may also drive tumor angiogenesis. Nonetheless, it is clear that tumors with high TYMP expression are likely to have dense microvascular systems.

4.2 TYMP-driven tumorigenesis through epigenetic modification

TYMP also influences tumor progression through its role in DNA methylation regulation. A 2016 study revealed that TYMP catalyzes the conversion of thymidine to thymine and 2-deoxy-D-ribose (2DDR), which then binds to integrin αVβ3/α5β1 on progenitor cells, activating the PI3K/Akt signaling pathway. This results in increased expression of DNA methyltransferase 3A (DNMT3A), leading to hypermethylation of key genes such as RUNX2, osterix, and IRF8 (48) (Figure 3). This mechanism is particularly significant in myeloma, where TYMP-induced hypermethylation of these genes contributes to reduced bone formation and enhanced bone resorption. TYMP overexpression is commonly observed in bone metastatic tumors, further supporting the potential of TYMP-targeted therapies for treating myeloma-related bone diseases.

4.3 TYMP-driven tumorigenesis through anti-apoptotic pathways

TYMP plays a key role in helping tumor cells resist apoptosis induced by hypoxia. Kitazono's study demonstrated that TYMP's metabolites, 2-deoxy-D-ribose and thymine, can partially counteract hypoxia-induced apoptosis in KB/TP cells by transfecting them with endothelial cell growth factor/thymidine phosphorylase (PD-ECGF/TP) cDNA (49). Additionally, research involving myocardial ischemia in dogs showed that PD-ECGF/TP improved ischemic conditions, alleviating apoptosis caused by hypoxia (50, 51). Furthermore, TYMP activates the PI3K/Akt signaling pathway (48), a key pathway involved in regulating cell apoptosis (52). Upon PI3K activation, phosphatidylinositol-4,5-bisphosphate (PIP2) is converted into phosphatidylinositol-3,4,5-triphosphate (PIP3) (53), leading to the phosphorylation of Akt *via* phosphoinositide-dependent kinase 1 (PDK1) and mammalian target of rapamycin complex 2 (mTORC2), thereby activating Akt (54). Activated Akt inhibits the Forkhead box O (FOXO) transcription factors, which initiate apoptosis, thereby promoting cell survival (55). Additionally, Akt can inhibit the expression of cell

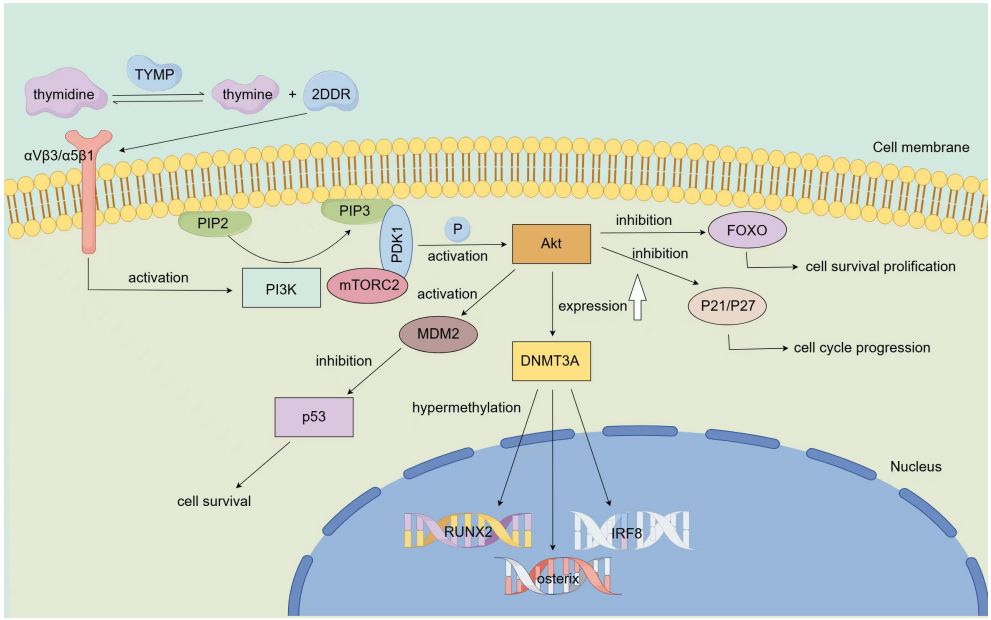

FIGURE 3
Mechanism *via* which TYMP modifies epigenetic and resists apoptosis TYMP catalyzes the conversion of thymidine to thymine and 2DDR, which binds to integrin αVβ3/α5β1 on progenitor cells, thereby activating the PI3K pathway. Once activated, PI3K promotes the conversion of PIP2 to PIP3, leading to the phosphorylation of Akt *via* PDK1 and mTORC2, completing Akt activation. Activated Akt inhibits FOXO, a key initiator of apoptosis, thereby promoting cell survival. Additionally, Akt can enhance tumor growth by suppressing the expression of tumor suppressor proteins P21 and P27. Furthermore, Akt acts on the MDM2 oncoprotein, negatively regulating the p53 tumor suppressor, thus resisting apoptosis and promoting tumor cell survival. Activated Akt also upregulates the expression of DNMT3A, leading to the hypermethylation of key genes such as RUNX2, osterix, and IRF8.

cycle regulators P21 and P27, further supporting tumor growth (56). Akt also negatively regulates the p53 tumor suppressor protein *via* MDM2, resisting apoptosis and promoting tumor cell survival (57) (Figure 3). Thus, TYMP can prevent cell apoptosis by activating the PI3K/Akt pathway, supporting tumor cells in resisting apoptosis induced by various treatments such as the immune response, hypoxia, radiotherapy, and chemotherapy. Understanding TYMP's anti-apoptotic role could enhance cancer therapies and offer insights into treating diseases caused by cellular hypoxia. The main signaling pathways of TYMP are summarized in Figure 3.

4.4 TYMP-driven tumorigenesis through stabilizing the thymidine pool

As a key enzyme in the nucleoside metabolic salvage pathway, TYMP helps maintain thymine pool stability, a key factor for DNA synthesis. Tumor cells reprogram their metabolic pathways to meet growth demands, with pyrimidine metabolism playing a central role. Studies have shown that the expression levels of thymidylate synthase (TYMS) and TYMP in tumor tissues are significantly higher than in adjacent normal tissues. Both TYMS and TYMP mRNA have the potential to serve as reliable diagnostic indicators for colon cancer (CC), but further research is required to confirm this (58). Given that tumor growth depends on cell division, TYMP's involvement in cell proliferation and tumor development suggests its critical role in cancer progression. Further investigation into the relationship between TYMP and tumors is needed.

5 Roles of TYMP in anti-cancer therapy

5.1 TYMP functions as a target for cancer therapy

Although TYMP exerts several promoting effects on tumor cell growth and development, it also holds therapeutic potential in cancer treatment. As a molecular target, TYMP is being explored for the development of cancer therapeutics (59). Investigating its biological functions in tumors may lead to the synthesis of TYMP inhibitors, which could prevent angiogenesis and slow tumor metastasis. However, research has indicated that certain TYMP activities can activate a variety of chemotherapeutic agents (40), which is crucial for cancer therapy. For instance, bevacizumab can enhance the metabolic activation of 5-fluorouracil (5-FU) through upregulation of TYMP (60). Furthermore, recent studies suggest that utilizing human mesenchymal stem cells (hMSCs) as carriers to deliver TYMP to cancer cells may facilitate the conversion of docifluridine (5′-DFUR) into the toxic 5-FU, promoting cancer cell death (61).

The activation of nucleic acid sensors in endothelial cells (ECs) triggers inflammation in various diseases, including cancer. Specifically, activation of the cytoplasmic RNA sensor retinoic acid-induced gene 1 (RIG-I) significantly contributes to decreased EC survival, with TYMP being the most upregulated gene in this process. Therefore, inhibiting TYMP could potentially alleviate endothelial dysfunction and enhance cancer treatment (62).

As previously discussed, TYMP activity can activate chemotherapy drugs, while TYMP inhibitors could mitigate its angiogenic effects, thereby indirectly impeding tumor cell growth. We summarized the TYMP inhibitors that are currently of certain research value and the chemotherapeutic drugs that rely on TYMP activity activation (Table 1). Although TYMP inhibitors may hold promise in cancer therapy (69), their safety remains uncertain, and long-term research is necessary to determine their clinical viability.

5.2 Targeting TYMP to alleviate resistance to cancer immunotherapy and chemotherapy

Immunotherapy and chemotherapy are widely used in cancer treatment; however, their efficacy is not always consistent. Over prolonged exposure to these therapies, tumor cells often develop drug resistance, which diminishes treatment effectiveness. This phenomenon is a key factor contributing to the continued challenges in achieving significant progress in cancer treatment.

Peri et al. observed the upregulation of TYMP in gastric cancer cells that were induced to become resistant to 5-fluorouracil, identifying TYMP gene mutations in tumor cells as a common cause of 5-fluorouracil resistance. Such mutations can enhance angiogenesis in gastric cancer cell lines (70). Another study found that TYMP-induced T cell exhaustion plays a critical role in immunotherapy resistance in colorectal cancer (CRC) (71). Targeted TYMP therapies could potentially improve the effectiveness of immunotherapy. In 2022, a research team explored whether demethylation of TYMP would increase cancer cell sensitivity to 5-FU. While the results did not demonstrate that TYMP demethylation alone enhanced 5-FU sensitivity, they suggested a potential strategy combining TYMP with other metabolic pathways to boost 5-FU responsiveness (72). These findings provide novel insights into drug resistance in tumor cells, thereby enhancing cancer treatment strategies.

5.3 Role of TYMP in prognostic evaluation of tumor therapies

The expression of TYMP is closely associated with rectal cancer treatment outcomes (73). Preoperative radiotherapy or chemoradiotherapy (CRT) is considered the standard treatment for locally advanced rectal cancer (74, 75), and studies have shown that TYMP expression can help predict the efficacy of CRT (76). Furthermore, TYMP's significance in CRC progression is evident, as a study demonstrated that the rs11479 polymorphism could predict the prognosis of patients with CRC receiving capecitabine-based adjuvant chemotherapy (77). This highlights that modulating TYMP mRNA expression could enhance the effectiveness of

TABLE 1 TYMP targeted drugs and their introduction.

Medicine	Introduction	References
2-thioxo-pyrazolo[1,5-a] [1,3,5]triazin-4-ones	A series of 2-thioxo-pyrazolo[1,5-a] [1,3,5]triazin-4-one derivatives were designed and synthesized, and their TYMP inhibitory potential was evaluated. Certain compounds were found to exhibit promising TYMP inhibitory activity. This provides a new direction for the design of novel TYMP inhibitors.	(63)
Ciprofloxacin analogs	A research team synthesized a series of ciprofloxacin and evaluated their inhibitory potential against TYMP. They found that some of the analogs had good inhibitory activity against thymidine phosphorylase. This drug may provide a new approach for treating tumors.	(64)
Tritylated inosine derivative 5'-O-triynyl sugar (formerly known as KIN59)	Acts as a non-competitive inhibitor of TYMP.	(65)
Polycyclic nitrogen heterocycles	As a potential TYMP inhibitor, it has certain research value.	(18)
Tipiracil hydrochloride (TPI)	TPI is a selective TYMP inhibitor that exerts its antithrombotic effect by blocking TYMP-mediated platelet activation through the inhibition of TYMP-LYN binding. The safety profile of TPI has been confirmed in experimental studies, demonstrating a lower bleeding risk even at high doses compared to commonly used clinical agents such as aspirin and clopidogrel. Currently, TPI has been approved for clinical use by the U.S. Food and Drug Administration (FDA).	(66)
Docifluridine and TYMP-expressing mesenchymal stem cells	Human mesenchymal stem cells are used as delivery vehicles to deliver a certain amount of TYMP activity to docifluridine, a prodrug of 5-fluorouracil, thereby converting the non-toxic prodrug docifluridine into the toxic chemotherapy drug 5-fluorouracil, thereby eliminating cancer cells.	(67)
Bevacizumab	Bevacizumab mediates the activation of 5-fluorouracil by upregulating TYMP, thereby achieving a therapeutic effect on tumors.	(60)
Capecitabine	Capecitabine relies on TYMP to activate the intermediate form 5'-deoxy-5-fluorouracil into the active form 5-fluorouracil, thereby achieving a therapeutic effect on tumors.	(68)

capecitabine-based therapy, thus improving survival rates in patients with CRC.

Additionally, TYMP expression in CRC tumor epithelial cells is linked to recurrence-free survival (RFS) in patients with CRC. Elevated TYMP expression may correlate with poor prognosis in these patients (78). Furthermore, research has shown that TYMP polymorphisms can influence the prognosis of patients with CRC undergoing chemotherapy by modulating TYMP mRNA expression (79, 80).

TYMP also serves as a valuable immune prognostic marker in various cancers, including renal clear cell carcinoma (81, 82) and low-grade glioma (83). Recent studies have shown that a reduction in TYMP expression can significantly affect the proliferation, migration, and invasion of renal cell carcinoma (RCC) cells *in vitro* (84). Furthermore, a 2016 study indicated a potential link between TYMP levels and the survival rate of patients with localized gastric cancer following radical gastrectomy (85). Additionally, the combined expression of TYMP and hypoxia-inducible factor α (HIF-1α) has been shown to predict the prognosis of patients with rectal cancer undergoing neoadjuvant chemoradiotherapy with oxaliplatin and capecitabine (XELOXART) (86). These findings underscore the pivotal role of TYMP in cancer treatment and prognosis prediction.

Despite its promising potential in cancer therapy, TYMP has certain limitations. Due to individual differences among patients, TYMP-targeting drugs may be effective for some cancer individuals, while less effective for others. Moreover, TYMP not only promotes tumor progression but also influences normal physiological functions, making it crucial to consider the potential side effects of TYMP-targeted therapies. Further research and clinical trials are needed to validate these effects. While significant progress has been made in understanding TYMP's role in disease, many aspects remain to be explored. The mechanisms underlying TYMP's involvement in tumors are complex, and the clinical effects of inhibiting TYMP have yet to be fully established. The potential for unknown side effects of TYMP inhibitors also warrants further investigation. Despite these uncertainties, TYMP remains a promising therapeutic target. It holds considerable potential in the understanding and treatment of cancer, making ongoing research into TYMP essential. However, considering the current state of research, significant progress is still required before TYMP-targeted therapies can be fully developed and applied.

6 Conclusions

TYMP, a protein found extensively in both prokaryotic and eukaryotic cells, performs critical physiological functions, including promoting platelet activation, osteoclast differentiation, and angiogenesis. Mutations in the TYMP gene can lead to genetic disorders such as MNGIE. Beyond its role in normal cells, TYMP is also pivotal in cancer cells, where it facilitates tumor angiogenesis, modifies epigenetics, and helps resist cell apoptosis. Additionally, TYMP functions as a key enzyme in the nucleoside metabolic rescue

pathway. Consequently, studying TYMP enhances our understanding of cancer mechanisms and is vital for cancer treatment. Targeting TYMP has emerged as a promising strategy for cancer therapy, and TYMP-activated anti-tumor drugs represent an important therapeutic approach. Despite existing limitations, further research on TYMP holds significant potential for advancing cancer treatment.

Author contributions

BH: Data curation, Investigation, Writing – original draft. QY: Writing – original draft, Conceptualization, Supervision. JS: Conceptualization, Supervision, Writing – original draft. CW: Writing – review & editing, Data curation, Investigation. DY: Conceptualization, Supervision, Writing – review & editing.

Funding

The author(s) declare that no financial support was received for the research and/or publication of this article.

Acknowledgments

We acknowledge Bullet Edits Limited for their linguistic editing and proofreading of the manuscript. We also extend our gratitude to the FigDraw platform for facilitating the creation of the illustrations. The three images included in this manuscript were designed with the assistance of the FigDraw platform and received approval. The approval numbers for the images are as follows: Figure 1 ID: UWPSO8ccc4; Figure 2 ID: RYUII43b78; Figure 3 ID: TIWUU7ee76.

Conflict of interest

The authors declare that the research was conducted in the absence of any commercial or financial relationships that could be construed as a potential conflict of interest.

Generative AI statement

The author(s) declare that no Generative AI was used in the creation of this manuscript.

Correction note

A correction has been made to this article. Details can be found at: 10.3389/fimmu.2025.1642752.

Publisher's note

References

1. Friedkin M, Roberts D. The enzymatic synthesis of nucleosides. I. Thymidine phosphorylase in mammalian tissue. *J Biol Chem*. (1954) 207:245–56. doi: 10.1016/S0021-9258(18)71264-7

2. Kubilus J, Lee LD, Baden HP. Purification of thymidine phosphorylase from human amniochorion. *Biochim Biophys Acta*. (1978) 527:221–8. doi: 10.1016/0005-2744(78)90271-1

3. Bray F, Laversanne M, Sung H, Ferlay J, Siegel RL, Soerjomataram I, et al. Global cancer statistics 2022: GLOBOCAN estimates of incidence and mortality worldwide for 36 cancers in 185 countries. *CA Cancer J Clin*. (2024) 74:229–63. doi: 10.3322/caac.21834

4. de Martel C, Georges D, Bray F, Ferlay J, Clifford GM. Global burden of cancer attributable to infections in 2018: a worldwide incidence analysis. *Lancet Glob Health*. (2020) 8:e180–90. doi: 10.1016/S2214-109X(19)30488-7

5. Siegel RL, Miller KD, Fuchs HE, Jemal A. Cancer statistics, 2022. *CA Cancer J Clin*. (2022) 72:7–33. doi: 10.3322/caac.21708

6. Yuan Q, Sun J, Hong Z, Shang D. Determining a robust prognostic biomarker for 804 patients with pancreatic cancer using a machine learning computational framework. *Int J Surg*. (2025) 111:1561–3. doi: 10.1097/JS9.0000000000002016

7. Pu N, Wu W, Liu S, Xie Y, Yin H, Chen Q, et al. Survival benefit and impact of adjuvant chemotherapy following systemic neoadjuvant chemotherapy in patients with resected pancreas ductal adenocarcinoma: a retrospective cohort study. *Int J Surg*. (2023) 109:3137–46. doi: 10.1097/JS9.0000000000000589

8. Liang H, Yan X, Li Z, Chen X, Qiu Y, Li F, et al. Clinical outcomes of conversion surgery following immune checkpoint inhibitors and chemotherapy in stage IV gastric cancer. *Int J Surg*. (2023) 109:4162–72. doi: 10.1097/JS9.0000000000000738

9. Nishino I, Spinazzola A, Hirano M. Thymidine phosphorylase gene mutations in MNGIE, a human mitochondrial disorder. *Science*. (1999) 283:689–92. doi: 10.1126/science.283.5402.689

10. Walter MR, Cook WJ, Cole LB, Short SA, Koszalka GW, Krenitsky TA, et al. Three-dimensional structure of thymidine phosphorylase from Escherichia coli at 2.8 A resolution. *J Biol Chem*. (1990) 265:14016–22. doi: 10.1016/S0021-9258(18)77450-4

11. Barton GJ, Ponting CP, Spraggon G, Finnis C, Sleep D. Human platelet-derived endothelial cell growth factor is homologous to Escherichia coli thymidine phosphorylase. *Protein Sci*. (1992) 1:688–90. doi: 10.1002/pro.5560010514

12. Li W, Gigante A, Perez-Perez MJ, Yue H, Hirano M, McIntyre TM, et al. Thymidine phosphorylase participates in platelet signaling and promotes thrombosis. *Circ Res*. (2014) 115:997–1006. doi: 10.1161/CIRCRESAHA.115.304591

13. Tabata S, Yamamoto M, Goto H, Hirayama A, Ohishi M, Kuramoto T, et al. Thymidine catabolism as a metabolic strategy for cancer survival. *Cell Rep*. (2017) 19:1313–21. doi: 10.1016/j.celrep.2017.04.061

14. Mitsiki E, Papageorgiou AC, Iyer S, Thiyagarajan N, Prior SH, Sleep D, et al. Structures of native human thymidine phosphorylase and in complex with 5-iodouracil. *Biochem Biophys Res Commun*. (2009) 386:666–70. doi: 10.1016/j.bbrc.2009.06.104

15. Miyadera K, Sumizawa T, Haraguchi M, Yoshida H, Konstanty W, Yamada Y, et al. Role of thymidine phosphorylase activity in the angiogenic effect of platelet derived endothelial cell growth factor/thymidine phosphorylase. *Cancer Res*. (1995) 55:1687–90.

16. Bronckaers A, Aguado L, Negri A, Camarasa MJ, Balzarini J, Pérez-Pérez MJ, et al. Identification of aspartic acid-203 in human thymidine phosphorylase as an important residue for both catalysis and non-competitive inhibition by the small molecule "crystallization chaperone" 5'-O-tritylinosine (KIN59). *Biochem Pharmacol*. (2009) 78:231–40. doi: 10.1016/j.bcp.2009.04.011

17. Grierson JR, Brockenbrough JS, Rasey JS, Wiens L, Vesselle H. Synthesis and *in vitro* evaluation of 5-fluoro-6-[(2-iminopyrrolidin-1-YL)methyl]uracil, TPI(F): an

inhibitor of human thymidine phosphorylase (TP). *Nucleosides Nucleotides Nucleic Acids*. (2010) 29:49–54. doi: 10.1080/15257770903451603

18. Aknin K, Bontemps A, Farce A, Merlet E, Belmont P, Helissey P, et al. Polycyclic nitrogen heterocycles as potential thymidine phosphorylase inhibitors: synthesis, biological evaluation, and molecular docking study. *J Enzyme Inhib Med Chem*. (2022) 37:252–68. doi: 10.1080/14756366.2021.2001806

19. Babur Ö, Melrose AR, Cunliffe JM, Klimek J, Pang J, Sepp AI, et al. Phosphoproteomic quantitation and causal analysis reveal pathways in GPVI/ITAM-mediated platelet activation programs. *Blood*. (2020) 136:2346–58. doi: 10.1182/blood.2020005496

20. Dütting S, Bender M, Nieswandt B. Platelet GPVI: a target for antithrombotic therapy?! *Trends Pharmacol Sci*. (2012) 33:583–90. doi: 10.1016/j.tips.2012.07.004

21. Séverin S, Nash CA, Mori J, Zhao Y, Abram C, Lowell CA, et al. Distinct and overlapping functional roles of Src family kinases in mouse platelets. *J Thromb Haemost*. (2012) 10:1631–45. doi: 10.1111/j.1538-7836.2012.04814.x

22. Cicmil M, Thomas JM, Sage T, Barry FA, Leduc M, Bon C, et al. Collagen, convulxin, and thrombin stimulate aggregation-independent tyrosine phosphorylation of CD31 in platelets. Evidence for the involvement of Src family kinases. *J Biol Chem*. (2000) 275:27339–47. doi: 10.1016/S0021-9258(19)61516-4

23. Ming Z, Hu Y, Xiang J, Polewski P, Newman PJ, Newman DK. Lyn and PECAM-1 function as interdependent inhibitors of platelet aggregation. *Blood*. (2011) 117:3903–6. doi: 10.1182/blood-2010-09-304816

24. Wei W, Peng C, Gu R, Yan X, Ye J, Xu Z, et al. Urolithin A attenuates RANKL-induced osteoclastogenesis by co-regulating the p38 MAPK and Nrf2 signaling pathway. *Eur J Pharmacol*. (2022) 921:174865. doi: 10.1016/j.ejphar.2022.174865

25. Teitelbaum SL. Osteoclasts: what do they do and how do they do it? *Am J Pathol*. (2007) 170:427–35. doi: 10.2353/ajpath.2007.060834

26. Karin M, Cao Y, Greten FR, Li ZW. NF-kappaB in cancer: from innocent bystander to major culprit. *Nat Rev Cancer*. (2002) 2:301–10. doi: 10.1038/nrc780

27. Teitelbaum SL, Ross FP. Genetic regulation of osteoclast development and function. *Nat Rev Genet*. (2003) 4:638–49. doi: 10.1038/nrg1122

28. Xue C, Luo H, Wang L, Deng Q, Kui W, Da W, et al. Aconine attenuates osteoclast-mediated bone resorption and ferroptosis to improve osteoporosis via inhibiting NF-κB signaling. *Front Endocrinol (Lausanne)*. (2023) 14:1234563. doi: 10.3389/fendo.2023.1234563

29. Takayanagi H, Kim S, Koga T, Nishina H, Isshiki M, Yoshida H, et al. Induction and activation of the transcription factor NFATc1 (NFAT2) integrate RANKL signaling in terminal differentiation of osteoclasts. *Dev Cell*. (2002) 3:889–901. doi: 10.1016/S1534-5807(02)00369-6

30. Kim HJ, Warren JT, Kim SY, Chappel JC, DeSelm CJ, Ross FP, et al. Fyn promotes proliferation, differentiation, survival and function of osteoclast lineage cells. *J Cell Biochem*. (2010) 111:1107–13. doi: 10.1002/jcb.v111:5

31. Matsumae G, Shimizu T, Tian Y, Takahashi D, Ebata T, Alhasan H, et al. Targeting thymidine phosphorylase as a potential therapy for bone loss associated with periprosthetic osteolysis. *Bioeng Transl Med*. (2021) 6:e10232. doi: 10.1002/btm2.10232

32. Fox SB, Moghaddam A, Westwood M, Turley H, Bicknell R, Gatter KC, et al. Platelet-derived endothelial cell growth factor/thymidine phosphorylase expression in normal tissues: an immunohistochemical study. *J Pathol*. (1995) 176:183–90. doi: 10.1002/path.1711760212

33. Bijnsdorp IV, Capriotti F, Kruyt FA, Losekoot N, Fukushima M, Griffioen AW, et al. Thymidine phosphorylase in cancer cells stimulates human endothelial cell migration and invasion by the secretion of angiogenic factors. *Br J Cancer*. (2011) 104:1185–92. doi: 10.1038/bjc.2011.74

34. Hotchkiss KA, Ashton AW, Schwartz EL. Thymidine phosphorylase and 2-deoxyribose stimulate human endothelial cell migration by specific activation of the integrins alpha 5 beta 1 and alpha V beta 3. *J Biol Chem*. (2003) 278:19272–9. doi: 10.1074/jbc.M212670200

35. Kučerová L, Dolina J, Dastych M, Bartušek D, Honzík T, Mazanec J, et al. Mitochondrial neurogastrointestinal encephalomyopathy imitating Crohn's disease: a rare cause of malnutrition. *J Gastrointestin Liver Dis*. (2018) 27:321–5. doi: 10.15403/jgld.2014.1121.273.kuc

36. Shah SAY, Shakeel HA, Hassan WU. Rare pathogenic mutation in the thymidine phosphorylase gene (TYMP) causing mitochondrial neurogastrointestinal encephalomyelopathy. *BMJ Neurol Open*. (2022) 4:e000287. doi: 10.1136/bmjno-2022-000287

37. Mojtabavi H, Fatehi F, Shahkarami S, Rezaei N, Nafissi S. Novel mutations of the TYMP gene in mitochondrial neurogastrointestinal encephalomyopathy: case series and literature review. *J Mol Neurosci*. (2021) 71:2526–33. doi: 10.1007/s12031-021-01822-w

38. Filosto M, Cotti Piccinelli S, Caria F, Gallo Cassarino S, Baldelli E, Galvagni A, et al. Mitochondrial neurogastrointestinal encephalomyopathy (MNGIE-MTDPS1). *J Clin Med*. (2018) 7(11):389. doi: 10.3390/jcm7110389

39. Wang L, Huang X, Chen Y, Jin X, Li Q, Yi TN. Prognostic value of TP/PD-ECGF and thrombocytosis in gastric carcinoma. *Eur J Surg Oncol*. (2012) 38:568–73. doi: 10.1016/j.ejso.2012.04.008

40. Bronckaers A, Gago F, Balzarini J, Liekens S. The dual role of thymidine phosphorylase in cancer development and chemotherapy. *Med Res Rev*. (2009) 29:903–53. doi: 10.1002/med.20159

41. Yao L, Itoh S, Furuta I. Thymidine phosphorylase expression in oral squamous cell carcinoma. *Oral Oncol*. (2002) 38:584–90. doi: 10.1016/S1368-8375(01)00113-0

42. Chujo M, Miura T, Kawano Y, Miyawaki M, Imakiire T, Hayashita Y, et al. Thymidine phosphorylase levels and dihydropyrimidine dehydrogenase levels in non-small cell lung cancer tissues. *Oncol Rep*. (2006) 16:777–80. doi: 10.3892/or.16.4.777

43. Sadahiro S, Suzuki T, Tanaka A, Okada K, Nagase H, Uchida J. Association of right-sided tumors with high thymidine phosphorylase gene expression levels and the response to oral uracil and tegafur/leucovorin chemotherapy among patients with colorectal cancer. *Cancer Chemother Pharmacol*. (2012) 70:285–91. doi: 10.1007/s00280-012-1909-8

44. Hasegawa K, Okamoto H, Kawamura K, Kato R, Kobayashi Y, Sekiya T, et al. The effect of chemotherapy or radiotherapy on thymidine phosphorylase and dihydropyrimidine dehydrogenase expression in cancer of the uterine cervix. *Eur J Obstetrics Gynecology Reprod Biol*. (2012) 163:67–70. doi: 10.1016/j.ejogrb.2012.03.014

45. Shimabukuro T, Matsuyama H, Baba Y, Jojima K, Suyama K, Aoki A, et al. Expression of thymidine phosphorylase in human superficial bladder cancer. *Int J Urol*. (2005) 12:29–34. doi: 10.1111/j.1442-2042.2004.00992.x

46. Bijnsdorp IV, de Bruin M, Laan AC, Fukushima M, Peters GJ. The role of platelet-derived endothelial cell growth factor/thymidine phosphorylase in tumor behavior. *Nucleosides Nucleotides Nucleic Acids*. (2008) 27:681–91. doi: 10.1080/15257770802143988

47. O'Byrne KJ, Koukourakis MI, Giatromanolaki A, Cox G, Turley H, Steward WP, et al. Vascular endothelial growth factor, platelet-derived endothelial cell growth factor and angiogenesis in non-small-cell lung cancer. *Br J Cancer*. (2000) 82:1427–32. doi: 10.1054/bjoc.1999.1129

48. Liu H, Liu Z, Du J, He J, Lin P, Amini B, et al. Thymidine phosphorylase exerts complex effects on bone resorption and formation in myeloma. *Sci Transl Med*. (2016) 8:353ra113. doi: 10.1126/scitranslmed.aad8949

49. Kitazono M, Takebayashi Y, Ishitsuka K, Takao S, Tani A, Furukawa T, et al. Prevention of hypoxia-induced apoptosis by the angiogenic factor thymidine phosphorylase. *Biochem Biophys Res Commun*. (1998) 253:797–803. doi: 10.1006/bbrc.1998.9852

50. Li W, Tanaka K, Ihaya A, Fujibayashi Y, Takamatsu S, Morioka K, et al. Gene therapy for chronic myocardial ischemia using platelet-derived endothelial cell growth factor in dogs. *Am J Physiol Heart Circ Physiol*. (2005) 288:H408–15. doi: 10.1152/ajpheart.00176.2004

51. Li W, Tanaka K, Morioka K, Takamori A, Handa M, Yamada N, et al. Long-term effect of gene therapy for chronic ischemic myocardium using platelet-derived endothelial cell growth factor in dogs. *J Gene Med*. (2008) 10:412–20. doi: 10.1002/jgm.v10:4

52. Fresno Vara JA, Casado E, de Castro J, Cejas P, Belda-Iniesta C, González-Barón M. PI3K/Akt signalling pathway and cancer. *Cancer Treat Rev*. (2004) 30:193–204. doi: 10.1016/j.ctrv.2003.07.007

53. Miricescu D, Totan A, Stanescu-Spinu II, Badoiu SC, Stefani C, Greabu M. PI3K/AKT/mTOR signaling pathway in breast cancer: from molecular landscape to clinical aspects. *Int J Mol Sci*. (2021) 22:173. doi: 10.3390/ijms22010173

54. Tian L-Y, Smit DJ, Jücker M. The role of PI3K/AKT/mTOR signaling in hepatocellular carcinoma metabolism. *Int J Mol Sci*. (2023) 24:2652. doi: 10.3390/ijms24032652

55. Farhan M, Wang H, Gaur U, Little PJ, Xu J, Zheng W. FOXO signaling pathways as therapeutic targets in cancer. *Int J Biol Sci*. (2017) 13:815–27. doi: 10.7150/ijbs.20052

56. Guo Q, Xiong Y, Song Y, Hua K, Gao S. ARHGAP17 suppresses tumor progression and up-regulates P21 and P27 expression via inhibiting PI3K/AKT signaling pathway in cervical cancer. *Gene*. (2019) 692:9–16. doi: 10.1016/j.gene.2019.01.004

57. Mayo LD, Donner DB. A phosphatidylinositol 3-kinase/Akt pathway promotes translocation of Mdm2 from the cytoplasm to the nucleus. *Proc Natl Acad Sci U.S.A*. (2001) 98:11598–603. doi: 10.1073/pnas.181181198

58. Ramadan RA, Moghazy TF, Hafez R, Morsi H, Samir M, Shamesya M. Significance of expression of pyrimidine metabolizing genes in colon cancer. *Arab J Gastroenterol*. (2020) 21:189–93. doi: 10.1016/j.ajg.2020.07.006

59. Deves C, Rostirolla DC, Martinelli LK, Bizarro CV, Santos DS, Basso LA. The kinetic mechanism of Human Thymidine Phosphorylase - a molecular target for cancer drug development. *Mol Biosyst*. (2014) 10:592–604. doi: 10.1039/C3MB70453J

60. Liu W, Zhang J, Yao X, Jiang C, Ni P, Cheng L, et al. Bevacizumab-enhanced antitumor effect of 5-fluorouracil via upregulation of thymidine phosphorylase through vascular endothelial growth factor A/vascular endothelial growth factor receptor 2-specificity protein 1 pathway. *Cancer Sci*. (2018) 109:3294–304. doi: 10.1111/cas.2018.109.issue-10

61. Tarar A, Alyami EM, Peng CA. Mesenchymal stem cells anchored with thymidine phosphorylase for doxifluridine-mediated cancer therapy. *RSC Adv*. (2021) 11:1394–403. doi: 10.1039/D0RA10263F

62. Baris A, Fraile-Bethencourt E, Eubanks J, Khou S, Anand S. Thymidine phosphorylase facilitates retinoic acid inducible gene-I induced endothelial dysfunction. *Cell Death Dis*. (2023) 14:294. doi: 10.1038/s41419-023-05821-0

63. Bera H, Ojha Pk, Tan BJ, Sun L, Dolzhenko AV, Chui WK, et al. Discovery of mixed type thymidine phosphorylase inhibitors endowed with antiangiogenic properties: synthesis, pharmacological evaluation and molecular docking study of 2-

thioxo-pyrazolo[1,5-a][1,3,5]triazin-4-ones. Part II. *Eur J Med Chem*. (2014) 78:294–303. doi: 10.1016/j.ejmech.2014.03.063

64. Shahzad SA, Sarfraz A, Yar M, Khan ZA, Naqvi SAR, Naz S, et al. Synthesis, evaluation of thymidine phosphorylase and angiogenic inhibitory potential of ciprofloxacin analogues: Repositioning of ciprofloxacin from antibiotic to future anticancer drugs. *Bioorg Chem*. (2020) 100:103876. doi: 10.1016/j.bioorg.2020.103876

65. Bronckaers A, Aguado L, Negri A, Camarasa MJ, Balzarini J, Pérez-Pérez MJ, et al. Identification of aspartic acid-203 in human thymidine phosphorylase as an important residue for both catalysis and non-competitive inhibition by the small molecule "crystallization chaperone" 5'-O-tritylinosine (KIN59). *Biochem Pharmacol*. (2009) 78:231–40. doi: 10.1016/j.bcp.2009.04.011

66. Belcher A, Zulfiker AHM, Li OQ, Yue H, Gupta AS, Li W. Targeting thymidine phosphorylase with tipiracil hydrochloride attenuates thrombosis without increasing risk of bleeding in mice. *Arterioscler Thromb Vasc Biol*. (2021) 41:668–82. doi: 10.1161/ATVBAHA.120.315109

67. Wang X, Peng I, Peng CA. Eradication of cancer cells using doxifluridine and mesenchymal stem cells expressing thymidine phosphorylase. *Bioengineering (Basel)*. (2024) 11(12):1194. doi: 10.3390/bioengineering11121194

68. Toi M, Bando H, Horiguchi S, Takada M, Kataoka A, Ueno T, et al. Modulation of thymidine phosphorylase by neoadjuvant chemotherapy in primary breast cancer. *Br J Cancer*. (2004) 90:2338–43. doi: 10.1038/sj.bjc.6601845

69. Pérez-Pérez MJ, Priego EM, Hernández AI, Camarasa MJ, Balzarini J, Liekens S. Thymidine phosphorylase inhibitors: recent developments and potential therapeutic applications. *Mini Rev Med Chem*. (2005) 5:1113–23. doi: 10.2174/138955705774933301

70. Peri S, Biagioni A, Versienti G, Andreucci E, Staderini F, Barbato G, et al. Enhanced vasculogenic capacity induced by 5-fluorouracil chemoresistance in a gastric cancer cell line. *Int J Mol Sci*. (2021) 22(14):7698. doi: 10.3390/ijms22147698

71. Paladhi A, Daripa S, Mondal I, Hira SK. Targeting thymidine phosphorylase alleviates resistance to dendritic cell immunotherapy in colorectal cancer and promotes antitumor immunity. *Front Immunol*. (2022) 13:988071. doi: 10.3389/fimmu.2022.988071

72. Koyama M, Osada E, Akiyama N, Eto K, Manome Y. Effect of thymidine phosphorylase gene demethylation on sensitivity to 5-fluorouracil in colorectal cancer cells. *Anticancer Res*. (2022) 42:837–44. doi: 10.21873/anticanres.15541

73. Derwinger K, Lindskog EB, Palmqvist E, Wettergren Y. Changes in thymidine phosphorylase gene expression related to treatment of rectal cancer. *Anticancer Res*. (2013) 33:2447–51.

74. Peeters KC, Marijnen CA, Nagtegaal ID, Kranenbarg EK, Putter H, Wiggers T, et al. The TME trial after a median follow-up of 6 years: increased local control but no survival benefit in irradiated patients with resectable rectal carcinoma. *Ann Surg*. (2007) 246:693–701. doi: 10.1097/01.sla.0000257358.56863.ce

75. Sauer R, Liersch T, Merkel S, Fietkau R, Hohenberger W, Hess C, et al. Preoperative versus postoperative chemoradiotherapy for locally advanced rectal cancer: results of the German CAO/ARO/AIO-94 randomized phase III trial after a median follow-up of 11 years. *J Clin Oncol*. (2012) 30:1926–33. doi: 10.1200/JCO.2011.40.1836

76. Sadahiro S, Suzuki T, Tanaka A, Okada K, Saito G, Kamijo A, et al. Increase in gene expression of TYMP, DPYD and HIF1A are associated with response to preoperative chemoradiotherapy including S-1 or UFT for rectal cancer. *Anticancer Res*. (2016) 36:2433–40.

77. Jia X, Zhang T, Sun J, Lin H, Bai T, Qiao Y, et al. Rs11479 in thymidine phosphorylase associated with prognosis of patients with colorectal cancer who received capecitabine-based adjuvant chemotherapy. *Pharmgenomics Pers Med*. (2023) 16:277–89. doi: 10.2147/PGPM.S397382

78. Kaidi D, Szeponik L, Yrlid U, Wettergren Y, Bexe Lindskog E. Impact of thymidine phosphorylase and CD163 expression on prognosis in stage II colorectal cancer. *Clin Transl Oncol*. (2022) 24:1818–27. doi: 10.1007/s12094-022-02839-2

79. Goto T, Shinmura K, Yokomizo K, Sakuraba K, Kitamura Y, Shirahata A, et al. Expression levels of thymidylate synthase, dihydropyrimidine dehydrogenase, and thymidine phosphorylase in patients with colorectal cancer. *Anticancer Res*. (2012) 32:1757–62.

80. Du YB, Zhang TF, Cui K, Jin SL, Xi Y, Ma W. The influence of Thymidine Phosphorylase genetic variation on clinical outcomes and safety of colorectal cancer patients received adjuvant chemotherapy after R0 resection. *Zhonghua Yi Xue Za Zhi*. (2018) 98:2569–73. doi: 10.3760/cma.j.issn.0376-2491.2018.32.007

81. Chen SA, Zhang JP, Wang N, Chen J. Identifying TYMP as an immune prognostic marker in clear cell renal cell carcinoma. *Technol Cancer Res Treat*. (2023) 22:15330338231194555. doi: 10.1177/15330338231194555

82. Liu M, Pan Q, Xiao R, Yu Y, Lu W, Wang L. A cluster of metabolism-related genes predict prognosis and progression of clear cell renal cell carcinoma. *Sci Rep*. (2020) 10:12949. doi: 10.1038/s41598-020-67760-6

83. Yang Y, Jiang L, Wang S, Chen H, Yi M, Wu Y, et al. A comprehensive pan-cancer analysis on the immunological role and prognostic value of TYMP in human cancers. *Transl Cancer Res*. (2022) 11:3187–208. doi: 10.21037/tcr-22-502

84. Li Y, Fan C, Hu Y, Zhang W, Li H, Wang Y, et al. Multi-cohort validation: A comprehensive exploration of prognostic marker in clear cell renal cell carcinoma. *Int Immunopharmacol*. (2024) 135:112300. doi: 10.1016/j.intimp.2024.112300

85. Huang L, Liu S, Lei Y, Wang K, Xu M, Chen Y, et al. Systemic immune-inflammation index, thymidine phosphorylase and survival of localized gastric cancer patients after curative resection. *Oncotarget*. (2016) 7:44185–93. doi: 10.18632/oncotarget.v7i28

86. Lin S, Lai H, Qin Y, Chen J, Lin Y.. Thymidine phosphorylase and hypoxia-inducible factor 1-α expression in clinical stage II/III rectal cancer: association with response to neoadjuvant chemoradiation therapy and prognosis. *Int J Clin Exp Pathol*. (2015) 8:10680–8.

frontiers | Frontiers in Immunology

TYPE Review
PUBLISHED 30 April 2025
DOI 10.3389/fimmu.2025.1576283

OPEN ACCESS

EDITED BY
Pengpeng Liu,
University of Massachusetts Medical School, United States

REVIEWED BY
Yi Liu,
Stanford University, United States
Qiuxia Zhao,
The University of Texas at Austin, United States
Zhimin Hu,
University of California, San Diego, United States

*CORRESPONDENCE
Guanghui Wu
ndwgh@163.com
Yisheng Chen
capydora@qq.com
Xianjun Li
lixianjun1978@126.com
Ming Liu
liuming_2011@outlook.com
Jiancheng Shen
190996473@qq.com

RECEIVED 13 February 2025
ACCEPTED 02 April 2025
PUBLISHED 30 April 2025

CITATION
Wu G, Chen Y, Chen C, Liu J, Wu Q, Zhang Y, Chen R, Xiao J, Su Y, Shi H, Yu C, Wang M, Ouyang Y, Jiang A, Chen Z, Ye X, Shen C, Reheman A, Li X, Liu M and Shen J (2025) Role and mechanisms of exercise therapy in enhancing drug treatment for glioma: a review. *Front. Immunol.* 16:1576283. doi: 10.3389/fimmu.2025.1576283

Role and mechanisms of exercise therapy in enhancing drug treatment for glioma: a review

Guanghui Wu[1,2*], Yisheng Chen[1,2,3,4,5,6*], Chong Chen[7], Jianling Liu[3], Qiaowu Wu[3], Yazhen Zhang[8], Runqiong Chen[3], Jianzhong Xiao[3], Yusheng Su[3], Haojun Shi[9], Chunsheng Yu[3], Miao Wang[3], Yifan Ouyang[3], Airong Jiang[3], Zhengzhou Chen[3], Xiao Ye[3], Chengwan Shen[3], Aikebaier Reheman[3], Xianjun Li[3*], Ming Liu[1,2*] and Jiancheng Shen[1,2*]

[1]Department of Neurosurgery, Ningde Clinical Medical College, Fujian Medical University, Ningde, Fujian, China, [2]Department of Neurosurgery, Ningde Municipal Hospital, Ningde Normal University, Ningde, Fujian, China, [3]Fujian Key Laboratory of Toxicant and Drug Toxicology, Medical College, Ningde Normal University, Ningde, Fujian, China, [4]Department of Neurosurgery, School of Medicine, Loma Linda University, Loma Linda, CA, United States, [5]Department of Physiology and Pharmacology, School of Medicine, Loma Linda University, Loma Linda, CA, United States, [6]Department of Neurosurgery and Anesthesiology, School of Medicine, Loma Linda University, Loma Linda, CA, United States, [7]NHC Key Laboratory of Diagnosis and Treatment on Brain Functional Diseases, The First Affiliated Hospital of Chongqing Medical University, Chongqing, China, [8]School of Physical Education, Ningde Normal University, Ningde, Fujian, China, [9]Faculty of Chinese Medicine and State Key Laboratory of Quality Research in Chinese Medicines, Macau University of Science and Technology, Macau, Macau SAR, China

Gliomas, particularly glioblastoma (GBM), are among the most aggressive and challenging brain tumors to treat. Although current therapies such as chemotherapy, radiotherapy, and targeted treatments have extended patient survival to some extent, their efficacy remains limited and is often accompanied by severe side effects. In recent years, exercise therapy has gained increasing attention as an adjunctive treatment in clinical and research settings. Exercise not only improves patients' physical function and cognitive abilities but may also enhance the efficacy of conventional drug treatments by modulating the immune system, suppressing inflammatory responses, and improving blood-brain barrier permeability. This review summarizes the potential mechanisms of exercise in glioma treatment, including enhancing immune surveillance through activation of natural killer (NK) cells and T cells, and increasing drug penetration by improving blood-brain barrier function. Additionally, studies suggest that exercise can synergize with chemotherapy and immunotherapy, improving treatment outcomes while reducing drug-related side effects. Although the application of exercise therapy in glioma patients is still in the exploratory phase, existing evidence indicates its significant clinical value as an adjunctive approach, with the potential to become a new standard in glioma treatment in the future.

KEYWORDS

glioma, exercise therapy, drug treatment, immune system, blood-brain barrier

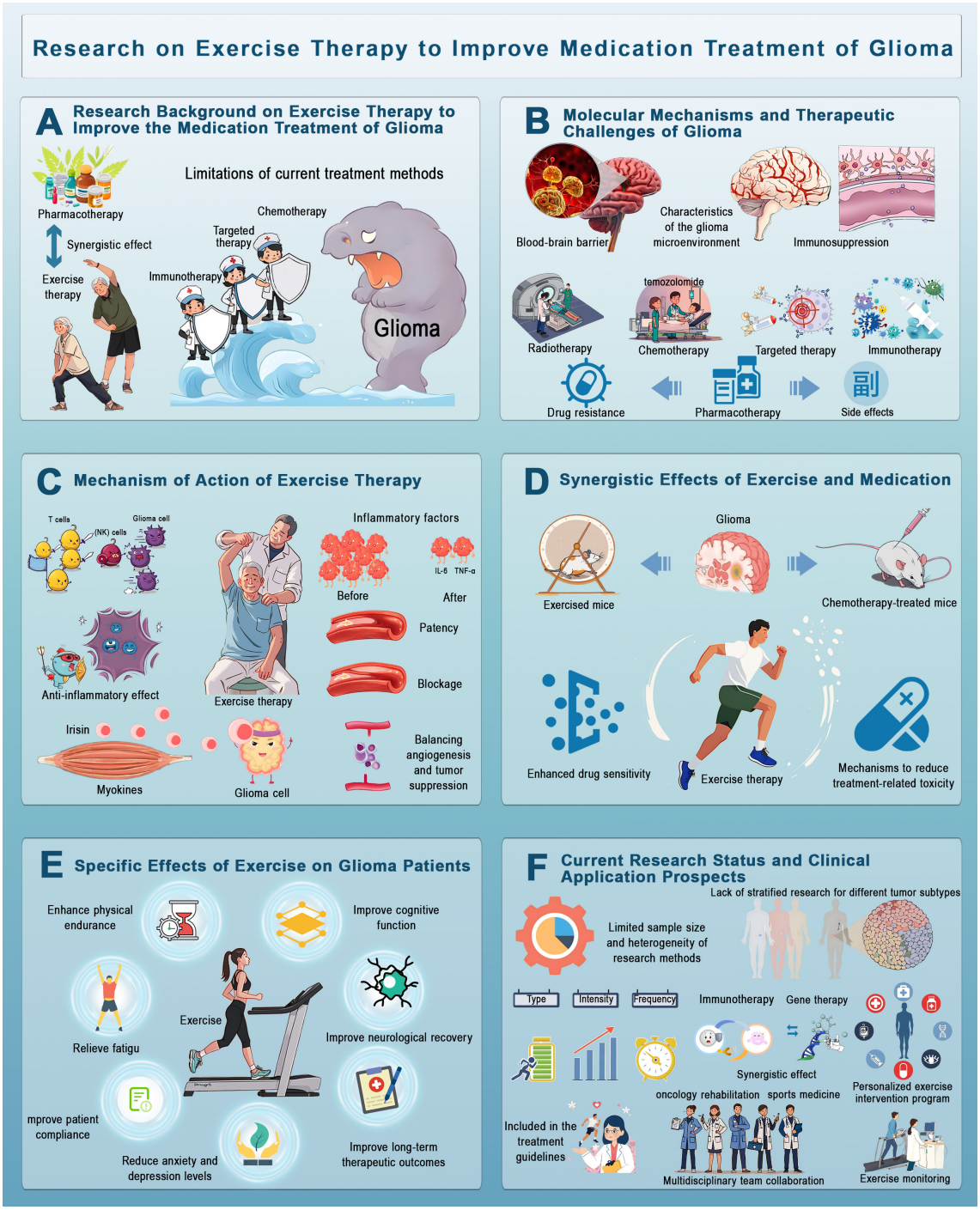

GRAPHICAL ABSTRACT

Research on Exercise Therapy in Improving Drug Treatment for Glioma This figure illustrates the potential of exercise therapy to enhance glioma treatment. **(A)** Conventional therapies face limitations, such as drug resistance and side effects. **(B)** Glioma treatment is challenged by the blood-brain barrier, tumor microenvironment and immunosuppression. **(C)** Exercise modulates the immune response, reduces inflammation, and promotes tumor suppression via myokines. **(D)** Exercise enhances drug sensitivity and reduces chemotherapy resistance. **(E)** It improves physical endurance, cognitive function, neurological recovery and mental well-being. **(F)** Despite research gaps, integrating exercise into clinical oncology through personalized programs and multidisciplinary collaboration holds promise for the management of glioma.

1 Introduction

1.1 Epidemiology and clinical burden

Gliomas, especially glioblastomas (GBM), are among the most common and aggressive brain tumors (1). With a high degree of malignancy and poor prognosis, current treatment options such as chemotherapy, targeted therapy, and immunotherapy have many limitations (2). Glioblastomas account for approximately 48% of adult brain malignancies, with standard treatment primarily relying on radiotherapy and temozolomide chemotherapy (3). However, these therapies have not significantly improved long-term survival and quality of life for patients (4). The biological characteristics of glioblastomas present numerous challenges during treatment. These tumors are characterized by dense vasculature and are often accompanied by vasogenic edema and mass effects, which exacerbate neurological symptoms and lead to a poor quality of life (5). Additionally, glioblastomas exhibit a highly immunosuppressive microenvironment, which further complicates treatment efforts. Although there have been significant advances in cancer treatment in recent years, therapeutic outcomes for gliomas remain limited, particularly in patients with high-grade gliomas (HGGs) (6). The primary treatment goal for patients with HGG is to achieve progression-free survival and delay cognitive and neurological decline as much as possible (7). For these patients, health-related quality of life (HRQOL) has become a critical measure for evaluating treatment effectiveness (8).

Although brain tumors account for a relatively small proportion of all malignancies (1. 4%), their negative impact on both physical and mental health is profound (9). Patients with brain tumors often suffer from functional impairments, experiencing not only physical dysfunction but also significant reductions in cognitive abilities and social psychological well-being. Consequently, cancer rehabilitation, particularly research focused on patients with brain tumors, has become a prominent area of study. With advancements in early diagnosis and treatment, the overall survival rate of patients with cancer has significantly improved (10). However, the challenge of maintaining quality of life after treatment remains severe for patients with gliomas. This is particularly important given the frequent occurrence of neurological deficits, fatigue, and cognitive decline that persist after conventional treatment. In this context, complementary therapies, such as exercise, may offer potential benefits by improving both physical function and cognitive outcomes.

The incidence of brain tumors increases with age, and survival rates decline with age at diagnosis. The median age at diagnosis of most brain tumors is 56 years. However, it is important to note that brain tumors remain one of the most common malignant cancers in children (11). The incidence of different types of brain tumors varies significantly across age groups. In children, embryonal/neuroectodermal tumors and pilocytic astrocytomas are more prevalent, whereas in adults, meningiomas and malignant gliomas are more common (12). The impact of brain tumors on patient health extends beyond physical effects and includes a decline in social and psychological functioning (13). Treatments such as surgery, radiotherapy, and chemotherapy not only cause direct physical damage but can also lead to long-term side effects, further impairing a patient's ability to work and interact socially (14). Therefore, glioma treatment should focus not only on prolonging survival but also on enhancing post-treatment functional recovery and quality of life. Moreover, emerging evidence suggests that incorporating physical exercise during or after treatment could offer additional benefits by modulating the immune response, reducing inflammation, and improving drug delivery.

1.2 Burden of brain cancer and other central nervous system cancers

Although brain cancer and other central nervous system (CNS) tumors account for a relatively small proportion of all cancers, their disease burden on patients is extremely heavy. Glioma is the most common malignant brain tumor in adults, accounting for 80% of all primary brain cancers. According to statistics, the five-year relative survival rate for brain cancer is only 22%, which is significantly lower than that of other common cancers, such as breast cancer and prostate cancer, and much lower than the overall cancer survival rate (10, 15). Despite advancements in treatment, gliomas, especially glioblastomas, remain highly aggressive and have a poor prognosis, making them a major challenge for clinicians and researchers. Although treatment methods such as chemoradiotherapy (temozolomide) have somewhat improved patient survival rates, treatment-related side effects, particularly their impact on physical, cognitive, and social psychological functions, remain significant. These side effects persist throughout the treatment process and affect various stages of a patient's life (16).

1.3 Potential of exercise as an adjunctive therapy

Ongoing research continues to unravel the intricate regulatory mechanisms through which physical activity modulates various biological processes. These findings are instrumental in advancing the refinement of intervention strategies and identification of novel therapeutic targets (16–18). In recent years, exercise has been increasingly recognized for its potential benefits as an adjunctive therapy for cancer patients. Research has shown that appropriate exercise interventions can significantly improve physical, social psychological, and cognitive functions in both healthy individuals and cancer patients (19). Exercise not only aids in the brain repair process in mice but also enhances cognitive abilities in both mice and humans (20). Although it remains unclear whether these benefits can be replicated in adult brain tumor patients undergoing treatment, animal studies have demonstrated the restorative effects of exercise on neurological function (21). In particular, the potential of exercise interventions in patients with brain tumors warrants further investigation.

A meta-analysis indicated that patients who engaged in physical activity after diagnosis had significantly higher disease-free survival and

overall survival rates than those with the least physical activity (22). Furthermore, cancer-specific and all-cause mortality rates were reduced by 59% and 64%, respectively. This evidence highlights the importance of exercise as a potential therapeutic strategy for improving physical function, modulating immune responses, and enhancing overall treatment efficacy (23–25). The American College of Sports Medicine's exercise prescription guidelines also provide strong evidence supporting the role of exercise interventions in managing anxiety, depressive symptoms, fatigue, quality of life (QoL), and physical function. Notably, exercise interventions have also shown benefits for bone health and sleep (26).

2 Molecular mechanisms of glioma and treatment challenges

2.1 Molecular and biological characteristics of glioma

Glioma, particularly GBM, is a significant concern because of its high invasiveness, heterogeneity, and strong resistance to current treatments as shown in Figure 1. The heterogeneity of glioma cells is reflected not only in cell morphology but also in gene expression, epigenetic modifications, metabolic characteristics, and the

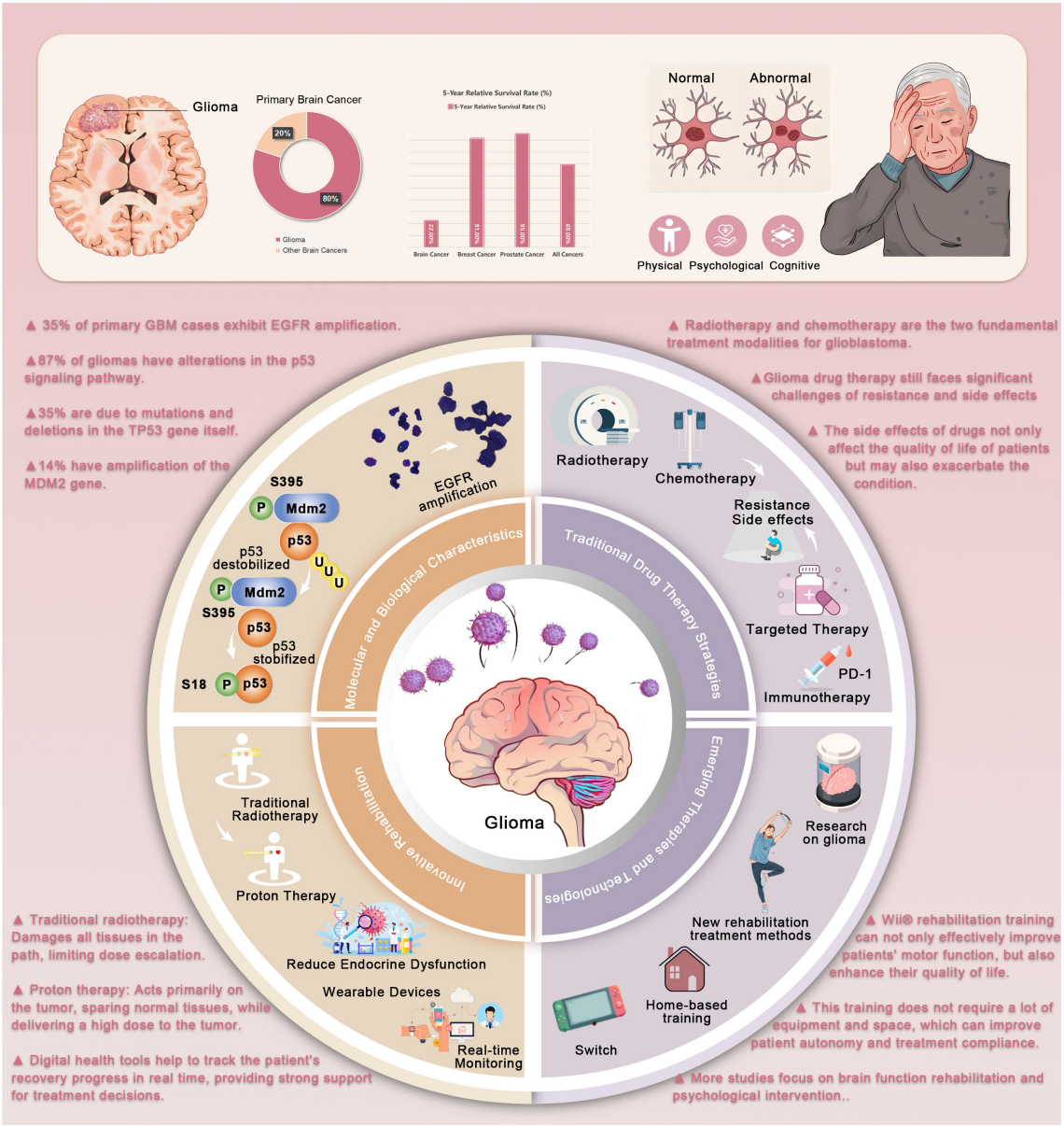

FIGURE 1
Molecular Characteristics, Treatment Strategies, and Emerging Technologies for Glioma Management. This figure outlines glioma pathophysiology, traditional treatments, and emerging therapies. The p53 pathway's dysregulation, influenced by phosphorylation, is key in glioma progression. Traditional treatments, including radiotherapy and chemotherapy, face resistance and side effects. New approaches, like PD-1 inhibitors and immunotherapy, are being explored. Proton therapy offers more precise targeting of tumors, sparing healthy tissues. Rehabilitation technologies like home training and digital monitoring improve patient autonomy and compliance.

complexity of the immune microenvironment (27). This heterogeneity contributes to the difficulty in effectively treating gliomas, as traditional therapies often fail to address all tumor subpopulations, leading to tumor recurrence (28). At the molecular level, gliomas are typically characterized by gene mutations, chromosomal aberrations, and epigenetic alterations (29). For instance, amplification of the EGFR gene and mutations in TP53 are common genetic features of glioblastoma. These mutations are closely associated with the high invasiveness, rapid growth, and treatment resistance observed in gliomas. Further studies have shown that EGFR amplification activates a series of oncogenic signaling pathways, such as the PI3K/AKT and Ras/MAPK pathways, promoting glioma growth, proliferation, and migration (30). Additionally, the methylation status of the MGMT (O-6-methylguanine-DNA methyltransferase) gene is closely linked to the response of patients with glioma to temozolomide (31). MGMT methylation suppresses its expression, enhancing patient sensitivity to chemotherapy drugs (31).

In addition to genetic mutations, the metabolic characteristics of glioma cells reflect their high heterogeneity. Studies have found that glioma cells often exhibit abnormal glucose metabolism, such as the phenomenon of "aerobic glycolysis" (the Warburg effect) (32). This metabolic process allows tumor cells to preferentially generate energy through glycolysis, even in the presence of sufficient oxygen (33). This not only provides the energy needed for tumor cell growth but also leads to the accumulation of lactate, altering the tumor microenvironment and promoting tumor invasiveness (34). The immune microenvironment of gliomas is also a crucial factor contributing to therapeutic resistance. Research indicates that glioma cells suppress antitumor immune responses through multiple mechanisms (35). For example, gliomas often upregulate immune checkpoint molecules, such as PD-L1, inhibiting T-cell immune responses (36). Furthermore, the infiltration of tumor-associated macrophages (TAMs) and other immune-suppressive cell populations is one of the reasons for glioma's resistance to treatment (37). This immunosuppressive microenvironment not only shields tumor cells from immune surveillance but also fosters tumor progression and metastasis (38).Investigating the intricate interplay of biomolecular mechanisms in gliomas-including signaling pathways activated by genetic mutations, metabolic reprogramming, and immune microenvironment regulation – enables comprehensive elucidation of tumorigenic processes, thereby informing strategic development of targeted therapeutic agents (39, 40).

2.2 Traditional and emerging pharmacological treatment strategies

2.2.1 Radiotherapy and chemotherapy

Radiotherapy and chemotherapy are the two mainstay treatments for glioblastoma. Despite their essential role in clinical treatment, their effectiveness is often limited (41). Radiotherapy kills tumor cells through high-energy radiation but is also challenging to target solely at tumor cells, often causing damage to normal brain tissue (42). This is particularly problematic in pediatric patients, in whom long-term cognitive dysfunction caused by radiotherapy remains a serious side effect. In addition to cognitive damage, radiotherapy may lead to brain atrophy, endocrine dysfunction, and other neurological impairments (43). To reduce these side effects, increasing attention is being paid to more precise radiotherapy techniques, such as stereotactic radiotherapy (SRT) and proton beam radiotherapy (PBRT), which enhance targeting accuracy and reduce damage to healthy tissue (44). Temozolomide (TMZ) is a standard drug used in the treatment of glioblastoma. It kills tumor cells by interfering with the DNA repair processes. However, due to the resistance of tumor cells, the efficacy of temozolomide is often limited (45). The resistance mechanisms may involve the expression levels of the MGMT gene, changes in the tumor microenvironment, and autophagy (46). To address this issue, researchers are exploring combination therapies with temozolomide to overcome tumor resistance and enhance the therapeutic efficacy.

2.2.2 Targeted therapy and immunotherapy

In recent years, targeted therapy and immunotherapy have become popular topics in glioma research. Targeted therapy inhibits specific molecular targets within tumor cells to block their growth. For instance, targeted drugs against EGFR mutations and VEGF antibodies have been used in glioma treatment (47). However, owing to the molecular heterogeneity of gliomas, single-target drugs often fail to address the tumor's diversity and resistance. In addition to single-target therapies, combination therapies targeting multiple pathways are being explored (28). Bioinformatics technologies have played a pivotal role in unraveling gene expression and regulatory mechanisms in gliomas, providing critical insights into the molecular basis of tumorigenesis and progression (48–50).Immunotherapy represents a revolutionary advancement in cancer treatment. By utilizing immune checkpoint inhibitors, the immune system is activated to enhance its recognition and destruction of tumor cells (51). Immunotherapy has provided new hope for patients with gliomas. However, the immune evasion mechanisms of gliomas render immunotherapy less effective than in other cancer types. The highly immunosuppressive microenvironment of gliomas and the frequent upregulation of immune checkpoints are major obstacles to the success of immunotherapy (52). Therefore, overcoming immune evasion mechanisms and improving the effectiveness of immunotherapy remain key challenges in the treatment of gliomas. In glioma immunotherapy, integrating bioinformatics with experimental approaches, such as epigenetic profiling, metabolic regulation analysis, and intercellular communication studies, uncovers novel immune cell mechanisms, thereby informing the optimization of therapeutic strategies (38, 53).

2.2.3 Drug resistance and side effects

Despite continuous advancements in treatment strategies, drug resistance and side effects remain significant challenges in the treatment of gliomas. Tumor cell resistance to current treatments is not only closely linked to genetic mutations but also involves factors such as the tumor microenvironment, drug metabolism

pathways, and the efficacy of the blood-brain barrier (54). The tumor microenvironment plays a crucial role in facilitating drug resistance by creating physical, biochemical, and immune barriers (55). For instance, overcoming the blood-brain barrier (BBB) for drug delivery in glioma requires interdisciplinary approaches that integrate pharmaceutics, materials science, and bioinformatics (38). Long-term treatment side effects are also a dilemma for patients with glioma. The side effects of drugs not only affect patients' quality of life but can also exacerbate their conditions. For instance, while dexamethasone can alleviate brain edema and increased intracranial pressure in patients with glioma, prolonged use may lead to a range of side effects, such as osteoporosis, diabetes, and muscle atrophy (56). These chronic side effects can significantly reduce the patient's functional capacity and quality of life, further complicating glioma management. These side effects highlight the need for more individualized treatment strategies to minimize the negative impact on patients' health.

2.3 Emerging treatment methods and technologies

With technological advancements, emerging treatment methods and technologies have brought new hope for glioma treatment. Proton beam radiotherapy (PBRT) is a precise radiotherapy technique that offers greater targeting accuracy and fewer side effects than traditional photon radiotherapy (XRT). Proton beam radiotherapy can precisely focus radiation on the tumor site, minimizing radiation exposure to surrounding healthy tissues, and thus significantly reducing the risk of neurocognitive damage (57). Although large-scale clinical trial data remain limited, existing studies have shown that proton beam radiotherapy offers clear advantages in glioma treatment, particularly in reducing endocrine dysfunction and lowering the risk of tumor recurrence (58). In addition, the application of digital health technologies is gradually gaining attention in glioma treatment. By using wearable devices to monitor patients' physiological data in real time, physicians can better understand the patient's condition and adjust the treatment plan accordingly. These devices can monitor indicators such as activity levels, heart rate, and blood oxygen levels, and can also assess patients' mobility and cognitive function (59). Meanwhile, AI-empowered CADD has advanced to high-throughput multi-scale simulations, providing intelligent frameworks for glioma-targeted therapies. Nanodelivery systems (NDS) optimize stem cell niches and enhance targeted delivery, while synergizing with exercise therapy to improve drug penetration and immune activation, thus overcoming blood-brain barrier and immunosuppressive challenges (60–62).Glioma research has established an integrated framework combining bioinformatics, advanced imaging technologies, and single-cell transcriptomics to systematically elucidate pathological mechanisms and white matter repair processes. The single-cell transcriptomic analysis methodology, developed based on references (63, 64), employs single-cell sequencing and high-dimensional omics technologies to characterize disease pathogenesis and cellular/molecular features within tumor immune microenvironments, offering novel perspectives for understanding disease progression and therapeutic responses (65–67). The synergistic application of bioinformatic tools and single-cell sequencing has enabled researchers to identify microenvironment-specific immune reaction patterns, providing empirical support for personalized treatment strategies (68, 69). These technological advancements have facilitated the implementation of multi-omics approaches (transcriptomics, metabolomics, proteomics) in clinical sample analysis, revealing disease-associated molecular signatures that inform early diagnosis and precision medicine (70, 71).

Clinical implementations demonstrate that CT-based multitask deep learning models can predict tumor-stroma ratios and treatment outcomes, while machine learning algorithms effectively identify lymph node metastasis patterns in gliomas, establishing evidence-based foundations for individualized therapy (72–76).Digital health monitoring systems significantly enhance rehabilitation management through real-time progression tracking (77). The integration of big data analytics and bioinformatics has become pivotal in glioma biomarker discovery and prognostic evaluation, with transcriptomic data mining enabling precise identification of critical genes and signaling pathways that inform drug development and early diagnostic markers (78–80). Cutting-edge approaches combining multi-omics integration, advanced bioinformatic analysis, and nanotechnology have elucidated potential therapeutic mechanisms of various agents (81, 82). Current investigations in glioma and other malignancies focus on extracellular vesicle (EV) applications as drug delivery systems through combined cellular biology and immune microenvironment analysis, creating novel paradigms for therapeutic innovation and prognostic assessment (83, 84).

3 Mechanisms of exercise therapy

3.1 Systemic antitumor effects

3.1.1 The broad role of exercise in antitumor therapy

Accumulating evidence underscores the capacity of exercise to modulate diverse biological processes, thereby facilitating the optimization of intervention strategies and identification of novel therapeutic targets (16–18). In recent years, exercise, as a natural health behavior, has been increasingly demonstrated to have potential in antitumor therapy (85). Exercise not only helps improve physical fitness, enhances cardiovascular function, and boosts the immune system, but also provides active support against tumor occurrence, progression, and recurrence through various mechanisms (86). This effect is particularly prominent in the treatment of highly malignant brain tumors, such as GBM. Owing to the limitations imposed by drug resistance, the BBB, and adverse factors in the tumor microenvironment, exercise as a non-pharmacological therapy has garnered significant attention for its potential antitumor effects (87). The antitumor effects of exercise

can operate through various mechanisms, particularly by modulating the immune system, exerting anti-inflammatory effects, and improving the tumor microenvironment, thereby enhancing the body's resistance to tumors (88). Studies have shown that moderate exercise can significantly improve immune system function by increasing the activity of immune cells, thereby enhancing the body's ability to recognize and eliminate tumors as shown in Figure 2 (89).

3.1.2 Modulation of the immune system by exercise

The impact of exercise on the immune system is considered a core mechanism underlying its antitumor effects. The immune system plays a crucial role in tumor initiation and development (90). Tumor cells often evade detection by the host immune system through various mechanisms, whereas exercise enhances immune system function through multiple pathways, making it an effective strategy for preventing tumor progression (91). Studies have shown that moderate exercise enhances immune surveillance by regulating the quantity and activity of natural killer (NK) cells (25). NK cells are key components of the innate immune system, serving as the body's first line of defense by effectively recognizing and eliminating tumor cells (92). By increasing the number and activity of these cells, exercise promotes immune system surveillance and attacks tumors (93). Furthermore, exercise can regulate T cell function, especially by enhancing the effectiveness of cytotoxic T cells, thereby promoting the clearance of tumor cells (94). Cytotoxic T cells recognize and kill tumor cells, assisting the body in eliminating tumors. By enhancing the function of these immune cells, exercise helps lower the incidence of tumors and slow their progression (50).

In addition to modulating T cells and NK cells, exercise regulates the expression of immunosuppressive factors (95). In the tumor microenvironment, immunosuppressive factors (such as IL-10 and TGF-β) often suppress immune cell function, allowing tumor cells to escape immune system attack (96). Research indicates that Exercise can lower the levels of these immunosuppressive factors, thereby enhancing the immune system's ability to eliminate tumors (97). Chronic inflammation plays a key role in the occurrence and progression of tumors, and chronic inflammation in the tumor microenvironment is considered one of the primary factors

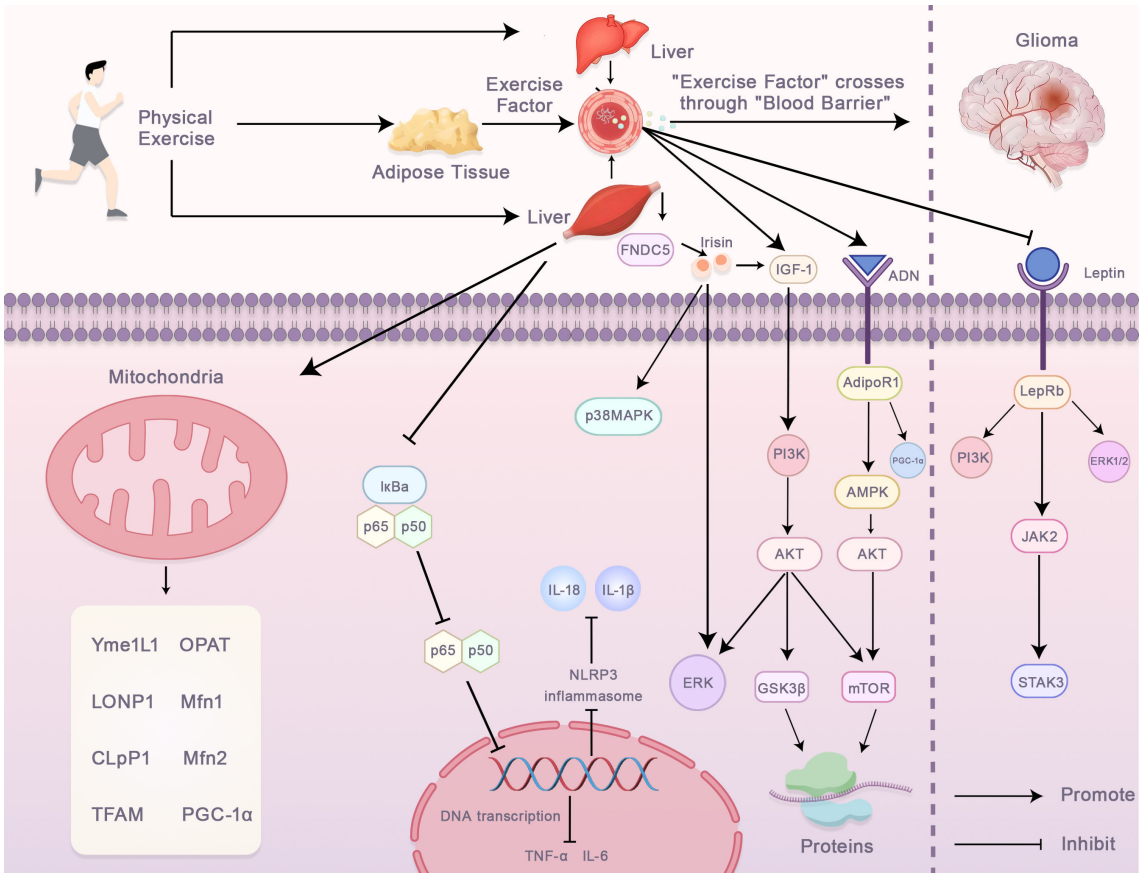

FIGURE 2
Molecular Mechanisms Underlying the Effects of Exercise on Glioma Progression. This figure shows how physical exercise influences glioma progression through systemic and intracellular pathways. Exercise releases factors like FNDC5, Irisin, IGF-1, and adiponectin from adipose tissue and the liver, which cross the blood-brain barrier and regulate glioma cells. These factors activate pathways that enhance mitochondrial function, reduce inflammation, and regulate glioma signaling. Exercise activates p38MAPK, inhibiting the NLRP3 inflammasome and lowering pro-inflammatory cytokines. IGF-1 and adiponectin activate survival pathways like PI3K/AKT, ERK, and GSK3β, promoting cellular homeostasis. Leptin also regulates glioma progression through the PI3K/JAK2/STAT3 axis. These adaptations suggest exercise therapy could complement glioma treatment.

promoting tumor growth and metastasis (98). Pro-inflammatory factors activate tumor cell proliferation, migration, and metastasis (99). Exercise, by reducing the expression of these pro-inflammatory factors, contributes to a less favorable environment for tumor growth and spread (100). The temporal dynamics of exercise-induced immune modulation are critical in this regard. Intermittent high-intensity interval training (HIIT) induces acute increases in cytotoxic T-cell infiltration within 24 h, whereas sustained moderate exercise promotes macrophage polarization toward the anti-tumor M1 phenotype. In glioma-bearing mice, HIIT reduced tumor volume by 25% compared to that in sedentary controls, whereas continuous exercise primarily improved survival rates. Clinical protocols should balance intensity and duration based on the treatment phase.

3.1.3 Regulation of inflammatory response by exercise

Exercise is widely regarded as an effective anti-inflammatory agent, capable of modulating the immune system through various mechanisms and reducing the release of pro-inflammatory factors, thereby inhibiting tumor growth and metastasis (101). Studies have found that moderate exercise promotes the production of anti-inflammatory factors such as IL-10 and TGF-β (102, 103). These anti-inflammatory factors downregulate the expression of pro-inflammatory factors, thereby reducing chronic inflammation. For example, IL-10 inhibits the activation of T cells and macrophages, reducing inflammation, whereas TGF-β reduces immune cell activity, helping restore immune tolerance (104). Exercise can directly lower the expression of proinflammatory factors by modulating cellular signaling pathways. IL-6 and TNF-α, which are closely associated with chronic inflammation, are significantly reduced by exercise, alleviating inflammation in the tumor microenvironment (105). By reducing the release of pro-inflammatory factors, exercise can effectively inhibit tumor cell proliferation, migration, and metastasis, further suppressing tumor growth (106). Studies have shown that exercise boosts the activity of immune cells, such as T cells, NK cells, and macrophages, helping the immune system to more effectively recognize and eliminate tumor cells (101). Enhanced immune function not only directly combats tumors but also reduces the impact of chronic inflammation, which supports tumor growth (107).

3.1.4 The potential of exercise in cancer immunotherapy

As immunotherapy emerges as a promising approach in cancer treatment, the immune-regulating effects of exercise have gained widespread attention. Immunotherapies, such as immune checkpoint inhibitors and CAR-T cell therapy, have shown significant efficacy against various tumor types (108). However, the effectiveness of immunotherapy is often hindered by immunosuppressive and pro-inflammatory factors in the tumor microenvironment. As a natural immune regulator, exercise can enhance immune cell activity, promote antitumor immune responses, and improve the effectiveness of immunotherapy (109). For instance, research has shown that exercise enhances the function of NK and T cells, enabling them to more effectively recognize and kill tumor cells (93). Exercise also improves blood supply in the tumor microenvironment, boosting immune cell infiltration in the tumor and enhancing the effects of immunotherapy (110).

3.1.5 Exercise and immune checkpoint blockade

Immune checkpoint blockade (ICB) therapy, which includes inhibitors targeting PD-1, PD-L1, and CTLA-4, has revolutionized cancer treatment by reactivating the immune response against tumor cells. However, the clinical effectiveness of immune checkpoint inhibitors (ICIs) is often limited by the immunosuppressive tumor microenvironment (TME), which dampens the immune system's ability to recognize and attack cancer cells. Exercise has emerged as a promising strategy to enhance the efficacy of immune checkpoint blockade therapy by modulating the TME and boosting immune cell function. Exercise can significantly improve immune surveillance by increasing the activity of immune cells, such as natural killer (NK) cells, cytotoxic T lymphocytes (CTLs), and dendritic cells (DCs). These immune cells are crucial for the recognition and elimination of tumor cells. Research has shown that exercise-induced systemic inflammation, characterized by increased cytokine release, can enhance the recruitment of immune cells to the tumor site, thereby sensitizing tumors to ICB therapy (25). Moreover, exercise reduces immune suppression in the TME, which often arises from the accumulation of regulatory T cells (Tregs) and myeloid-derived suppressor cells (MDSCs). By inhibiting these immunosuppressive cells, exercise helps enhance the antitumor immune response, making tumors more responsive to immune checkpoint inhibitors.

3.1.6 Exercise's role in systemic inflammation regulation

Exercise not only affects local inflammation but also regulates systemic inflammation, improving the overall immune status. Epidemiological studies have shown that individuals who engage in regular exercise have generally lower levels of chronic inflammation, which may be one of the key reasons for their lower cancer incidence (111). Moderate exercise reduces systemic inflammation by improving blood circulation, metabolism, and immune response, thereby lowering the risk of tumor occurrence (112). Chronic inflammation is a risk factor for various types of cancer, especially colorectal and breast cancers (111). Exercise significantly reduces systemic inflammation by improving blood circulation, modulating immune responses, and promoting metabolism, thereby supporting cancer prevention (86).

3.1.7 Exercise's role in inhibiting tumor metastasis

Tumor metastasis is often accompanied by intensification of local inflammation, with high levels of pro-inflammatory factors stimulating the invasiveness of tumor cells (98). Exercise can effectively inhibit the invasiveness of tumor cells by reducing local inflammation, thereby lowering the risk of metastasis (106). Studies have shown that exercise can slow tumor metastasis by reducing the levels of proinflammatory factors, such as IL-6 and TNF-α. Moreover, exercise improves endothelial function, inhibits tumor

angiogenesis, and reduces the chances of tumor cell metastasis through the blood or lymphatic systems. Numerous animal experiments and clinical studies have demonstrated that regular exercise significantly lowers the risk of tumor metastasis and delays tumor progression (88).

3.1.8 Synergistic effects of exercise and antitumor drugs

In addition to directly improving the tumor microenvironment and reducing inflammation, exercise has synergistic effects with traditional antitumor treatments, such as chemotherapy and radiotherapy. Research indicates that moderate exercise enhances the efficacy of chemotherapy drugs while reducing side effects (113). Exercise improves immune system function and reduces inflammation, helping chemotherapy drugs exert greater efficacy within the tumor microenvironment (24, 114). Specifically, exercise improves blood circulation, enhances drug delivery efficiency, and alleviates immune suppression in the tumor microenvironment, allowing chemotherapy drugs to target tumor cells more effectively (90, 110). Research also shows that exercise enhances the effects of immunotherapy, improving immune recognition and the elimination of tumor cells (50, 115).

3.1.9 Clinical studies on the anti-inflammatory effects of exercise

Numerous clinical studies have validated the anti-inflammatory effects of exercise in reducing tumor-related inflammation (90). For instance, breast cancer patients undergoing chemotherapy demonstrated that regular low-intensity exercise significantly reduced the levels of inflammatory factors in the blood and improved their quality of life (116). Similar results have been confirmed in studies on colorectal cancer and other tumor types, demonstrating the potential of exercise in clinical cancer treatment (50, 117).

3.2 The remodeling of the tumor microenvironment by Exercise

3.2.1 Altering immune and inflammatory factors in the tumor microenvironment

The TME plays a critical role in tumor growth, metastasis, and resistance to treatment. Exercise can effectively inhibit tumor progression by altering the levels of immune and inflammatory factors in the tumor microenvironment, particularly in the treatment of GBM (118). Moderate exercise can improve the tumor microenvironment by increasing NK and T cell infiltration, reducing the expression of immunosuppressive factors, and enhancing the effectiveness of immunotherapy (118).

3.2.2 Improving blood-brain barrier permeability

The BBB is a complex structure composed of brain endothelial cells, basal membrane, astrocytes, and other cells that serves as a highly selective barrier to protect the brain from harmful substances. This barrier prevents the entry of pathogens, toxins, and other potentially harmful substances while limiting the effective delivery of many drugs, especially antitumor drugs. The BBB ensures the stability of the brain microenvironment and maintains neuronal function (119). However, its protective role complicates drug delivery in cancer treatments, particularly for invasive brain tumors such as glioblastoma, where the BBB becomes a major obstacle to treatment (120). In tumor therapy, especially for brain tumors, the ability to effectively penetrate the BBB and deliver drugs to the tumor site is crucial for improving treatment efficacy (121). Although various methods to enhance drug penetration through the BBB have been proposed, such as nanocarriers and drug delivery systems, these approaches often have limitations or potential side effects (122). Therefore, exploring natural physiological methods to improve BBB permeability has become an important area of research. Increasing evidence suggests that exercise, particularly regular aerobic exercise, may be a natural and effective way to improve BBB permeability (123, 124). Exercise, as a physical activity, influences multiple functions of blood circulation, the immune system, and the nervous system, and it has been increasingly shown to play a vital role in enhancing brain health. Specifically, exercise can improve BBB function through a series of complex physiological reactions, enhancing the permeability of the BBB to therapeutic drugs, thereby increasing the efficacy of antitumor medications in the brain (25, 123).

Studies have shown that regular aerobic exercise can improve endothelial cell function in the BBB through several mechanisms. Endothelial cells are the basic building blocks of the BBB and form tight junctions that control the selective permeability of substances. Exercise improves endothelial cell blood supply, promotes angiogenesis, and regulates the expression of molecules involved in cell-cell tight junctions, thereby increasing BBB permeability (123). Specifically, exercise has been shown to increase the levels of certain molecules in the blood, such as vascular endothelial growth factor (VEGF), matrix metalloproteinases (MMPs), and adrenomedullin, which can promote the "opening" of the BBB, making it easier for drugs to cross into the brain, thus enhancing drug efficacy (125). Exercise enhances BBB permeability through dual mechanisms (1): upregulation of vascular endothelial growth factor (VEGF) and erythropoietin (EPO), which promote endothelial cell proliferation and transiently loosen tight junction proteins (e.g., claudin-5, occluding); and (2) inhibition of matrix metalloproteinase-9 (MMP-9), which reduces the degradation of the basement membrane. Pharmacological agents targeting these pathways (e.g., anti-VEGF monoclonal antibodies) partially mimic the effects of exercise but lack systemic anti-inflammatory benefits. Notably, animal studies have demonstrated that voluntary running increases temozolomide penetration by 40% in orthotopic glioma models. Exercise-induced VEGF activates the PI3K/Akt signaling pathway in endothelial cells, promoting angiogenesis and transiently increasing BBB permeability. Concurrently, exercise reduces oxidative stress by upregulating antioxidant enzymes (e.g., SOD and Gaps), thereby stabilizing BBB integrity. Pharmacological agents mimicking these effects, such as anti-VEGF monoclonal antibodies (e.g., bevacizumab), show partial efficacy but lack the systemic benefits of exercise. Moreover, exercise can regulate neuroplasticity in the brain (126).

Neuroplasticity is the brain's ability to adapt to external changes, and exercise promotes neuroplasticity, which strengthens the interaction between neurons and endothelial cells, further improving BBB function (127). Notably, after prolonged exercise training, studies have shown enhanced blood supply to the brain and significant improvement in BBB permeability (123). This means that exercise not only improves drug delivery by enhancing blood circulation but also facilitates drug penetration by improving the adaptability of neural structures (128).

In addition to its direct effects on endothelial cell function, exercise enhances antioxidant capacity and reduces systemic inflammation, thereby reducing BBB damage (123). This mechanism is particularly important in brain tumor treatment, as the tumor microenvironment is often accompanied by significant inflammatory responses, which not only promote tumor cell growth but also damage the BBB (129). Therefore, exercise can alleviate these negative impacts through its anti-inflammatory and antioxidant effects, improving BBB function and enhancing drug efficacy (90, 130). These effects of exercise have been confirmed in animal studies and clinical research. In animal experiments, regular aerobic exercise (such as running and swimming) has been shown to significantly increase the permeability of antitumor drugs in the brain (131). In some studies, after several weeks of exercise training, the size of brain tumors in experimental animals was significantly reduced, and the concentration of drugs in the tumor region was notably higher (132). Although these studies are still mostly in the experimental phase, their potential has attracted widespread attention in the scientific community. Furthermore, exercise can enhance drug penetration by regulating molecular pathways related to the BBB (123). For instance, exercise increases ATP production, activating critical signaling pathways, such as the PI3K/Akt, MAPK, and NF-κB pathways, all of which play important roles in maintaining BBB integrity (133, 134). Exercise also regulates the function of cell adhesion molecules (such as tight junction proteins like ZO-1, occluding, and claudins) and transporters (e.g., P-glycoprotein), thereby modifying the selective permeability of the BBB (123). Through these mechanisms, exercise enables drugs that would typically struggle to penetrate the BBB, especially chemotherapeutic and immunotherapeutic drugs targeting tumors, to be delivered more effectively to the tumor site. It should be noted that the effect of exercise on BBB permeability may vary depending on the type, intensity, and duration of the exercise (123). Excessive and intense exercise may induce excessive stress responses in the body, leading to adverse effects (135). Therefore, moderate and consistent exercise is considered the optimal approach for improving BBB function (123). Many studies recommend engaging in at least three to four sessions of moderate-intensity aerobic exercise per week, with each session lasting more than 30 min, to achieve the best results (136). For patients with brain tumors, a personalized exercise plan can improve treatment outcomes and reduce side effects (137).

In summary, exercise improves BBB function through multiple pathways, enhancing the permeability of antitumor drugs and thus improving the efficacy of brain tumor treatments (138). Although most current studies are still in the animal or preclinical stage, the findings provide valuable insights into the potential of exercise as an adjunctive therapeutic approach for patients with cancer. In the future, with further clinical research, exercise may become an essential part of treatment regimens for patients with brain tumors, helping to enhance treatment outcomes and improve the quality of life. However, when exercise is used as an adjunctive therapy, individualized exercise plans must be developed based on the patient's physical condition and treatment needs, and the plans should be implemented under the guidance of a professional medical team to ensure safety and effectiveness (139).

3.2.3 Improving tumor blood supply and angiogenesis

Tumor growth and expansion largely depend on blood supply. As tumors continue to grow, their demand for oxygen and nutrients gradually increases, forcing tumor cells to secrete various growth factors, such as vascular endothelial growth factor (VEGF), to stimulate angiogenesis and ensure an adequate supply of nutrients and oxygen (140). Angiogenesis is not only a critical mechanism in tumor growth and metastasis but also directly impacts the tumor's response to drug therapy (141). Tumor blood vessels are often structurally abnormal and functionally incomplete, resulting in an uneven blood supply and sometimes regional hypoxia (142). This promotes tumor cell metabolism, proliferation and dissemination. To overcome this inadequate blood supply, scientists have proposed strategies to enhance tumor treatment effectiveness by improving angiogenesis and blood supply within the tumor microenvironment (50, 143). Exercise, as a natural physiological modulator, has been shown to significantly influences tumor blood supply and angiogenesis (144). Although exercise enhances VEGF-mediated vascular normalization, it does not promote pathological angiogenesis. In GBM models, exercise reduced hypoxia-inducible factor-1α (HIF-1α) expression, thereby inhibiting aberrant vessel formation and improving perfusion for drug delivery.

The effect of exercise on tumor blood supply and angiogenesis primarily occurs by regulating various physiological responses in the body (145). Exercise enhances overall blood circulation, improving blood flow and oxygen transport, thereby increasing blood supply to the tumor region (146). This process serves a dual role in cancer therapy: on one hand, it provides more oxygen and nutrients, supporting tumor cell metabolism and growth; on the other hand, it enhances the delivery of antitumor drugs, enabling them to reach the tumor tissue more effectively and exert therapeutic effects (147). Additionally, exercise regulates local blood flow, preventing blood stagnation and reducing the negative impact of local hypoxia on tumor cells, thereby improving the tumor microenvironment and reducing tumor invasiveness (146).

Exercise also plays a critical role in improving the tumor microenvironment by directly modulating angiogenesis (148). Angiogenesis is the formation of new blood vessels, a process that is crucial for tumor growth. Tumor cells secrete angiogenesis-promoting factors, such as VEGF and basic fibroblast growth factor (bFGF), to stimulate blood vessel growth and ensure adequate oxygen and nutrient supply to the tumor. However, tumor blood vessels often have abnormal morphology and loose structures, leading to

impaired blood flow and inadequate oxygen and nutrient supply (149). Exercise enhances endothelial cell function, promotes new blood vessel formation, and regulates angiogenesis, thereby optimizing the tumor blood supply and microenvironment, ultimately improving therapeutic outcomes (150).

However, it is important to note that angiogenesis within the tumor microenvironment is not a simple physiological process, and its changes have profound effects on tumor progression, metastasis, and therapy outcomes. Excessive angiogenesis can lead to structurally abnormal tumor blood vessels, resulting in impaired blood flow and creating a vicious cycle that may facilitate tumor cell invasion and metastasis (151). Therefore, exercise not only promotes angiogenesis but also regulates its extent, ensuring balanced angiogenesis that favors treatment (152). In cancer therapy, maintaining moderate angiogenesis improves blood supply to the tumor, enhancing its oxygen and nutrient status while avoiding the negative effects of excessive angiogenesis, such as tumor spread and metastasis (153).

In clinical practice, the application of exercise as an adjunctive treatment is gaining increasing attention (154). Many patients with cancer undergo regular exercise alongside standard treatments to improve their overall health and treatment outcomes. Exercise not only enhances physical strength and immune function but also improves the tumor microenvironment blood supply, thereby enhancing the effectiveness of therapeutic drugs and improving patients' quality of life (115). However, exercise therapy is not suitable for all patients, particularly those who are physically weak or in the early stages of treatment (155). The intensity and type of exercise should be individualized according to the patient's physical condition (154). Therefore, exercise should be conducted under the supervision of a professional medical team to ensure safety and effectiveness (156).

In summary, exercise improves the tumor microenvironment by regulating blood supply and angiogenesis in the tumor region, offering new approaches and methods for cancer treatment that warrant further investigation. By enhancing oxygen and nutrient supply to the tumor, exercise not only supports tumor cell metabolism and growth but also enhances the effectiveness of antitumor drugs, improving overall treatment outcomes (110). In future cancer therapies, exercise may become an important adjunctive treatment, providing a more comprehensive therapeutic regimen and improving patients' quality of life.

3.3 Exercise-induced molecular factors

Irisin is a molecule secreted by muscles during physical activity, and as an exercise-induced myokine, it has garnered widespread attention in the scientific community (157). Initially discovered in relation to fat metabolism, irisin promotes the transformation of white fat into brown fat, helping to regulate energy expenditure and metabolic balance (158). However, as research deepened, it became evident that irisin's functions extend far beyond metabolism alone. Growing evidence suggests that irisin plays a significant role in tumor suppression, immune regulation, and exercise performance (159). Notably, in the field of cancer treatment, irisin, a natural molecule, has demonstrated unique antitumor potential (160). By inducing tumor cell cycle arrest, increasing apoptosis, and inhibiting tumor cell proliferation, irisin provides novel targets and strategies for the treatment of malignant tumors (161).

The antitumor effects of irisin are first reflected in its ability to inhibit tumor cell growth (162). Specifically, irisin upregulates the expression of p21, which inhibits the expression of key cell cycle proteins, such as Cyclin D and Cyclin E, preventing cells from progressing from the G1 phase to the S phase (161). As a cell cycle inhibitor, p21 binds to cyclin-dependent kinases (CDKs), inhibiting CDK activity, leading to cell cycle arrest in the G1 phase, and preventing further tumor cell proliferation (163). This mechanism has been confirmed *in vitro* and in mouse models. By promoting p21 expression, irisin significantly inhibits tumor cell proliferation, slows tumor growth, and enhances the effectiveness of antitumor therapies (164).

In addition to inducing cell cycle arrest, irisin plays an essential role in regulating tumor cell apoptosis (160). Research indicates that irisin activates apoptotic pathways, promoting programmed cell death in tumor cells (165). Irisin enhances oxidative stress within cells, increasing the levels of reactive oxygen species (ROS) (166). Elevated ROS levels lead to damage to proteins, lipids, and DNA, activating apoptotic signaling pathways and ultimately resulting in tumor cell death (25, 167). More importantly, irisin regulates the expression of Bcl-2 family proteins, affecting the balance between pro-apoptotic and anti-apoptotic factors within cells (168). Irisin upregulates pro-apoptotic factors, such as Bax, and downregulates anti-apoptotic factors, such as Bcl-2, thereby activating mitochondrial-mediated apoptosis pathways and promoting tumor cell death (165). Through this mechanism, irisin not only effectively inhibits tumor cell proliferation but also enhances tumor cell death, offering new strategies for cancer treatment (161).

The potential of irisin in cancer therapy extends beyond the regulation of cell-cycle arrest and apoptosis. Recent studies suggest that irisin can also inhibit tumor invasion and metastasis by improving the tumor microenvironment (160). Tumor metastasis, a leading cause of cancer-related deaths, is closely associated with the tumor microenvironment, which provides favorable conditions for tumor cell growth and spread, including hypoxia, acidosis, and immune suppression (169). Irisin modulates immune cell functions in the tumor microenvironment, enhancing the immune system's ability to clear tumor cells and thereby suppressing tumor metastasis (170). For instance, studies have shown that irisin can regulate the activity of natural killer (NK) cells, enhancing the immune system's surveillance and clearance of tumor cells and reducing the likelihood of tumor cells invading the blood and lymphatic systems (164). Additionally, irisin improves the structure and function of tumor blood vessels, reducing hypoxia within tumor tissues and thereby inhibiting tumor cell spread (50, 170).Another remarkable effect of irisin in antitumor treatment is its supportive role in enhancing the efficacy of anticancer drugs (171). Research has shown that irisin enhances the permeability of drugs in tumors, helping drugs reach tumor sites more effectively and exert their therapeutic effects (172). Tumor cells often exhibit strong drug resistance, particularly during

chemotherapy and radiotherapy, which leads to diminished treatment efficacy. Irisin improves drug delivery by modulating the tumor microenvironment, overcoming drug resistance, and enhancing treatment effectiveness (173). For example, irisin upregulates vascular endothelial growth factor (VEGF), enhancing blood vessel permeability in the tumor region, which facilitates better penetration of antitumor drugs into the tumor tissue (164). Irisin not only increases drug accumulation in tumors but also improves immune cell function in the tumor microenvironment, increasing tumor cell sensitivity to drugs (171).

The antitumor effects of irisin have shown great potential in the treatment of highly malignant tumors, such as glioblastoma multiforme (GBM) (161). GBM is a highly aggressive brain tumor that is notoriously difficult to treat because of the severe limitations posed by the blood-brain barrier (BBB) on drug permeability (174). However, irisin has been found to improve the permeability of the blood-brain barrier, allowing antitumor drugs to penetrate the BBB more effectively and reach the tumor (120). This mechanism positions irisin as a promising new strategy for treating brain tumors, such as glioblastoma, offering better therapeutic prospects for patients (161).

The antitumor effects of irisin are not limited to glioblastoma. Studies have shown that irisin inhibits various types of cancer cells, including breast, lung, and colorectal cancer cells (170). Through its multiple mechanisms of action, irisin not only effectively inhibits tumor cell proliferation but also enhances tumor cell sensitivity to treatment, thereby improving treatment outcomes (172). As a natural molecule, irisin offers good safety and tolerance, making it a promising adjunct to cancer therapy (170).

Although clinical trials directly testing irisin in patients with glioma are lacking, phase I trials in breast cancer (NCT04350463) show that recombinant irisin (100 μg/kg, biweekly IV) is well tolerated and reduces circulating IL-6. Translational strategies for glioma include intranasal delivery to bypass the BBB and CRISPR-activation of FNDC5 (Irisin precursor) in muscle. Beyond irisin, high-throughput sequencing analyses in gene expression regulation studies have identified exercise-induced miR-210 as a novel mediator. This microRNA demonstrates dual oncogenic effects by targeting tumor suppressor genes while activating PI3K/AKT and Wnt/β-catenin signaling pathways, thereby promoting glioma cell proliferation and chemoresistance. These findings reveal potential therapeutic targets underlying the paradoxical effects of exercise intervention (175).

Although the potential of irisin in cancer treatment has been widely studied and validated, its clinical application faces several challenges. Future research should further explore the efficacy of irisin in different cancer types, assess its combined effects with other therapies (such as chemotherapy, radiotherapy, and immunotherapy), and determine optimal treatment regimens. Additionally, the mechanisms of action of irisin require further investigation to reveal its multi-layered effects in cancer treatment (170). These studies lay a solid foundation for the clinical application of irisin and offer new insights and methods for cancer treatment (176).

4 Synergistic effects of exercise and drug therapy

4.1 Experimental and clinical evidence

4.1.1 Efficacy of combined exercise and chemotherapy in mouse models

Research has shown that the synergistic effect of exercise and drug therapy, particularly with natural compounds, plays a significant role in cancer treatment (113). In mouse model experiments, we found that Nutlin-3a, a natural compound and MDM2 inhibitor, effectively inhibited glioma cell proliferation and activated the p53 pathway (177). The efficacy of Nutlin-3a may be affected by MDM2 overexpression; however, exercise can reverse this effect (177). This was further validated in a mouse model of LGG, where the combination of physical exercise and Nutlin-3a improved the physical function of tumor-bearing mice with MDM2 expression deficiency (20). This finding highlights the synergistic effects of exercise and natural products and reveals their role in immune modulation, suggesting that the combination of exercise and natural compounds may be a new approach for glioma treatment (178) as shown in Figure 3.

4.1.2 Exercise and reduction in brain cancer mortality risk

Epidemiological studies have demonstrated that exercise significantly reduces the risk of mortality in patients with brain cancer (179). However, while existing studies emphasize the impact of exercise on brain cancer mortality, the direct relationship between physical exercise and glioma progression remains unclear (180). In an experiment using a high-grade glioma mouse model, we investigated the effect of voluntary physical exercise on tumor proliferation and exercise ability in mice (20). The study found that voluntary exercise significantly reduced the proliferation rate of cortical motor tumors in mice and delayed the onset of motor dysfunction caused by gliomas (20, 25). Thus, physical exercise may serve as an adjunctive intervention in neuro-oncology, helping patients preserve motor function and mitigate the behavioral effects of gliomas.

4.1.3 Impact of exercise interventions on quality of life and treatment outcomes in clinical trials

A systematic review assessed the effects of exercise interventions on the health outcomes of patients with brain cancer. By searching databases such as PubMed and EMBASE, the review identified studies related to brain cancer, and the results indicated that higher levels of physical activity were associated with fewer disease symptoms and better quality of life in patients with brain cancer (180). Preliminary evidence suggests that exercise benefits various aspects, including cancer symptoms, quality of life, and body composition, and has a positive effect on alleviating cancer-related symptoms (181). However, the strength of this evidence remains weak, and high-quality studies are required to confirm these findings.

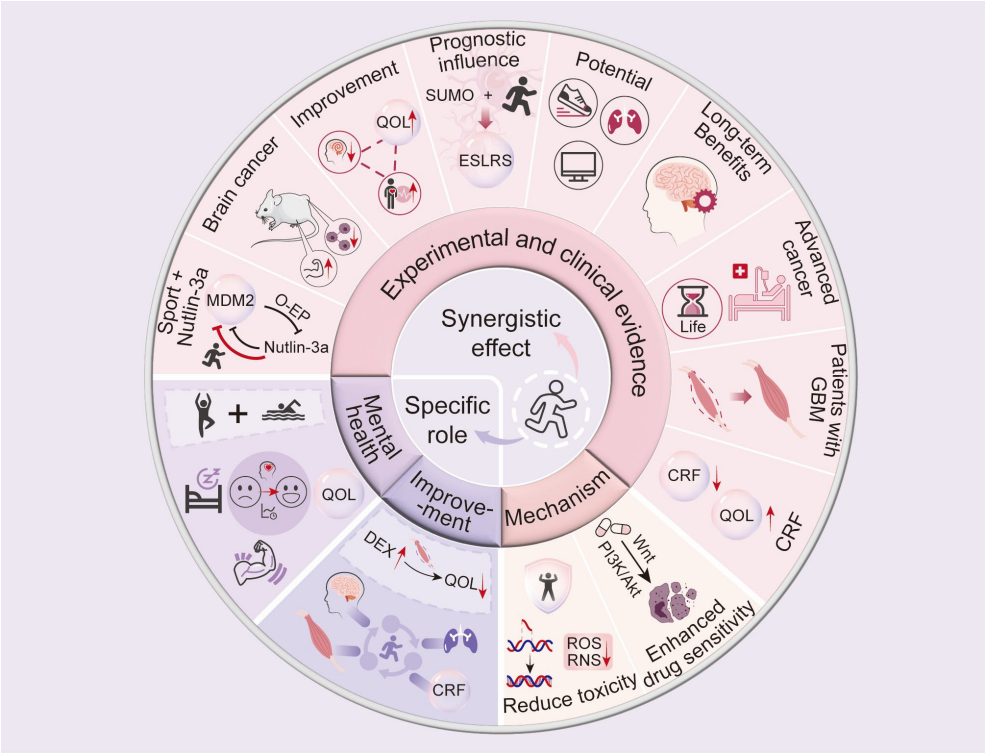

FIGURE 3
Synergistic Effects of Exercise on Glioblastoma Treatment: Experimental and Clinical Evidence. This figure shows experimental and clinical evidence supporting exercise as a beneficial addition to glioblastoma (GBM) treatment. Exercise enhances quality of life, mental health, and treatment efficacy by modulating biological pathways, reducing drug toxicity, and increasing sensitivity to therapies targeting the MDM2-p53 axis. It affects molecular pathways like Wnt/β-catenin, PI3K/AKT, and oxidative stress regulation, aiding cellular protection and tumor suppression. Exercise can reduce cancer-related fatigue, offer long-term benefits, and improve prognosis. Prognostic markers like SUMO and ESRLS suggest exercise may improve survival outcomes. This emphasizes the importance of integrating exercise into GBM treatment to boost therapeutic efficacy and patient well-being.

4.1.4 exercise and prognosis in glioma patients

Recent research has indicated that exercise significantly influences the prognosis of patients with glioma (182). Furthermore, the identification of glioma-specific biomarkers and analysis of molecular pathways enable researchers to predict disease progression and treatment response with enhanced precision (183–185).Exercise not only reduces the risk of mortality but may also promote neuroregeneration (186). In recent years, researchers have focused on the role of small ubiquitin-like modifier (SUMO) proteins in the anticancer effects of exercise and have developed exercise and SUMO-related gene signatures (ESLRS) using machine learning methods (187). This signature reveals how exercise improves the prognosis of low-grade gliomas and other cancers (182).In evaluating treatment efficacy and prognostic indicators, integrating factors such as glioma metabolic profiles and immune cell signatures provides a multidimensional perspective for assessing disease progression and therapeutic responses (188, 189) as shown in Figure 3.

4.1.5 Exercise potential in brain tumor treatment

Exercise has the potential to mitigate various health impairments during brain tumor treatment. A systematic review of the impact of exercise on children with brain tumors found that exercise positively affects neuroimaging, physical fitness, and cardiopulmonary function (21). While the effects of exercise on cognition remain unclear, the overall results suggest that exercise interventions can improve physical fitness and quality of life in patients without exacerbating symptoms (190). Therefore, exercise may be an essential component of pediatric brain tumor treatment.

4.1.6 Long-term benefits of exercise for brain tumor survivors

Brain tumor survivors often face a range of complications due to the complexities of the treatment and tumor pathology (14). Research has shown that exercise has a positive effect on the recovery and quality of life of these patients (191). Exercise helps survivors improve cognitive function, enhances motor abilities, and shows improvements in brain structure as detected by magnetic resonance imaging (192, 193). Furthermore, exercise therapy is linked to cognitive performance improvements, particularly in children who have undergone brain tumor treatment, where exercise effectively restores neurocognitive functions (194).

4.1.7 Exercise effects on advanced cancer patients

Patients with advanced cancer often face issues such as fatigue and reduced physical function (19). In recent years, an increasing body of evidence has supported the use of exercise interventions in palliative

and end-of-life care (195). Studies have found that over 90% of patients with advanced cancer can undergo exercise therapy (196). Exercise not only improves physical strength but also benefits caregivers (197). Despite some challenges, exercise intervention is considered a feasible and effective approach for treating patients with advanced cancer (198).

4.1.8 Exercise and glioblastoma multiforme patients

Exercise intervention studies in patients with glioblastoma (GBM) have shown that exercise can improve functional performance and quality of life (199). Regular exercise interventions during treatment help patients regain strength, enhance muscle function, and improve their quality of life (200). The results of this study suggest that exercise rehabilitation can play a positive role in the treatment of patients with GBM (201).

4.1.9 Exercise and cancer-related fatigue

Cancer-related fatigue (CRF) is a common symptom among patients with cancer, significantly affecting their quality of life (202). Studies have shown that exercise interventions help alleviate CRF and improve patients' quality of life (203). Exercise intervention has been shown to relieve fatigue, improve quality of life, and is highly feasible in patients with high-grade gliomas (204). These results suggest that exercise may be an effective intervention for combating cancer-related fatigue (203).

4.2 Mechanistic analysis

4.2.1 Exercise enhances drug sensitivity by regulating PI3K/Akt, Wnt pathways

The benefits of exercise in cancer treatment extend beyond improving physical health, as it also enhances drug sensitivity by regulating intracellular signaling pathways (106). Studies have found that exercise can modulate tumor cell growth and differentiation through pathways such as PI3K/Akt and Wnt, thereby increasing the cytotoxic effect of drugs on tumor cells (110). Integrative metabolomics and bioinformatics analyses in cellular metabolism studies reveal progesterone's therapeutic enhancement mechanism. The hormone potentiates antiglioma drug efficacy through AMPK/mTOR pathway modulation, establishing novel pharmacological optimization strategies (205). Furthermore, innovative nanodrug delivery systems, such as near-infrared light-activated upconversion nanoparticle/curcumin hybrid formulations, have demonstrated significant therapeutic potential by inducing differentiation and elimination of glioma stem cells (206). This combinatorial approach may offer enhanced treatment efficacy via multitargeted regulatory mechanisms, thereby presenting novel avenues for precision glioma therapy.

4.2.2 Mechanisms of reducing treatment-related toxicity

Cancer treatments, particularly chemotherapy and radiotherapy, are often associated with severe side effects (207). Exercise reduces treatment-related toxicity through several mechanisms, such as decreasing oxidative stress, enhancing immune function, and repairing DNA damage (208). These effects not only improve the patient's quality of life but also enhance overall treatment efficacy (113). Therefore, exercise can be an effective adjunctive therapy in cancer treatment, helping to mitigate the adverse effects of drugs and treatments (110).

4.2.3 Summary

Overall, the combination of exercise and drug therapy offers a new treatment strategy for patients with brain tumors. Experimental and clinical studies have shown that exercise can not only improve patients' physiological functions but also enhance treatment outcomes by regulating cellular signaling pathways, increasing drug sensitivity, and reducing treatment-related toxicity (113, 209, 210). Future research should continue to explore the synergistic effects of exercise interventions and drug therapy and develop personalized exercise treatment plans to maximize their clinical application.

5 Specific effects of exercise on glioma patients

Exercise has a broad and profound impact on patients with glioma, influencing physical function, quality of life, psychological health, and other aspects. According to current research, exercise can not only enhance patients' physical and cognitive abilities but also significantly improve their mental health, alleviate fatigue, reduce anxiety and depression, and improve treatment adherence and quality of life (211). The following is a detailed exploration of the specific effects of exercise interventions on patients with glioma.

5.1 Improvement of physical function and quality of life

Enhancing physical endurance and alleviating fatigue are among the most direct benefits of exercise in patients with glioma (204). Long-term or high-dose use of steroid drugs, such as dexamethasone (DEX), leads to muscle atrophy in 10%-60% of patients with glioblastoma, significantly affecting their physical function and quality of life (QOL) (212). Consequently, an increasing number of studies support exercise as an effective adjunctive therapy to help improve functional capacity and reduce treatment-related side effects. Particularly in the context of resistance training, research has shown that such training can increase muscle mass, strength, and functional fitness in older adults and certain cancer patients (213). Although research on exercise interventions in patients with glioblastoma is relatively limited, preliminary evidence suggests that exercise is safe and feasible (180). For example, a systematic review of exercise interventions in childhood cancer survivors (CCS) who had completed anti-cancer treatment at least one year prior indicated that, despite low methodological quality, early evidence suggests that exercise interventions could improve brain volume and structure in childhood brain tumor survivors (21).

Additionally, patients with glioma often experience cognitive impairments, which severely impact their quality of life and interfere with daily life, social, and professional activities (214). Increasing evidence shows that exercise promotes experience-dependent brain plasticity, which helps in the structural and functional recovery of the brain following damage (215). For instance, a randomized controlled trial (RCT) in patients with glioma demonstrated that exercise intervention helped improve cognitive functions, including attention, information processing speed, verbal memory, and executive function (201). Moreover, exercise interventions significantly improved self-reported fatigue, mood, sleep quality, and health-related quality of life (216). Specifically, during a six-month intervention, the exercise group outperformed the control group in various cognitive tests, although the exercise group showed slightly poorer results in sustained selective attention (217). Furthermore, exercise interventions have been shown to improve neurocognitive function, body composition, and motor ability (218). In exercise studies on other cancer patients, aerobic and resistance training have been proven to enhance muscle strength, endurance, and aerobic capacity (156). Studies on patients with glioma also support this conclusion, showing that even small-sample trials can yield positive clinical effects (219).

5.2 Psychological health effects

Exercise also has a significant positive impact on the psychological health of patients with glioma (192). Several studies have shown that exercise interventions can effectively reduce negative emotions, such as anxiety and depression, and improve patients' psychological health (220, 221). A study on a novel independent home exercise program found that patients with glioma who engaged in exercise generally demonstrated better adherence and improved quality of life (222). In this study, nine out of 14 participants (60%) adhered to the exercise regimen for a month. Patients who exercised more frequently tended to have higher marital satisfaction and income levels and showed positive trends in quality-of-life scores. Another study reported the effects of a 12-week exercise intervention involving two patients with glioma (192). The participants completed biweekly 1-hour aerobic and resistance-training sessions. At the 6- and 12-week assessments, the patients showed improvements in strength, cardiovascular health, and psychological well-being (e.g., reduced depression and anxiety and improved quality of life). In particular, patients generally experienced a reduction in psychological distress in self-reported anxiety and depression. Additionally, a randomized controlled trial on patients with high-grade glioma investigated the effects of endurance and resistance training on psychological health, sleep quality, and quality of life (223). The results showed that patients who received exercise interventions showed significant improvements in physical strength, sleep quality, and anxiety symptoms. Compared with the control group, the exercise intervention group demonstrated more substantial improvements in psychological health and sleep quality. Furthermore, combining aerobic exercise with flexibility training has been shown to have significant effects on both psychological health and physiological function in patients with glioma (192). In one study, a female patient who underwent 36 sessions of aerobic and flexibility training experienced a 20% reduction in fatigue and nearly a 70% improvement in quality of life (224). However, despite the positive effects on psychological and physiological health, improvements in cognitive function require further investigation. Overall, although research on exercise interventions in patients with glioma is relatively sparse, existing evidence suggests that exercise not only improves physical function and cognitive abilities but also enhances psychological health, reduces anxiety and depression, and improves treatment adherence and quality of life (225). Therefore, exercise holds significant clinical and research value as an adjunctive therapy for patients with glioma.

5.3 Conclusion and outlook

In conclusion, exercise interventions for patients with glioma not only improve physical health but also positively affect psychological health, quality of life, and cognitive function (201). Although existing research provides preliminary evidence, many questions remain unanswered. For instance, how to design more personalized exercise programs and how to quantify the long-term benefits of exercise for patients with glioma. Addressing these issues will provide more scientific evidence for glioma treatment and promote the widespread clinical application of exercise interventions in this context.

Future research should further explore the mechanisms underlying exercise interventions in patients with glioma and investigate the optimal timing, intensity, and frequency of different types of exercise (201). This will allow for more effective and personalized treatment plans for patients. Moreover, based on the broad benefits of exercise interventions for patients with glioma, exercise therapy is likely to become a standard adjunctive treatment, offering comprehensive treatment support.

6 Research status and limitations

6.1 Limitations of current research

Despite the broad positive impact of exercise on cancer patients' rehabilitation, research specifically focused on patients with brain tumors, particularly those with high-grade glioma (HGG), remains insufficient as shown in Figure 4.

6.1.1 Limited sample size and heterogeneity in research methods

Although multiple studies have been conducted on exercise interventions, research specifically targeting patients with brain tumors, particularly those with high-grade gliomas, remains limited (180). Existing studies often face challenges of small sample sizes and a lack of consistency in study design, making it difficult to draw broadly applicable conclusions (180). For example, physical fitness, cardiopulmonary function, muscle mass, and

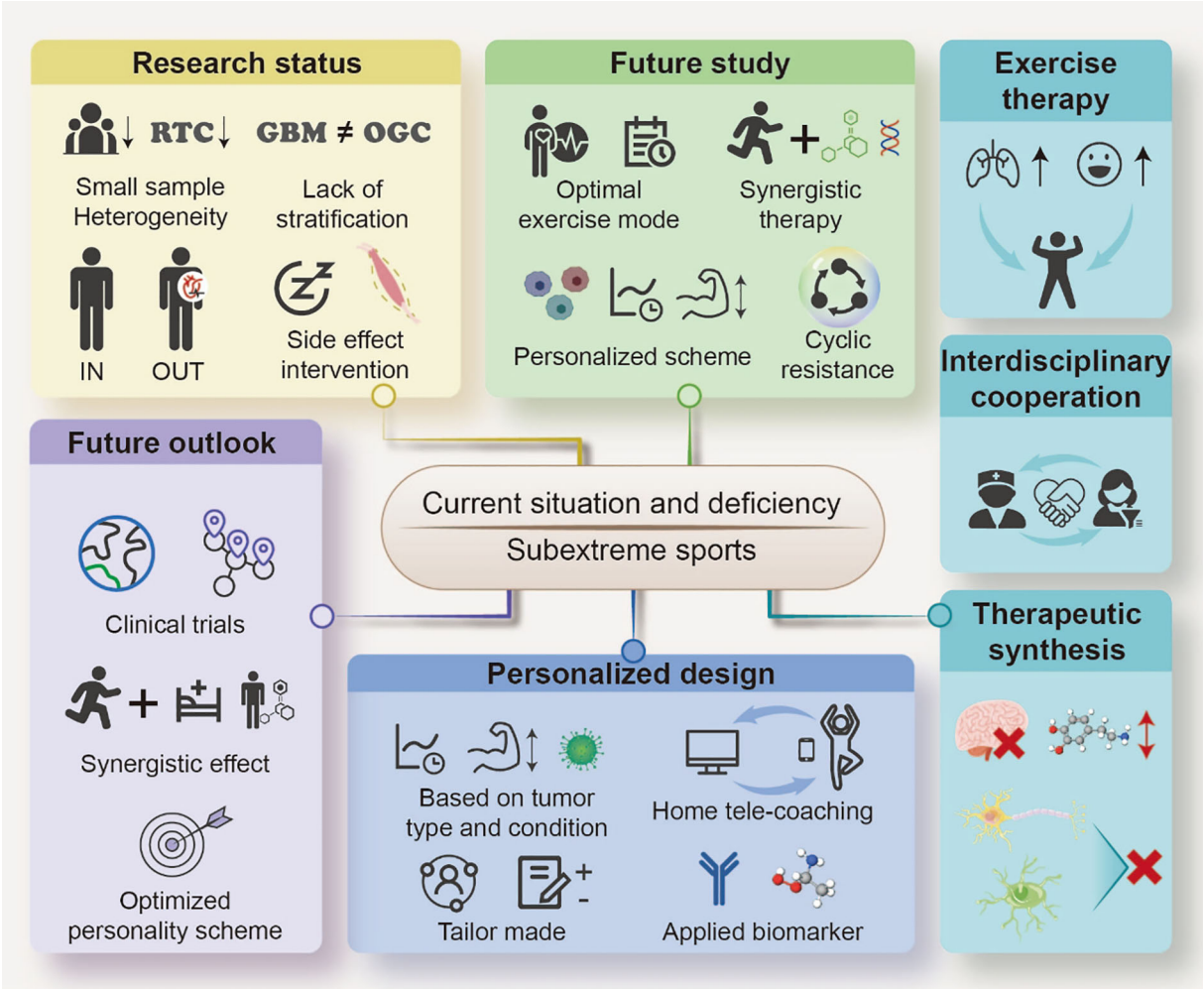

FIGURE 4
Current Situation, Deficiencies, and Future Directions of Exercise Therapy for Glioma Treatment. This figure summarizes the existing challenges, research status, and future perspectives of exercise therapy as an adjunctive treatment for gliomas. The current situation and deficiencies highlight the need to refine exercise-based interventions for cancer care. The research status section outlines key limitations, including small sample sizes, heterogeneity, lack of stratification between GBM and other glioma cancers (OGC), and the necessity for intervention for side effects. The future study section emphasizes the need to optimize exercise modes, implement synergistic therapy, and utilize cyclic resistance training, with a focus on personalized treatment schemes. The future outlook discusses the potential of clinical trials, synergistic effects of exercise and therapy, and development of optimized personality schemes for patient-centered care. The personalized design section highlights the importance of tailoring exercise regimens based on tumor type and patient condition, incorporating home tele-coaching, and applying biomarkers to improve the treatment efficacy. Furthermore, exercise therapy is linked to interdisciplinary cooperation and therapeutic synthesis, advocating integrated strategies that enhance patient outcomes and mitigate treatment-related side effects. This framework underscores the necessity for continued research and clinical application of exercise-based interventions for glioma management.

strength in brain tumor patients are often affected during treatment. However, exercise intervention studies for this group are still less abundant compared to other cancer populations (Ballard-Barbash et al., 2012; Singh et al., 2013; Buffart et al., 2014) (192). The heterogeneity of these studies is primarily manifested in differences in research methods and data collection, including the absence of systematic randomized controlled trials (RCTs).

6.1.2 Lack of stratified research on different tumor subtypes

There has been insufficient comparative research on the effects of exercise interventions in patients with different types of brain tumors, particularly low-grade and high-grade gliomas (226). Each tumor type has distinct biological characteristics; therefore, there may be significant differences in the effects of exercise interventions (227). However, most current studies do not conduct stratified analyses by tumor subtype or offer detailed intervention strategies or effect comparisons. For example, patients with glioblastoma (GBM) may have different exercise tolerance and outcomes compared to patients with oligodendrogliomas; however, this aspect has not been fully explored in the existing literature.

6.1.3 Limitations in research methods

Most current research on exercise interventions for brain tumor survivors is observational, with small sample sizes and relatively high attrition rates (228). Since patients with brain tumors often

have comorbidities (e.g., heart disease, neurological deficits), these patients are often excluded from studies, leading to recruitment bias (229). This bias is particularly significant in patients with brain cancer, as only those in relatively good health are likely to participate in exercise intervention studies.

6.1.4 Recruitment and retention issues in exercise interventions

Despite the potential benefits of exercise interventions, recruitment and retention remain major challenges in brain tumor research (228). Since brain tumor treatment often involves multiple side effects (e.g., fatigue, cognitive impairment, and muscle wasting), these side effects may affect patients' willingness to participate and their adherence to interventions (230). This makes it more complex to conduct exercise intervention studies and difficult to generalize the findings to a broader patient population.

6.2 Future research directions

6.2.1 Investigating the optimal type, intensity, and frequency of exercise

Future research should further explore the effects of different types of exercise interventions (e.g., aerobic exercise, resistance training) and the optimal intensity and frequency for patients with brain tumors, particularly those with high-grade gliomas. Although existing studies have shown the benefits of aerobic and resistance training for individuals with cancer, most of these studies have focused on other cancer populations, and the specific needs and intervention effects for individuals with brain tumors have not been thoroughly studied (192). Therefore, future studies should systematically analyze the specific effects of different exercise programs on patients with brain tumors and identify the most suitable exercise types and intervention intensities.

6.2.2 In-depth study on the synergistic effects of exercise and emerging therapies

Emerging therapies, such as immunotherapy and gene therapy, have become important directions in glioma treatment (231). Future research should investigate the synergistic effects of exercise in combination with these emerging therapies. Novel targeted therapeutic strategies are emerging as potential game-changers, offering the dual benefits of enhanced treatment efficacy and minimized side effects while advancing precision medicine frontiers (232). It is worth exploring whether exercise can enhance the effects of immunotherapy or gene therapy or whether it can alleviate the side effects of these treatments (91). Research on this synergistic effect could lead to more personalized and comprehensive treatment plans for patients (233, 234).

6.2.3 Development of personalized exercise intervention programs

Given the significant differences in pathology, treatment responses, and side effects among patients with brain tumors, future research should focus on developing personalized exercise intervention programs (154). Studies have tailored exercise regimens to individual patients based on factors such as cancer type, treatment stage, and physical fitness level (235). Personalized interventions not only increase patient adherence but also maximize the effectiveness of exercise in improving functional capacity, reducing fatigue, and enhancing quality of life (236).

6.2.4 Verifying the effectiveness of circuit resistance training for glioblastoma patients

Existing research has shown that personalized circuit resistance training can improve functional fitness in patients with cancer and may help mitigate steroid-induced myopathy (237). Studies on patients with glioblastoma have also indicated that personalized exercise interventions can effectively enhance physical fitness and overall quality of life (192, 204). Future studies should further verify these findings and explore the applicability and effectiveness of circuit resistance training in patients with different types of brain tumors. Future research should also consider factors such as patients' lifestyle, disease activity, and the feasibility of exercise interventions.

7 Exploring the safety and efficacy of submaximal exercise for glioma patients

Submaximal exercise refers to physical activities that do not exceed a patient's maximum heart rate but effectively activate cardiovascular function and muscle strength (238). A program named ActiNO has demonstrated that submaximal exercise is both safe and effective in patients with glioma (239). Future research should focus on exploring the long-term effects of this exercise regimen, particularly its potential to extend survival and improve quality of life. These studies could help in the development of more targeted exercise programs tailored to patients with brain tumors.

Enhancing Quality of Life——To achieve this, exercise therapy should be incorporated into the comprehensive treatment plan for glioma, becoming a routine part of care.

7.1 Incorporating exercise therapy into glioma comprehensive treatment guidelines

Currently, the primary treatments for gliomas rely on surgery, radiotherapy, and chemotherapy (240). However, these therapies often come with significant side effects, such as cognitive decline, fatigue, and motor dysfunction, which severely affect the patient's daily life and quality of life (41). Therefore, including exercise therapy in the treatment guidelines is crucial for improving recovery outcomes. Studies have found that exercise not only alleviates fatigue but also enhances muscle strength, boosts cardiovascular endurance, and improves cognitive function, all of which contribute to better overall health (241).

7.2 Multidisciplinary team collaboration

Treatment for patients with glioma requires a multidisciplinary team, typically consisting of oncologists, rehabilitation specialists, exercise medicine experts, nutritionists, and psychologists. This collaborative approach ensures comprehensive treatment, addressing the patient's physical, psychological, and social recovery needs (242). Based on the patient's specific requirements, the team can create personalized treatment plans and adjust them according to the patient's responses. This integrated treatment model allows patients to effectively cope with the side effects of tumor treatment while improving their quality of life and functional independence during the process (243).

7.3 Enhancing the comprehensiveness of rehabilitation treatment

Patients with glioma often experience a variety of sequelae, such as cognitive impairments, fatigue, and visual perception changes, which severely impact their quality of life (214). A more comprehensive rehabilitation model is urgently needed to address these issues. Patient recovery should not be limited to directly addressing the effects of tumor treatment but should also consider interventions for various complications, including cognitive impairment, emotional fluctuations, and motor dysfunction (244, 245). With a more refined rehabilitation model, it is possible to effectively slow the functional decline of patients and help them regain the ability to perform daily activities. The advantages of multidisciplinary collaboration lie in the ability to jointly assess and intervene, continuously identifying and addressing functional limitations (246).

Research has shown that early multidisciplinary rehabilitation interventions can significantly reduce disability rates and improve daily living abilities in patients with glioma. For example, in a study involving patients with brain tumors, after 12 weeks of rehabilitation intervention, patients showed significant improvements in physical function scores, cognitive function, and social functioning ($P < 0.0001$) (247). This demonstrates the effectiveness of early multidisciplinary rehabilitation in reducing symptoms and improving the quality of life.

7.4 Personalized program design

7.4.1 Exercise interventions based on tumor type and disease status

Each patient with glioma has unique circumstances, including disease stage, physical condition, treatment responses, and side effects. Therefore, exercise interventions must be personalized to suit individuals. This involves selecting the appropriate types of exercise (such as aerobic exercise and resistance training), intensity, and frequency, as well as considering the patient's disease stage, functional level, and the toxicity of their treatments. For example, some patients may experience significant physical decline due to the tumor or treatment side effects, whereas others may have better physical capacity and tolerate higher-intensity interventions. Personalized exercise prescriptions can ensure that patients maximize the benefits of exercise while ensuring safety (248).

7.4.2 Feasibility of home-based remote exercise interventions

A pilot study involving patients with glioma explored the feasibility of home-based remote exercise interventions (222). The study, designed as a randomized controlled trial (RCT), involved stable grade II and III glioma patients who underwent a six-month intervention. The patients exercised at home three times per week, with the intensity set at 60%-85% of their maximum heart rate. Heart rate monitors were worn by the patients, and data were monitored and feedback was provided through an online platform. The results of this study showed that home-based remote interventions were feasible for a small group of willing participants and could significantly improve cardiovascular function, physical activity, and body mass index. This further supports the need for large-scale exercise intervention trials in patients with glioma.

7.4.3 Tailored exercise prescriptions

Patients with glioma often experience fluctuating disease stages and various side effects from treatment; therefore, exercise interventions need to be flexibly adjusted based on individual conditions (199). Exercise prescriptions should be designed according to factors such as the patient's physical condition, treatment toxicity, and disease progression. For example, some patients may be too weak post-treatment to engage in high-intensity exercise, whereas others may tolerate higher exercise volumes. Tailored exercise prescriptions can maximize physical strength and quality of life and minimize the risk of injury or adverse reactions associated with exercise.

7.4.4 Application of biomarkers in exercise interventions

To monitor the effects of exercise interventions more precisely, future research should develop biomarkers to evaluate the therapeutic impact of exercise. These biomarkers reflect the physiological state, immune function, and other health indicators influenced by exercise, providing objective data support (249). For example, certain immune system biomarkers or blood metabolic products may partially reflect the physiological regulation induced by exercise (250). Thus, combining biomarker monitoring with exercise could help assess the short-term effects and predict the long-term outcomes of interventions (53).

7.5 Challenges in exercise adherence

Although exercise interventions offer significant benefits for patients with glioma, adherence to exercise programs remains a major challenge. Several factors contribute to low adherence rates, including physical limitations, psychological distress, and lack of motivation owing to the severity of the disease. Patients often experience fatigue, pain, and cognitive impairment, which can hinder their ability to engage in regular physical activity (197).

Additionally, psychological factors, such as depression, anxiety, and fear of treatment side effects, can negatively affect adherence to exercise protocols (198).

To address these challenges, solutions must focus on enhancing patient motivation and providing support to overcome physical and emotional barriers. For instance, interventions involving regular monitoring, personalized support, and motivational strategies, such as goal-setting or feedback mechanisms, have been shown to improve adherence in cancer populations (199). Implementing supervised exercise sessions or combining physical activity with psychological support (e.g., counseling or group exercises) may also increase participation rates. Additionally, the use of digital platforms, such as mobile apps or online exercise programs, could offer more flexible and accessible ways to support exercise adherence in patients with gliomas (200).

Moreover, clinicians should emphasize the importance of exercise as an integral part of the treatment regimen and address any concerns that patients may have regarding safety and feasibility. Educating patients on the benefits of exercise for symptom management and improving their quality of life can help reduce their resistance to participating in exercise interventions. By addressing these barriers, exercise interventions can become a more effective and sustainable adjunctive therapy for patients with glioma.

7.6 Future research directions and challenges

7.6.1 Large-scale, multicenter clinical trials

Owing to the low incidence of brain cancer, single-center studies may struggle to recruit sufficient patient samples. Therefore, large-scale, multicenter international cooperative trials are needed to ensure that the findings are statistically significant and applicable across diverse populations (251). These studies will help validate the effectiveness of exercise interventions in patients with different types of brain tumors.

7.6.2 Further exploration of the synergistic effects between exercise and other treatments

Although research has shown that exercise can improve physical function and quality of life in patients with glioma, the synergistic effects of exercise with other treatments (such as radiotherapy, chemotherapy, and immunotherapy) require further investigation (154, 252). Exploring these interactions could provide more comprehensive treatment strategies, thereby improving the overall treatment efficacy.

7.6.3 Optimization and application of personalized exercise programs

With the development of precision medicine, personalized exercise interventions have become a key component of glioma treatment (253). Future research should focus on optimizing exercise prescriptions and developing more refined and individualized exercise plans. In particular, in the rehabilitation of patients with brain tumors, precise interventions based on functional status, treatment responses, and lifestyle will be an important direction for future research (254, 255).

8 Conclusion

Gliomas, particularly glioblastoma multiforme (GBM), are highly aggressive brain tumors that present numerous treatment challenges. Although current therapies, such as radiotherapy, chemotherapy, and targeted treatment, have extended patient survival to some extent, these therapies have limited efficacy and are often accompanied by significant side effects. The biological characteristics of gliomas, including blood-brain barrier permeability, tumor cell heterogeneity, and an immunosuppressive microenvironment, make treatment even more difficult. Moreover, glioblastoma often leads to long-term side effects, such as cognitive dysfunction and neurological decline, which greatly affect the patients' quality of life. As the incidence of glioma rises globally, particularly with age, improving patients' quality of life and prolonging survival have become important issues in brain tumor research. In this context, exercise as an adjunctive treatment has gained increasing attention. Exercise not only helps improve physical function and cognitive abilities but may also enhance the patient's antitumor capacity by regulating the immune system and suppressing inflammation (16–18). Studies have shown that appropriate exercise can significantly reduce the mortality risk in patients with brain cancer and positively influence glioma treatment outcomes.

Exercise interventions in glioma treatment work through several key mechanisms. Firstly, exercise boosts the immune system by activating NK cells and T cells, enhancing immune surveillance and aiding in tumor cell elimination. Secondly, it reduces inflammation in the tumor microenvironment by lowering pro-inflammatory cytokines, helping to slow glioma growth and spread. Additionally, exercise improves blood-brain barrier permeability, increasing the delivery and effectiveness of anti-tumor drugs. Exercise-induced factors, like irisin, may also inhibit tumor cell growth and invasion. Studies show that combining exercise with drug therapies, such as chemotherapy and immunotherapy, improves drug efficacy, reduces side effects, and enhances patients' quality of life. Though the precise mechanisms are not fully clear, early evidence highlights exercise as a promising adjunctive treatment, with potential to improve survival and prognosis in glioma patients. Further research could solidify its role in future clinical glioma management.

Author contributions

GW: Conceptualization, Data curation, Formal analysis, Investigation, Methodology, Resources, Software, Visualization, Writing – original draft, Writing – review & editing. YC: Conceptualization, Data curation, Formal analysis, Investigation, Methodology, Software, Supervision, Visualization, Writing – original draft, Writing – review & editing. CC: Conceptualization, Formal analysis, Investigation, Methodology, Software, Writing – original draft, Writing – review & editing. JL: Conceptualization, Data

curation, Formal analysis, Investigation, Validation, Writing – original draft, Writing – review & editing. QW: Conceptualization, Investigation, Methodology, Writing – original draft, Writing – review & editing. YZ: Conceptualization, Formal analysis, Investigation, Supervision, Writing – original draft, Writing – review & editing. RC: Formal analysis, Resources, Validation, Writing – original draft, Writing – review & editing. JX: Data curation, Formal analysis, Methodology, Validation, Writing – original draft, Writing – review & editing. YS: Formal analysis, Investigation, Software, Writing – original draft, Writing – review & editing. HS: Conceptualization, Data curation, Formal analysis, Software, Writing – original draft, Writing – review & editing. CY: Formal analysis, Investigation, Project administration, Writing – original draft, Writing – review & editing. MW: Methodology, Software, Writing – original draft, Writing – review & editing. YO: Formal analysis, Resources, Writing – original draft, Writing – review & editing. AJ: Data curation, Formal analysis, Writing – original draft, Writing – review & editing. ZC: Data curation, Supervision, Writing – original draft, Writing – review & editing. XY: Investigation, Software, Writing – original draft, Writing – review & editing. CS: Formal analysis, Methodology, Writing – original draft, Writing – review & editing. XL: Investigation, Supervision, Writing – original draft, Writing – review & editing. AR: Formal analysis, Validation, Writing – original draft, Writing – review & editing. ML: Conceptualization, Data curation, Resources, Writing – original draft, Writing – review & editing. JS: Conceptualization, Investigation, Validation, Writing – original draft, Writing – review & editing.

Funding

The author(s) declare that financial support was received for the research and/or publication of this article. This research was funded by the National Scholarship for Studying Abroad (202306100231) and the 2024 Research Project of Ningde Normal University (Project No. 000059091501).

Conflict of interest

The authors declare that the research was conducted in the absence of any commercial or financial relationships that could be construed as a potential conflict of interest.

Generative AI statement

The author(s) declare that Generative AI was used in the creation of this manuscript. We utilized ChatGPT-4.0 for language refinement to enhance the accuracy and fluency of the paper's expression. This tool was solely employed for grammatical corrections and language optimization, and it did not partake in the writing of academic content such as research design, data analysis, or interpretation of results. Therefore, the use of this tool aligns with academic ethical standards and does not compromise the independence and authenticity of the research.

Publisher's note

References

1. Davis M. Glioblastoma: overview of disease and treatment. *CJON*. (2016) 20:S2–8. doi: 10.1188/16.CJON.S1.2-8

2. Yalamarty SSK, Filipczak N, Li X, Subhan MA, Parveen F, Ataide JA, et al. Mechanisms of resistance and current treatment options for glioblastoma multiforme (GBM). *Cancers*. (2023) 15:2116. doi: 10.3390/cancers15072116

3. Fernandes C, Costa A, Osório L, Lago RC, Linhares P, Carvalho B, et al. Current standards of care in glioblastoma therapy. *Exon Publications*. (2017), 197–241. doi: 10.15586/codon.glioblastoma.2017.ch11

4. Janjua TI, Rewatkar P, Ahmed-Cox A, Saeed I, Mansfeld FM, Kulshreshtha R, et al. Frontiers in the treatment of glioblastoma: Past, present and emerging. *Adv Drug Div Rev*. (2021) 171:108–38. doi: 10.1016/j.addr.2021.01.012

5. Alexander BM, Cloughesy TF. Adult glioblastoma. *JCO*. (2017) 35:2402–9. doi: 10.1200/JCO.2017.73.0119

6. Chelliah SS, Paul EAL, Kamarudin MNA, Parhar I. Challenges and perspectives of standard therapy and drug development in high-grade gliomas. *Mol*. (2021) 26:1169. doi: 10.3390/molecules26041169

7. Pellerino A, Franchino F, Soffietti R, Rudà R. Overview on current treatment standards in high-grade gliomas. *Q J Nucl Med Mol Imaging*. (2018) 62(3):225–38. doi: 10.23736/S1824-4785.18.03096-0

8. Gabel N, Altshuler DB, Brezzell A, Briceño EM, Boileau NR, Miklja Z, et al. Health related quality of life in adult low and high-grade glioma patients using the national institutes of health patient reported outcomes measurement information system (PROMIS) and neuro-QOL assessments. *Front Neurol*. (2019) 10:212. doi: 10.3389/fneur.2019.00212

9. Bates A, Gonzalez-Viana E, Cruickshank G, Roques T. Primary and metastatic brain tumours in adults: summary of NICE guidance. *BMJ*. (2018) 362:k2924. doi: 10.1136/bmj.k2924

10. Miller KD, Ostrom QT, Kruchko C, Patil N, Tihan T, Cioffi G, et al. Brain and other central nervous system tumor statistics, 2021. *CA A Cancer J Clin*. (2021) 71:381–406. doi: 10.3322/caac.21693

11. Thorbinson C, Kilday J-P. Childhood Malignant brain tumors: balancing the bench and bedside. *Cancers*. (2021) 13:6099. doi: 10.3390/cancers13236099

12. Zhang AS, Ostrom QT, Kruchko C, Rogers L, Peereboom DM, Barnholtz-Sloan JS. Complete prevalence of Malignant primary brain tumors registry data in the United States compared with other common cancers, 2010. *NEUONC*. (2016) 19(5):now252. doi: 10.1093/neuonc/now252

13. Noll K, King AL, Dirven L, Armstrong TS, Taphoorn MJB, Wefel JS. Neurocognition and health-related quality of life among patients with brain tumors. *Hematol/Oncol Clin North Am*. (2022) 36:269–82. doi: 10.1016/j.hoc.2021.08.011

14. Alemany M, Velasco R, Simó M, Bruna J. Late effects of cancer treatment: consequences for long-term brain cancer survivors. *Neuro-Oncol Pract*. (2021) 8:18–30. doi: 10.1093/nop/npaa039

15. Ostrom QT, Truitt G, Gittleman H, Brat DJ, Kruchko C, Wilson R, et al. Relative survival after diagnosis with a primary brain or other central nervous system tumor in

the National Program of Cancer Registries, 2004 to 2014. *Neuro-Oncol Pract*. (2020) 7:306–12. doi: 10.1093/nop/npz059

16. Chen Y, Chen X, Luo Z, Kang X, Ge Y, Wan R, et al. Exercise-induced reduction of IGF1R sumoylation attenuates neuroinflammation in APP/PS1 transgenic mice. *J Adv Res*. (2025) 69:279–97. doi: 10.1016/j.jare.2024.03.025

17. Chen Y, Huang L, Luo Z, Han D, Luo W, Wan R, et al. Pantothenate-encapsulated liposomes combined with exercise for effective inhibition of CRM1-mediated PKM2 translocation in Alzheimer's therapy. *J Controlled Rel*. (2024) 373:336–57. doi: 10.1016/j.jconrel.2024.07.010

18. Chen Y, Luo Z, Sun Y, Li F, Han Z, Qi B, et al. Exercise improves choroid plexus epithelial cells metabolism to prevent glial cell-associated neurodegeneration. *Front Pharmacol*. (2022) 13:1010785. doi: 10.3389/fphar.2022.1010785

19. Dittus KL, Gramling RE, Ades PA. Exercise interventions for individuals with advanced cancer: A systematic review. *Prev Med*. (2017) 104:124–32. doi: 10.1016/j.ypmed.2017.07.015

20. Tantillo E, Colistra A, Baroncelli L, Costa M, Caleo M, Vannini E. Voluntary physical exercise reduces motor dysfunction and hampers tumor cell proliferation in a mouse model of glioma. *IJERPH*. (2020) 17:5667. doi: 10.3390/ijerph17165667

21. Sharma B, Allison D, Tucker P, Mabbott D, Timmons BW. Exercise trials in pediatric brain tumor: A systematic review of randomized studies. *J Pediatr Hematol/Oncol*. (2021) 43:59–67. doi: 10.1097/MPH.0000000000001844

22. Wang Y, Song H, Yin Y, Feng L. Cancer survivors could get survival benefits from postdiagnosis physical activity: A meta-analysis. *Evidence-Based Complement. Altern Med*. (2019) 2019:1–10. doi: 10.1155/2019/1940903

23. Zhang W, Liu Y, Zhou J, Qiu T, Xie H, Pu Z. *Chicoric acid* advanced PAQR3 ubiquitination to ameliorate ferroptosis in diabetes nephropathy through the relieving of the interaction between PAQR3 and P110α pathway. *Clin Exp HTN*. (2024) 46:2326021. doi: 10.1080/10641963.2024.2326021

24. Xu W, Gao X, Luo H, Chen Y. FGF21 attenuates salt-sensitive hypertension via regulating HNF4α/ACE2 axis in the hypothalamic paraventricular nucleus of mice. *Clin Exp HTN*. (2024) 46:2361671. doi: 10.1080/10641963.2024.2361671

25. Liu X, Su Y, Liu J, Liu D, Yu C. Inhibition of Th17 cell differentiation by aerobic exercise improves vasodilatation in diabetic mice. *Clin Exp HTN*. (2024) 46:2373467. doi: 10.1080/10641963.2024.2373467

26. Campbell KL, Winters-Stone KM, Wiskemann J, May AM, Schwartz AL, Courneya KS, et al. Exercise guidelines for cancer survivors: consensus statement from international multidisciplinary roundtable. *Med Sci Sports Exercise*. (2019) 51:2375–90. doi: 10.1249/MSS.0000000000002116

27. DeCordova S, Shastri A, Tsolaki AG, Yasmin H, Klein L, Singh SK, et al. Molecular heterogeneity and immunosuppressive microenvironment in glioblastoma. *Front Immunol*. (2020) 11:1402. doi: 10.3389/fimmu.2020.01402

28. Nicholson JG, Fine HA. Diffuse glioma heterogeneity and its therapeutic implications. *Cancer Discov*. (2021) 11:575–90. doi: 10.1158/2159-8290.CD-20-1474

29. Uddin M, Mamun AA, Alghamdi BS, Tewari D, Jeandet P, Sarwar MdS, et al. Epigenetics of glioblastoma multiforme: From molecular mechanisms to therapeutic approaches. *Semin Cancer Biol*. (2022) 83:100–20. doi: 10.1016/j.semcancer.2020.12.015

30. Oprita A, Baloi S-C, Staicu G-A, Alexandru O, Tache DE, Danoiu S, et al. Updated insights on EGFR signaling pathways in glioma. *IJMS*. (2021) 22:587. doi: 10.3390/ijms22020587

31. Pandith AA, Qasim I, Zahoor W, Shah P, Bhat AR, Sanadhya D, et al. Concordant association validates MGMT methylation and protein expression as favorable prognostic factors in glioma patients on alkylating chemotherapy (Temozolomide). *Sci Rep*. (2018) 8:6704. doi: 10.1038/s41598-018-25169-2

32. Strickland M, Stoll EA. Metabolic reprogramming in glioma. *Front Cell Dev Biol*. (2017) 5:43. doi: 10.3389/fcell.2017.00043

33. Johar D, Elmehrath AO, Khalil RM, Elberry MH, Zaky S, Shalabi SA, et al. Protein networks linking Warburg and reverse Warburg effects to cancer cell metabolism. *BioFactors*. (2021) 47:713–28. doi: 10.1002/biof.1768

34. De La Cruz-López KG, Castro-Muñoz LJ, Reyes-Hernández DO, García-Carrancá A, Manzo-Merino J. Lactate in the regulation of tumor microenvironment and therapeutic approaches. *Front Oncol*. (2019) 9:1143. doi: 10.3389/fonc.2019.01143

35. Rafii S, Kandoussi S, Ghouzlani A, Naji O, Reddy KP, Ullah Sadiqi R, et al. Deciphering immune microenvironment and cell evasion mechanisms in human gliomas. *Front Oncol*. (2023) 13:1135430. doi: 10.3389/fonc.2023.1135430

36. Romani M, Pistillo MP, Carosio R, Morabito A, Banelli B. Immune checkpoints and innovative therapies in glioblastoma. *Front Oncol*. (2018) 8:464. doi: 10.3389/fonc.2018.00464

37. Grégoire H, Roncali L, Rousseau A, Chérel M, Delneste Y, Jeannin P, et al. Targeting tumor associated macrophages to overcome conventional treatment resistance in glioblastoma. *Front Pharmacol*. (2020) 11:368. doi: 10.3389/fphar.2020.00368

38. Ni G, Sun Y, Jia H, Xiahou Z, Li Y, Zhao F, et al. MAZ-mediated tumor progression and immune evasion in hormone receptor-positive breast cancer: Targeting tumor microenvironment and PCLAF+ subtype-specific therapy. *Trans Oncol*. (2025) 52:102280. doi: 10.1016/j.tranon.2025.102280

39. Fang J, Lin L, Cao Y, Tan J, Liang Y, Xiao X, et al. Targeting the CD24-siglec10 axis: a potential strategy for cancer immunotherapy. *BIOI*. (2024) 5(1):997. doi: 10.15212/bioi-2023-0022

40. Fu Q, Yang H, Huang J, Liu F, Fu Y, Saw PE, et al. The circHAS2/RPL23/MMP9 axis facilitates brain tumor metastasis. *BIOI*. (2024) 5(1):e999. doi: 10.15212/bioi-2023-0013

41. Zhang H, Wang R, Yu Y, Liu J, Luo T, Fan F. Glioblastoma treatment modalities besides surgery. *J Cancer*. (2019) 10:4793–806. doi: 10.7150/jca.32475

42. Witzmann K, Raschke F, Troost EGC. MR image changes of normal-appearing brain tissue after radiotherapy. *Cancers*. (2021) 13:1573. doi: 10.3390/cancers13071573

43. Brook I. Late side effects of radiation treatment for head and neck cancer. *Radiat Oncol J*. (2020) 38:84–92. doi: 10.3857/roj.2020.00213

44. Romesser PB, Cahlon O, Scher E, Zhou Y, Berry SL, Rybkin A, et al. Proton beam radiation therapy results in significantly reduced toxicity compared with intensity-modulated radiation therapy for head and neck tumors that require ipsilateral radiation. *Radiother Oncol*. (2016) 118:286–92. doi: 10.1016/j.radonc.2015.12.008

45. Singh N, Miner A, Hennis L, Mittal S. Mechanisms of temozolomide resistance in glioblastoma - a comprehensive review. *CDR*. (2020) 4(1):17. doi: 10.20517/cdr.2020.79

46. Woo Peter YM, Li Y, Chan Anna HY, Ng Stephanie CP, Loong Herbert HF, Chan Danny TM, et al. A multifaceted review of temozolomide resistance mechanisms in glioblastoma beyond O-6-methylguanine-DNA methyltransferase. *Glioma*. (2019) 2:68. doi: 10.4103/glioma.glioma_3_19

47. Lin L, Cai J, Jiang C. Recent advances in targeted therapy for glioma. *CMC*. (2017) 24(13):1365–81. doi: 10.2174/0929867323666161223150242

48. Du Y, Liu H. Exercise-induced modulation of miR-149-5p and MMP9 in LPS-triggered diabetic myoblast ER stress: licorice glycoside E as a potential therapeutic target. *Tradit Med Res*. (2024) 9:45. doi: 10.53388/TMR20230121002

49. Yao J-Y, Yang Y-L, Chen W-J, Fan H-Y. Exploring the therapeutic potential of Qi Teng Mai Ning recipe in ischemic stroke and vascular cognitive impairment. *Tradit Med Res*. (2024) 9:57. doi: 10.53388/TMR20240214001

50. Ramirez-Hernandez D, Lezama-Martinez D, Velazco-Bejarano B, Valencia-Hernandez I, Lopez-Sanchez P, Fonseca-Coronado S, et al. The beneficial effects of swimming training preconditioning on reducing vascular reactivity in chronic myocardial infarction: Independent of NO production. *J Renin Ang ALD Syst*. (2024) 25:14703203241294029. doi: 10.1177/14703203241294029

51. Wang H, Xu T, Huang Q, Jin W, Chen J. Immunotherapy for Malignant glioma: current status and future directions. *Trends Pharmacol Sci*. (2020) 41:123–38. doi: 10.1016/j.tips.2019.12.003

52. Miyazaki T, Ishikawa E, Sugii N, Matsuda M. Therapeutic strategies for overcoming immunotherapy resistance mediated by immunosuppressive factors of the glioblastoma microenvironment. *Cancers*. (2020) 12:1960. doi: 10.3390/cancers12071960

53. Qin S, Xie B, Wang Q, Yang R, Sun J, Hu C, et al. New insights into immune cells in cancer immunotherapy: from epigenetic modification, metabolic modulation to cell communication. *MedComm*. (2024) 5:e551. doi: 10.1002/mco2.551

54. Ou A, Yung WKA, Majd N. Molecular mechanisms of treatment resistance in glioblastoma. *IJMS*. (2020) 22:351. doi: 10.3390/ijms22010351

55. Li Y, Wang Z, Ajani JA, Song S. Drug resistance and Cancer stem cells. *Cell Commun Signal*. (2021) 19:19. doi: 10.1186/s12964-020-00627-5

56. Afshari AR, Sanati M, Aminyavari S, Shakeri F, Bibak B, Keshavarzi Z, et al. Advantages and drawbacks of dexamethasone in glioblastoma multiforme. *Crit Rev Oncol/Hematol*. (2022) 172:103625. doi: 10.1016/j.critrevonc.2022.103625

57. Thomas H, Timmermann B. Paediatric proton therapy. *Br J Radiol*. (2020) 93:20190601. doi: 10.1259/bjr.20190601

58. Chambrelant I, Eber J, Antoni D, Burckel H, Noël G, Auvergne R. Proton therapy and gliomas: A systematic review. *Radiation*. (2021) 1:218–33. doi: 10.3390/radiation1030019

59. Garg S, Williams NL, Ip A, Dicker AP. Clinical integration of digital solutions in health care: an overview of the current landscape of digital technologies in cancer care. *JCO Clin Cancer Inf*. (2018) 2(2):1–9. doi: 10.1200/CCI.17.00159

60. Chen C, Wu Z-H, Lu X-J, Shi J-L. *BRIP1* induced ferroptosis to inhibit glioma cells and was associated with increased oxidative stress. *Discov Med*. (2024) 36:2264. doi: 10.24976/Discov.Med.202436190.208

61. Rajendran A, Rajan RA, Balasubramaniyam S, Elumalai K. Nano delivery systems in stem cell therapy: Transforming regenerative medicine and overcoming clinical challenges. *Nano TransMed*. (2025) 4:100069. doi: 10.1016/j.ntm.2024.100069

62. Nascimento IJDS, De Aquino TM, Da Silva-Júnior EF. The new era of drug discovery: the power of computer-aided drugDesign (CADD). *LDDD*. (2022) 19:951–5. doi: 10.2174/1570180819666220405225817

63. Sui S, Tian Y, Wang X, Zeng C, Luo OJ, Li Y. Single-cell RNA sequencing gene signatures for classifying and scoring exhausted $CD8^+$ T cells in B-cell acute lymphoblastic leukaemia. *Cell Prolif*. (2024) 57:e13583. doi: 10.1111/cpr.13583

64. Sui S, Wei X, Zhu Y, Feng Q, Zha X, Mao L, et al. Single-cell multiomics reveals TCR clonotype-specific phenotype and stemness heterogeneity of T- ALL cells. *Cell Prolif*. (2024):e13786. doi: 10.1111/cpr.13786

65. Wang X, Wen D, Xia F, Fang M, Zheng J, You C, et al. Single-cell transcriptomics revealed white matter repair following subarachnoid hemorrhage. *Transl Stroke Res*. (2024), 1–17. doi: 10.1007/s12975-024-01265-6

66. Han D, Han Y, Guo W, Wei W, Yang S, Xiang J, et al. High-dimensional single-cell proteomics analysis of esophageal squamous cell carcinoma reveals dynamic alterations of the tumor immune microenvironment after neoadjuvant therapy. *J Immunother Cancer*. (2023) 11:e007847. doi: 10.1136/jitc-2023-007847

67. Komuro H, Shinohara S, Fukushima Y, Demachi-Okamura A, Muraoka D, Masago K, et al. Single-cell sequencing on $CD8^+$ TILs revealed the nature of exhausted T cells recognizing neoantigen and cancer/testis antigen in non-small cell lung cancer. *J Immunother Cancer*. (2023) 11:e007180. doi: 10.1136/jitc-2023-007180

68. Chauleau J-Y, Trassin M. Sensing multiferroic states non-invasively using optical second harmonic generation. *Microstructures*. (2024) 4(1):2024005. doi: 10.20517/microstructures.2023.50

69. Jang J, Choi S-Y. Reduced dimensional ferroelectric domains and their characterization techniques. *Microstruct*. (2024) 4(2). doi: 10.20517/microstructures.2023.67

70. Qin H, Ji Z, Zhao Q, Wang K, Mao F, Han H, et al. Contrast-enhanced ultrasound features of primary hepatic lymphoepithelioma-like carcinoma: comparison with hepatocellular carcinoma. *BIOI*. (2024) 5(1):996. doi: 10.15212/bioi-2023-0019

71. Wu M, Chen J, Kuang X, Chen Y, Wang Y, Huang L, et al. Sarcopenia-related traits, body mass index and ovarian cancer risk: investigation of causal relationships through multivariable mendelian randomization analyses. *BIOI*. (2024) 5(1):995. doi: 10.15212/bioi-2023-0020

72. Cui Y, Zhao K, Meng X, Mao Y, Han C, Shi Z, et al. A CT-based multitask deep learning model for predicting tumor stroma ratio and treatment outcomes in patients with colorectal cancer: a multicenter cohort study. *Int J Surg*. (2024) 110(7):2. doi: 10.1097/JS9.0000000000001161

73. Huang X, Wang Q, Xu W, Liu F, Pan L, Jiao H, et al. Machine learning to predict lymph node metastasis in T1 esophageal squamous cell carcinoma: a multicenter study. *Int J Surg*. (2024) 110:7852–9. doi: 10.1097/JS9.0000000000001694

74. Han X, Cai C, Deng W, Shi Y, Li L, Wang C, et al. Landscape of human organoids: Ideal model in clinics and research. *Innov*. (2024) 5:100620. doi: 10.1016/j.xinn.2024.100620

75. Atiku SM, Kasozi D, Campbell K. Single nucleotide variants (SNVs) of angiotensin-converting enzymes (ACE1 and ACE2): A plausible explanation for the global variation in COVID-19 prevalence. *J Renin Ang ALD Syst*. (2023) 2023:9668008. doi: 10.1155/2023/9668008

76. Karimi F, Maleki M, Movahedpour A, Alizadeh M, Kharazinejad E, Sabaghan M. Overview of the renin-angiotensin system in diabetic nephropathy. *J Renin Ang ALD Syst*. (2024) 25:14703203241302966. doi: 10.1177/14703203241302966

77. Rončević A, Koruga N, Soldo Koruga A, Rončević R, Rotim T, Šimundić T, et al. Personalized treatment of glioblastoma: current state and future perspective. *Biomed*. (2023) 11:1579. doi: 10.3390/biomedicines11061579

78. He M-X, Tahir AT, Waris S, Cheng W-B, Kang J. Network pharmacology analysis combined with experimental verification of the molecular mechanism of Xihuang pill in treating liver cancer. *Tradit. Med Res*. (2023) 8:33. doi: 10.53388/TMR20221221002

79. Chu C, Sun W, Chen S, Jia Y, Ni Y, Wang S, et al. Squid-inspired anti-salt skin-like elastomers with superhigh damage resistance for aquatic soft robots. *Adv Matls*. (2024) 36:2406480. doi: 10.1002/adma.202406480

80. Ni Y, Li B, Chu C, Wang S, Jia Y, Cao S, et al. One-step fabrication of ultrathin porous Janus membrane within seconds for waterproof and breathable electronic skin. *Sci Bull*. (2025) 70:712–21. doi: 10.1016/j.scib.2024.12.040

81. Tang Y, Tang R. Health neuroscience—How the brain/mind and body affect our health behavior and outcomes. *J Integr Neurosci*. (2024) 23:69. doi: 10.31083/j.jin2304069

82. Wu S, Fu Z, Wang S, Zheng F, Qiu W, Xu G, et al. Disrupted functional brain network architecture in sufferers with boxing-related repeated mild traumatic brain injury: A resting-state EEG study. *J Integr Neurosci*. (2024) 23:102. doi: 10.31083/j.jin2305102

83. Lin H, Zhou J, Ding T, Zhu Y, Wang L, Zhong T, et al. Therapeutic potential of extracellular vesicles from diverse sources in cancer treatment. *Eur J Med Res*. (2024) 29:350. doi: 10.1186/s40001-024-01937-x

84. Zhang X-M, Huang J, Ni X-Y, Zhu H-R, Huang Z-X, Ding S, et al. Current progression in application of extracellular vesicles in central nervous system diseases. *Eur J Med Res*. (2024) 29:15. doi: 10.1186/s40001-023-01606-5

85. Iyengar NM, Jones LW. Development of exercise as interception therapy for cancer: A review. *JAMA Oncol*. (2019) 5:1620. doi: 10.1001/jamaoncol.2019.2585

86. Wang Q, Zhou W. Roles and molecular mechanisms of physical exercise in cancer prevention and treatment. *J Sport Health Sci*. (2021) 10:201–10. doi: 10.1016/j.jshs.2020.07.008

87. Da Ros M, De Gregorio V, Iorio AL, Giunti L, Guidi M, De Martino M, et al. Glioblastoma chemoresistance: the double play by microenvironment and blood-brain barrier. *IJMS*. (2018) 19:2879. doi: 10.3390/ijms19102879

88. Ruiz-Casado A, Martín-Ruiz A, Pérez LM, Provencio M, Fiuza-Luces C, Lucia A. Exercise and the hallmarks of cancer. *Trends Cancer*. (2017) 3:423–41. doi: 10.1016/j.trecan.2017.04.007

89. Sitlinger A, Brander DM, Bartlett DB. Impact of exercise on the immune system and outcomes in hematologic Malignancies. *Blood Adv*. (2020) 4:1801–11. doi: 10.1182/bloodadvances.2019001317

90. Chong Y, Wu X, Wang Y, Gu Q, Zhang J, Meng X, et al. USP18 reduces the inflammatory response of LPS-induced SA-AKI by inhibiting the PI3K-AKT-NF-κB pathway and regulate apoptosis of cells. *J Renin Ang ALD Syst*. (2024) 25:14703203241265218. doi: 10.1177/14703203241265218

91. Zhu C, Ma H, He A, Li Y, He C, Xia Y. Exercise in cancer prevention and anticancer therapy: Efficacy, molecular mechanisms and clinical information. *Cancer Lett*. (2022) 544:215814. doi: 10.1016/j.canlet.2022.215814

92. Maskalenko NA, Zhigarev D, Campbell KS. Harnessing natural killer cells for cancer immunotherapy: dispatching the first responders. *Nat Rev Drug Discov*. (2022) 21:559–77. doi: 10.1038/s41573-022-00413-7

93. Idorn M, Hojman P. Exercise-dependent regulation of NK cells in cancer protection. *Trends Mol Med*. (2016) 22:565–77. doi: 10.1016/j.molmed.2016.05.007

94. Rundqvist H, Veliça P, Barbieri L, Gameiro PA, Bargiela D, Gojkovic M, et al. Cytotoxic T-cells mediate exercise-induced reductions in tumor growth. *eLife*. (2020) 9:e59996. doi: 10.7554/eLife.59996

95. Dorneles GP, Dos Passos AAZ, Romão PRT, Peres A. New insights about regulatory T cells distribution and function with exercise: the role of immunometabolism. *CPD*. (2020) 26:979–90. doi: 10.2174/1381612826666200305125210

96. Munn DH, Bronte V. Immune suppressive mechanisms in the tumor microenvironment. *Curr Opin Immunol*. (2016) 39:1–6. doi: 10.1016/j.coi.2015.10.009

97. Lyu D. Immunomodulatory effects of exercise in cancer prevention and adjuvant therapy: a narrative review. *Front Physiol*. (2024) 14:1292580. doi: 10.3389/fphys.2023.1292580

98. Hibino S, Kawazoe T, Kasahara H, Itoh S, Ishimoto T, Sakata-Yanagimoto M, et al. Inflammation-induced tumorigenesis and metastasis. *IJMS*. (2021) 22:5421. doi: 10.3390/ijms22115421

99. Shang G-S, Liu L, Qin Y-W. IL-6 and TNF-α promote metastasis of lung cancer by inducing epithelial-mesenchymal transition. *Oncol Lett*. (2017) 13:4657–60. doi: 10.3892/ol.2017.6048

100. Koelwyn GJ, Zhuang X, Tammela T, Schietinger A, Jones LW. Exercise and immunometabolic regulation in cancer. *Nat Metab*. (2020) 2:849–57. doi: 10.1038/s42255-020-00277-4

101. Spiliopoulou P, Gavriatopoulou M, Kastritis E, Dimopoulos M, Terzis G. Exercise-induced changes in tumor growth via tumor immunity. *Sports*. (2021) 9:46. doi: 10.3390/sports9040046

102. Cabral-Santos C, De Lima Junior EA, Fernandes IMDC, Pinto RZ, Rosa-Neto JC, Bishop NC, et al. Interleukin-10 responses from acute exercise in healthy subjects: A systematic review. *J Cell Physiol*. (2019) 234:9956–65. doi: 10.1002/jcp.27920

103. Rosa L, Teixeira A, Lira F, Tufik S, Mello M, Santos R. Moderate acute exercise (70% VO_2 peak) induces TGF -β, α-amylase and IgA in saliva during recovery. *Oral Dis*. (2014) 20:186–90. doi: 10.1111/odi.12088

104. Komai T, Inoue M, Okamura T, Morita K, Iwasaki Y, Sumitomo S, et al. Transforming growth factor-β and interleukin-10 synergistically regulate humoral immunity via modulating metabolic signals. *Front Immunol*. (2018) 9:1364. doi: 10.3389/fimmu.2018.01364

105. Daou HN. Exercise as an anti-inflammatory therapy for cancer cachexia: a focus on interleukin-6 regulation. *Am J Physiology-Regulatory Integr Comp Physiol*. (2020) 318:R296–310. doi: 10.1152/ajpregu.00147.2019

106. Hojman P, Gehl J, Christensen JF, Pedersen BK. Molecular mechanisms linking exercise to cancer prevention and treatment. *Cell Metab*. (2018) 27:10–21. doi: 10.1016/j.cmet.2017.09.015

107. Shalapour S, Karin M. Immunity, inflammation, and cancer: an eternal fight between good and evil. *J Clin Invest*. (2015) 125:3347–55. doi: 10.1172/JCI80007

108. Inthagard J, Edwards J, Roseweir AK. Immunotherapy: enhancing the efficacy of this promising therapeutic in multiple cancers. *Clin Sci*. (2019) 133:181–93. doi: 10.1042/CS20181003

109. Gustafson MP, Wheatley-Guy CM, Rosenthal AC, Gastineau DA, Katsanis E, Johnson BD, et al. Exercise and the immune system: taking steps to improve responses to cancer immunotherapy. *J Immunother Cancer*. (2021) 9:e001872. doi: 10.1136/jitc-2020-001872

110. Ashcraft KA, Warner AB, Jones LW, Dewhirst MW. Exercise as adjunct therapy in cancer. *Semin Radiat Oncol*. (2019) 29:16–24. doi: 10.1016/j.semradonc.2018.10.001

111. Michels N, Van Aart C, Morisse J, Mullee A, Huybrechts I. Chronic inflammation towards cancer incidence: A systematic review and meta-analysis of epidemiological studies. *Crit Rev Oncol/Hematol*. (2021) 157:103177. doi: 10.1016/j.critrevonc.2020.103177

112. Jurdana M. Physical activity and cancer risk. Actual knowledge and possible biological mechanisms. *Radiol Oncol*. (2021) 55:7–17. doi: 10.2478/raon-2020-0063

113. Yang L, Morielli AR, Heer E, Kirkham AA, Cheung WY, Usmani N, et al. Effects of exercise on cancer treatment efficacy: A systematic review of preclinical and clinical studies. *Cancer Res*. (2021) 81:4889–95. doi: 10.1158/0008-5472.CAN-21-1258

114. Holmen Olofsson G, Jensen AWP, Idorn M, Thor Straten P. Exercise oncology and immuno-oncology; A (Future) dynamic duo. *IJMS*. (2020) 21:3816. doi: 10.3390/ijms21113816

115. Idorn M, Thor Straten P. Exercise and cancer: from "healthy" to "therapeutic"? *Cancer Immunol Immunother*. (2017) 66:667–71. doi: 10.1007/s00262-017-1985-z

116. Schauer T, Mazzoni A-S, Henriksson A, Demmelmaier I, Berntsen S, Raastad T, et al. Exercise intensity and markers of inflammation during and after (neo-) adjuvant cancer treatment. *Endocrine-Related Cancer*. (2021) 28:191–201. doi: 10.1530/ERC-20-0507

117. Van Rooijen SJ, Engelen MA, Scheede-Bergdahl C, Carli F, Roumen RMH, Slooter GD, et al. Systematic review of exercise training in colorectal cancer patients during treatment. *Scand Med Sci Sports*. (2018) 28:360–70. doi: 10.1111/sms.12907

118. Zhang X, Ashcraft KA, Betof Warner A, Nair SK, Dewhirst MW. Can exercise-induced modulation of the tumor physiologic microenvironment improve antitumor immunity? *Cancer Res*. (2019) 79:2447–56. doi: 10.1158/0008-5472.CAN-18-2468

119. Alahmari A. Blood-brain barrier overview: structural and functional correlation. *Neural Plast*. (2021) 2021:1–10. doi: 10.1155/2021/6564585

120. Wang D, Wang C, Wang L, Chen Y. A comprehensive review in improving delivery of small-molecule chemotherapeutic agents overcoming the blood-brain/brain tumor barriers for glioblastoma treatment. *Drug Dlv*. (2019) 26:551–65. doi: 10.1080/10717544.2019.1616235

121. Mitusova K, Peltek OO, Karpov TE, Muslimov AR, Zyuzin MV, Timin AS. Overcoming the blood–brain barrier for the therapy of Malignant brain tumor: current status and prospects of drug delivery approaches. *J Nanobiotechnol*. (2022) 20:412. doi: 10.1186/s12951-022-01610-7

122. Markowicz-Piasecka M, Darłak P, Markiewicz A, Sikora J, Kumar Adla S, Bagina S, et al. Current approaches to facilitate improved drug delivery to the central nervous system. *Eur J Pharm BCS*. (2022) 181:249–62. doi: 10.1016/j.ejpb.2022.11.003

123. Małkiewicz MA, Szarmach A, Sabisz A, Cubała WJ, Szurowska E, Winklewski PJ. Blood-brain barrier permeability and physical exercise. *J NI*. (2019) 16:15. doi: 10.1186/s12974-019-1403-x

124. Iqbal I, Saqib F, Mubarak Z, Latif MF, Wahid M, Nasir B, et al. Alzheimer's disease and drug delivery across the blood–brain barrier: approaches and challenges. *Eur J Med Res*. (2024) 29:313. doi: 10.1186/s40001-024-01915-3

125. Lundy DJ, Lee K-J, Peng I-C, Hsu C-H, Lin J-H, Chen K-H, et al. Inducing a transient increase in blood–brain barrier permeability for improved liposomal drug therapy of glioblastoma multiforme. *ACS Nano*. (2019) 13:97–113. doi: 10.1021/acsnano.8b03785

126. Lin T-W, Tsai S-F, Kuo Y-M. Physical exercise enhances neuroplasticity and delays alzheimer's disease. *BPL*. (2018) 4:95–110. doi: 10.3233/BPL-180073

127. Nishijima T, Torres-Aleman I, Soya H. Exercise and cerebrovascular plasticity. *Prog Brain Res*. (2016) 225:243–68. doi: 10.1016/bs.pbr.2016.03.010

128. He Q, Liu J, Liang J, Liu X, Li W, Liu Z, et al. Towards improvements for penetrating the blood–brain barrier—Recent progress from a material and pharmaceutical perspective. *Cells*. (2018) 7:24. doi: 10.3390/cells7040024

129. Alghamri MS, McClellan BL, Hartlage CS, Haase S, Faisal SM, Thalla R, et al. Targeting neuroinflammation in brain cancer: uncovering mechanisms, pharmacological targets, and neuropharmaceutical developments. *Front Pharmacol*. (2021) 12:680021. doi: 10.3389/fphar.2021.680021

130. Martínez-Guardado I, Arboleya S, Grijota FJ, Kaliszewska A, Gueimonde M, Arias N. The therapeutic role of exercise and probiotics in stressful brain conditions. *IJMS*. (2022) 23:3610. doi: 10.3390/ijms23073610

131. Betof AS, Lascola CD, Weitzel D, Landon C, Scarbrough PM, Devi GR, et al. Modulation of murine breast tumor vascularity, hypoxia, and chemotherapeutic response by exercise. *J Natl Cancer Inst*. (2015) 107(5):djv040. doi: 10.1093/jnci/djv040

132. Pedersen L, Idorn M, Olofsson GH, Lauenborg B, Nookaew I, Hansen RH, et al. Voluntary running suppresses tumor growth through epinephrine- and IL-6-dependent NK cell mobilization and redistribution. *Cell Metab*. (2016) 23:554–62. doi: 10.1016/j.cmet.2016.01.011

133. Wang Z-G, Cheng Y, Yu X-C, Ye L-B, Xia Q-H, Johnson NR, et al. bFGF protects against blood-brain barrier damage through junction protein regulation via PI3K-akt-rac1 pathway following traumatic brain injury. *Mol Neurobiol*. (2016) 53:7298–311. doi: 10.1007/s12035-015-9583-6

134. Vega RB, Konhilas JP, Kelly DP, Leinwand LA. Molecular mechanisms underlying cardiac adaptation to exercise. *Cell Metab*. (2017) 25:1012–26. doi: 10.1016/j.cmet.2017.04.025

135. Da Rocha AL, Pinto AP, Kohama EB, Pauli JR, De Moura LP, Cintra DE, et al. The proinflammatory effects of chronic excessive exercise. *Cytokine*. (2019) 119:57–61. doi: 10.1016/j.cyto.2019.02.016

136. Lippi G, Mattiuzzi C, Sanchis-Gomar F. Updated overview on interplay between physical exercise, neurotrophins, and cognitive function in humans. *J Sport Health Sci*. (2020) 9:74–81. doi: 10.1016/j.jshs.2019.07.012

137. Ayotte SL, Harro CC. Effects of an individualized aerobic exercise program in individuals with a brain tumor undergoing inpatient rehabilitation: A feasibility study. *Rehabil Oncol*. (2017) 35:163–71. doi: 10.1097/01.REO.0000000000000069

138. Song Y, Hu C, Fu Y, Gao H. Modulating the blood–brain tumor barrier for improving drug delivery efficiency and efficacy. *VIEW*. (2022) 3:20200129. doi: 10.1002/VIW.20200129

139. Stout NL, Brown JC, Schwartz AL, Marshall TF, Campbell AM, Nekhlyudov L, et al. An exercise oncology clinical pathway: Screening and referral for personalized interventions. *Cancer*. (2020) 126:2750–8. doi: 10.1002/cncr.32860

140. Carmeliet P. VEGF as a key mediator of angiogenesis in cancer. *Oncol*. (2005) 69:4–10. doi: 10.1159/000088478

141. Teleanu RI, Chircov C, Grumezescu AM, Teleanu DM. Tumor angiogenesis and anti-angiogenic strategies for cancer treatment. *JCM*. (2019) 9:84. doi: 10.3390/jcm9010084

142. Hughes VS, Wiggins JM, Siemann DW. Tumor oxygenation and cancer therapy—then and now. *BJR*. (2018) 92(1093):20170955. doi: 10.1259/bjr.20170955

143. Stylianopoulos T, Munn LL, Jain RK. Reengineering the tumor vasculature: improving drug delivery and efficacy. *Trends Cancer*. (2018) 4:258–9. doi: 10.1016/j.trecan.2018.02.010

144. Esteves M, Monteiro MP, Duarte JA. Role of regular physical exercise in tumor vasculature: favorable modulator of tumor milieu. *Int J Sports Med*. (2021) 42:389–406. doi: 10.1055/a-1308-3476

145. Pedersen L, Christensen JF, Hojman P. Effects of exercise on tumor physiology and metabolism. *Cancer J*. (2015) 21:111–6. doi: 10.1097/PPO.0000000000000096

146. Wiggins JM, Opoku-Acheampong AB, Baumfalk DR, Siemann DW, Behnke BJ. Exercise and the tumor microenvironment: potential therapeutic implications. *Exercise Sport Sci Rev*. (2018) 46:56–64. doi: 10.1249/JES.0000000000000137

147. Giordo R, Wehbe Z, Paliogiannis P, Eid AH, Mangoni AA, Pintus G. Nano-targeting vascular remodeling in cancer: Recent developments and future directions. *Semin Cancer Biol*. (2022) 86:784–804. doi: 10.1016/j.semcancer.2022.03.001

148. Buss LA, Dachs GU. Effects of exercise on the tumour microenvironment. In: Birbrair A, editor. *Tumor microenvironment. Advances in experimental medicine and biology*. Springer International Publishing, Cham (2020). p. 31–51. doi: 10.1007/978-3-030-35727-6_3

149. Matuszewska K, Pereira M, Petrik D, Lawler J, Petrik J. Normalizing tumor vasculature to reduce hypoxia, enhance perfusion, and optimize therapy uptake. *Cancers*. (2021) 13:4444. doi: 10.3390/cancers13174444

150. SChadler KL, Thomas NJ, Galie PA, Bhang DH, Roby KC, Addai P, et al. Tumor vessel normalization after aerobic exercise enhances chemotherapeutic efficacy. *Oncotarget*. (2016) 7:65429–40. doi: 10.18632/oncotarget.11748

151. Treps L, Gavard J. L'angiogenèse tumorale: Quand l'arbre de vie tourne mal. *Med Sci (Paris)*. (2015) 31:989–95. doi: 10.1051/medsci/20153111013

152. Kwak S-E, Lee J-H, Zhang D, Song W. Angiogenesis: focusing on the effects of exercise in aging and cancer. *JENB*. (2018) 22:21–6. doi: 10.20463/jenb.2018.0020

153. Jiménez-Valerio G, Casanovas O. Angiogenesis and metabolism: entwined for therapy resistance. *Trends Cancer*. (2017) 3:10–8. doi: 10.1016/j.trecan.2016.11.007

154. Cormie P, Nowak AK, Chambers SK, Galvão DA, Newton RU. The potential role of exercise in neuro-oncology. *Front Oncol*. (2015) 5:85. doi: 10.3389/fonc.2015.00085

155. Van Der Leeden M, Huijsmans RJ, Geleijn E, De Rooij M, Konings IR, Buffart LM, et al. Tailoring exercise interventions to comorbidities and treatment-induced adverse effects in patients with early stage breast cancer undergoing chemotherapy: a framework to support clinical decisions. *Disability Rehabil*. (2018) 40:486–96. doi: 10.1080/09638288.2016.1260647

156. Piraux E, Caty G, Aboubakar Nana F, Reychler G. Effects of exercise therapy in cancer patients undergoing radiotherapy treatment: a narrative review. *SAGE Open Med*. (2020) 8:2050312120922657. doi: 10.1177/2050312120922657

157. Korta P, Pocheć E, Mazur-Biały A. Irisin as a multifunctional protein: implications for health and certain diseases. *Medicina*. (2019) 55:485. doi: 10.3390/medicina55080485

158. Arhire LI, Mihalache L, Covasa M. Irisin: A hope in understanding and managing obesity and metabolic syndrome. *Front Endocrinol*. (2019) 10:524. doi: 10.3389/fendo.2019.00524

159. Tsiani E, Tsakiridis N, Kouvelioti R, Jaglanian A, Klentrou P. Current evidence of the role of the myokine irisin in cancer. *Cancers*. (2021) 13:2628. doi: 10.3390/cancers13112628

160. Zhang D, Tan X, Tang N, Huang F, Chen Z, Shi G. Review of research on the role of irisin in tumor. *OTT*. (2020) 13:4423–30. doi: 10.2147/OTT.S245178

161. Huang C, Chang Y, Lee H, Wu J, Huang J, Chung Y, et al. Irisin, an exercise myokine, potently suppresses tumor proliferation, invasion, and growth in glioma. *FASEB J*. (2020) 34:9678–93. doi: 10.1096/fj.202000573RR

162. Zhang D, Zhang P, Li L, Tang N, Huang F, Kong X, et al. Irisin functions to inhibit Malignant growth of human pancreatic cancer cells via downregulation of the PI3K/AKT signaling pathway. *OTT*. (2019) 12:7243–9. doi: 10.2147/OTT.S214260

163. Abbas T, Dutta A. p21 in cancer: intricate networks and multiple activities. *Nat Rev Cancer*. (2009) 9:400–14. doi: 10.1038/nrc2657

164. Pinkowska A, Podhorska-Okołów M, Dzięgiel P, Nowińska K. The role of irisin in cancer disease. *Cells*. (2021) 10:1479. doi: 10.3390/cells10061479

165. Alshanqiti KH, Alomar SF, Alzoman N, Almomen A. Irisin induces apoptosis in metastatic prostate cancer cells and inhibits tumor growth *In Vivo*. *Cancers*. (2023) 15:4000. doi: 10.3390/cancers15154000

166. Ho M-Y, Wen M-S, Yeh J-K, Hsieh I-C, Chen C-C, Hsieh M-J, et al. Excessive irisin increases oxidative stress and apoptosis in murine heart. *Biochem Biophys Res Commun*. (2018) 503:2493–8. doi: 10.1016/j.bbrc.2018.07.005

167. Nakamura H, Takada K. Reactive oxygen species in cancer: Current findings and future directions. *Cancer Sci*. (2021) 112:3945–52. doi: 10.1111/cas.15068

168. Liu S, Du F, Li X, Wang M, Duan R, Zhang J, et al. Effects and underlying mechanisms of irisin on the proliferation and apoptosis of pancreatic β cells. *PLoS One*. (2017) 12:e0175498. doi: 10.1371/journal.pone.0175498

169. Damgaci S, Ibrahim-Hashim A, Enriquez-Navas PM, Pilon-Thomas S, Guvenis A, Gillies RJ. Hypoxia and acidosis: immune suppressors and therapeutic targets. *Immunol*. (2018) 154:354–62. doi: 10.1111/imm.12917

170. Sumsuzzman D, Jin Y, Choi J, Yu J-H, TH L, Hong Y. Pathophysiological role of endogenous irisin against tumorigenesis and metastasis: Is it a potential biomarker and therapeutic? *Tumour Biol*. (2019) 41:101042831989279. doi: 10.1177/1010428319892790

171. Liu J, Huang Y, Liu Y, Chen Y. Irisin enhances doxorubicin-induced cell apoptosis in pancreatic cancer by inhibiting the PI3K/AKT/NF-κB pathway. *Med Sci Monit*. (2019) 25:6085–96. doi: 10.12659/MSM.917625

172. Gannon NP, Vaughan RA, Garcia-Smith R, Bisoffi M, Trujillo KA. Effects of the exercise-inducible myokine irisin on Malignant and non-malignant breast epithelial cell behavior *in vitro*. *Intl J Cancer*. (2015) 136(4):E197–E202. doi: 10.1002/ijc.29142

173. Zhou Y, Chen X, Cao J, Gao H. Overcoming the biological barriers in the tumor microenvironment for improving drug delivery and efficacy. *J Mater Chem B*. (2020) 8:6765–81. doi: 10.1039/D0TB00649A

174. Dréan A, Goldwirt L, Verreault M, Canney M, Schmitt C, Guehennec J, et al. Blood-brain barrier, cytotoxic chemotherapies and glioblastoma. *Expert Rev Neurother*. (2016) 16:1285–300. doi: 10.1080/14737175.2016.1202761

175. Bei Y, Wang H, Liu Y, Su Z, Li X, Zhu Y, et al. Exercise-Induced miR-210 Promotes Cardiomyocyte Proliferation and Survival and Mediates Exercise-Induced Cardiac Protection against Ischemia/Reperfusion Injury. *Research*. (2024) 7:327. doi: 10.34133/research.0327

176. Maalouf G-E, El Khoury D. Exercise-induced irisin, the fat browning myokine, as a potential anticancer agent. *J Obes*. (2019) 2019:1–8. doi: 10.1155/2019/6561726

177. Chen Y, Fan Z, Luo Z, Kang X, Wan R, Li F, et al. Impacts of Nutlin-3a and exercise on murine double minute 2–enriched glioma treatment. *Neural Regen Res*. (2025) 20:1135–52. doi: 10.4103/NRR.NRR-D-23-00875

178. Vengoji R, Macha MA, Batra SK, Shonka NA. Natural products: a hope for glioblastoma patients. *Oncotarget*. (2018) 9:22194–219. doi: 10.18632/oncotarget.25175

179. Cormie P, Zopf EM, Zhang X, Schmitz KH. The impact of exercise on cancer mortality, recurrence, and treatment-related adverse effects. *Epidemiol Rev*. (2017) 39:71–92. doi: 10.1093/epirev/mxx007

180. Sandler CX, Matsuyama M, Jones TL, Bashford J, Langbecker D, Hayes SC. Physical activity and exercise in adults diagnosed with primary brain cancer: a systematic review. *J Neurooncol*. (2021) 153:1–14. doi: 10.1007/s11060-021-03745-3

181. Thomas R, Kenfield SA, Yanagisawa Y, Newton RU. Why exercise has a crucial role in cancer prevention, risk reduction and improved outcomes. *Br Med Bull*. (2021) 139:100–19. doi: 10.1093/bmb/ldab019

182. Lu L, Hu Y, Wang C, Jiang F, Wu C. Methylation and expression of the exercise-related TLR1 gene is associated with low grade glioma prognosis and outcome. *Front Mol Biosci*. (2021) 8:747933. doi: 10.3389/fmolb.2021.747933

183. Murasawa S, Kageyama K, Usutani M, Asari Y, Kinoshita N, Nakada Y, et al. Biochemical evaluation by confirmatory tests after unilateral adrenalectomy for primary aldosteronism. *J Renin Ang ALD Syst*. (2023) 2023:5732812. doi: 10.1155/2023/5732812

184. Luoyi H, Yan P, Qihong F. Relationship between angiotensin-converting enzyme insertion/deletion polymorphism and the risk of COVID-19: A meta-analysis. *J Renin Ang ALD Syst*. (2023) 2023:3431612. doi: 10.1155/2023/3431612

185. Park Y, Kang D, Sinn DH, Kim H, Hong YS, Cho J, et al. Effect of renin-angiotensin system inhibitor in incident cancer among chronic hepatitis B patients: An emulated target trial using a nationwide cohort. *J Renin Ang ALD Syst*. (2024) 25:14703203241294037. doi: 10.1177/14703203241294037

186. Sujkowski A, Hong L, Wessells RJ, Todi SV. The protective role of exercise against age-related neurodegeneration. *Ageing Res Rev*. (2022) 74:101543. doi: 10.1016/j.arr.2021.101543

187. Kroonen JS, Vertegaal ACO. Targeting SUMO signaling to wrestle cancer. *Trends Cancer*. (2021) 7:496–510. doi: 10.1016/j.trecan.2020.11.009

188. Lee W, Oh M, Kim JS, Sung M, Hong K, Kwak BJ, et al. Metabolic tumor burden as a prognostic indicator after neoadjuvant chemotherapy in pancreatic cancer. *Int J Surg*. (2024) 110:4074–82. doi: 10.1097/JS9.0000000000001389

189. Lu Y, Yao Y, Zhai S, Ni F, Wang J, Chen F, et al. The role of immune cell signatures in the pathogenesis of ovarian-related diseases: a causal inference based on Mendelian randomization. *Int J Surg*. (2024) 110:6541–50. doi: 10.1097/JS9.0000000000001814

190. Dauwan M, Begemann MJH, Slot MIE, Lee EHM, Scheltens P, Sommer IEC. Physical exercise improves quality of life, depressive symptoms, and cognition across chronic brain disorders: a transdiagnostic systematic review and meta-analysis of randomized controlled trials. *J Neurol*. (2021) 268:1222–46. doi: 10.1007/s00415-019-09493-9

191. Gerritsen JKW, Vincent AJPE. Exercise improves quality of life in patients with cancer: a systematic review and meta-analysis of randomised controlled trials. *Br J Sports Med*. (2016) 50:796–803. doi: 10.1136/bjsports-2015-094787

192. Levin GT, Greenwood KM, Singh F, Tsoi D, Newton RU. Exercise improves physical function and mental health of brain cancer survivors: two exploratory case studies. *Integr Cancer Ther*. (2016) 15:190–6. doi: 10.1177/1534735415600068

193. Szulc-Lerch KU, Timmons BW, Bouffet E, Laughlin S, De Medeiros CB, Skocic J, et al. Repairing the brain with physical exercise: Cortical thickness and brain volume increases in long-term pediatric brain tumor survivors in response to a structured exercise intervention. *NeuroImage Clin*. (2018) 18:972–85. doi: 10.1016/j.nicl.2018.02.021

194. Cox E, Bells S, Timmons BW, Laughlin S, Bouffet E, De Medeiros C, et al. A controlled clinical crossover trial of exercise training to improve cognition and neural communication in pediatric brain tumor survivors. *Clin Neurophysiol*. (2020) 131:1533–47. doi: 10.1016/j.clinph.2020.03.027

195. Vira P, Samuel SR, Amaravadi SK, Saxena PP, Rai Pv S, Kurian JR, et al. Role of physiotherapy in hospice care of patients with advanced cancer: A systematic review. *Am J Hosp Palliat Care*. (2021) 38:503–11. doi: 10.1177/1049909120951163

196. Heywood R, McCarthy AL, Skinner TL. Efficacy of exercise interventions in patients with advanced cancer: A systematic review. *Arch Phys Med Rehabil*. (2018) 99:2595–620. doi: 10.1016/j.apmr.2018.04.008

197. Doyle KL, Toepfer M, Bradfield AF, Noffke A, Ausderau KK, Andreae S, et al. Systematic review of exercise for caregiver–care recipient dyads: what is best for spousal caregivers—Exercising together or not at all? *Gerontol*. (2021) 61:e283–301. doi: 10.1093/geront/gnaa043

198. De Lazzari N, Niels T, Tewes M, Götte M. A systematic review of the safety, feasibility and benefits of exercise for patients with advanced cancer. *Cancers*. (2021) 13:4478. doi: 10.3390/cancers13174478

199. Hansen A, Søgaard K, Minet LR. Development of an exercise intervention as part of rehabilitation in a glioblastoma multiforme survivor during irradiation treatment: a case report. *Disability Rehabil*. (2019) 41:1608–14. doi: 10.1080/09638288.2018.1432707

200. Sweegers MG, Altenburg TM, Chinapaw MJ, Kalter J, Verdonck-de Leeuw IM, Courneya KS, et al. Which exercise prescriptions improve quality of life and physical function in patients with cancer during and following treatment? A systematic review and meta-analysis of randomised controlled trials. *Br J Sports Med*. (2018) 52:505–13. doi: 10.1136/bjsports-2017-097891

201. Gehring K, Stuiver MM, Visser E, Kloek C, Van Den Bent M, Hanse M, et al. A pilot randomized controlled trial of exercise to improve cognitive performance in patients with stable glioma: a proof of concept. *Neuro-Oncol*. (2020) 22:103–15. doi: 10.1093/neuonc/noz178

202. Singh GK, Varghese L, Menon N, Dale O, Patil VM. Cancer-related fatigue and its impact on quality of life in patients with central nervous system tumors: A cross-sectional analysis. *Cancer Res Stats Treat*. (2021) 4:44–9. doi: 10.4103/crst.crst_364_20

203. Scott K, Posmontier B. Exercise interventions to reduce cancer-related fatigue and improve health-related quality of life in cancer patients. *Holist Nurs Pract*. (2017) 31:66–79. doi: 10.1097/HNP.0000000000000194

204. Spencer J, Staffileno B. Exercise intervention: A pilot study to assess the feasibility and impact on cancer-related fatigue and quality of life among patients with high-grade glioma. *CJON*. (2021) 25:194–200. doi: 10.1188/21.CJON.194-200

205. Wu N, Zhang X, Fang C, Zhu M, Wang Z, Jian L, et al. Progesterone enhances niraparib efficacy in ovarian cancer by promoting palmitoleic-acid-mediated ferroptosis. *Research*. (2024) 7:371. doi: 10.34133/research.0371

206. Jing G, Li Y, Sun F, Liu Q, Du A, Wang H, et al. Near-infrared light-activatable upconversion nanoparticle/curcumin hybrid nanodrug: a potent strategy to induce the differentiation and elimination of glioma stem cells. *Adv Compos Hybrid Mater*. (2024) 7:82. doi: 10.1007/s42114-024-00886-7

207. Zhang Q-Y, Wang F-X, Jia K-K, Kong L-D. Natural product interventions for chemotherapy and radiotherapy-induced side effects. *Front Pharmacol*. (2018) 9:1253. doi: 10.3389/fphar.2018.01253

208. Kleckner IR, Dunne RF, Asare M, Cole C, Fleming F, Fung C, et al. Exercise for toxicity management in cancer—A narrative review. *Oncol Hematol Rev (US)*. (2018) 14:28. doi: 10.17925/OHR.2018.14.1.28

209. Tan J, Peeraphong L, Ruchawapol C, Zhang J, Zhao J, Fu W, et al. Emerging role of HJURP as a therapeutic target in cancers. *Acta Matls Med*. (2023) 2(2):157–71. doi: 10.15212/AMM-2023-0008

210. Wang Z, Liu Z, Qu J, Sun Y, Zhou W. Role of natural products in tumor therapy from basic research and clinical perspectives. *Acta Matls Med*. (2024) 3(2):163–206. doi: 10.15212/AMM-2023-0050

211. Dolezal BA, Neufeld EV, Boland DM, Martin JL, Cooper CB. Interrelationship between sleep and exercise: A systematic review. *Adv Prev Med*. (2017) 2017:1–14. doi: 10.1155/2017/1364387

212. Armstrong TS, Ying Y, Wu J, Acquaye AA, Vera-Bolanos E, Gilbert MR, et al. The relationship between corticosteroids and symptoms in patients with primary brain

tumors: utility of the Dexamethasone Symptom Questionnaire–Chronic. *Neuro Oncol*. (2015) 17:1114–20. doi: 10.1093/neuonc/nov054

213. Lee J. The effects of resistance training on muscular strength and hypertrophy in elderly cancer patients: A systematic review and meta-analysis. *J Sport Health Sci*. (2022) 11:194–201. doi: 10.1016/j.jshs.2021.02.002

214. Allen DH, Loughan AR. Impact of cognitive impairment in patients with gliomas. *Semin Oncol Nurs*. (2018) 34:528–46. doi: 10.1016/j.soncn.2018.10.010

215. Narayanasetti Pt N, Thomas Pt A. Exercise and neural plasticity-A review study. *J Neurol Neurosci*. (2017) 08(05). doi: 10.21767/2171-6625.1000216

216. Mishra SI, Scherer RW, Snyder C, Geigle P, Gotay C. The effectiveness of exercise interventions for improving health-related quality of life from diagnosis through active cancer treatment. *Oncol Nurs Forum*. (2015) 42:E33–53. doi: 10.1188/15.ONF.E33-E53

217. Jonasson LS, Nyberg L, Kramer AF, Lundquist A, Riklund K, Boraxbekk C-J. Aerobic exercise intervention, cognitive performance, and brain structure: results from the physical influences on brain in aging (PHIBRA) study. *Front Aging Neurosci*. (2017) 8:336. doi: 10.3389/fnagi.2016.00336

218. Levin O, Netz Y, Ziv G. The beneficial effects of different types of exercise interventions on motor and cognitive functions in older age: a systematic review. *Eur Rev Aging Phys Act*. (2017) 14:20. doi: 10.1186/s11556-017-0189-z

219. Vanderbeek AM, Rahman R, Fell G, Ventz S, Chen T, Redd R, et al. The clinical trials landscape for glioblastoma: is it adequate to develop new treatments? *Neuro-Oncol*. (2018) 20:1034–43. doi: 10.1093/neuonc/noy027

220. Wang X, Cai Z, Jiang W, Fang Y, Sun W, Wang X. Systematic review and meta-analysis of the effects of exercise on depression in adolescents. *Child Adolesc Psychiatry Ment Health*. (2022) 16:16. doi: 10.1186/s13034-022-00453-2

221. Wegner M, Helmich I, MaChado S, Nardi A, Arias-Carrion O, Budde H. Effects of exercise on anxiety and depression disorders: review of meta- analyses and neurobiological mechanisms. *CNSNDDT*. (2014) 13:1002–14. doi: 10.2174/1871527313666140612102841

222. Gehring K, Kloek CJ, Aaronson NK, Janssen KW, Jones LW, Sitskoorn MM, et al. Feasibility of a home-based exercise intervention with remote guidance for patients with stable grade II and III gliomas: a pilot randomized controlled trial. *Clin Rehabil*. (2018) 32:352–66. doi: 10.1177/0269215517728326

223. Cordier D, Gerber M, Brand S. Effects of two types of exercise training on psychological well-being, sleep, quality of life and physical fitness in patients with high-grade glioma (WHO III and IV): study protocol for a randomized controlled trial. *Cancer Commun*. (2019) 39:1–10. doi: 10.1186/s40880-019-0390-8

224. Abdelaziz GN, Ramzy GM, Fayed LH, Ahmed SM, Ahmed MG. The effect of physical therapy rehabilitation on fatigue and pain in female patients with fibromyalgia. *Sportk*. (2024) 34. doi: 10.6018/sportk.581811

225. Mahindru A, Patil P, Agrawal V. Role of physical activity on mental health and well-being: A review. *Cureus*. (2023) 15(1):7. doi: 10.7759/cureus.33475

226. Miklja Z, Gabel N, Altshuler D, Wang L, Hervey-Jumper SL, Smith S. Exercise improves health-related quality of life sleep and fatigue domains in adult high- and low-grade glioma patients. *Supp Care Cancer*. (2022) 30:1493–500. doi: 10.1007/s00520-021-06566-2

227. Jones LW. Precision oncology framework for investigation of exercise as treatment for cancer. *JCO*. (2015) 33:4134–7. doi: 10.1200/JCO.2015.62.7687

228. Sheill G, Guinan E, Brady L, Hevey D, Hussey J. Exercise interventions for patients with advanced cancer: A systematic review of recruitment, attrition, and exercise adherence rates. *Pall Supp Care*. (2019) 17:686–96. doi: 10.1017/S1478951519000312

229. Duma N, Kothadia SM, Azam TU, Yadav S, Paludo J, Vera Aguilera J, et al. Characterization of comorbidities limiting the recruitment of patients in early phase clinical trials. *Oncol*. (2019) 24:96–102. doi: 10.1634/theoncologist.2017-0687

230. Cramer CK, Cummings TL, Andrews RN, Strowd R, Rapp SR, Shaw EG, et al. Treatment of radiation-induced cognitive decline in adult brain tumor patients. *Curr Treat Opt Oncol*. (2019) 20:42. doi: 10.1007/s11864-019-0641-6

231. Rong L, Li N, Zhang Z. Emerging therapies for glioblastoma: current state and future directions. *J Exp Clin Cancer Res*. (2022) 41:142. doi: 10.1186/s13046-022-02349-7

232. Vargas-Sierra O, Hernández-Juárez J, Uc-Uc PY, Herrera LA, Domínguez-Gómez G, Gariglio P, et al. Role of SLC5A8 as a tumor suppressor in cervical cancer. *Front Biosci. (Landmark Ed)*. (2024) 29:16. doi: 10.31083/j.fbl2901016

233. Figueredo VM. The heart renaissance. *Rev Cardiovasc Med*. (2024) 25:91. doi: 10.31083/j.rcm2503091

234. Li M, Liu X, Jiang M, Lei Y, Li Z, Li S, et al. Prognostic capability of clinical SYNTAX score in patients with complex coronary artery disease and chronic renal insufficiency undergoing percutaneous coronary intervention. *Rev Cardiovasc Med*. (2024) 25:18. doi: 10.31083/j.rcm2501018

235. Buffart LM, Sweegers MG, May AM, Chinapaw MJ, Van Vulpen JK, Newton RU, et al. Targeting exercise interventions to patients with cancer in need: an individual patient data meta-analysis. *J Natl Cancer Inst*. (2018) 110:1190–200. doi: 10.1093/jnci/djy161

236. Campanella R, Guarnaccia L, Caroli M, Zarino B, Carrabba G, La Verde N, et al. Personalized and translational approach for Malignant brain tumors in the era of precision medicine: the strategic contribution of an experienced neurosurgery laboratory in a modern neurosurgery and neuro-oncology department. *J Neurol Sci*. (2020) 417:117083. doi: 10.1016/j.jns.2020.117083

237. Keats MR, Grandy SA, Blanchard C, Fowles JR, Neyedli HF, Weeks AC, et al. The impact of resistance exercise on muscle mass in glioblastoma in survivors (RESIST): protocol for a randomized controlled trial. *JMIR Res Protoc*. (2022) 11: e37709. doi: 10.2196/37709

238. De Los Monteros CTE, Harteveld LM, Kuipers IM, Rammeloo L, Hazekamp MG, Blom NA, et al. Prognostic value of maximal and submaximal exercise performance in fontan patients < 15 years of age. *Am J Cardiol*. (2021) 154:92–8. doi: 10.1016/j.amjcard.2021.05.049

239. Jost J, Müther M, Brandt R, Altuner U, Lemcke L, Stummer W, et al. Conceptual development of an intensive exercise program for glioma patients (ActiNO): summary of clinical experience. *J Neurooncol*. (2023) 163:367–76. doi: 10.1007/s11060-023-04354-y

240. Rajaratnam V, Islam M, Yang M, Slaby R, Ramirez H, Mirza S. Glioblastoma: pathogenesis and current status of chemotherapy and other novel treatments. *Cancers*. (2020) 12:937. doi: 10.3390/cancers12040937

241. Falck RS, Davis JC, Best JR, Crockett RA, Liu-Ambrose T. Impact of exercise training on physical and cognitive function among older adults: a systematic review and meta-analysis. *Neurobiol Aging*. (2019) 79:119–30. doi: 10.1016/j.neurobiolaging.2019.03.007

242. Bozzao A, Weber D, Crompton S, Braz G, Csaba D, Dhermain F, et al. European cancer organisation essential requirements for quality cancer care: adult glioma. *J Cancer Policy*. (2023) 38:100438. doi: 10.1016/j.jcpo.2023.100438

243. Walbert T, Chasteen K. "Palliative and supportive care for glioma patients". In: Raizer J, Parsa A, editors. Current understanding and treatment of gliomas. *Cancer treatment and research*. Springer International Publishing, Cham (2015). p. 171–84. doi: 10.1007/978-3-319-12048-5_11

244. Bai L, Yu E. A narrative review of risk factors and interventions for cancer- related cognitive impairment. *Ann Transl Med*. (2021) 9:72–2. doi: 10.21037/atm-20-6443

245. Park J, Park YG. Brain tumor rehabilitation: symptoms, complications, and treatment strategy. *Brain Neurorehabil*. (2022) 15:e25. doi: 10.12786/bn.2022.15.e25

246. Berardi R, Morgese F, Rinaldi S, Torniai M, Mentrasti G, Scortichini L, et al. Benefits and limitations of a multidisciplinary approach in cancer patient management. *CMAR*. (2020) 12:9363–74. doi: 10.2147/CMAR.S220976

247. Hojan K, Gerreth K. Can multidisciplinary inpatient and outpatient rehabilitation provide sufficient prevention of disability in patients with a brain tumor?—A case-series report of two programs and A prospective, observational clinical trial. *IJERPH*. (2020) 17:6488. doi: 10.3390/ijerph17186488

248. Zubin Maslov P, Schulman A, Lavie CJ, Narula J. Personalized exercise dose prescription. *Eur Heart J*. (2018) 39:2346–55. doi: 10.1093/eurheartj/ehx686

249. Costache A-D, Costache I-I, R-Ştefan M, Stafie C-S, Leon-Constantin M-M, Roca M, et al. Beyond the finish line: the impact and dynamics of biomarkers in physical exercise—A narrative review. *JCM*. (2021) 10:4978. doi: 10.3390/jcm10214978

250. Wang J, Liu S, Li G, Xiao J. Exercise regulates the immune system. In: Xiao J, editor. *Physical exercise for human health. Advances in experimental medicine and biology*. Springer Nature Singapore, Singapore (2020). p. 395–408. doi: 10.1007/978-981-15-1792-1_27

251. Wen Z, Nie X, Chen L, Liu P, Lan C, Mossa-Basha M, et al. A decision tree model to help treatment decision-making for unruptured intracranial aneurysms: A multi-center, long-term follow-up study in a large chinese cohort. *Transl Stroke Res*. (2024), 1–13. doi: 10.1007/s12975-024-01280-7

252. Cirocchi R, Matteucci M, Lori E, D'Andrea V, Arezzo A, Pironi D, et al. Sutureless FOCUS harmonic scalpel versus clamp-and-tie techniques for thyroidectomy: a meta-analysis of 43 randomized controlled trials. *Int J Surg*. (2024) 110:8083–96. doi: 10.1097/JS9.0000000000002113

253. Holland E, Ene C. Personalized medicine for gliomas. *Surg Neurol Int*. (2015) 6:89. doi: 10.4103/2152-7806.151351

254. Zhuo Z, Zhang D, Lu W, Wu X, Cui Y, Zhang W, et al. Reversal of tamoxifen resistance by artemisinin in ER+ breast cancer: bioinformatics analysis and experimental validation. *OR*. (2024) 32:1093–107. doi: 10.32604/or.2024.047257

255. Hu Q, Wang M, Wang J, Tao Y, Niu T. Development of a cell adhesion-based prognostic model for multiple myeloma: Insights into chemotherapy response and potential reversal of adhesion effects. *OR*. (2024) 32:753–68. doi: 10.32604/or.2023.043647

frontiers | Frontiers in Oncology

TYPE Systematic Review
PUBLISHED 01 July 2025
DOI 10.3389/fonc.2025.1621666

OPEN ACCESS

EDITED BY
Lei Huang,
University of Massachusetts Medical School, United States

REVIEWED BY
Fu Gao,
Yale University, United States
Yue Liu,
The University of Texas at Austin, United States
Zhimin Hu,
University of California, San Diego, United States

*CORRESPONDENCE
Huanhuan Ma
mahuanhuan@stu.gzy.edu.cn
Hongguan Jiao
jiaohg@gzy.edu.cn

RECEIVED 01 May 2025
ACCEPTED 06 June 2025
PUBLISHED 01 July 2025

CITATION
Ma H, Ding R, Wang J, Du G, Zhang Y, Lu Q, Hou Y, Chen H and Jiao H (2025) Global research trends in tryptophan metabolism and cancer: a bibliometric and visualization analysis (2005–2024). *Front. Oncol.* 15:1621666. doi: 10.3389/fonc.2025.1621666

Global research trends in tryptophan metabolism and cancer: a bibliometric and visualization analysis (2005–2024)

Huanhuan Ma[1*], Ran Ding[2], Junwen Wang[3], Guangying Du[1], Yun Zhang[1], Qiuchen Lu[1], Yingyue Hou[1], Haosong Chen[1] and Hongguan Jiao[2*]

[1]School of Information Engineering, Guizhou University of Traditional Chinese Medicine, Guiyang, China, [2]College of Basic Traditional Chinese Medicine, Guizhou University of Traditional Chinese Medicine, Guiyang, China, [3]Institute of Basic Theory of Traditional Chinese Medicine, China Academy of Chinese Medical Sciences, Beijing, China

Background: In recent years, tryptophan metabolism has gained increasing attention for its pivotal role in shaping the tumor immune microenvironment and promoting cancer progression. As a result, it has become a central topic in cancer metabolism and tumor immunology. This study applies a comprehensive bibliometric approach to analyze global research trends in tryptophan metabolism within the context of cancer. By identifying emerging hotspots, leading contributors, and patterns of international collaboration, this work aims to provide meaningful insights to guide future therapeutic strategies targeting metabolic pathways in oncology.

Methods: A systematic literature search was performed using the Web of Science Core Collection to retrieve publications related to tryptophan metabolism in cancer from 2005 to 2024. Bibliometric and visual analyses were conducted using CiteSpace, VOSviewer, and Python to examine publication trends, national and institutional contributions, author productivity, journal influence, co-citation networks, and keyword co-occurrence patterns.

Results: A total of 1,927 publications were identified, authored by 11,134 researchers from 70 countries and published in 781 academic journals. The volume of publications showed a steady increase, peaking in 2021. The United States and China emerged as the dominant contributors, excelling in both research output and international collaboration. Dietmar Fuchs was identified as the most prolific author, with 61 publications. The Medical University of Innsbruck was the leading institution, with 144 publications. *Frontiers in Immunology* demonstrated strong citation performance and academic impact. Co-citation and keyword analysis revealed key research themes, including "IDO (indoleamine 2,3-dioxygenase)," "tryptophan catabolism," "cancer," and "dendritic cells," as well as emerging topics such as "gut microbiota," "tumor microenvironment," "aryl hydrocarbon receptor," and "cancer immunotherapy."

Conclusion: This study highlights the growing significance of tryptophan metabolism research in cancer, underlining the complex interactions between metabolic pathways and immune responses. Further investigations are needed to explore the therapeutic potential of these metabolic pathways, which could lead to novel cancer treatment strategies.

KEYWORDS

tryptophan metabolism, cancer, kynurenine, TME, bibliometrics, visualization

1 Introduction

Cancer is a highly complex and heterogeneous disease characterized by the dysregulation of normal cellular control mechanisms, leading to the abnormal proliferation and dissemination of malignant cells (1). This uncontrolled growth threatens patients' physical and mental well-being and adversely affects family dynamics and interpersonal relationships. According to the World Health Organization (WHO), cancer is the second leading cause of death worldwide after cardiovascular diseases, causing approximately 10 million deaths annually. Projections indicate that from 2020 to 2050, the global economic burden of cancer will reach $25.2 trillion, equivalent to an average annual tax burden of 0.55% of the global gross domestic product (GDP) (2). By 2050, the global incidence of cancer is projected to rise to 35.3 million new cases—a 76.6% increase—while cancer-related mortality may reach 18.5 million, representing an 89.7% increase (3). Despite advances in conventional treatments such as surgery, chemotherapy, and radiotherapy, drug resistance remains a major unresolved challenge. To overcome this, modern approaches including targeted therapy, immunotherapy, gene therapy, stem cell therapy, natural antioxidants, photodynamic therapy, nanoparticles, and precision medicine are being applied to cancer diagnosis and treatment (4–8). Among these, metabolic therapy has attracted considerable interest for its promising therapeutic potential (9).

Drug resistance primarily arises from tumors establishing compensatory signaling pathways, alterations in target proteins, changes in the tumor microenvironment, tumor heterogeneity, and adaptation to targeted therapies. The interaction of these factors drives the development of acquired resistance to targeted treatments (10). To date, the U.S. Food and Drug Administration (FDA) has approved drugs targeting over 30 distinct molecular targets (11–13), offering new hope to patients. Advances in technologies such as whole-genome sequencing, targeted high-throughput sequencing, and deep sequencing have enabled the detection of aberrant tumor genes with greater precision. Immunotherapies—including immune checkpoint inhibitors, CAR-T cell therapies, and cancer vaccines (14, 15) —leverage the host immune system to selectively eliminate malignant cells while sparing normal tissues (16). Notably, PD-1/PD-L1 antibody therapies have shown remarkable efficacy and durable responses across various cancers, with fewer side effects than conventional treatments (17, 18).

Studies have demonstrated that tumor cells preferentially metabolize glucose into lactate via glycolysis even in the presence of oxygen, a phenomenon known as the Warburg effect. This metabolic reprogramming provides a theoretical foundation for tumor metabolic therapy (19). Among metabolic pathways, tryptophan metabolism has attracted significant attention due to its essential role in regulating inflammation, metabolism, immune responses, and neurological functions (20). Beyond these physiological processes, tryptophan metabolism has been implicated in tumor progression by suppressing anti-tumor immunity and promoting tumor cell malignancy (21). In particular, enzymes involved in the kynurenine pathway—such as IDO and tryptophan 2,3-dioxygenase (TDO)—have been correlated with poor prognosis in multiple cancer types (22).

As research on tryptophan metabolism in cancer advances, there is an increasing need to explore the current status and

Abbreviations: WHO, World Health Organization; GDP, Global gross Domestic Product; FDA, Food and Drug Administration; IDO, Indoleamine 2,3-dioxygenase; TDO, Tryptophan 2,3-dioxygenase; DKFZ, German Cancer Research Center; LC, Local Citations; GC, Global Citations; KMO, Kynurenine 3-monooxygenase; KYN, Kynurenine; TME, Tumor Microenvironment; NAD^+, Nicotinamide Adenine Dinucleotide; AhR, Aryl hydrocarbon Receptor; IFN-γ, Interferon-gamma; IL-2, Interleukin-2; TGF-β, Transforming Growth Factor-beta; IL-10, Interleukin-10; NK, Natural Killer; MAPK, Mitogen-Activated Protein Kinase; PI3K/AKT, Phosphoinositide 3-kinase/Protein Kinase B; EMT, Epithelial-Mesenchymal Transition; PFS, Progression-Free Survival; OS, Overall Survival; KP, Kynurenine Pathway; LUAD, Lung Adenocarcinoma; 5-HT, 5-Hydroxytryptamine; TPH1, Tryptophan Hydroxylase 1; HIF-1α, Hypoxia-Inducible Factor-1α; PKM2, Pyruvate Kinase M2; AC, Adenylate Cyclase; PKA, Protein Kinase A; TAMs, Tumor-Associated Macrophages; CSC, Cancer Stem Cell; 5-HIAA, 5-hydroxyindoleacetic acid; GPR35, G Protein-coupled Receptor 35; TE, Telotristat Ethyl; CPA, P-Chlorophenylalanine; SSRIs, Selective Serotonin Reuptake Inhibitors; MAOA, Monoamine Oxidase A; I3A, Indole-3-Aldehyde; IA, Indoleacrylic Acid; IAA, Indole-3-Acetic Acid; IS, Indoxyl Sulfate; 3-HK, 3-Hydroxykynurenine; ICB, Immune Checkpoint Blockade; I3P, Indole-3-pyruvic acid; KYN/Trp, Kynurenine/Tryptophan; ADT, Arginine Deprivation Therapy.

emerging trends in this field. Bibliometrics has become a powerful and widely used tool for analyzing and evaluating scientific literature across disciplines. As an interdisciplinary science, bibliometrics employs mathematical and statistical methods alongside visualization techniques to quantitatively analyze large bodies of literature within specific research domains, thereby revealing patterns and trends in the development of scientific topics (23). This quantitative approach offers an objective and intuitive assessment of past academic activities and achievements, minimizing potential biases arising from subjective evaluation (24). By quantifying research output, bibliometrics enables comparisons of scholarly productivity across countries, institutions, authors, and journals, and facilitates the identification of cutting-edge research and publication trends (25). Although bibliometric analyses have been widely conducted in many fields, no comprehensive bibliometric study has yet addressed tryptophan metabolism in cancer. Therefore, this study employs bibliometric analysis to comprehensively examine the literature on tryptophan metabolism in cancer from 2005 to 2024. It aims to identify the developmental trajectory, current research landscape, and emerging trends, while providing guidance for future research directions and therapeutic strategies (see Figure 1).

2 Materials and methods

2.1 Data acquisition and search strategy

The Web of Science is globally recognized as a leading authoritative database, indexing a wide range of high-quality academic journals, conference papers, books, patents, and other scholarly works. We conducted a literature search in the Web of Science Core Collection for documents related to tryptophan metabolism and cancer, utilizing the following search strategy: Topic: ((TS=(cancer* OR tumor* OR tumour* OR neoplas* OR malignan* OR carcinoma* OR adenocarcinoma* OR choricarcinoma* OR leukemia* OR leukaemia* OR metastat* OR sarcoma* OR teratoma* OR melanoma* OR lymphoma* OR myeloma*)) NOT TS=("benign neoplasms" OR "benign neoplasm" OR "neoplasms, benign" OR "neoplasm, benign" OR "benign tumor" OR "non-malignant neoplasms" OR "non-cancerous tumor" OR "non-neoplastic lesion")) AND TS=("tryptophan metabolism" OR "trp metabolism" OR "tryptophan catabolic pathway*" OR "tryptophan degradation*" OR "tryptophan breakdown" OR "indole metabolism" OR "kynurenine pathway" OR "serotonin metabolism" OR "tryptophan catabolism*" OR "tryptophan degradation pathway*" OR "tryptophan metabolic pathway*" OR "tryptophan oxidation" OR "tryptophan turnover" OR "tryptophan biotransformation" OR "tryptophan metabolite*" OR "tryptophan metabolism regulation" OR "tryptophan metabolic network").

2.2 Inclusion and exclusion criteria

Preliminary searches revealed that the earliest publication addressing the role of tryptophan metabolism in cancer development dates back to 1955, marking the initial exploration of this field. From 1955 to 2004, a total of 313 relevant publications were retrieved, accounting for 13.3% of the overall dataset (2,352 articles). However, the annual publication output during this period remained low, with most years recording fewer than ten articles, and only 20 articles published in 2004. These findings suggest that, although early research laid a foundational basis, the field was still in its infancy and lacked sustained and systematic development. In contrast, the period from 2005 to 2024 witnessed a significant acceleration in research activity, characterized by a steady increase in annual publication volume. A total of 2,039 articles were retrieved during this stage, indicating greater academic interest and a more robust research output.

To ensure the scientific rigor and reliability of the analysis, this study focused on publications from August 1, 2005, to July 31, 2024. Only English-language original research articles and reviews were included, while unrelated or retracted publications were excluded. After applying these criteria, 1,927 high-quality articles were retained for analysis. All retrieved records were exported in plain text format in multiple batches, each named as "download_xxx.txt," including full records and cited references. The data were then imported into CiteSpace software for duplicate removal, resulting in a final dataset comprising 1,927 valid articles. The entire data retrieval and preprocessing process was completed on August 1, 2024. A detailed workflow is illustrated in Figure 2. To enhance the comprehensiveness and transparency of this study—and to acknowledge the contributions of early researchers—Supplementary Table S1 provides the annual publication distribution from 1955 to 2004, along with a brief summary of several representative early studies.

2.3 Analysis tools

This study employed a range of visualization tools to intuitively and systematically present and analyze bibliometric data, including Python, CiteSpace (6.3.R1), VOSviewer (1.6.19), and R Bibliometrix. Python was primarily used for flexible data processing and the generation of customized visualizations, such as annual publication trends and comparative metric charts. CiteSpace facilitated data cleaning and comprehensive visual analyses, including institutional collaboration networks, co-cited references, keyword co-occurrence, and clustering. VOSviewer and R Bibliometrix were applied to construct collaboration and co-occurrence networks among countries, authors, and journals, providing a clear depiction of global research collaboration patterns and the distribution of academic influence.

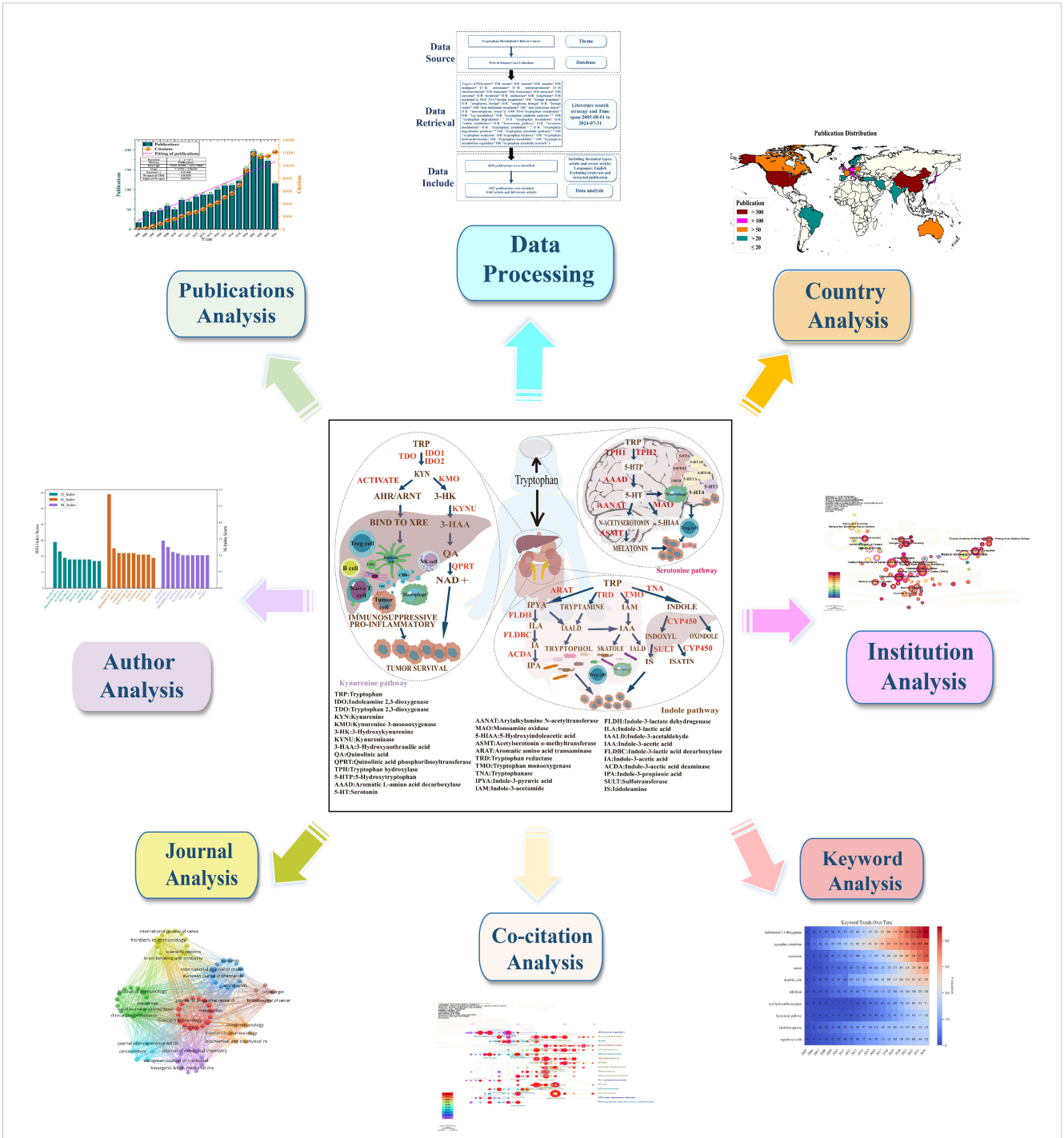

FIGURE 1
Graphical abstract illustrating the bibliometric analysis of tryptophan metabolism in cancer. Publications related to tryptophan metabolism in cancer were retrieved from the Web of Science Core Collection (WOSCC). Visualization analyses were conducted using multiple tools, covering various perspectives including annual publication trends, leading countries, prolific authors, influential institutions, journals, co-cited references, and keyword co-occurrence.

To systematically evaluate the research landscape and identify emerging trends in tryptophan metabolism and cancer, several core bibliometric indicators were applied. The number of publications was used to assess research activity and temporal evolution, while citation frequency reflected academic impact. Author and institutional performance were evaluated using the H-index, G-index, and M-index. Keyword co-occurrence frequency and centrality helped identify key research hotspots and core themes. Additionally, burst detection was conducted to uncover rapidly emerging topics within specific timeframes. Clustering analyses of keywords and co-cited references were also performed. The quality and robustness of the clustering structure were assessed using

modularity (Q) and silhouette (S) scores. A Q value greater than 0.3 indicates statistically significant clustering. An S value above 0.5 suggests reasonable cluster quality, while a value above 0.7 reflects high reliability and efficiency.

3 Results

3.1 Analysis of publications and citations

Between 2005 and 2024, a total of 1,927 publications related to tryptophan metabolism in cancer were identified (see Figure 3). The field began with just 17 publications in 2005 and has since demonstrated steady growth. Notably, research activity accelerated significantly after 2019, reaching a peak of 196 publications in 2021. Although there was a slight decline in output in 2022 and 2023, the overall upward trajectory remains strong. This temporary dip may be partly attributed to the global COVID-19 pandemic, which disrupted research activities worldwide. Simultaneously, citation counts increased dramatically—from zero in 2005 to 12,102 by 2024—indicating growing academic attention and influence. Linear regression analysis demonstrated a strong positive correlation between publication volume and year (R^2 = 0.83659, Adjusted R^2 = 0.82751), suggesting a high degree of model fit and confirming the robust upward trend. These findings highlight the increasing importance of tryptophan metabolism in cancer research and the expanding interest in this topic over the past two decades.

3.2 Analysis of the top producing countries/regions

A total of 1,927 publications related to tryptophan metabolism in cancer were contributed by researchers from 70 countries. As shown in Table 1, the United States leads in publication output with 537 papers and 40,276 citations, and demonstrates a total link strength of 320, highlighting its strong academic influence and extensive research collaborations. China ranks second with 529 publications, a total link strength of 120, and 14,522 citations. Although China's publication count nearly matches that of the United States, a significant gap in citation frequency suggests room for improvement in research quality and international impact. Germany, despite publishing only 161 papers, has garnered

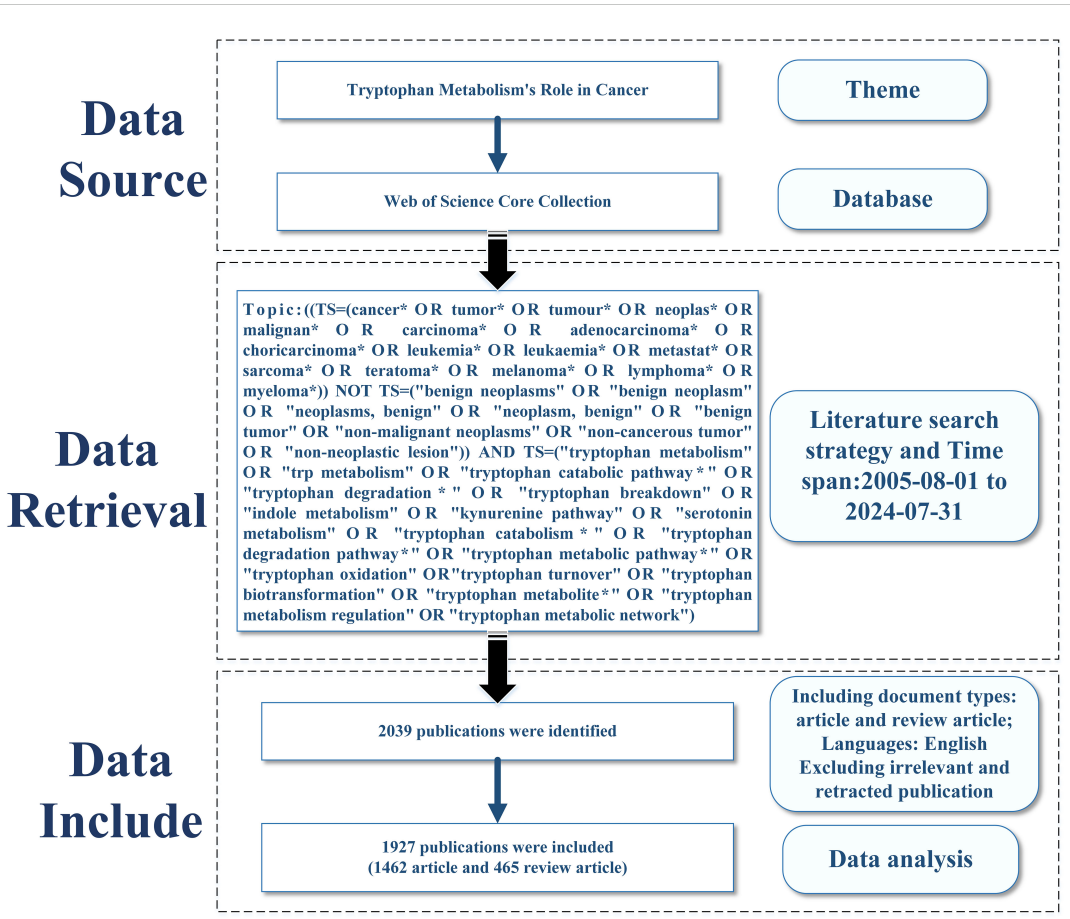

FIGURE 2
Flowchart of the literature screening process.

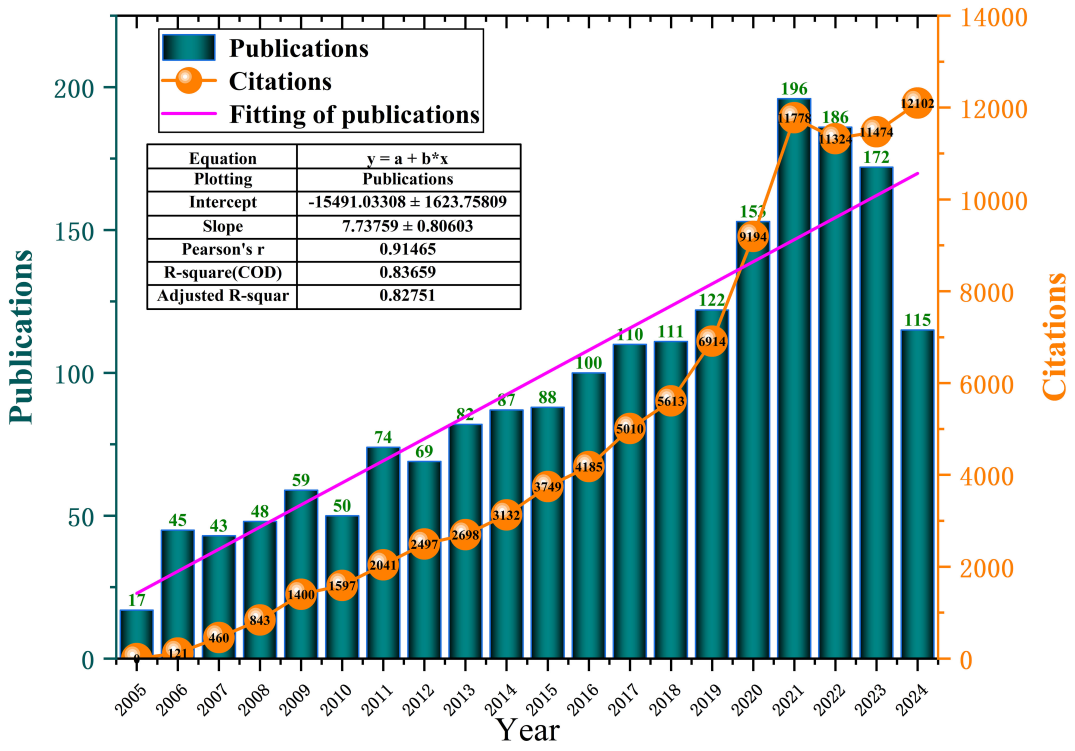

FIGURE 3
Annual publication and citations on tryptophan metabolism in cancer research from 2005 to 2024.

TABLE 1 Top 10 countries/regions and institutions contributing to tryptophan metabolism research in cancer.

Rank	Country	Publications	Citations	Total link strength	Institutions	Publications	Institutions	Citations
1	USA	537	40276	320	Medical University of Innsbruck	144	German Cancer Research Center (DKFZ)	3508
2	China	529	14522	120	Wayne State University	135	Thomas Jefferson University	3285
3	Germany	161	10810	214	Helmholtz Association	122	Lankenau Institute for Medical Research	3243
4	Italy	120	8383	130	German Cancer Research Center (DKFZ)	107	Medical College of Georgia	2959
5	United Kingdom	119	6181	205	Ruprecht Karls University Heidelberg	105	University of Perugia	2888
6	Japan	109	6121	39	University of Texas System	100	Innsbruck Medical University	2421
7	Austria	85	4451	73	University of California System	96	University of Illinois	2321
8	Australia	79	4945	114	Harvard University	89	Catholic University of Louvain	2303
9	France	79	5925	160	Northwestern University	79	University of Padua	2108
10	Netherlands	75	4987	119	Medical University of Lublin	78	University of Sydney	1986

10,810 citations and achieved a total link strength of 214, reflecting its prominent role within the European research network and its high academic influence.

The global distribution of research efforts (see Figures 4A, B) shows that the United States and China dominate in both publication volume and citation frequency. In contrast, European countries such as Germany, the United Kingdom, and France exhibit a clear advantage in research quality and international collaboration. Radar charts (see Figures 4C, D) further illustrate the comparative academic output and collaborative strengths of leading countries. Cluster analysis (Figure 4E) reveals the formation of several regional and international research alliances, underscoring a pattern of strong transnational collaboration. The United States plays a central role in the global research network, engaging extensively with partners across Europe, Asia, and beyond. In comparison, countries in South America, Africa, and parts of Southeast Asia remain underrepresented, with their research activities often relying on collaborations with major

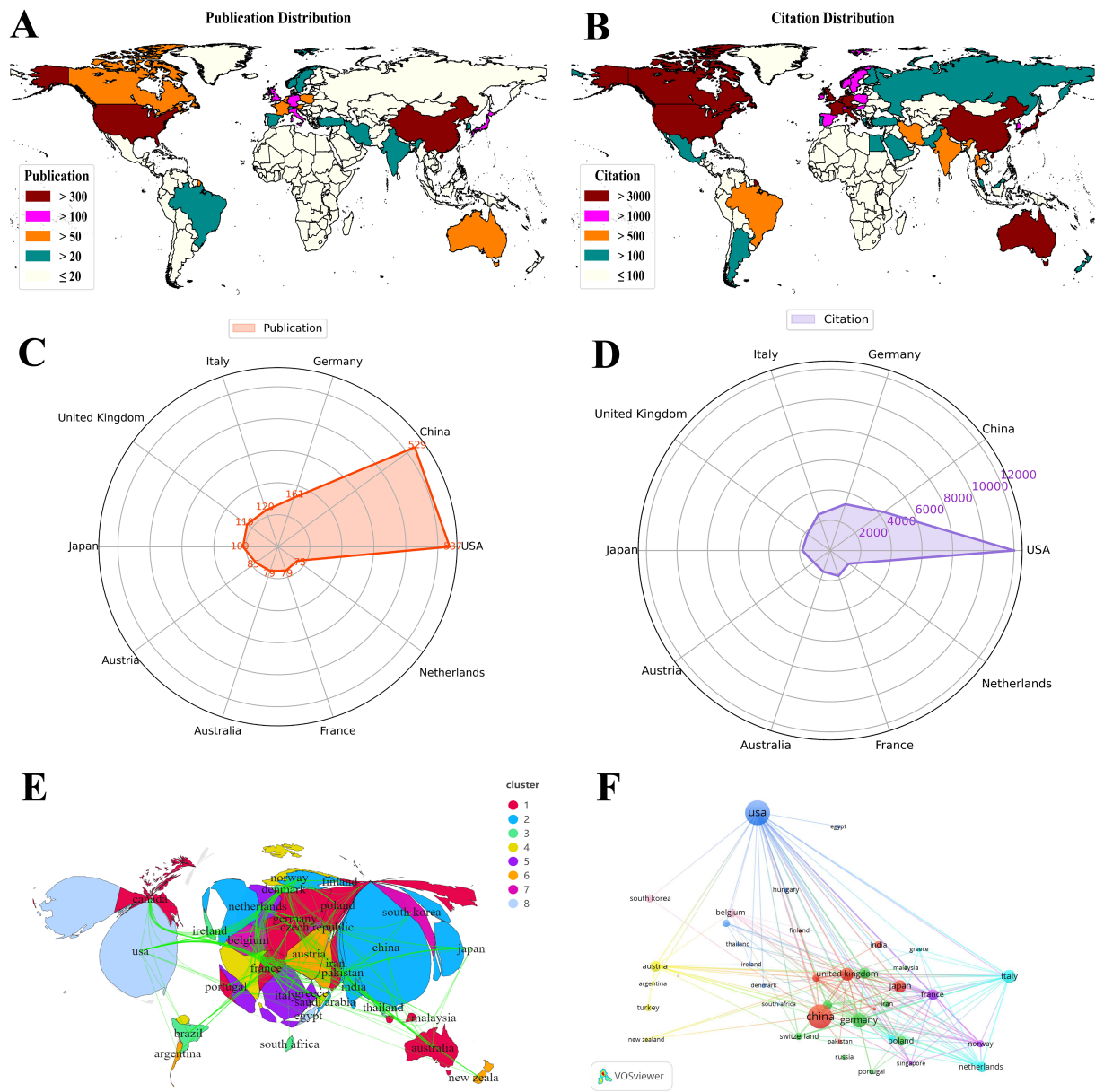

FIGURE 4
Global distribution of tryptophan metabolism in cancer research. **(A)** Global distribution of publications on tryptophan metabolism in cancer, with colors representing varying publication volumes, and darker red indicating higher counts. **(B)** Global distribution of citations on tryptophan metabolism in cancer, with colors representing varying citation frequencies, and darker red indicating higher counts. **(C)** Visualization map of country publications in tryptophan metabolism and cancer. **(D)** Visualization map of country citations in tryptophan metabolism and cancer. **(E)** Geographic clustering visualization of countries/regions. **(F)** Collaboration network diagram of countries/regions in tryptophan metabolism and cancer, where nodes represent countries, node size reflects publication volume, and links indicate collaboration strength.

contributors such as the United States and China. To further visualize national contributions, 41 countries with at least five publications were selected for network mapping (see Figure 4F). The resulting distribution confirms clear regional and collaborative patterns, highlighting both the global scope and the geographic disparities in research on tryptophan metabolism and cancer.

3.3 Analysis of the top-producing authors

A total of 11,134 authors worldwide have contributed to 1,927 publications in the field of tryptophan metabolism and cancer. The top ten authors, ranked by the number of publications (NP), were further evaluated based on key bibliometric indicators, including citation frequency, H-index, G-index, and M-index (see Table 2). The H-index measures a researcher's sustained impact by quantifying the number of publications (h) that have been cited at least h times. The G-index builds on this by giving additional weight to highly cited papers, thus reflecting the breadth of a scholar's influence. The M-index, calculated as H/N (where N is the number of years since the researcher's first publication), captures the pace of academic impact over time, with higher values indicating a more rapid trajectory of influence (26).

Among the top contributors, Fuchs, Dietmar ranks first with 61 publications and holds the highest H-index (29), G-index (59), and M-index (1.526), reflecting both prolific output and sustained scholarly influence. Although Prendergast, George C has authored fewer papers (25), he has received 3,628 citations—surpassing Fuchs—and his M-index of 1.15 suggests a fast-growing academic presence. Mittal, Sandeep, Takikawa, Osamu, and Guillemin, Gilles J show comparable H-indices (18, 18, and 16, respectively) and G-indices (all 22), indicating similar levels of research contribution. However, Mittal's M-index (1.125) points to a faster growth rate in scholarly influence compared to Takikawa (0.9) and Guillemin (0.889). Although Müller, Alexander J has the fewest publications (19), his H-index (18) and M-index (0.9) indicate a relatively high quality of work with steady, albeit slower, impact growth. Overall, Fuchs, Prendergast, and Mittal stand out as key figures in the field, each demonstrating unique patterns of academic influence (see Figures 5A, B).

Regarding collaboration networks, Juhasz, Csaba and Mittal, Sandeep play central roles, with total link strengths of 100 and 99, respectively, underscoring their importance in facilitating scientific collaboration. Co-authorship network visualizations (Figures 5C, D) further illustrate these relationships. In Figure 5C, clusters are color-coded by research themes, node size represents publication volume, and line thickness indicates the strength of collaboration. The red cluster, containing the largest number of authors, represents a robust collaborative group, while the purple cluster shows strong connections to other clusters, highlighting cross-disciplinary interactions. Figure 5D adds a temporal dimension, showing that Juhasz was most actively involved in collaborative work between 2016 and 2018. In recent years, researchers such as Jayaraman, Arul, Chapkin, Robert S, and Opitz, Christiane A have emerged as active participants in evolving collaboration networks.

3.4 Analysis of the top-producing institutions

In the visualization analysis of institutional output, influence, and collaboration in tryptophan metabolism and cancer research, Figures 6A, B display the top ten institutions ranked by publication volume and citation frequency, respectively. Publication volume—a direct measure of institutional output—shows that the Medical University of Innsbruck leads the field with 144 publications, indicating its high level of research activity. It is followed by Wayne State University (135 publications) and the Helmholtz Association (122 publications). The German Cancer Research Center (DKFZ) ranks fourth with 107 publications, reflecting its sustained contributions to the field (see Table 1). Figure 6B, which highlights citation frequency as a measure of academic impact, shows that DKFZ leads with 3,508 citations, underscoring both the volume and influence of its research. Thomas Jefferson University and the Lankenau Institute for Medical Research follow with 3,285 and 3,243 citations, respectively, further emphasizing their

TABLE 2 Top 10 authors contributing to tryptophan metabolism research in cancer.

Rank	Author	NP	TC	h_index	g_index	m_index	PY_start
1	Fuchs, Dietmar	61	3560	29	59	1.526	2006
2	Prendergast, George C	25	3628	23	25	1.15	2005
3	Mittal, Sandeep	22	631	18	22	1.125	2009
4	Takikawa, Osamu	22	1934	18	22	0.9	2005
5	Guillemin, Gilles J	22	1775	16	22	0.889	2007
6	Wang Y	22	861	11	22	0.786	2011
7	Platten, Michael	21	3178	19	21	1.056	2007
8	Saito, Kuniaki	21	785	18	21	0.947	2006
9	Juhász, Csaba	21	635	17	21	0.895	2006
10	Muller, Alexander J	19	2762	18	19	0.9	2005

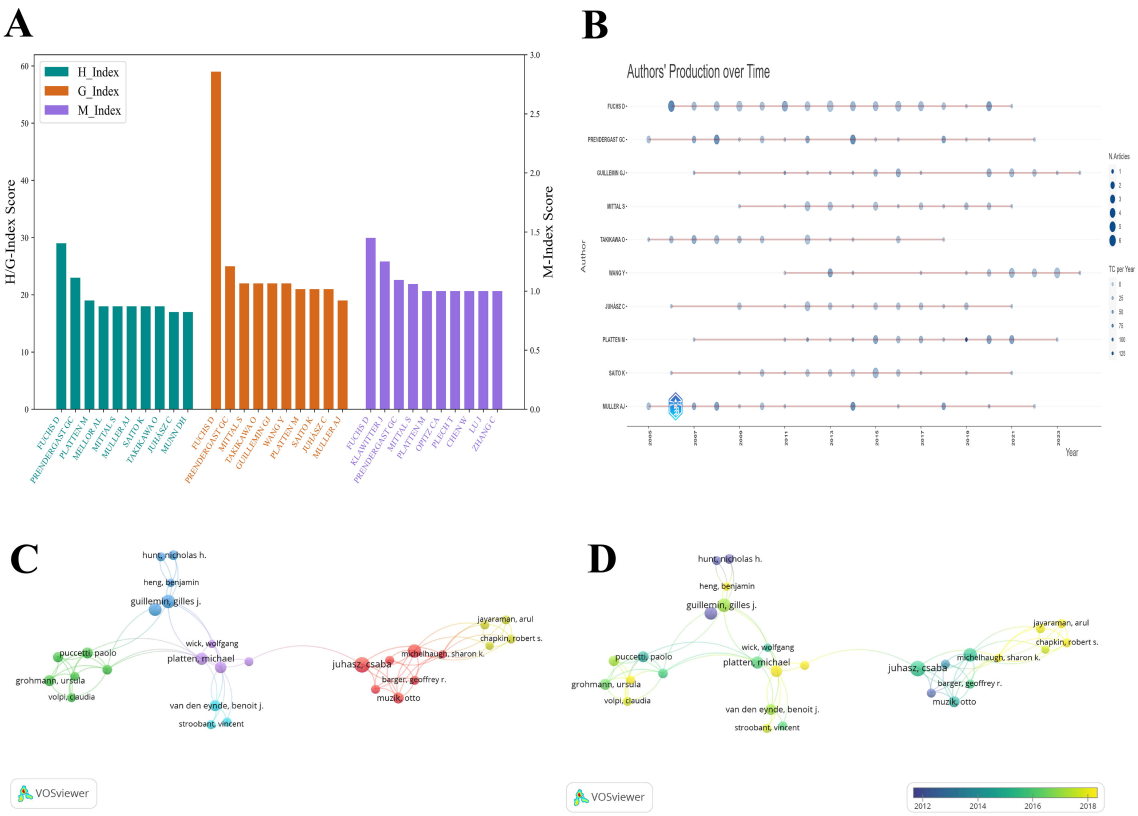

FIGURE 5
Visualization of the top authors in tryptophan metabolism research in cancer. **(A)** Visualization map of H-index, G-index, and M-index for the top 10 authors by publication volume, with colors representing different impact metrics. **(B)** Publication volume of the top 10 authors over time. Node size represents the number of articles, and color intensity reflects total citations. **(C)** Author co-citation network map in tryptophan metabolism and cancer, with colors representing distinct collaboration groups. **(D)** Temporal trend graph of the author co-citation network in tryptophan metabolism and cancer, with color intensity ranging from purple to yellow to represent the progression of years from past to present.

significant academic standing in this domain. A comparison of Figures 6A, B reveals that academic institutions dominate both in output and impact, likely due to their central roles in conducting foundational and innovative research. These data provide valuable insights into the current institutional landscape and offer direction for future research efforts and collaborative partnerships.

Figure 6C visualizes the collaborative network among institutions from 2005 to 2024. Each node represents a research institution, with node size proportional to its publication volume, and line thickness indicating the strength of collaboration. The Medical University of Innsbruck appears as the largest node, reflecting its dominant role in the field, followed by the Helmholtz Association, Institut National de la Santé et de la Recherche Médicale (Inserm), the Chinese Academy of Sciences, and DKFZ. The purple outer ring around each node represents betweenness centrality, which reflects an institution's role as a connector within the collaborative network. A total of eight institutions have a betweenness centrality ≥ 0.2, highlighting their key positions in facilitating inter-institutional cooperation. Gustave Roussy exhibits the highest betweenness centrality (0.43), underscoring its pivotal bridging role. Both the Chinese Academy of Sciences and the National Center for Geriatrics & Gerontology show values of 0.28, further indicating their strategic importance within the global collaboration network.

3.5 Analysis of the top-producing journals

The academic impact of a journal serves as a key indicator of its standing within the scientific community. By examining metrics such as the H-index, G-index, and M-index, a more comprehensive evaluation of a journal's citation performance and scholarly value can be obtained. In the field of tryptophan metabolism and cancer, a total of 781 journals have contributed to the dissemination of research, playing a critical role in advancing knowledge and academic communication. To gain deeper insights into the publication patterns within this field, we conducted a focused analysis of the top ten journals by publication volume (see Table 3). Among them, *Frontiers in Immunology* demonstrated outstanding performance across multiple metrics, including publication volume, citation frequency, H-index, G-index, and M-index, highlighting its significant academic influence in the field of immunology (see Figure 7A). The *International Journal of Molecular Sciences* and *Plos One* ranked second and third in

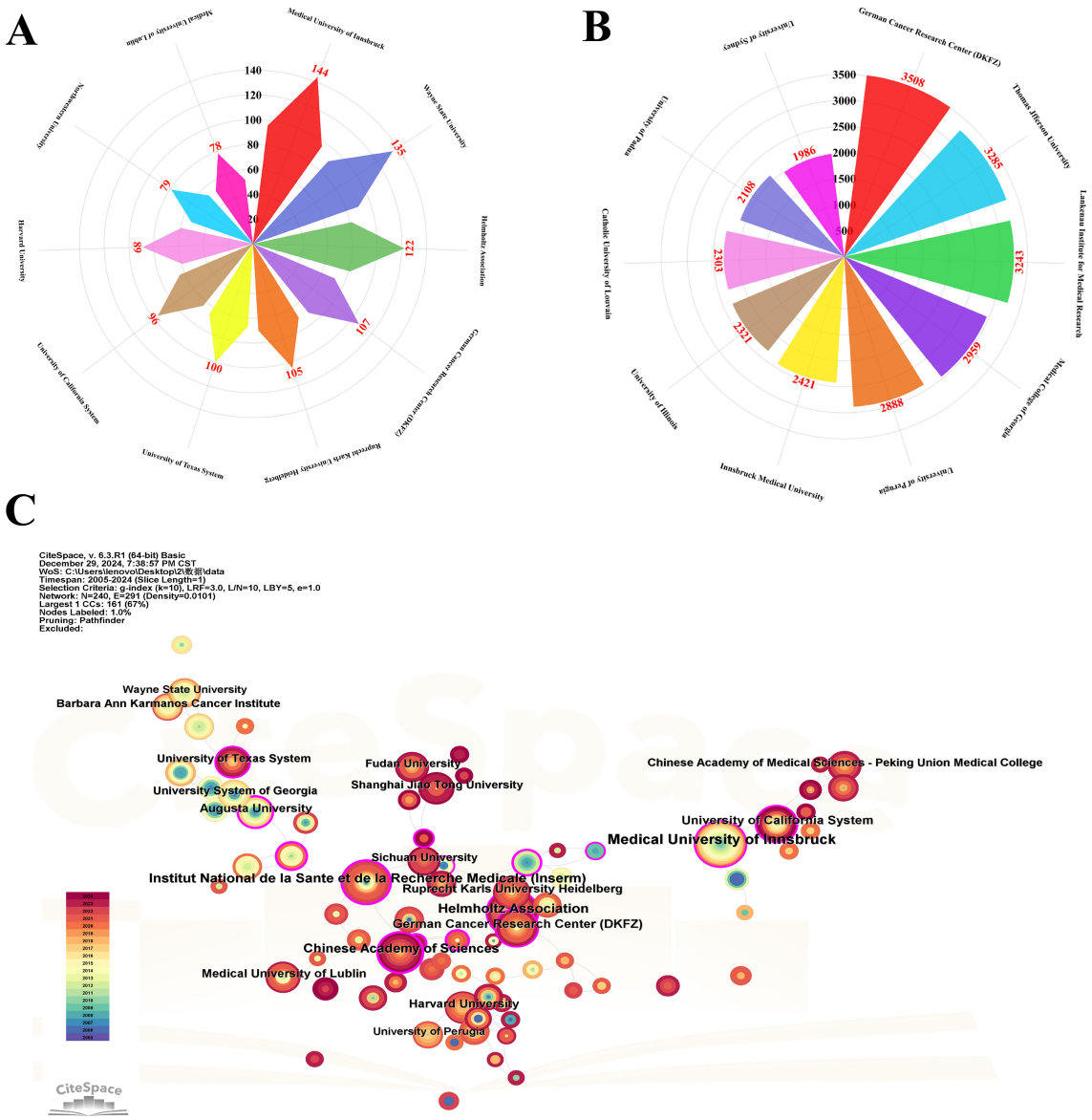

FIGURE 6
Visualization of the top institutions in tryptophan metabolism research in cancer. **(A)** Visualization map of the top 10 institutions based on publication volume. **(B)** Visualization map of the top 10 institutions based on citation count. **(C)** Collaborative relationship map among research institutions. Nodes represent individual institutions, with node size corresponding to publication volume. The thickness of connecting lines reflects collaboration strength, and the purple outer ring around each node indicates betweenness centrality.

terms of publication volume, respectively. However, *Plos One* recorded a substantially higher citation count. Although *Frontiers in Oncology* published a comparable number of papers to *Plos One*, its total citations remained lower, indicating a relatively lesser impact. Notably, several journals—such as *Journal of Immunology*, *Cancer Research*, and *Journal of Medicinal Chemistry* — published fewer articles but achieved high citation frequencies, reflecting the strong academic recognition of their contributions. Furthermore, eight out of the ten leading journals are classified as Q1 journals, underscoring the high visibility and scholarly esteem that research on tryptophan metabolism and cancer has garnered within the scientific community.

The journal thematic clustering map (see Figure 7B) offers a clear visualization of the thematic distribution of journals within the field of tryptophan metabolism and cancer, revealing their affiliations based on subject similarity. In the figure, nodes of different colors represent distinct clusters, each corresponding to collaborative networks centered around specific research themes. Overall, the clusters form interconnected structures, highlighting the interdisciplinary nature of this research area. The yellow cluster primarily focuses on immunology, with core journals including *Frontiers in Immunology*, *Scientific Reports*, *Brain*, *Behavior*, and *Immunity*, and *International Journal of Cancer*. Among these, *Frontiers in Immunology* emerges as the most influential node,

TABLE 3 Top 10 journals contributing to tryptophan metabolism research in cancer.

Rank	Source	NP	TC	h_index	g_index	m_index	IF	JCR
1	*Frontiers in Immunology*	61	3379	30	58	2.308	5.7	Q1
2	*International Journal of Molecular Sciences*	34	656	14	25	1	4.9	Q1
3	*Plos One*	30	1107	18	30	1.2	2.9	Q1
4	*Frontiers in Oncology*	30	496	13	21	1.625	3.5	Q2
5	*Scientific Reports*	29	646	15	25	1.364	3.8	Q1
6	*Cancers*	25	391	13	19	1.625	4.5	Q1
7	*Journal of Immunology*	24	1671	19	24	0.95	3.6	Q2
8	*Cancer Research*	18	2535	17	18	0.81	12.5	Q1
9	*European Journal of Medicinal Chemistry*	18	512	15	18	0.938	6.0	Q1
10	*Journal of Medicinal Chemistry*	18	1223	14	18	0.778	6.8	Q1

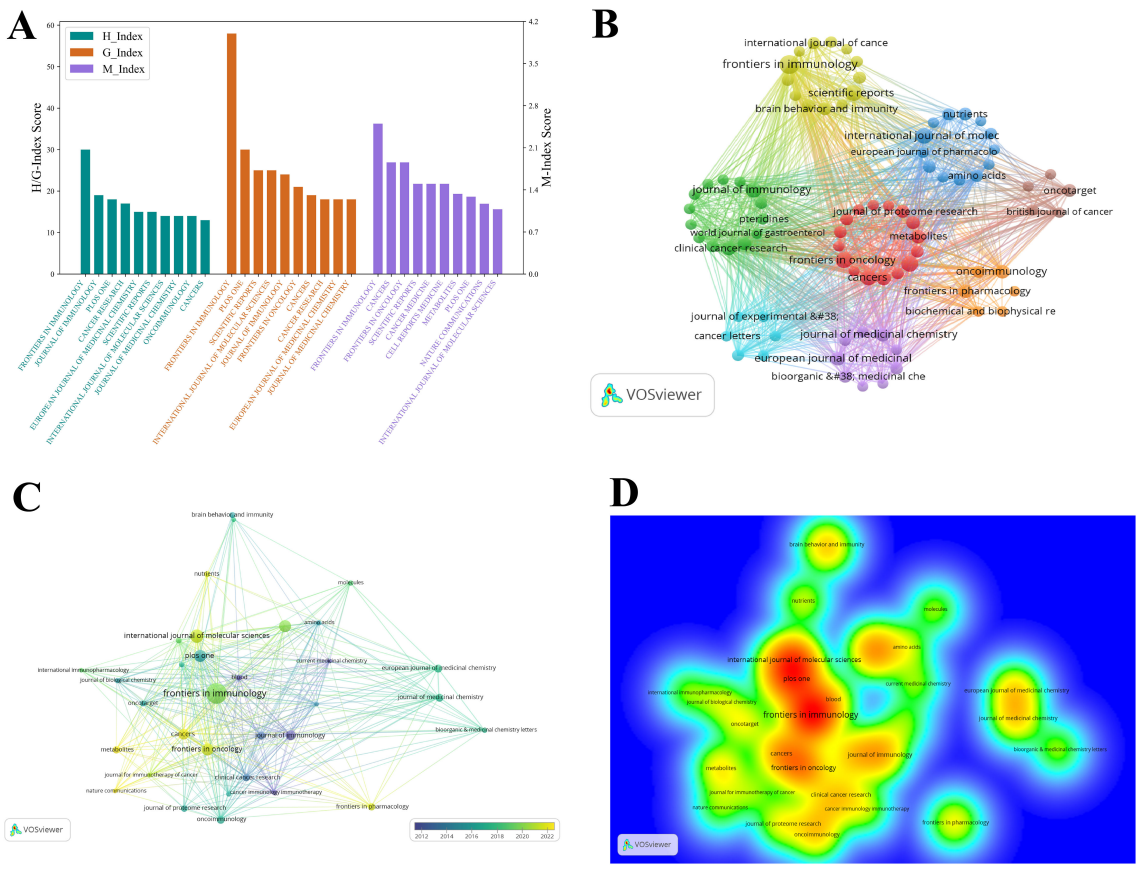

FIGURE 7
Visualization of the top journals in tryptophan metabolism research in cancer. **(A)** Visualization map of H-index, G-index, and M-index for the top 10 journals by publication volume, with colors representing different impact metrics. **(B)** Journal thematic clustering map of tryptophan metabolism and cancer research. Nodes represent distinct journal clusters, with colors denoting different research themes. **(C)** Temporal trend graph of the journal collaboration network in tryptophan metabolism and cancer, with color intensity shifting towards yellow indicating increased collaboration in recent years. **(D)** The item density map visualizes the distribution density of journals within the collaboration network, with color intensity reflecting citation frequency and collaboration strength.

distinguished by its high publication volume, citation frequency, and academic impact. This highlights the central role of immunological mechanisms—particularly immunometabolic regulation and immunotherapy—in research on tryptophan metabolism and cancer. The red cluster is predominantly associated with cancer research, encompassing themes such as cancer metabolism, proteomics, and clinical treatment strategies. Representative journals within this cluster include *Frontiers in Oncology*, *Cancers*, *Journal of Proteome Research*, and *Metabolites*. The high thematic coherence and strong inter-journal connections observed in this cluster underscore the critical role of tryptophan metabolism in cancer initiation, progression, and therapeutic development.

The blue cluster is primarily associated with molecular biology and pharmacology research. Key journals in this cluster include the *European Journal of Pharmacology*, *Amino Acids*, and *Nutrients*. The presence of this cluster underscores the significance of tryptophan metabolism not only in cancer pathophysiology but also in areas such as molecular signaling, nutritional metabolism, and drug development. Research within this domain typically adopts a multidisciplinary approach, integrating biochemistry, bioinformatics, and pharmacology, and thereby offering innovative strategies and insights for cancer therapy. The green cluster focuses predominantly on clinical applications, particularly in the fields of immunology and cancer treatment. Representative journals include *Journal of Immunology* and *Clinical Cancer Research*. The formation of this cluster reflects the increasing convergence of basic research and clinical translation, with discoveries in tryptophan metabolism being progressively applied to precision medicine and the development of personalized therapeutic strategies. In recent years, growing attention has been directed toward the role of immunometabolic regulation in cancer therapy, and the existence of this cluster further substantiates this emerging trend.

To further investigate the evolution of journals in this field, we analyzed temporal trends to reveal changes in academic influence and shifting research hotspots (see Figure 7C). Between 2018 and 2022, journals such as *Frontiers in Immunology*, *Frontiers in Pharmacology*, *Frontiers in Oncology*, and *International Journal of Molecular Sciences* have shown increased activity within the collaboration network, indicating their rising prominence in tryptophan metabolism and cancer research. Conversely, some established journals, including the *Journal of Immunology*, despite maintaining high academic influence, are gradually losing centrality in the network to these emerging outlets. This transition reflects a shift in research focus from traditional immune mechanism studies toward more interdisciplinary directions, particularly at the intersection of immunotherapy and cancer metabolism. The density map (see Figure 7D) further illustrates the spatial distribution of collaboration hotspots and centers of influence among journals. High-density regions (red) cluster around *Frontiers in Immunology*, *Plos One*, and *International Journal of Molecular Sciences*, underscoring their pivotal roles in citation frequency and collaborative engagement, thereby forming the core of the field's influence. Medium-density areas (yellow) include journals such as *Frontiers in Oncology*, *Cancers*, and *Journal of Immunology*, which exert notable influence within specific subdomains but have yet to integrate fully into the core collaborative network. Journals situated in low-density regions (blue) occupy the periphery, often representing niche or emerging topics, thus reflecting unique research trajectories and collaboration patterns within the broader field.

3.6 Analysis of the top-cited references

Local Citations (LC) and Global Citations (GC) are critical metrics for assessing the scholarly impact of individual publications. LC measures a paper's influence within a specific research domain —such as tryptophan metabolism in cancer—while GC captures its overall recognition across the broader scientific community. The LC/GC ratio (local-to-global citation ratio) provides further insight into the paper's relative impact: a higher ratio indicates strong influence within a specialized field, but potentially limited reach beyond it. As shown in Table 4, Platten M (2019, Nat Rev Drug Discov) received 166 local citations and 897 global citations, highlighting its substantial academic impact both within the field and across related disciplines, such as drug development and immunotherapy. In contrast, Pilotte L (2012, P Natl Acad Sci USA) accumulated 192 Local Citations but only 471 Global Citations, suggesting concentrated recognition within tryptophan metabolism and cancer research, yet more limited dissemination in the wider scientific landscape.

Citation frequency is a key indicator of a publication's academic impact, often reflecting its contribution to theoretical innovation, methodological advancement, or technological application. Highly cited studies frequently serve as foundational or landmark references, guiding subsequent research in the field. As illustrated in Figure 8A, each bubble represents a publication, with its position corresponding to the number of citations received in a given year. The size and color of the bubbles indicate citation magnitude—larger, red bubbles denote high citation counts, while smaller, blue ones reflect lower frequencies. Platten M (2019, Nat Rev Drug Discov) has shown a significant rise in citations since 2019, reaching 223 citations by 2024, making it one of the most highly cited publications in the dataset. Similarly, Gao J (2018, Front Cell Infect Microbiol) experienced a rapid increase in citations from 2020 to 2024, reflecting its growing academic attention in later years. In contrast, earlier publications such as Bronte V (2005, Nat Rev Immunol) maintained high citation levels from 2010 to 2021 but have since shown a gradual decline, suggesting a waning influence over time. Figure 8B presents a thematic clustering map of the cited literature, identifying 16 distinct research themes. Each colored region represents a thematic cluster, with node size indicating citation frequency and color denoting thematic category. Cluster #0, labeled "immune regulation," is the largest, suggesting it is the most extensively studied area and likely represents a central research axis in the field. The partial overlap among clusters underscores the interdisciplinary nature of tryptophan metabolism research, highlighting the close integration of immunology, oncology, metabolism, and therapeutic development.

TABLE 4 Top 10 most cited references on tryptophan metabolism in cancer.

Rank	Document	DOI	Year	Local citations	Global citations	LC/GC ratio (%)	Normalized local citations	Normalized global citations
1	CLIN CANCER RES (27)	10.1158/1078-0432.CCR-05-1966	2006	206	522	39.46	11.21	4.68
2	P NATL ACAD SCI USA (28)	10.1073/pnas.1113873109	2012	192	471	40.76	12.96	6.1
3	J CLIN INVEST (29)	10.1172/JCI31178	2007	185	872	21.22	6.99	6.14
4	PLATTEN M, 2019, NAT REV DRUG DISCOV (30)	10.1038/s41573-019-0016-5	2019	166	897	18.51	29.06	20.25
5	CANCER RES (31)	10.1158/0008-5472.CAN-07-1872	2007	163	408	39.95	6.16	2.87
6	CANCER RES (32)	10.1158/0008-5472.CAN-12-0569	2012	156	539	28.94	10.53	6.98
7	BLOOD (33)	10.1182/blood-2009-09-246124	2010	122	440	27.73	8.28	5.37
8	CANCER IMMUNOL IMMUN (34)	10.1007/s00262-008-0513-6	2009	109	260	41.92	7.13	2.53
9	J CLIN INVEST (35)	10.1172/JCI31911	2007	107	665	16.09	4.04	4.68
10	NAT REV CANCER (36)	10.1038/nrc2639	2009	103	360	28.61	6.74	3.5

Figure 8C presents a timeline visualization of citation trends and the evolution of research themes in the field. Red circles denote highly cited publications, with their size proportional to citation frequency, while connecting lines illustrate thematic or citation linkages between studies. This timeline effectively captures the emergence, development, and transition of key research foci over time. Between 2015 and 2019, themes such as #0 immune regulation and #10 kynurenine pathway experienced rapid growth, with associated publications receiving substantial academic attention. Notably, since 2019, newer themes—such as #15 major depressive disorder and #3 ulcerative colitis—have shown a significant increase in citation frequency, reflecting a shift in research interest toward the broader implications of tryptophan metabolism in neuroimmunological and inflammatory disorders. Key studies, including Platten M (2019) and Opitz CA (2011), occupy pivotal positions on the timeline, suggesting their role as landmark contributions that have shaped the trajectory of the field. Collectively, the visualization underscores not only the dynamic nature of research priorities but also the expanding interdisciplinary relevance of tryptophan metabolism in cancer and related pathologies.

Figure 8D highlights the top 20 publications with the highest burst strength, reflecting research that experienced a rapid and concentrated increase in scholarly attention over specific time intervals. Red bars indicate the duration of each citation burst, illustrating both the timing and intensity of influence. Most citation bursts occurred between 2015 and 2020, suggesting that this timeframe marked a critical phase in the maturation of the field. The majority of these burst-identified publications focus on key themes such as immune regulation, metabolic pathways, and clinical therapeutics, emphasizing their centrality in shaping research directions. Among them, Platten M (2019) stands out with a burst strength of 26.18, beginning in 2019 and continuing through 2024, signifying its profound and sustained academic impact. In contrast, Opitz CA (2011), though published earlier, experienced its burst primarily during 2015–2016, indicating a delayed but notable rise in recognition. Similarly, Munn DH (2013) and Bessede A (2014) showed pronounced bursts from 2015 to 2018, likely corresponding to inflection points in the development of immunometabolic and therapeutic research within the field.

3.7 Analysis of the top keywords

By analyzing the keywords in the field of tryptophan metabolism and cancer, we can delve into the research hotspots and future trends within this domain. The heatmap in Figure 9A provides a clear illustration of the temporal trends in keyword co-occurrence frequency. The gradient from blue to red intuitively reflects the transition from lower to higher frequency values. Notably, the keywords “indoleamine 2,3-dioxygenase” and “tryptophan catabolism” have shown a consistent upward trend, underscoring their central role in the expanding intersection of immunology and cancer biology. Similarly, the increasing prevalence of terms such as “cancer” and “dendritic cells” reflects the rapid evolution of cancer immunotherapy and dendritic cell-based research. In recent years, keywords like “aryl-hydrocarbon receptor” and “kynurenine pathway” have exhibited accelerated growth, suggesting heightened interest in their roles as emerging regulators of immune response and

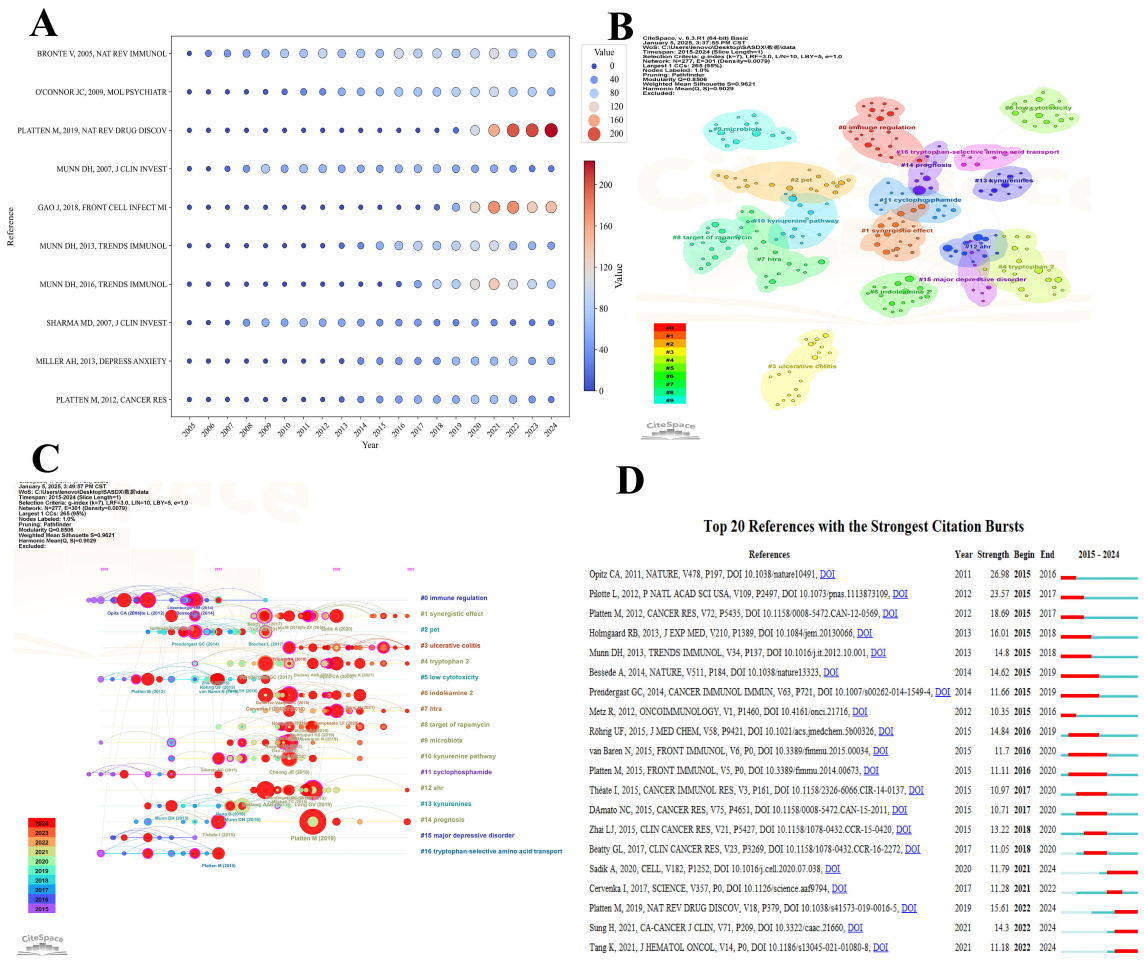

FIGURE 8
Visualization of the top cited references in tryptophan metabolism research in cancer. **(A)** Visualization map of the top 10 most cited references over the past 20 years, illustrating the temporal variation in citation frequency. Each bubble represents a publication, with its position corresponding to the citation count in a specific year. The size and color intensity of the bubbles reflect the citation frequency of the publication. **(B)** Thematic clustering map of the cited literature, where node size reflects citation frequency and node color represents distinct research themes. **(C)** The top sixteen clusters timeline distribution. Each node signifies a publication, with its size corresponding to the citation frequency in its respective year. The node colors transition from blue (2015) to red (2023), representing the temporal progression. Lines connect publications within the same cluster across various years, showcasing the temporal continuity and evolutionary paths of research within each cluster. **(D)** The top 20 references with the highest citation burst. A red bar represents a significant increase in citations during the corresponding year.

potential therapeutic targets. In contrast, foundational terms such as "expression" and "inhibition" have maintained relatively stable frequency, indicating their enduring relevance across various mechanistic studies. Additionally, the sustained rise in keywords such as "interferon-gamma" and "regulatory T cells" highlights their continued importance in immune-related research. The recurring prominence of "tryptophan catabolism", "kynurenine pathway", and "aryl-hydrocarbon receptor" further suggests a strong current focus on metabolic reprogramming and immunoregulatory mechanisms. Importantly, the heatmap reveals a marked surge in keyword activity between 2013 and 2015, coinciding with major advances in cancer immunology—particularly the clinical emergence of immune checkpoint inhibitors and other immunomodulatory therapies. These breakthroughs likely catalyzed the intensified research interest observed during this pivotal period.

The ridge plot presented in Figure 9B illustrates the distribution characteristics of the top 10 most frequently co-occurring keywords in the field. Among these, "indoleamine 2,3-dioxygenase" exhibits a distribution range of approximately between 50 and 550, indicating a high and relatively uniform occurrence frequency across this interval. This pattern suggests sustained research interest in this topic throughout the examined timeframe. Similarly, "tryptophan catabolism" displays a broad distribution from around 0 to 500, with particularly high frequencies between 300 and 400, underscoring its prominent role in the literature. In contrast, the keyword "expression" demonstrates a narrower distribution, ranging from approximately 50 to 400. Although its span is more limited, it still reflects consistent and substantial scholarly attention. Meanwhile, keywords such as "aryl-hydrocarbon receptor" and "kynurenine pathway" are primarily concentrated within the 0 to

10.3389/fonc.2025.1621666

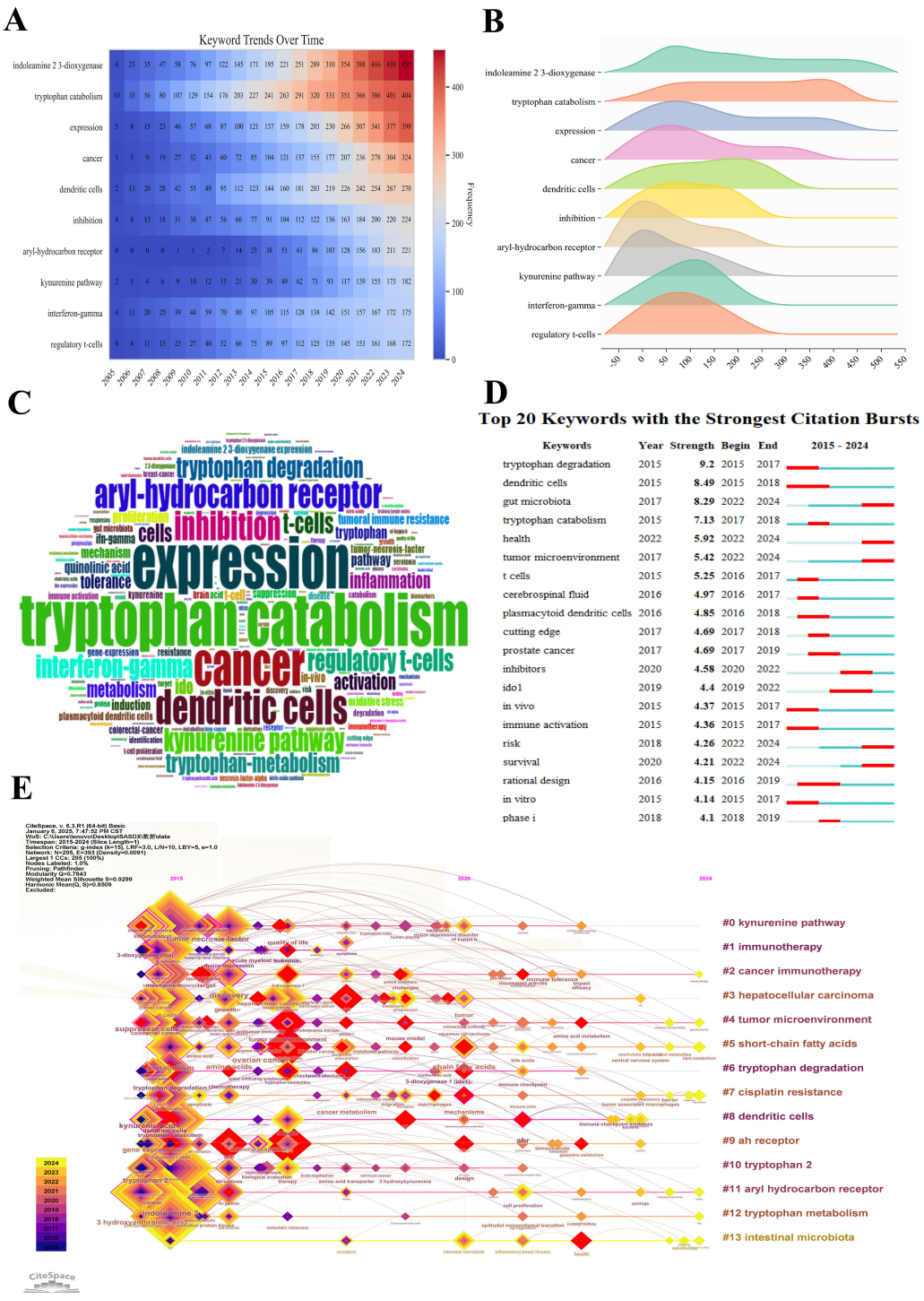

FIGURE 9
Visualization of the top keywords in tryptophan metabolism research in cancer. **(A)** Heatmap of keyword distribution over time in tryptophan metabolism and cancer research. The redder the color, the higher the co-occurrence frequency of keywords. **(B)** Ridge plot depicting the distribution patterns of the top 10 most frequently co-occurring keywords in tryptophan metabolism and cancer research. The length of each color distribution indicates a higher frequency of occurrence within that range, signifying the sustained attention these keywords have received in the literature. **(C)** Word cloud of the top 200 keywords in tryptophan metabolism and cancer research. The size of the keywords is proportional to their co-occurrence frequency. **(D)** The top 20 keywords with the strongest citation bursts. A red bar represents a significant increase in citations during the corresponding year. **(E)** Timeline visualization of keyword evolution based on CiteSpace. Node size reflects the research impact of keywords, with larger nodes indicating greater influence. Colors shift from purple (earlier years) to yellow (later years), showing time progression. Lines show connections between keywords, highlighting research topic relationships and development trends.

50 range, suggesting that these topics were not focal points in the early stages of research but may have gained prominence more recently. Figure 9C lists the top 200 co-occurring keywords, showing a positive correlation between word frequency and occurrence rate, which reinforces the trends identified in the ridge plot. Collectively, these findings indicate that research on tryptophan metabolism and its associated immunological mechanisms has emerged as a major hotspot in recent years, reflecting the growing interest in metabolic-immunological interplay in cancer biology.

Figure 9D highlights the top 20 keywords with the highest burst strength in the field of tryptophan metabolism and cancer. Between 2015 and 2017, "tryptophan degradation" exhibited the strongest citation burst (strength = 9.2), ranking first among all keywords. This was followed by "dendritic cells" (8.49) and "gut microbiota" (8.29), which ranked second and third, respectively. Notably, from 2022 to 2024, keywords such as "gut microbiota", "health", "tumor microenvironment", "risk", and "survival" remained highly active, indicating a sustained and growing interest in the interplay between tryptophan metabolism, immune regulation, and the tumor microenvironment. Additionally, keywords like "inhibitors" and "IDO1" experienced marked increases in burst strength between 2019 and 2022, a trend likely driven by the rapid advancements in tumor immunotherapy. Although other keywords—such as "plasmacytoid dendritic cells", "prostate cancer", "*in vivo*", "immune activation", "rational design", "*in vitro*", and "phase I"—exhibited comparatively lower burst intensities, they still demonstrated notable research activity during different time periods. These keywords collectively span a wide range of research topics, from basic biological mechanisms to clinical translational applications, reflecting the depth and multidimensional nature of the field. Figure 9E depicts the temporal evolution of keyword clusters, categorizing research themes into 13 groups. Each node represents a specific theme, with node size corresponding to its frequency in a given year. The color gradient—from purple (2011) to yellow (2024)—visually traces the chronological development of these themes. Among them, the "kynurenine pathway" cluster stands out as a dominant and sustained hotspot, as indicated by the large node size and continued presence over time. The connecting lines between nodes illustrate co-occurrence frequencies, providing insights into the interrelationships among various research domains and emphasizing the integrative, interdisciplinary nature of this evolving field.

4 Discussion

4.1 General information

In the field of tryptophan metabolism and cancer research, a total of 1,927 papers have been published across 781 academic journals by 11,134 researchers from 70 countries worldwide. Overall, both the number of publications and citation frequency have shown a steady upward trend over the years. However, this growth has decelerated in the past two years, likely due to the global disruptions caused by the COVID-19 pandemic. The United States leads the field in terms of research output, consistently maintaining a dominant position. Among individual researchers, Dietmar Fuchs ranks first in publication count, while the Medical University of Innsbruck stands out for its sustained productivity in this domain. The German Cancer Research Center has garnered significant attention due to the high citation frequency of its publications. *Frontiers in Immunology* has emerged as a key publication platform in this domain. Notably, the review by Platten et al. (2019), published in *Nature Reviews Drug Discovery*, is among the most highly cited works in the field. This seminal paper systematically assessed the therapeutic potential of key enzymes—IDO1, IDO2, TDO, and KMO (Kynurenine 3-monooxygenase)—highlighting their roles in immune modulation and tumor immune evasion. By offering a comprehensive framework for understanding the immunological functions of tryptophan metabolism, the study has laid the groundwork for translational advances in cancer therapy.

Co-citation analyses indicate that current research on tryptophan metabolism primarily focuses on several major solid tumors, including glioblastoma, breast cancer, lung cancer, colorectal cancer, and melanoma. In glioblastoma, studies have largely concentrated on IDO1-mediated immunosuppression and its pivotal role in resistance to immune checkpoint inhibitors. Research on breast and lung cancers has highlighted the kynurenine–aryl hydrocarbon receptor (AhR) axis and serotonin signaling as critical pathways contributing to tumor progression and immune evasion. In colorectal cancer, increasing attention has been paid to gut microbiota-derived indole metabolites and their regulatory roles in host–tumor interactions. Notably, melanoma has emerged as a key model for integrating tryptophan metabolism with cancer immunotherapy, particularly in clinical trials combining IDO1 inhibitors with PD-1/PD-L1 blockade. Collectively, these findings underscore tryptophan metabolism as a highly conserved and targetable pathway across diverse tumor types, offering a solid theoretical foundation for the development of both broad-spectrum and tumor-specific therapeutic strategies.

To date, the majority of studies have relied on *in vitro* cancer cell lines and *in vivo* murine models, primarily utilizing syngeneic or xenograft systems. Bibliometric analysis reveals that "*in vitro*" and "*in vivo*" were prominent burst keywords during 2015–2017, indicating a research focus heavily oriented toward basic experimental studies during this period. In recent years, however, there has been a marked shift toward clinical relevance, with increasing use of patient-derived materials such as tumor biopsies, plasma samples, and immune profiling data. The emergence of "inhibitors" as a burst keyword between 2020 and 2022 reflects a transition from mechanistic investigation to therapeutic intervention and translational application. Further keyword burst analysis reveals evolving frontiers in this field. High-frequency terms such as "gut microbiota," "tumor microenvironment," "aryl hydrocarbon receptor," and "cancer immunotherapy" suggest a paradigmatic shift from single-pathway metabolic studies toward integrated perspectives that encompass metabolic–immune–microbial interactions. Future

research on tryptophan metabolism is expected to place increasing emphasis on multidimensional mechanistic integration, clinical translation, and the advancement of precision oncology.

4.2 Mechanisms of tryptophan metabolism in cancer

Tryptophan is an essential amino acid that cannot be synthesized by the human body and must be obtained through dietary intake. Within the human body, tryptophan plays a crucial role in various biological processes, including protein synthesis, neurotransmitter production, and maintaining the normal function of the immune system (37). In recent years, the intricate metabolic pathways and regulatory mechanisms of tryptophan have garnered increasing attention in cancer research. Studies have shown that tryptophan metabolism is closely associated with tumorigenesis and treatment response, and it also serves as a key regulator in the immune evasion process. It modulates malignant phenotypes and contributes to the reprogramming of the tumor immune microenvironment (38). Disruptions in tryptophan metabolism have emerged as critical drivers of cancer progression, through mechanisms involving immune suppression, enhanced cell proliferation, metastasis, and metabolic reprogramming (39). The major metabolic pathways of tryptophan include the kynurenine (KYN) pathway, the serotonin (5-HT) pathway, and the gut microbiota metabolic pathway (40). Among these, the kynurenine pathway accounts for approximately 95% of total tryptophan metabolism, followed by the serotonin pathway (1–2%) and the microbial metabolic pathway (4–6%). Figure 10 illustrates the mechanisms of tryptophan metabolism in cancer.

4.2.1 Kynurenine pathway

The kynurenine (KYN) pathway, a major route of tryptophan catabolism, plays a pivotal role in tumor immune evasion (41). Bibliometric analysis shows a rising frequency of keywords such as "IDO1," "AhR," "inhibitors," and "kynurenine pathway" in recent years, reflecting sustained interest in this metabolic axis and its translational potential in oncology. In the tumor microenvironment (TME), expression of key enzymes—IDO1 and TDO—is markedly elevated (42). These enzymes convert tryptophan into KYN and downstream metabolites, including quinolinic acid and nicotinamide adenine dinucleotide (NAD^+), leading to local tryptophan depletion and KYN accumulation (30). Elevated KYN activates the aryl hydrocarbon receptor (AhR), triggering potent immunosuppressive effects. Mechanistically, KYN–AhR signaling suppresses the proliferation and cytotoxicity of effector T cells ($CD4^+$, $CD8^+$, and $CD25^+$) and inhibits the secretion of pro-inflammatory cytokines such as interferon-gamma (IFN-γ) and interleukin-2 (IL-2) (43). At the same time, it promotes the differentiation of naïve $CD4^+$ T cells into regulatory T cells (Tregs), increasing the release of immunosuppressive cytokines including transforming growth factor-beta (TGF-β) and interleukin-10 (IL-10) (44). KYN also impairs the activation and receptor expression of natural killer (NK) cells, reducing their antitumor activity. Beyond immunosuppression, KYN and its metabolites activate oncogenic signaling pathways such as MAPK and PI3K/AKT, thereby promoting tumor cell proliferation, survival, epithelial–mesenchymal transition (EMT), and metastatic potential (45).

Given its central role in these processes, IDO1, the rate-limiting enzyme in tryptophan degradation, has emerged as a key therapeutic target in cancer immunotherapy. Among the ten most co-cited references, eight highlight IDO's role in immune evasion—particularly in cancer—and emphasize the therapeutic promise of IDO inhibitors. The remaining two focus on the role of gut microbiota in modulating immunity and intestinal barrier function via tryptophan metabolism, and on the kynurenine pathway's relevance as a biomarker and potential target in neuropsychiatric and inflammatory disorders. Collectively, these studies underscore the prominence of "IDO" as a frequently co-occurring keyword, reinforcing its importance in tumor immunology. Preclinical studies have shown that IDO1 inhibitors such as epacadostat can enhance the antitumor efficacy of PD-1 blockade, fueling enthusiasm for targeting this pathway. This enthusiasm is mirrored in bibliometric data, where "IDO" consistently ranks among the top co-occurring terms. However, clinical development has faced significant setbacks. In 2018, the phase III ECHO-301/KEYNOTE-252 trial revealed that combining epacadostat with pembrolizumab failed to improve progression-free survival (PFS) or overall survival (OS) in advanced melanoma patients, raising considerable concern. Similarly, the combination of navoximod with atezolizumab did not achieve its primary efficacy endpoints. These failures have been attributed to issues such as suboptimal dosing, inadequate suppression of intratumoral KYN levels, and potential paradoxical activation of AhR by certain inhibitors, highlighting the complexity of this pathway and the need for deeper mechanistic insights. Consequently, several companies have discontinued related drug development programs (46–48).

Despite these challenges, bibliometric trends indicate a continued—albeit slower—growth in publications, suggesting ongoing interest and a shift in research direction. One emerging focus is the development of predictive biomarkers; for instance, the KYN/Trp ratio is being investigated as a surrogate marker for IDO1 or TDO activity to aid in therapeutic response assessment and patient stratification (49, 50). Another priority is identifying compensatory mechanisms and alternative targets. For example, TDO2 is highly expressed in lung adenocarcinoma, and its inhibition has been shown to downregulate PD-L1 and improve immune responsiveness (51). Kynureninase, an enzyme that degrades KYN and limits AhR activation, has also shown therapeutic potential (52). In parallel, AhR antagonists such as BAY-218 are under investigation as alternatives to IDO1 blockade due to their ability to prevent Treg induction and checkpoint molecule expression (53). Dual inhibitors like RG70099 and CMG017, which simultaneously target IDO1 and TDO2, have demonstrated the ability to reduce systemic KYN levels, offering a strategy to overcome the limitations of monotherapies (54, 55). Synthetic biology approaches are also being explored to integrate

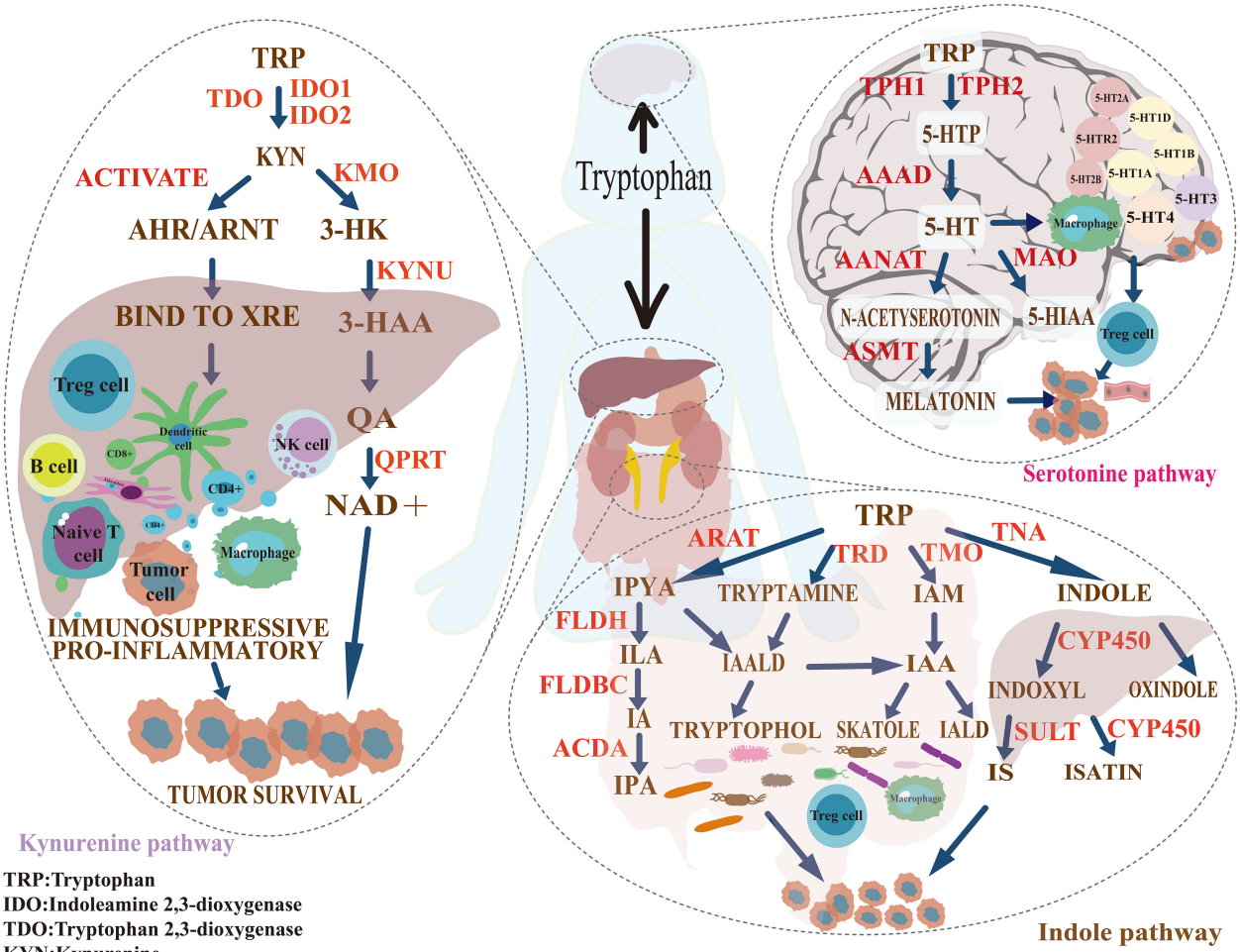

FIGURE 10
Mechanism illustration of tryptophan metabolism in cancer. Tryptophan is an essential amino acid that must be obtained through dietary intake. Its metabolism primarily occurs via three pathways: the kynurenine (KYN) pathway (approximately 95%), the serotonin (5-HT) pathway (about 1–2%), and the gut microbiota metabolic pathway (around 4–6%). These pathways play important roles in tumorigenesis, immune regulation, and cancer progression.

IDO1 inhibition with T cell engineering, aiming to enhance antitumor immunity (56). Moreover, noncanonical regulatory mechanisms have attracted attention—for instance, the USP14 inhibitor IU1 has been reported to downregulate IDO1 expression and restore T cell–mediated antitumor responses in colorectal cancer models (57).

4.2.2 5-HT pathways

The 5-hydroxytryptamine (5-HT) metabolic pathway has recently emerged as a crucial regulator in tumor biology, particularly through its involvement in remodeling the tumor microenvironment (TME), mediating immune suppression, and driving metabolic reprogramming. Bibliometric co-occurrence analysis highlights a high frequency of keywords such as “tumor microenvironment,” “immune regulation,” “dendritic cells,” and “metabolic reprogramming,” underscoring the close association between the 5-HT pathway and these cutting-edge research areas. Tumor cells metabolize tryptophan into 5-HT via the enzyme tryptophan hydroxylase 1 (TPH1) (58). Subsequently, 5-HT activates specific receptors, including 5-HT receptor 2B (HTR2B) and 5-HT receptor 7 (HTR7), which initiate signaling cascades that promote metabolic reprogramming and suppress immune

responses (59, 60). For instance, 5-HT signaling through 5-HTR2A/C receptors activates Jak1, leading to phosphorylation of STAT3 (61). This event upregulates hypoxia-inducible factor-1α (HIF-1α) and pyruvate kinase M2 (PKM2), thereby enhancing glycolysis and glucose uptake to support rapid tumor proliferation. Concurrently, 5-HT stimulates adenylate cyclase (AC), elevating intracellular cAMP levels, which activate protein kinase A (PKA) and promote phosphorylation of CREB. This pathway improves mitochondrial function, enabling tumor cells to survive under hypoxic and nutrient-deprived conditions (62). By reducing lactate accumulation and tumor acidosis, this cascade also restricts immune cell infiltration. Furthermore, 5-HT activates the PI3K/Akt/mTOR signaling pathway, which further facilitates metabolic reprogramming and immune evasion in the tumor context (63).

Beyond its direct role in metabolic regulation, 5-HT also modulates the tumor immune microenvironment, consistent with bibliometric analyses that highlight "immune regulation" and "dendritic cells" as key research focuses. It promotes the polarization of tumor-associated macrophages (TAMs) toward the M2 phenotype. These M2-type TAMs secrete immunosuppressive cytokines, such as IL-10 and TGF-β, which inhibit the activity of effector T cells and NK cells, thereby facilitating tumor immune evasion (64–66). The immunosuppressive milieu established by M2 TAMs further supports tumor growth and metastasis. In colorectal cancer models, knockout of TPH2 significantly suppresses tumor growth, suggesting that TPH2-positive neurons in the gut promote cancer stem cell (CSC) proliferation through 5-HT secretion (67). Moreover, 5-HT stabilizes β-catenin and stimulates CSC expansion by activating the Wnt/β-catenin signaling pathway, thereby driving tumor progression and metastasis. Its metabolite, 5-hydroxyindoleacetic acid (5-HIAA), enhances neutrophil migration and inflammatory responses via activation of the G protein-coupled receptor 35 (GPR35), which further contributes to immune evasion (68). Additionally, 5-HT functions in an autocrine manner through the HTR2B receptor to increase aerobic glycolysis in tumor cells under metabolic stress, supplying essential substrates for tumor growth (69). This mechanism reinforces the concept of "metabolic reprogramming," as identified in keyword cluster analyses.

Despite the role of 5-HT metabolites in promoting tumor immune evasion, this pathway's activity can be effectively modulated through pharmacological interventions. TPH1 inhibitors, such as telotristat ethyl (TE), have received FDA approval for treating carcinoid syndrome and exhibit potent inhibition of 5-HT synthesis (70). Preclinical studies have demonstrated that TE suppresses tumor growth across various cancer types and enhances the antitumor efficacy of immune checkpoint inhibitors. Other TPH inhibitors, including LP-533401 and p-chlorophenylalanine (CPA), have shown antitumor activity in breast cancer and cholangiocarcinoma models (71, 72). These findings correspond with bibliometric data that frequently highlight keywords such as "immune checkpoint" and "inhibitor," underscoring the translational potential of targeting the 5-HT pathway. Beyond TPH1 inhibition, alternative strategies targeting 5-HT signaling have garnered increasing attention. Selective serotonin reuptake inhibitors (SSRIs), such as fluoxetine and sertraline, have demonstrated antitumor effects in models of breast cancer, colorectal cancer, hepatocellular carcinoma, and glioblastoma (73–76). Their mechanisms of action likely involve induction of apoptosis, inhibition of cell proliferation, and activation of the p53 signaling pathway. Furthermore, both agonists and antagonists of 5-HT receptors show promise in cancer therapy. For example, tropisetron and palonosetron, two 5-HT3 receptor antagonists commonly used to alleviate chemotherapy-induced side effects, have also been found to inhibit the growth and metastasis of colorectal and lung cancers (77). Monoamine oxidase A (MAOA), which is highly expressed in prostate cancer and associated with increased tumor aggressiveness and poor prognosis, represents another therapeutic target. MAOA inhibitors such as clorgyline and phenelzine have demonstrated the ability to slow tumor progression in prostate cancer models and may restore sensitivity to enzalutamide (78, 79). Early clinical evidence further suggests that phenelzine may benefit patients with biochemically recurrent castration-sensitive prostate cancer, and its combination with docetaxel may enhance antitumor efficacy (80).

4.2.3 Indole pathway

Keyword burst analysis highlights a recent surge in terms such as "gut microbiota," "immune checkpoint blockade," and "metabolic reprogramming" between 2022 and 2024, reflecting the expanding use of multi-omics technologies in tryptophan metabolism research. Single-cell transcriptomics, metabolomics, and microbiome sequencing are increasingly deployed to dissect how tryptophan-derived metabolites modulate immune dynamics and shape the TME (81). A landmark study by Gao et al. (2018) defined a mechanistic framework linking microbial tryptophan metabolism to immune regulation and epithelial integrity, laying the foundation for the "microbiota–tryptophan–immune axis" (82). Indole derivatives generated by gut microbes—e.g., indole-3-aldehyde (I3A), indole acrylic acid (IA), indole-3-acetic acid (IAA), and indoxyl sulfate (IS)—activate the aryl hydrocarbon receptor (AhR), thereby orchestrating immune cell behavior and TME remodeling (83). Certain metabolites, particularly those linked to indole-3-pyruvate (I3P), drive M2-like polarization of tumor-associated macrophages (TAMs) through AhR signaling, fostering immune suppression and tumor growth (84). Others inhibit indoleamine 2,3-dioxygenase 1 (IDO1), reducing kynurenine (KYN) levels and partially reversing immune evasion (85). Downstream products such as 3-hydroxykynurenine (3-HK) suppress tryptophan hydroxylase 1 (TPH1), lowering serotonin (5-HT) synthesis, which exerts dual immunoregulatory effects (86).

IL4I1, an L-amino acid oxidase, metabolizes tryptophan into I3P and its derivatives. Its elevated expression in immune checkpoint blockade (ICB)-resistant tumors suggests a key role in immunosuppression via AhR activation and positions IL4I1 as a potential therapeutic target (87, 88). This mechanistic insight mirrors bibliometric trends highlighting increased interest in metabolic reprogramming and immune escape. Microbial indole metabolites also show strain-specific immunological consequences. Bacteroides fragilis-derived I3A promotes barrier integrity and immune

homeostasis via AhR activation (89), whereas Porphyromonas gingivalis-derived IAA drives immune tolerance and invasive tumor phenotypes (90). These metabolites not only influence local immunity but also reprogram the TME and affect tumor evolution. Synthetic biology provides emerging tools to engineer microbial pathways and therapeutically manipulate tryptophan metabolism (91). Engineered bacteria can be programmed to colonize tumors and deliver immunomodulatory payloads, including cytokines, cytotoxins, or RNA therapeutics. Incorporation of gene circuits—featuring suicide switches, quorum sensing, and logic gates—enhances the safety and precision of these approaches, addressing limitations of conventional therapies (92). Bibliometric trends reflect increasing convergence between microbiome engineering and immunometabolism. Preclinical models show that combining a low-tryptophan diet with IDO1 inhibition produces synergistic anti-tumor effects by limiting Trp availability and suppressing KYN-driven immune evasion. However, microbial compensation via alternative Trp pathways necessitates balancing dietary interventions with microbiome stability (93). Biomarkers like the plasma KYN/Trp ratio have been associated with immunotherapy outcomes, while microbial-derived indoles are being explored as prognostic indicators (49).

4.3 Comparative analysis of tryptophan metabolism and other cancer-related metabolic pathways

In recent years, cancer metabolism research has advanced significantly across multiple metabolic pathways. The development of multi-omics metabolomic technologies has greatly improved our ability to elucidate complex interactions among these pathways, facilitating systematic comparative analyses and the development of precise therapeutic strategies. Among these, the metabolic pathways of glutamine, arginine, glucose, and tryptophan have garnered sustained attention. Although no systematic bibliometric analysis has specifically targeted glutamine metabolism in cancer, some studies have explored its association with diabetes. Between 2001 and 2022, a total of 945 relevant publications were identified, showing a steady growth in output since 2007 and reaching a peak around 2017 (94). Arginine metabolism demonstrates significant potential in tumor immunoregulation, particularly through ASS1 downregulation-mediated arginine deprivation therapy (ADT) and its impact on T cell function as well as the expansion of MDSCs and Tregs. These mechanisms have been observed across various cancers, including pancreatic, liver, small-cell lung, and colorectal carcinomas (95). However, systematic bibliometric analyses on this metabolic pathway remain limited. Glucose metabolism, due to its central role in energy metabolic reprogramming, was among the earliest focal points in cancer metabolism research. Taking breast cancer as an example, 957 related publications were identified between 2004 and 2024. The number of publications has risen markedly since 2015, nearly tripling compared to 2010, and peaked in 2022 with over 100 articles, reflecting sustained and active research interest in this field (96). Bibliometric research on tryptophan metabolism is comparatively abundant, with 1,927 relevant publications included from 2005 to 2024. The overall trend demonstrates steady growth, with a pronounced acceleration between 2019 and 2021, culminating in an annual peak of 196 publications in 2021. Although its period of heightened activity began slightly later than that of glutamine metabolism, the peak publication volume notably surpasses those of glutamine and glucose metabolism, reflecting a rapid increase in research interest within this field in recent years.

4.4 Limitations

This study presents the first bibliometric analysis that systematically investigates the global research landscape on tryptophan metabolism in cancer from 2005 to 2024. By leveraging multidimensional visualization tools, including CiteSpace, VOSviewer, Python, and R Bibliometrix, this study provides a comprehensive overview of research trends, key contributors, and emerging topics, offering valuable insights into the evolution of this field. Despite its significant academic contributions, this study has certain limitations. First, the dataset is exclusively sourced from the Web of Science Core Collection and only includes English-language publications. This restriction may lead to the exclusion of relevant studies published in other languages, potentially limiting the comprehensiveness of global research insights. Second, discrepancies in algorithmic approaches and metric calculations among different visualization tools may introduce variations in analytical results. Future studies should consider integrating data from multiple databases, incorporating multilingual literature, and adopting diverse analytical methodologies to enhance the robustness and comprehensiveness of bibliometric assessments.

5 Conclusions

This study systematically analyzed the research progress on tryptophan metabolism in cancer from 2005 to 2024 using bibliometric methods, highlighting the rapid expansion and growing importance of this research field. Our analysis confirms that tryptophan metabolism—particularly via the kynurenine pathway—plays a pivotal role in tumor progression, immune suppression, and therapeutic resistance. Despite significant advances, several knowledge gaps remain. First, most current studies are preclinical, and the translation of findings into clinical applications remains limited. The precise molecular mechanisms by which different branches of tryptophan metabolism—kynurenine, serotonin, and microbial indole pathways—interact with immune cells in the tumor microenvironment require further elucidation. Second, there is a lack of validated biomarkers for predicting treatment response or guiding patient stratification, especially in the context of immune checkpoint blockade. Third, the therapeutic potential of targeting multiple metabolic pathways simultaneously has yet to be fully explored.

Future research should prioritize translational studies that bridge basic mechanistic findings with clinical outcomes, including the validation of plasma or tissue-based biomarkers such as the KYN/Trp ratio or microbiota-derived metabolites. Additionally, therapeutic strategies that combine metabolic enzyme inhibitors (e.g., IDO1/TDO, IL4I1) with immunotherapy warrant deeper investigation, particularly in resistant tumors. Integrative multi-omics approaches and systems biology tools will be essential for mapping the complex network of tryptophan metabolism and its crosstalk with other oncogenic pathways. Moreover, synthetic biology and engineered microbial therapeutics offer promising platforms for modulating tryptophan metabolism in a tumor-specific manner. International and interdisciplinary collaborations will be crucial in developing precise, multi-targeted interventions aimed at overcoming tumor immune escape and improving patient outcomes.

Data availability statement

The original contributions presented in the study are included in the article/Supplementary Material. Further inquiries can be directed to the corresponding authors.

Author contributions

HM: Conceptualization, Data curation, Formal analysis, Methodology, Visualization, Writing – original draft, Writing – review & editing. RD: Conceptualization, Data curation, Formal analysis, Methodology, Visualization, Writing – review & editing. JW: Conceptualization, Data curation, Formal analysis, Methodology, Visualization, Writing – review & editing. GD: Formal analysis, Methodology, Visualization, Writing – review & editing. YZ: Data curation, Methodology, Visualization, Writing – review & editing. QL: Data curation, Methodology, Visualization, Writing – review & editing. YH: Methodology, Visualization, Writing – review & editing. HC: Methodology, Visualization, Writing – review & editing. HJ: Data curation, Formal analysis, Funding acquisition, Methodology, Project administration, Supervision, Visualization, Writing – original draft, Writing – review & editing.

Funding

The author(s) declare that financial support was received for the research and/or publication of this article. This study was supported by a subproject of the National Key Research and Development Program of China (Grant No. 2020YFC2006002-03).

Acknowledgments

The authors would like to express gratitude to all the staff members who participated in this research.

Conflict of interest

The authors declare that the research was conducted in the absence of any commercial or financial relationships that could be construed as a potential conflict of interest.

Generative AI statement

The author(s) declare that no Generative AI was used in the creation of this manuscript.

Publisher's note

Supplementary material

The Supplementary Material for this article can be found online at: https://www.frontiersin.org/articles/10.3389/fonc.2025.1621666/full#supplementary-material

References

1. Brown JS, Amend SR, Austin RH, Gatenby RA, Hammarlund EU, Pienta KJ. Updating the definition of cancer. *Mol Cancer Res*. (2023) 21:1142–7. doi: 10.1158/1541-7786

2. Chen SM, Cao Z, Prettner K, Kuhn M, Yang JT, Jiao LR, et al. Estimates and projections of the global economic cost of 29 cancers in 204 countries and territories from 2020 to 2050. *JAMA Oncol*. (2023) 9:465–72. doi: 10.1001/jamaoncol.2022.7826

3. Bizuayehu HM, Ahmed KY, Kibret GD, Dadi AF, Belachew SA, Bagade T, et al. Global disparities of cancer and its projected burden in 2050. *JAMA Netw Open*. (2024) 7:e2443198. doi: 10.1001/jamanetworkopen.2024.43198

4. Kaur R, Bhardwaj A, Gupta S. Cancer treatment therapies: traditional to modern approaches to combat cancers. *Mol Biol Rep*. (2023) 50:9663–76. doi: 10.1007/s11033-023-08809-3

5. Nazari A, Osati P, Fakhr SS, Faghihkhorasani F, Ghanaatian M, Faghihkhorasani F, et al. New emerging therapeutic strategies based on manipulation of the redox regulation against therapy resistance in cancer. *Antioxid Redox Signaling*. (2024). doi: 10.1089/ars.2023.0491

6. Nobari SA, Doustvandi MA, Yaghoubi SM, Oskouei SSS, Alizadeh E, Nour MA, et al. Emerging trends in quantum dot-based photosensitizers for enhanced photodynamic therapy in cancer treatment. *J Pharm Invest*. (2024) 55:55–90. doi: 10.1007/s40005-024-00698-3

7. Shamaeizadeh A, Beigi A, Naghib SM, Tajabadi M, Rahmanian M, Mozafari MR. Smart nanobiomaterials for gene delivery in localized cancer therapy: an overview from emerging materials and devices to clinical applications. *Curr Cancer Drug Targets*. (2024) 8:1012–42. doi: 10.2174/0115680096288917240404060506

8. Zhao YT, Sun JQ, Xu XL, Su J, Du YZ. The potential of nanosystems in disrupting adenosine signaling pathways for tumor immunotherapy. *Expert Opin Drug Deliv*. (2024) 21:1755–70. doi: 10.1080/17425247.2024.2417687

9. Liu Y, Zhou Q, Song SL, Tang S. Integrating metabolic reprogramming and metabolic imaging to predict breast cancer therapeutic responses. *Trends Endocrinol Metab*. (2021) 32:762–75. doi: 10.1016/j.tem.2021.07.001

10. Chen Z, Li Y, Tan B, Zhao Q, Fan L, Li F, et al. Progress and current status of molecule-targeted therapy and drug resistance in gastric cancer. *Drugs Today*. (2020) 56:469–82. doi: 10.1358/dot.2020.56.7.3112071

11. Martins AC, Oshiro MY, Albericio F, de la Torre BG. Food and drug administration (Fda) approvals of biological drugs in 2023. *Biomedicines*. (2024) 12:1992. doi: 10.3390/biomedicines12091992

12. Yuan S, Yu B, Liu HM. New drug approvals for 2019: synthesis and clinical applications. *Eur J Med Chem*. (2020) 205:112667. doi: 10.1016/j.ejmech.2020.112667

13. Brown DG, Wobst HJ. A decade of fda-approved drugs (2010-2019): trends and future directions. *J Med Chem*. (2021) 64:2312–38. doi: 10.1021/acs.jmedchem.0c01516

14. Mathlouthi S, Kuryk L, Prygiel M, Lupo MG, Zasada AA, Pesce C, et al. Extracellular vesicles powered cancer immunotherapy: targeted delivery of adenovirus-based cancer vaccine in humanized melanoma model. *J Controlled Release*. (2024) 376:777–93. doi: 10.1016/j.jconrel.2024.10.057

15. Chen QQ, Guo XJ, Ma WX. Opportunities and challenges of cd47-targeted therapy in cancer immunotherapy. *Oncol Res*. (2024) 32:49–60. doi: 10.32604/or.2023.042383

16. Joshi DC, Sharma A, Prasad S, Singh K, Kumar M, Sherawat K, et al. Novel therapeutic agents in clinical trials: emerging approaches in cancer therapy. *Discov Oncol*. (2024) 15:342. doi: 10.1007/s12672-024-01195-7

17. Meira M, Frey A, Chekkat N, Rybczynska M, Sellam Z, Park JS, et al. Targeting rgmb interactions: discovery and preclinical characterization of potent anti-rgmb antibodies blocking multiple ligand bindings. *Mabs*. (2024) 16:2432403. doi: 10.1080/19420862.2024.2432403

18. Wang Y, Zhao LW, Zhang Z, Liu P. Immunogenic cell death inducers and pd-1 blockade as neoadjuvant therapy for rectal cancer. *Oncoimmunology*. (2024) 13:2416558. doi: 10.1080/2162402x.2024.2416558

19. Arner EN, Rathmell JC. Metabolic programming and immune suppression in the tumor microenvironment. *Cancer Cell*. (2023) 41:421–33. doi: 10.1016/j.ccell.2023.01.009

20. Xue C, Li G, Zheng Q, Gu X, Shi Q, Su Y, et al. Tryptophan metabolism in health and disease. *Cell Metab*. (2023) 35:1304–26. doi: 10.1016/j.cmet.2023.06.004

21. Zárate LV, Miret NV, Candia AJN, Zappia CD, Pontillo CA, Chiappini FA, et al. Breast cancer progression and kynurenine pathway enzymes are induced by hexachlorobenzene exposure in a her2-positive model. *Food Chem Toxicol*. (2023) 177:113822. doi: 10.1016/j.fct.2023.113822

22. Perez-Castro L, Garcia R, Venkateswaran N, Barnes S, Conacci-Sorrell M. Tryptophan and its metabolites in normal physiology and cancer etiology. *FEBS J*. (2023) 290:7–27. doi: 10.1111/febs.16245

23. Wu XA, Jin B, Liu X, Mao YL, Wan XS, Du SD. Research trends of cellular immunotherapy for primary liver cancer: A bibliometric analysis. *Hum Vaccines Immunotherapeut*. (2024) 20:2426869. doi: 10.1080/21645515.2024.2426869

24. Li JQ, Li XX, Fu YY, Meng HB, Xu D, Hou WY. Visualizing immunotherapy for multiple myeloma worldwide from 2013 to 2023: A bibliometric analysis. *Hum Vaccines Immunotherapeut*. (2024) 20:2433304. doi: 10.1080/21645515.2024.2433304

25. Chen YM, Lu XJ, Peng GY, Liu SJ, Wang M, Hou HM. A bibliometric analysis of research on pd-1/pd-L1 in urinary tract tumors. *Hum Vaccines Immunotherapeut*. (2024) 20:2390727. doi: 10.1080/21645515.2024.2390727

26. Zheng DT, Chen LZ, Tian HT, Yang QP, Wu JY, Ji ZQ, et al. A scientometric analysis of research trends on emerging contaminants in the field of cancer in 2012-2021. *Front Public Health*. (2022) 10:1034585. doi: 10.3389/fpubh.2022.1034585

27. Brandacher G, Perathoner A, Ladurner R, Schneeberger S, Obrist P, Winkler C, et al. Prognostic Value of Indoleamine 2,3-Dioxygenase Expression in Colorectal Cancer: Effect on Tumor-Infiltrating T Cells. *Clin Cancer Res*. (2006) 12:1144–51. doi: 10.1158/1078-0432.CCR-05-1966

28. Pilotte L, Larrieu P, Stroobant V, Colau D, Dolusic E, Frederick R, et al. Reversal of Tumoral Immune Resistance by Inhibition of Tryptophan 2,3-Dioxygenase. *Proc Natl Acad Sci U S A*. (2012) 109:2497–502. doi: 10.1073/pnas.1113873109

29. Munn DH, Mellor AL. Indoleamine 2,3-Dioxygenase and Tumor-Induced Tolerance. *J Clin Invest*. (2007) 117:1147–54. doi: 10.1172/JCI31178

30. Platten M, Nollen EAA, Röhrig UF, Fallarino F, Opitz CA. Tryptophan metabolism as a common therapeutic target in cancer, neurodegeneration and beyond. *Nat Rev Drug Discov*. (2019) 18:379–401. doi: 10.1038/s41573-019-0016-5

31. Metz R, Duhadaway JB, Kamasani U, Laury-Kleintop L, Muller AJ, Prendergast GC. Novel Tryptophan Catabolic Enzyme Ido2 Is the Preferred Biochemical Target of the Antitumor Indoleamine 2,3-Dioxygenase Inhibitory Compound D-1-Methyl-Tryptophan. *Cancer Res*. (2007) 67:7082–7087. doi: 10.1158/0008-5472.CAN-07-1872

32. Platten M, Wick W, Van den Eynde BJ. Tryptophan Catabolism in Cancer: Beyond Ido and Tryptophan Depletion. *Cancer Res*. (2012) 72:5435–5440. doi: 10.1158/0008-5472.CAN-12-0569

33. Liu X, Shin N, Koblish HK, Yang G, Wang Q, Wang K, et al. Selective Inhibition of Ido1 Effectively Regulates Mediators of Antitumor Immunity. *Blood*. (2010) 115:3520–3530. doi: 10.1182/blood-2009-09-246124

34. Lob S, Konigsrainer A, Zieker D, Brucher BL, Rammensee HG, Opelz G, et al. Ido1 and Ido2 Are Expressed in Human Tumors: Levo- but Not Dextro-1-Methyl Tryptophan Inhibits Tryptophan Catabolism. *Cancer Immunol Immunother*. (2009) 58:153–157. doi: 10.1007/s00262-008-0513-6

35. Sharma MD, Baban B, Chandler P, Hou DY, Singh N, Yagita H, et al. Plasmacytoid Dendritic Cells from Mouse Tumor-Draining Lymph Nodes Directly Activate Mature Tregs Via Indoleamine 2,3-Dioxygenase. *J Clin Invest*. (2007) 117:2570–2582. doi: 10.1172/JCI31911

36. Lob S, Konigsrainer A, Rammensee HG, Opelz G, Terness P. Inhibitors of Indoleamine-2,3-Dioxygenase for Cancer Therapy: Can We See the Wood for the Trees? *Nat Rev Cancer*. (2009) 9:445–452. doi: 10.1038/nrc2639

37. Zhang HL, Zhang AH, Miao JH, Sun H, Yan GL, Wu FF, et al. Targeting regulation of tryptophan metabolism for colorectal cancer therapy: A systematic review. *Rsc Adv*. (2019) 9:3072–80. doi: 10.1039/c8ra08520j

38. Zhang SX, Chen SL, Wang ZH, Li JH, Yuan YB, Feng WT, et al. Prognosis prediction and tumor immune microenvironment characterization based on tryptophan metabolism-related genes signature in brain glioma. *Front Pharmacol*. (2022) 13:1061597. doi: 10.3389/fphar.2022.1061597

39. Li F, Hu HY, Li LY, Ding LF, Lu ZY, Mao XD, et al. Integrated machine learning reveals the role of tryptophan metabolism in clear cell renal cell carcinoma and its association with patient prognosis. *Biol Direct*. (2024) 19:132. doi: 10.1186/s13062-024-00576-w

40. Hou YJ, Li J, Ying SH. Tryptophan metabolism and gut microbiota: A novel regulatory axis integrating the microbiome, immunity, and cancer. *Metabolites*. (2023) 13:1166. doi: 10.3390/metabo13111166

41. Tan QW, Deng SH, Xiong LJ. Role of kynurenine and its derivatives in liver diseases: recent advances and future clinical perspectives. *Int J Mol Sci*. (2025) 26:968. doi: 10.3390/ijms26030968

42. Seo S-K, Kwon B. Immune regulation through tryptophan metabolism. *Exp Mol Med*. (2023) 55:1371–9. doi: 10.1038/s12276-023-01028-7

43. Yang T, Li QQ, Liu YM, Yang B. T cells in pancreatic cancer stroma: tryptophan metabolism plays an important role in immunoregulation. *World J Gastroenterol*. (2023) 29:2701–3. doi: 10.3748/wjg.v29.i17.2701

44. Xu XL, Yuan HY, Lv QJ, Wu ZJ, Fan WH, Liu JJ. Indoleamine 2, 3-dioxygenase regulates the differentiation of T lymphocytes to promote the growth of gastric cancer cells through the pi3k/akt/mtor pathway. *Cell Biochem Biophysics*. (2024) 83:2289–99. doi: 10.1007/s12013-024-01641-x

45. Wang LX, Zhou X, Yan HS, Miao YP, Wang BB, Gu YH, et al. Deciphering the role of tryptophan metabolism-associated genes echs1 and aldh2 in gastric cancer: implications for tumor immunity and personalized therapy. *Front Immunol*. (2024) 15:1460308. doi: 10.3389/fimmu.2024.1460308

46. De Martino M, Rathmell JC, Galluzzi L, Vanpouille-Box C. Cancer cell metabolism and antitumour immunity. *Nat Rev Immunol*. (2024) 24:654–69. doi: 10.1038/s41577-024-01026-4

47. Luke JJ, Fakih M, Schneider C, Chiorean EG, Bendell J, Kristeleit R, et al. Phase I/ii sequencing study of azacitidine, epacadostat, and pembrolizumab in advanced solid tumors. *Br J Cancer*. (2023) 128:2227–35. doi: 10.1038/s41416-023-02267-1

48. Lu ZH, Zhang CC, Zhang J, Su W, Wang GY, Wang ZQ. The kynurenine pathway and indole pathway in tryptophan metabolism influence tumor progression. *Cancer Med*. (2025) 14:e70703. doi: 10.1002/cam4.70703

49. Mandarano M, Orecchini E, Bellezza G, Vannucci J, Ludovini V, Baglivo S, et al. Kynurenine/tryptophan ratio as a potential blood-based biomarker in non-small cell lung cancer. *Int J Mol Sci*. (2021) 22:4403. doi: 10.3390/ijms22094403

50. Meireson A, Ferdinande L, Haspeslagh M, Hennart B, Allorge D, Ost P, et al. Clinical relevance of serum kyn/trp ratio and basal and ifnγ-upregulated ido1 expression in peripheral monocytes in early stage melanoma. *Front Immunol*. (2021) 12:736498. doi: 10.3389/fimmu.2021.736498

51. Jin E, Yin ZD, Zheng XX, Yan CH, Xu K, Eunice FY, et al. Potential of targeting tdo2 as the lung adenocarcinoma treatment. *J Proteome Res*. (2024) 23:1341–50. doi: 10.1021/acs.jproteome.3c00746

52. Labadie BW, Bao RY, Luke JJ. Reimagining ido pathway inhibition in cancer immunotherapy via downstream focus on the tryptophan-kynurenine-aryl hydrocarbon axis. *Clin Cancer Res*. (2019) 25:1462–71. doi: 10.1158/1078-0432.Ccr-18-2882

53. Gutcher I, Kober C, Roese L, Roewe J, Schmees N, Prinz F, et al. Blocking tumor-associated immune suppression with bay-218, a novel, selective aryl hydrocarbon receptor (Ahr) inhibitor. *Cancer Res*. (2019) 79:Abstract nr 1288. doi: 10.1158/1538-7445.Am2019-1288

54. Gyulveszi G, Fischer C, Mirolo M, Stern M, Green L, Ceppi M, et al. Rg70099: A novel, highly potent dual ido1/tdo inhibitor to reverse metabolic suppression of immune cells in the tumor micro-environment. *Cancer Res*. (2016) 76:Abstract nr LB-085. doi: 10.1158/1538-7445.Am2016-lb-085

55. Kim C, Kim JH, Kim JS, Chon HJ, Kim JH. A novel dual inhibitor of 100 and tdo, cmg017, potently suppresses the kynurenine pathway and overcomes resistance to

immune checkpoint inhibitors. *J Clin Oncol*. (2019) 37:e14228. doi: 10.1200/JCO.2019.37.15_suppl.e14228

56. Wang H, Xu F, Yao CL, Dai HX, Xu JL, Wu BB, et al. Engineering bacteria for cancer immunotherapy by inhibiting ido activity and reprogramming cd8+T cell response. *Proc Natl Acad Sci United States America*. (2024) 121:e2412070121. doi: 10.1073/pnas.2412070121

57. Shi DN, Wu XQ, Jian YT, Wang JY, Huang CM, Mo S, et al. Usp14 promotes tryptophan metabolism and immune suppression by stabilizing ido1 in colorectal cancer. *Nat Commun*. (2022) 13:5644. doi: 10.1038/s41467-022-33285-x

58. Siddiqui EJ, Thompson CS, Mikhailidis DP, Mumtaz FH. The role of serotonin in tumour growth (Review). *Oncol Rep*. (2005) 14:1593–7. doi: 10.3892/or.14.6.1593

59. Julius D, Livelli TJ, Jessell TM, Axel R. Ectopic expression of the serotonin 1c receptor and the triggering of Malignant transformation. *Science*. (1989) 244:1057–62. doi: 10.1126/science.2727693

60. Sola-Penna M, Paixao LP, Branco JR, Ochioni AC, Albanese JM, Mundim DM, et al. Serotonin activates glycolysis and mitochondria biogenesis in human breast cancer cells through activation of the jak1/stat3/erk1/2 and adenylate cyclase/pka, respectively. *Br J Cancer*. (2020) 122:194–208. doi: 10.1038/s41416-019-0640-1

61. Wehde BL, Radler PD, Shrestha H, Johnson SJ, Triplett AA, Wagner KU. Janus kinase 1 plays a critical role in mammary cancer progression. *Cell Rep*. (2018) 25:2192–207 e5. doi: 10.1016/j.celrep.2018.10.063

62. Jiang SH, Li J, Dong FY, Yang JY, Liu DJ, Yang XM, et al. Increased serotonin signaling contributes to the warburg effect in pancreatic tumor cells under metabolic stress and promotes growth of pancreatic tumors in mice. *Gastroenterology*. (2017) 153:277–91.e19. doi: 10.1053/j.gastro.2017.03.008

63. Zheng YY, Li LF, Shen ZB, Wang LH, Niu XY, Wei YJ, et al. Mechanisms of neural infiltration-mediated tumor metabolic reprogramming impacting immunotherapy efficacy in non-small cell lung cancer. *J Exp Clin Cancer Res*. (2024) 43:284. doi: 10.1186/s13046-024-03202-9

64. Ye D, Xu HJ, Tang QL, Xia HW, Zhang CL, Bi F. The role of 5-ht metabolism in cancer. *Biochim Et Biophys Acta-Reviews Cancer*. (2021) 1876:188618. doi: 10.1016/j.bbcan.2021.188618

65. Yu HF, Qu TY, Yang JL, Dai Q. Serotonin acts through yap to promote cell proliferation: mechanism and implication in colorectal cancer progression. *Cell Commun Signaling*. (2023) 21:75. doi: 10.1186/s12964-023-01096-2

66. Ge C, Yan J, Yuan X, Xu G. A positive feedback loop between tryptophan hydroxylase 1 and beta-catenin/zbp-89 signaling promotes prostate cancer progression. *Front Oncol*. (2022) 12:923307. doi: 10.3389/fonc.2022.923307

67. Zhu PP, Lu TK, Chen ZZ, Liu BY, Fan DD, Li C, et al. 5-hydroxytryptamine produced by enteric serotonergic neurons initiates colorectal cancer stem cell self-renewal and tumorigenesis. *Neuron*. (2022) 110:2268. doi: 10.1016/j.neuron.2022.04.024

68. De Giovanni M, Chen HW, Li XC, Cyster JG. Gpr35 and mediators from platelets and mast cells in neutrophil migration and inflammation. *Immunol Rev*. (2023) 317:187–202. doi: 10.1111/imr.13194

69. Karmakar S, Lal G. Role of serotonin receptor signaling in cancer cells and anti-tumor immunity. *Theranostics*. (2021) 11:5296–312. doi: 10.7150/thno.55986

70. Schneider MA, Heeb L, Beffinger MM, Pantelyushin S, Linecker M, Roth L, et al. Attenuation of peripheral serotonin inhibits tumor growth and enhances immune checkpoint blockade therapy in murine tumor models. *Sci Trans Med*. (2021) 13:eabc8188. doi: 10.1126/scitranslmed.abc8188

71. Gwynne WD, Hallett RM, Girgis-Gabardo A, Bojovic B, Dvorkin-Gheva A, Aarts C, et al. Serotonergic system antagonists target breast tumor initiating cells and synergize with chemotherapy to shrink human breast tumor xenografts. *Oncotarget*. (2017) 8:32101–16. doi: 10.18632/oncotarget.16646

72. Alpini G, Invernizzi P, Gaudio E, Venter J, Kopriva S, Bernuzzi F, et al. Serotonin metabolism is dysregulated in cholangiocarcinoma, which has implications for tumor growth. *Cancer Res*. (2008) 68:9184–93. doi: 10.1158/0008-5472.Can-08-2133

73. Gil-Ad I, Zolokov A, Lomnitski L, Taler M, Bar M, Luria D, et al. Evaluation of the potential anti-cancer activity of the antidepressant sertraline in human colon cancer cell lines and in colorectal cancer-xenografted mice. *Int J Oncol*. (2008) 33:277–86. doi: 10.3892/ijo_00000007

74. Duarte D, Cardoso A, Vale N. Synergistic growth inhibition of ht-29 colon and mcf-7 breast cancer cells with simultaneous and sequential combinations of antineoplastics and cns drugs. *Int J Mol Sci*. (2021) 22:7408. doi: 10.3390/ijms22147408

75. Duarte D, Rema A, Amorim I, Vale N. Drug combinations: A new strategy to extend drug repurposing and epithelial-mesenchymal transition in breast and colon cancer cells. *Biomolecules*. (2022) 12:190. doi: 10.3390/biom12020190

76. Bhagavathula AS, Woolf B, Rahmani J, Vidyasagar K, Tesfaye W. Selective serotonin reuptake inhibitor use and the risk of hepatocellular carcinoma: A systematic review and dose-response analysis of cohort studies with one million participants. *Eur J Clin Pharmacol*. (2022) 78:547–55. doi: 10.1007/s00228-021-03264-0

77. Chen L, Huang S, Wu X, He W, Song M. Serotonin signalling in cancer: emerging mechanisms and therapeutic opportunities. *Clin Transl Med*. (2024) 14:e1750. doi: 10.1002/ctm2.1750

78. Gaur S, Gross ME, Liao CP, Qian B, Shih JC. Effect of monoamine oxidase a (Maoa) inhibitors on androgen-sensitive and castration-resistant prostate cancer cells. *Prostate*. (2019) 79:667–77. doi: 10.1002/pros.23774

79. Wang KL, Luo J, Yeh SY, You BS, Meng JL, Chang P, et al. The mao inhibitors phenelzine and clorgyline revert enzalutamide resistance in castration resistant prostate cancer. *Nat Commun*. (2020) 11:2689. doi: 10.1038/s41467-020-15396-5

80. Gross ME, Agus DB, Dorff TB, Pinski JK, Quinn D, Castellanos O, et al. Phase 2 trial of monoamine oxidase inhibitor phenelzine in biochemical recurrent prostate cancer. *Prostate Cancer Prostatic Dis*. (2021) 24:61–8. doi: 10.1038/s41391-020-0211-9

81. Rauth S, Malafa M, Ponnusamy MP, Batra SK. Emerging trends in gastrointestinal cancer targeted therapies: harnessing tumor microenvironment, immune factors, and metabolomics insights. *Gastroenterology*. (2024) 167:867–84. doi: 10.1053/j.gastro.2024.05.005

82. Gao J, Xu K, Liu H, Liu G, Bai M, Peng C, et al. Impact of the gut microbiota on intestinal immunity mediated by tryptophan metabolism. *Front Cell Infect Microbiol*. (2018) 8:13. doi: 10.3389/fcimb.2018.00013

83. Hubková B, Valko-Rokytovská M, Cizmárová B, Zábavníková M, Mareková M, Birková A. Tryptophan: its metabolism along the kynurenine, serotonin, and indole pathway in Malignant melanoma. *Int J Mol Sci*. (2022) 23:9160. doi: 10.3390/ijms23169160

84. Pan JL, Lin Y, Liu XY, Zhang XZ, Liang TB, Bai XL. Harnessing amino acid pathways to influence myeloid cell function in tumor immunity. *Mol Med*. (2025) 31:44. doi: 10.1186/s10020-025-01099-4

85. Fong W, Li Q, Ji FF, Liang W, Lau HCH, Kang X, et al. Lactobacillus gallinarum-derived metabolites boost anti-pd1 efficacy in colorectal cancer by inhibiting regulatory T cells through modulating ido1/kyn/ahr axis. *Gut*. (2023) 72:2272–85. doi: 10.1136/gutjnl-2023-329543

86. Wyatt M, Greathouse KL. Targeting dietary and microbial tryptophan-indole metabolism as therapeutic approaches to colon cancer. *Nutrients*. (2021) 13:1189. doi: 10.3390/nu13041189

87. Zuo M, Fang J, Huang P, Liu S, Hou P, Wang S, et al. Il4i1-catalyzed tryptophan metabolites mediate the anti-inflammatory function of cytokine-primed human muscle stem cells. *Cell Death Discov*. (2023) 9:269. doi: 10.1038/s41420-023-01568-x

88. Sadik A, Somarribas Patterson LF, Öztürk S, Mohapatra SR, Panitz V, Secker PF, et al. Il4i1 is a metabolic immune checkpoint that activates the ahr and promotes tumor progression. *Cell*. (2020) 182:1252–70.e34. doi: 10.1016/j.cell.2020.07.038

89. Hu J, Chen JW, Xu XJ, Hou QL, Ren J, Yan XH. Gut microbiota-derived 3-phenylpropionic acid promotes intestinal epithelial barrier function via ahr signaling. *Microbiome*. (2023) 11:102. doi: 10.1186/s40168-023-01551-9

90. Ternes D, Tsenkova M, Pozdeev VI, Meyers M, Koncina E, Atatri S, et al. The gut microbial metabolite formate exacerbates colorectal cancer progression. *Nat Metab*. (2022) 4:458. doi: 10.1038/s42255-022-00558-0

91. Gurbatri CR, Arpaia N, Danino T. Engineering bacteria as interactive cancer therapies. *Science*. (2022) 378:858–63. doi: 10.1126/science.add9667

92. Jiawen Chen JH, Sun H. Current developments in the use of engineered bacteria for cancer therapy. *Synthetic Biol J*. (2023) 4:690–702. doi: 10.12211/2096-8280.2022-062

93. Bender MJ, McPherson AC, Phelps CM, Pandey SP, Laughlin CR, Shapira JH, et al. Dietary tryptophan metabolite released by intratumoral lactobacillus reuteri facilitates immune checkpoint inhibitor treatment. *Cell*. (2023) 186:1846. doi: 10.1016/j.cell.2023.03.011

94. Zhao M, Wang K, Lin R, Mu F, Cui J, Tao X, et al. Influence of glutamine metabolism on diabetes development:A scientometric review. *Heliyon*. (2024) 10:e25258. doi: 10.1016/j.heliyon.2024.e25258

95. Feng T, Xie F, Lyu Y, Yu P, Chen B, Yu J, et al. The arginine metabolism and its deprivation in cancer therapy. *Cancer Lett*. (2025) 620:217680. doi: 10.1016/j.canlet.2025.217680

96. Huang L, Zhao W, Sun L, Niu D, Zhu X, Jin C. Research progresses and hotspots on glucose metabolic reprogramming in breast cancer: A bibliometric analysis over the past two decades. *Front Oncol*. (2024) 14:1493996. doi: 10.3389/fonc.2024.1493996

frontiers | Frontiers in Immunology

TYPE Original Research
PUBLISHED 04 July 2025
DOI 10.3389/fimmu.2025.1592416

OPEN ACCESS

EDITED BY
Dan Liu,
Wuhan University, China

REVIEWED BY
Til Ber,
Kotebe University of Education, Ethiopia
Huan Lan,
Genentech Inc., United States

*CORRESPONDENCE
En-Yu Liu
liuenyu@163.com
Su-Qing Zhang
zsq7829@163.com
Wei-Hua Cai
cwhntsy@163.com

†These authors have contributed equally to this work and share first authorship

‡These authors have contributed equally to this work and share last authorship

RECEIVED 12 March 2025
ACCEPTED 11 April 2025
PUBLISHED 04 July 2025

CITATION
Wang R, Qin G-H, Jiang Y, Chen F-X, Wang Z-H, Ju L-L, Chen L, Fu D, Liu E-Y, Zhang S-Q and Cai W-H (2025) Integrated multiomics analysis identifies PHLDA1+ fibroblasts as prognostic biomarkers and mediators of biological functions in pancreatic cancer.
Front. Immunol. 16:1592416.
doi: 10.3389/fimmu.2025.1592416

Integrated multiomics analysis identifies PHLDA1+ fibroblasts as prognostic biomarkers and mediators of biological functions in pancreatic cancer

Rui Wang[1,2†], Guan-Hua Qin[2,3†], Yifei Jiang[4†], Fu-Xiang Chen[2,3], Zi-Han Wang[1,2], Lin-Ling Ju[5], Lin Chen[5], Da Fu[6], En-Yu Liu[7*‡], Su-Qing Zhang[3*‡] and Wei-Hua Cai[1*‡]

[1]Department of Hepatobiliary Surgery, Affiliated Nantong Hospital 3 of Nantong University, Nantong, Jiangsu, China, [2]Medical School of Nantong University, Nantong, Jiangsu, China, [3]Department of Hepatobiliary and Pancreatic Surgery, Affiliated Tumor Hospital of Nantong University, Nantong, Jiangsu, China, [4]Department of Nuclear Medicine, Ruijin Hospital, Shanghai Jiaotong University School of Medicine, Shanghai, China, [5]Nantong Institute of Liver Disease, Affiliated Nantong Hospital 3 of Nantong University, Nantong, Jiangsu, China, [6]Department of General Surgery, Ruijin Hospital, Shanghai Jiaotong University School of Medicine, Shanghai, China, [7]Department of General Surgery, Qilu Hospital, Cheeloo College of Medicine, Shandong University, Jinan, Shandong, China

Background: Pancreatic cancer (PC) is marked by extensive heterogeneity, posing significant challenges to effective treatment. The tumor microenvironment (TME), particularly cancer-associated fibroblasts (CAFs), plays a critical role in driving PC progression. However, the prognostic and functional contributions of distinct CAF subtypes remain inadequately understood. Here, we introduce a novel 7-gene risk model that not only robustly stratifies PC patients but also unveils the unique role of PHLDA1 as a key mediator in tumor-stroma crosstalk.

Methods: By integrating single-cell RNA sequencing (scRNA-seq), spatial transcriptomics, and bulk RNA sequencing data, we comprehensively characterized the heterogeneity of CAFs in PC. We identified five CAF subtypes and focused on matrix CAFs (mCAFs), which were strongly associated with poor prognosis. A 7-gene mCAF-associated risk model was constructed using advanced machine learning algorithms, and the biological significance of PHLDA1 was validated through co-culture experiments and pan-cancer analyses.

Results: Our multiomics analysis revealed that the novel 7-gene model (comprising USP36, KLF5, MT2A, KDM6B, PHLDA1, REL, and DDIT4) accurately predicts patient survival, immunotherapy response, and TME status. Notably, PHLDA1 was uniquely overexpressed in CAFs and correlated with the activation of key protumorigenic pathways, including EMT, KRAS, and TGF-β, underscoring its central role in modulating the crosstalk between CAFs and malignant ductal cells. Pan-cancer analysis further supported PHLDA1's prognostic and immunomodulatory significance across multiple tumor types.

Conclusion: Our study presents a novel 7-gene prognostic model that significantly enhances risk stratification in PC and identifies PHLDA1+ CAFs as promising prognostic biomarkers and therapeutic targets. These findings provide new insights into the TME of PC and open avenues for personalized treatment strategies.

KEYWORDS

pancreatic cancer, PHLDA1, prognostic biomarker, tumor microenvironment (TME), spatial transcriptomics

Background

Pancreatic cancer (PC) is an aggressive neoplasm of the digestive system and may be expected to emerge as the major frequent cause of cancer-related fatality by 2030 (1). Despite the incremental progress in diagnostic modalities and therapeutic strategies, the overall survival (OS) rate for PC continues strikingly low, at less than 10% (2). This grim prognosis is attributed to the fact that over 80% patients preclude the possibility of curative surgery and increases the risk of tumor recurrence (3). For patients with unresectable PC, chemotherapy regimens based on fluorouracil or gemcitabine, has shown limited efficacy, with survival extension not exceeding 12 months (4–6). Therefore, to improve clinical outcomes, there is an imperative need to elucidate the intricate biological underpinnings of pancreatic cancer cells and their associated cellular milieu comprehensively.

The tumor microenvironment (TME) has recently assumed a central focus on oncological research and drug development, encompassing a diverse array of cellular and noncellular elements, comprising immune cells, cancer-associated fibroblasts (CAFs) or cytokines (7–9). The intricate interplay within the TME is pivotal in modulating malignancy progression (10). CAFs, a predominant cell type in the stromal constituents, is closely associated with invasion, metastasis, or poor prognosis in a variety of malignant tumors (11, 12). Single-cell analyses have revealed distinct CAF subtypes, each characterized by unique genetic signatures or functional attributes. The heterogeneity of fibroblasts has been investigated across various cancers, including colorectal (13, 14), chordoma (15), breast (16, 17), and head and neck cancer (18), among others. The variability in CAF types and functions across different tumor types highlights the complexity of their functional role within the TME, indicating a need for further investigation into their multifaceted contributions. Given the marked heterogeneity within the CAF population, we hypothesize that distinct CAF subtypes exert unique influences on pancreatic cancer progression. In particular, we postulate that a specific subset characterized by elevated PHLDA1 expression plays a pivotal role in mediating the crosstalk between malignant ductal cells and the tumor microenvironment. We propose that PHLDA1+ CAFs contribute to tumor growth and immune modulation by activating protumorigenic signaling pathways—such as PI3K/Akt, TGF-β, and KRAS—which, in turn, may impact patient prognosis and therapeutic response. This hypothesis underpins our investigation into the prognostic and functional significance of PHLDA1+ CAFs in pancreatic cancer.

In recent years, machine learning (ML) approaches have become indispensable for extracting robust prognostic and biological insights from high-dimensional cancer datasets (19). Supervised methods—such as Lasso-Cox regression, Random Forests, and Support Vector Machines—have been widely applied to bulk and single-cell transcriptomic profiles to derive multi-gene signatures that accurately stratify patients by survival risk and therapeutic response. Unsupervised algorithms, including consensus clustering and non-negative matrix factorization, have facilitated the identification of novel TME cellular subtypes by grouping cells with shared expression patterns, thereby revealing heterogeneity that is otherwise obscured in bulk analyses (20). More recently, deep learning frameworks have been integrated with spatial transcriptomics to infer spatially resolved cell–cell interactions, enabling the construction of predictive models that link the spatial distribution of immune and stromal populations to clinical outcomes (21). In pancreatic cancer and other malignancies, such integrative ML pipelines have successfully uncovered prognostic signatures within CAFs, predicted immunotherapy responders based on TME composition, and highlighted key signaling pathways driving tumor–stroma crosstalk. By leveraging these advanced algorithms, our study not only constructs a robust 7-gene risk model but also situates PHLDA1+ CAFs within a framework of ML-driven TME analysis, underlining their relevance for precision prognostication and therapeutic targeting.

ScRNA-seq technology has enabled the characterization of tumor cell heterogeneity with single-cell resolution, thereby laying a more robust foundation for the comprehensive elucidation of tumor pathogenesis, therapeutic strategies, and prognostic outcomes (22, 23). Spatial transcriptomics (ST) methodologies facilitate the acquisition of whole-transcriptome data within tissue sections, concurrently preserving the spatial context of cellular localization (24).

In this research, multi-omics data were used to elucidate the contributions of CAFs in the malignant progression from a multidimensional perspective. Furthermore, we sought to

investigate the influence of CAFs on the prognosis of patients with PC and their possible predictive value for the response to immunotherapy. Our research contributes to clarifying the biological roles of CAFs in the development of PC and offers guidance for creating innovative treatment approaches.

Methods

Data collection

All data were obtained from GEO database (https://www.ncbi.nlm.nih.gov/geo/) and Xena database (https://xena.ucsc.edu/). ScRNA data consisted of GSE154778, GSE155698, and GSE231535 datasets, comprising 38 samples of primary pancreatic cancer and control tissues (25–27). Spatial transcriptomic data were derived from the GSE235315 dataset, used for deconvolution of single-cell data to observe cell type distribution (28). The bulk datasets were divided into three parts: 1. The dataset for training the prognostic model was sourced from the TCGA-PAAD cohort, including 176 pancreatic cancer patients with survival and clinical information. 2. The datasets for validating the prognostic model were obtained from the GSE28735, GSE57495, and GSE62452 datasets, all containing survival information for pancreatic cancer patients (29–31). 3. The dataset for expression analysis was created by batch-correcting and merging the TCGA-PAAD cohort with the GTEX pancreatic cohort to increase the number of control samples, totaling 176 pancreatic cancer tissues and 167 control pancreatic tissues.

Data processing

For single-cell data, analyses were conducted using Seurat 4.2.2. Data were normalized for dimensionality reduction and clustering. The Harmony algorithm was employed to correct batch effects across datasets and samples. Cell annotation was performed using SingleR and existing methods. The percentage of cells was displayed using the "ggalluvial" software package after identifying marker genes for cell types.

For spatial transcriptomic data, the "cell2location" package was installed in a Python 3.9 environment for analysis. The "scanpy" package was used to import spatial transcriptomic data, filtering out low-quality cells after removing mitochondrial genes. A negative binomial regression model was used to train a feature matrix from single-cell data, achieving optimal results with max_epochs set to 250. Shared genes between single-cell and spatial data were identified as reference signatures for deconvolution analysis, predicting cell abundance. Considering the availability of data and code, we supplemented the analyzed relevant code with Seurat objects to the supplemental notebook.

For bulk transcriptomic data, the "sva" package facilitated batch correction and merging of TCGA and GTEX data. The data were then analyzed for different expression and survival.

Identification of CAF subtypes

To define and annotate cancer-associated fibroblast (CAF) subtypes, we first performed dimensionality reduction and unsupervised clustering within the CAF across all three scRNA-seq cohorts (GSE154778, GSE155698, GSE231535). Clustering was conducted in Seurat v4.2.2 using principal component analysis (PCA) followed by the Louvain algorithm (resolution = 0.6). Marker genes for each cluster were identified with FindMarkers ($\log_2$ fold change > 0.25, adjusted $P < 0.05$). We required that each putative CAF subtype exhibit at least five independently validated "signature" genes (e.g., FAP, POSTN, COL1A1 for matrix CAFs (mCAFs); CXCL1, IL6, CXCL12 for iCAFs) with significant overexpression relative to other fibroblast clusters.

To assess consistency across datasets, we reclustered CAFs independently in each cohort under identical parameters (Harmony for batch correction, followed by Louvain clustering). Each of the five subtypes (iCAFs, proCAFs, mCAFs, $MT2A^+$ myCAFs, $CXCL14^+$ myCAFs) appeared in all three cohorts, and the adjusted Rand index (ARI) between integrated and per-dataset cluster assignments exceeded 0.85 in each case. Finally, to verify that subtype definitions were not an artifact of a single clustering technique, we repeated the CAF subtyping using a Leiden algorithm (resolution = 0.5) and hierarchical clustering on z-score–normalized expression profiles; subtype identities and relative proportions differed by less than 5% compared to the Louvain result.

Identification of malignant versus non-malignant cells

First, we sorted the input expression matrix according to the order of genes in the genome, followed by data normalization. The cells were then clustered based on Euclidean distance or correlation. A Gaussian mixture model (GMM) was used to estimate the variance of each cluster, with the cluster showing the least variance serving as the diploid reference (i.e., normal cells) for subsequent analysis. When calculating copy number alterations (CNA) through gene expression, CopyKAT grouped every 25 genes into a detection window and assessed the significance of the mean expression differences between adjacent windows. Windows with significant differences were identified as chromosomal breakpoints. Finally, hierarchical clustering using CNA data was performed to distinguish between aneuploid tumor cells and diploid normal cells. This process was carried out using the R package "CopyKAT".

Inference of cell–cell communication networks

The underlying mechanisms of cell-to-cell communication were uncovered by the "CellChat" v1.5.0. The netVisual_circle function visualized the number and strength of communications between

cells, whereas the netAnalysis_computeCentrality function inferred the input and output weights of specific signaling pathways.

Estimation of cell-type proportions in TCGA-PAAD cohort

The deconvolution algorithm extracted representative features from high-dimensional data and mapped them to a lower-dimensional space to identify the proportions of elements in the high-dimensional data. To perform deconvolution, the "IOBR" package was used. First, the generateRef_seurat function extracted feature genes from single-cell data to construct a deconvolution feature expression matrix. The deconvo_tme function then applied the SVR algorithm to deconvolve the abundance of all cell types in the TCGA-PAAD dataset.

Identification of core gene modules through high-dimensional co-expression analysis

hdWGCNA (high-dimensional WGCNA) is a systems biology method that analyzes high-throughput gene expression data to uncover relationships between genes. Specifically, the SetupForWGCNA function constructs a WGCNA object, and the MetacellsByGroups function creates metacell information. Gene module analysis was performed based on the soft threshold of the co-expression network, and module eigengenes were calculated to identify core genes.

Machine learning and prognostic model construction

To develop a prognostic risk model, ten machine learning methods were used for selection and modeling: Lasso, Enet, StepCox, SurvivalSVM, CoxBoost, SuperPC, Ridge, plsRcox, RSF, and GBM. These were combined in various ways to create 101 different algorithms to assess the diagnostic efficiency of the models.

Cross-validation and model selection

To mitigate the risk of overfitting associated with testing 101 algorithms, we implemented a rigorous 10-fold cross-validation procedure on the training set. Specifically, the TCGA-PAAD cohort was randomly partitioned into 10 equal subsets. In each iteration, 9 folds were used to train the model, while the remaining fold served as the validation set. We computed performance metrics, including the concordance index (c-index) and the area under the receiver operating characteristic curve (AUC), for each fold. The final model was selected based on the highest average performance across the 10 folds. Additionally, sensitivity analyses were performed to assess the stability of model parameters. The selected model was further validated using independent external datasets to ensure its generalizability.

Immune infiltration and immunotherapy assessment

To analyze the overall immune microenvironment and potential for immunotherapy in high- and low-risk patients, the CIBERSORT algorithm was performed. Additionally, the expression of key factors such as chemokines, TNF family factors and HLA family molecules in high- and low-risk groups was further investigated. Overall activation of the immune microenvironment was assessed by the "ESTIMATE" package.

The "IOBR" package was used for evaluating tumor TME-related gene sets. The TIDE website (http://tide.dfci.harvard.edu/) was subsequently performed to analyze immunoreactivity and to assess immunotherapy sensitivity based on factors, such as co-mutation frequency, tumor mutation burden, and immune checkpoint expression. Finally, the external immunotherapy datasets IMvigor210 and GSE91061 were used for validation (32).

Enrichment analysis

All genes were ranked by logFC values. HALLMARK enrichment analysis was conducted using the "GSEA" and "clusterProfiler" packages, with a significance threshold of adjusted $P < 0.05$.

Drug screening and molecular docking

Drug screening was primarily conducted using the DSigDB database available on the Enrichr website. Drugs with an adjusted $P < 0.01$ were selected. The top 20 drugs were selected for display according to the binding score. The top1 drug was chosen for further analysis. For molecular docking, AutoDock Tools 1.5.6 was used to set charges, add polar and nonpolar hydrogens, and define rotatable bonds. The receptor grid files were generated by AutoDock Tools. AutoDock Vina 1.2.5 was then employed to dock the ligand structures with the generated receptor grid files. The results were visualized, analyzed, and plotted using PyMOL 3.2.

Pan-cancer analysis

Pan-cancer data were derived in accordance with UCSC Xena (https://xenabrowser.net), encompassing 24 tumor types from TCGA. The "Limma" package was used for uniform standardization and normalization of all datasets. Survival analysis was then performed. Gene sets related to angiogenesis, cell cycle, and EMT were sourced from previous studies (33–35). Correlation scatter plots were created using "ggplot2".

Clinical samples

Tumor tissues and paired adjacent tissues were obtained from Ruijin Hospital, Shanghai Jiao Tong University School of Medicine. The detail patient clinicopathologic information can be viewed in Supplementary Table S1. The research protocol was approved by the Research Ethics Committee of Ruijin Hospital, Shanghai Jiao Tong University School of Medicine. All the participants agreed to participate in this cohort study and provided written informed consent.

Cell culture and transfection

PATU-8988 and PANC-1 were purchased from the Cell Bank of the Chinese Academy of Sciences. Cancer-associated fibroblasts (CAFs) were obtained from the tumor tissues. The above were cultured in RPMI-1640 medium containing 10% fetal bovine serum (FBS) and 1% penicillin/streptomycin (P/S). The incubation temperature was 37°C and the incubator was 5% CO_2. Short hairpin RNA of PHLDA1 was provided by Genechem (Shanghai, China). For transfections, proper plasmids were introduced into the supernatant using HilyMax (Dojindo,Japan). After 8–12 hours, the medium was replaced and then validated.

Immunohistochemistry and immunofluorescence

After being formalin-fixed and paraffin-embedded, the tumor tissue samples were sectioned onto slides. IHC was then performed to validate the expression of PHLDA1.

Following deparaffinization and rehydration, the slides were subjected to antigen repair. This was subsequently followed by antibody incubation, color development and sealing. Finally, representative images were captured under a microscope. Similar to the IHC protocol, IF was carried out.

RNA extraction and real-time quantitative PCR

Total RNA was abstracted by TRIzol reagent (Invitrogen, USA). cDNA was gotten by reverse transcription using HiScript III RT SuperMix (Vazyme, Nanjing, China). RT-qPCR was performed with the ChamQ SYBR qPCR Master Mix (Vazyme Biotech, China) according to the manufacturer's instructions.

Patient-derived organoid construction and evaluation

Pancreatic tumor tissues from patients were quickly separated in RPMI-1640 medium that had been chilled beforehand and digested for 30 minutes at 37°C using collagenase. Individual cells were subsequently placed into Matrigel (Corning, USA) and filtered through a Falcon 40 μm cell screen (Corning, USA). They were then grown in the full organoid medium (OmaStem, China). Following the manufacturer's instructions, the CellTiter-Glo 3D cell viability assay (Promega, USA) was used to measure the relative activity of the organoids after being co-cultured with CAFs.

Western blot

RIPA buffer (Epizyme, China) combined with protease inhibitors (Epizyme, China) was used to extract proteins from cells. Separated from 10% SDS-PAGE, proteins were transferred to PVDF membranes. PHLDA1 primary antibody (Abcam, UK) and the relevant secondary antibody were used for incubation. Finally, protein expression levels were determined using ECL reagents (Epizyme, China).

Cell proliferation assay

For the Cell Counting Kit-8 (CCK-8; MeilunBio, China) assay, 2000 cells were plated in a 96-well plate and then cultivated at 37°C in an incubator with 5% CO2. Following the addition of 90 μL of growth media and 10 μL of CCK-8 to each well at specified times, the cells were cultured for an additional 2 hours, and the optical density (OD) values of each group were measured at 450 nm. For colony formation, the cells were seeded at a density of 1000 cells per well in a 6-well plate, and the medium was replaced every three days. The cells were subsequently fixed and stained with 0.1% crystal violet at room temperature for 30 minutes. ImageJ software was used to quantify the number of colonies after they were imaged.

Cell migration assay

For the migration assay, the upper chamber was filled with pancreatic cancer cells (5×10^4) suspended in 200 μL of serum-free media, while 1×10^6 CAFs were seeded in lower chamber culture plates containing 700 μl of RPMI-1640 medium supplemented with 10% FBS. After 24 hours, the cells that had moved to the lower side of the membrane were fixed and stained for 15 minutes at room temperature with a 1% crystal violet solution. ImageJ software was used to count the number of moving cells.

Statistical analysis

Statistical analyses were performed using GraphPad Prism 9.0. Continuous variables are presented as mean ± standard deviation (SD), and their distribution was assessed by the Shapiro–Wilk test. For comparisons between two independent groups, an unpaired two-tailed Student's t-test was applied when data were normally distributed; otherwise, the Mann–Whitney U test was used. For

comparisons among three or more independent groups, one-way analysis of variance (ANOVA) followed by Tukey's multiple comparisons test was employed. Categorical variables were compared using Pearson's chi-square test; when any expected cell count was less than 5, Fisher's exact test was used instead. Survival curves were generated by the Kaplan–Meier method, and differences between survival curves were evaluated by the log-rank test. All statistical tests were two-tailed, and a P value < 0.05 was considered statistically significant.

Results

Characterization of the single-cell landscape in pancreatic cancer

Based on methodological quality control standards, we retained 5,805 normal control group cells and 56,853 pancreatic cancer cells for downstream analysis. These included 12,458 from GSE154778, 37,583 from GSE155698, and 12,617 from GSE231535. After batch effect removal, 34 clusters of cells labeled 0–33 were identified (Figure 1A). Using SingleR and existing methods, we annotated these 34 clusters into 11 cell types. The markers for each cell type included ductal cells (KRT19, KRT8, and CFTR), macrophages (LYZ, CD68, and C1QB), T cells (CD3D, CD3E, and NKG7), acinar cells (CLPS, CELA2A, and CELA3A), cancer-associated fibroblasts (FAP, COL1A1, and POSTN), endothelial cells (VWF, CDH5, and ERG), plasma cells (JCHAIN, MZB1, and JSRP1), pericytes (ACTA2, RGS5, and TAGLN), mast cells (KIT, CPA3, and TPSAB1), B cells (CD79A, CD79B, and MS4A1), and endocrine cells (GCG, INS, and GAS5) (Figures 1B, C). The changes in each cell type of consistency were compared and we found that proportions of ductal cells, CAFs, and plasma cells increased, whereas those of acinar cells and pericytes decreased. These findings suggested that ductal cells, CAFs, and plasma cells may be associated with the malignant progression (Figure 1D). Additionally, we found that most malignant cells originated from ductal cells using the CopyKAT (Figure 1E). This raised the question of whether malignant ductal cells have significant biological differences from nonmalignant ductal cells, accelerating progression of pancreatic cancer.

Crosstalk between cancer-associated fibroblasts and malignant ductal cells

To address this, we divided the ductal cells in the single-cell data into tumor-associated ductal cells and normal ductal cells based on whether they were diploid and calculated their communication with other cell components in the microenvironment. The results revealed that CAF or pericytes were most closely interconnected with malignant ductal cells (Figures 2A, B). In terms of specific communication signals, tumor-associated ductal cells increase the output of signals such as ALCAM and OCLN and the input of signals such as CD96 and CD6 (Figure 2C). To explore whether CAFs or pericytes play a more important role in promoting disease, we extracted a reference set of feature genes from the single-cell expression matrix and deconvoluted them into ordinary transcriptome data. We found that the abundance of CAFs was significantly related to overall survival, with a higher proportion of CAFs associated with worse overall survival (Figures 2D, E). In addition, CAFs had a substantial positive correlation with the quantity of tumor-associated ductal cells, suggesting that CAFs may be the most important cells involved in malignant progression via affecting ductal cells (Figure 2F). At the same time, CAFs were also related to clinical stage, with worse stages such as G3/G4 or Stage III/IV having a higher proportion of CAFs (Figures 2G–I). Elucidating the characteristics and functions of CAFs may be important for understanding pancreatic cancer.

mCAFs correlate with clinical prognosis in pancreatic cancer

Next, by secondary dimensionality reduction and clustering on the CAFs, and based on their respective expression characteristics, five cell subgroups were derived: inflammatory CAFs (iCAFs), progenitor CAFs (proCAFs), matrix CAFs (mCAFs), and myogenic CAFs (two subtypes with high expression of MT2A and CXCL14 respectively) (Figures 3A, B). Univariate Cox analysis revealed that among these five types of cells, only mCAFs had a significant correlation with overall survival. The survival curve also revealed that a greater abundance of mCAFs was related to worse prognosis, suggesting mCAFs constituted the most significant malignant CAF subtype (Figures 3C, D). HdWGCNA is an important means to mine core genes. To parse the characteristic genes of mCAFs, hdWGCNA was performed. Given a soft threshold of 12, we achieved the best attributes of the scale-free topological network model and good connectivity (Figure 3E). At this time, all genes were divided into eight color series module genes, including yellow, blue, turquoise, green, pink, brown, red, and black modules (Figures 3F, G). By calculating the correlation of each module gene with different CAF subtypes, we found that the black module genes had the highest correlation with mCAFs, indicating that the module genes most closely fit the characteristics of mCAFs (Figure 3H). This module gene has a total of 125 genes. Through differential expression analysis, we retained genes whose expression significantly differed, which will be used as candidate genes for the next step of core prognostic gene screening. (Figure 3I).

Performance of a prognostic model

Before constructing a prognostic model, we prescreened survival for the candidate genes. By Univariate Cox regression analysis, a total of 32 genes were substantial correlated with overall survival (Figure 4A). We constructed a protein interaction network of these 32 genes, and the MCODE algorithm extracted two core submodules from it (Figure 4B). Enrichment analysis

10.3389/fimmu.2025.1592416

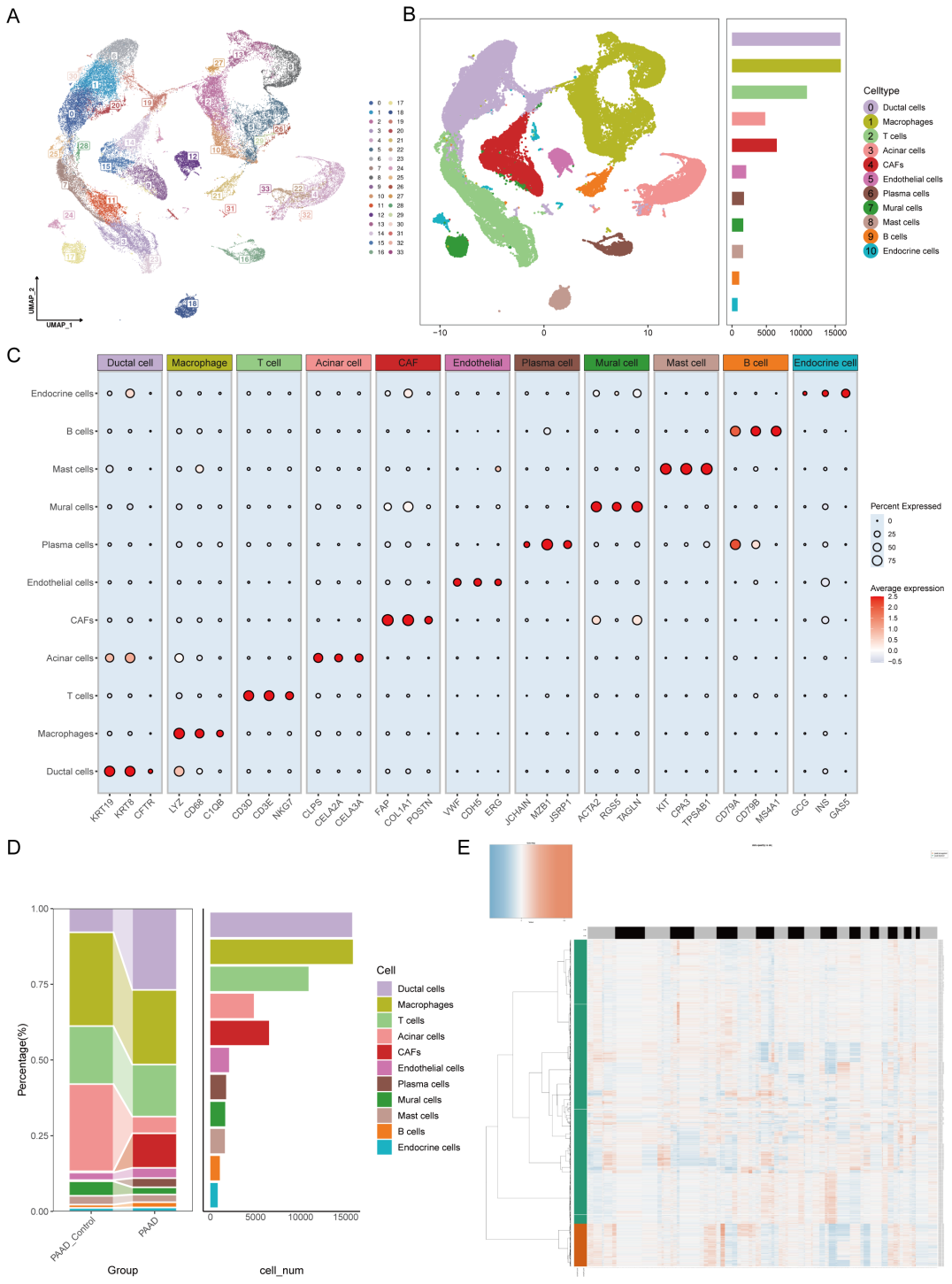

FIGURE 1
Single-cell atlas features of pancreatic cancer construction. **(A)** UMAP visualization analysis of 56,853 cells from 34 clusters by integrating the GSE154778, GSE155698 and GSE231535 datasets. **(B)** The number of each cell type in the integrated dataset. **(C)** Percentages and abundances of marker genes expressed in different cell types. The horizontal axis represents marker genes in different cell types, and the vertical axis represents different cell subpopulations. The size of the dots represents the percentage of expression, and the color shading represents the average expression level. **(D)** Histograms of the percentages and numbers of various types of cells in normal and pancreatic tumor tissues. **(E)** The CopyKAT algorithm suggested that most ductal cells were malignant.

10.3389/fimmu.2025.1592416

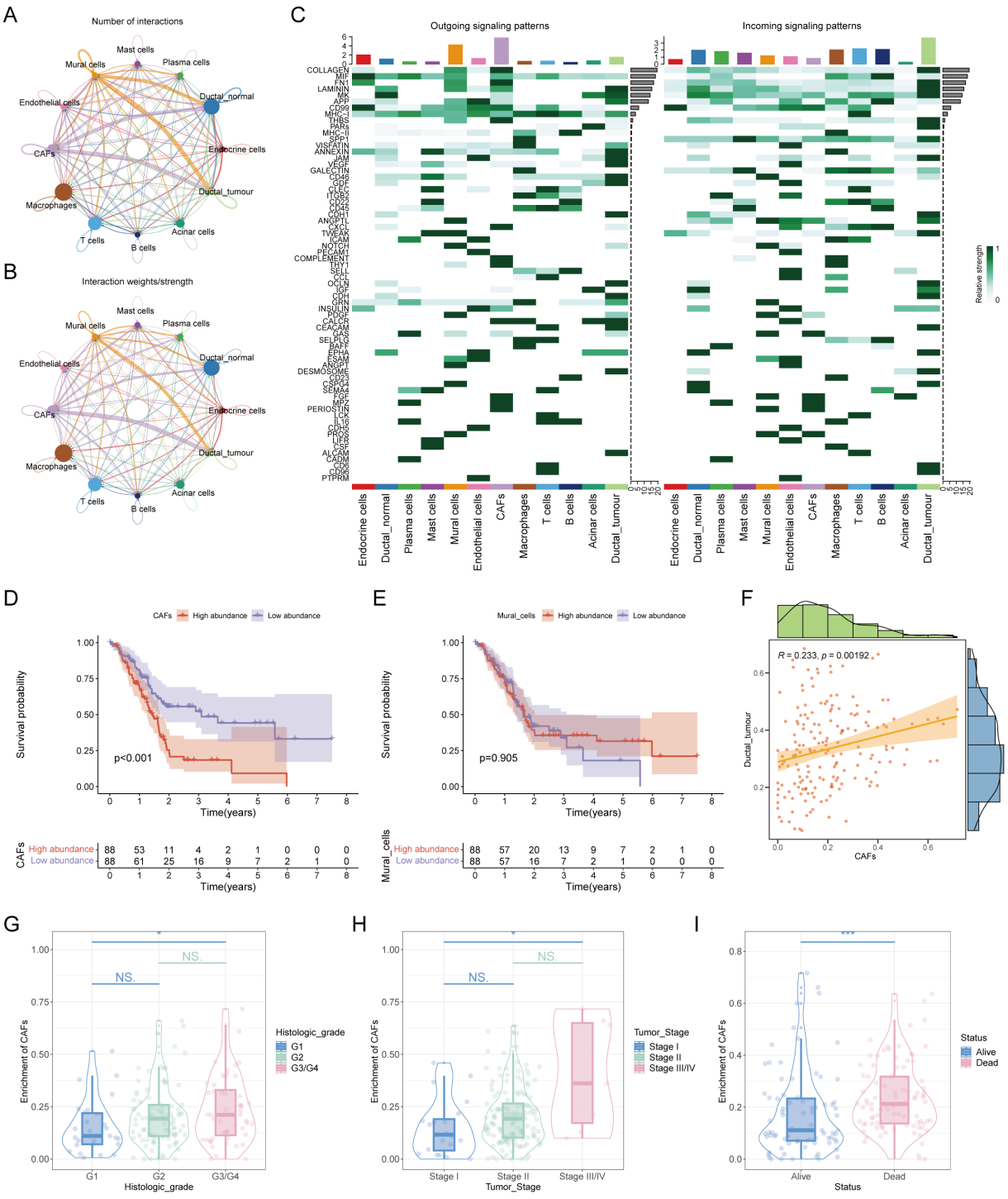

FIGURE 2
In-depth analysis of mutual crosstalk between ductal cells and cancer-associated fibroblasts. **(A)** Number of interactions between different cell subpopulations. **(B)** Interaction weights/strengths among each cell type. **(C)** Outgoing signaling patterns and incoming signaling patterns of all cell types. **(D)** Survival analysis revealed that the abundance of CAFs was correlated with poor prognosis in patients with pancreatic cancer. **(E)** KM plot showing the relationship between the abundance of mural cells and patient prognosis. **(F)** Correlation analysis of the abundance between CAFs and malignant ductal cells. **(G)** The abundance of CAFs was correlated with clinical stage. **(H)** A positive association was found between the number of CAFs and the pathological stage of patients. **(I)** There was an association between the number of CAFs and the survival status of patients. * represents p<0.05; *** represents p<0.001.

10.3389/fimmu.2025.1592416

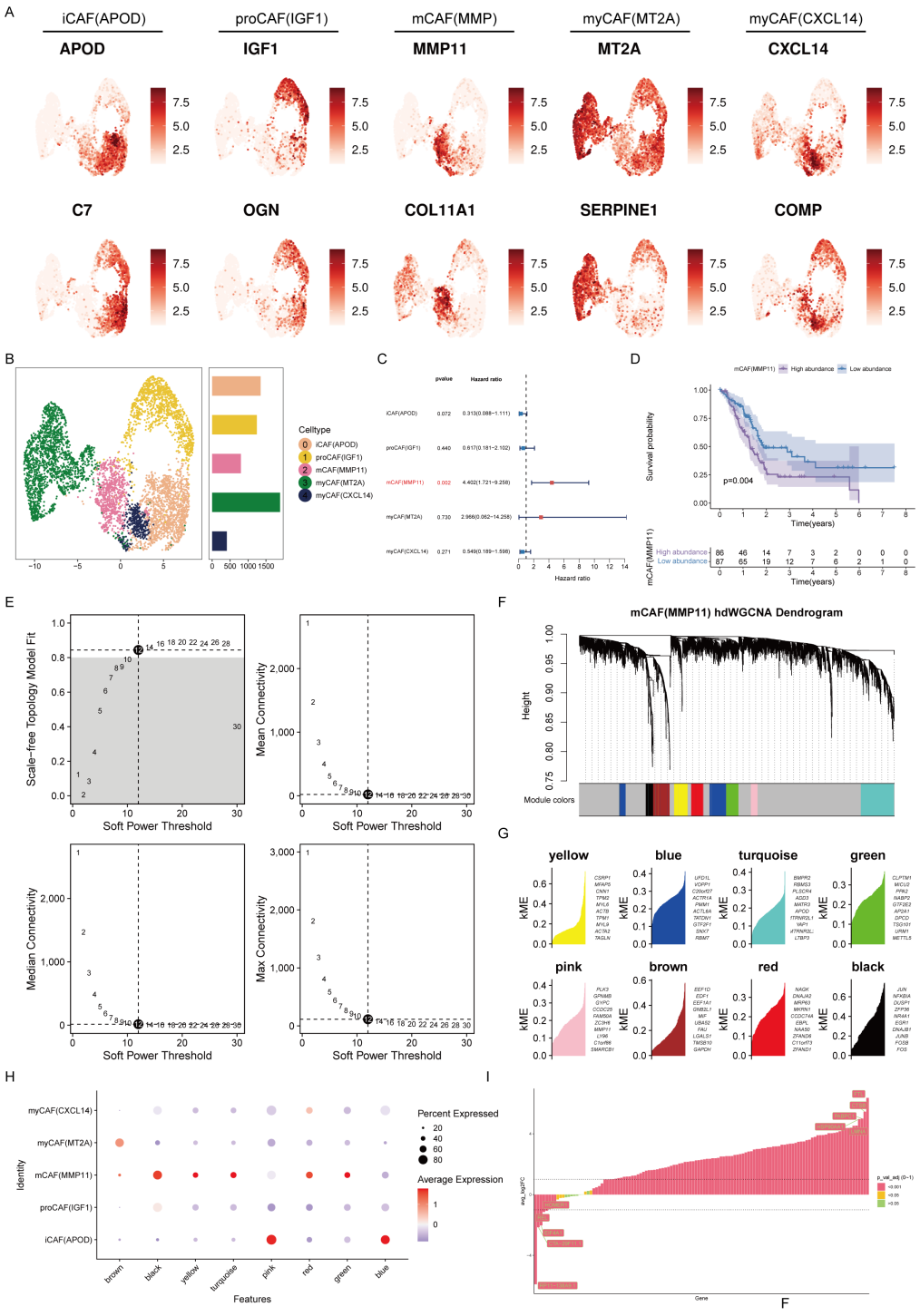

FIGURE 3
mCAFs are associated with poor prognosis in pancreatic cancer patients. **(A)** Expression levels of marker genes for 5 different CAF subtypes. The color shading represents the intensity of expression. **(B)** UMAP plot demonstrating the distribution of the five different CAF subtypes. Histograms indicate the number of cells in each type of subpopulation. **(C)** Univariate Cox analysis to assess the impact of five different CAF subtypes on the prognosis of patients with pancreatic cancer. **(D)** Survival analysis revealed that the abundance of mCAFs was correlated with poor prognosis in patients with pancreatic cancer. **(E)** The selection of the optimal soft threshold. **(F)** Scale-free topological network models were built using an ideal soft threshold of 12, and genes were partitioned into modules to create gene clustering trees. **(G)** The feature-based gene connectivity for each gene in the scale-free topological network analysis was calculated to determine the highly connected genes in each module. **(H)** Bubble plots illustrating the associations of different color modular genes with different CAF isoforms, with the black module gene having the highest correlation with mCAFs. **(I)** Differential expression analysis of black module genes.

revealed that these survival-related mCAF characteristic genes were enriched mainly in processes promoting tumors, such as hypoxia, angiogenesis, and apoptosis (Figure 4C). The results of feature gene screening and model construction based on 101 survival analyses revealed that after CoxBoost was used for core gene screening and StepCox was used for prognostic model construction, the best prognostic model was obtained. The average concordance index (C-index) reached 0.748, indicating excellent predictive performance (Figure 4D). The genes involved in the construction of this prognostic model included USP36, KLF5, MT2A, KDM6B, PHLDA1, REL, and DDIT4. According to this prognostic model, pancreatic cancer patients were stratified by disease status. Patients in the low-risk group had a better prognosis than those in the high-risk group (Figures 4E–H). The model exhibited consistently robust predictive ability in both the training and validation cohorts, particularly at the second and third years of follow-up, where the area under the ROC curves (AUCs) exceeded 0.7 and even reached above 0.8(Figures 4I–L), suggesting that the reliability and accuracy of the constructed prognostic model.

Immune atlas of high- and low-risk groups

Furthermore, we assessed the immune status of different groups patients. CIBERSORT analysis revealed that high-risk patients had fewer immune activation-related cells, such as memory B cells and follicular helper T cells, but more mast cells. These findings suggested that high-risk patients may have certain defects in assisting the activation of adaptive immunity (Figure 5A). In terms of immune activity factors, chemokines and the TNF family are common cell factors that induce immune cell aggregation and activate inflammatory responses. The risk score was markedly positively corresponded to these two molecules, suggesting that high-risk patients experienced a high degree of cytokine storm, which strongly promoted continuous chronic progression and delay of tumor development (Figure 5B). The HLA family comprises common antigen-presenting-related molecules. Except for MT2A and REL in the prognostic model, which are significantly positively correlated with the HLA family, most molecules are unrelated or even negatively correlated with the HLA family. These findings suggest that there was no obvious antigen presentation activation in the high-risk group (Figure 5C). Microenvironment scoring revealed a more active immune status and a smaller proportion of tumor cells in the low-risk group. Conversely, patients in the high-risk group exhibited a state of immune deficiency and high tumor tissue infiltration (Figures 5D–F). In addition, we evaluated many gene sets related to the tumor microenvironment, including genes related to mismatch repair, EMT, and various biological metabolisms, all of which had positive risk scores (HRs). The high-risk group had higher CAF scores, EMT scores, etc., suggesting that the high-risk group was overall in a state of low antitumor immunity and an accelerated protumor environment (Figures 5G, H).

Immunotherapy response assessment by risk score

To further demonstrate the immunotherapy sensitivity of patients by degree of risk, we first assessed their mutation status. The proportion of mutations was higher in patients in the low-risk group (92.77%), especially in KRAS, with a mutation rate reaching 81%. Furthermore, the tumor mutational load is higher in low-risk individuals, representing that immunotherapy may be more likely to be beneficial for these patients (Figures 6A–C). Besides, the high-risk group's higher TIDE scores suggested a lesser chance of benefit since they showed signs of rejection and immunological dysregulation. (Figures 6D–F). The low-risk group also showed higher expression of conventional immune checkpoints like CTLA-4 and PD1, indicating that these patients are better suited to start immunotherapy. (Figure 6G). To prove that the prognostic model could help assess the possibility of immunotherapy, we used two external treatment cohorts for validation. In the IMvigor210 cohort, high-risk patients assessed by our prognostic model also had significantly lower overall survival probabilities, and the risk scores of patients with complete remission and partial remission were also significantly lower than those of patients with stable disease and progressive disease (Figure 6H). Another immunotherapy dataset also revealed that immunoreactive patients had lower risk scores (Figure 6I), illustrating our model's strong immunological response prediction capabilities.

Crosstalk between PHLDA1^{+} CAFs and malignant ductal cells

Subsequently, we further confirmed the most important genes could be used as molecular markers and intervention targets. Through the examination of seven key genes' expression levels, only PHLDA1 was highly expressed in CAFs in the pancreatic cancer group, suggesting that this gene could be a potential procancer CAF marker (Figure 7A). In four pancreatic cancer datasets, including the TCGA-GTEX cohort, PHLDA1 expression was remarkably elevated in the pancreatic cancer samples (Figures 7B–E). Meanwhile, PHLDA1 was related to TNM stage, and poorer TNM stages are associated with higher PHLDA1 expression (Figures 7F–H). Further enrichment analysis demonstrated that high PHLDA1 expression activated classic protumor pathways such as the EMT, KRAS, and TGFB pathways (Figure 7I). Moreover, patients with high PHLDA1 expression also presented increased expression of chemokines and TNF family members, including CCL5, CCR1, and TNFRSF1B (Figures 7J, K). Spatial transcriptome analysis can better observe the spatial location of cells based on more spatial information. Unrolling cell types into tissue sections revealed significant colocalization of CAFs and ductal cells, indicating a clear spatial interaction between the two (Figure 8A). Moreover, the expression of PHLDA1 and the CAF marker POSTN was also concentrated in the colocalization area of CAFs and ductal cells, indicating that PHLDA1 may mediate their interaction (Figures 8B, C).

10.3389/fimmu.2025.1592416

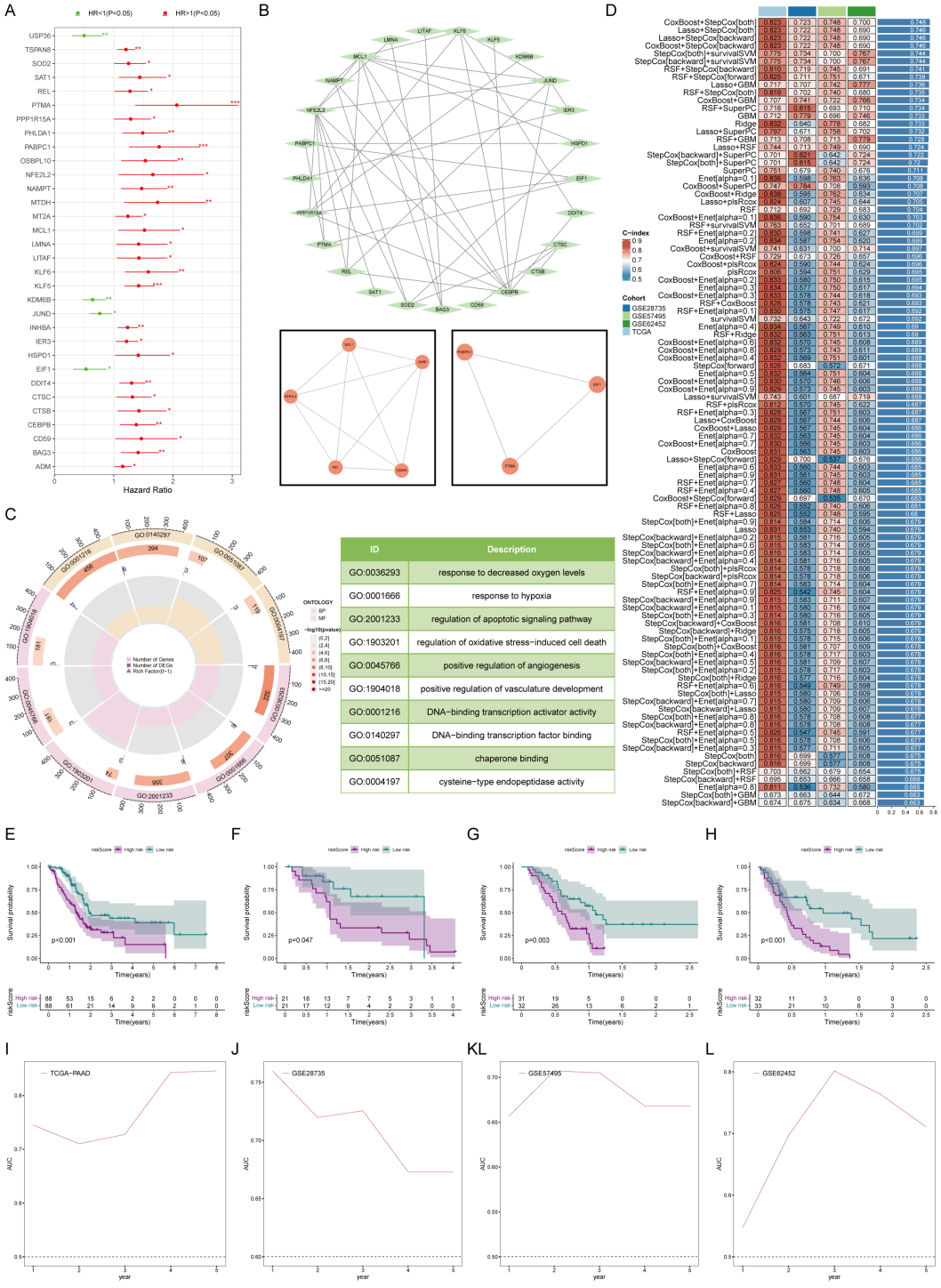

FIGURE 4
Establishment and testing of the prognostic model. **(A)** Univariate Cox analysis revealed 32 marker genes associated with survival in patients with pancreatic cancer. **(B)** Network map of protein interactions of 32 survival-related genes. **(C)** Gene ontology enrichment analysis suggested that survival-related mCAF marker genes activated protumor-related biological processes. **(D)** 101 machine learning algorithms for marker gene screening and prognostic model construction. **(E–H)** Overall survival was compared between the high- and low-risk groups in K-M plots in both the training **(E)** and validation cohorts **(F–H)**. **(I–L)** Time-dependent ROC curves for estimating 1-, 3-, and 5-year overall survival in the training **(I)** and validation **(J–L)** cohorts. * represents p<0.05; ** represents p<0.01; *** represents p<0.001.

10.3389/fimmu.2025.1592416

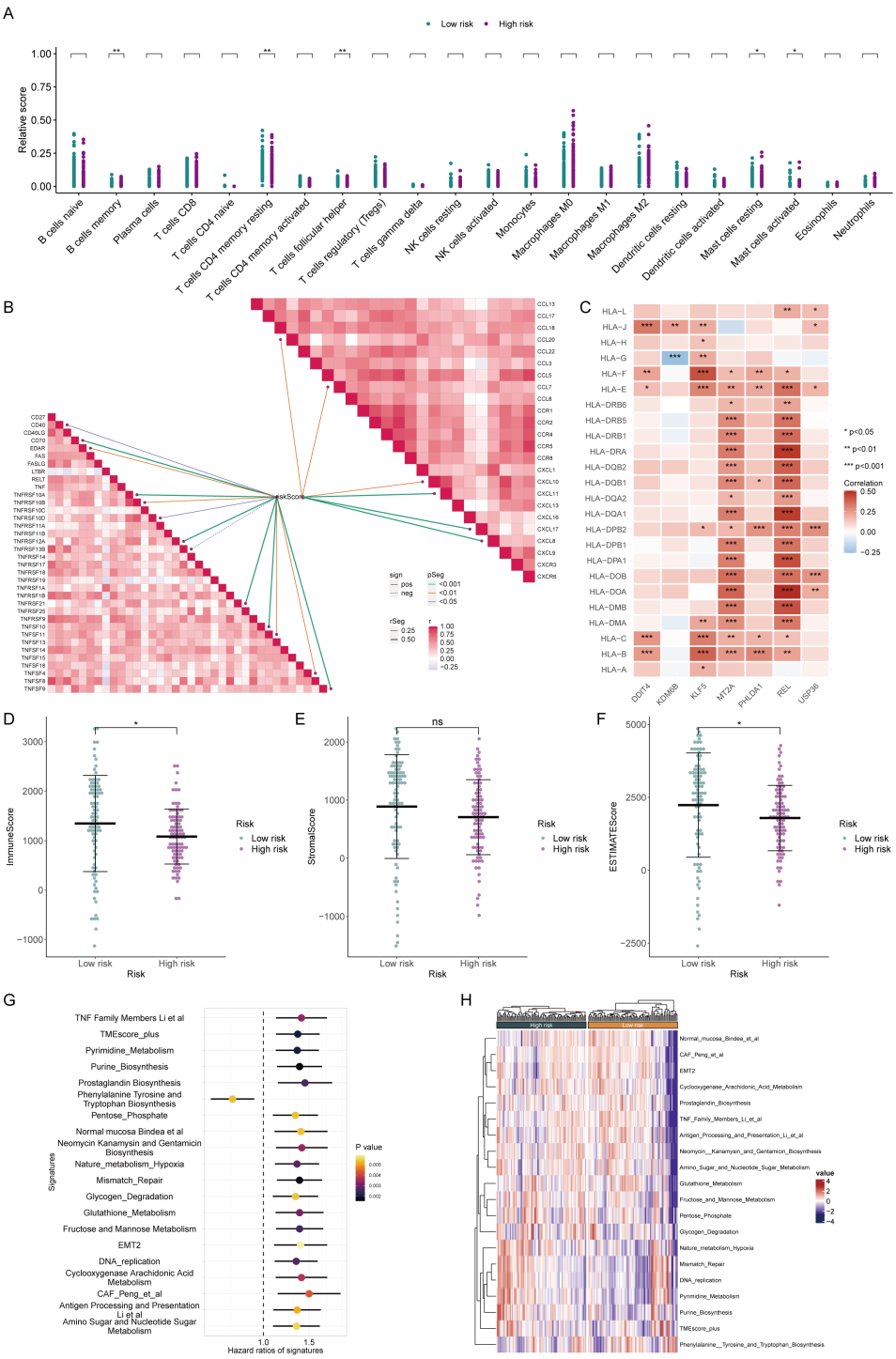

FIGURE 5
Assessment of the immune microenvironment in patients in high and low-risk groups. **(A)** The CIBERSORT algorithm demonstrated enrichment levels of various types of immune cells in patients from different risk groups. **(B)** Correlation analysis of different immunoreactive factors with the risk score. **(C)** Relationships of core genes with molecules associated with antigen presentation. **(D–F)** The ESTIMATE algorithm evaluated the ImmuneScore **(D)**, StromalScore **(E)**, and ESTIMATEScore **(F)** in patients from the high- and low-risk groups. **(G, H)** Assessment of hazard ratios (HRs) and activation levels for gene sets associated with the tumor microenvironment.

10.3389/fimmu.2025.1592416

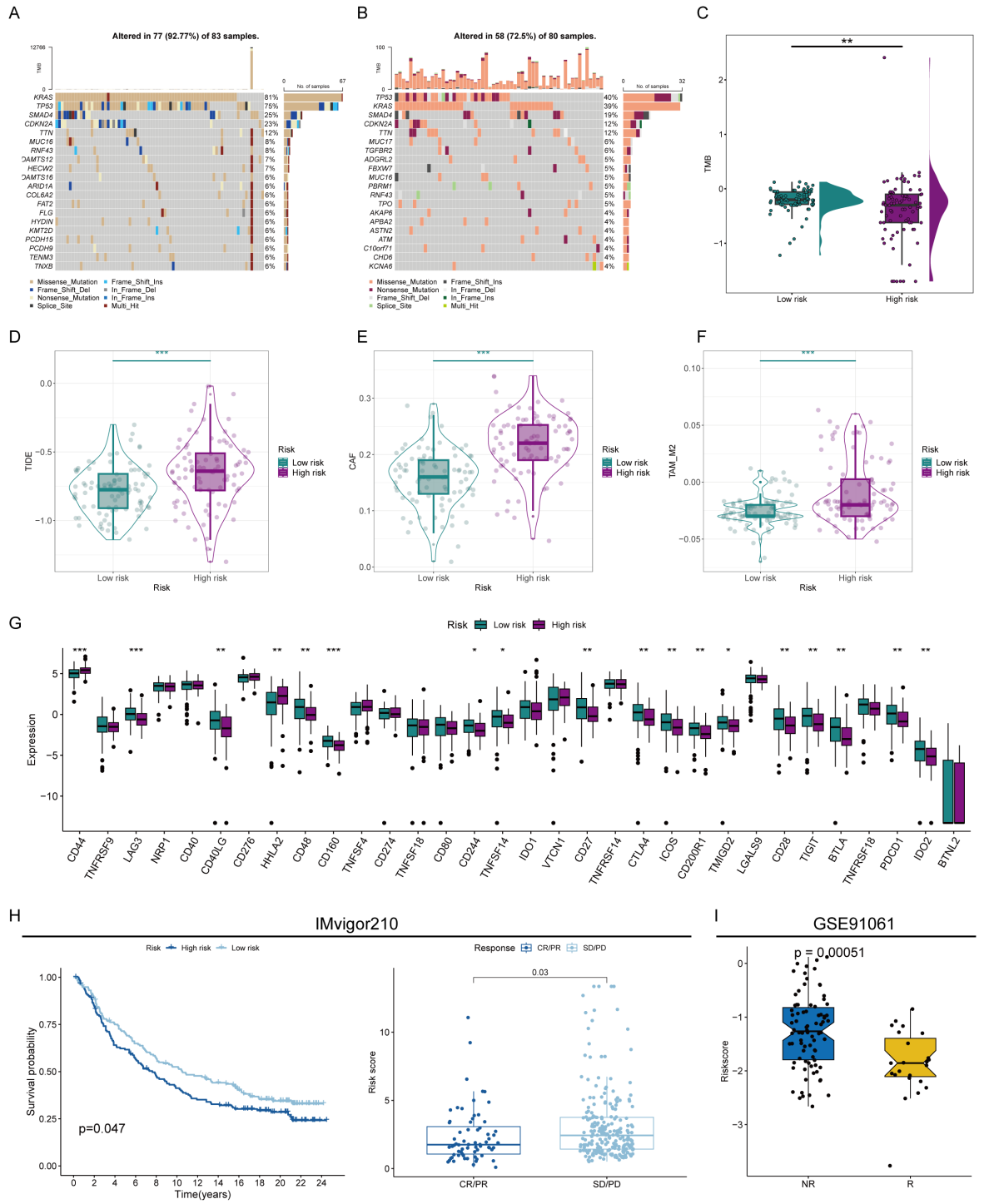

FIGURE 6
Prediction of immunotherapy sensitivity. **(A)** Mutation analysis of patients in the high- and low-risk groups. **(B)** Correlation analysis of different immunoreactive factors with the risk score. **(C)** Comparison of tumor mutation burden (TMB) in patients in the high- and low-risk groups. **(D)** TIDE scores of high- and low-risk score patients. **(E, F)** Comparison of CAF **(E)** and TAM_M2 **(F)** infiltration levels in the immune microenvironment of patients in the high- and low-risk groups. **(G)** Assessment of the expression abundance of immune checkpoint molecules. **(H, I)** Prediction of immunotherapy efficacy by risk score in immunotherapy cohorts. * represents p<0.05; ** represents p<0.01; *** represents p<0.001.

10.3389/fimmu.2025.1592416

FIGURE 7
Screening of key molecular markers and intervention targets. **(A)** Box plots representing the expression levels of 7 model genes in pancreatic cancer and normal tissues. **(B–E)** Expression of PHLDA1 in different datasets. **(F–H)** The expression levels of PHLDA1 at different T stages **(F)**, N stages **(G)**, and M stages **(H)** were compared. **(I)** GSEA revealed enriched pathways in patients with high or low PHLDA1 expression in pancreatic cancer. **(J, K)** Differences in the expression levels of chemokines **(J)** and TNF family molecules **(K)** in patients with high or low PHLDA1 expression in pancreatic cancer. * represents p<0.05; ** represents p<0.01; *** represents p<0.001.

Screening of small molecule drugs and molecular docking

Drug screening is an essential step for the clinical translation of molecular targets. To screen for potential drugs targeting PHLDA1, we carried out a drug screening based on DSigDB and identified the top 20 drugs according to their binding scores. Among them, three drugs, TTNPB, securinine, and myricetin, had the highest binding scores (Figure 8D). To further determine which drug has the best binding rate with PHLDA1, molecular docking was performed

10.3389/fimmu.2025.1592416

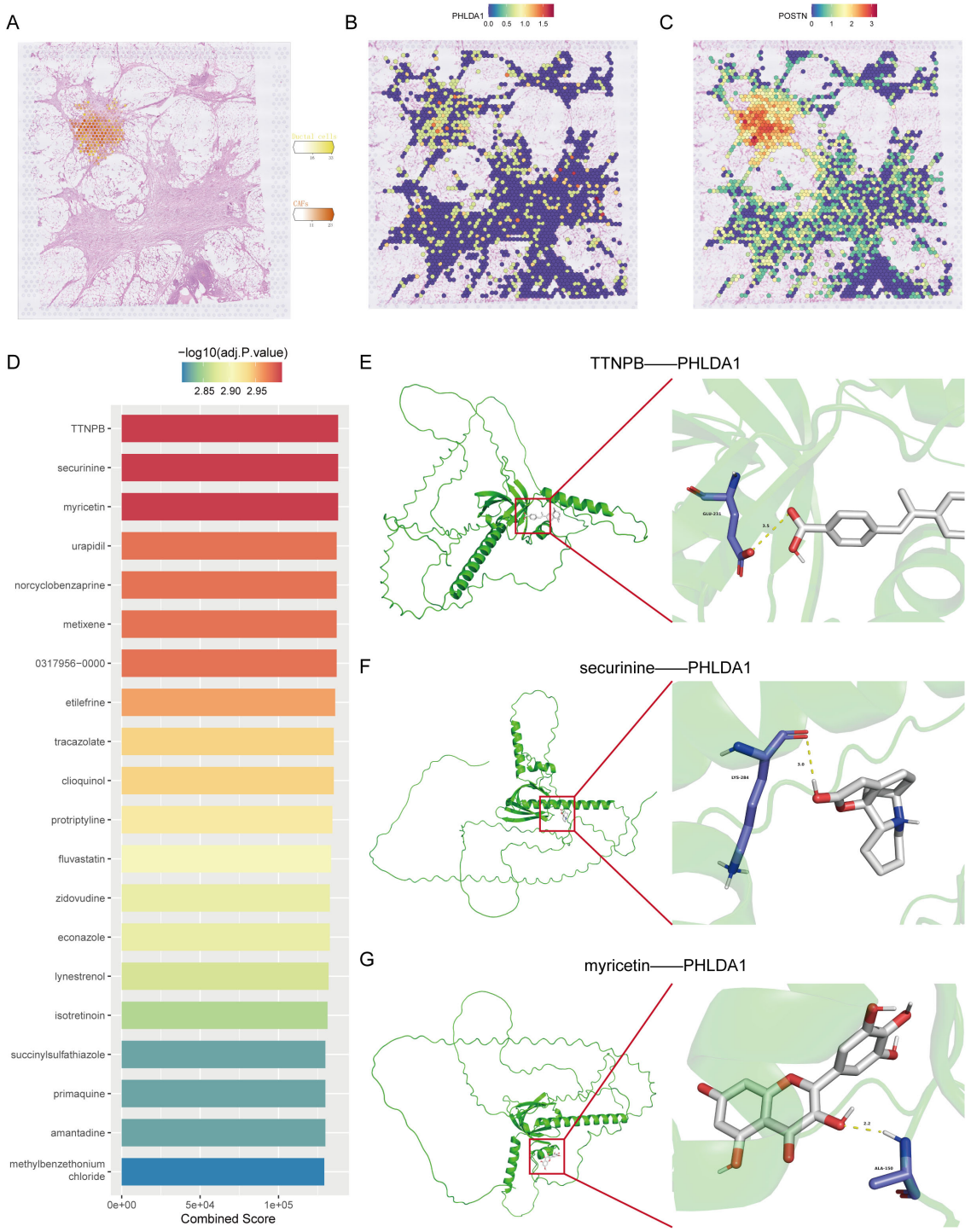

FIGURE 8
Spatial transcriptomic analysis and target molecule docking of PHLDA1. **(A)** Spatial distribution of CAFs and malignant ductal cells in pancreatic cancer. **(B, C)** Distribution of PHLDA1 **(B)** and POSTN **(C)** expression in the region of colocalization of CAFs with malignant duct cells. **(D)** Top 20 drugs targeting PHLDA1 in the DSigDB database. **(E, G)** Three-dimensional structure of the molecular docking of PHLDA1 with TTNPB **(E)**, securinine **(F)** and myricetin **(G)**.

separately for the three drugs with PHLDA1. As seen in Figures 8E–G, TTNPB presented the lowest binding energy of -6.816 kcal/mol, indicating that it bound most stably with PHLDA1 and could potentially be a PHLDA1-targeted drug.

In our drug-screening pipeline, TTNPB emerged as the top candidate for PHLDA1 targeting based on its lowest docking energy among the top 20 ranked compounds. TTNPB is a well-characterized synthetic retinoic acid receptor (RAR) agonist that

has previously been shown to modulate fibroblast differentiation and extracellular matrix remodeling in various contexts. Although no studies to date have directly linked TTNPB to PHLDA1 inhibition, several reports indicate that RAR activation can suppress profibrotic signaling cascades (e.g., TGF-β/Smad) in stromal fibroblasts, which raises the possibility that TTNPB may indirectly attenuate PHLDA1-driven CAF activation. Moreover, retinoid signaling has been reported to downregulate key EMT-associated transcription factors—many of which overlap with PHLDA1 downstream effectors—thereby providing a mechanistic rationale for TTNPB's potential efficacy in disrupting CAF–tumor crosstalk. Future work should therefore prioritize *in vivo* validation of TTNPB in CAF-rich pancreatic cancer models, such as co-implantation of PHLDA1-high CAFs with orthotopic tumor cells, to assess whether pharmacologic RAR activation can reduce tumor stiffness, limit desmoplasia, and enhance anti-tumor immunity. Additionally, given the established immunosuppressive role of CAFs, combining TTNPB with immune-checkpoint inhibitors (e.g., anti-PD-1/PD-L1) or other stroma-modulating agents may further potentiate therapeutic responses. Such combinatorial strategies could help overcome the stromal barriers that frequently limit drug delivery and immunotherapy efficacy in pancreatic cancer.

PHLDA1^{+} CAFs promote malignant progression in pancreatic cancer

Next, we investigated the role of PHLDA1 in the development of pancreatic cancer. According to survival analysis, patients with high PHLDA1 expression had a worse prognosis than patients with low PHLDA1 expression, which suggested that PHLDA1 could be a possible prognostic marker for pancreatic cancer (Figures 9A, B). Also, the expression of PHLDA1 in clinical samples of patients with pancreatic cancer was subsequently described. It could be observed higher mRNA expression of PHLDA1 in tumor tissues (Figure 9C). At the same time, it was linked to lymph node metastases and worse pathological staging characteristics according to paired tumor tissues and adjacent tissues (Figures 9D, E) (Supplementary Table S1). Moreover, PHLDA1 was shown to be expressed differently in tumor and adjuvant tumor tissues by further western blot and IHC staining (Figures 9F, G). Following the previous analysis, immunofluorescence was performed on the tumor sample and adjuvant tumor sample, and the findings indicated that PHLDA1 was expressed primarily in CAFs in pancreatic cancer (Figure 9H). As demonstrated in Figures 10A–C, downregulating PHLDA1 in CAFs dramatically decreased tumor cell proliferation activity, and similar results were achieved in colony formation assays. Additionally, patient-derived organoids were cocultured with CAFs, and we discovered that when PHLDA1 expression was reduced in CAFs, organoid proliferation ability was limited (Figures 10D, E). To ascertain if PHLDA1 in CAFs aided in the migration of pancreatic cancer cells, transwell experiments were yd. As expected, PHLDA1 considerably increased the migration capacity of PATU-8988 and PANC-1 cells (Figure 10F). Together, our findings suggest that PHLDA1 serves as a prognostic biomarker in pancreatic cancer and influences tumor growth by modulating cancer-cell proliferation and migration.

PHLDA1 reflects prognosis and immune status in multiple tumors

Finally, to broaden the application of PHLDA1, we analyzed its applicability across various types of cancer. It could be seen that melanomas exhibited the highest PHLDA1 expression, while thymomas showed the lowest (Figure 11A). The expression of this gene varies among different tumors. Specifically, PHLDA1 was highly expressed in the control group for bladder cancer, breast cancer, cholangiocarcinoma, renal papillary cell carcinoma, liver cancer, prostate cancer, and thyroid cancer, whereas it was highly expressed in the tumor groups for colorectal cancer, glioma, renal clear cell carcinoma, lung squamous cell carcinoma, rectal cancer, and gastric cancer (Figure 11B). PHLDA1 was found to be substantially associated with disease-free survival in patients with thyroid cancer, head and neck squamous cell carcinoma, pancreatic cancer, soft tissue sarcoma, bladder cancer, and endometrial cancer, as well as with overall survival in these patients. It was also significantly related to progression-free survival in patients with colorectal cancer, lung adenocarcinoma, pancreatic cancer, lung squamous cell carcinoma, thyroid cancer, and endometrial cancer (Figures 11C–E), suggesting that this indicator could be used to guide survival prognosis in these types of cancer. Additionally, PHLDA1 and the quantity of activated mast cells in practically all cancer types showed a strong positive connection, according to immune infiltration study, indicating that mast cells may contribute to the development of cancer (Figure 11F). Finally, the correlation analysis uncovered that angiogenesis, cell cycle, and EMT were significantly positively correlated with PHLDA1 in all types of cancer, further suggesting the cancer-promoting role of PHLDA1 (Figures 11G–I).

Discussion

An increasing body of research has highlighted the pronounced intratumoral heterogeneity within pancreatic cancer (PC), posing significant challenges for the development of effective therapeutic strategies. Therefore, finding innovative treatment strategies is crucial to raising PC patients' overall survival rates. A growing body of research suggests that the complex tumor microenvironment's (TME) neoplastic and stromal cells' intercellular communication is closely related to the tumor cells' malignant biological activities (36–38). As essential components of the TME, cancer-associated fibroblasts (CAFs) are known to influence important facets of carcinogenesis, such as metastasis, angiogenesis, proliferation, and resistance to different treatment modalities in a variety of cancers (12, 39, 40). Additionally, mounting data emphasizes how crucial CAFs are in initiating drug susceptibility in pancreatic cancer to immunotherapy,

10.3389/fimmu.2025.1592416

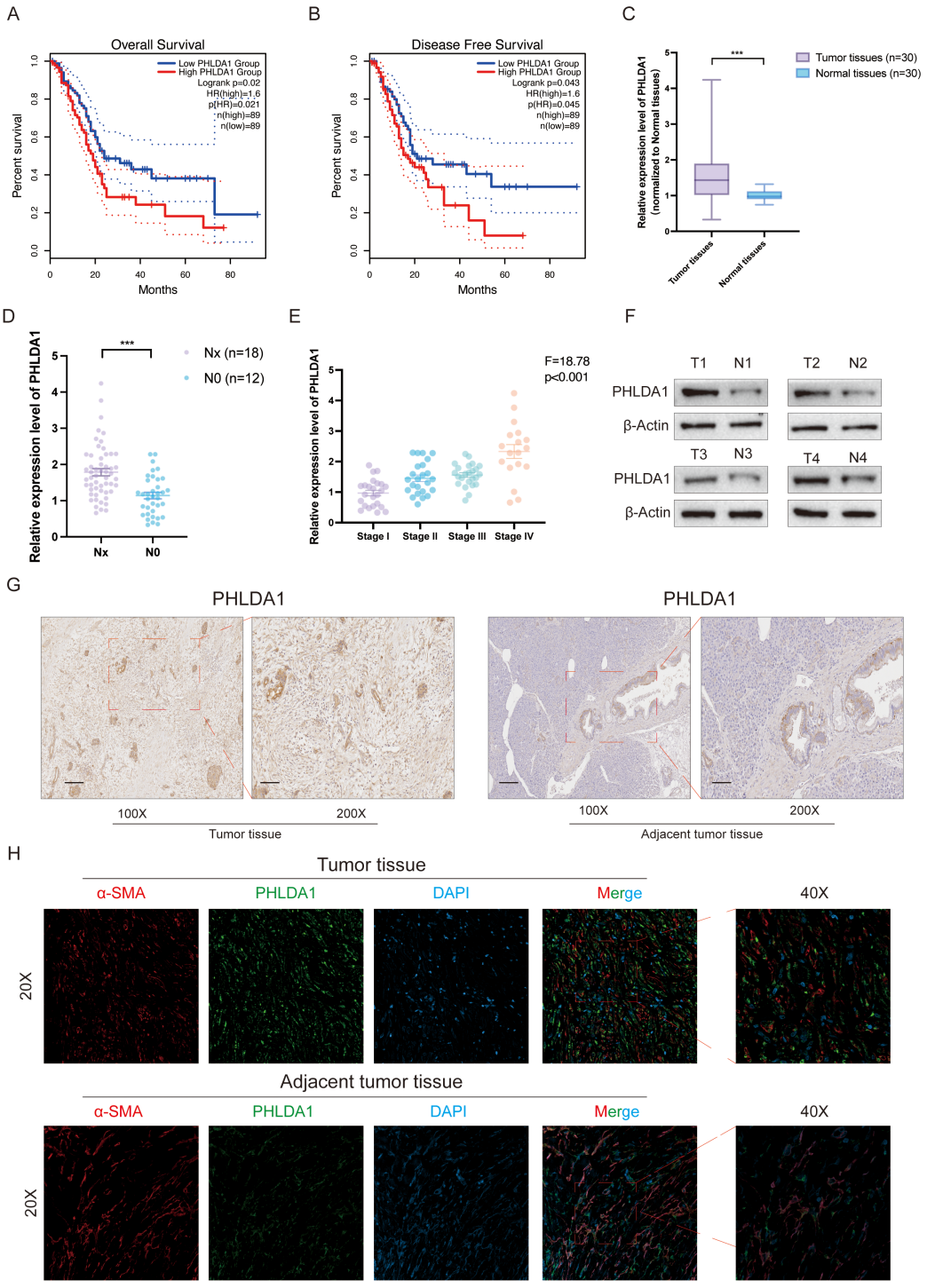

FIGURE 9
PHLDA1 is highly expressed and associated with poor prognosis in pancreatic cancer patients. **(A, B)** The overall survival **(A)** and disease-free survival **(B)** analysis of PHLDA1 in pancreatic cancer patients. **(C)** The mRNA expression level of PHLDA1 in tumor tissues (n=30) and paired adjacent tumor tissues (n=30). **(D)** The mRNA expression level of PHLDA1 in patients with lymph node metastasis. **(E)** PHLDA1 expression in patients with different pathological stages (n=30). **(F)** Western blot showing the protein level of PHLDA1 in tumor tissues and paired normal tissues (n=4). **(G)** IHC staining showing the expression level of PHLDA1 in tumor tissues and paracancerous tissues. **(H)** Colocalized distribution of PHLDA1 with the CAF marker α-SMA in cancer and adjacent tumor tissues.

10.3389/fimmu.2025.1592416

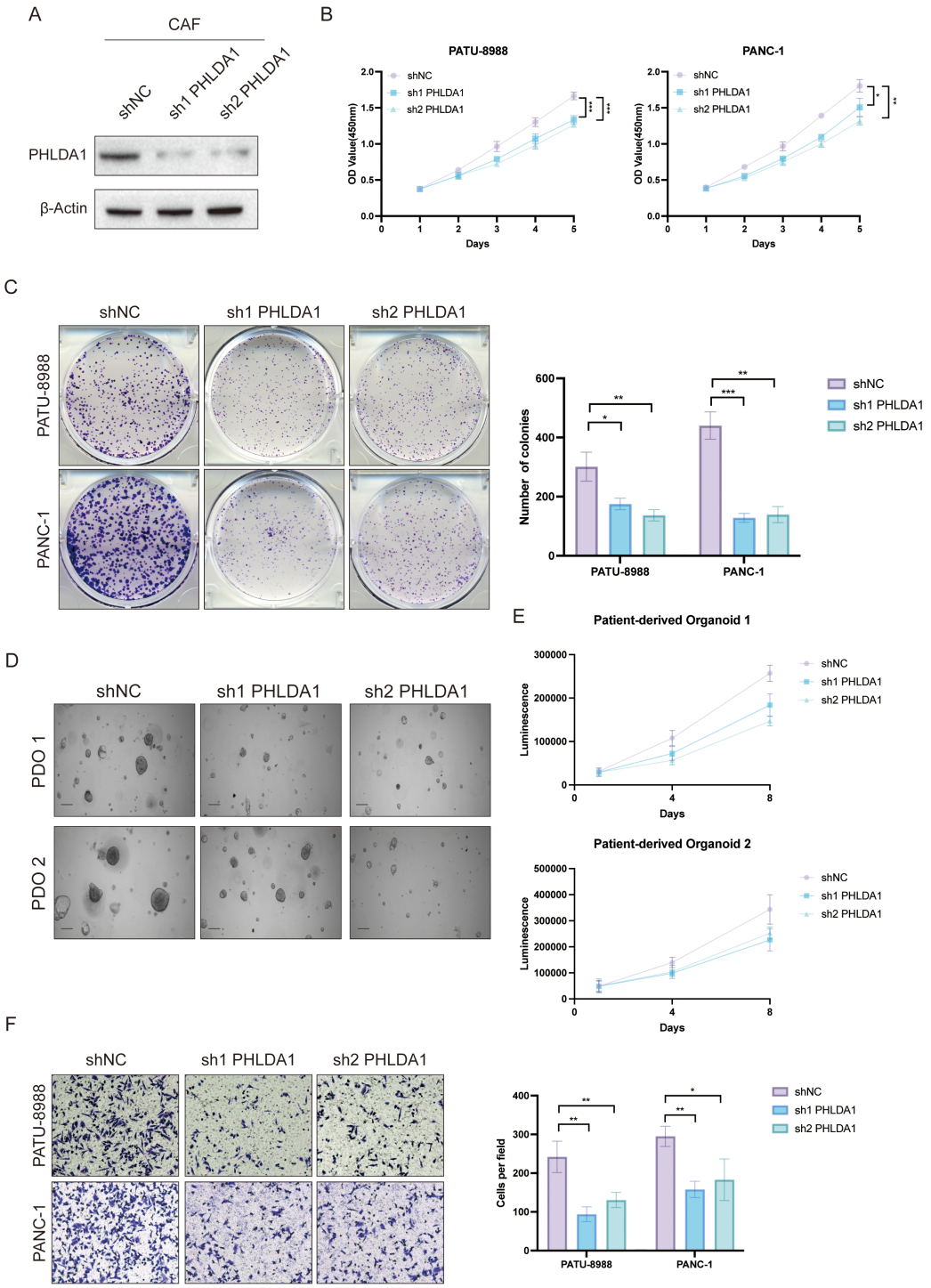

FIGURE 10
PHLDA1^{+} CAF facilitated malignant biological behavior in pancreatic cancer. **(A)** Knockdown efficiency of PHLDA1 at the protein level in CAFs. **(B)** When PHLDA1 was inhibited, CCK8 assays were used to detect the proliferative activity of PANC-1 or PATU-8988 cells when cocultured with CAFs. **(C)** Colony formation assays in PATU-8988 and PANC1 cells after cocultured with CAFs (shNC, sh1 PHLDA1, sh2 PHLDA1). **(D)** Representative images of PDO 1 or PDO 2 co-cultured with CAFs. **(E)** CTG assays revealed the proliferative capacity of different patient-derived organoids after cocultured with CAFs in Days 1, 4, and 8. **(F)** Evaluation of the migration capacity of PATU-8988 and PANC-1 cells after cocultured with CAFs (shNC, sh1 PHLDA1, sh2 PHLDA1). * represents p<0.05; ** represents p<0.01; *** represents p<0.001.

10.3389/fimmu.2025.1592416

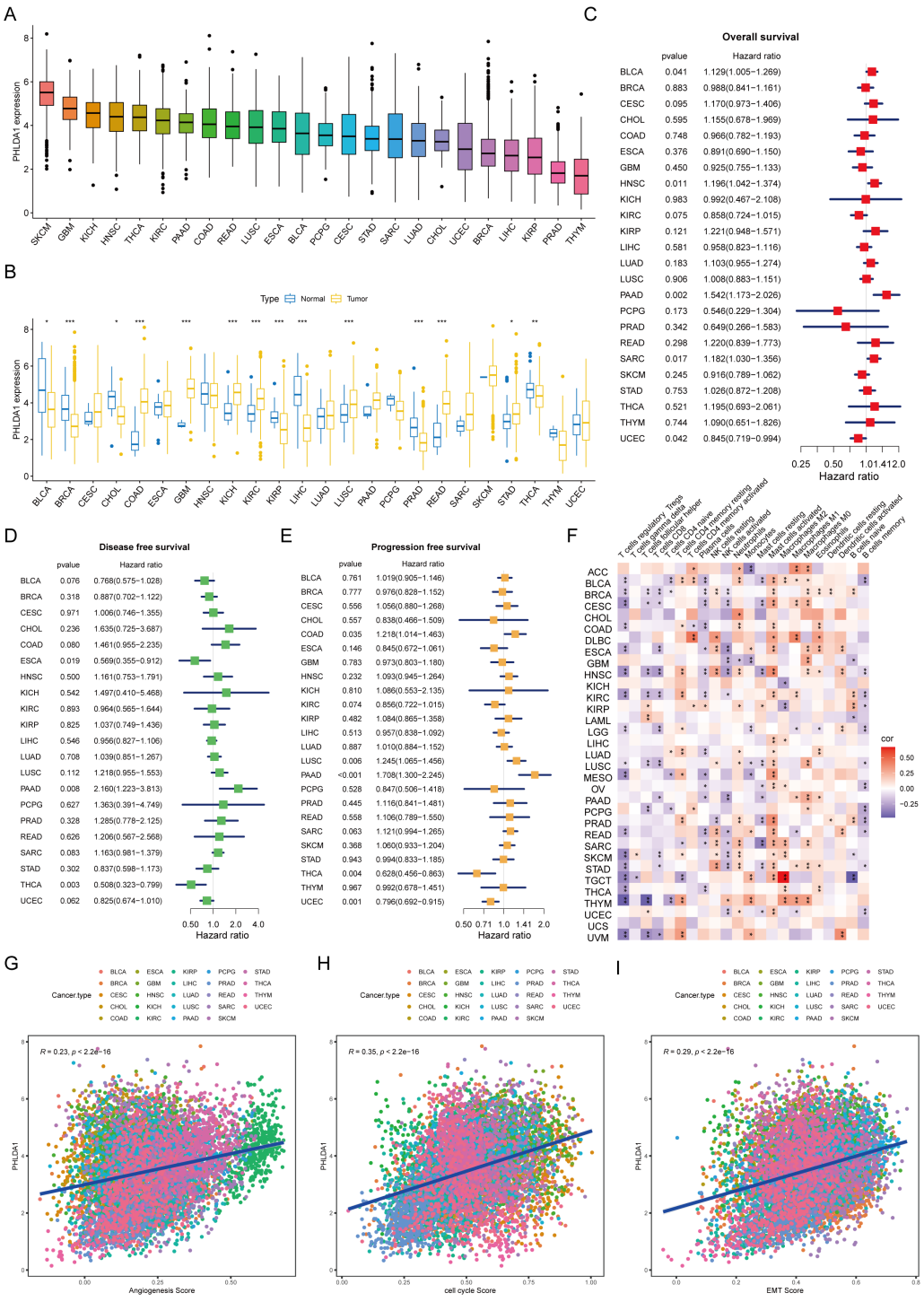

FIGURE 11
The applicability of PHLDA1 at the pan-cancer level. **(A)** The mRNA expression level of PHLDA1 in various cancer types. **(B)** PHLDA1 expression in the tumor and adjacent tumor tissues of different tumors. **(C–E)** The overall survival **(C)**, disease-free survival **(D)** and progression-free survival **(E)** of PHLDA1 at the pan-cancer level. **(F)** Correlations of PHLDA1 with the infiltration of various immune cells in multiple tumor types. **(G, H)** Evaluation of PHLDA1 expression, angiogenesis score, cell cycle score and EMT score in a range of cancers. * represents p<0.05; ** represents p<0.01; *** represents p<0.001.

targeted treatment, chemotherapy, and radiation (41, 42). According to certain report, the formation and spread of cancer are directly linked to the interactions between various cell types inside the TME (43). Our analysis of published single-cell RNA sequencing (scRNA-seq) data revealed an increased proportion of ductal and CAF cells in PC tissues, along with enhanced interactions between these cell types as shown by CellChat analysis. In addition, a higher prevalence of CAFs was correlated

with advanced disease stages and poorer overall survival. These observations indicate a potential involvement of CAFs in PC progression.

CAFs are a heterogeneous population arising from various cell types across solid tumors, activated by multiple signaling pathways (44). Their diverse origins and activation mechanisms generate a spectrum of phenotypes, resulting in functional heterogeneity. CAFs were first divided into two subgroups (CAF-A and CAF-B) via single-cell sequencing in colorectal cancer (45). In recent years, CAFs have been divided into three groups based on their roles in lung, prostate, and triple-negative breast cancer: myofibroblastic CAFs (myCAFs), inflammatory CAFs (iCAFs), and matrix CAFs (mCAFs) (46–48). Our goal in this study was to clarify how CAFs affect PC's biological behavior. Comprehensive analysis revealed the existence of five distinct CAF subpopulations, namely, iCAFs, progenitor cell CAFs (proCAFs), mCAFs, MT2A-expressing myofibroblastic CAFs (MT2A+ myCAFs), and CXCL14-expressing myofibroblastic CAFs (CXCL14+ myCAFs). Among these, mCAFs have emerged as the most critical malignant CAF subgroup with the potential to predict the prognosis of PC patients. We developed a 7-gene mCAF-related gene risk model, which allowed us to accurately forecast the survival rates of patients by classifying them into high-risk and low-risk groups. This stratification approach holds promise for improving prognostic accuracy and may inform personalized treatment strategies for PC patients.

CAFs are intricately involved in the progression of PC and are closely linked to metastasis, immune evasion, and resistance to immunotherapy (49). Within the TME, CAFs engage tumor cells and other stromal components, producing excess extracellular matrix proteins, soluble mediators, and matrix-degrading enzymes. These activities result in increased matrix deposition, increased interstitial pressure, and compression of blood vessels, which collectively contribute to hypoxia and nutrient deprivation (50, 51). Consequently, this environment restricts the administration of chemotherapeutic drugs and prevents immune cells from infiltrating.

In this study, we employed our established risk model to assess the immune profiles of patients, as well as their potential response to immunotherapy. Our findings showed that high-risk patients exhibited a pronounced inflammatory cytokine surge, which correlates with chronic tumor progression (52). Moreover, the high-risk group displayed immune dysfunction, weakened antitumor responses, and an intensified protumorigenic microenvironment. Our risk model demonstrated statistically significant predictive accuracy for immunotherapy outcomes in PC patients, suggesting its potential utility in guiding patient care and clinical decision-making.

Prior investigation has emphasized how crucial the temporal and spatial dynamics within the TME are in promoting tumor heterogeneity (53). Malignant tumor invasiveness, metastatic potential, and clinical outcomes have been found to be substantially associated with the density and spatial distribution of immune cells across different tissue subregions (54). These conclusions are supported by published data, which also confirm that the spatial variability of CAFs significantly affects cancer patients' survival (55). These observations highlight the importance of considering the spatial architecture of the TME when examining the biology of cancer and its response to therapy. Although previous studies have characterized CAF signatures based on a limited set of markers (56), our study extends these findings by identifying a distinct PHLDA1-positive CAF subtype that is significantly associated with poor prognosis and tumor-stroma interactions. Recent advancements in single-cell and spatial transcriptomic technologies have revealed that specific CAF subpopulations play critical roles in mediating immunotherapy resistance and overall patient outcomes (8, 17). Importantly, our data suggest that targeting PHLDA1-positive CAFs could serve as a novel therapeutic strategy, thereby bridging the gap between conventional CAF classifications and personalized treatment approaches (16). In this context, our findings not only refine the existing CAF paradigm but also enhance its clinical applicability by providing a more robust biomarker for prognostic stratification and therapeutic decision-making.

Consistent with these findings, our analysis revealed that mCAFs are in close proximity to malignant ductal cells and that their spatial distribution and density within tumor tissues are correlated with the aggressiveness and prognosis of PC. According to these findings, mCAFs most likely promote PC development by having a direct impact on the biological activity of ductal cells. Notably, mCAFs' spatial heterogeneity may play a role in the regulation of tumor behavior. Specifically, mCAFs located at different spatial distances from ductal cells may carry out unique biological tasks that could influence tumor growth and invasion through a variety of mechanisms of action, ultimately accelerating the advancement of the tumor. Further mechanistic analysis revealed that elevated expression of PHLDA1 promotes CAF activation and proliferation by activating key signaling pathways such as TGF-β and KRAS, thereby inducing epithelial-mesenchymal transition (EMT) and enhancing extracellular matrix (ECM) deposition and remodeling. This ECM remodeling increases tissue stiffness and density, creating physical barriers that restrict immune infiltration and therapeutic drug penetration, consequently facilitating invasion and migration of pancreatic cancer cells and leading to poor patient prognosis. These findings uncover the underlying mechanisms by which PHLDA1+ CAFs shape the tumor microenvironment and drive pancreatic cancer progression.

To provide more direct evidence for PHLDA1's functional involvement in key protumorigenic pathways, we examined both published mechanistic studies and our own co-culture results. PHLDA1 has been identified as a direct TGF-β/SMAD target, with TGF-β1 treatment increasing PHLDA1 mRNA expression approximately threefold in keratinocyte models, and chromatin immunoprecipitation confirmed SMAD3/SMAD4 binding to a regulatory region upstream of PHLDA1 (57). In addition, PHLDA1 overexpression can induce β-catenin nuclear localization, disrupt adherens junctions, and trigger EMT-associated transcriptional programs—specifically upregulating SNAI1 and VIM—consistent with a functional role in EMT induction (58). And, PHLDA1 augments KRAS pathway activity

by stabilizing the RAS–ERK axis: in glioblastoma, PHLDA1 binds to Ras and competitively inhibits Src-mediated Ras phosphorylation, resulting in sustained Ras-GTP levels, increased RAF/MEK/ERK signaling, and elevated downstream MYC transcription; conversely, PHLDA1 knockdown reduces phospho-ERK1/2 levels by approximately 50 % (59).

PHLDA1 (also known as TDAG51) is a pleckstrin homology domain-containing protein originally implicated in regulating apoptosis, cell proliferation, and cellular stress responses. Under physiological conditions, PHLDA1 plays a role in maintaining cellular homeostasis and signaling balance, as well as in specific differentiation processes. Notably, prior studies have reported that PHLDA1 is involved in several key signaling pathways, including the PI3K/Akt, TGF-β, and KRAS pathways. In our study, elevated PHLDA1 expression was associated with the activation of protumorigenic pathways such as EMT, KRAS, and TGF-β, suggesting that it may contribute to the regulation of tumor cell transformation, invasion, and migration. Moreover, the high expression of PHLDA1 in CAFs and its significant correlation with poor prognosis indicate that it plays an important role in modulating the tumor microenvironment. Therefore, targeting PHLDA1 might not only disrupt the detrimental crosstalk between CAFs and tumor cells but also enhance the efficacy of conventional therapies, offering a promising new avenue for pancreatic cancer treatment. Further studies are needed to fully elucidate its mechanisms and validate its potential as a therapeutic target.

Although we applied established batch-correction tools (e.g., Harmony for single-cell data and sva for bulk RNA-seq), some technical variability from library preparation, sequencing platforms, and sample handling likely persists. These residual batch effects may obscure subtle transcriptomic differences, especially among rare cell populations. Moreover, although pan-cancer analysis highlights the broad prognostic and immunomodulatory relevance of PHLDA1, interpretation of these cross-tumor associations must be tempered by the fact that expression patterns and downstream signaling networks can vary dramatically between tumor lineages. In particular, tissue-specific microenvironmental cues and distinct oncogenic drivers in each cancer type may confound the generalizability of PHLDA1's functional role. Future work incorporating uniformly processed samples and validation in lineage-matched models will be essential to disentangle true biological signals from cohort-specific artifacts.

Although our study focused on the enrichment of PHLDA1 in mCAFs and its association with ECM remodeling and tumor invasion, it is important to place these findings within the broader context of CAF heterogeneity. In contrast to inflammatory CAFs (iCAFs), which are marked by high cytokine secretion, and myofibroblastic CAFs (myCAFs), known for their contractile and matrix-remodeling functions, our data indicate that PHLDA1+ mCAFs preferentially activate TGF-β and KRAS signaling pathways. This suggests that targeting PHLDA1+ mCAFs, either alone or in combination with interventions aimed at other CAF subtypes, could provide a more comprehensive strategy for disrupting tumor–stroma interactions and improving therapeutic outcomes in pancreatic cancer. Unlike traditional CAF markers such as FAP and α-SMA—which mainly indicate matrix remodeling and myofibroblastic activation, respectively—our results show that PHLDA1 specifically marks a CAF subset that is strongly associated with protumorigenic pathways (e.g., EMT, KRAS, and TGF-β signaling). In our study, high PHLDA1 expression correlated with advanced TNM stage and poorer overall survival, a relationship that was less pronounced for FAP and α-SMA. Furthermore, PHLDA1 knockdown in CAFs significantly impaired tumor cell proliferation and migration. These findings suggest that PHLDA1 not only offers superior prognostic value but also plays a direct role in mediating tumor-stroma crosstalk, thereby representing a promising therapeutic target.

In addition to molecular targeting of PHLDA1, recent bioengineering platforms offer promising avenues to overcome stromal barriers and reshape the tumor microenvironment. For example, Huang et al. developed a Christmas tree–shaped microneedle patch that achieved spatiotemporal delivery of FOLFIRINOX directly into orthotopic pancreatic tumors by layering oxaliplatin/leucovorin and irinotecan/fluorouracil within hierarchical microneedle tiers, significantly enhancing intratumoral penetration and drug retention. Such a device could be adapted to co-deliver PHLDA1 inhibitors alongside chemotherapeutics or CAF-modulating agents, thereby improving drug distribution in desmoplastic lesions. Similarly, Zetrini et al. engineered polymer–lipid manganese dioxide nanoparticles that consume hydrogen (60) peroxide to generate oxygen and buffer acidity, reoxygenating hypoxic tumors and driving macrophage polarization toward an M1 phenotype when combined with radiotherapy (61). Translating this platform to PHLDA1^high CAF-rich pancreatic tumors could normalize the microenvironment, attenuate CAF-mediated immunosuppression, and potentiate the efficacy of PHLDA1-targeted therapies and immune checkpoint blockade. Future studies should investigate the integration of microneedle-based spatiotemporal delivery and redox-active nanoparticle strategies in lineage-matched pancreatic cancer models to evaluate synergistic effects on stromal depletion and antitumor immunity.

In addition to molecular and delivery-based innovations, emerging spatial genomics platforms and integrin–mTOR signaling studies offer novel avenues for future PHLDA1 research. For example, the recently described Perturb-DBiT technology enables simultaneous *in vivo* CRISPR screening and spatial transcriptomics, providing single-cell resolution maps of how genetic perturbations affect both coding and noncoding RNAs within their native microenvironment (62). By applying Perturb-DBiT to CAF populations, researchers could uncover PHLDA1's spatially resolved downstream effectors and identify context-dependent interactions between CAFs and tumor cells *in situ*. Likewise, insights from integrin-mediated mTOR/TGF-β overactivity in fibrotic valve disease illuminate how integrin–mTOR axes drive profibrotic signaling and immune cell recruitment (63). Translating these findings to CAF biology suggests that integrin–mTOR inhibitors may synergize with PHLDA1-targeted approaches to normalize the stroma and enhance anti-tumor immunity. Altogether, integrating spatial

CRISPR screens with targeted modulation of integrin–mTOR pathways could accelerate the development of more precise, microenvironment-focused therapies.

Conclusion

In conclusion, our study found a novel CAF cluster with strong predictive significance and offered a thorough examination of ductal cells and fibroblasts in the PC tumor microenvironment. According to comprehensive RNA-seq and ST findings, the mCAF subset may facilitate PC development by directly interacting with ductal cells. Through additional pan-cancer analysis tests, we investigated the function of PHLDA1. To sum up, we detailed the variety of CAFs in PC and discovered a distinct mCAF isoform and target linked to tumor growth, which enables us to better comprehend why immunotherapy is so ineffective in this situation. The present research offers a workable concept for upcoming PC medication interventions.

Data availability statement

The original contributions presented in the study are included in the article/Supplementary Material. Further inquiries can be directed to the corresponding authors.

Ethics statement

The study was approved by the Research Ethics Committee of Ruijin Hospital, School of Medicine, Shanghai Jiao Tong University, and complied with the Helsinki Declaration (No. 2021-161). All samples were collected with documented informed consent from the enrolled patients.

Author contributions

RW: Data curation, Formal Analysis, Visualization, Writing – original draft. G-HQ: Data curation, Formal Analysis, Writing – original draft. YJ: Writing – review & editing, Supervision, Formal analysis, Funding acquisition, Investigation. F-XC: Visualization, Writing – original draft. Z-HW: Investigation, Writing – original draft. L-LJ: Investigation, Writing – review & editing. LC: Supervision, Writing – review & editing. DF: Supervision, Writing – review & editing. E-YL: Conceptualization, Investigation, Resources, Writing – review & editing. S-QZ: Conceptualization, Writing – review & editing. W-HC: Conceptualization, Funding acquisition, Resources, Supervision, Visualization, Writing – review & editing.

Funding

The author(s) declare that financial support was received for the research and/or publication of this article. This research is funded by the Postgraduate Research & Practice Innovation Program of Jiangsu Province (SJCX24-2071).

Conflict of interest

The authors declare that the research was conducted in the absence of any commercial or financial relationships that could be construed as a potential conflict of interest.

Generative AI statement

The author(s) declare that no Generative AI was used in the creation of this manuscript.

Publisher's note

Supplementary material

The Supplementary Material for this article can be found online at: https://www.frontiersin.org/articles/10.3389/fimmu.2025.1592416/full#supplementary-material

References

1. Rahib L, Smith BD, Aizenberg R, Rosenzweig AB, Fleshman JM, Matrisian LM. Projecting cancer incidence and deaths to 2030: the unexpected burden of thyroid, liver, and pancreas cancers in the United States. *Cancer Res.* (2014) 74:2913–21. doi: 10.1158/0008-5472.Can-14-0155

2. Siegel RL, Miller KD, Fuchs HE, Jemal A. Cancer statistics, 2022. *CA Cancer J Clin.* (2022) 72:7–33. doi: 10.3322/caac.21708

3. Neoptolemos JP, Kleeff J, Michl P, Costello E, Greenhalf W, Palmer DH. Therapeutic developments in pancreatic cancer: current and future perspectives. *Nat Rev Gastroenterol Hepatol.* (2018) 15:333–48. doi: 10.1038/s41575-018-0005-x

4. Yoo C, Kang J, Kim KP, Lee JL, Ryoo BY, Chang HM, et al. Efficacy and safety of neoadjuvant folfirinox for borderline resectable pancreatic adenocarcinoma: improved efficacy compared with gemcitabine-based regimen. *Oncotarget.* (2017) 8:46337–47. doi: 10.18632/oncotarget.17940

5. Conroy T, Desseigne F, Ychou M, Bouché O, Guimbaud R, Bécouarn Y, et al. Folfirinox versus gemcitabine for metastatic pancreatic cancer. *N Engl J Med.* (2011) 364:1817–25. doi: 10.1056/NEJMoa1011923

6. Von Hoff DD, Ervin T, Arena FP, Chiorean EG, Infante J, Moore M, et al. Increased survival in pancreatic cancer with nab-paclitaxel plus gemcitabine. *N Engl J Med.* (2013) 369:1691–703. doi: 10.1056/NEJMoa1304369

7. Hinshaw DC, Shevde LA. The tumor microenvironment innately modulates cancer progression. *Cancer Res*. (2019) 79:4557–66. doi: 10.1158/0008-5472.Can-18-3962

8. Chen X, Song E. Turning foes to friends: targeting cancer-associated fibroblasts. *Nat Rev Drug Discov*. (2019) 18:99–115. doi: 10.1038/s41573-018-0004-1

9. Yang C, Geng H, Yang X, Ji S, Liu Z, Feng H, et al. Targeting the immune privilege of tumor-initiating cells to enhance cancer immunotherapy. *Cancer Cell*. (2024) 42:2064–81.e19. doi: 10.1016/j.ccell.2024.10.008

10. Jin MZ, Jin WL. The updated landscape of tumor microenvironment and drug repurposing. *Signal Transduct Target Ther*. (2020) 5:166. doi: 10.1038/s41392-020-00280-x

11. Liu T, Han C, Wang S, Fang P, Ma Z, Xu L, et al. Cancer-associated fibroblasts: an emerging target of anti-cancer immunotherapy. *J Hematol Oncol*. (2019) 12:86. doi: 10.1186/s13045-019-0770-1

12. Sahai E, Astsaturov I, Cukierman E, DeNardo DG, Egeblad M, Evans RM, et al. A framework for advancing our understanding of cancer-associated fibroblasts. *Nat Rev Cancer*. (2020) 20:174–86. doi: 10.1038/s41568-019-0238-1

13. Pelka K, Hofree M, Chen JH, Sarkizova S, Pirl JD, Jorgji V, et al. Spatially organized multicellular immune hubs in human colorectal cancer. *Cell*. (2021) 184:4734–52.e20. doi: 10.1016/j.cell.2021.08.003

14. Khaliq AM, Erdogan C, Kurt Z, Turgut SS, Grunvald MW, Rand T, et al. Refining colorectal cancer classification and clinical stratification through a single-cell atlas. *Genome Biol*. (2022) 23:113. doi: 10.1186/s13059-022-02677-z

15. Zhang TL, Xia C, Zheng BW, Hu HH, Jiang LX, Escobar D, et al. Integrating single-cell and spatial transcriptomics reveals endoplasmic reticulum stress-related caf subpopulations associated with chordoma progression. *Neuro Oncol*. (2024) 26:295–308. doi: 10.1093/neuonc/noad173

16. Cords L, Tietscher S, Anzeneder T, Langwieder C, Rees M, de Souza N, et al. Cancer-associated fibroblast classification in single-cell and spatial proteomics data. *Nat Commun*. (2023) 14:4294. doi: 10.1038/s41467-023-39762-1

17. Kieffer Y, Hocine HR, Gentric G, Pelon F, Bernard C, Bourachot B, et al. Single-cell analysis reveals fibroblast clusters linked to immunotherapy resistance in cancer. *Cancer Discov*. (2020) 10:1330–51. doi: 10.1158/2159-8290.Cd-19-1384

18. Puram SV, Tirosh I, Parikh AS, Patel AP, Yizhak K, Gillespie S, et al. Single-cell transcriptomic analysis of primary and metastatic tumor ecosystems in head and neck cancer. *Cell*. (2017) 171:1611–24.e24. doi: 10.1016/j.cell.2017.10.044

19. Libbrecht MW, Noble WS. Machine learning applications in genetics and genomics. *Nat Rev Genet*. (2015) 16:321–32. doi: 10.1038/nrg3920

20. Brunet JP, Tamayo P, Golub TR, Mesirov JP. Metagenes and molecular pattern discovery using matrix factorization. *Proc Natl Acad Sci U.S.A*. (2004) 101:4164–9. doi: 10.1073/pnas.0308531101

21. Longo SK, Guo MG, Ji AL, Khavari PA. Integrating single-cell and spatial transcriptomics to elucidate intercellular tissue dynamics. *Nat Rev Genet*. (2021) 22:627–44. doi: 10.1038/s41576-021-00370-8

22. Zhang Q, Fei L, Han R, Huang R, Wang Y, Chen H, et al. Single-cell transcriptome reveals cellular hierarchies and guides P-emt-targeted trial in skull base chordoma. *Cell Discov*. (2022) 8:94. doi: 10.1038/s41421-022-00459-2

23. Sun G, Li Z, Rong D, Zhang H, Shi X, Yang W, et al. Single-cell Rna sequencing in cancer: applications, advances, and emerging challenges. *Mol Ther Oncolytics*. (2021) 21:183–206. doi: 10.1016/j.omto.2021.04.001

24. Tian L, Chen F, Macosko EZ. The expanding vistas of spatial transcriptomics. *Nat Biotechnol*. (2023) 41:773–82. doi: 10.1038/s41587-022-01448-2

25. Lin W, Noel P, Borazanci EH, Lee J, Amini A, Han IW, et al. Single-cell transcriptome analysis of tumor and stromal compartments of pancreatic ductal adenocarcinoma primary tumors and metastatic lesions. *Genome Med*. (2020) 12:80. doi: 10.1186/s13073-020-00776-9

26. Halbrook CJ, Thurston G, Boyer S, Anaraki C, Jiménez JA, McCarthy A, et al. Differential integrated stress response and asparagine production drive symbiosis and therapy resistance of pancreatic adenocarcinoma cells. *Nat Cancer*. (2022) 3:1386–403. doi: 10.1038/s43018-022-00463-1

27. Oh K, Yoo YJ, Torre-Healy LA, Rao M, Fassler D, Wang P, et al. Coordinated single-cell tumor microenvironment dynamics reinforce pancreatic cancer subtype. *Nat Commun*. (2023) 14:5226. doi: 10.1038/s41467-023-40895-6

28. Kim S, Leem G, Choi J, Koh Y, Lee S, Nam SH, et al. Integrative analysis of spatial and single-cell transcriptome data from human pancreatic cancer reveals an intermediate cancer cell population associated with poor prognosis. *Genome Med*. (2024) 16:20. doi: 10.1186/s13073-024-01287-7

29. Zhang G, He P, Tan H, Budhu A, Gaedcke J, Ghadimi BM, et al. Integration of metabolomics and transcriptomics revealed a fatty acid network exerting growth inhibitory effects in human pancreatic cancer. *Clin Cancer Res*. (2013) 19:4983–93. doi: 10.1158/1078-0432.Ccr-13-0209

30. Yang S, He P, Wang J, Schetter A, Tang W, Funamizu N, et al. A novel Mif signaling pathway drives the Malignant character of pancreatic cancer by targeting Nr3c2. *Cancer Res*. (2016) 76:3838–50. doi: 10.1158/0008-5472.Can-15-2841

31. Chen DT, Davis-Yadley AH, Huang PY, Husain K, Centeno BA, Permuth-Wey J, et al. Prognostic fifteen-gene signature for early stage pancreatic ductal adenocarcinoma. *PloS One*. (2015) 10:e0133562. doi: 10.1371/journal.pone.0133562

32. Riaz N, Havel JJ, Makarov V, Desrichard A, Urba WJ, Sims JS, et al. Tumor and microenvironment evolution during immunotherapy with nivolumab. *Cell*. (2017) 171:934–49.e16. doi: 10.1016/j.cell.2017.09.028

33. Masiero M, Simões FC, Han HD, Snell C, Peterkin T, Bridges E, et al. A core human primary tumor angiogenesis signature identifies the endothelial orphan receptor Eltd1 as a key regulator of angiogenesis. *Cancer Cell*. (2013) 24:229–41. doi: 10.1016/j.ccr.2013.06.004

34. Yu TJ, Ma D, Liu YY, Xiao Y, Gong Y, Jiang YZ, et al. Bulk and single-cell transcriptome profiling reveal the metabolic heterogeneity in human breast cancers. *Mol Ther*. (2021) 29:2350–65. doi: 10.1016/j.ymthe.2021.03.003

35. Sanchez-Vega F, Mina M, Armenia J, Chatila WK, Luna A, La KC, et al. Oncogenic signaling pathways in the cancer genome atlas. *Cell*. (2018) 173:321–37.e10. doi: 10.1016/j.cell.2018.03.035

36. Shiga K, Hara M, Nagasaki T, Sato T, Takahashi H, Takeyama H. Cancer-associated fibroblasts: their characteristics and their roles in tumor growth. *Cancers (Basel)*. (2015) 7:2443–58. doi: 10.3390/cancers7040902

37. Zhang W, Huang P. Cancer-stromal interactions: role in cell survival, metabolism and drug sensitivity. *Cancer Biol Ther*. (2011) 11:150–6. doi: 10.4161/cbt.11.2.14623

38. Cano P, Godoy A, Escamilla R, Dhir R, Onate SA. Stromal-epithelial cell interactions and androgen receptor-coregulator recruitment is altered in the tissue microenvironment of prostate cancer. *Cancer Res*. (2007) 67:511–9. doi: 10.1158/0008-5472.Can-06-1478

39. Zhou B, Chen WL, Wang YY, Lin ZY, Zhang DM, Fan S, et al. A role for cancer-associated fibroblasts in inducing the epithelial-to-mesenchymal transition in human tongue squamous cell carcinoma. *J Oral Pathol Med*. (2014) 43:585–92. doi: 10.1111/jop.12172

40. Kato T, Noma K, Ohara T, Kashima H, Katsura Y, Sato H, et al. Cancer-associated fibroblasts affect intratumoral Cd8(+) and Foxp3(+) T cells via Il6 in the tumor microenvironment. *Clin Cancer Res*. (2018) 24:4820–33. doi: 10.1158/1078-0432.Ccr-18-0205

41. Steer A, Cordes N, Jendrossek V, Klein D. Impact of cancer-associated fibroblast on the radiation-response of solid xenograft tumors. *Front Mol Biosci*. (2019) 6:70. doi: 10.3389/fmolb.2019.00070

42. Ogier C, Colombo PE, Bousquet C, Canterel-Thouennon L, Sicard P, Garambois V, et al. Targeting the Nrg1/Her3 pathway in tumor cells and cancer-associated fibroblasts with an anti-neuregulin 1 antibody inhibits tumor growth in pre-clinical models of pancreatic cancer. *Cancer Lett*. (2018) 432:227–36. doi: 10.1016/j.canlet.2018.06.023

43. Liu Y, He S, Wang XL, Peng W, Chen QY, Chi DM, et al. Tumour heterogeneity and intercellular networks of nasopharyngeal carcinoma at single cell resolution. *Nat Commun*. (2021) 12:741. doi: 10.1038/s41467-021-21043-4

44. Lv K, He T. Cancer-associated fibroblasts: heterogeneity, tumorigenicity and therapeutic targets. *Mol BioMed*. (2024) 5:70. doi: 10.1186/s43556-024-00233-8

45. Li H, Courtois ET, Sengupta D, Tan Y, Chen KH, Goh JJL, et al. Reference component analysis of single-cell transcriptomes elucidates cellular heterogeneity in human colorectal tumors. *Nat Genet*. (2017) 49:708–18. doi: 10.1038/ng.3818

46. Hu H, Piotrowska Z, Hare PJ, Chen H, Mulvey HE, Mayfield A, et al. Three subtypes of lung cancer fibroblasts define distinct therapeutic paradigms. *Cancer Cell*. (2021) 39:1531–47.e10. doi: 10.1016/j.ccell.2021.09.003

47. Sebastian A, Hum NR, Martin KA, Gilmore SF, Peran I, Byers SW, et al. Single-cell transcriptomic analysis of tumor-derived fibroblasts and normal tissue-resident fibroblasts reveals fibroblast heterogeneity in breast cancer. *Cancers (Basel)*. (2020) 12(5):1307. doi: 10.3390/cancers12051307

48. Chen Z, Zhou L, Liu L, Hou Y, Xiong M, Yang Y, et al. Single-cell rna sequencing highlights the role of inflammatory cancer-associated fibroblasts in bladder urothelial carcinoma. *Nat Commun*. (2020) 11:5077. doi: 10.1038/s41467-020-18916-5

49. Sun Q, Zhang B, Hu Q, Qin Y, Xu W, Liu W, et al. The impact of cancer-associated fibroblasts on major hallmarks of pancreatic cancer. *Theranostics*. (2018) 8:5072–87. doi: 10.7150/thno.26546

50. Provenzano PP, Cuevas C, Chang AE, Goel VK, Von Hoff DD, Hingorani SR. Enzymatic targeting of the stroma ablates physical barriers to treatment of pancreatic ductal adenocarcinoma. *Cancer Cell*. (2012) 21:418–29. doi: 10.1016/j.ccr.2012.01.007

51. Diop-Frimpong B, Chauhan VP, Krane S, Boucher Y, Jain RK. Losartan inhibits collagen I synthesis and improves the distribution and efficacy of nanotherapeutics in tumors. *Proc Natl Acad Sci U.S.A*. (2011) 108:2909–14. doi: 10.1073/pnas.1018892108

52. von Bernstorff W, Voss M, Freichel S, Schmid A, Vogel I, Jöhnk C, et al. Systemic and local immunosuppression in pancreatic cancer patients. *Clin Cancer Res*. (2001) 7:925s–32s. doi: 10.1159/000048515

53. Wu R, Guo W, Qiu X, Wang S, Sui C, Lian Q, et al. Comprehensive analysis of spatial architecture in primary liver cancer. *Sci Adv*. (2021) 7:eabg3750. doi: 10.1126/sciadv.abg3750

54. Gartrell RD, Marks DK, Hart TD, Li G, Davari DR, Wu A, et al. Quantitative analysis of immune infiltrates in primary melanoma. *Cancer Immunol Res*. (2018) 6:481–93. doi: 10.1158/2326-6066.Cir-17-0360

55. Pellinen T, Paavolainen L, Martín-Bernabé A, Papatella Araujo R, Strell C, Mezheyeuski A, et al. Fibroblast subsets in non-small cell lung cancer: associations with

survival, mutations, and immune features. *J Natl Cancer Inst*. (2023) 115:71–82. doi: 10.1093/jnci/djac178

56. Öhlund D, Handly-Santana A, Biffi G, Elyada E, Almeida AS, Ponz-Sarvise M, et al. Distinct populations of inflammatory fibroblasts and myofibroblasts in pancreatic cancer. *J Exp Med*. (2017) 214:579–96. doi: 10.1084/jem.20162024

57. Budi EH, Hoffman S, Gao S, Zhang YE, Derynck R. Integration of Tgf-B-induced smad signaling in the insulin-induced transcriptional response in endothelial cells. *Sci Rep*. (2019) 9:16992. doi: 10.1038/s41598-019-53490-x

58. Nagai MA. Pleckstrin homology-like domain, family a, member 1 (Phlda1) and cancer. *BioMed Rep*. (2016) 4:275–81. doi: 10.3892/br.2016.580

59. Wang J, Yao N, Hu Y, Lei M, Wang M, Yang L, et al. Phlda1 promotes glioblastoma cell growth via sustaining the activation state of ras. *Cell Mol Life Sci*. (2022) 79:520. doi: 10.1007/s00018-022-04538-1

60. Huang D, Fu X, Zhang X, Zhao Y. Christmas tree-shaped microneedles as folfirinox spatiotemporal delivery system for pancreatic cancer treatment. *Res (Wash D C)*. (2022) 2022:9809417. doi: 10.34133/2022/9809417

61. Zetrini AE, Lip H, Abbasi AZ, Alradwan I, Ahmed T, He C, et al. Remodeling tumor immune microenvironment by using polymer-lipid-manganese dioxide nanoparticles with radiation therapy to boost immune response of castration-resistant prostate cancer. *Res (Wash D C)*. (2023) 6:247. doi: 10.34133/research.0247

62. Fan R, Baysoy A, Tian X, Zhang F, Renauer P, Bai Z, et al. Spatially resolved panoramic *in vivo* Crispr screen via Perturb-Dbit. *Res Sq*. (2025) 8:rs.3.rs-6481967. doi: 10.21203/rs.3.rs-6481967/v1

63. Gao F, Chen Q, Mori M, Li S, Ferrari G, Krane M, et al. Integrin-mediated mtor signaling drives Tgf-B Overactivity and myxomatous mitral valve degeneration in hypomorphic fibrillin-1 mice. *J Clin Invest*. (2025) 20:e183558. doi: 10.1172/jci183558

frontiers | Frontiers in Immunology

TYPE Original Research
PUBLISHED 21 July 2025
DOI 10.3389/fimmu.2025.1633034

OPEN ACCESS

EDITED BY
Paul Takam Kamga,
Université de Versailles Saint-Quentin-en-Yvelines, France

REVIEWED BY
Jie Ren,
Dalian Medical University, China
Tibera Rugambwa,
Central South University, China

*CORRESPONDENCE
Wei Cao
11009049@qq.com
Zhen He
1170756710@qq.com
Huimin Han
2221881941@qq.com

†These authors have contributed equally to this work

RECEIVED 22 May 2025
ACCEPTED 07 July 2025
PUBLISHED 21 July 2025

CITATION
Xu Y, Liu Y, Han H, He Z and Cao W (2025) The predictive value of the neutrophil/eosinophil ratio in cancer patients undergoing immune checkpoint inhibition: a meta-analysis and a validation cohort in hepatocellular carcinoma.
Front. Immunol. 16:1633034.
doi: 10.3389/fimmu.2025.1633034

The predictive value of the neutrophil/eosinophil ratio in cancer patients undergoing immune checkpoint inhibition: a meta-analysis and a validation cohort in hepatocellular carcinoma

Yang Xu†, Yang Liu†, Huimin Han*, Zhen He* and Wei Cao*

Department of Oncology, Wuhan Third Hospital, Tongren Hospital of Wuhan University, Wuhan, Hubei, China

Objective: This study was conducted to determine the prognostic relevance of neutrophil/eosinophil ratio (NER) in cancer patients receiving immune checkpoint inhibition therapy.

Methods: A comprehensive search of the literature was carried out across PubMed, EMBASE, and the Cochrane Library to identify relevant studies published before May 2025. Key clinical endpoints included overall survival (OS), progression-free survival (PFS), objective response rate (ORR), and disease control rate (DCR). Additionally, a retrospective cohort analysis involving 67 hepatocellular carcinoma (HCC) patients who received ICIs at our center was undertaken to evaluate the prognostic significance of NER with respect to OS and PFS.

Results: This meta-analysis incorporated 12 studies comprising a total of 1,716 patients. Higher baseline NER was consistently associated with poorer clinical outcomes, including shorter OS (HR = 1.82, 95% CI: 1.57–2.11, $p < 0.001$) and PFS (HR = 1.62, 95% CI: 1.34–2.97, $p < 0.001$), as well as lower ORR (HR = 0.50, 95% CI: 0.37–0.68, $p < 0.001$) and DCR (OR = 0.44, 95% CI: 0.31–0.61, $p < 0.001$). Complementing these findings, analysis of a retrospective cohort from our institution involving HCC patients revealed that individuals with higher NER experienced significantly worse OS ($p = 0.006$) and PFS ($p = 0.033$) when compared to those with lower NER levels.

Conclusion: These findings underscore the prognostic significance of pretreatment NER in cancer patients receiving ICI therapy. Integrating NER into standard clinical evaluation may enhance risk stratification and contribute to the personalization of treatment strategies.

KEYWORDS

immune checkpoint inhibitors, neutrophil-to-eosinophil ratio, prognosis, cancer, hepatocellular carcinoma

1 Introduction

Cancer remains the leading cause of death worldwide and continues to impose an increasingly severe threat to global health systems (1). The advent of monoclonal antibodies that inhibit immune checkpoints has ushered in a new era in oncology therapeutics (2, 3). Therapies based on immune checkpoint inhibitors (ICIs), particularly those targeting programmed cell death protein 1 (PD-1)/programmed death-ligand 1 (PD-L1) and cytotoxic T-lymphocyte–associated protein 4 (CTLA-4) pathways, have emerged as central pillars in modern immuno-oncology (4, 5). By reinvigorating immune responses or augmenting existing antitumor immunity, these approaches have shown substantial efficacy across a wide range of malignancies (6). Nonetheless, the clinical benefits are often limited to a subset of patients, and the absence of dependable predictive biomarkers remains a significant challenge (7). This highlights an urgent need to discover not only novel immunotherapeutic targets but also accessible, blood-derived biomarkers that can guide treatment selection. Such advances would expand the reach of ICI strategies and enhance their clinical impact across diverse cancer populations.

Neutrophils and eosinophils are both derived from myeloid progenitor cells but play distinct roles in the tumor microenvironment. Increasing evidence indicates a dynamic interplay between these two granulocyte populations (8, 9). Neutrophils often promote tumor progression through immunosuppressive mechanisms and facilitation of metastasis (8, 9), whereas eosinophils may exert anti-tumor effects by enhancing cytotoxic immune responses and secreting chemokines that recruit T cells. The NER, therefore, reflects a balance between pro-tumor and anti-tumor inflammatory forces. Given this biological rationale, NER has the potential to serve as an integrative prognostic biomarker, particularly in patients undergoing immune checkpoint inhibitor (ICI) therapy.

Emerging evidence suggests a potential link between a low baseline neutrophil/eosinophil ratio (NER) and favorable clinical outcomes in cancer patients receiving ICI therapy (10–12). In contrast, studies by Pozorski et al. and Zhuang et al. found no significant association between pretreatment NER and progression-free survival (PFS) in cancer patients (13, 14). To reconcile these contradictory results, the current study integrates both a meta-analytic framework and retrospective cohort analysis to comprehensively investigate the prognostic significance of NER in cancer patients treated with ICIs.

2 Methods

2.1 Literature search strategy, inclusion and exclusion criteria for the meta-analysis

Beginning in May 2025, a comprehensive electronic search was conducted across PubMed, EMBASE, and the Cochrane Library databases. The search utilized keywords such as "Neutrophil-to-Eosinophil Ratio" and "Neutrophil/Eosinophil Ratio." The complete search syntax is available in the Supplementary Material. In addition to database retrieval, grey literature was reviewed via Google Scholar, and the reference lists of all eligible studies were manually screened for additional sources.

Studies were included if they met the following criteria: (1) enrolled patients diagnosed with cancer; (2) involved treatment with ICIs; (3) stratified patients into high and low NER groups; and (4) reported at least one relevant clinical endpoint—namely, overall survival (OS), PFS, objective response rate (ORR), or disease control rate (DCR). Studies were excluded if they were conference abstracts or commentary articles. When multiple publications reported on overlapping patient cohorts, only the version with the most complete dataset and rigorous methodology was included (15).

2.2 Data extraction and quality evaluation for the meta-analysis

Key information was systematically extracted from each eligible study, including the first author's name, year of publication, study period, geographic location, tumor classification, treatment strategy, sample size, participant demographics (such as age and sex), and the cutoff value. When available, hazard ratios (HRs) from multivariate analyses were preferred over those from univariate models (16).

The methodological quality of the included observational studies was assessed using the Newcastle–Ottawa Scale (NOS) for cohort studies. This scale evaluates three broad domains: (1) Selection of study groups (up to 4 points), including representativeness of the exposed cohort, selection of the non-exposed cohort, ascertainment of exposure, and demonstration that outcome of interest was not present at the start of the study; (2) Comparability of cohorts based on design or analysis (up to 2 points); and (3) Outcome assessment (up to 3 points), including assessment of outcome, follow-up duration, and adequacy of follow-up. Studies scoring more than six points were considered high quality. All steps were performed independently by two reviewers. Any discrepancies between reviewers were resolved through consultation with the senior author.

2.3 Retrospective study cohort and data acquisition

This study received approval from the institutional ethics committee. Owing to its retrospective design, the requirement for informed consent was waived. A historical cohort analysis was conducted involving patients diagnosed with hepatocellular carcinoma (HCC) who underwent treatment with ICIs combined with anti-angiogenic agents at our center between Mar 2019 and May 2023. Inclusion criteria mandated at least one measurable tumor lesion as defined by RECIST version 1.1 (17).

Clinical and demographic information was extracted from electronic medical records and included patient age, gender, Eastern Cooperative Oncology Group performance status (ECOG PS), underlying hepatitis type, presence of cirrhosis, Barcelona Clinic Liver Cancer (BCLC) stage, Child–Pugh score, number of

lesions, macrovascular invasion status, treatment line, modified albumin–bilirubin (mALBI) grade, and serum alpha-fetoprotein (AFP) levels. Tumor response and progression were evaluated according to RECIST version 1.1 criteria. Follow-up imaging via CT was routinely conducted at intervals of one to three months after treatment initiation. PFS was defined as the time from the first dose of immune checkpoint blockade to radiographic progression or death, while OS was measured from treatment initiation to death from any cause.

2.4 Statistical methods

Categorical data were expressed as absolute frequencies accompanied by their respective percentages. Survival outcomes across different subgroups were evaluated using the Kaplan–Meier estimator in conjunction with the Cox proportional hazards regression model. Meta-analytical computations were performed with Stata version 18.0, and the results were graphically summarized using forest plots. To quantify heterogeneity across included studies, both the I^2 statistic and Cochran's Q test were applied. A heterogeneity level was considered significant if the I^2 exceeded 50% or the corresponding p-value was below 0.1 (18). When substantial variability was detected, the DerSimonian–Laird random-effects model was employed; otherwise, a fixed-effect model using the Inverse Variance method was applied.

Publication bias was investigated through Begg's and Egger's statistical tests (19). Sensitivity analyses were also conducted by sequentially omitting individual studies to assess the influence of each on the pooled HRs and overall effect estimates (20). Furthermore, subgroup analyses were conducted by stratifying data according to NER cutoff values and the type of Cox regression model used. A two-tailed p-value of less than 0.05 was considered to indicate statistical significance.

3 Results

3.1 Search results and study characteristics

An initial search across the databases, supplemented by manual screening of reference lists, yielded a total of 208 potentially relevant records. Following the removal of 54 duplicate entries, 125 studies were excluded after evaluation of titles and abstracts, as they did not meet the predefined inclusion criteria. A full-text assessment of the remaining 32 articles resulted in the exclusion of 20 papers that failed to satisfy the eligibility standards. Consequently, 12 studies were ultimately included in the meta-analysis (10–14, 21–27) (Figure 1).

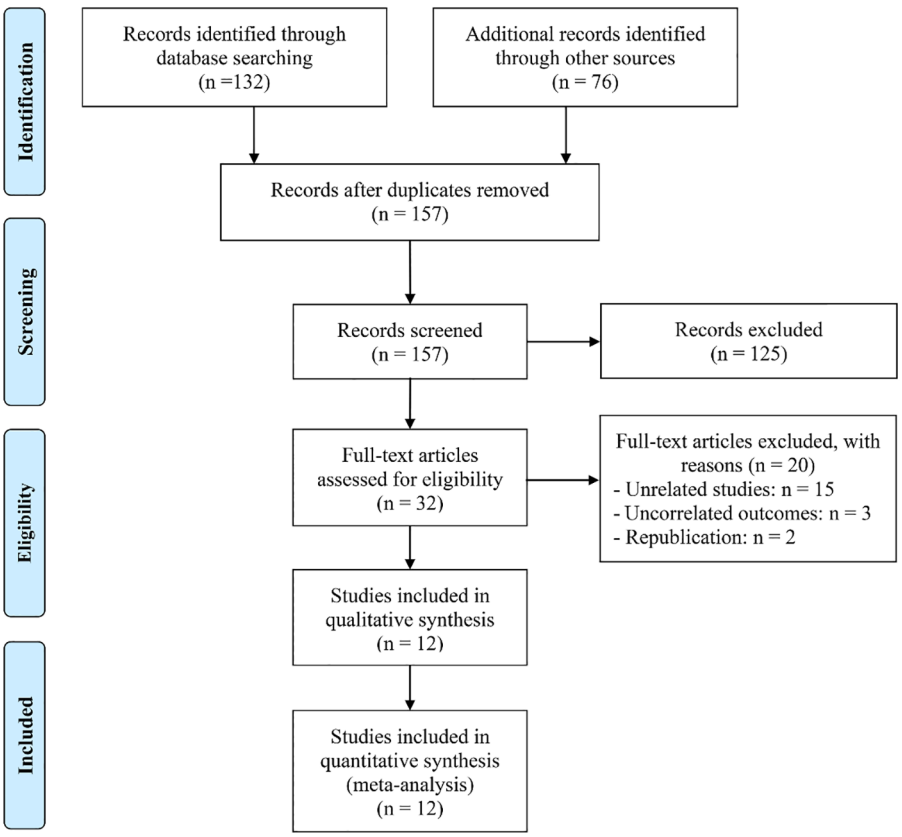

FIGURE 1
The flow diagram of identifying eligible studies.

Table 1 provides an overview of the key characteristics of the included studies. In total, 1,716 individuals were enrolled, with sample sizes ranging from 21 to 401 per study. Of the 12 studies, five were conducted in the USA and two in Japan. Five studies involved patients with renal cell carcinoma, two with urothelial carcinoma, and two were pan-cancer studies. All studies employed a retrospective design. Based on the NOS, quality scores ranged from 6 to 8, indicating a low risk of bias (Table 1).

3.2 Baseline neutrophil/eosinophil ratio and overall survival

This meta-analysis incorporated 12 qualified studies involving a total of 1,716 patients to assess the prognostic relevance of the NER on OS in individuals receiving ICI therapy. The aggregated HR indicated a significant association between higher NER levels and poorer OS outcomes (HR = 1.82, 95% CI: 1.57–2.11, $p < 0.001$; Figure 2A). Between-study variability was negligible, as reflected by Cochran's Q test and an I^2 value ($I^2 = 0$, $p = 0.444$), supporting the use of a fixed-effects model.

Robustness of the pooled results was validated through sensitivity analysis, which involved the stepwise exclusion of each individual study. The overall estimates for OS remained consistent throughout this process (Figure 2B). Furthermore, assessments for publication bias using Begg's and Egger's tests revealed no statistically significant evidence of bias (Begg's $p = 0.118$; Egger's $p = 0.108$).

Subgroup analyses demonstrated that both univariate (HR = 1.71, 95% CI: 1.42–2.08, $p < 0.001$) and multivariate regression approaches (HR = 1.98, 95% CI: 1.57–2.49, $p < 0.001$) consistently revealed a statistically significant link between elevated NER values and reduced OS (Figure 3). Moreover, this inverse association remained evident when the NER threshold exceeded 30 (HR = 1.91, 95% CI: 1.56–2.34, $p < 0.001$) or fell within the 20–30 range (HR = 1.81, 95% CI: 1.38–2.36, $p < 0.001$, Supplementary Figure S1). In contrast, when the cut-off point was below 20, NER failed to show prognostic value in predicting OS among cancer patients (HR = 1.67, 95% CI: 0.73–3.81, $p = 0.227$, Supplementary Figure S1).

3.3 Baseline neutrophil/eosinophil ratio and progression-free survival

This meta-analysis included nine eligible studies encompassing 1,504 patients to investigate the prognostic impact of the NER on PFS among individuals treated with ICIs. The pooled HR indicated a strong correlation between elevated NER and unfavorable PFS

TABLE 1 Main characteristics of the studies included.

Study	Country	Cancer type	Treatment	Study period	Sample size	Age	Gender (male/female)	Cut point	NOS
Yildirim et al., 2025 (24)	USA	RCC	ICIs	01/2018-08/2023	401	66 (18–95)[b]	283/118	43.1	7
Pozorski et al., 2023 (14)	USA	Melanoma	Nivolumab or pembrolizumab	2011-2022	183	–	113/70	35.0	7
Tucker et al., 2024 (25)	USA	RCC	Avelumab plus axitinib or sunitinib	–	383	–	–	29.2	8
Zhuang et al., 2025 (13)	USA	pSCC	Nivolumab or pembrolizumab	2012-2023	21	56 (38–76)[b]	–	49.4	6
Gambale et al., 2024 (10)	Italian	UC	Avelumab	2021-2023	109	72 (54 -77)[a]	89/20	28.1	7
Suzuki et al., 2022 (22)	Japan	HNSCC	Nivolumab	10/2017-12/2021	47	67 (29–84)[b]	39/8	32	6
Beulque et al., 2024 (11)	UK, Belgium	RCC	Nivolumab with or without ipilimumab	2012-2022	201	67 (31-90)[b]	149/52	33.8	7
Liang et al., 2023 (21)	China	Pan-cancer	Anti-PD-(L)1	01/2019-12/2021	46	64 (57.5-67)[a]	41/6	18.43	7
Tucker et al., 2021 (26)	USA	RCC	Nivolumab plus ipilimumab	2016-2020	110	60.5 (54-69)[a]	84/26	26.4	7
Varayathu et al., 2021 (23)	India	Pan-cancer	Nivolumab or pembrolizumab	2017-2021	61	58[c]	42/19	24.3	7
Furubayashi et al., 2021 (27)	Japan	UC	Pembrolizumab	01/2018-06/2021	105	72 (67-77)[a]	75/30	13.7	7
Gil et al., 2022 (12)	Portugal	RCC	Nivolumab	06/2017-04/2021	49	61(28-85)[b]	42/7	48.0	6

[a]median (IQR), [b]median (range), [c]median. ICIs, immune checkpoint inhibitors; RCC, renal cell carcinoma; UC, uothelial carcinoma; HNSCC, head and neck squamous cell carcinoma; pSCC, penile squamous cell carcinoma.

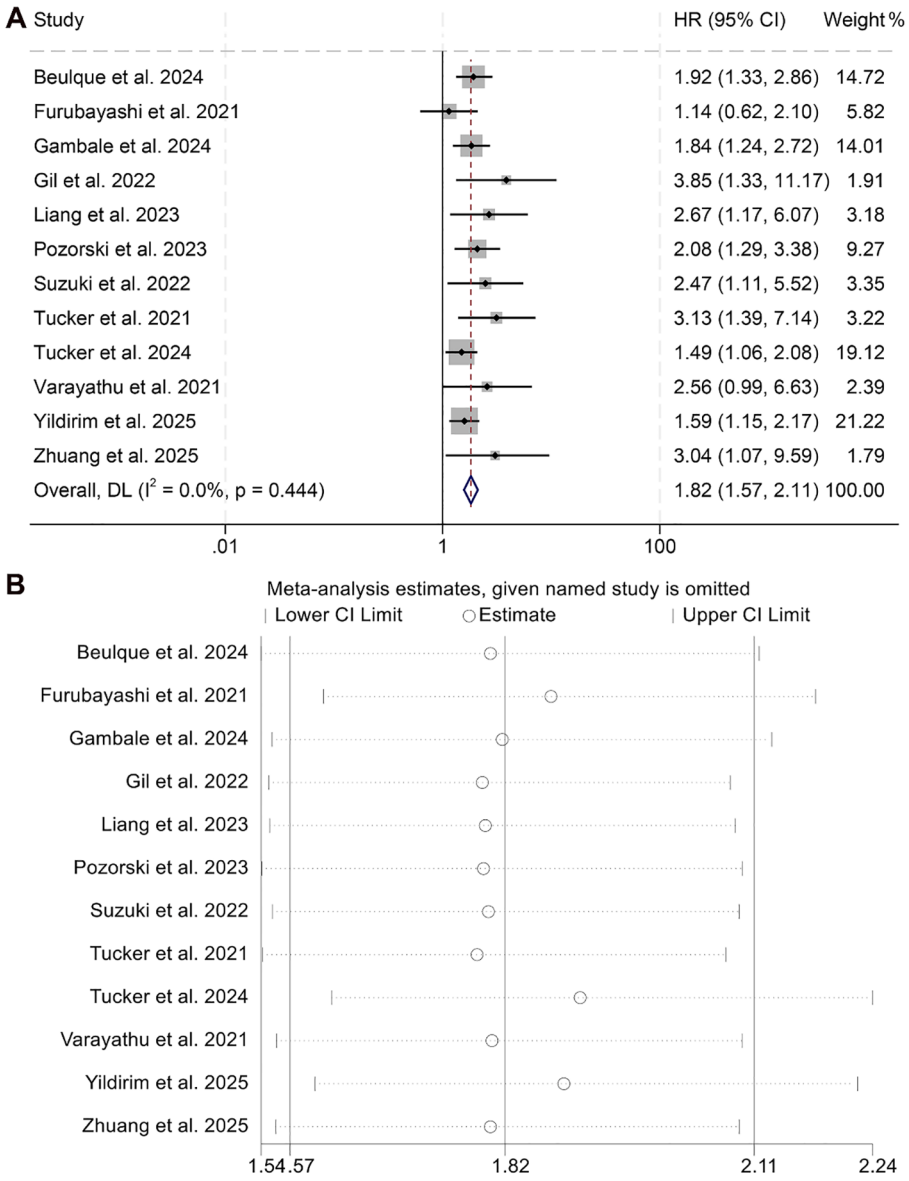

FIGURE 2
Forest plots depicting the association between the baseline neutrophil/eosinophil ratio and overall survival in cancer patients treated with ICIs **(A)**. Sensitivity analysis of the association between baseline neutrophil/eosinophil ratio and overall survival in cancer patients treated with ICIs **(B)**. HR, hazard ratio; CI, confidence interval.

outcomes (HR = 1.62, 95% CI: 1.34–2.97, $p < 0.001$; Figure 4A). Substantial heterogeneity was observed among the studies (I^2 = 41.8%, $p = 0.089$), warranting the use of a random-effects model.

Sensitivity analysis, performed through sequential removal of each study, confirmed the stability of the combined PFS estimates (Figure 4B). In addition, assessments for potential publication bias using Begg's and Egger's tests did not indicate statistical evidence of asymmetry (Begg's $p = 0.129$; Egger's $p = 0.145$).

Subgroup analyses further supported the association between high baseline NER and reduced PFS, with consistent results observed in both univariate (HR = 1.90, 95% CI: 1.32–2.75, $p < 0.001$) and multivariate models (HR = 1.46, 95% CI: 1.20–1.79, $p < 0.001$, Figure 5). Notably, this negative prognostic relationship was maintained when the NER cut-off was greater than 30 (HR = 1.66, 95% CI: 1.31–2.10, $p < 0.001$) or within the 20–30 range (HR = 1.62, 95% CI: 1.07–2.45, $p < 0.001$, Supplementary Figure S2).

3.4 Baseline neutrophil/eosinophil ratio and objective response rate

Our study further investigated the association between NER and ORR, incorporating data from six studies involving a total of 973 cancer patients. As no significant heterogeneity was observed across these studies, a fixed-effect model was applied (I^2 = 42.4%, $p = 0.123$). The meta-analysis demonstrated that patients with

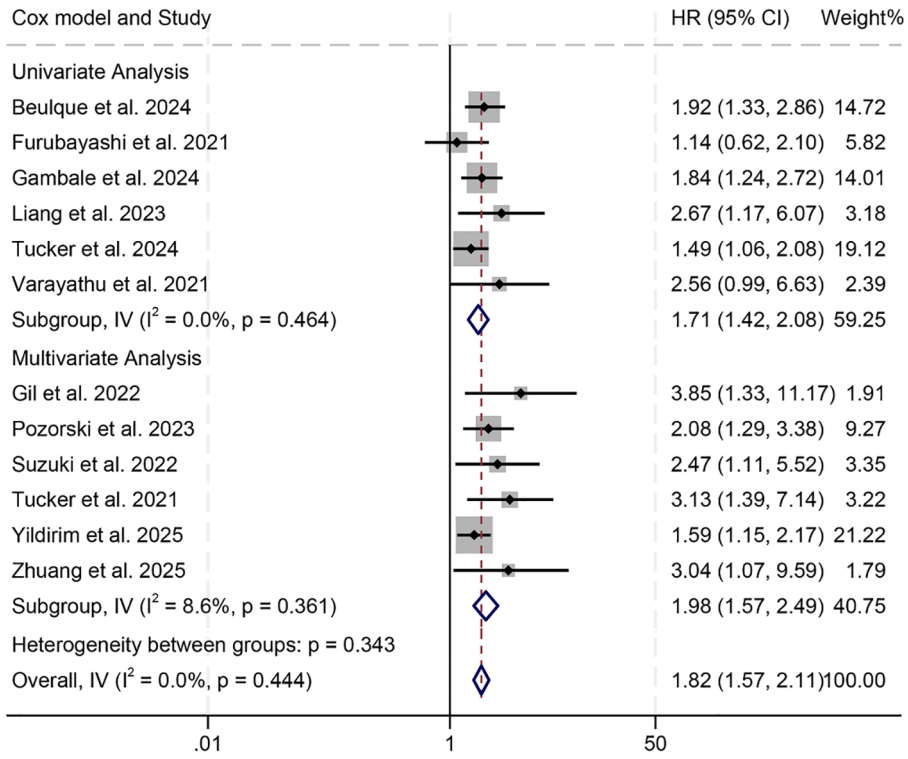

FIGURE 3
Subgroup analysis based on the Cox model revealed the relationship between the baseline neutrophil/eosinophil ratio and the overall survival of cancer patients treated with immune checkpoint inhibitors. HR, hazard ratio; CI, confidence interval.

elevated NER had a significantly lower ORR compared to those in the low-NER group (OR = 0.50, 95% CI: 0.37–0.68, $p < 0.001$; Figure 6A).

Sensitivity analysis confirmed the robustness of this finding, as sequential exclusion of individual studies did not materially alter the overall effect estimate (Figure 6B). Assessments for publication bias using Begg's and Egger's tests revealed no statistically significant evidence of bias (Begg's $p = 0.328$; Egger's $p = 0.428$). Moreover, subgroup analysis based on different NER cut-off values consistently supported the observed association, indicating that the inverse relationship between NER and ORR remained stable across various threshold definitions (Supplementary Figure S3).

3.5 Baseline neutrophil/eosinophil ratio and disease control rate

The relationship between NER and DCR among cancer patients was analyzed based on four studies comprising 759 individuals. As the analysis revealed no significant heterogeneity ($I^2 = 0$, $p = 0.586$), a fixed-effects model was deemed appropriate. The aggregated findings demonstrated that higher NER levels were significantly correlated with a lower DCR compared to patients with lower NER values (OR = 0.44, 95% CI: 0.31–0.61, $p < 0.001$; Figure 7A).

To assess the reliability of these results, sensitivity analyses were performed by systematically excluding each study. The consistency of the effect estimates across iterations confirmed the robustness and stability of the pooled outcome for DCR (Figure 7B).

3.6 Prognostic role of neutrophil/eosinophil ratio in our HCC cohort

In view of the limited literature addressing the prognostic relevance of the NER in hepatocellular carcinoma (HCC), we conducted an analysis using patient data from our institution to enhance current insights into NER as a prognostic biomarker in oncology.

Supplementary Table 1 presents the baseline demographic and clinical profiles of the 67 patients with HCC included in our cohort. The median age was 58.2 years, with an age range spanning from 40.2 to 81.23 years. A predominance of male participants was observed, accounting for 67.16% (n = 45) of the total. Regarding performance status, 62.69% (n = 42) had an ECOG PS score of 0, while the remaining 37.31% (n = 25) had a score of 1. Chronic viral hepatitis was documented in 77.61% (n = 52) of the cohort, and cirrhosis of the liver was present in 67.16% (n = 45). According to the BCLC staging system, 5.97% (n = 4) were categorized as early stage, 41.79% (n = 28) as intermediate stage, and 52.24% (n = 35) as advanced stage. Microvascular invasion was identified in 35.82% (n = 24) of patients, and AFP levels exceeded 400 ng/mL in 58.21% (n = 39) of cases.

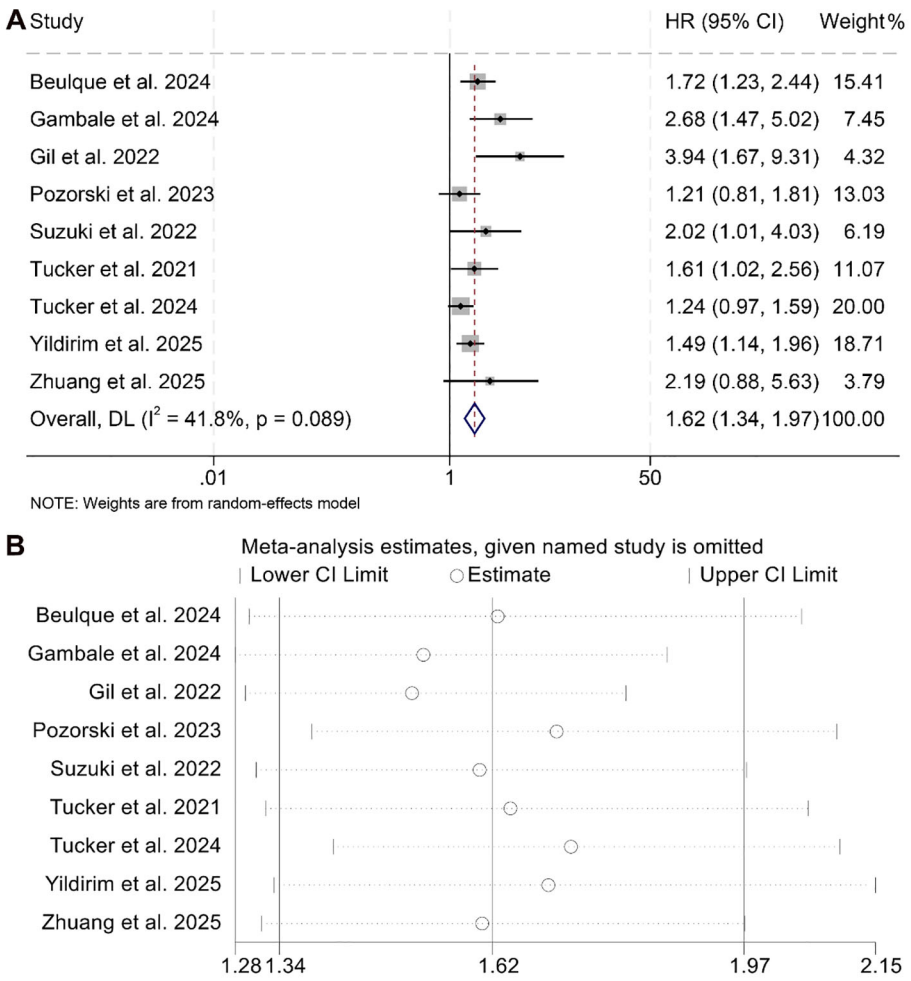

FIGURE 4
Forest plots depicting the association between the baseline neutrophil/eosinophil ratio and progression-free survival in cancer patients treated with ICIs **(A)**. Sensitivity analysis of the association between baseline neutrophil/eosinophil ratio and progression-free survival in cancer patients treated with ICIs **(B)**. HR, hazard ratio; CI, confidence interval. OR, odds ratio; CI, confidence interval.

Patients were stratified into two subgroups according to the median baseline NER threshold. Kaplan–Meier analysis demonstrated that individuals with higher NER exhibited markedly reduced OS (p = 0.006) as well as PFS (p = 0.033) when compared to those with lower NER values (Figure 8).

4 Discussion

As a biomarker easily obtainable through routine hematological testing, the NER offers a cost-efficient and widely accessible measure. In this study, elevated baseline NER was significantly associated with worse survival outcomes among cancer patients. Furthermore, its prognostic relevance remained robust across varying regression models and stratifications based on different threshold definitions.

Earlier investigations have demonstrated that increased circulating neutrophil counts, along with their accumulation within the tumor microenvironment, are linked to unfavorable responses to immune checkpoint blockade therapies (8, 9). Tumor-associated neutrophils (TANs) contribute to poor clinical outcomes by promoting processes such as aerobic glycolysis, angiogenic signaling, formation of neutrophil extracellular traps (NETs), and activation of immunosuppressive mechanisms (28–31).

While eosinophils are well-recognized for their involvement in allergic conditions, parasitic infections, and certain viral responses, their functions within the tumor microenvironment (TME) remain comparatively underexplored relative to other immune cell subsets (32). A growing body of literature has underscored their role in tumor progression and metastasis. *In vitro* experiments suggest that eosinophils contribute to tumor cell eradication by engaging in complex cellular interactions with B lymphocytes, Th1/Th2 $CD4^+$ T cells, and other granulocytes (33). Upon encountering tumor-associated molecular signatures and receiving cues from the immune milieu, eosinophils undergo degranulation, releasing a spectrum of effector molecules—such as TNF-α, granzymes, major basic protein (MBP), and metalloproteinases—that facilitate immune cell recruitment, enhance antigen presentation, and directly induce tumor cytotoxicity (34, 35).

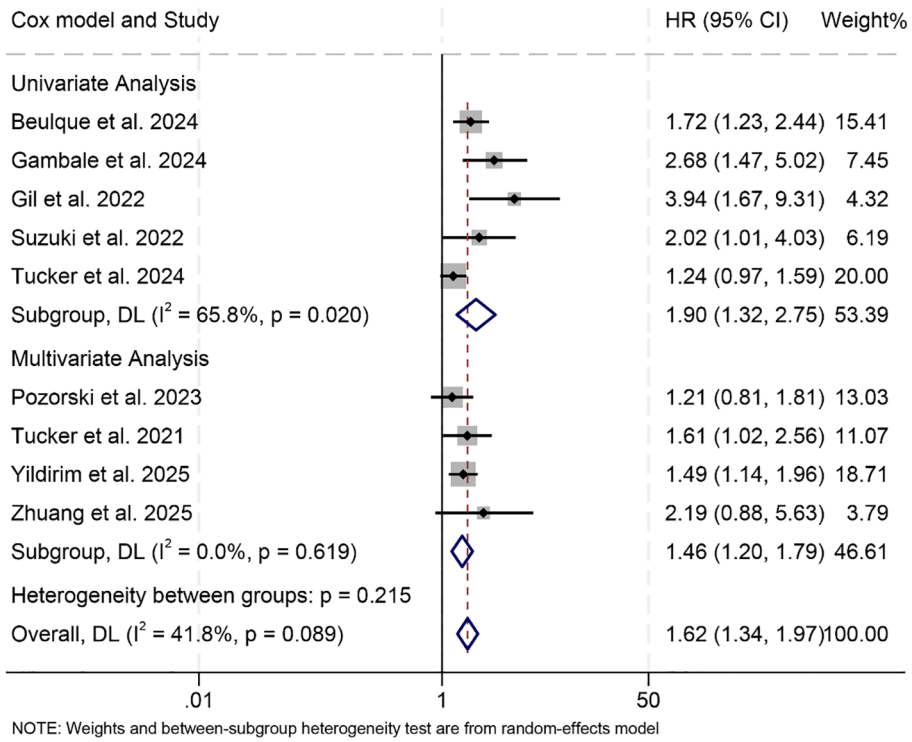

FIGURE 5
Subgroup analysis based on the Cox model revealed the relationship between the baseline neutrophil/eosinophil ratio and the progression-free survival of cancer patients treated with immune checkpoint inhibitors. HR, hazard ratio; CI, confidence interval. OR, odds ratio; CI, confidence interval.

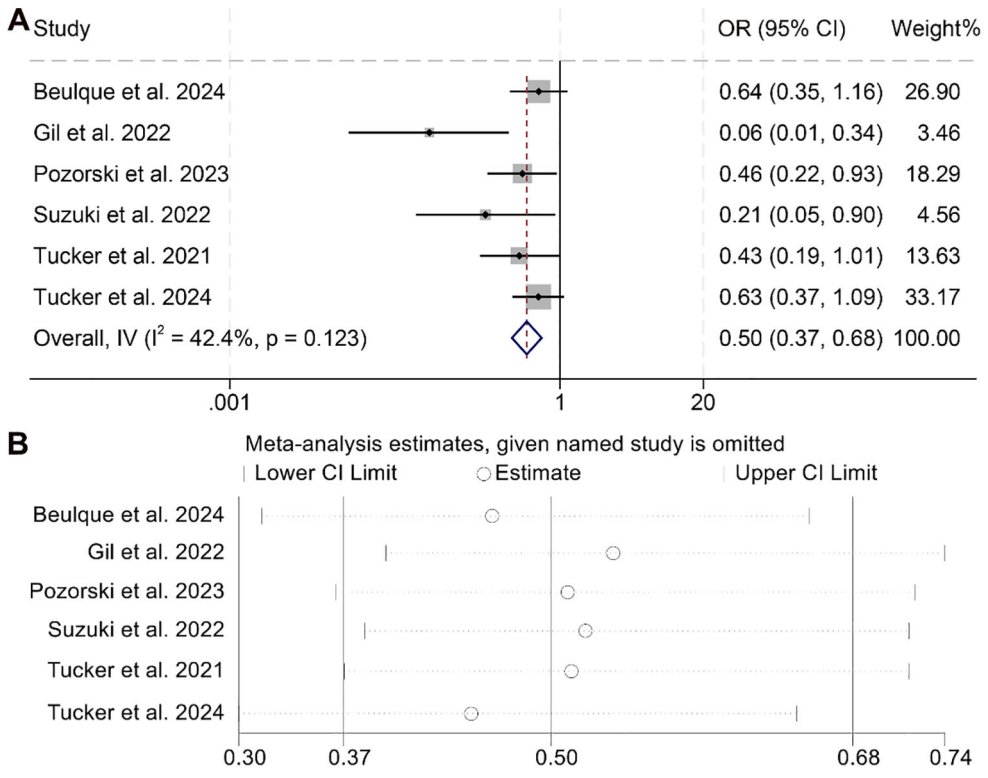

FIGURE 6
Forest plots depicting the association between the baseline neutrophil/eosinophil ratio and objective response rate in cancer patients treated with ICIs **(A)**. Sensitivity analysis of the association between baseline neutrophil/eosinophil ratio and objective response rate in cancer patients treated with ICIs **(B)**. OR, odds ratio; CI, confidence interval.

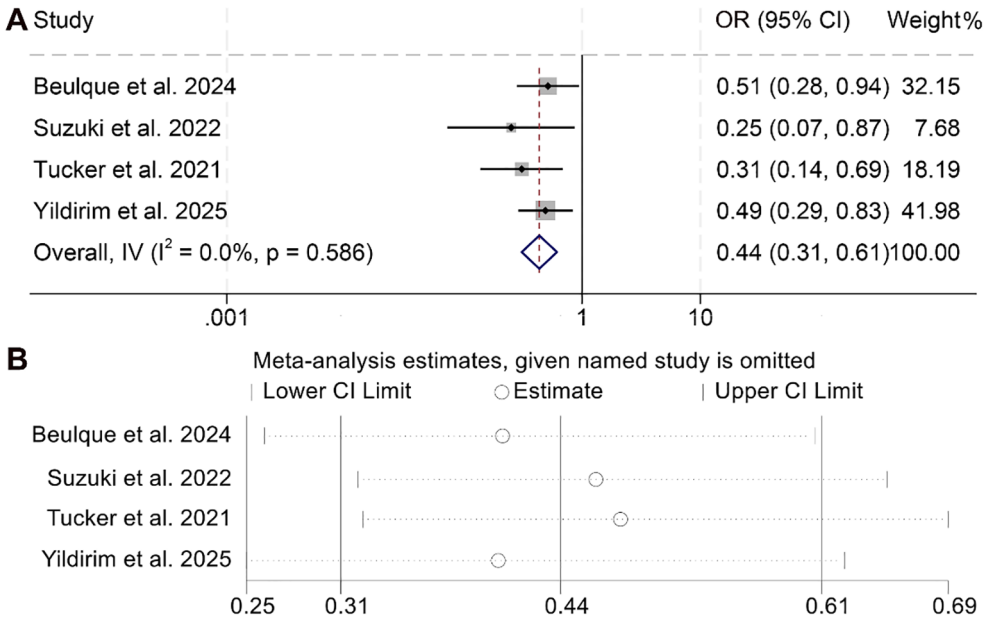

FIGURE 7
Forest plots depicting the association between the baseline neutrophil/eosinophil ratio and disease control rate in cancer patients treated with ICIs **(A)**. Sensitivity analysis of the association between baseline neutrophil/eosinophil ratio and disease control rate in cancer patients treated with ICIs **(B)**. OR, odds ratio; CI, confidence interval.

Moreover, eosinophils secrete ribonucleases and cationic proteins capable of forming extracellular traps that promote tumor cell lysis. *In vivo* models have demonstrated that CC-chemokines play a critical role in guiding eosinophils into tumors and enhancing their cytotoxic activity. Chemokines such as C-C motif chemokine ligand 5 (CCL5), C-C motif chemokine ligand 11 (CCL11), C-X-C motif chemokine ligand 9 (CXCL9), and C-X-C motif chemokine ligand 10 (CXCL10) are believed to be primary mediators of eosinophil-driven tumor necrosis. Notably, diminished expression of CCL11 has been linked to increased tumor load and reduced eosinophil infiltration in preclinical mouse models (36, 37).

Previous studies using melanoma models indicate that tumor cell apoptosis itself may serve as a recruitment signal for eosinophils. Although the precise mechanisms remain to be elucidated, retrospective clinical evidence in melanoma has hinted at a favorable association between lower baseline NER or elevated eosinophil counts and enhanced response to first-line immunotherapy (38, 39). These mechanistic insights offer strong biological support for the findings observed in our present study.

In addition to NER, several other peripheral blood-based biomarkers have shown potential in predicting outcomes in cancer patients undergoing immune checkpoint inhibitor therapy (15, 28, 35, 37, 40). These include the neutrophil-to-lymphocyte ratio (NLR), platelet-to-lymphocyte ratio (PLR), and systemic immune-inflammation index (SII), all of which reflect systemic inflammation and immune status (28). For instance, elevated NLR has been associated with worse prognosis in various malignancies treated with ICIs (28, 35). While these markers may offer complementary insights, there is currently no consensus on which

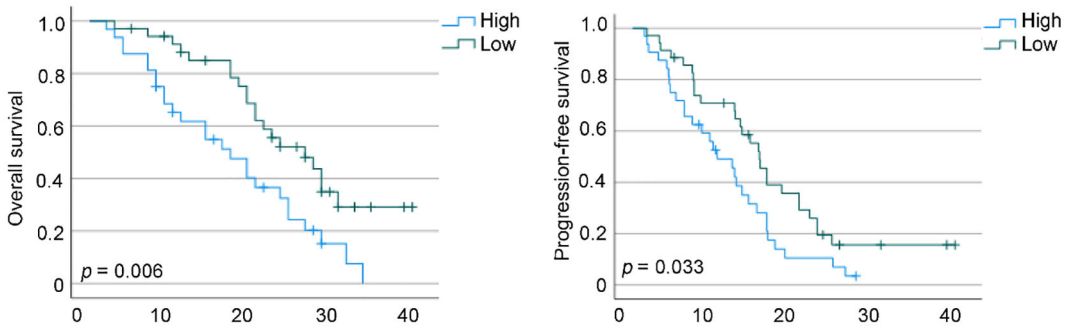

FIGURE 8
Kaplan–Meier survival estimates for overall survival and progression-free survival are presented, stratified by baseline neutrophil-to-eosinophil ratio levels in our cohorts. HR, hazard ratio; CI, confidence interval.

parameter provides the most reliable predictive value. Future prospective studies are needed to directly compare the prognostic performance of NER with these alternative indices and to determine their utility in composite prognostic models.

Although this meta-analysis provides valuable insights, several inherent limitations must be acknowledged. Most notably, the analysis is based solely on retrospective cohort studies, which may compromise the robustness and accuracy of the pooled estimates. Additionally, variation in the definition of NER cut-off values across the included studies introduces methodological inconsistencies. To address these concerns, future investigations should focus on prospective, multicenter trials employing harmonized protocols, thereby improving the generalizability and clinical applicability of NER as a prognostic indicator in oncology.

5 Conclusion

These findings underscore the prognostic utility of the pretreatment NER in cancer patients receiving immune checkpoint inhibitors. As a readily accessible and cost-effective biomarker, NER could be integrated into standard oncology workflows to support pre-treatment risk stratification. Future prospective studies are warranted to validate standardized NER thresholds and to assess its integration into clinical decision-making algorithms for optimizing immunotherapy outcomes.

Data availability statement

The original contributions presented in the study are included in the article/Supplementary Material. Further inquiries can be directed to the corresponding authors.

Ethics statement

The studies involving humans were approved by Ethics Committee of Wuhan Third Hospital. The studies were conducted in accordance with the local legislation and institutional requirements. The ethics committee/institutional review board waived the requirement of written informed consent for participation from the participants or the participants' legal guardians/next of kin because this is a retrospective study utilizing clinical data collected during patients' hospitalization. Written informed consent was obtained from the individual(s) for the publication of any potentially identifiable images or data included in this article.

Author contributions

YX: Investigation, Methodology, Project administration, Software, Visualization, Writing – original draft. YL: Conceptualization, Data curation, Methodology, Software, Validation, Writing – original draft. HH: Conceptualization, Formal analysis, Project administration, Resources, Supervision, Writing – original draft. ZH: Conceptualization, Data curation, Methodology, Resources, Supervision, Validation, Writing – review & editing. WC: Conceptualization, Funding acquisition, Methodology, Project administration, Resources, Supervision, Writing – review & editing.

Funding

The author(s) declare that no financial support was received for the research and/or publication of this article.

Conflict of interest

The authors declare that the research was conducted in the absence of any commercial or financial relationships that could be construed as a potential conflict of interest.

Generative AI statement

The author(s) declare that no Generative AI was used in the creation of this manuscript.

Publisher's note

Supplementary material

The Supplementary Material for this article can be found online at: https://www.frontiersin.org/articles/10.3389/fimmu.2025.1633034/full#supplementary-material

References

1. Murray CJ, Atkinson C, Bhalla K, Birbeck G, Burstein R, Chou D, et al. The state of US health, 1990-2010: burden of diseases, injuries, and risk factors. *JAMA*. (2013) 310:591–608. doi: 10.1001/jama.2013.13805

2. Sordo-Bahamonde C, Lorenzo-Herrero S, Granda-Díaz R, Martínez-Pérez A, Aguilar-García C, Rodrigo JP, et al. Beyond the anti-PD-1/PD-L1 era: promising role of the BTLA/HVEM axis as a future target for cancer immunotherapy. *Mol Cancer*. (2023) 22:142. doi: 10.1186/s12943-023-01845-4

3. Dolton G, Rius C, Wall A, Szomolay B, Bianchi V, Galloway SAE, et al. Targeting of multiple tumor-associated antigens by individual T cell receptors during successful cancer immunotherapy. *Cell*. (2023) 186:3333–49.e27. doi: 10.1016/j.cell.2023.06.020

4. Sattiraju A, Kang S, Giotti B, Chen Z, Marallano VJ, Brusco C, et al. Hypoxic niches attract and sequester tumor-associated macrophages and cytotoxic T cells and reprogram them for immunosuppression. *Immunity*. (2023) 56:1825–43.e6. doi: 10.1016/j.immuni.2023.06.017

5. Hoos A. Development of immuno-oncology drugs - from CTLA4 to PD1 to the next generations. *Nat Rev Drug Discov*. (2016) 15:235–47. doi: 10.1038/nrd.2015.35

6. Chen Y, Hu H, Yuan X, Fan X, Zhang C. Advances in immune checkpoint inhibitors for advanced hepatocellular carcinoma. *Front Immunol*. (2022) 13:896752. doi: 10.3389/fimmu.2022.896752

7. Le DT, Durham JN, Smith KN, Wang H, Bartlett BR, Aulakh LK, et al. Mismatch repair deficiency predicts response of solid tumors to PD-1 blockade. *Science*. (2017) 357:409–13. doi: 10.1126/science.aan6733

8. Schalper KA, Carleton M, Zhou M, Chen T, Feng Y, Huang SP, et al. Elevated serum interleukin-8 is associated with enhanced intratumor neutrophils and reduced clinical benefit of immune-checkpoint inhibitors. *Nat Med*. (2020) 26:688–92. doi: 10.1038/s41591-020-0856-x

9. Zer A, Sung MR, Walia P, Khoja L, Maganti M, Labbe C, et al. Correlation of neutrophil to lymphocyte ratio and absolute neutrophil count with outcomes with PD-1 axis inhibitors in patients with advanced non-small-cell lung cancer. *Clin Lung Cancer*. (2018) 19:426–34.e1. doi: 10.1016/j.cllc.2018.04.008

10. Gambale E, Maruzzo M, Messina C, De Gennaro Aquino I, Vascotto IA, Rossi V, et al. Neutrophil-to-eosinophil ratio predicts the efficacy of avelumab in patients with advanced urothelial carcinoma enrolled in the MALVA study (Meet-URO 25). *Clin Genitourin Cancer*. (2024) 22:102099. doi: 10.1016/j.clgc.2024.102099

11. Beulque Y, Kinget L, Roussel E, Mobaraki S, Laenen A, Debruyne PR, et al. Baseline neutrophil-to-eosinophil-ratio and outcome in metastatic clear-cell renal cell carcinoma treated with nivolumab or ipilimumab/nivolumab. *Acta Oncol*. (2024) 63:658–68. doi: 10.2340/1651-226x.2024.40390

12. Gil L, Alves FR, Silva D, Fernandes I, Fontes-Sousa M, Alves M, et al. Prognostic impact of baseline neutrophil-to-eosinophil ratio in patients with metastatic renal cell carcinoma treated with nivolumab therapy in second or later lines. *Cureus*. (2022) 14: e22224. doi: 10.7759/cureus.22224

13. Zhuang TZ, Goyal S, Case KB, Olsen TA, Vemuru S, Yildirim A, et al. Real-world outcomes in patients with advanced penile squamous cell carcinoma receiving immune checkpoint inhibitors: A single institution experience. *J Immunother Precis Oncol*. (2025) 8:1–10. doi: 10.36401/jipo-24-19

14. Pozorski V, Park Y, Mohamoud Y, Tesfamichael D, Emamekhoo H, Birbrair A, et al. Neutrophil-to-eosinophil ratio as a biomarker for clinical outcomes in advanced stage melanoma patients treated with anti-PD-1 therapy. *Pigment Cell Melanoma Res*. (2023) 36:501–11. doi: 10.1111/pcmr.13109

15. Zhang L, Kuang T, Chai D, Deng W, Wang P, Wang W. The use of antibiotics during immune checkpoint inhibitor treatment is associated with lower survival in advanced esophagogastric cancer. *Int Immunopharmacol*. (2023) 119:110200. doi: 10.1016/j.intimp.2023.110200

16. Zhang L, Chen C, Chai D, Li C, Kuang T, Liu L, et al. Effects of PPIs use on clinical outcomes of urothelial cancer patients receiving immune checkpoint inhibitor therapy. *Front Pharmacol*. (2022) 13:1018411. doi: 10.3389/fphar.2022.1018411

17. Schwartz LH, Litière S, de Vries E, Ford R, Gwyther S, Mandrekar S, et al. "*RECIST 1.1-Update and clarification: From the RECIST committee*". *European J Cancer* (Oxford, England : 1990) (2016) 62:132–7. doi: 10.1016/j.ejca.2016.03.081

18. Ma W, Shi Q, Zhang L, Qiu Z, Kuang T, Zhao K, et al. Impact of baseline body composition on prognostic outcomes in urological Malignancies treated with immunotherapy: a pooled analysis of 10 retrospective studies. *BMC Cancer*. (2024) 24:830. doi: 10.1186/s12885-024-12579-x

19. Zhang L, Li X, Wang K, Wu M, Liu W, Wang W. Prognostic impact of body composition in hepatocellular carcinoma patients with immunotherapy. *Ann Med*. (2024) 56:2395062. doi: 10.1080/07853890.2024.2395062

20. Zhang L, Wang K, Liu R, Kuang T, Chen C, Yao F, et al. Body composition as a prognostic factor in cholangiocarcinoma: a meta-analysis. *Nutr J*. (2024) 23:145. doi: 10.1186/s12937-024-01037-w

21. Liang L, Cui C, Lv D, Li Y, Huang L, Feng J, et al. Inflammatory biomarkers in assessing severity and prognosis of immune checkpoint inhibitor-associated cardiotoxicity. *ESC Heart Fail*. (2023) 10:1907–18. doi: 10.1002/ehf2.14340

22. Suzuki S, Abe T, Endo T, Kaya H, Kitabayashi T, Kawasaki Y, et al. Association of pretreatment neutrophil-to-eosinophil ratio with clinical outcomes in patients with recurrent or metastatic head and neck squamous cell carcinoma treated with nivolumab. *Cancer Manag Res*. (2022) 14:3293–302. doi: 10.2147/CMAR.S382771

23. Varayathu H, Sarathy V, Thomas BE, Mufti SS, Sangi L, Thungappa SC, et al. Translational relevance of baseline peripheral blood biomarkers to assess the efficacy of anti-programmed cell death 1 use in solid Malignancies. *J Cancer Res Ther*. (2021) 17:114–21. doi: 10.4103/jcrt.jcrt_910_20

24. Yildirim A, Wei M, Liu Y, Nazha B, Brown JT, Carthon BC, et al. Association of baseline inflammatory biomarkers and clinical outcomes in patients with advanced renal cell carcinoma treated with immune checkpoint inhibitors. *Ther Adv Med Oncol*. (2025) 17:17588359251316243. doi: 10.1177/17588359251316243

25. Tucker M, Chen YW, Voss MH, McGregor BA, Bilen MA, Grimm MO, et al. Association between neutrophil-to-eosinophil ratio and efficacy outcomes with avelumab plus axitinib or sunitinib in patients with advanced renal cell carcinoma: *post hoc* analyses from the JAVELIN Renal 101 trial. *BMJ Oncol*. (2024) 3:e000181. doi: 10.1136/bmjonc-2023-000181

26. Tucker MD, Brown LC, Chen YW, Kao C, Hirshman N, Kinsey EN, et al. Association of baseline neutrophil-to-eosinophil ratio with response to nivolumab plus ipilimumab in patients with metastatic renal cell carcinoma. *biomark Res*. (2021) 9:80. doi: 10.1186/s40364-021-00334-4

27. Furubayashi N, Minato A, Negishi T, Sakamoto N, Song Y, Hori Y, et al. The association of clinical outcomes with posttreatment changes in the relative eosinophil counts and neutrophil-to-eosinophil ratio in patients with advanced urothelial carcinoma treated with pembrolizumab. *Cancer Manag Res*. (2021) 13:8049–56. doi: 10.2147/CMAR.S333823

28. Zhang L, Feng J, Kuang T, Chai D, Qiu Z, Deng W, et al. Blood biomarkers predict outcomes in patients with hepatocellular carcinoma treated with immune checkpoint Inhibitors: A pooled analysis of 44 retrospective sudies. *Int Immunopharmacol*. (2023) 118:110019. doi: 10.1016/j.intimp.2023.110019

29. Xue R, Zhang Q, Cao Q, Kong R, Xiang X, Liu H, et al. Liver tumour immune microenvironment subtypes and neutrophil heterogeneity. *Nature*. (2022) 612:141–7. doi: 10.1038/s41586-022-05400-x

30. Quail DF, Amulic B, Aziz M, Barnes BJ, Eruslanov E, Fridlender ZG, et al. Neutrophil phenotypes and functions in cancer: A consensus statement. *J Exp Med*. (2022) 219:e20220011. doi: 10.1084/jem.20220011

31. Teijeira A, Garasa S, Ochoa MC, Villalba M, Olivera I, Cirella A, et al. IL8, neutrophils, and NETs in a collusion against cancer immunity and immunotherapy. *Clin Cancer Res*. (2021) 27:2383–93. doi: 10.1158/1078-0432.ccr-20-1319

32. Huang L, Appleton JA. Eosinophils in helminth infection: defenders and dupes. *Trends Parasitol*. (2016) 32:798–807. doi: 10.1016/j.pt.2016.05.004

33. Lilong Z, Kuang T, Li M, Li X, Hu P, Deng W, et al. Sarcopenia affects the clinical efficacy of immune checkpoint inhibitors in patients with gastrointestinal cancers. *Clin Nutr*. (2024) 43:31–41. doi: 10.1016/j.clnu.2023.11.009

34. Legrand F, Driss V, Delbeke M, Loiseau S, Hermann E, Dombrowicz D, et al. Human eosinophils exert TNF-α and granzyme A-mediated tumoricidal activity toward colon carcinoma cells. *J Immunol*. (2010) 185:7443–51. doi: 10.4049/jimmunol.1000446

35. Kuang T, Qiu Z, Wang K, Zhang L, Dong K, Wang W. Pan-immune inflammation value as a prognostic biomarker for cancer patients treated with immune checkpoint inhibitors. *Front Immunol*. (2024) 15:1326083. doi: 10.3389/fimmu.2024.1326083

36. Xing Y, Tian Y, Kurosawa T, Matsui S, Touma M, Yanai T, et al. CCL11-induced eosinophils inhibit the formation of blood vessels and cause tumor necrosis. *Genes Cells*. (2016) 21:624–38. doi: 10.1111/gtc.12371

37. Zhang L, Ma W, Qiu Z, Kuang T, Wang K, Hu B, et al. Prognostic nutritional index as a prognostic biomarker for gastrointestinal cancer patients treated with immune checkpoint inhibitors. *Front Immunol*. (2023) 14:1219929. doi: 10.3389/fimmu.2023.1219929

38. Moreira A, Leisgang W, Schuler G, Heinzerling L. Eosinophilic count as a biomarker for prognosis of melanoma patients and its importance in the response to immunotherapy. *Immunotherapy*. (2017) 9:115–21. doi: 10.2217/imt-2016-0138

39. Zhang L, Chen C, Chai D, Li C, Qiu Z, Kuang T, et al. Characterization of the intestinal fungal microbiome in patients with hepatocellular carcinoma. *J Transl Med*. (2023) 21:126. doi: 10.1186/s12967-023-03940-y

40. Zhang L, Wang K, Kuang T, Deng W, Hu P, Wang W. Low geriatric nutritional risk index as a poor prognostic biomarker for immune checkpoint inhibitor treatment in solid cancer. *Front Nutr*. (2023) 10:1286583. doi: 10.3389/fnut.2023.1286583

frontiers | Frontiers in Immunology

TYPE Original Research
PUBLISHED 02 October 2025
DOI 10.3389/fimmu.2025.1599252

OPEN ACCESS

EDITED BY
Lei Huang,
University of Massachusetts Medical School, United States

REVIEWED BY
Yue Du,
AstraZeneca, United Kingdom
Zhouxuan Li,
University of Texas MD Anderson Cancer Center, United States
Yanyu Zhu,
Stanford University, United States

*CORRESPONDENCE
Bo Li
liboer2002@126.com
Xiaoli Yang
344920646@qq.com
Maoshan Chen
snscms@126.com

†These authors have contributed equally to this work

RECEIVED 24 March 2025
ACCEPTED 29 August 2025
PUBLISHED 02 October 2025

CITATION
Fan J, Chen J, Wang R, Peng Y, Tan S, Zhang X, Tang H, Chen M, Li B and Yang X (2025) Suppressing glutamine metabolism in the pancreatic cancer microenvironment can enhance the anti-tumor effect of CD8 T cells and promote the efficacy of immunotherapy.
Front. Immunol. 16:1599252.
doi: 10.3389/fimmu.2025.1599252

Suppressing glutamine metabolism in the pancreatic cancer microenvironment can enhance the anti-tumor effect of CD8 T cells and promote the efficacy of immunotherapy

Jun Fan[1,2,3†], Jianfei Chen[4†], Rui Wang[2,3†], Yisheng Peng[5], Sunde Tan[2,3], Xi Zhang[2,3], Hao Tang[2,3], Maoshan Chen[1*], Bo Li[2,3*] and Xiaoli Yang[2,3*]

[1]Department of Breast and Thyroid Surgery, Suining Central Hospital, Suining, Sichuan, China, [2]Department of General Surgery (Hepatopancreatobiliary Surgery), The Affiliated Hospital of Southwest Medical University, Luzhou, China, [3]Academician (Expert) Workstation of Sichuan Province, Metabolic Hepatobiliary and Pancreatic Diseases Key Laboratory of Luzhou City, The Affiliated Hospital of Southwest Medical University, Luzhou, China, [4]Department of Thyroid and Breast Surgery, The First People's Hospital of Zigong, Zigong, Sichuan, China, [5]State Key Laboratory of Molecular Vaccinology and Molecular Diagnostics, Center for Molecular Imaging and Translational Medicine, School of Public Health, Xiamen University, Xiamen, China

Objective: This study aims to investigate the relationship between tumor cell glutamine metabolism and CD8 T cells, with the goal of providing new insights to improve immunotherapy for pancreatic cancer.

Methods: Using the The Cancer Genome Atlas – Pancreatic Adenocarcinoma (TCGA-PAAD) cohort, we computed gene expression scores related to glutamine metabolism and stratified patients into high- and low-score groups. Prognosis and differences in immune cell anti-tumor activity were compared between these groups. We further utilized single-cell RNA sequencing data to quantitatively assess the expression of glutamine metabolism-related pathways in tumor cells. Based on tumor-specific glutamine metabolism gene expression, patients were again classified into high- and low-score groups. The immune remodeling effects exerted by tumor cell glutamine metabolism on CD8 T cells were subsequently investigated. To examine the impact of perturbing glutamine metabolism within the tumor microenvironment on CD8 T cell phenotype and the efficacy of PD-1 inhibitors, we conducted *in vivo* animal experiments.

Results: we analyzed the pancreatic cancer dataset in the cancer gene atlas database. We found that tumor glutamine metabolism was negatively correlated with patient prognosis and anti-tumor activity. Next, we defined two types of CD8 effector T cells in single-cell RNA sequencing data, namely, effector memory T cells (CD8-Tem) and terminally differentiated effector memory T cells (CD8-Temra). Under the pressure of high glutamine metabolism in tumor cells, the cytotoxicity of the CD8-Tem subset was reduced, and its immaturity score increased, while the exhaustion score of the CD8-Temra subset increased. Pseudotime analysis showed that CD8-Tn in the low-scoring group mainly developed into CD8-Tem subset, and its immune activation pathway was significantly upregulated. In addition, we found that the glutamine metabolism

inhibitor JHU083 promoted the infiltration of CD4 and CD8 T cells and T lymphocyte differentiation, and increased the efficacy of PD-1 inhibitors. Glutamine inhibitors can inhibit the apoptosis of immune cells in the tumor microenvironment, while promoting CD8 T cells activation and cytotoxicity increase.

Conclusion: Inhibition of glutamine metabolism within the pancreatic cancer microenvironment results in reduced apoptosis of immune cells, heightened activation and cytotoxicity of CD8 T cells, and a substantial enhancement in the therapeutic efficacy of immunotherapy.

KEYWORDS

pancreatic cancer, glutamine, CD8 T cells, immunotherapy, JHU083

1 Introduction

Pancreatic cancer is highly invasive, and patients have a poor prognosis (1–5). Currently, the efficacy of immunotherapy is unsatisfactory (6–16). T lymphocytes are the main immune cells infiltrating the tumor microenvironment of pancreatic cancer (17). CD8 T cells play a critical role in eliminating malignant cells and can provide long-term protective immunity (18–20). In tumor tissues, high abundance of CD8 effector T cells is positively correlated with the prognosis of pancreatic cancer patients (21, 22). However, CD8 T cells generally exhibit low infiltration and low cytotoxicity in pancreatic cancer (23–25). Existing studies have shown that the tumor microenvironment in which CD8 T cells reside is correlated with their developmental trajectory and determines their immune response. That is, the tumor microenvironment determines the anti-tumor ability of CD8 T cells (26). The classical theory has long held that tumor cells mainly obtain energy by taking up glucose in the immune microenvironment, and high glucose metabolism of tumor cells is a core factor that reshapes the metabolic microenvironment of tumors and prevents CD8 T cells from exerting their anti-tumor ability (27–29). Inhibition of glucose metabolism has long been regarded as an important strategy for treating tumors. However, effective inhibitors of glucose metabolism for tumor treatment have not been proven clinically so far. Recently, Professor Kimryn Rathmell's research found that in the tumor immune microenvironment, tumor cells uptake more glutamine than glucose. At the same time, they found that immune cells in the tumor immune microenvironment are not lacking in glucose. In contrast, the amount of glutamine uptake by a single tumor cell is four times that of CD8 T cells (30). Therefore, it is possible that the high metabolism of glutamine in tumor cells in the tumor immune microenvironment leads to a change in the developmental trajectory of CD8 T cells, resulting in a decrease in their anti-tumor effect.

Rapidly proliferating cells, such as tumor cells, exhibit unique metabolic features to meet their high energy demands and increasing synthesis requirements for structural materials such as amino acids, nucleotides, and lipids, enabling sustained proliferation (31–34). Studies have also found increased expression levels of the glutamine transporter in various tumors (35), such as solute carrier family 1 member 5 (SLC1A5). The Myc oncogene can directly promote upregulation of SLC1A5 (36). These unique metabolic features increase the demand of tumor cells for glutamine (Gln) to promote synthetic metabolism. These findings suggest that tumor cells in the tumor microenvironment are dependent on glutamine. We may have overlooked the impact of tumor cell glutamine metabolism reshaping the tumor metabolic microenvironment on the phenotype of CD8 T cells.

Therefore, it is hypothesized that the anti-tumor effect of CD8T cell subpopulations may be diminished when pancreatic cancer remodels the tumor microenvironment through high glutamine metabolism. Disrupting such aberrant pancreatic cancer metabolic microenvironments may potentially enhance the infiltration and cytotoxicity of CD8 T cells, thereby increasing the efficacy of immune checkpoint inhibitors.It is worth noting that overcoming the immunosuppressive microenvironment often requires combination strategies. For example, accumulated evidence has shown that exercise can modulate a variety of cytokines, affect transcriptional pathways, and reprogram certain metabolic processes, ultimately promoting anti-tumor immunity and enhancing the efficacy of immune checkpoint inhibitors in cancer patients (37). Nonetheless, successfully targeting metabolic pathways or integrating adjunctive therapies remains challenging due to the highly complex and heterogeneous nature of the tumor microenvironment, which poses obstacles for designing selective and effective treatment strategies (38).

2 Methods

2.1 Source and data cleaning of pancreatic cancer tissue block sequencing data

The FPKM gene expression matrix of pancreatic cancer tissue block RNA sequencing data, as well as the corresponding clinical follow-up information, can be downloaded from the Cancer

Genome Atlas database (index number TCGA-PAAD) (https://portal.gdc.cancer.gov/). All patients were diagnosed with pancreatic cancer through pathology. After excluding patients with missing clinical follow-up information, we obtained transcriptomic expression matrices of 176 patients and their corresponding clinical pathological parameters. By comparing with the genome annotation file GRCh38, we screened 18,965 protein coding genes and included them in the next analysis after removing duplicate probes.

2.2 Downstream analysis of pancreatic cancer tissue RNA sequencing data

According to the genes related to glutamine metabolism (ALDH18A1, GAPDH, GCLM, GLS, GOT1, MTHFS, OAT, SLC1A5, SLC38A1, SLC38A5, SLC7A5), we used the "ssGSEA" function in the "GSVA" package to calculate the expression scores of glutamine metabolism-related genes in tumor cells of each patient. Similarly, as cytotoxicity-related genes (GZMK, GZMH, GZMB, PRF1, IFNG, EOMES, NKG7), immune cell exhaustion-related genes (PDCD1, TIGIT, HAVCR2, LAG3, CTLA4), and immaturity-related genes (LEF1, SELL, TCF7, CCR7) are specifically expressed in immune cells, tissue block sequencing data can also be used to calculate the cytotoxicity scores of immune cell subgroups in each patient to evaluate the immune phenotype of immune cells in the immune microenvironment. After setting the median score of glutamine metabolism-related gene expression in patients' pancreatic tissue as the grouping intercept value, 176 patients were divided into high and low score groups, and the relationship between the two groups and prognosis was explored.

2.3 The origin and data cleaning of single-cell RNA sequencing data

The single-cell RNA sequencing data used in this study were obtained from the Gene Expression Omnibus (GEO) with accession number GSE155698 (https://www.ncbi.nlm.nih.gov/geo/query/acc.cgi?acc=GSE155698) (39). Specifically, tumor tissues from 12 pancreatic cancer patients were selected for inclusion (4 patients were excluded due to fewer than 10 tumor cells). Cells with gene counts of 50 or more were included in downstream analysis if the same gene was expressed in at least 3 or more cells. Additionally, cells were excluded if their mitochondrial gene ratio was greater than 4%, ribosomal gene ratio was less than 2%, or hemoglobin gene ratio was greater than 10%. Finally, genes and cells meeting the aforementioned criteria were used for downstream analysis.

2.4 Clustering and biological annotation of single-cell RNA sequencing data

The software R (version 4.1.2) was utilized for the analysis of single-cell RNA sequencing data and tissue block sequencing data. The gene expression matrix of all cells was normalized using the built-in function "NormalizeData" from the Seurat package, with the scaling factor set to 10,000. The "vst" algorithm from the "FindVariableFeatures" function was employed to identify 3,000 highly variable genes. The expression matrix was then normalized using the "ScalData" function, with all genes used as reference genes. Principal component analysis was performed to identify statistically significant principal components (P-value < 0.05). To reduce data dimensionality, we used the t-distributed stochastic neighbor embedding algorithm with the top 15 principal components' genes and performed clustering on all cells, with a resolution of 0.1. Based on molecular markers summarized in previous literature, we annotated the clustered cells as different biological subgroups, including neutrophils (ITGAM, ITGAX), epithelial cells (EPCAM, KRT18, KRT19), fibroblasts (TIMP1, FN1, ACTA2), mast cells (FCER1A, KIT), acinar cells (CTRB1, CELA3A, PLA2G1B), macrophages (CD68, CD163, LYZ), B cells (CD38, TNFRSF17), and NK and T cells (KLRB1, PRF1, CD2, CD3E, CD3D).

Identification of malignant epithelial cells: Since both malignant and normal epithelial cells express similar molecular markers, it is difficult to annotate the two subgroups based solely on differential gene expression. As malignant tumor cells originate from normal epithelial cells, the degree of malignancy often accompanies variations in chromosome structure and number. Therefore, in this study, we used the R package "infercnv" (https://github.com/broadinstitute/inferCNV) to calculate copy number variations (CNVs) in each of the 22 chromosomes of each cell based on its transcriptome, thereby defining malignant tumor cells and normal epithelial cells. The CNVs of each cell were sorted and classified by the position of the genes on the chromosome, and a moving average was applied to the relative expression values using a sliding window of 100 genes per chromosome. The reference cells were set as 1000 fibroblasts and 1000 T cells. Based on the obtained CNV matrix, an unsupervised clustering algorithm was used to divide all unidentified cells into multiple subgroups with varying copy numbers, with the subgroup with the lowest copy number and closest to the reference cell line defined as normal epithelial cells, and the rest defined as malignant tumor cells.

After extracting NK cell and T cell subpopulations, we used the 'Harmony' package to remove batch effects and reduce any unnecessary biological or technical factors. Next, the same standardization and dimension reduction procedures were applied to the T cell subpopulations. The functions 'FindNeighbors' and 'FindClusters' were used to identify individual cell subpopulations,

with a resolution set at 0.8. The biological background of each subpopulation was annotated using known molecular markers. CD4 T cell subpopulations included CD4Tn (TCF7, SELL, IL7R, CCR7, LEF1, MAL), CD4Trg (FOXP3, PDCD1, CTLA4, TIGIT, BATF), CD4Tm (S100A4, S100A10, ANXA1, IL7R, KLF2), CD4Th17 (CCR6, IL2, DPP4, RORA, IFNGR1), and CD4Tfh (CXCL13, GNG4, CD200, IGFL2, TOX2). CD8 T cell subpopulations included CD8Tem (CD8 effector memory cells) (GZMK, GZMH, DUSP2, ITM2C, CD74, EOMES, CST7), CD8Trm (ZNF683, IL7R, ANXA1, CD55, GZMA, HOPX, CXCR6, ITGA1), CD8Temra (CD8 terminally differentiated effector memory cells) (GZMA, GZMH, GZMB, ZEB2, TBX21, NKG7, PLEK, KLRD1), CD8Tc17 (SLC4A10, CEBPD, NCR3, IFNGR1, RORA, LTK), and CD8Tn (CD8 naive T cells) (CCR7, LEF1, TCF7, SELL). The NK cell subpopulations included NK-FCGR3A (+) cells (NCAM1, CD160, FCGR3A) and NK-FCGR3A (-) cells (NCAM1, CD160). Some T cell subpopulations could not be mapped to known molecular markers after clustering (40) and were therefore not biologically annotated.

2.5 Patient grouping and pathway enrichment score calculation

Based on the glutamine metabolism-related genes (ALDH18A1, GAPDH, GCLM, GLS, GOT1, MTHFS, OAT, SLC1A5, SLC38A1, SLC38A5, SLC7A5), we calculated the expression scores of glutamine metabolism-related genes in tumor cells (GStumor) and CD8 T cells (GSimmune) using the "ssGSEA" algorithm in the "GSVA" package. After dividing the patients into high-score and low-score groups based on the median of GStumor scores from 12 patients, we compared the differences in the scores of cytotoxicity-related gene sets (GZMK, GZMH, GZMB, PRF1, IFNG, EOMES, NKG7), exhaustion-related gene sets (PDCD1, TIGIT, HAVCR2, LAG3, CTLA4), and naive-related gene sets (LEF1, SELL, TCF7, CCR7) between the different GStumor groups in CD8T subpopulations (CD8Tem and CD8-Temra).

2.6 Gene set enrichment analysis of tumor-infiltrating CD8 T cells

Gene Set Enrichment Analysis (GSEA) is a statistical method used to calculate the distribution trend of genes and determine their contribution to a specified phenotype, based on the comparison of sorted genes related to the phenotype and predefined gene sets. Compared to GO and KEGG enrichment analysis, GSEA can avoid the influence of subjective bias and retain more effective information, while also allowing for quantitative assessment of pathway activation. In this study, we downloaded multiple gene sets, including C2: CP: KEGG, C2: CP: REACTOME, and C5: GO (BP, MF, and CC) from the MsigDB website (https://www.gsea-msigdb.org/gsea/msigdb/). We selected the CD8Tem and CD8-Temra subsets, used the "FindAllMarkers" function to select differentially expressed genes that were upregulated and downregulated in the CD8Tem subset of patients in the low-score group, and calculated the fold change corresponding to these genes. Finally, we used the "GSEA" function in the "clusterProfiler" package to sort the gene sets according to fold change from high to low and perform enrichment analysis, obtaining enrichment scores for different pathways. The same method was used to process the CD8-Temra subset. We used the "AUCell_exploreThresholds" function to distinguish between high and low AUC values, which automatically defines the threshold for the bimodal distribution to determine the "activation" or "inactivation" status of cells in the relevant pathway gene set, respectively.

2.7 Under the influence of tumor cell glutamine metabolism, the developmental trajectory of tumor-infiltrating CD8 effector T cells

To investigate the differences of tumor-infiltrating CD8 effector T cells under different tumor cell glutamine metabolism pressures, we calculated the cytotoxic scores and cell proportions of these three CD8 T cell subsets (CD8-Tn, CD8-Tem, and CD8-Temra) and their changes between the two patient groups and performed pseudo-time gene dynamic analysis on the three CD8 T cell subsets (CD8-Tn, CD8-Tem, and CD8-Temra) using the "Monocle2" package in R. Monocle2 can use unsupervised machine learning and reverse graph embedding algorithms based on single-cell transcriptome expression matrices to place cells on different branches of the developmental trajectory to simulate the biological process of the cell population, forming a "one-root-two-branches" cell development tree diagram, in which cells on the same branch have the same gene expression features and differentiation status. This pseudo-time analysis can infer the differentiation trajectory of cells or the evolution process of cell subtypes during development, and identify key genes and pathway changes that affect branch formation. We extracted three objects, including gene expression matrix, gene information, and cell phenotype information, and constructed them into a "CellDataSet" object. The "estimateSizeFactors" function can standardize the transcriptome expression matrix. Using the "FindAllMarkers" function, we screened for upregulated genes in CD8-Tef (CD8-Tem and CD8-Temra) under these two metabolic modes, and then used the "DDRTree" algorithm to project all cells onto a two-dimensional plane and arrange them in order of branching.

2.8 Establishment, grouping, and drug intervention of a mouse model

A cell suspension of 0.1 ml at a concentration of 1×10^6/ml Panc02 tumor cells (i.e., 1×10^5 cells per mouse) was inoculated into the right groin area of each mouse. On day 6 post-inoculation, the length and width of the subcutaneous tumors in the mice were

observed and recorded, and the volume of the subcutaneous tumors was calculated using the formula: V (mm^3) = length (mm) × width (mm) × width (mm) × π/6. Twenty mice with subcutaneous tumors of similar volumes were selected and randomly divided into four groups (five mice per group):

1. Control group (VEH): orally administered with 100 μL of 0.9% saline solution per day and intraperitoneally injected with 100 μL of 0.9% saline solution once every three days for 20 consecutive days.
2. Glutamine metabolism inhibitor group (JHU083): orally administered with 100 μL of JHU083 solution in saline (1 mg/kg/d) per day and intraperitoneally injected with 100 μL of 0.9% saline solution once every three days for 20 consecutive days.
3. Immune checkpoint inhibitor group (Anti-PD-1): intraperitoneally injected with 100 μL of PD-1 monoclonal antibody solution in saline (1 mg/kg/d) once every three days and orally administered with 100 μL of 0.9% saline solution per day for 20 consecutive days.
4. Combination of glutamine metabolism inhibitor and immune checkpoint inhibitor group (JHU083+Anti-PD-1): orally administered with 100 μL of JHU083 solution in saline (1 mg/kg/d) per day and intraperitoneally injected with 100 μL of PD-1 monoclonal antibody solution in saline (1 mg/kg/d) once every three days for 20 consecutive days.

The length and width of the tumors were measured every two days, and the volume of the subcutaneous tumors was calculated accordingly. All mice were euthanized after being fed for 27 days, and subcutaneous tumor samples were harvested immediately after euthanasia. To ensure humane euthanasia, mice were placed in a CO_2chamber with a flow rate set at 30% of the chamber volume per minute, following approved welfare guidelines. The CO_2concentration was gradually increased to induce unconsciousness, followed by respiratory and cardiac arrest.

2.9 Quantitative real-time polymerase chain reaction

Approximately 50 mg tumor tissue was grind and crushed, add an appropriate amount of Trizol lysis solution to it and lyse it thoroughly on ice. The lysate was then transferred to an enzyme-free EP tube and centrifuged at 4°C, 12,000 rpm/min for 10 min; the supernatant obtained by centrifugation was then transferred to another EP tube, chloroform was added, the supernatant and chloroform were mixed and left to stand for 15 min, next centrifuged at 4°C, 8,000 rpm/min for 15 min. Wash with 75% ethanol solution, centrifuge for 15 min at 4°C at 12000 rpm/min, add 20 μl DEPC water to the precipitate, wait for the precipitate to dissolve, measure the mRNA concentration. mRNA was collected and reverse transcribed into cDNA, which were amplified in triplicate using SYBR Green PCR Master Mix (Guangzhou RiboBio Co), 10 pmol of primer (Supplementary Table S1), and 20 ng of cDNA per reaction with the StepOnePlus (Roche LightCycler 96). Quantitation was performed using the ΔΔCt method.

2.10 Immunohistochemistry

All pathological diagnoses were made independently by 2 senior physicians in the Department of Pathology, and controversial diagnoses were assessed by a third physician and then decided by joint consultation. The specific steps of staining were as follows.

1. Dewaxing and hydration: The slices were placed in the oven at a temperature of 60°C for 90 min, then placed in xylene for 30 min for dewaxing, then the slices were immersed in ethanol (anhydrous ethanol, 95% ethanol, 75% ethanol) in a gradient from high to low concentration for 5 min, and finally rinsed repeatedly with double-distilled water for 5 min.
2. Antigen repair and peroxidase removal: The treated tissue sections were placed in a repair cassette with 200 ml of ethylene glycol tetraacetic acid (EDTA) solution, then placed in an autoclave with double-distilled water, first heated to vapour, then allowed to cool, and then rinsed with double-distilled water. The sections were then placed in 3% hydrogen peroxide solution (H2O2) for 10 min incubation protected from light, allowed to cool and then soaked 3 times with double distilled water for 5 min each and rinsed with PBS for 5 min.
3. Addition of antibody, colour development, re-staining and blocking: sections were added dropwise with antibody (KI67, CD3 and CD8) diluted at 1:200 and refrigerated overnight at 4°C. The next day the sections were washed three times with PBS for 5 min each time. Second day, the sections were washed three times with PBS for 5 min each time, shaken dry, incubated with secondary antibody for 30 min, and washed three times with PBS for 5 min each time. The reaction was terminated by adding a drop of DAB staining solution to the sections and observing a positive reaction under the microscope. After washing, the sections were fractionated with ethanol hydrochloride solution, then washed, dehydrated, sealed and labelled.
4. After the above steps were completed, the pathological sections were observed under an inverted fluorescent microscope. The expression levels of KI67, CD3 and CD8 proteins were measured with Image J software.

2.11 Flow cytometry

Immune cell populations were identified via flow cytometry from respective dissociated whole tumor cell suspensions.

(1) After mechanically cutting the tumor tissue, it was filtered with 300 mesh filter cloth, centrifuged with 300 g for 5 min, and the cell concentration was adjusted to 10*6/mL with PBS. (2) 1 μg antibody (CD8a, CD3, cd49b, CD45, CD4, LIVE/DEAD) were add into 100 μL cell suspension in the sterile EP tube. Dye at 4 °C for 30 min without light after mixing. (3) Adding 1000 μL PBS to wash the mixture, the supernatant was removed after centrifuging with 300g for 5min. (4) Cells were resuspended by 400 μL PBS and then detected by ZE5 flow cytometry, flow cytometry data were analyzed using FlowJo software.

2.12 Immunocyte apoptosis detection

(1) Take 100 μL of the immunocyte suspension separated from "Flow cytometry (1)" and centrifuge at 300g for 5 minutes. Discard the supernatant and resuspend the cells in 100 μL of binding buffer. (2) Add 5 μL of Annexin V-FITC staining fluorescent dye and incubate for 10 minutes at room temperature in the dark. (3) Add 10 μL of PI staining dye and incubate for 5 minutes at room temperature in the dark. Add 400 μL of PBS and resuspend the cells. Immediately detect the cells using a flow cytometer. (4) Analyze the data using FlowJo software and a ZE5 flow cytometer.

2.13 Statistical analysis

The statistical analysis of the experimental data was performed using R software (version 4.1.2) in accordance with the conventions of medical academic papers. In this study, Kaplan-Meier survival analysis was performed to compare overall survival (OS) among different groups. In this study, overall survival (OS) was defined as the time interval from the date of diagnosis (the starting point) to the date of death from any cause (the endpoint). For patients who were still alive or lost to follow-up by the time of analysis cutoff, their OS time was censored at the date of the last known follow-up. All OS and follow-up data were obtained from clinical follow-up records within the TCGA database. If the data were normally distributed, t-test was used for comparison. If not, Wilcoxon rank sum test was used instead. P value less than 0.05 was considered statistically significant. $0.05 \leq P$ value < 0.10 as indicative of borderline significance. Wilcoxon and t-tests were adjusted for using the Benjamini–Hochberg method via the p.adjust function in R.

3 Result

3.1 The scoring of genes related to glutamine metabolism in tumor tissue is negatively correlated with patient prognosis and anti-tumor immune presentation

To distinguish between high and low metabolism of glutamine and to clarify the relationship between glutamine metabolism levels and prognosis of pancreatic cancer patients, we scored the expression of glutamine metabolism-related genes (ALDH18A1, GAPDH, GCLM, GLS, GOT1, MTHFS, OAT, SLC1A5, SLC38A1, SLC38A5, SLC7A5) in tumor cells of 176 patients in TCGA cohort, and divided them into high and low scoring groups based on the median value (Figure 1A). Hierarchical clustering results also demonstrated the expression differences of glutamine metabolism-related genes between these two patient groups, indicating that unsupervised clustering algorithms can significantly separate these 176 pancreatic cancer patients based on glutamine metabolism-related genes (Figure 1B). Kaplan-Meier curves showed that patients in the high scoring group had a worse prognosis. In the high scoring group, the overall survival rates at 1, 3, and 5 years were 63.1%, 27.1%, and 22.6%, respectively. However, in the low scoring group, the overall survival rates at 1, 3, and 5 years were 82.1%, 41.0%, and 27%, respectively, suggesting a negative correlation between glutamine metabolism and pancreatic cancer prognosis (Figure 1C). The baseline characteristics of the patients are detailed in Supplementary Table S3.

In order to investigate whether the metabolism of glutamine in tumor cells affects the anti-tumor activity of immune cells in pancreatic cancer, we used single-sample gene set enrichment analysis (ssCSEA) to study the relationship between glutamine metabolism in tumor cells and immune infiltration, cytotoxic gene set (GZMK, GZMH, GZMB, PRF1, IFNG, EOMES, NKG7), immune exhaustion gene set (PDCD1, TIGIT, HAVCR2, LAG3, CTLA4), and immature-related gene set (LEF1, SELL, TCF7, CCR7) in the pancreatic cancer microenvironment. Immune infiltration analysis revealed a trend toward higher CD8+ T cell infiltration in the tumor immune microenvironment of the low glutamine score group compared to the high glutamine score group ($P = 0.059$) (Figure 1D). In the low score group, the immune cell cytotoxicity-related gene score was significantly higher than that in the high score group (Figure 1E). By plotting the glutamine score and immune cell cytotoxicity score of the two groups, we found that there was a negative correlation between tumor cell glutamine metabolism and immune cell cytotoxicity in the high score group (Figure 1F). In terms of immune exhaustion score, we found that the low score group was significantly higher than the high score group (Figure 1G), which indicates a negative correlation between tumor cell glutamine metabolism and immune cell exhaustion. To determine whether the low immune cell exhaustion score in the high glutamine score group is related to the level of immature immune cells, we plotted the glutamine score and immature-related gene set (LEF1, SELL, TCF7, CCR7) of the two groups, and found that as the glutamine score increased in tumors with high glutamine metabolism, the expression of immature immune cell genes increased significantly (Figure 1I). This may suggest that the decrease in immune cell cytotoxicity in the high glutamine metabolism group of tumor cells is related to the level of immature immune cells. The results of this study indicate that as the glutamine metabolism in tumors increases, immune cells become more immature, while the scores of immune cell cytotoxicity and exhaustion decrease.

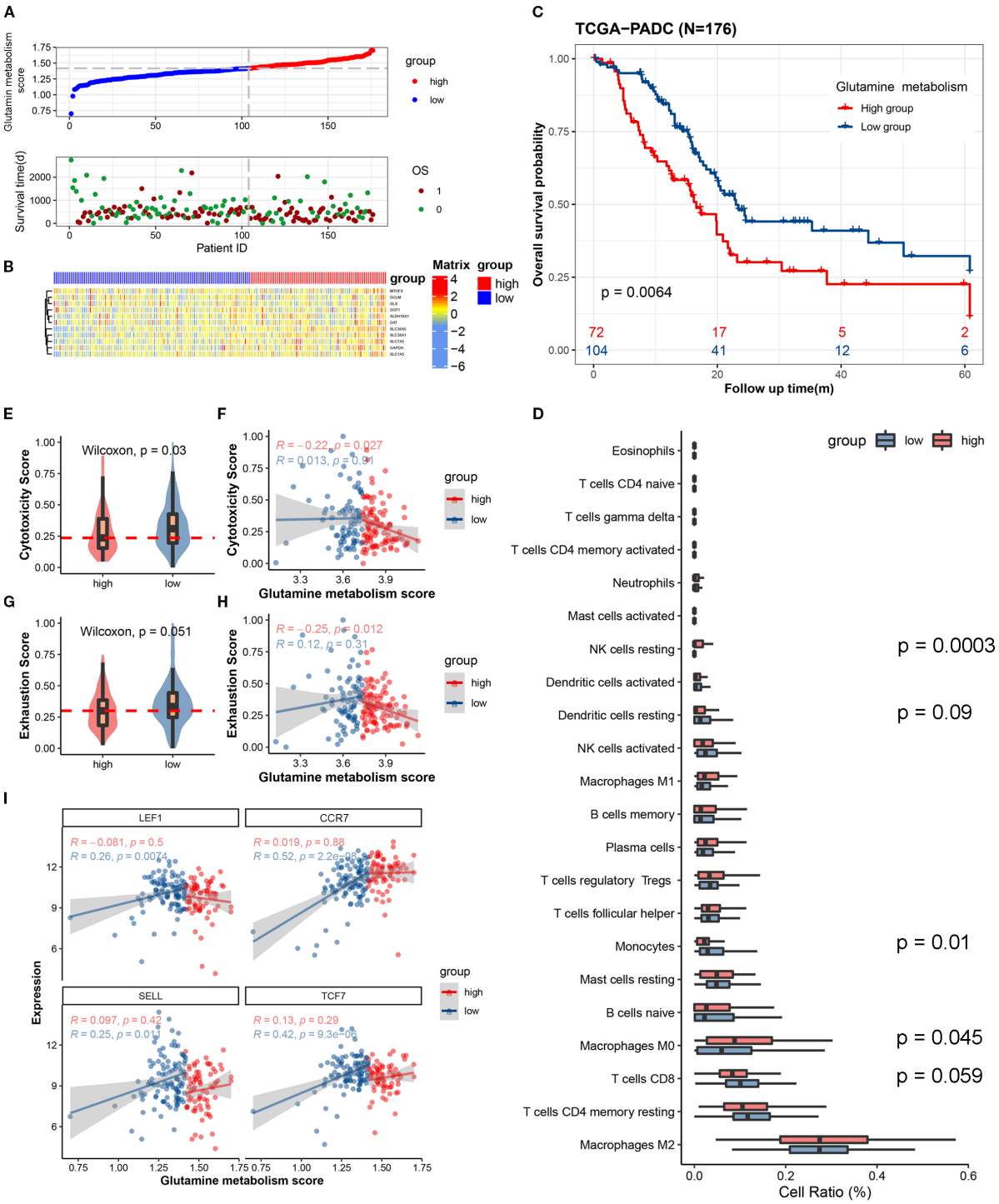

FIGURE 1
The expression scores of glutamine metabolism-related genes in the tumor microenvironment of pancreatic cancer are closely correlated with the anti-tumor activity of immune cells and the prognosis of patients. **(A)** The upper curve shows the distribution of glutamine metabolism-related gene expression scores in tumor cells of all pancreatic cancer patients. The lower dot plot shows the survival status and survival time of all patients sorted by tumor glutamine metabolism-related gene expression scores from low to high. **(B)** The heatmap shows the expression levels of glutamine metabolism-related genes between two groups. Blue represents low metabolism group, and red represents high metabolism group. **(C)** This Kaplan-Meier curve shows the difference in overall survival rate between different groups. **(D)** The box plot shows the degree of infiltration of 22 immune cells in the tumor microenvironment. (**E**, **G**) Differences in cell toxicity score and exhaustion score of CD8T cells between the two groups. (**F**, **H**) Fitting curves of glutamine metabolism score of tumors in the two groups with cell toxicity score and exhaustion score. The correlation coefficient and significance test were calculated and marked in the upper left corner. **(I)** Fitting curves of glutamine metabolism score of tumor cells in the two groups with expression levels of immature-related genes. The correlation coefficient and significance test were calculated and marked in the upper left corner.

3.2 Identification of subpopulations and patient stratification using single-cell transcriptome sequencing data

To obtain a comprehensive single-cell gene expression atlas of the pancreatic cancer immune microenvironment, we used the program package 'Seurat' to identify differential genes and cell types in 12 pancreatic cancer patients. A total of 39,719 qualified cells were annotated as nine major cell subtypes and one undefined cell subtype (Figure 2A). The major cell subtypes include neutrophils (ITGAM, ITGAX), epithelial cells (EPCAM, KRT18, KRT19), fibroblasts (TIMP1, FN1, ACTA2), mast cells (FCER1A, KIT), acinar cells (CTRB1, CELA3A, PLA2G1B), macrophages (CD68, CD163, LYZ), B cells (CD38, TNFRSF17), and NK/T cells (KLRB1, PRF1, CD2, CD3E, CD3D) (Figure 2C). Tumor cells were identified using the INFERCNV algorithm (https://github.com/broadinstitute/inferCNV). As no known molecular markers were mapped to the undefined cell subtype, it was not included in this study.

In order to investigate the impact of tumor cell glutamine metabolism on immune subpopulations in the immune microenvironment of pancreatic cancer, we divided 12 patients into a high-scoring group (P01, P6, P5, P16, P3, P11) and a low-scoring group (P8, P2, P13, P15, P7, P8) based on the expression scores of glutamine metabolism-related genes in tumor cell subpopulations (Figure 2F). At the same time, we found that in the low-scoring group of tumor cell glutamine metabolism, the glutamine scores of T cells and NK cells were mostly higher than those of tumor cell glutamine scores. In contrast, the opposite was true in the high-scoring group of tumor cell glutamine metabolism (Figures 2G, I). Interestingly, compared with the low-scoring group, the high-scoring group had more tumor cells (24% vs 19%) and fewer T cells and NK cells (21% vs 23%) (Figures 2H, J). This suggests that in the immune microenvironment of pancreatic cancer, high tumor cell glutamine metabolism will be accompanied by low metabolism of immune cells and low infiltration of T cells and NK cells.

3.3 In the immune microenvironment of pancreatic cancer, the glutamine metabolism of tumor cells can affect the anti-tumor activity of CD8 T cells

To further investigate the effect of tumor cell glutamine metabolism on CD8 effector T cells, we identified 8700 T cells and NK cells into 12 known cell subpopulations and one undefined cell subpopulation based on known molecular markers (Figures 3A, B). CD4 T cell subpopulations included CD4Tn (TCF7, SELL, IL7R, CCR7, LEF1, MAL), CD4Trg (FOXP3, PDCD1, CTLA4, TIGIT, BATF), CD4Tm (S100A4, S100A10, ANXA1, IL7R, KLF2), CD4Th17 (CCR6, IL2, DPP4, RORA, IFNGR1), and CD4Tfh (CXCL13, GNG4, CD200, IGFL2, TOX2). CD8 T cell subpopulations included CD8Tem (GZMK, GZMH, DUSP2, ITM2C, CD74, EOMES, CST7), CD8Trm (ZNF683, IL7R, ANXA1, CD55, GZMA, HOPX, CXCR6, ITGA1), CD8Temra (GZMA, GZMH, GZMB, ZEB2, TBX21, NKG7, PLEK, KLRD1), CD8Tc17 (SLC4A10, CEBPD, NCR3, IFNGR1, RORA, LTK), and CD8Tn (CCR7, LEF1, TCF7, SELL). NK cells included NK-FCGR3A(+) cells (NCAM1, CD160, FCGR3A) and NK-FCGR3A(-) cells (NCAM1, CD160). Both CD8Tem and CD8Temra subpopulations belonged to CD8-Tef (Figures 3A, B). Some T cells could not be mapped to known molecular markers after grouping, so they were not biologically annotated. The two t-SNE plots and pie charts show the composition ratio of T cell and NK cell subpopulations in the two populations (Figure 3I).

3.3.1 Influence of tumor cells glutamine metabolism on CD8 effector T cells cytotoxicity

To investigate the effect of tumor cell glutamine metabolism on CD8 effector T cell cytotoxicity, we calculated a cytotoxicity score for each T cell based on the expression levels of immune cell cytotoxicity-related genes (GZMK, GZMH, GZMB, PRF1, IFNG, EOMES, and NKG7). The cytotoxicity score of T cells in the high glutamine metabolism group of tumor cells was significantly lower than that in the low glutamine metabolism group, and the difference was statistically significant (Wilcoxon test, $p = 2.8 \times 10{-}6$). Further study of CD8 effector T cells (CD8T-Tem and CD8T-Temra) revealed that the immune cell cytotoxicity score of CD8T-Tem in the high glutamine metabolism group was significantly lower than that in the low glutamine metabolism group, and the difference was statistically significant (Wilcoxon test, $p = 4.7 \times 10{-}5$). However, there was no statistically significant difference in the immune cell cytotoxicity score of CD8T-Temra between the high and low glutamine metabolism groups (Figure 3C). These findings suggest that high tumor cell glutamine metabolism is associated with a decrease in cytotoxicity of the CD8T-Tem subset, while there is no apparent correlation between the cytotoxicity of the CD8T-Temra subset and tumor cell glutamine metabolism.

3.3.2 Influence of tumor cells glutamine metabolism on CD8 effector T cells exhaustion

In order to investigate the impact of tumor cell glutamine metabolism on CD8 effector T cell exhaustion, we calculated an exhaustion score for each T cell based on the expression levels of immune exhaustion-related genes (PDCD1, TIGIT, HAVCR2, LAG3, and CTLA4). In T cells, the immune exhaustion score of the high glutamine metabolism group was significantly lower than that of the low group, with a statistically significant difference (Wilcoxon test, $p = 2.2 \times 10{-}16$), but this difference was not significant in CD8-Tem (Wilcoxon test, $p = 0.081$). In CD8-Temra, the immune exhaustion score of the high glutamine metabolism group was actually higher than that of the low group, with a statistically significant difference (Wilcoxon test, $p = 0.0046$) (Figure 3D). This suggests that high glutamine metabolism in tumor cells is associated with exhaustion in the CD8-Temra subset, but not with exhaustion in the CD8-Tem subset.

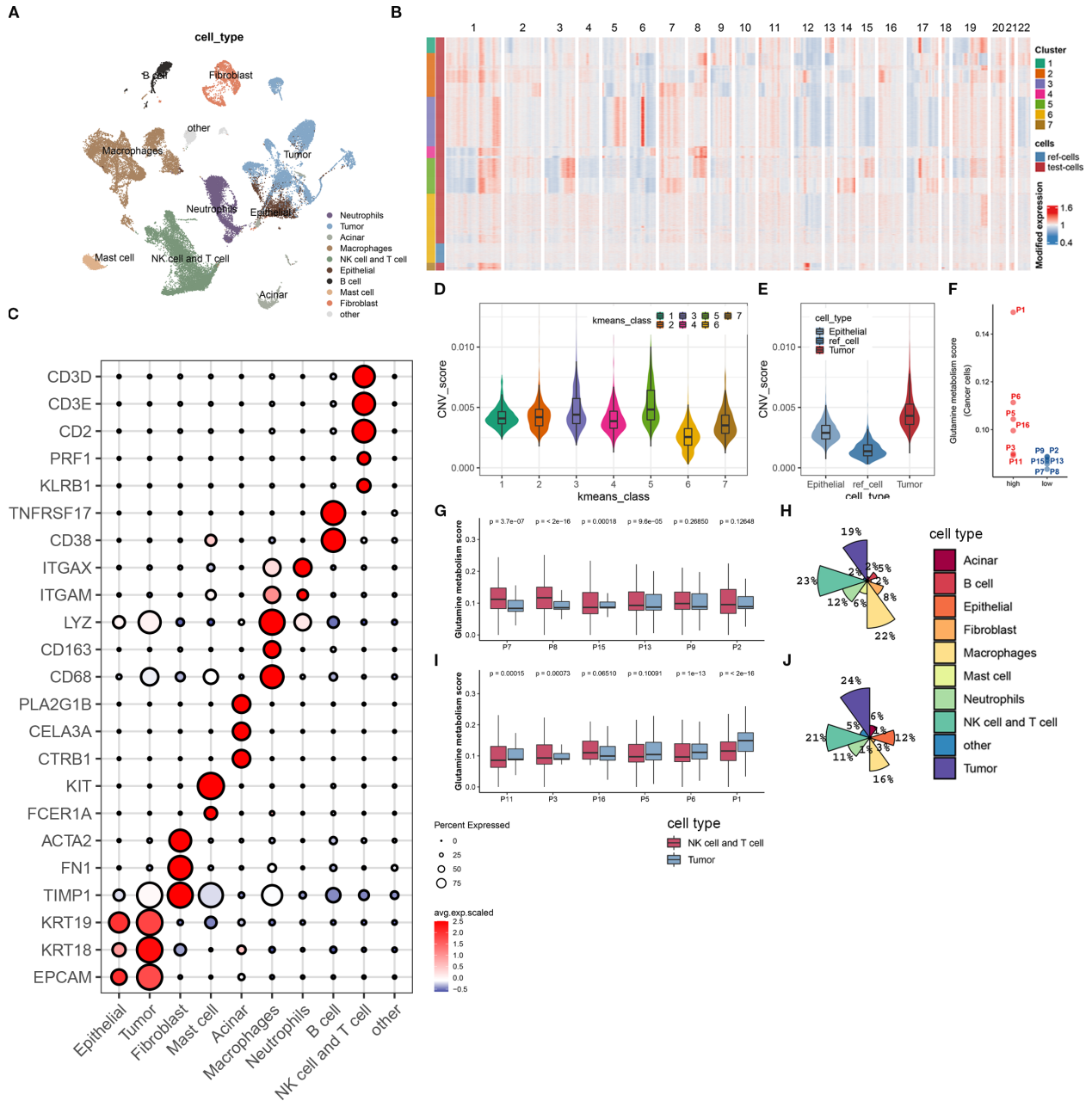

FIGURE 2
Biological annotation of single-cell sequencing data. **(A)** The t-SNE plot displays all the cellular subpopulations present in the tumor microenvironment of pancreatic cancer patients. Different colors represent different cell types. The cellular subpopulations are annotated as shown in the figure. **(B)** The heatmap shows copy number variations of all genes on 22 chromosomes in normal epithelial cells and malignant epithelial cells. All cells are classified into 7 groups using unsupervised clustering algorithm. The group with the lowest copy number variation is identified as normal epithelial cells, while the rest are malignant epithelial cells. **(C)** The bubble plot shows the expression levels of molecular marker genes and cell proportions in each cellular subpopulation. The color of the dot represents the average expression level of the gene, with red indicating high expression and blue indicating low expression; the size of the dot represents the cell proportion. **(D)** This boxplot shows the difference in copy number variation scores between the 7 epithelial cell subpopulations. **(E)** We demonstrate the difference in copy number variation scores between the reference cell line, normal epithelial cells, and malignant epithelial cells (tumor cells) after biological annotation. **(F)** This scatterplot divides 12 pancreatic cancer patients into high- and low-metabolism groups based on the expression score of glutamine metabolism-related genes in tumor cells. **(G, H)** The boxplot **(G)** displays the expression score of glutamine metabolism-related genes in tumor cells, T cells, and NK cells of 6 low-metabolism group patients, while the pie chart **(H)** shows the composition ratio of all cell subpopulations in this group. **(I, J)** The boxplot **(I)** displays the expression score of glutamine metabolism-related genes in tumor cells, T cells, and NK cells of 6 high-metabolism group patients, while the pie chart **(J)** shows the composition ratio of all cell subpopulations in this group.

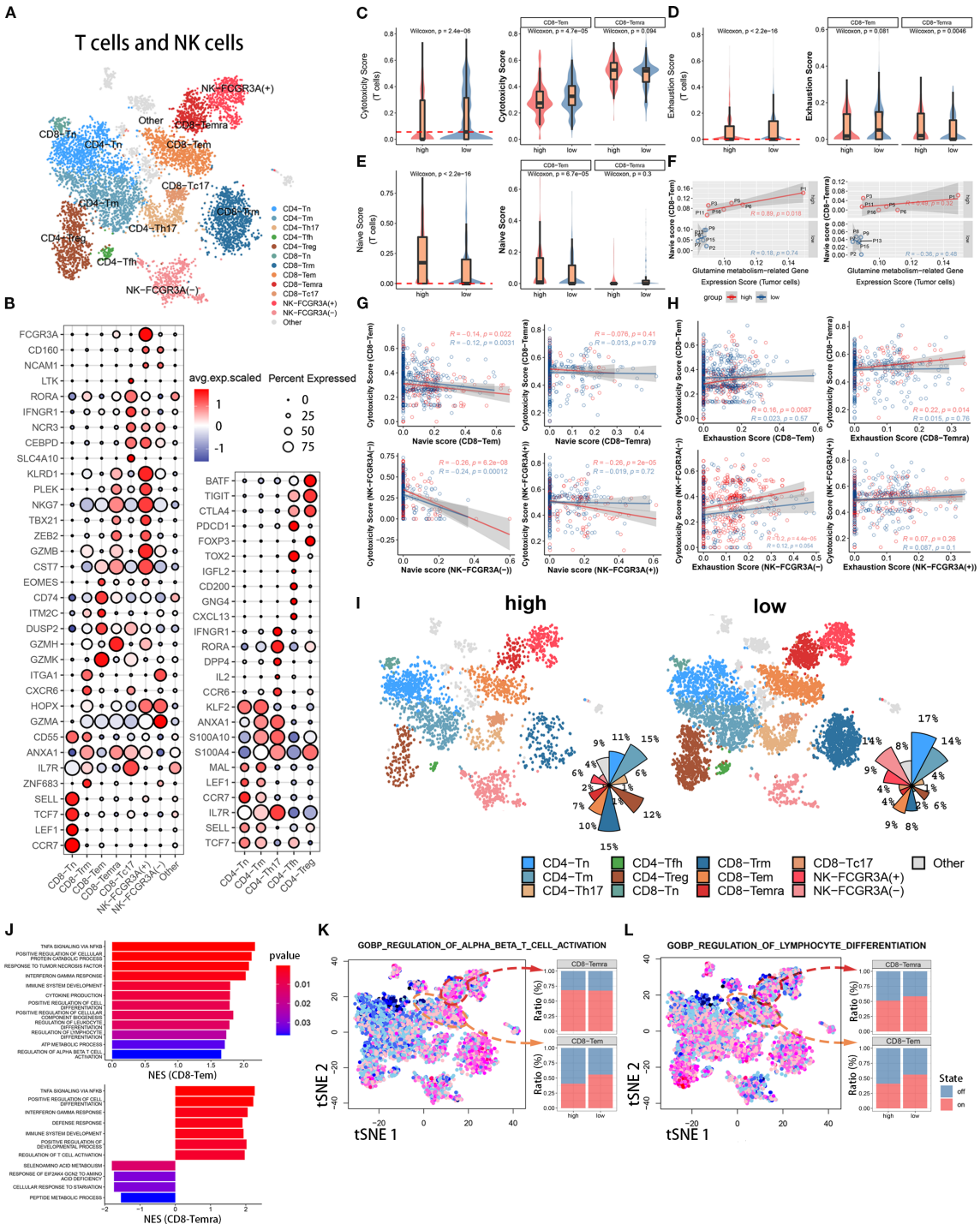

FIGURE 3
Immune functional differences of CD8+ T cell subsets among different populations. **(A)** The t-SNE plot displays T cell and NK cell subpopulations from the tumor microenvironment of pancreatic cancer patients. Different colors represent different cell types. Subpopulation annotations are shown in the figure. **(B)** The bubble plot shows the expression levels and cell proportions of molecular markers in each cell subpopulation. The color of the dots represents the average expression level of the gene, with red indicating high expression and blue indicating low expression. The size of the dots represents the cell proportion. **(C-E)** These three sets of boxplots show the differences in cell cytotoxicity score, exhaustion score, and naive score of the entire T cell subpopulation and its CD8-Tem and CD8-Temra subpopulations between two groups. **(F)** We show the fitting curve between the tumor cell glutamine metabolism-related gene expression score of the two groups and the naive score of CD8-Tem and CD8-Temra subpopulations. **(G, H)** We separately display the fitting curves between the naive score and exhaustion score and cell cytotoxicity score of four subpopulations (CD8-Tem, CD8-Temra, NK-FCGR3A(-), and NK-FCGR3A(+)) in the high and low metabolism groups. **(I)** Two sets of t-SNE plots and pie charts show the composition ratio of T cell and NK cell subpopulations in two groups. **(J)** The bar graph displays the pathway enrichment differences between CD8-Tem and CD8-Temra subpopulations between the two groups. **(K, L)** The t-SNE plots on the left show the enrichment levels of two pathways in all T cells and NK cells, and the bar graphs on the right show the activation ratio of the two pathways between CD8-Tem and CD8-Temra subpopulations.

3.3.3 Influence of tumor cells glutamine metabolism on CD8 effector T cells maturity

In order to investigate the impact of tumor cell glutamine metabolism on the development of CD8 effector T cells, we used immature immune cell-related genes (LEF1, SELL, TCF7, CCR7) to score the immaturity of each T cell. In the high glutamine metabolism group of tumor cells, the immature scores of T cells and CD8-Tem were significantly higher than those in the low score group, with significant statistical differences (Wilcoxon test, $p = 2.2 \times 10-16$, $p = 6.7 \times 10-5$), while there was no statistical difference in immature scores between the two groups of CD8-Temra (Figure 3E). We analyzed the fitting curves of tumor cell glutamine metabolism score and immature scores of CD8-Tem and CD8-Temra subsets in the two groups and found that in the high glutamine metabolism group of tumor cells, the immature scores increased with the increase of tumor cell glutamine metabolism score, and the difference in CD8-Tem subset had statistical significance ($R = 0.89$, $p = 0.018$) (Figure 3F). This indicates that the higher the level of tumor cell glutamine metabolism, the more immature the CD8-Tem subset, and the immaturity level of CD8-Temra subset may not be related to tumor cell glutamine metabolism.

3.3.4 Is there correlation between CD8 effector T cells cytotoxicity and between immaturity scores and exhaustion scores?

The Figure 3G shows the fitted curves between the cytotoxicity scores and the immaturity scores of four cell subpopulations (CD8-Tem, CD8-Temra, NK-FCGR3A(-), and NK-FCGR3A(+)) of tumor cells with high and low glutamine scores. The immune cell cytotoxicity of CD8-Tem (high score group: R=-0.14, p=0.022; low score group: R=-0.12, p=0.0031), NK-FCGR3A(-) (high score group: R=-0.26, $p=6.2\times10-8$; low score group: R=-0.24, p=0.00012), and NK-FCGR3A(+) (high score group: R=-0.26, $p=2\times10-5$; low score group: R=-0.019, p=0.72) subpopulations decreased as the immaturity scores increased, especially in the high glutamine score group of tumor cells. However, there was no significant correlation between the cytotoxicity of CD8-Temra subpopulation and the immaturity scores. The Figure 3H shows the fitted curves between the cytotoxicity scores of four subpopulations (CD8-Tem, CD8-Temra, NK-FCGR3A(-), and NK-FCGR3A(+)) of tumor cells with high and low glutamine scores and the exhaustion scores. The two t-SNE plots and pie charts show the composition ratio of T cell and NK cell subpopulations in the two populations (Figure 3I). The immune cell cytotoxicity of CD8-Temra and NK-FCGR3A(-) subpopulations increased as the exhaustion scores increased, while there was no significant correlation between the cytotoxicity of CD8-Tem and NK-FCGR3A(+) subpopulations and the exhaustion scores. Through the above research, we found that the high metabolism of glutamine in tumor cells may reduce the cytotoxicity of CD8-Tem cells by inhibiting their development and inducing their immaturity. Additionally, the high metabolism of glutamine in tumor cells may promote the exhaustion of CD8-Temra subpopulation. In general, the high metabolism of glutamine in tumor cells is negatively correlated with the anti-tumor activity of CT8 effector T cells.

3.3.5 Influence of tumor cells metabolism on immune cell activation pathways

To further elucidate the mechanism underlying the anti-tumor activity of CD8 effector T cells through the inhibition of tumor cell glutamine metabolism, we used gene set enrichment analysis (GSEA) to quantitatively calculate the pathway enrichment scores of high and low scoring groups in CD8-Tem and CD8-Temra subsets. In the low scoring group, the immune cell activation pathways of CD8-Tem subset were significantly upregulated, such as αβ T cell activation, interferon-gamma pathway, tumor necrosis factor pathway, cytokine production, lymphocyte and leukocyte differentiation, etc. These immune cell activation pathways were also significantly upregulated in the CD8-Temra subset in the low scoring group (Figure 3J). In the low scoring group, the T cell activation pathway (CD8-Tem subset) and lymphocyte differentiation pathway (CD8-Tem and CD8-Temra subsets) were significantly higher than those in the high scoring group (Figures 3K, L). These studies demonstrate that when tumor cell glutamine metabolism is reduced, the immune activation pathways of CD8-Tem and CD8-Temra subsets are significantly upregulated.

3.3.6 Conclusions

In the microenvironment of pancreatic cancer, high glutamine metabolism in tumor cells has different effects on different CD8Tef subsets. High glutamine metabolism in tumor cells reduces the cytotoxicity and differentiation of CD8-Tem subset, and increases the CD8-Temra exhaustion score. In conclusion, high glutamine metabolism in tumor cells ultimately reduces the anti-tumor activity of CD8-Tef(CD8-Tem and CD8-Temra).

3.4 Under the influence of tumor cell glutamine metabolism, CD8 effector T cells have a distinct immune status

In order to study the developmental differences and dynamic changes in genes and pathways of CD8-Tem and CD8-Temra subsets in different levels of tumor cell glutamine metabolism, we used the Monocle package to plot the developmental trajectory of cells (CD8-Tem subset, CD8-Temra subset, and CD8Tn subset) and observed changes in the immune status of CD8 effector T cell subsets. Cells were sequentially arranged on the trajectory tree according to a pseudotime of 0 to 10 (Figure 4A), with the early part of the trajectory defined as stage 1. After stage 1, CD8 T cells began to develop in different directions; some cells developed towards stage 2 (fate 1), while others developed towards stages 3, 4, and 5 (fate 2) (Figure 4B). Each cell on the pseudotemporal trajectory was scored for cytotoxicity and then mapped to the trajectory tree according to color, showing the dynamic changes in cytotoxicity of CD8T cell subsets between tumor cell high-metabolism and low-metabolism groups (Figure 4C). We

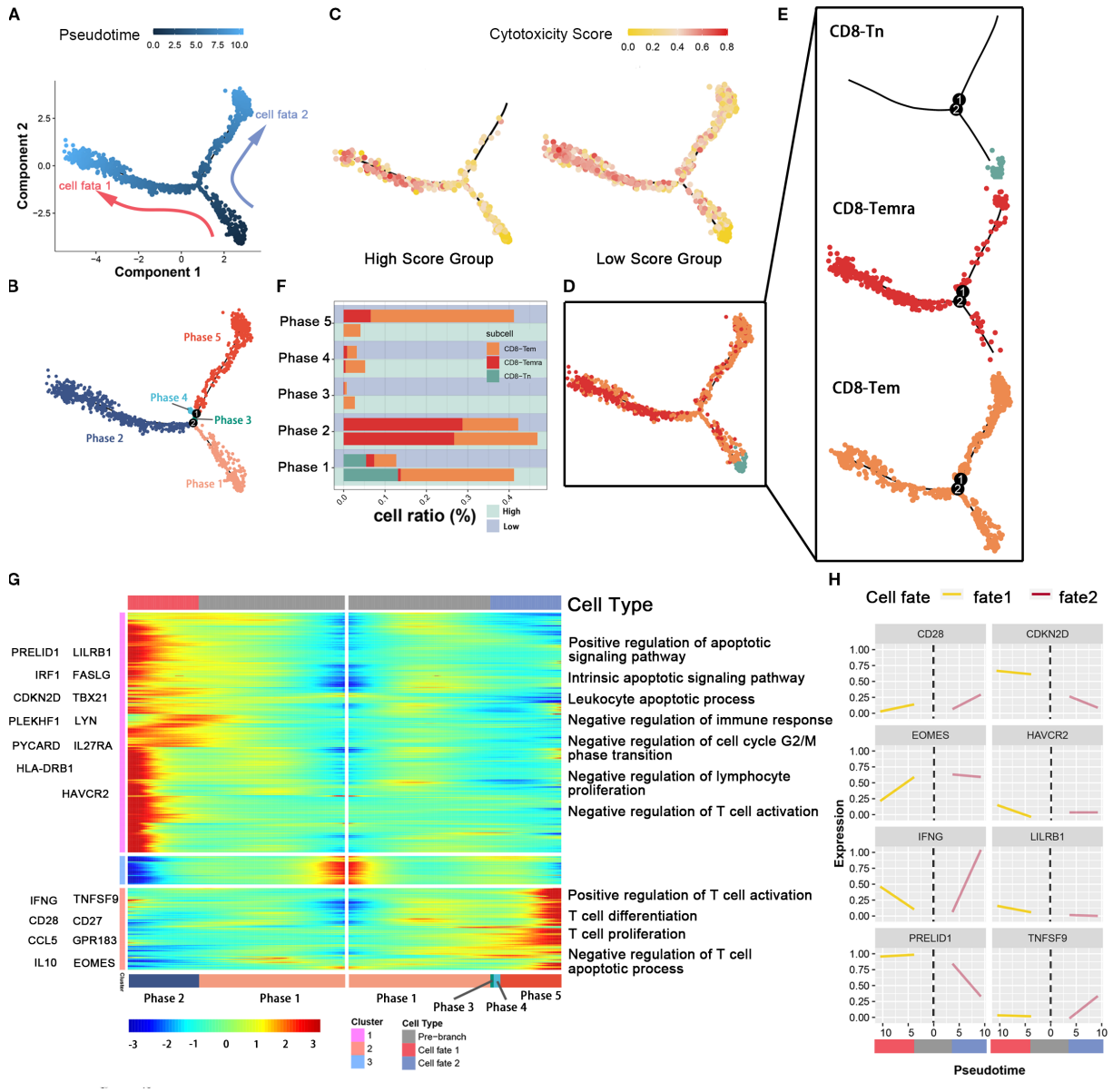

FIGURE 4
The association between glutamine metabolism of pancreatic cancer cells and the developmental trajectory of CD8+ T cells. **(A)** Pseudotime analysis of CD8-Tem, CD8-Tn, and CD8-Temra subpopulations. Arrows indicate the direction of cell differentiation. **(B)** CD8T cells ordered by pseudotime were divided into five trajectory periods and indicated by different colors. **(C)** Each cell on the pseudotime trajectory was assigned a cytotoxicity score and mapped to the trajectory tree according to color, demonstrating the dynamic changes of cytotoxicity in CD8T cell subpopulations between high metabolic and low metabolic tumor cell groups. **(D, E)** The trajectory tree shows the distribution of three CD8T cell subpopulations along the developmental trajectory. CD8-Tn is indicated by light blue, CD8-Temra by deep red, and CD8-Tem by orange-yellow. **(F)** This histogram shows the cell distribution of CD8-Tn, CD8-Temra, and CD8-Tem subpopulations in five periods among different populations, indicated by different colors for CD8T cell subpopulations. **(G)** The heatmap displays the dynamic changes of gene expression over pseudotime. Representative genes of gene clusters 1 and 2 are listed on the left of the heatmap. Immune regulation-related pathways enriched are labeled on the right of the heatmap. **(H)** The two-dimensional fitting curve shows the dynamic expression of immune-related genes during pseudotime in two developmental pathways.

observed that the cytotoxicity of CD8T cell subsets in the low-glutamine metabolism group of tumor cells was higher than that in the high-glutamine metabolism group at all stages, especially in stages 3, 4, and 5 (fate 2). We also visualized the distribution of CD8-Tem, CD8-Temra, and CD8-Tn subsets on the trajectory tree (Figures 5D, E). We calculated the cell proportions of these three T cell subsets at five stages (Figure 4F). We observed that the proportion of CD8 T cells in the low-glutamine metabolism group of tumor cells that developed towards fate 2 was significantly higher than that in the high-glutamine metabolism group. There was no significant relationship between the development of CD8 T cells towards fate 1 and tumor cell glutamine metabolism. Pseudotemporal analysis showed that the development of CD8 T cells towards fate 2 mainly upregulated

10.3389/fimmu.2025.1599252

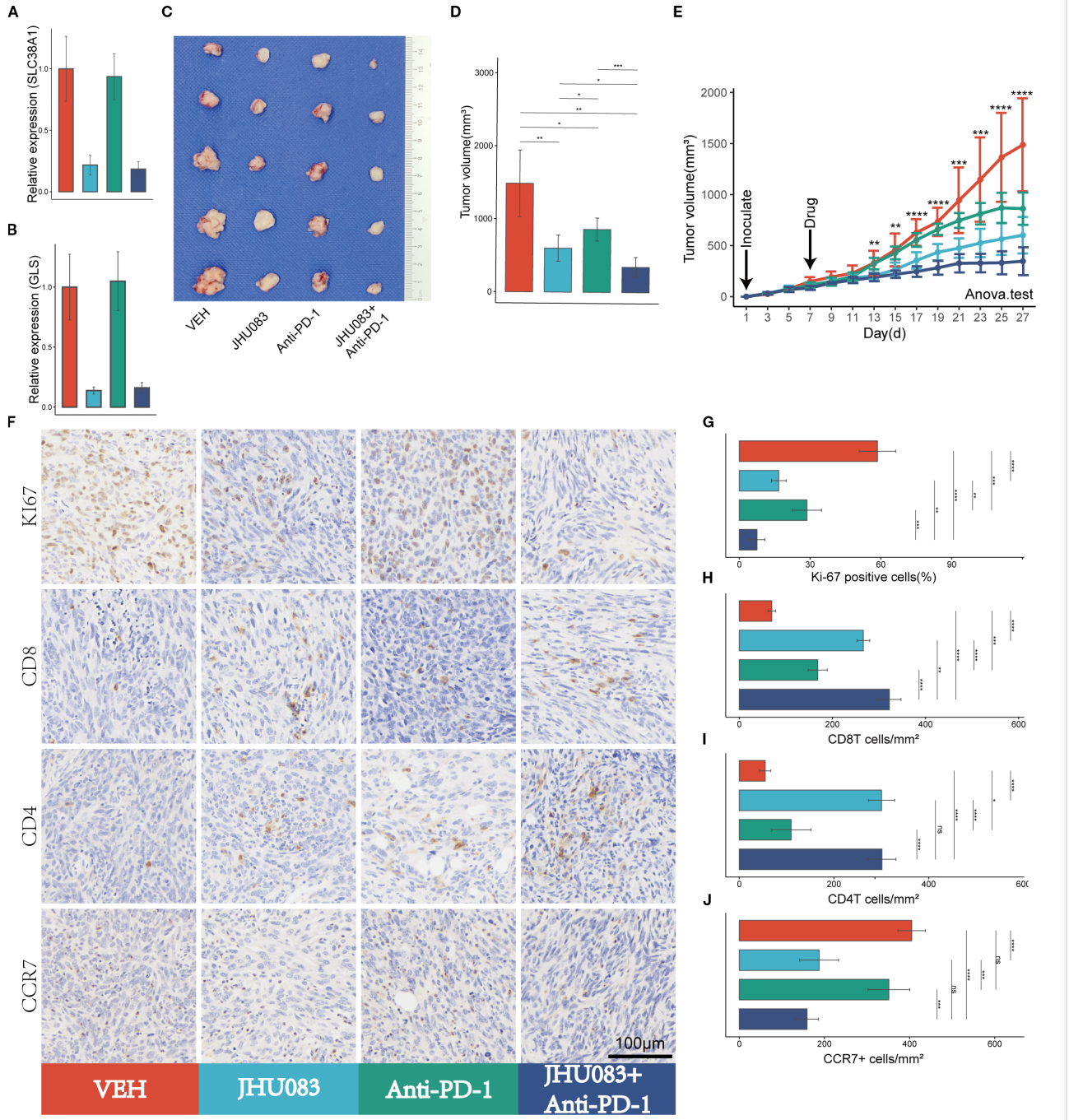

FIGURE 5
Glutamine metabolism inhibitors (JHU083) exhibit anti-tumor effects and enhance the anti-tumor efficacy of PD-1 inhibitors. Different colors were used to mark the groups: red, blue, green, and purple represent VEH, JHU083, antiPD-1, and JHU083+antiPD-1 groups, respectively. NS indicates no statistical significance; *p < 0.05; **p < 0.01; ***p < 0.001; ****p < 0.0001. **(A, B)** The relative expression levels of SLC38A1 and GLS RNA in tumor tissue after drug treatment. **(C)** Images of mouse tumor specimens collected 26 days after inoculation. **(D)** A bar chart showing the differences in tumor volume among groups of mice collected 26 days after inoculation. **(E)** Tumor growth curves showing the growth rate of tumors in different groups. Panc02 cells were inoculated on day 1 and drug treatment was started on day 7. Tumor volume was measured every 2 days. Significance testing was performed using analysis of variance. **(F)** Immunohistochemical staining of Ki67, CD8, CD3, and CCR7. **(G-J)** Bar charts showing quantitative analysis of immunohistochemical staining for Ki67, CD8, CD4, and CCR7.

immune activation-related pathways, such as T cell activation pathway, T cell differentiation and proliferation pathway, and T cell apoptosis inhibition pathway, and many pro-immune-related genes, such as CD28, EOMES, INFG, and TNFSF9, were also upregulated. The development of CD8 T cells towards fate 1 mainly upregulated immune inhibition-related pathways, such as immune cell apoptosis activation pathway, inhibition of immune response, inhibition of lymphocyte proliferation, and inhibition of T cell activation, and many genes related to proliferation and immune inhibition, such as PRELID1, LILRB1, CDKN2D, and HAVCR2, were also upregulated (Figures 4G, H). In general, the differentiation status and immune function of CD8 T cells exhibit significant heterogeneity between different pancreatic cancer cell glutamine metabolism levels. When tumor cell glutamine metabolism is weaker, CD8 T cells are more likely to acquire stronger anti-tumor activity.

3.5 The glutamine metabolism inhibitor JHU083 enhances the anti-tumor effect of immune checkpoint inhibitors (PD-1 inhibitors)

3.5.1 Glutamine metabolism inhibitor JHU083 impact on mRNA expression levels of the glutamine metabolism genes

After treatment with JHU083, the mRNA expression levels of the genes SLC38A1 and GLS decreased significantly, indicating successful inhibition of glutamine metabolism in subcutaneous pancreatic cancer tissue (Figures 5A, B).

3.5.2 Glutamine metabolism inhibitor JHU083 impact on tumor volume

To investigate the therapeutic effect of the glutamine metabolism inhibitor JHU083 on pancreatic cancer, we compared the efficacy of four groups of mice treated with different drugs, including the VEH group, JHU083 group, Anti-PD-1 group, and JHU083+Anti-PD-1 group. Compared with the VEH group, both the JHU083 group and the Anti-PD-1 group showed a significant decrease in subcutaneous tumor volume. In addition, the JHU083 group showed a more significant decrease in subcutaneous tumor volume than the Anti-PD-1 group. The combination of JHU083 and PD-1 inhibitor not only significantly inhibited tumor growth but also demonstrated stronger efficacy than using JHU083 or Anti-PD-1 alone (Figures 5C-E). These results suggest that JHU083 is effective in treating pancreatic cancer and enhances the anti-tumor effect of immune checkpoint inhibitors (PD-1 inhibitors).

3.5.3 Glutamine metabolism inhibitor JHU083 impact on tumor immune microenvironment

In order to clarify the effect of glutamine metabolism enzyme inhibitor JHU083 on the immune microenvironment of pancreatic cancer, we performed immunohistochemical staining on tumor tissues, including Ki-61, CD8, CD4 and CCR7 (Figure 5F). We found that the percentage of Ki-67 positive cells in the JHU083 group, Anti-PD-1 group, and JHU083+Anti-PD-1 group was lower than that in the VEH group, and the difference was statistically significant. Meanwhile, the percentage of Ki-67 positive cells in the JHU083 group was significantly lower than that in the Anti-PD-1 group. The percentage of Ki-67 positive cells in the JHU083+Anti-PD-1 group was significantly lower than that in the JHU083 group and the Anti-PD-1 group, and the difference was statistically significant, indicating that both JHU083 and PD-1 inhibitors can effectively inhibit the proliferation of pancreatic cancer cells. The effect of JHU083 alone was better than that of PD-1 inhibitor alone, and the inhibitory effect of the combination of the two drugs on tumor cell growth was significantly enhanced compared to either drug alone (Figure 5G). The CD8T cell density in the JHU083 group, Anti-PD-1 group, and JHU083+Anti-PD-1 group was significantly higher than that in the VEH group, and the difference was statistically significant. The CD8T cell density in the JHU083 group was significantly higher than that in the Anti-PD-1 group, and the CD8T cell density in the JHU083+Anti-PD-1 group was higher than that in either single-drug group (Figure 5H). The CD4 T cell density in the JHU083 group, Anti-PD-1 group, and JHU083+Anti-PD-1 group was significantly higher than that in the VEH group, and the difference was statistically significant. The CD8T cell density in the JHU083 group was significantly higher than that in the Anti-PD-1 group, while the CD8T cell density in the JHU083+Anti-PD-1 group was significantly higher than that in the Anti-PD-1 group, with no significant difference from the JHU083 group (Figure 5I). This indicates that JHU083 can enhance the immune infiltration of both CD8T and CD4 T cells in the pancreatic cancer microenvironment, while PD-1 inhibitors can only enhance the immune infiltration of CD8 T cells. Compared to JHU083 or PD-1 inhibitor alone, the combination of the two drugs can enhance the infiltration of CD8 T cells in the pancreatic cancer immune microenvironment. There was no statistically significant difference in the CCR7+ cell density between the JHU083 group and the JHU083+Anti-PD-1 group, but it was significantly higher than that in the VEH group and the Anti-PD-1 group, while there was no statistically significant difference in the CCR7+ cell density between the VEH group and the Anti-PD-1 group (Figure 5J). This indicates that JHU083 can reduce the proportion of immature T lymphocytes in the tumor immune microenvironment, while PD-1 inhibitors have no such effect. Overall, JHU083 alone has a clear anti-tumor effect on pancreatic cancer and enhances the anti-tumor effect of PD-1 inhibitors.

3.6 The glutamine metabolism enzyme inhibitor (JHU083) can inhibit the apoptosis of immune cells in the tumor immune microenvironment and enhance the anti-tumor effect of CD8 T cells

In order to investigate the effect of the glutamine metabolism inhibitor JHU083 on CD8 T cells infiltration and immune phenotype in the immune microenvironment, we used flow cytometry to perform immune typing of CD8 T cells in tumor

10.3389/fimmu.2025.1599252

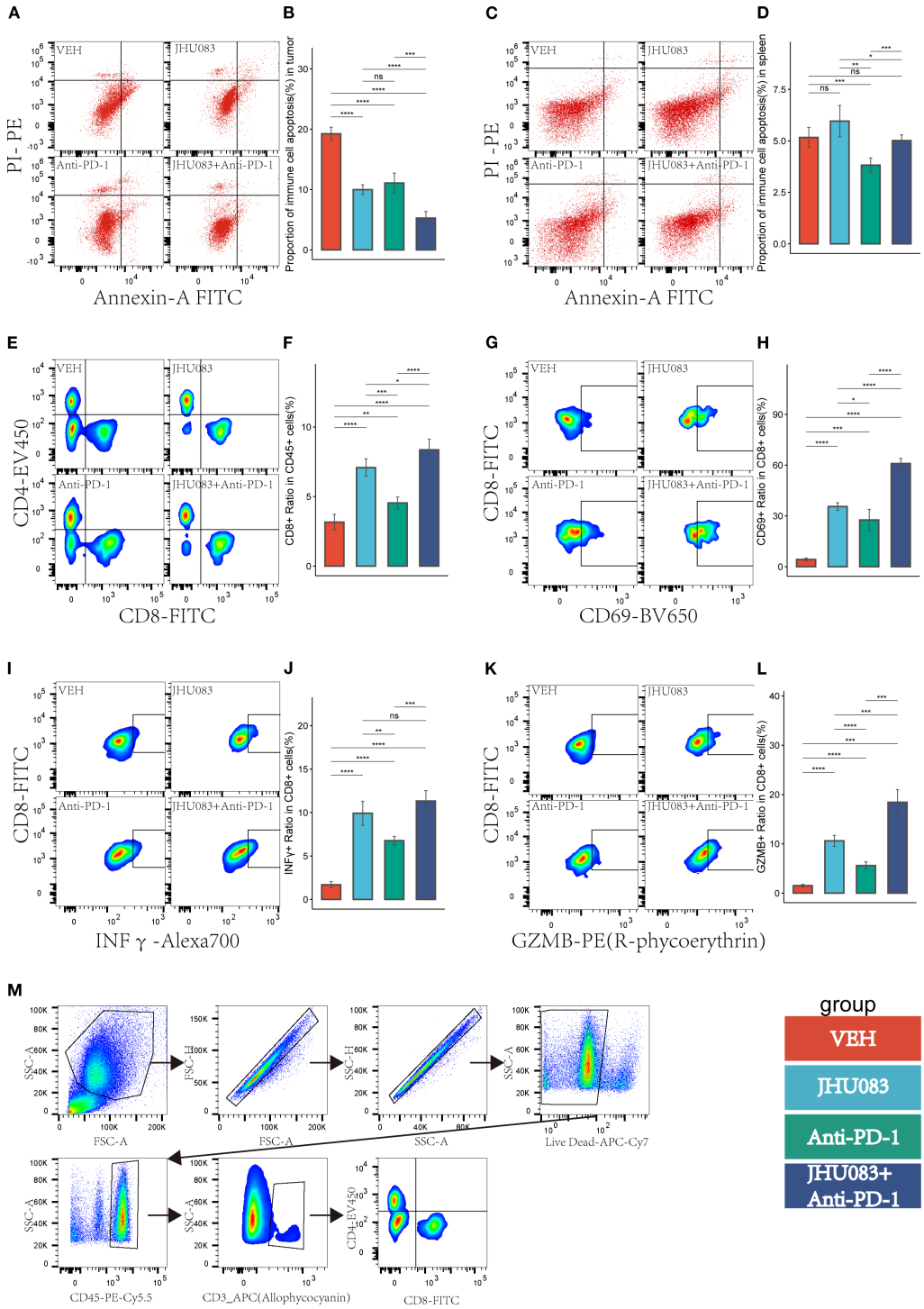

FIGURE 6
In the pancreatic cancer microenvironment, the inhibition of glutamine metabolism can suppress the apoptosis of immune cells, increase immune cell infiltration, reshape the CD8 T-cell immune phenotype, and enhance the immune therapy response. Different colors were used to mark the groups: red, blue, green, and purple represent VEH, JHU083, antiPD-1, and JHU083+antiPD-1 groups, respectively. NS indicates no statistical significance; *p < 0.05; **p < 0.01; ***p < 0.001; ****p < 0.0001. (**A**, **C**) show the flow cytometry of the tumor microenvironment of subcutaneous tumors in each group of mice and the apoptosis of immune cells in the spleen, respectively. (**B**, **D**) show the statistical analysis of immune cell apoptosis in the tumor microenvironment and spleen, respectively. **(E)** shows the flow cytometry cell sorting diagram, including T cells, CD8+ T cells, and CD4+ T cells. **(F)** shows the difference in the proportion of CD8T cells in CD45 cells in each group. (**G**, **I**, **K**) are flow cytometry cell sorting diagrams, including CD8+CD69+ T cells, CD8+INFγ+ T cells, and CD8+GZMB+ T cells. (**H**, **J**, **L**) show the percentage of the above cells in CD8T cells in a bar graph. **(M)** shows the gating diagram for flow cytometry cell sorting.

tissue (CD69 as a T cell activation marker, INFγ and GZMB as cell cytotoxicity markers). The proportion of CD8 T cells in CD45 T cells in the JHU083 group, Anti-PD-1 group, and JHU083+Anti-PD-1 group was significantly higher than that in the VEH group. The proportion of CD8 T cells in CD45 T cells in the JHU083 group was significantly higher than that in the Anti-PD-1 group. The proportion of CD8 T cells in CD45 T cells in the JHU083+Anti-PD-1 group was significantly higher than that in the single drug group (Figures 6E, F). These results indicate that both JHU083 and Anti-PD-1 can increase the proportion of CD8 T cells in CD45 T cells in the immune microenvironment, and single-use JHU083 is superior to Anti-PD-1, while the combination of the two is better than single drugs. The proportion of CD8+CD69+ T cells in CD8 T cells in the JHU083 group, Anti-PD-1 group, and JHU083+Anti-PD-1 group was significantly higher than that in the VEH group. The proportion of CD8+CD69+ T cells in CD8 T cells in the JHU083 group was significantly higher than that in the Anti-PD-1 group. The proportion of CD8+CD69+T cells in CD8 T cells in the JHU083+Anti-PD-1 group was significantly higher than that in the single drug group (Figures 6G, H), indicating that single-use JHU083 and Anti-PD-1 can both stimulate CD8 T cells activation, but single-use JHU083 is superior to Anti-PD-1, and the combination of the two is better than single drugs.

The proportion of CD8+ INFγ+ T cells in CD8 T cells was significantly higher in the JHU083 group, Anti-PD-1 group, and JHU083+Anti-PD-1 group than in the VEH group. The proportion of CD8+ INFγ+ T cells in the JHU083 group was significantly higher than that in the Anti-PD-1 group. The proportion of CD8+ INFγ+ T cells in the JHU083+Anti-PD-1 group was significantly higher than that in the Anti-PD-1 group, but there was no statistically significant difference between the JHU083 group and the JHU083+Anti-PD-1 group. The proportion of CD8+ GZMB+ T cells in CD8 T cells was significantly higher in the JHU083 group, Anti-PD-1 group, and JHU083+Anti-PD-1 group than in the VEH group. The proportion of CD8+ GZMB+ T cells in the JHU083 group was significantly higher than that in the Anti-PD-1 group. The proportion of CD8+ GZMB+ T cells in the JHU083+Anti-PD-1 group was significantly higher than that in the single drug groups. These results indicate that both the JHU083 group and the Anti-PD-1 group can enhance the cytotoxicity of CD8 T cells to a certain extent, but JHU083 alone is superior to Anti-PD-1, and the combination of the two is better than using a single drug. In summary, the glutaminase inhibitor JHU083 can inhibit the apoptosis of immune cells in the tumor immune microenvironment and enhance the anti-tumor effect of CD8 T cells. Furthermore, it can enhance the anti-tumor effect of PD-1 inhibitors.

4 Discussion

Pancreatic cancer is known to be glutamine-dependent (41–43), yet how tumor cell glutamine metabolism influences immune cells in the tumor microenvironment is still unclear. In this study, based on the pancreatic cancer dataset in the TCGA database, we found that the tumor glutamine metabolism of patients was negatively correlated with patient prognosis and immune cell cytotoxicity, and positively correlated with immune cell immaturity score. After analyzing the pancreatic cancer single-cell dataset in the GEO database, we found that high glutamine metabolism in tumor cells would inhibit the anti-tumor effect of CD8 T cells. Through *in vivo* experiments in mice, we observed that the glutamine metabolism inhibitor has an anti-tumor effect and can inhibit immune cell apoptosis in the tumor microenvironment, while increasing the cytotoxicity of CD8 T cells and enhancing the anti-tumor efficacy of PD-1 inhibitors.

In recent years, the incidence of pancreatic cancer has been on the rise. It accounts for approximately 2% of all cancers and is associated with 5% of cancer-related deaths (2, 44). The pancreatic cancer microenvironment is considered an immune-suppressive environment (45–51). In the pancreatic cancer microenvironment, most T lymphocytes are CD4 T cells, with CD8 T cells accounting for only a small proportion. The CD4 T cells in the pancreatic cancer microenvironment are mainly Th2 cells, rather than Th1 cells. Th2 cells are associated with tumor immune tolerance, while Th1 cells can increase the tumor-killing effect of CD8 T cells (24, 25). In addition, Treg cells within the CD4 T cell population gradually increase in the development of pancreatic cancer (24, 52). Interestingly, Treg cells play an important role in immune evasion in pancreatic cancer through various immunosuppressive mechanisms (24, 52, 53). These may be the reasons why immune checkpoint inhibitors have not achieved satisfactory therapeutic effects. Therefore, a thorough investigation into the formation mechanism of the immune-suppressive microenvironment in pancreatic cancer is an important approach to improving the efficacy of pancreatic cancer immunotherapy. In this study, through transcriptome sequencing of tissue blocks, we found that the expression score of tumor glutamine metabolism-related genes was negatively correlated with patient prognosis, immune cell toxicity, and immune cell differentiation. Meanwhile, single-cell sequencing data analysis results showed that the anti-tumor activity of CD8T effector cells in the tumor immune microenvironment of patients with high tumor glutamine metabolism was reduced. High tumor glutamine metabolism in tumor cells reduced the cytotoxicity and differentiation degree of CD8-Tem subsets and increased the CD8-Temra exhaustion score. Through GSEA analysis, we observed a negative correlation between tumor cell glutamine metabolism and the activation and differentiation of CD8-Tem and CD8-Temra subsets. Through the above studies, we hypothesize that high tumor glutamine metabolism reshapes the tumor metabolic microenvironment, causing a decrease in the anti-tumor effect of CD8-Tef. Disrupting such abnormal tumor metabolic microenvironments may improve the anti-tumor activity of CD8-Tef, and the efficacy of immune checkpoint inhibitors may also improve.

According to existing research, the tumor microenvironment where CD8 T cells are located is closely related to their developmental trajectory (26). This suggests that the abnormal metabolism of tumor cell glutamine may reshape the metabolic

microenvironment of the tumor and alter the developmental trajectory of CD8 T cells. Gene dynamic time analysis and gene set enrichment analysis show that the proportion of CD8 T cells in fate 2 development in the high glutamine score group of tumor cells is significantly lower than that in the low glutamine score group. When CD8 T cells develop into fate 2, they mainly up-regulate immune activation-related pathways. Based on the above data, we speculate that CD8 T cells in the tumor microenvironment with high glutamine metabolism are more likely to lead to weakened anti-tumor activity. When tumor cell glutamine metabolism is inhibited, the developmental trajectory of CD8 T cells returns to normal, and their anti-tumor activity also recovers.

The efficacy of PD-1 inhibitors was found to depend on the infiltration of immune cells in the tumor microenvironment (54, 55). Previous research suggests that blocking the high metabolism of glutamine in tumor cells may increase immune infiltration and promote the differentiation of immune cells, while also potentially enhancing the anti-tumor effect of CD8 T cells. In a subcutaneous pancreatic cancer mouse model, we demonstrated that a glutamine inhibitor can increase the infiltration of CD4 T and CD8 T cells in the tumor microenvironment, promote the differentiation of immune cells, inhibit the rapid proliferation of tumor cells, and enhance the inhibitory effect of PD-1 inhibitors on tumor growth. After treatment with the glutamine inhibitor, the tumor volume significantly decreased, and the growth rate slowed significantly. We found that the anti-tumor effect of using only the glutamine inhibitor was superior to using only PD-1 inhibitor, but the combined use of the two significantly improved the anti-tumor effect. We also observed that the glutamine inhibitor can inhibit the apoptosis of immune cells in the tumor microenvironment, and the combined use of the glutamine inhibitor and PD-1 inhibitor had a stronger effect in inhibiting immune cell apoptosis. Interestingly, the proportion of immune cell apoptosis in the spleen decreased significantly after using only PD-1, but after the combined use of the glutamine inhibitor, the proportion of apoptosis returned to normal levels. Therefore, we speculate that JHU083 not only increases the anti-tumor effect of PD-1 but may also reduce the toxic side effects of PD-1 in normal tissues. Through flow cytometry cell sorting, we found that the glutamine inhibitor can promote the infiltration and activation of CD8 T cells, as well as increase their toxicity, and its effect was significantly enhanced when combined with PD-1 inhibitors. We speculate that the excellent efficacy of JHU083 may be closely related to the increased cytotoxicity of CD8 T cells and the inhibition of tumor cell growth. The effect of the glutamine inhibitor on these two cell subsets has already been confirmed in colon cancer (56). In addition, inhibiting the activity of GLS can reduce the accumulation of intracellular alpha-ketoglutarate and confer a high proliferative and long-lived phenotype to CD8 T cells (56, 57). Even when the glutamine metabolism pathway is completely inhibited, CD8 T cells can still compensate by taking up glucose, increasing the activity of pyruvate carboxylase, and enhancing the activity of the acetyl-CoA metabolism pathway, leading to increased cellular metabolism (58). However, this flexible metabolic compensation mechanism is lacking in tumor cells.

However, our study still has some shortcomings. Although we have demonstrated that inhibiting glutamine metabolism in the tumor microenvironment can increase the infiltration density of CD4 T cells, we have not proven the subtype of CD4 T cells that increased in the tumor microenvironment (TME). Therefore, we cannot determine whether the increased CD4 T cell subtype promotes the enhanced function of CD8 T cells as Th1 cells or promotes immune evasion of pancreatic cancer as Treg cells, or other subtypes. Furthermore, although inhibiting glutamine metabolism in the TME can enhance the cytotoxicity of CD8 T cells, we still do not know the specific mechanism. We have demonstrated that a glutamine inhibitor can enhance the anti-tumor effect of PD-1 inhibitors, but we are not sure whether the enhanced ability of PD-1 to fight tumors is related to the increased cytotoxicity of CD8 T cells. Finally, the animal model we used only includes some pathological and clinical features of human pancreatic cancer, so the sensitizing effect of the glutamine inhibitor on PD-1 inhibitors needs further validation in clinical trials.

Data availability statement

Publicly available datasets were analyzed in this study. This data can be found here: GSE155698, https://www.ncbi.nlm.nih.gov/geo/query/acc.cgi?acc=GSE155698.

Ethics statement

The animal study was approved by the Animal Experimental Ethics Committee of Southwest Medical University. The study was conducted in accordance with the local legislation and institutional requirements.

Author contributions

JF: Software, Conceptualization, Data curation, Validation, Writing – review & editing, Formal Analysis, Writing – original draft. JC: Writing – original draft. RW: Writing – original draft. YP: Writing – original draft. ST: Writing – original draft. XZ: Writing – original draft. HT: Writing – original draft. MC: Writing – review & editing, Data curation, Funding acquisition, Investigation. BL: Writing – original draft. XY: Writing – original draft, Writing – review & editing, Funding acquisition.

Funding

The author(s) declare financial support was received for the research and/or publication of this article. This work was supported by Clinical Research Project of Wu Jie-Ping Medical Foundation (No. 320.6750.2022-19-20) and the Key Research and Development Project of the Science & Technology Department of Sichuan Province (Nos.2021YFS0231).

Conflict of interest

The authors declare that the research was conducted in the absence of any commercial or financial relationships that could be construed as a potential conflict of interest.

Generative AI statement

The author(s) declare that no Generative AI was used in the creation of this manuscript.

Any alternative text (alt text) provided alongside figures in this article has been generated by Frontiers with the support of artificial intelligence and reasonable efforts have been made to ensure accuracy, including review by the authors wherever possible. If you identify any issues, please contact us.

Publisher's note

Supplementary material

The Supplementary Material for this article can be found online at: https://www.frontiersin.org/articles/10.3389/fimmu.2025.1599252/full#supplementary-material

References

1. Siegel RL, Miller KD, Fuchs HE, Jemal A. Cancer statistics, 2021. *CA: Cancer J Clin*. (2021) 71:7–33. doi: 10.3322/caac.21654

2. Rahib L, Smith BD, Aizenberg R, Rosenzweig AB, Fleshman JM, Matrisian LM. Projecting cancer incidence and deaths to 2030: the unexpected burden of thyroid, liver, and pancreas cancers in the United States. *Cancer Res*. (2014) 74:2913–21. doi: 10.1158/0008-5472.CAN-14-0155

3. Kommalapati A, Tella SH, Goyal G, Shroff RT. Contemporary management of localized resectable pancreatic cancer. *Cancers*. (2018) 10. doi: 10.3390/cancers10010024

4. Mizrahi JD, Surana R, Valle JW, Shroff RT. Pancreatic cancer. *Lancet (London England)*. (2020) 395:2008–20. doi: 10.1016/S0140-6736(20)30974-0

5. Kamisawa T, Wood LD, Itoi T, Takaori K. Pancreatic cancer. *Lancet (London England)*. (2016) 388:73–85. doi: 10.1016/S0140-6736(16)00141-0

6. Brahmer JR, Tykodi SS, Chow LQ, Hwu WJ, Topalian SL, Hwu P, et al. Safety and activity of anti-PD-L1 antibody in patients with advanced cancer. *New Engl J Med*. (2012) 366:2455–65. doi: 10.1056/NEJMoa1200694

7. Weiss GJ, Waypa J, Blaydorn L, Coats J, McGahey K, Sangal A, et al. A phase Ib study of pembrolizumab plus chemotherapy in patients with advanced cancer (PembroPlus). *Br J Cancer*. (2017) 117:33–40. doi: 10.1038/bjc.2017.145

8. Sharma P, Sohn J, Shin SJ, Oh DY, Keam B, Lee HJ, et al. Efficacy and tolerability of tremelimumab in locally advanced or metastatic urothelial carcinoma patients who have failed first-line platinum-based chemotherapy. *Clin Cancer Res*. (2020) 26:61–70. doi: 10.1158/1078-0432.CCR-19-1635

9. Royal RE, Levy C, Turner K, Mathur A, Hughes M, Kammula US, et al. Phase 2 trial of single agent Ipilimumab (anti-CTLA-4) for locally advanced or metastatic pancreatic adenocarcinoma. *J immunother (Hagerstown Md: 1997)*. (2010) 33:828–33. doi: 10.1097/CJI.0b013e3181eec14c

10. Aglietta M, Barone C, Sawyer MB, Moore MJ, Miller WH Jr, Bagalà C, et al. A phase I dose escalation trial of tremelimumab (CP-675,206) in combination with gemcitabine in chemotherapy-naive patients with metastatic pancreatic cancer. *Ann Oncol*. (2014) 25:1750–5. doi: 10.1093/annonc/mdu205

11. Kamath SD, Kalyan A, Kircher S, Nimeiri H, Fought AJ, Benson A 3rd, et al. Ipilimumab and gemcitabine for advanced pancreatic cancer: A phase ib study. *oncologist*. (2020) 25:e808–e15. doi: 10.1634/theoncologist.2019-0473

12. O'reilly EM, Oh DY, Dhani N, Renouf DJ, Lee MA, Sun W, et al. Durvalumab with or without tremelimumab for patients with metastatic pancreatic ductal adenocarcinoma: A phase 2 randomized clinical trial. *JAMA Oncol*. (2019) 5:1431–8. doi: 10.1001/jamaoncol.2019.1588

13. Overman M, Javle M, Davis RE, Vats P, Kumar-Sinha C, Xiao L, et al. Randomized phase II study of the Bruton tyrosine kinase inhibitor acalabrutinib, alone or with pembrolizumab in patients with advanced pancreatic cancer. *J immunother Cancer*. (2020) 8. doi: 10.1136/jitc-2020-000587

14. Ready NE, Ott PA, Hellmann MD, Zugazagoitia J, Hann CL, de Braud F, et al. Nivolumab monotherapy and nivolumab plus ipilimumab in recurrent small cell lung cancer: results from the checkMate 032 randomized cohort. *J Thorac Oncol*. (2020) 15:426–35. doi: 10.1016/j.jtho.2019.10.004

15. Le DT, Lutz E, Uram JN, Sugar EA, Onners B, Solt S, et al. Evaluation of ipilimumab in combination with allogeneic pancreatic tumor cells transfected with a GM-CSF gene in previously treated pancreatic cancer. *J immunother (Hagerstown Md: 1997)*. (2013) 36:382–9. doi: 10.1097/CJI.0b013e31829fb7a2

16. Nevala-Plagemann C, Hidalgo M, Garrido-Laguna I. From state-of-the-art treatments to novel therapies for advanced-stage pancreatic cancer. *Nat Rev Clin Oncol*. (2020) 17:108–23. doi: 10.1038/s41571-019-0281-6

17. Poschke I, Faryna M, Bergmann F, Flossdorf M, Lauenstein C, Hermes J, et al. Identification of a tumor-reactive T-cell repertoire in the immune infiltrate of patients with resectable pancreatic ductal adenocarcinoma. *Oncoimmunology*. (2016) 5:e1240859. doi: 10.1080/2162402X.2016.1240859

18. Mabrouk N, Tran T, Sam I, Pourmir I, Gruel N, Granier C, et al. CXCR6 expressing T cells: Functions and role in the control of tumors. *Front Immunol*. (2022) 13:1022136. doi: 10.3389/fimmu.2022.1022136

19. Raskov H, Orhan A, Christensen JP, Gögenur I. Cytotoxic CD8(+) T cells in cancer and cancer immunotherapy. *Br J Cancer*. (2021) 124:359–67. doi: 10.1038/s41416-020-01048-4

20. Jansen CS, Prokhnevska N, Master VA, Sanda MG, Carlisle JW, Bilen MA, et al. An intra-tumoral niche maintains and differentiates stem-like CD8 T cells. *Nature*. (2019) 576:465–70. doi: 10.1038/s41586-019-1836-5

21. Balachandran VP, Łuksza M, Zhao JN, Makarov V, Moral JA, Remark R, et al. Identification of unique neoantigen qualities in long-term survivors of pancreatic cancer. *Nature*. (2017) 551:512–6. doi: 10.1038/nature24462

22. Peng J, Sun BF, Chen CY, Zhou JY, Chen YS, Chen H, et al. Single-cell RNA-seq highlights intra-tumoral heterogeneity and Malignant progression in pancreatic ductal adenocarcinoma. *Cell Res*. (2019) 29:725–38. doi: 10.1038/s41422-019-0195-y

23. Ajina R, Weiner LM. T-cell immunity in pancreatic cancer. *Pancreas*. (2020) 49:1014–23. doi: 10.1097/MPA.0000000000001621

24. Ino Y, Yamazaki-Itoh R, Shimada K, Iwasaki M, Kosuge T, Kanai Y, et al. Immune cell infiltration as an indicator of the immune microenvironment of pancreatic cancer. *Br J Cancer*. (2013) 108:914–23. doi: 10.1038/bjc.2013.32

25. Foucher ED, Ghigo C, Chouaib S, Galon J, Iovanna J, Olive D. Pancreatic ductal adenocarcinoma: A strong imbalance of good and bad immunological cops in the tumor microenvironment. *Front Immunol*. (2018) 9:1044. doi: 10.3389/fimmu.2018.01044

26. Phan AT, Goldrath AW, Glass CK. Metabolic and epigenetic coordination of T cell and macrophage immunity. *Immunity*. (2017) 46:714–29. doi: 10.1016/j.immuni.2017.04.016

27. Thommen DS, Schumacher TN. T cell dysfunction in cancer. *Cancer Cell*. (2018) 33:547–62. doi: 10.1016/j.ccell.2018.03.012

28. Zacharakis N, Chinnasamy H, Black M, Xu H, Lu YC, Zheng Z, et al. Immune recognition of somatic mutations leading to complete durable regression in metastatic breast cancer. *Nat Med*. (2018) 24:724–30. doi: 10.1038/s41591-018-0040-8

29. Guo D, Tong Y, Jiang X, Meng Y, Jiang H, Du L, et al. Aerobic glycolysis promotes tumor immune evasion by hexokinase2-mediated phosphorylation of IκBα. *Cell Metab*. (2022) 34:1312–24.e6. doi: 10.1016/j.cmet.2022.08.002

30. Reinfeld BI, Madden MZ, Wolf MM, Chytil A, Bader JE, Patterson AR, et al. Cell-programmed nutrient partitioning in the tumour microenvironment. *Nature*. (2021) 593:282–8. doi: 10.1038/s41586-021-03442-1

31. Wise DR, Thompson CB. Glutamine addiction: a new therapeutic target in cancer. *Trends Biochem Sci*. (2010) 35:427–33. doi: 10.1016/j.tibs.2010.05.003

32. Hensley CT, Wasti AT, Deberardinis RJ. Glutamine and cancer: cell biology, physiology, and clinical opportunities. *J Clin Invest*. (2013) 123:3678–84. doi: 10.1172/JCI69600

33. Youngblood VM, Kim LC, Edwards DN, Hwang Y, Santapuram PR, Stirdivant SM, et al. The ephrin-A1/EPHA2 signaling axis regulates glutamine metabolism in HER2-positive breast cancer. *Cancer Res*. (2016) 76:1825–36. doi: 10.1158/0008-5472.CAN-15-0847

34. Nakazawa MS, Keith B, Simon MC. Oxygen availability and metabolic adaptations. *Nat Rev Cancer*. (2016) 16:663–73. doi: 10.1038/nrc.2016.84

35. Fuchs BC, Bode BP. Amino acid transporters ASCT2 and LAT1 in cancer: partners in crime? *Semin Cancer Biol*. (2005) 15:254–66. doi: 10.1038/nrc.2016.84

36. Wise DR, Deberardinis RJ, Mancuso A, Sayed N, Zhang XY, Pfeiffer HK, et al. Myc regulates a transcriptional program that stimulates mitochondrial glutaminolysis and leads to glutamine addiction. *Proc Natl Acad Sci United States America*. (2008) 105:18782–7. doi: 10.1073/pnas.0810199105

37. Liu J, Liu W, Wan Y, Mao W. Crosstalk between exercise and immunotherapy: current understanding and future directions. *Res (Wash D C)*. (2024) 7:0360. doi: 10.34133/research.0360

38. Liang H, Lu Q, Yang J, Yu G. Supramolecular biomaterials for cancer immunotherapy. *Res (Wash D C)*. (2023) 6:0211. doi: 10.34133/research.0211

39. Steele NG, Carpenter ES, Kemp SB, Sirihorachai VR, The S, Delrosario L, et al. Multimodal mapping of the tumor and peripheral blood immune landscape in human pancreatic cancer. *Nat Cancer*. (2020) 1:1097–112. doi: 10.1038/s43018-020-00121-4

40. Zheng L, Qin S, Si W, Wang A, Xing B, Gao R, et al. Pan-cancer single-cell landscape of tumor-infiltrating T cells. *Sci (New York NY)*. (2021) 374:abe6474. doi: 10.1126/science.abe6474

41. Raho S, Capobianco L, Malivindi R, Vozza A, Piazzolla C, De Leonardis F, et al. KRAS-regulated glutamine metabolism requires UCP2-mediated aspartate transport to support pancreatic cancer growth. *Nat Metab*. (2020) 2:1373–81. doi: 10.1038/s42255-020-00315-1

42. Kerk SA, Papagiannakopoulos T, Shah YM, Lyssiotis CA. Metabolic networks in mutant KRAS-driven tumours: tissue specificities and the microenvironment. *Nat Rev Cancer*. (2021) 21:510–25. doi: 10.1038/s41568-021-00375-9

43. Son J, Lyssiotis CA, Ying H, Wang X, Hua S, Ligorio M, et al. Glutamine supports pancreatic cancer growth through a KRAS-regulated metabolic pathway. *Nature*. (2013) 496:101–5. doi: 10.1038/nature12040

44. Zhang X, Liu Q, Liao Q, Zhao Y. Pancreatic cancer, gut microbiota, and therapeutic efficacy. *J Cancer*. (2020) 11:2749–58. doi: 10.7150/jca.37445

45. Zhou W, Zhou Y, Chen X, Ning T, Chen H, Guo Q, et al. Pancreatic cancer-targeting exosomes for enhancing immunotherapy and reprogramming tumor microenvironment. *Biomaterials*. (2021) 268:120546. doi: 10.1016/j.biomaterials.2020.120546

46. Feig C, Jones JO, Kraman M, Wells RJ, Deonarine A, Chan DS, et al. Targeting CXCL12 from FAP-expressing carcinoma-associated fibroblasts synergizes with anti-PD-L1 immunotherapy in pancreatic cancer. *Proc Natl Acad Sci United States America*. (2013) 110:20212–7. doi: 10.1073/pnas.1320318110

47. Topalian SL, Drake CG, Pardoll DM. Immune checkpoint blockade: a common denominator approach to cancer therapy. *Cancer Cell*. (2015) 27:450–61. doi: 10.1016/j.ccell.2015.03.001

48. Tumeh PC, Harview CL, Yearley JH, Shintaku IP, Taylor EJ, Robert L, et al. PD-1 blockade induces responses by inhibiting adaptive immune resistance. *Nature*. (2014) 515:568–71. doi: 10.1038/nature13954

49. Balachandran VP, Beatty GL, Dougan SK. Broadening the impact of immunotherapy to pancreatic cancer: challenges and opportunities. *Gastroenterology*. (2019) 156:2056–72. doi: 10.1053/j.gastro.2018.12.038

50. Neesse A, Bauer CA, Öhlund D, Lauth M, Buchholz M, Michl P, et al. Stromal biology and therapy in pancreatic cancer: ready for clinical translation? *Gut*. (2019) 68:159–71. doi: 10.1136/gutjnl-2018-316451

51. Wörmann SM, Diakopoulos KN, Lesina M, Algül H. The immune network in pancreatic cancer development and progression. *Oncogene*. (2014) 33:2956–67. doi: 10.1038/onc.2013.257

52. Hiraoka N, Onozato K, Kosuge T, Hirohashi S. Prevalence of FOXP3+ regulatory T cells increases during the progression of pancreatic ductal adenocarcinoma and its premalignant lesions. *Clin Cancer Res*. (2006) 12:5423–34. doi: 10.1158/1078-0432.CCR-06-0369

53. Jang JE, Hajdu CH, Liot C, Miller G, Dustin ML, Bar-Sagi D. Crosstalk between regulatory T cells and tumor-associated dendritic cells negates anti-tumor immunity in pancreatic cancer. *Cell Rep*. (2017) 20:558–71. doi: 10.1016/j.celrep.2017.06.062

54. Zhang J, Huang D, Saw PE, Song E. Turning cold tumors hot: from molecular mechanisms to clinical applications. *Trends Immunol*. (2022) 43:523–45. doi: 10.1016/j.it.2022.04.010

55. Mansurov A, Ishihara J, Hosseinchi P, Potin L, Marchell TM, Ishihara A, et al. Collagen-binding IL-12 enhances tumour inflammation and drives the complete remission of established immunologically cold mouse tumours. *Nat Biomed Eng*. (2020) 4:531–43. doi: 10.1038/s41551-020-0549-2

56. Leone RD, Zhao L, Englert JM, Sun IM, Oh MH, Sun IH, et al. Glutamine blockade induces divergent metabolic programs to overcome tumor immune evasion. *Sci (New York NY)*. (2019) 366:1013–21. doi: 10.1126/science.aav2588

57. Chisolm DA, Savic D, Moore AJ, Ballesteros-Tato A, León B, Crossman DK, et al. CCCTC-binding factor translates interleukin 2- and α-ketoglutarate-sensitive metabolic changes in T cells into context-dependent gene programs. *Immunity*. (2017) 47:251–67.e7. doi: 10.1016/j.immuni.2017.07.015

58. Tyrakis PA, Palazon A, Macias D, Lee KL, Phan AT, Veliça P, et al. S-2-hydroxyglutarate regulates CD8(+) T-lymphocyte fate. *Nature*. (2016) 540:236–41. doi: 10.1038/nature20165

Frontiers in Immunology

Explores novel approaches and diagnoses to treat immune disorders.

The official journal of the International Union of Immunological Societies (IUIS) and the most cited in its field, leading the way for research across basic, translational and clinical immunology.

Discover the latest Research Topics

See more →

Frontiers

Avenue du Tribunal-Fédéral 34
1005 Lausanne, Switzerland
frontiersin.org

Contact us

+41 (0)21 510 17 00
frontiersin.org/about/contact